

The synthesis of novel olfactory receptor agonists and explorations in the selective fluorination of the *tert*-butyl group for bioactives discovery

Luca Dobson

A thesis submitted for the degree of PhD
at the
University of St Andrews



2024

Full metadata for this item is available in
St Andrews Research Repository
at:

<https://research-repository.st-andrews.ac.uk/>

Identifier to use to cite or link to this thesis:

DOI: <https://doi.org/10.17630/sta/853>

This item is protected by original copyright

Candidate's declaration

I, Luca Dobson, do hereby certify that this thesis, submitted for the degree of PhD, which is approximately 38,000 words in length, has been written by me, and that it is the record of work carried out by me, or principally by myself in collaboration with others as acknowledged, and that it has not been submitted in any previous application for any degree. I confirm that any appendices included in my thesis contain only material permitted by the 'Assessment of Postgraduate Research Students' policy.

I was admitted as a research student at the University of St Andrews in May 2019.

I received funding from an organisation or institution and have acknowledged the funder(s) in the full text of my thesis.

10/04/24

Date

Signature of candidate

Supervisor's declaration

I hereby certify that the candidate has fulfilled the conditions of the Resolution and Regulations appropriate for the degree of PhD in the University of St Andrews and that the candidate is qualified to submit this thesis in application for that degree. I confirm that any appendices included in the thesis contain only material permitted by the 'Assessment of Postgraduate Research Students' policy.

10/04/24

Date

Signature of supervisor

Permission for publication

In submitting this thesis to the University of St Andrews we understand that we are giving permission for it to be made available for use in accordance with the regulations of the University Library for the time being in force, subject to any copyright vested in the work not being affected thereby. We also understand, unless exempt by an award of an embargo as requested below, that the title and the abstract will be published, and that a copy of the work may be made and supplied to any bona fide library or research worker, that this thesis will be electronically accessible for personal or research use and that the library has the right to migrate this thesis into new electronic forms as required to ensure continued access to the thesis.

I, Luca Dobson, confirm that my thesis does not contain any third-party material that requires copyright clearance.

The following is an agreed request by candidate and supervisor regarding the publication of this thesis:

Printed copy

No embargo on print copy.

Electronic copy

No embargo on electronic copy.

10/04/24

Date

Signature of candidate

10/04/24

Date

Signature of supervisor

Underpinning Research Data or Digital Outputs

Candidate's declaration

I, Luca Dobson, understand that by declaring that I have original research data or digital outputs, I should make every effort in meeting the University's and research funders' requirements on the deposit and sharing of research data or research digital outputs.

10/04/24

Date

Signature of candidate

Permission for publication of underpinning research data or digital outputs

We understand that for any original research data or digital outputs which are deposited, we are giving permission for them to be made available for use in accordance with the requirements of the University and research funders, for the time being in force.

We also understand that the title and the description will be published, and that the underpinning research data or digital outputs will be electronically accessible for use in accordance with the license specified at the point of deposit, unless exempt by award of an embargo as requested below.

The following is an agreed request by candidate and supervisor regarding the publication of underpinning research data or digital outputs:

No embargo on underpinning research data or digital outputs.

10/04/24

Date

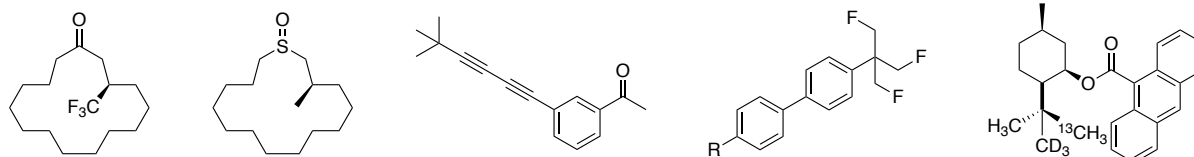
Signature of candidate

10/04/24

Date

Signature of supervisor

Abstract



In Chapter 1, an introduction to fluorine chemistry is given. The physical properties of fluorine are discussed, and examples of how the introduction of fluorine into a molecule can influence the structure and properties of a molecule are provided. Strategies for the incorporation of fluorine within a molecule are also discussed.

In Chapter 2, the structure and properties of (*R*)-muscone are discussed. The mechanism of olfaction is outlined, and the debate between the conformation and vibrational theories of olfaction is discussed. The development of a series of derivatives of (*R*)-muscone is explored, in particular trifluoromethyl, chloro and sulfoxide derivatives. Their effectiveness as olfactory molecules is compared to that of (*R*)-muscone to determine how altering the structure of (*R*)-muscone effects interactions with known olfactory receptors.

In Chapter 3, the structure and properties of synthetic musk compounds previously developed as alternatives to (*R*)-muscone is developed. The development of a new series of *bis*-acetylene compounds as prospective musk odorants is outlined. Their effectiveness as odorants is measured and targets are developed to determine the optimal shape and configuration of this class of molecule for interacting with olfactory receptors.

In Chapter 4, the effect of fluorine on the lipophilicity of compounds is outlined, and the *tert*-butyl group is discussed, particularly its uses in medicinal chemistry. The development of a new motif, the aryl β,β',β'' -trifluoro *tert*-butyl group is outlined, followed by an investigation into the structure, reactivity and properties of the group, to measure the effect of the fluorination of the *tert*-butyl group.

In Chapter 5, the chiral methyl group is introduced, and its use in biosynthetic studies is discussed. The development of a chiral *tert*-butyl group is outlined, and attempts to develop ^1H and ^{13}C NMR assays of the group are discussed.

Acknowledgements

First and foremost, I would like to thank my supervisor, Prof. David O'Hagan, for his support and guidance throughout my PhD. The aftermath of the BMS fire, COVID lockdowns, part-time working due to social distancing guidelines and a lack of lab space, then finally the move into the new BMS building made this a challenging time to do a PhD and David was a steadfast support through all this upheaval. David has an unfailing enthusiasm for organofluorine chemistry which is both inspiring and admirable, which has provided a great example and motivation to me and to the rest of his group.

I would like to thank members of the DOH group past and present for their support throughout my PhD. I would like to especially thank Dr Rifahath Mon Neyya Ppadath and Dr Qingzhi Zhang for their support and guidance, particularly at the beginning of my PhD. I would also like to thank Dr Phill Lowe, Dr. Marta Wojnowska, Dr. Xuan Feng, Dr. Zeguo Fang, Dr Joshua Clark, Dr Cihang Yu, Dr Yohann Renault, Yawen Chen, Tommy Poskin, Mengfan He, Dominic Spurling, Josephine Stewart, George Kingsley-Moore and Oluwayinka Oke for their support and all the interesting chats and group events that helped to keep me going through the PhD. I would also like to thank Eva Atraszkiewicz for beginning the project that led to the work in Chapter 5, and for being a great MChem student who never failed to cheer me up. I would also like to thank Ben McKay for beginning the project that led to the work in Chapter 4.

I would also like to thank our collaborators on the projects within this thesis: Dr Hanyi Zhuang and Dr Weihong Liu at Hanwang Technology Co. in Beijing, China for their work on the luciferase assays in Chapters 2 and 3; Bruno Piscelli and Dr Rodrigo Cormanich at State University of Campinas in Campinas, Brazil for their work on the computational studies in Chapter 4; Dr Mohd Faheem Khan and Prof. Cormac Murphy at University College Dublin in Dublin, Ireland for their work on the feeding studies in Chapter 4. I would also like to thank Prof Andy Smith and Prof Russell Morris for access to their laboratory space in the aftermath of the BMS fire and during the COVID-19 pandemic. I would also like to thank Dr Siobhan Smith, Prof Thomas Lebl and Dr Maria Papa for their help with NMR, Caroline Horsburgh,

Alan Taylor and the Edinburgh mass spectrometry centre for running my mass spectrometry samples, and Dr David Cordes for solving my X-Ray crystal structures.

I would again like to thank Yohann Renault and Maria Papa for being a great support through every step of the PhD, from start to finish, and Yohann and his godmother for providing free accommodation in Paris. I would also like to thank my family and friends for their emotional support throughout my PhD, without whom it would've been far more difficult to make it through these four and a half years.

I would like to thank the EPSRC DTP and University of St Andrews for funding my PhD.

Funding

This work was supported by the EPSRC DTP and University of St Andrews.

Research Data/Digital Outputs access statement

Research data underpinning this thesis are available at <https://doi.org/10.17630/786f436c-7dda-45d3-8ce1-6cd6418ec33c>

Abbreviations

ΔG	change in Gibbs free energy
acac	acetylacetone
AIBN	azobisisobutyronitrile
Ar	aromatic
atm	atmosphere
BINAP	(2,2'-bis(diphenylphosphino)-1,1'-binaphthyl
bpy	2,2'-bipyridine
CBS	Corey-Bakshi-Shibata catalyst
CFC	chlorofluorocarbon
COVID-19	Coronavirus disease 2019
CSD	Cambridge Structural Database
dap	2,9-bis(p-anisyl)-1,10-phenanthroline
DAST	diethylaminosulfur trifluoride
DCE	1,2-dichloroethane
DCM	dichloromethane
de	diastereomeric excess
DFT	Density functional theory
DMF	N,N-Dimethylformamide
DMSO	dimethylsulfoxide
DNP	2,4-dinitrophenol
dppf	1,1'-bis(diphenylphosphino)ferrocene
EC ₅₀	Half maximal effective concentration
ee	enantiomeric excess
equiv.	equivalents
FDA	The United States Food and Drug Administration
GC	Gas chromatography
GC-MS	Gas chromatography mass spectrometry
GWP	Global warming potential
HCFC	Hydrochlorofluorocarbon

HCl	Hydrochloric acid
HFC	Hydrofluorocarbon
HFO	Hydrofluoroolefin
HIV	Human immunodeficiency virus
HPLC	High-performance liquid chromatography
HRMS	High-resolution mass spectrometry
IR	Infrared
K	Association constant
LiHMDS	Lithium bis(trimethylsilyl)amide
logP	Log of the partition coefficient
<i>m</i> CPBA	<i>meta</i> -chloroperbenzoic acid
mRNA	Messenger RNA
MOR	Mouse olfactory receptor
m.p.	melting point
Ms	mesyl group
NADH	Reduced nicotinamide adenine dinucleotide
NADPH	Reduced nicotinamide adenine dinucleotide phosphate
NBS	N-bromosuccinimide
NHC	N-heterocyclic carbene
NMR	Nuclear magnetic resonance
ODS	Ozone-depleting substances
OECD	Organisation for Economic Co-operation and Development
OR1A1	Olfactory receptor family 1 subfamily A member 1
OR1A2	Olfactory receptor family 1 subfamily A member 2
OR5AN1	Olfactory receptor family 5 subfamily AN member 1
PAF	Platelet-activating factor receptor
PFAS	Per- and polyfluorinated alkyl substances
PFOA	Perfluorooctanoic acid
PFOS	Perfluorooctanesulfonic acid
phen	1,10-phenanthroline
pK _a	Negative log of K _a

pK _b	Negative log of K _b
PTFE	Polytetrafluoroethylene
OB	Olfactory bulb
OLED	Organic light-emitting diode
OR	Olfactory receptor
ppm	parts per million
RBF	round-bottomed flask
RNA	Ribonucleic acid
rt	room temperature
SAM	S-Adenosyl methionine
SCE	Saturated calomel electrode
SET	Single electron transfer
TBAB	Tetrabutylammonium bromide
TBAC	Tetrabutylammonium chloride
TBAF	Tetrabutylammonium fluoride
TBAI	Tetrabutylammonium fluoride
TBHP	<i>tert</i> -Butyl hydroperoxide
TBDMS	<i>tert</i> -Butyldimethylsilyl
Tf	triflyl group
TFA	trifluoroacetic acid
TFTB	tri-fluoro <i>tert</i> -butyl
THF	tetrahydrofuran
TLC	Thin-layer chromatography
tRNA	Transfer RNA
Ts	tosyl group

Contents

Abstract	v
Acknowledgements	vii
Abbreviations	ix
Contents	1
Chapter 1 - Introduction	5
1.1 Introduction to fluorine	5
1.2 Physical properties of fluorine	5
1.2.1 Electronegativity	5
1.2.2 The carbon-fluorine bond	6
1.2.3 Fluorine effects on pK_a	7
1.2.4 Fluorine effect on bond angles	9
1.2.5 Dipole-dipole interactions	10
1.2.6 Charge-dipole interactions.....	12
1.3 Fluorine in medicinal chemistry	13
1.3.1 Incorporation of fluorine to delay metabolism.....	14
1.3.2 Trifluoromethyl group in bioactives.....	15
1.4 Applications of synthetic fluorinated compounds	16
1.4.1 Chlorofluorocarbons (CFCs)	16
1.4.2 Per- and poly- fluoroalkyl substances (PFASs).....	18
1.4.3 Fluorous chemistry	20
1.5 Synthesis methods for introducing fluorine	21
1.5.1 Nucleophilic fluorination	21
1.5.2 Electrophilic fluorination	22
1.5.3 Radical perfluorination	25
1.6 Aims and objectives.....	29
Chapter 2 - Synthesis of cyclic musks	31
2.1 Introduction	31
2.1.1 Muscone	31
2.1.2 Muscone and the mechanism of olfaction	32

2.1.3 Fluorine in muscone	38
2.1.4 Recent cyclic musk developments	42
2.1.5 Olefin metathesis.....	43
2.1.6 Ring-closing metathesis	45
2.1.7 Sulfoxides and sulfones.....	47
2.1.8 Aims and objectives	48
2.2 Results and discussion.....	50
2.2.1 Synthesis of the CF ₃ containing muscone	50
2.2.2 Synthesis of a sulfoxide-derivative of (<i>R</i>)-muscone	62
2.3 Conclusions	73
Chapter 3 – Synthesis of acetylene musks.....	75
3.1 Introduction to polycyclic musks	75
3.1.1 Nitromusks.....	75
3.1.2 Polycyclic musks.....	81
3.1.3 Recent musk developments.....	84
3.1.4 Sonogashira cross-coupling.....	86
3.1.5 Cadiot-Chodkiewicz cross-coupling.....	88
3.1.6 The <i>gauche</i> effect	90
3.1.7 The anomeric effect	91
3.1.8 Fluorine as a hydrogen bond acceptor	92
3.1.9 Influencing the conformation of an aryl-carbonyl group.....	93
3.1.10 Aims and objectives	95
3.2 Synthesis of potential musks	96
3.2.1 Synthesis of monoacetylenes	96
3.2.2 Synthesis of initial <i>bis</i> -acetylene targets.....	100
3.2.3 Synthesis of indanone acetylenes.....	108
3.2.4 Synthesis of fluorinated <i>bis</i> -acetylenes	113
3.2.5 Synthesis of a <i>tris</i> -acetylene derivative	119
3.2.6 Synthesis of a dihydroisobenzylfuran <i>bis</i> -acetylene derivative	122
3.2.7 Synthesis of primary, tertiary and secondary alcohol <i>bis</i> -acetylenes	125
3.3 Conclusions.....	132
Chapter 4 – The tri-fluoro tert-butyl (TFTB) group.....	134

4.1 Introduction	134
4.1.1 Lipophilicity.....	134
4.1.2 Fluorine and lipophilicity	135
4.1.3 <i>tert</i> -Butyl group in nature and medicine	138
4.1.4 Tri-fluoro <i>tert</i> -butyl group.....	140
4.1.5 Suzuki cross-coupling reactions	143
4.1.6 Buchwald-Hartwig cross-coupling reactions.....	147
4.1.7 <i>Cunninghamella elegans</i>	152
4.1.8 Aims and objectives	153
4.2 Synthesis and properties of the tri-fluoro <i>tert</i>-butyl group	154
4.2.1 Development of a route to the aryl tri-fluoro <i>tert</i> -butyl group	154
4.2.2 Spectroscopic properties and lipophilicity of the aryl tri-fluoro <i>tert</i> -butyl group.....	156
4.2.3 Cross-coupling reactions of the tri-fluoro <i>tert</i> -butyl group	168
4.2.4 Conformational analysis of the aryl-TFTB group.....	173
4.2.5 Solubility of the aryl-TFTB group	177
4.2.6 Synthesis of an aryl-TFTB analogue of pyridaben	178
4.2.7 Other attempted reactions with the aryl trifluoro <i>tert</i> -butyl group	180
4.2.8 A study of the metabolism of the tri-fluoro <i>tert</i> -butyl group	183
4.3 Conclusions	189
Chapter 5 - Chiral <i>tert</i>-butyl group	190
5.1 Introduction	190
5.1.1 Biosynthetic origin of the <i>tert</i> -butyl group	190
5.1.2 The chiral methyl group.....	191
5.1.3 Applications of the chiral methyl group.....	195
5.1.4 The anthracene group.....	197
5.1.5 Aims and objectives	199
5.2 Synthesis and assay of the chiral <i>tert</i>-butyl group	200
5.2.1 Construction of the chiral <i>tert</i> -butyl group via conjugate addition	200
5.2.2 NMR assay and crystal structure.....	204
5.3 Conclusions	215
Chapter 6 – Conclusions and future work	216
Chapter 7 - Experimental	221

7.1 General experimental.....	221
7.2 Chapter 2	222
7.3 Chapter 3	249
7.4 Chapter 4	280
7.5 Chapter 5	302
7.6 Experimental details for computational analysis in Chapter 4.....	310
<i>Chapter 8 - References</i>	<i>312</i>

Chapter 1 - Introduction

1.1 Introduction to fluorine

Fluorine is the most abundant halogen and the 13th most abundant element in the earth's crust where it is found in fluoride-containing minerals. The most predominant of these is fluorite (CaF_2), originally known as fluorspar. Fluorite was first recorded in 1529 by Georgius Agricola. He recognised that fluorite could lower the melting point of solids in smelting processes.¹ In 1764, hydrofluoric acid was isolated by Andreas Sigismund Marggraf, who achieved this by heating fluorite with concentrated sulfuric acid. This was later repeated by Carl-Wilhelm Scheele in 1771.¹ The idea of isolating fluorine gas via electrolysis was first suggested by André-Marie Ampère in 1810, proposing the electrolysis of anhydrous hydrofluoric acid as a possible method to release fluorine gas. Following this, many chemists attempted to isolate fluorine gas via electrolysis. However, the violent reactivity of fluorine presented a significant challenge to this process, with numerous isolation attempts failing and some chemists even dying in their attempts.² The highly corrosive nature of hydrofluoric acid was in particular an issue when attempting electrolysis. However, it was not until 1886 that elemental fluorine was first isolated by Henri Moissan in Paris, work for which he was later awarded the Nobel Prize in 1906.³ He was able to achieve this via electrolysis of anhydrous hydrofluoric acid and with added potassium fluoride salt KHF_2 as an electrolyte, the latter of which was first isolated by Moissan's mentor Edmond Frémy in 1856. Moissan devised a platinum-based electrode system to conduct his electrolysis, operating at a low temperature using evacuated Dewar flasks. This had the effect of reducing corrosion during the process. However, large-scale isolation did not take place until World War II, when the USA required large amounts of fluorine to convert uranium into gaseous uranium hexafluoride (UF_6) for the Manhattan Project.⁴

1.2 Physical properties of fluorine

1.2.1 Electronegativity

Fluorine is an element with unique properties. It is the most electronegative element on the Pauling electronegativity scale (4.0), so a fluorine atom is highly electron-withdrawing.⁵ Also,

fluorine has the second-lowest atomic radius of all the elements (1.47 Å), second only to hydrogen. This is due to fluorine having the largest proton count of the period 2 elements, and therefore the highest effective nuclear charge of these elements. It follows that the valence electrons are held tightly to the nucleus, so the removal of an electron to generate F⁺ is a highly endothermic process (-401.2 kcal mol⁻¹). Conversely, the addition of an electron to fluorine is an exothermic process (+78.3 kcal mol⁻¹). This is because fluorine, with an electron configuration of 1s²2s²2p⁵, only requires one electron to fill its 2p subshell, so this process is energetically favourable. Furthermore, due to the high effective nuclear charge of the fluorine nucleus, the additional electron is well-stabilised.⁶

	H	C	N	O	F
Atomic radius (Å)	1.2	1.7	1.55	1.52	1.47
Pauling electronegativity	2.1	2.5	3.0	3.5	4.0

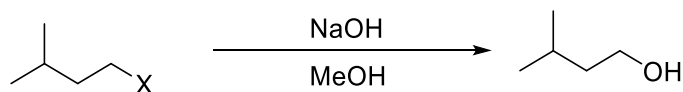
*Table 1.1 – Atomic radii and electronegativities of selected elements.*⁶

1.2.2 The carbon-fluorine bond

The carbon-fluorine bond is the strongest in organic chemistry, with C-F bond strengths ranging up to 130 kcal mol⁻¹.⁷ This is a result of the high electronegativity of fluorine polarising the carbon-fluorine bond, so carbon is essentially partially positively charged and fluorine is partially negatively charged. This gives the carbon-fluorine bond a strongly ionic character with a strong electrostatic attraction between the carbon and fluorine atoms. This is further exemplified by the decreasing carbon-fluorine bond lengths with the progressive replacement of hydrogen with fluorine in methane, and the carbon of tetrafluoromethane can be represented as C^{4δ+}. This increases the electrostatic attraction between the heavily polarised carbon and the fluorine atoms, shortening the bond length.⁸ Furthermore, fluorine and carbon have excellent overlap between their corresponding 2s and 2p orbitals due to their similar sizes again facilitating a strong and polarised C-F bond.

One result of this high bond strength is that fluorine is a poor leaving group, especially when compared to the other halogens, as shown in Table 1.2.⁶ This effect is pronounced in S_N2 reactions, where the rate of reaction for alkyl fluorides is lower than for alkyl chlorides and as much as three orders of magnitudes lower than for alkyl bromides or alkyl iodides. While

it could be expected that the polarisation of carbon by a geminal fluorine could make that carbon more electrophilic and so invite attack by a nucleophile, in reality, the strength of the carbon-fluorine bond disfavours the S_N2 reaction.



X	Relative rate of reaction
F	1
Cl	71
Br	3500
I	4500

Table 1.2 – Relative rates of S_N2 reactions of alkyl halides.⁶

However, fluorine has a propensity for elimination, particularly via an E1cB pathway, as illustrated in Figure 1.1.⁹ E1cB eliminations occur when there is an acidic proton *beta* to a weak leaving group, such as fluorine. The electronegative fluorine assists in polarising such a hydrogen by helping to stabilise the conjugate base (anion) through inductive effects. The anion then progresses to fluoride ion elimination.

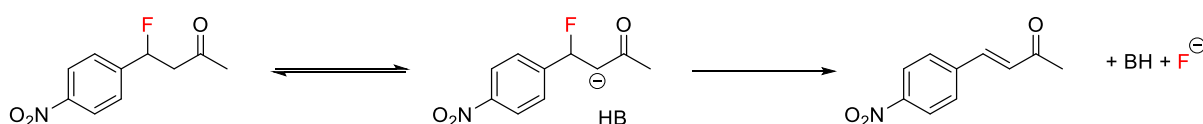


Figure 1.1 – An example of a fluorine-promoted E1cB reaction.⁹

1.2.3 Fluorine effects on pK_a

As a result of the low atomic radius of fluorine, it is often seen as a replacement for a hydrogen atom e.g. in medicinal chemistry, where there is a minimum steric impact when substituting hydrogen for fluorine. Yet the incorporation of even a single fluorine into an organic molecule can have a significant impact on its properties. For example, this incorporation can lead to a change in the pK_a of neighbouring functional groups.⁶ This is illustrated in the progressive fluorination of acetic acid as shown in Table 1.2, where increasing levels of fluorination decreases the pK_a , increasing the overall acidity. This is due

to the inductive effect of the electron-withdrawing fluorine stabilising the negative charge of the conjugate base.

Acetic acid analogue	pK_a
CH ₃ COOH	4.76
CH ₂ F ₁ COOH	2.59
CH ₂ F ₂ COOH	1.24
CF ₃ COOH	0.23

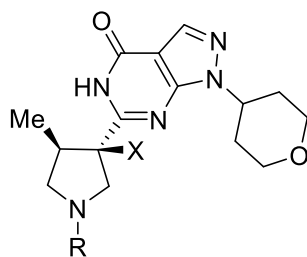
Table 1.2 – pK_a s of fluorinated analogues of acetic acid.⁶

Meanwhile, the introduction of fluorine can have a strong effect on basicity. One example of this is found in ethylamine, where the measured pK_b value and hence the basicity decreases with increasing levels of fluorination, as shown in Table 1.3. The effect is also illustrated by the decrease of the pK_b of aniline when the aromatic ring is perfluorinated. This is again due to the electron-withdrawing nature of fluorine causing an inductive effect, withdrawing the lone pair electron density on the nitrogen and making it less available, lowering the basicity.¹⁰

Ethylamine/aniline analogue	pK_b
CH ₃ CH ₂ NH ₂	10.7
CF ₃ CH ₂ NH ₂	5.9
C ₆ H ₅ NH ₂	4.6
C ₆ F ₅ NH ₂	-0.36

Table 1.3 – pK_b s of fluorinated analogues of ethylamine and aniline.¹⁰

This effect was shown by Juhl *et al.*, who synthesised fluorinated analogues of phosphodiesterase 9 (PDE9) inhibitors and measured the pK_a s and pK_b s of the inhibitors and their fluorinated analogues, as shown in Table 1.4.¹¹ PDE9 inhibitors can be used as potential therapeutics in the treatment of Alzheimer's disease.¹¹ They found that selective fluorination of the inhibitors lowered both the pK_a and pK_b of every inhibitor tested, increasing their acidity and lowering their basicity.



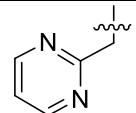
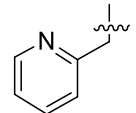
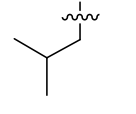
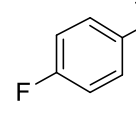
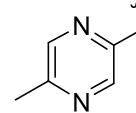
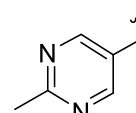
R	X	pK _a	pK _b
	H	9.6	6.8
	F	8.4	5.6
	H	9.6	7.0
	F	8.4	5.9
	H	10.1	8.4
	F	8.4	5.9
	H	9.7	7.9
	F	8.5	6.5
	H	9.7	8.8
	F	8.4	5.5
	H	9.5	7.7
	F	8.4	4.9

Table 1.4 – pK_a (at amine hydrogen) and pK_b (at pyrrolidine nitrogen) of fluorinated analogues of PDE9 inhibitors.¹¹

1.2.4 Fluorine effect on bond angles

Fluorine also has the ability to influence the structure and conformation of molecules. For example, the substitution of hydrogen by fluorine can affect the geometry at a carbon atom. The substitution of a single hydrogen atom for fluorine in fluoromethane **1.2** widens the H-C-H bond angle from 109.5° to 110.2° relative to methane, with the F-C-H bond angle narrowing to 108.7°, as illustrated in Figure 1.2.¹² A further substitution to difluoromethane

1.3 further widens the H-C-H bond angle to 113.8° and narrows the F-C-H bond angle to 108.4° .⁶ This phenomenon is due to the electronegative fluorine withdrawing electron density from the C-F bond to its low-lying 2p orbital. As a result of this, the carbon atom increases in sp^2 character, and so the H-C-H bond angle widens.

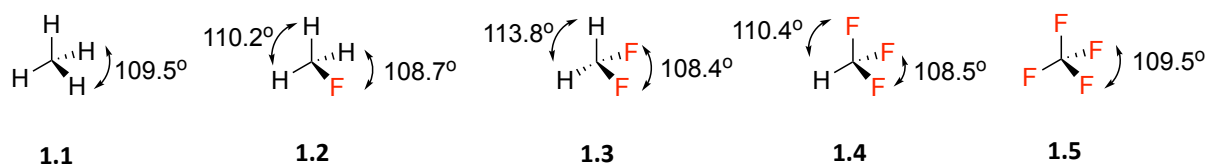


Figure 1.2 – Effect of fluorination on sp^3 carbon bond angle across the methane series as determined by dual-level variational transition state theory calculations.¹²

1.2.5 Dipole-dipole interactions

The significant electronegativity of fluorine and the ionic character of the C-F bond give rise to a large dipole moment. This dipole plays a significant role in determining the conformation of organic compounds as molecules will tend to orient to minimise their overall molecular dipole. This can be illustrated by various carbonyl-containing molecules as shown in Figure 1.3.¹³ The C-F bond has a strong preference to orient *anti*-planar to the carbonyl bond of amide **1.6**, minimising the net dipole of the molecule.¹³ This effect continues but reduces progressively for ester **1.7**,¹⁴ ketone **1.8**¹⁵ and aldehyde **1.9**¹⁶ as these motifs have progressively weaker dipoles.

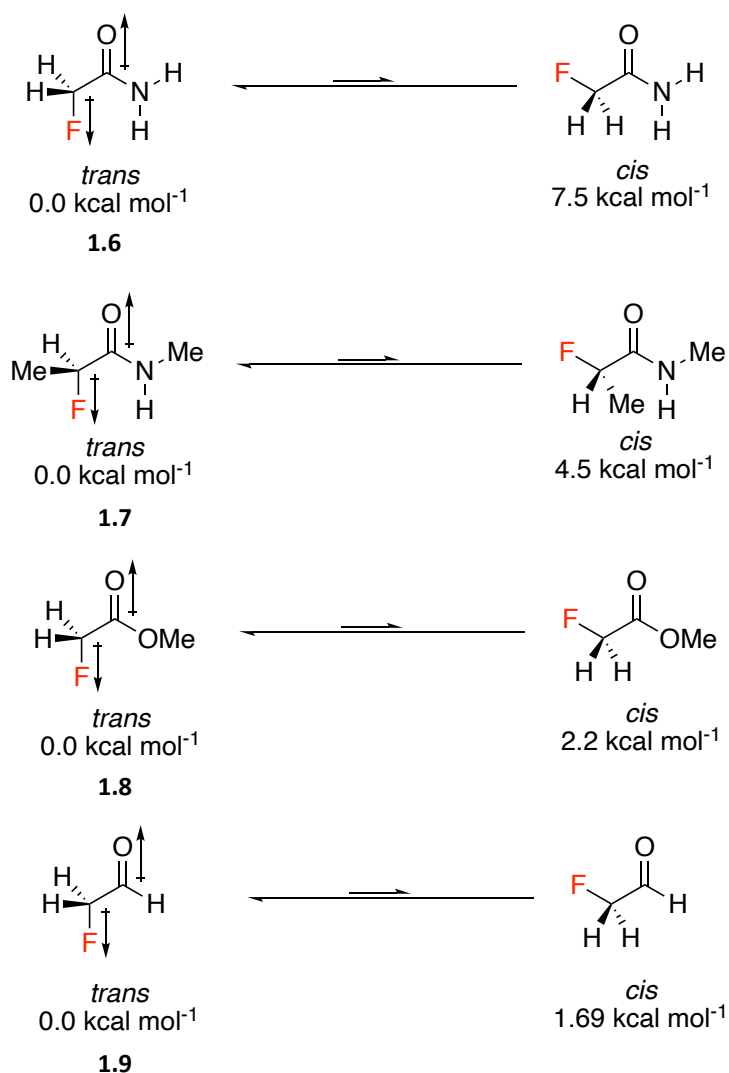


Figure 1.3 – Dipole-dipole interactions affecting the conformations of α -fluoroacyl molecules, as determined by *ab initio* calculations.¹³

Similar effects can be observed when fluorine atoms are placed 1,3 in a hydrocarbon chain. In 1,3-difluoroalkanes, molecules will preferentially orientate so that the fluorine atoms oppose each other, to minimise the overall dipole of the molecule. These molecules are further stabilised *via* hyperconjugation, with donation from the C-H bond to the C-F σ^* orbital. This has been explored using the example of 1,3-difluoropropane, as illustrated in Figure 1.4.¹⁷ The most stable conformer, GG **1.10**, has the fluorine atoms pointing away from each other, with two possible donations from the C-H bond to the $\sigma^*_{\text{C-F}}$ orbital. The next most stable conformer, GA **1.11**, has one possible donation from the C-H bond to the $\sigma^*_{\text{C-F}}$ orbital and then AA **1.12**, has no possible donation from the C-H bond to the $\sigma^*_{\text{C-F}}$

orbital, so there is no stabilising effect for this conformer. The disfavoured conformer, GG' **1.13**, features two possible stabilising donations of electron density from the C-H bond to the $\sigma^*_{\text{C-F}}$ orbital. However, with the fluorine atoms orienting in the same direction with the C-F bonds parallel, **1.13** is therefore destabilised by dipole repulsion and so this is the least stable conformer.

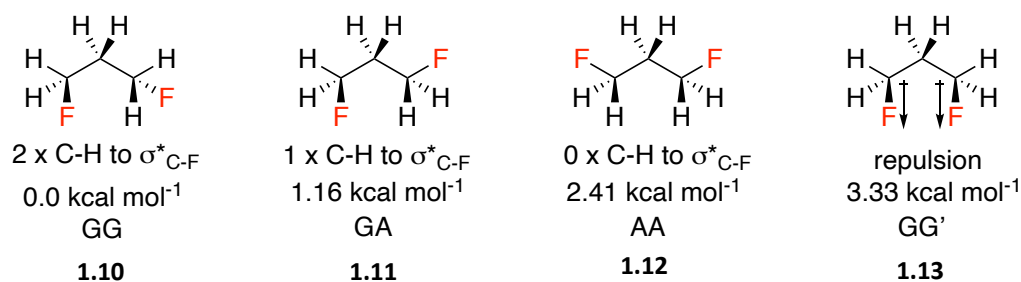


Figure 1.4 – Dipole-dipole interactions determining the conformation of 1,3-difluoropropanes, as determined by *ab initio* calculations.¹⁷

1.2.6 Charge-dipole interactions

The highly polarised C-F bond can also interact with formal charges. Molecules containing both a formal charge and a C-F bond will tend to orient to facilitate an electrostatic interaction. These interactions are much stronger than dipole-dipole interactions. This effect has been studied through 3-fluoropyridinium rings, as shown in Figure 1.5. The axial conformation of **1.14** is favoured by 5.4 kcal mol⁻¹ relative to the equatorial conformation, while the axial conformation of **1.15** is also favoured, by 4.0 kcal mol⁻¹.¹⁸ The effect has also been studied for protonated fluoroethylamine **1.16** and protonated fluoroethanol **1.17**, which favour their axial conformers by 5.8 kcal mol⁻¹ and 7.2 kcal mol⁻¹ respectively.¹⁹

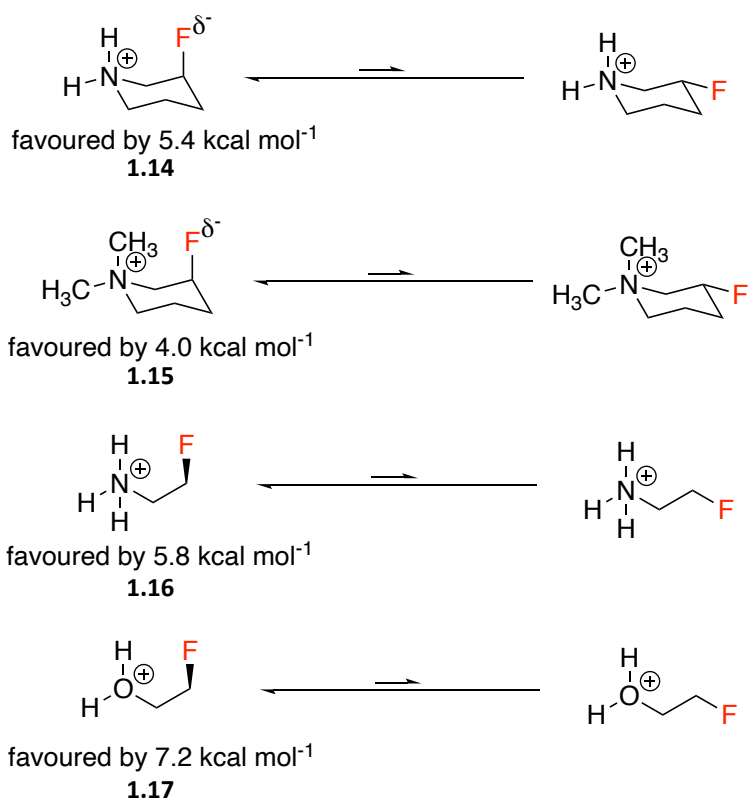


Figure 1.5 – Charge-dipole interactions influencing the conformations of organofluorine molecules, as determined by density functional theory, *ab initio* and MMFF force field calculations.

1.3 Fluorine in medicinal chemistry

An estimated 25% of all drugs contain at least one fluorine atom, including 30% of the top 30 drugs by sales.¹⁰ One example is Prozac **1.18**, the most widely used antidepressant worldwide, which features a *para*-trifluoromethyl group on an aromatic ring. Prozac is also used to treat obsessive-compulsive disorder, panic disorder and bulimia. It acts by inhibiting the uptake of serotonin, and it was found that Prozac is five times more effective at inhibiting serotonin uptake than its non-trifluoromethylated analogue.²² Lipitor **1.19**, a statin, is used to prevent cardiovascular disease by reducing the amount of cholesterol produced by a patient.²³ It contains an aryl *para*-fluorine atom. This drug was the second-most prescribed in the USA in 2017, with a total of 104,774,006 prescriptions. Another important example is Fluticasone propionate **1.20**, an anti-inflammatory used to treat asthma.²⁴ It contains multiple fluorine atoms including two at stereogenic centres. In 2017 it was the 15th most prescribed drug in the USA, with 32,049,111 prescriptions. Dolutegravir

1.21 is used in the treatment of HIV and acts as an inhibitor of HIV-integrase.²⁵ It acts on the strand transfer step, preventing HIV-1 genome integration into the host's chromosome. Dolutegravir is highly potent and is featured on the World Health Organisation's list of essential medicines. It contains two fluorine atoms on its phenyl ring.

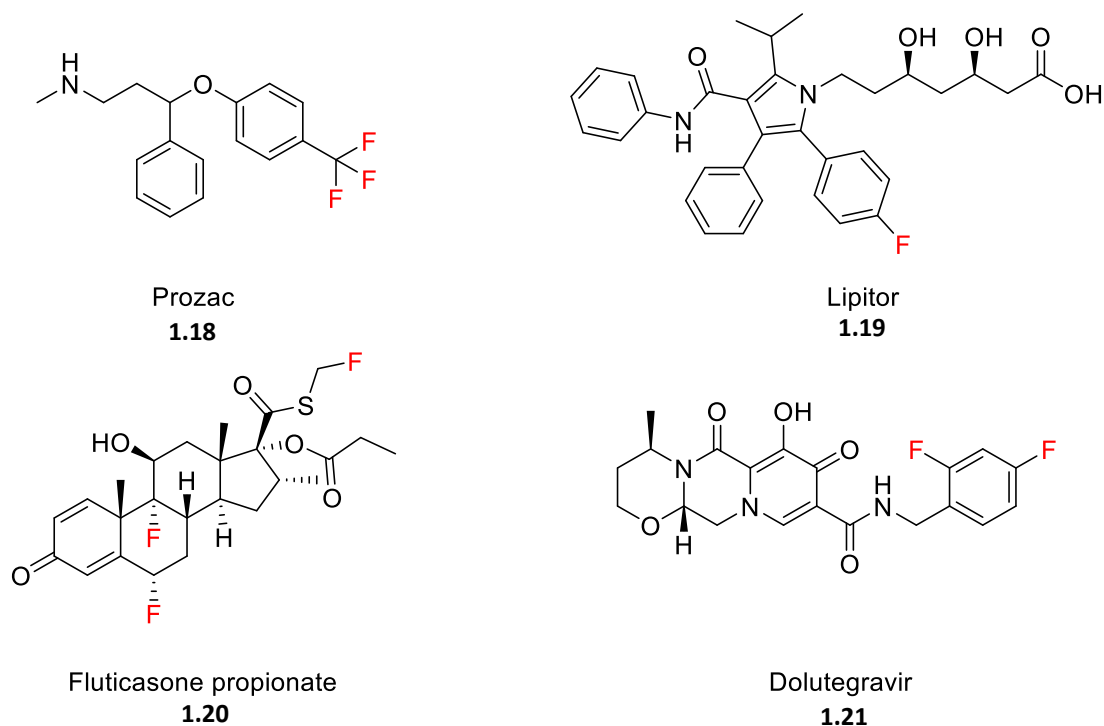
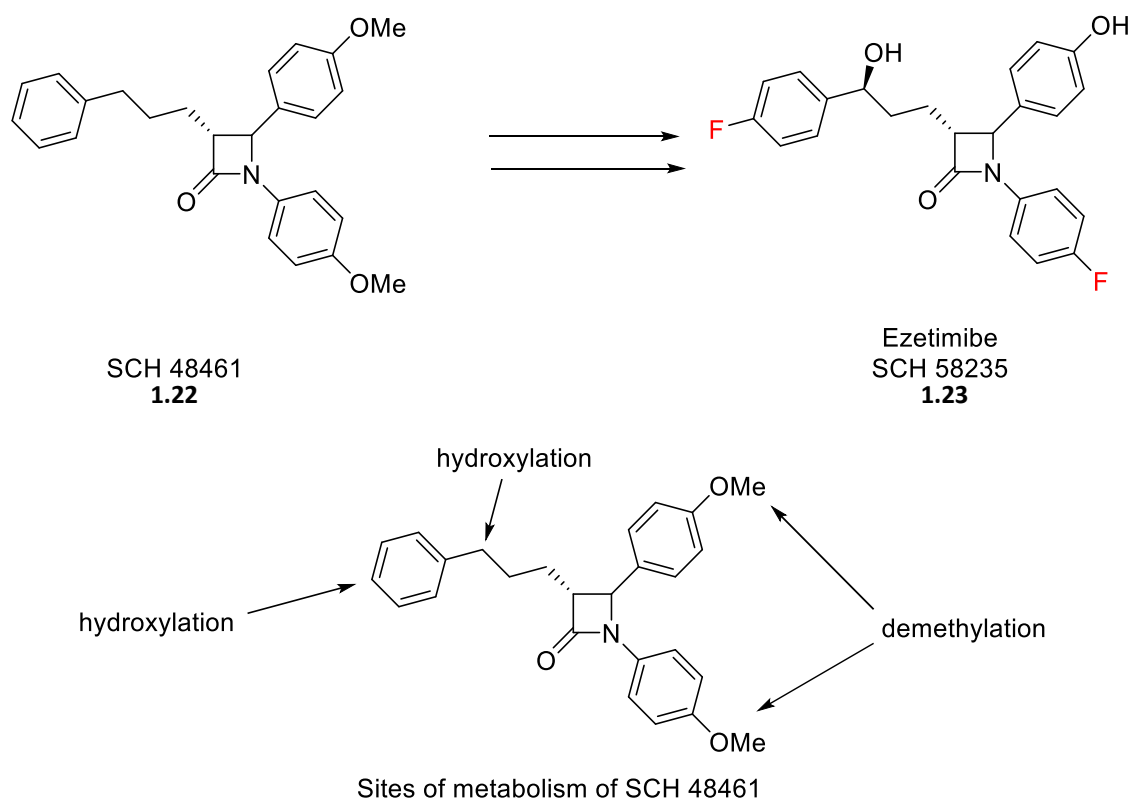


Figure 1.6 – Structures of Prozac **1.18**, Lipitor **1.19**, Fluticasone propionate **1.20** and Dolutegravir **1.21**.

1.3.1 Incorporation of fluorine to delay metabolism

Fluorine is often incorporated into drug molecules to delay their metabolism.²⁶ By incorporating fluorine into the metabolic site, or at positions adjacent to the metabolic site, the likelihood of enzymatic oxidation is reduced, as the C-F bond is less susceptible to enzymatic (cytochrome P₄₅₀) attack than the C-H bond. This is a result of the high bond strength of the C-F bond and also its electron-withdrawing power. One example of this effect is the development of the drug Ezetimibe **1.22**. This is a derivative of SCH 48461 **1.23**, which is a cholesterol absorption inhibitor. However, it has four sites at which it is susceptible to metabolic attack, as illustrated in Scheme 1.1. The introduction of fluorine at key positions led to the development of the fluorinated analogue Ezetimibe (SCH 58235),

which is metabolically more stable than SCH 48461 and shows a 50-fold increase in activity in hamsters as a result.²⁷



*Scheme 1.1 – Selective fluorination of SCH 48461 **1.22** to suppress metabolism.²⁷*

1.3.2 Trifluoromethyl group in bioactives

The trifluoromethyl group has long been incorporated into bioactive molecules, with a first introduction as early as 1928 by Lehmann *et al.*²⁸ The replacement of a methyl group with a trifluoromethyl group can have a large effect on the properties of a molecule without significantly altering its steric profile. The trifluoromethyl group has the effect of increasing the lipophilicity on aryl sites and lowering the lipophilicity on alkanes.¹⁰

One example of an FDA-approved drug containing a trifluoromethyl group is Ubrogapant **1.24**. This is used in the treatment of migraines, and acts as an antagonist of the calcitonin gene-related peptide receptor.²⁹ Pretomanid **1.25** is an antibiotic containing a trifluoromethyl group which is generally used in combination with bedaquiline and linezolid. It is used in the treatment of multi-drug-resistant tuberculosis.³⁰ Travopost **1.26** is a medication which is used to treat glaucoma. It works to relieve elevated intraocular pressure inside the eye by increasing the outflow of aqueous humour from the eyes.³¹

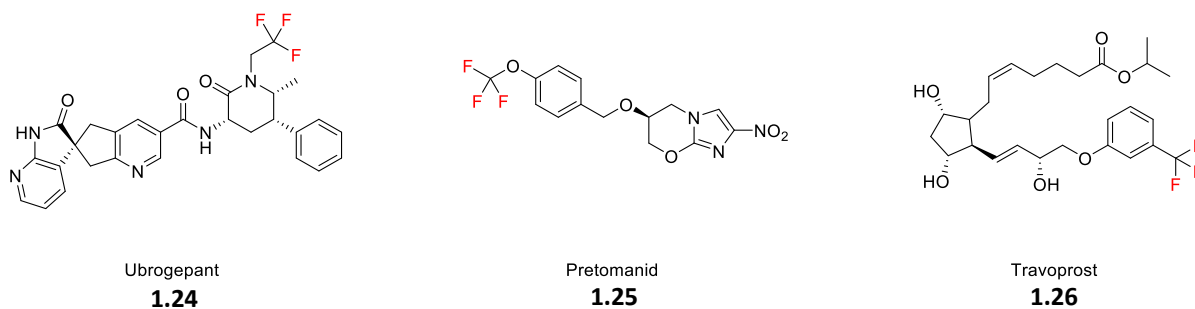
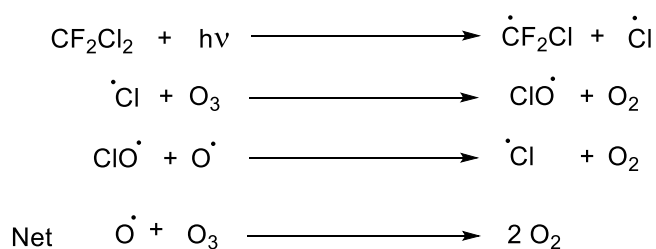


Figure 1.7 – Examples of drugs containing a trifluoromethyl group.

1.4 Applications of synthetic fluorinated compounds

1.4.1 Chlorofluorocarbons (CFCs)

The first synthetic fluorinated compounds which had widespread applications were the chlorofluorocarbons (CFCs). Initial research into CFCs was led by General Motors in the late 1920s by a team led by Thomas Midgeley Jr. They were seeking to develop safe gases to be used as refrigerants to replace the dangerous refrigerants in use at the time such as ammonia.³² The first of these to be developed was Freon-12 (dichlorodifluoromethane, CF_2Cl_2). Freon is a gas that was widely used as a refrigerant and coolant. Its non-toxic and non-flammable properties made it an ideal gas to be used in commercial products such as air-conditioners and refrigerators. It can be synthesised by the reaction of tetrachloromethane with antimony trifluoride.³³ Another notable CFC developed within this project was trichlorofluoromethane (Freon-11, CFCl_3). These compounds were widely used and accepted as safe until work published by Molina and Rowland in 1974 showed that CFCs break down in the atmosphere in a radical mechanism triggered by UV light, as shown in Scheme 1.2.³⁴ The resulting chloride free radicals then react with ozone gas which forms part of the Earth's protective ozone layer. This reaction causes the decomposition of ozone in the upper atmosphere, leading to the depletion of the ozone layer.³⁵



*Scheme 1.2 – Depletion of ozone by dichlorodifluoromethane.*³⁶

Following this realisation, action was taken to phase out the production and use of CFCs, which led to the development of the Montreal Protocol to reduce ozone-depleting substances (ODSs). The Montreal Protocol has been considered to be a success, with the use of ODSs being legislated against and this has resulted in significantly slowing and possibly reversing the depletion of the ozone layer.³⁷ As a result of the phase-out of CFCs, more widespread use of hydrochlorofluorocarbons (HCFCs), such as chlorodifluoromethane (Freon-22, CHF₂Cl), followed. While chlorodifluoromethane only has an ozone-depletion potential of 0.04 (dichlorodifluoromethane has an ozone-depletion potential of 1), it has a 100 year global warming potential (GWP) of 1810 years (carbon dioxide has a 100 year GWP of 1, dichlorodifluoromethane has a GWP of 10,200).^{38, 39} Therefore, HCFCs are considered to be potent greenhouse gases and they were considered “transitional substances” by the Montreal Protocol. These were gradually replaced by hydrofluorocarbons (HFCs). Commonly used HFCs include 1,1,2,2-tetrafluoroethane (HFC-134a) and difluoromethane (HFC-32), which due to the lack of chlorine have ozone-depletion potentials of 0. However, they both have high GWPs of 1360 and 705 respectively, so are considered to be greenhouse gases.⁴⁰ HFCs have been included in the Kyoto Protocol, meaning that the phase-out of these compounds as refrigerants is highly desired. The latest generation of refrigerants is the hydrofluoroolefins (HFOs). These are more environmentally friendly than CFCs, HCFCs and HFCs. For example, the most commonly used of the HFOs, 2,3,3,3-tetrafluoropropene (R-1234yf), has an ozone-depletion potential of 0 and a global warming potential of less than 1, less than carbon dioxide.⁴¹ These low values make HFOs promising potential replacements for CFCs, however, there is a growing concern that they rapidly convert to trifluoroacetic acid (TFA) in the lower atmosphere and TFA levels are increasing significantly in precipitation and surface water.

1.4.2 Per- and poly- fluoroalkyl substances (PFASs)

Per- and poly- fluoroalkyl substances (PFASs) are substances that contain at least one perfluoroalkyl group. An early definition by Franklin *et al.* stated that “PFASs are aliphatic substances containing one or more C atoms on which all the H substituents present in the nonfluorinated analogues from which they are notionally derived have been replaced by F atoms, in such a manner that PFASs contain the perfluoroalkyl moiety C_nF_{2n+1} ”.⁴² They further specified that per- and poly- fluoroalkyl substances must have all the hydrogen atoms bonded to carbon atoms replaced by fluorine atoms to qualify as PFASs. The definition of PFAS has been updated by the OECD in 2021 to be much broader in scope. They stated that “PFASs are defined as fluorinated substances that contain at least one fully fluorinated methyl or methylene carbon atom (without any H/Cl/Br/I atom attached to it), i.e., with a few noted exceptions, any chemical with at least a perfluorinated methyl group ($-CF_3$) or a perfluorinated methylene group ($-CF_2-$) is a PFAS”.⁴³

One highly common application of PFASs is as surfactants. This is due to the high hydrophobicity of the perfluoroalkyl moiety, which leads to a large reduction in the surface tension between the surfactant molecule and water. These were initially synthesised in 1948 via an electrochemical fluorination process. One notable example of this is perfluorooctanoic acid (PFOA) **1.27**. The compound was initially manufactured by 3M but was used by DuPont from 1951 in the manufacture of fluoropolymers such as Teflon. Another example of a PFAS is perfluorooctanesulfonic acid (PFOS) **1.28**. PFOS has many applications, for example as a protective coating for materials for fabrics and leather. Therefore, PFOS is able to act as a water and oil repellent and so was a key ingredient in Scotchgard, which was a fabric protector produced by 3M.

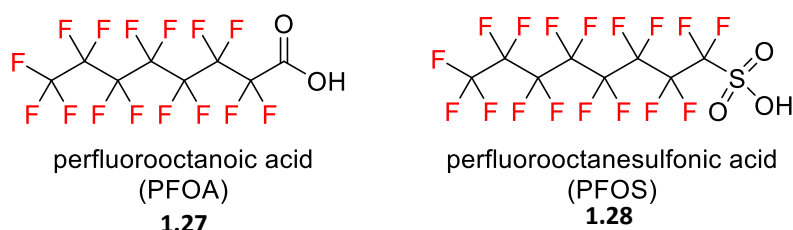


Figure 1.8 – Structures of PFOA **1.27** and PFOS **1.28**.

PFOA and PFOS have since been found to persist indefinitely within the environment and are considered to be “forever chemicals”. North Americans and Europeans are estimated to consume doses of 3 to 220 ng per kg of body weight per day of PFOS and 1 to 130 ng per kg of body weight per day of PFOA, likely consumed via contaminated foods and drinking water.⁴⁴ PFOA has a half-life of several years in humans, as it is unreactive and so is not metabolised by the human body. It has been found that even limited exposure to low levels of PFOA in drinking water can substantially increase total exposure to humans.⁴⁵ There has been much discussion and publicity about the safety of these chemicals, both due to their forever chemical status and because of the health effects caused by these chemicals. In 2001, residents living close to DuPont’s Washington Works plant in West Virginia filed a class action lawsuit against DuPont for contaminating groundwater with PFOA.⁴⁴ A report produced by epidemiologists as a result of this lawsuit found PFOA to be linked to six adverse health outcomes: kidney cancer, testicular cancer, thyroid disease, ulcerative colitis, high cholesterol and pregnancy-induced hypertension.^{44, 46} As a result of this, the phase-out of PFASs is highly desired.

Meanwhile, one of the most important examples of a polyfluoroalkyl substance is poly(tetrafluoroethylene) (PTFE) **1.29**, more widely known as Teflon. Teflon was first discovered by DuPont in 1938 by accident by Roy Plunkett, who was working on synthesising new CFCs.⁴⁷ It is synthesised via the free-radical polymerisation of tetrafluoroethylene.⁴⁸ The most commonly known application of PTFE is as the coating used for domestic non-stick frying pans. It is ideal for this use as it can withstand temperatures of up to 260 °C while remaining intact, and it also has a very low coefficient of friction, so substances cannot stick to its surface.⁴⁹ Above 260 °C, PTFE releases polymer fumes, and above 400 °C, PTFE decomposes into products such as tetrafluoroethylene and difluorocarbene radicals.⁵⁰

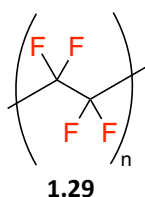


Figure 1.9 – Structure of PTFE **1.29**.

1.4.3 Fluorous chemistry

Another use of highly fluorinated compounds is in the area of fluorous chemistry. Fluorous solvents are those which are highly or fully fluorinated.⁵¹ Therefore, they are able to dissolve highly fluorinated compounds, while having a low affinity for non-fluorinated compounds. Fluorous solvents are also immiscible with organic and aqueous solvents, however, they can form a single phase with organic solvents when heated, as shown in Figure 1.10.⁵¹ These phases can then re-separate upon cooling. This functionality has been exploited within synthetic chemistry. In 1994, Hovárth and Rábai reported the first example of fluorous biphasic catalysis, developing a novel fluorous biphasic system for the hydroformylation of 1-octene.⁵² One key issue with the hydroformylation reaction is its use of triphenylphosphine, which leads to the production of triphenylphosphine oxide as a byproduct. This is often difficult to remove during a work-up. They developed a method to solve this problem using fluorous chemistry. By using $[\text{Rh}(\text{CO})_2(\text{acac})]$ and $\text{P}(\text{C}_2\text{H}_4\text{C}_6\text{F}_{13})_3$ as an alternative to triphenylphosphine in a toluene/perfluoromethylcyclohexane solvent system at 100 °C and 10 atm syngas, they were able to obtain the desired formylated product with a conversion of 85%. The use of the fluorinated alternative to triphenylphosphine allows for the facile extraction of its oxide, as it will be fully dissolved in the fluorous phase during a liquid-liquid extraction, thus eliminating the issue of extracting the triphenylphosphine oxide by-product.

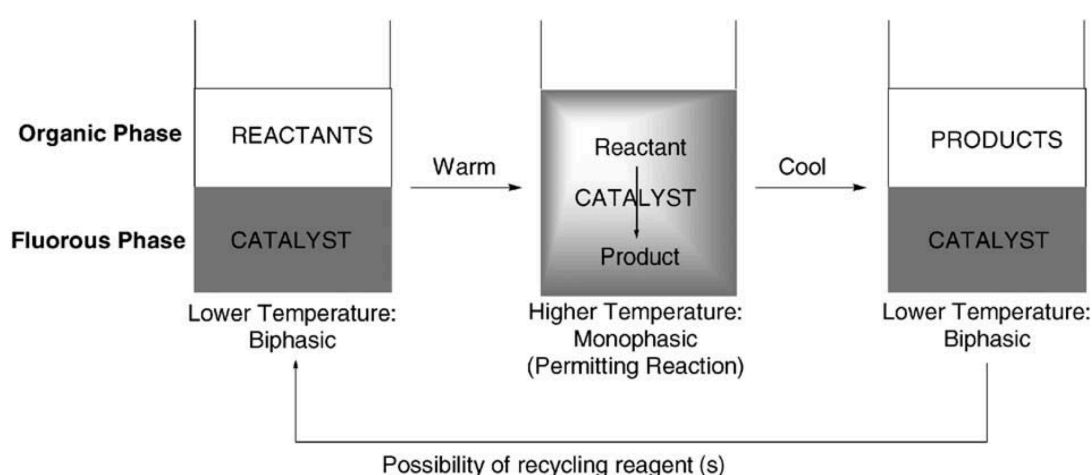


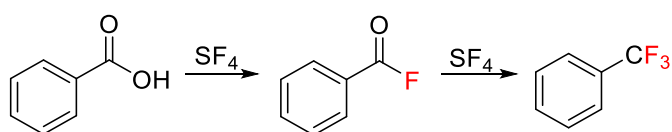
Figure 1.10 – The principle of fluorous biphasic catalysis.⁵¹

1.5 Synthesis methods for introducing fluorine

1.5.1 Nucleophilic fluorination

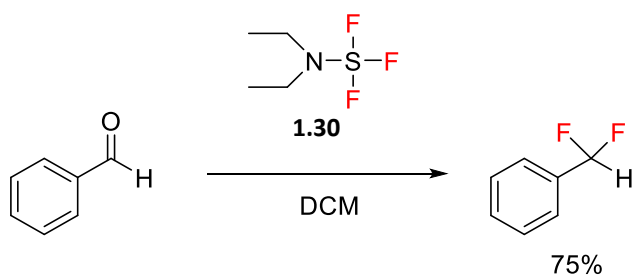
Fluoride ion itself is not usually used as a method to create C-F bonds as it is also highly basic, and this competes with its ability to react as a nucleophile. Also, the F^- ion is very poorly solvated in organic solvents, which reduces its utility in conventional organic chemistry. Therefore, alternative nucleophilic fluorinating agents have been developed.

One of the earliest was sulfur tetrafluoride (SF_4). SF_4 selectively replaces oxygen and sulfur atoms with fluorine atoms (deoxyfluorination).⁵³ For example, SF_4 will convert carboxylic acids into trifluoromethyl groups (Scheme 1.3) and aldehydes and ketones into geminal difluorides.⁵⁴ However, SF_4 is a gas and is difficult to handle. It is also corrosive and will release HF when it is exposed to water or moisture, therefore, it was attractive to develop nucleophilic fluorinating reagents that are safer and easier to handle.



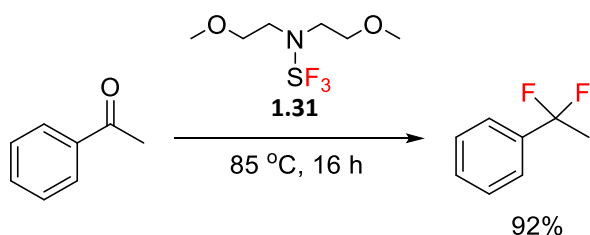
*Scheme 1.3 – Nucleophilic fluorination of a carboxylic acid using sulfur tetrafluoride.*⁵³

One such reagent is diethylaminosulfur trifluoride (DAST) **1.30**.⁵⁵ DAST is made after the reaction of SF_4 with diethylamine and is less reactive than SF_4 . It can also be used in deoxyfluorination reactions, converting alcohols to fluorine and aldehydes and ketones to difluoromethylene groups, as illustrated in Scheme 1.4.⁵⁶ However, DAST has been found to be thermally unstable.⁵⁷ When DAST reaches $90\text{ }^\circ\text{C}$, it decomposes into SF_4 and a diaminosulfur difluoride. Upon further heating, the sample can explode. Therefore, reagents that are more thermally stable than DAST were developed.



Scheme 1.4 – Deoxyfluorination of benzaldehyde using DAST **1.30**.⁵⁵

One such reagent is Deoxo-Fluor **1.31**, which has the same general reactivity as DAST, as shown in Scheme 1.5.⁵⁸ While Deoxo-Fluor decomposes at a similar temperature to DAST, it releases much less heat and at a far slower rate. Deoxo-Fluor was also found to have greater scope in terms of functional group transformations. In addition to fluorinating aldehydes and ketones, Deoxo-Fluor will convert carboxylic acids to $-CF_3$, whereas DAST will only convert carboxylic acids to acyl fluorides.

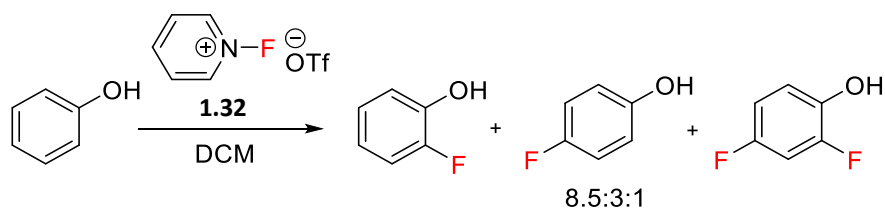


Scheme 1.5 – Deoxyfluorination of a ketone using Deoxo-Fluor **1.31**.⁵⁸

1.5.2 Electrophilic fluorination

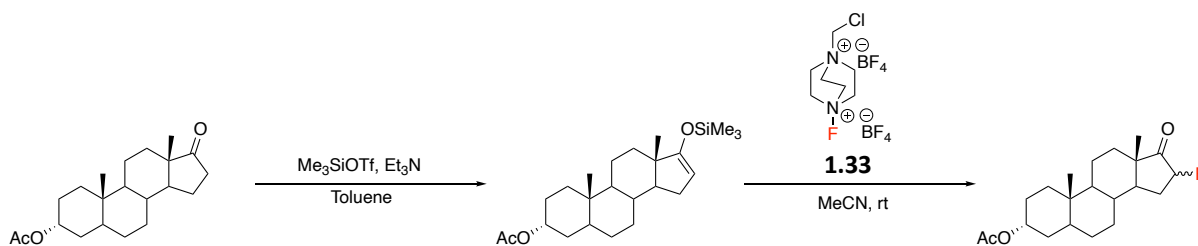
Electrophilic fluorination involves the attack of a nucleophile to an ‘apparent’ electrophilic fluorine atom. This is a process which involves a fluorine containing reagent, most often N-F reagents, as an oxidant which are reduced by single electron transfer from an electron-rich nucleophile. A fluorine atom (F^\cdot) then transfers back to form Nu-F. Many of these electrophilic fluorination reagents are commercially available and safe to handle.⁵⁹

The first class of these reagents to be developed were the *N*-fluoro-*N*-alkylsulfonamides.⁶⁰ However, while these reagents were stable, their scope was limited to fluorinating carbanions. This was followed by the development of *N*-fluoropyridinium salts by Umemoto, such as *N*-fluoropyridinium triflate **1.32**, reagents which were found to be very efficient for the fluorination of aromatics, silyl enol ethers and enolates, as shown in Scheme 1.6.⁶¹



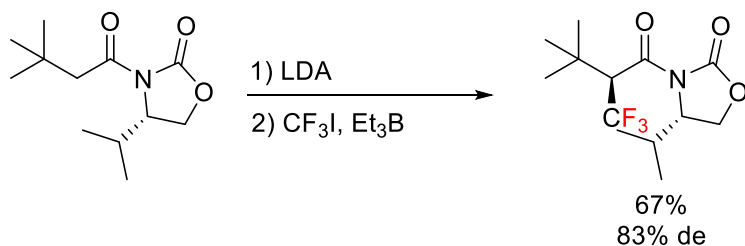
*Scheme 1.6 - Fluorination of phenol using an N-fluoropyridinium triflate salt.*⁶¹

The continuing development of N-F based electrophilic fluorinating reagents led to Selectfluor **1.33** by Banks.⁶² Selectfluor is also a stable, crystalline solid. One example of its utility is in the fluorination of steroids, as illustrated in Scheme 1.7. The steroid is converted to an enolate or to a silyl enol ether, which acts as a nucleophile and reacts with Selectfluor to fluorinate the α -carbon. This reaction is highly efficient, giving a yield of 90% from the enolate or 92% from the silyl enol ether.⁶²



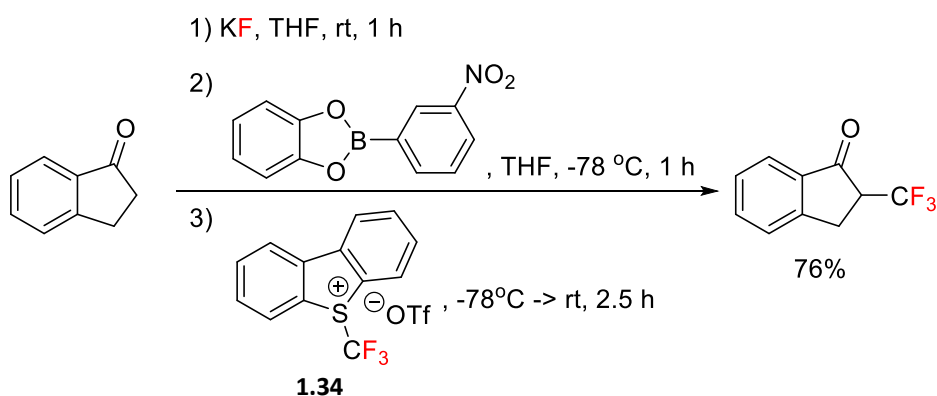
*Scheme 1.7 - The α -fluorination of steroids using Selectfluor **1.33**.*⁶²

Additionally, the incorporation of trifluoromethyl groups into molecules by the creation of C-CF₃ bonds has been developed in recent years. Early attempts to incorporate trifluoromethyl groups into molecules were largely based on radical methods. Initially, a non-stereoselective addition of a trifluoromethyl group to an alkene was developed by Utimoto *et al.*, who treated alkynes with perfluoroalkyl iodides in the presence of triethylborane, achieving yields of 61-86%.⁶³ Following this, Iseki *et al.* developed a method of asymmetric radical trifluoromethylation of N-acyloxazolidinones where trifluoroiodomethane acts as a CF₃-transfer reagent in a reaction that is initiated by triethylborane, as illustrated in Scheme 1.8.⁶⁴ These reactions achieved yields of 61-86% and diastereomeric excesses of 62-86%. However, the reaction is problematic as it requires a large excess of gaseous and expensive trifluoroiodomethane and it requires oxygen to initiate the radical process.⁶⁵



*Scheme 1.8 – Triethylborane mediated addition of a trifluoromethyl group to an oxazolidinone.*⁶⁴

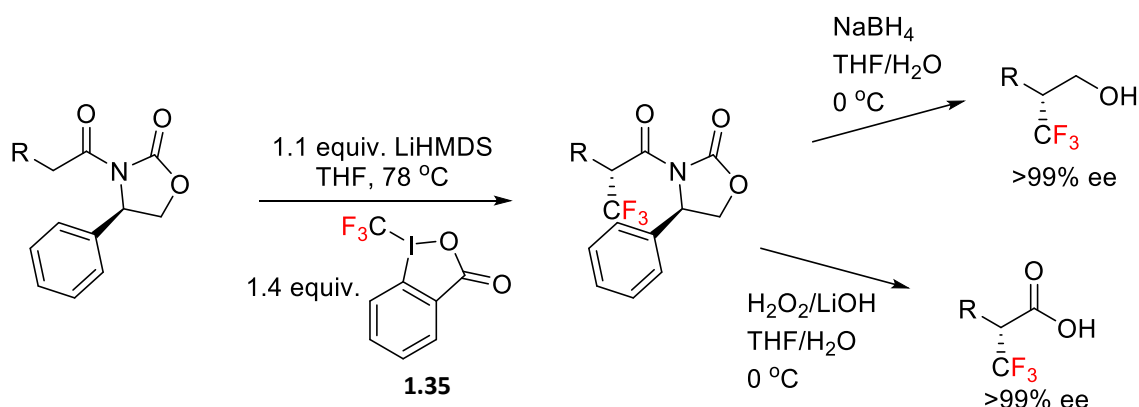
It was therefore attractive to develop CF₃-transfer reagents that were easier and safer to use. Umemoto *et al.*, developed reagents that feature S-CF₃ bonds.⁶⁶ These reagents are safer to handle than trifluoroiodomethane, and do not require a radical initiator to abstract iodide. Typically, as illustrated in Scheme 1.9, a ketone is reacted with a boronic acid to form an electron-rich boron-enolate. This initiates a SET process with the back transfer of a [•]CF₃ radical from the reduced Umemoto's reagent **1.34** to form the trifluoromethylated product. The selection of such a Lewis acid is key, as too weak a Lewis acid leads to the formation of trifluoromethane as a by-product, whereas too strong a Lewis acid leaves unreacted trifluoromethylating agent.⁶⁷ These reagents can give yields of up to 86%.



*Scheme 1.9 – Trifluoromethylation of 1-indanone using Umemoto's reagent **1.34**.*⁶⁶

Following this, Togni *et al.* developed hypervalent iodine CF₃-transfer reagents.⁶⁵ Reaction of chiral oxazolidinones at -78 °C in THF with LiHMDS and Togni's Reagent II **1.35** resulted in CF₃-substituted oxazolidinones with diastereomeric excesses of up to 94% and isolated yields of up to 91%, as illustrated in Scheme 1.10. These reagents give good stereoselectivity

while being easy and safe to handle. The chiral auxiliary can then be cleaved to give either a trifluoromethyl alcohol or trifluoromethyl carboxylic acid with high enantioselectivities.



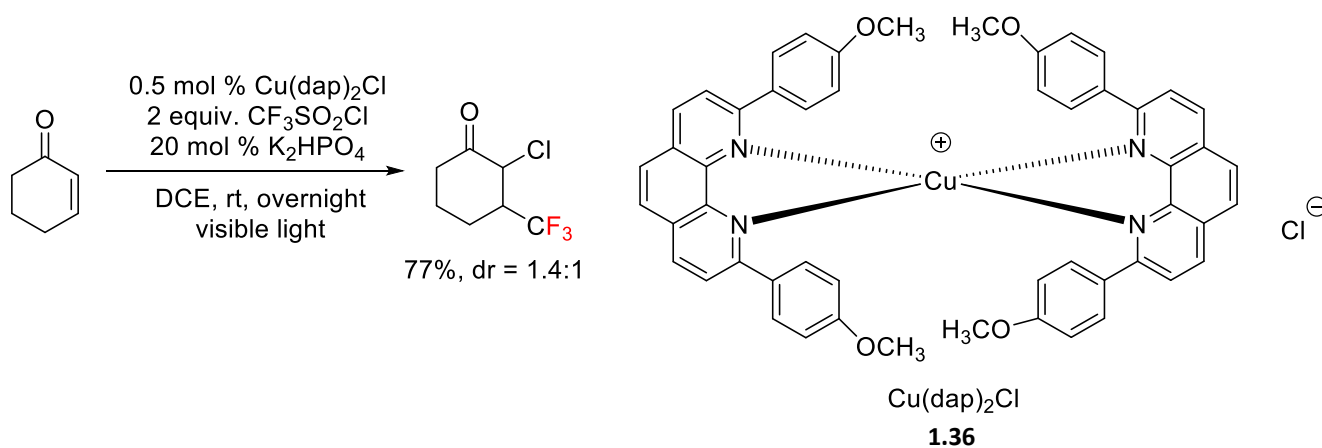
Scheme 1.10 – Trifluoromethylation reactions using Togni's reagent **1.35**.⁶⁵

1.5.3 Radical perfluorination

An alternative method to introduce fluorinated substituents into molecules involves the addition of perfluoro-radicals to alkenes, alkynes and arenes.⁶⁸ Early work in this area was carried out using radical initiators. One such example by Lacher *et al.*, found that when allyl alcohols were treated with perfluoroalkyl iodides under the influence of UV light, 1:1 adducts were formed.⁶⁹ The use of benzoyl peroxide as an initiator was found to be effective at catalysing this reaction. However, overall yields were poor. Another early example of the addition of perfluoroalkyl iodides to carbon-carbon multiple bonds was reported by Brace, who used AIBN as a radical initiator to mediate the addition of perfluoroalkyl iodides to malonic acid alkenes with 81% conversion.⁷⁰

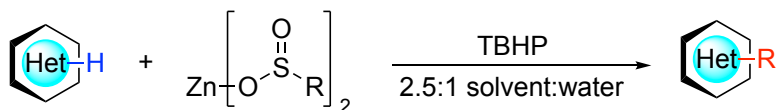
In 2015, Tang and Dolbier reported on a copper-catalysed addition reaction of fluoroalkylsulfonyl chlorides (RSO₂Cl) to electron-deficient alkenes in visible light conditions.⁷¹ This reaction involves the addition of a chlorine atom and an R group to opposite ends of an alkene to form a 1:1 adduct, as illustrated in Scheme 1.11. The photoredox catalyst [Cu(dap)₂Cl] **1.36** had previously been found to be effective at catalysing the additions of organic halides to electron-rich alkenes.⁷² This is due to it having high reductive ability in the excited state (-1.43 V vs SCE) compared to other photoredox catalysts such as [Ru(bpy)₃Cl₂] (-1.33 V vs SCE). When Dolbier's lab attempted the addition of CF₃SO₂Cl to N-methyl-N-phenylacrylamide with [Ru(bpy)₃Cl₂] as a photoredox catalyst,

they obtained only a trace amount of the desired product. However, when the same reaction was attempted with $[\text{Cu}(\text{dap})_2\text{Cl}]$, a 98% yield of the desired product was obtained. The reaction was catalysed using a visible light source to generate the radical. Various substrates were explored including α,β -unsaturated ketones to form α -chloro- β -trifluoromethyl ketones giving moderate to excellent yields. The reaction was also found to be successful with other fluoroalkylsulfonyl chlorides, such as $\text{HCF}_2\text{SO}_2\text{Cl}$, $\text{H}_2\text{CFSO}_2\text{Cl}$, $\text{CF}_3\text{CH}_2\text{SO}_2\text{Cl}$, and $\text{C}_4\text{F}_9\text{SO}_2\text{Cl}$. The resultant α -chloro- β -trifluoromethyl ketone product can then undergo reductive dehalogenation using zinc metal to yield a β -trifluoromethyl ketone.

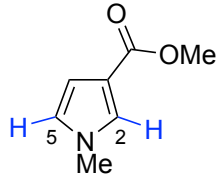


*Scheme 1.11 – Reaction of trifluoromethanesulfonyl chloride with electron-deficient alkenes catalysed by $\text{Cu}(\text{dap})_2\text{Cl}$ **1.36** (the identity of the major diastereomer was not indicated in the paper).^{71, 72}*

More recently, Baran *et al.* developed a method for the transfer of fluorinated alkyl radicals to nitrogen-rich heterocycles using zinc sulfinate salts, as illustrated in Figure 1.11.⁷³ This allowed for the functionalisation of the C-H bond using mild reaction conditions, often at room temperature and with a 2.5:1 mixture of solvent/water, although reactions can also be carried out without organic solvent and in open air. The reaction has been shown to be tolerant of a variety of functional groups, such as esters, nitriles, ketones, carboxylic acids and even aryl halides, rendering its use advantageous compared to more classical cross-coupling chemistry. This chemistry has since gone into use at Pfizer for medicinal chemistry, with building blocks **1.39**, **1.40**, **1.41** and **1.43** among those in use there.



Heterocycle	Zn salt, R			
	CF ₃	CF ₂ H	CH ₂ CF ₃	CH ₂ F
<p>1.37</p>	89 (100) [†]	73 (57) [†]	51#	80#
<p>1.38</p>	79 (100) [†]	72 (41) [†]	44#	75#
<p>1.39</p>	35 (77) [†] [4:1 C2:C3]	66 (100) [†] [only C2]	18 (85)# [4:1 C2:C3]	73¶ [17:1 C2:C2&C6]
<p>1.40</p>	66 (65) [†] [2.3:1 C6:C2]	60 (96) [†] [C2:C6:C4 3:2:1]	33# [1.4:1 C6:C4]	No reaction
<p>1.41</p>	75 (100) [†] [5 products]	50 (67) [†]	31 (77) [‡]	56#
<p>1.42</p>	42 (44) [2.7:1 C4:C5]	21 (44) [1.6:1 C4:C5]	21** [only C5]	No reaction
<p>1.43</p>	45 (90) [only C4]	57 (71) [6:1 C4:C5]	No reaction	No reaction

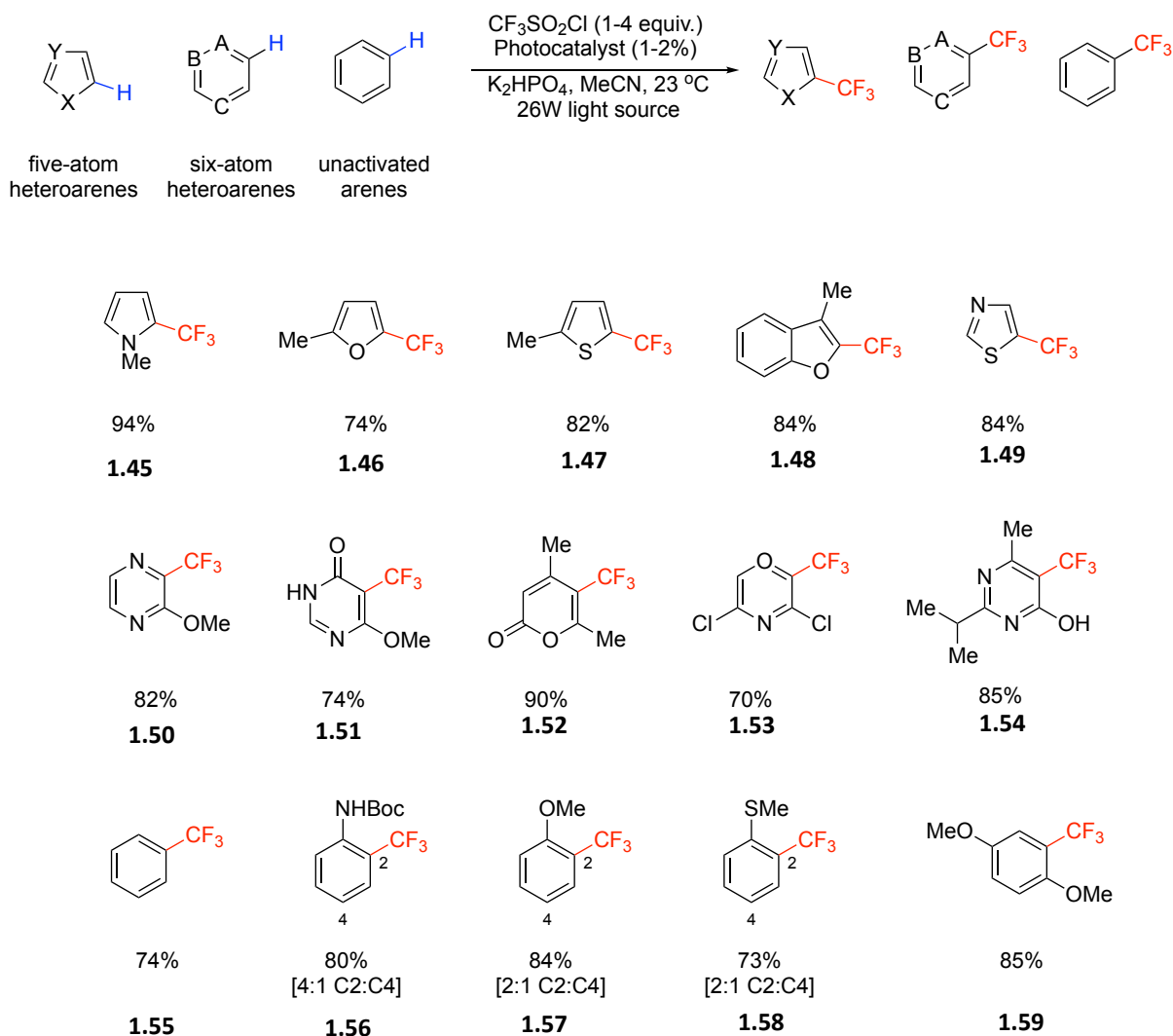
 <p style="text-align: center;">1.44</p>	76 (91) [†] [7.4:1 C2:C5]	65 (100) [†] [only C2]	58 ^{**} [1.4:1 C2:C5]	40 [§] [only C2]
--	---------------------------------------	------------------------------------	-----------------------------------	------------------------------

Isolated yields are shown. Percentage conversions by gas chromatography are indicated in parentheses, and regioselectivities are indicated in square brackets. * Standard conditions involve heterocycle (1.0 equiv.), zinc salt (2.0–3.0 equiv.), TBHP (3.0–5.0 equiv.) and solvent:water (2.5:1) at a specified temperature for a period of 3–12 h.

Solvent and temperature: [†]CH₂Cl₂, RT; [‡]ClCH₂CH₂Cl, RT; [§]ClCH₂CH₂Cl, 50 °C; ^{||}perfluorohexane, RT; [¶]perfluorotoluene, RT; [#]perfluorotoluene, 50 °C; ^{**}DMSO, 50 °C.

Figure 1.11 – Substrate scope for the radical alkylation of nitrogen-rich heterocycles as developed by Baran et al.⁷³

MacMillan further explored the use of radical chemistry to install CF₃ groups as an alternative to cross-coupling methods, as illustrated in Scheme 1.12.⁷⁴ This was envisaged as a method to enable the late-stage trifluoromethylation of a drug candidate as an alternative to relying on pre-fluorinated building blocks. MacMillan achieved this using trifluoromethylsulfonyl chloride as the source of radical CF₃, Ru(phen)₃Cl₂ photocatalyst and a household lightbulb to initiate the radical process. The reaction was effective for a wide range of substrates, such as five-membered heteroarenes **1.45-1.49**, six-membered heteroarenes **1.50-1.54** and unactivated arenes **1.55-1.59** and was shown to tolerate a variety of functional groups including aryl halides, allowing for the generation of products suitable for further coupling reactions.



*Scheme 1.12 – Radical trifluoromethylation of five-membered heteroarenes **1.45-1.49**, six-membered heteroarenes **1.50-1.54** and unactivated arenes **1.55-1.59** as developed by MacMillan with selected examples.⁷⁴*

1.6 Aims and objectives

This chapter has reviewed the basics of organofluorine chemistry, how the unique properties of fluorine can influence molecules and common strategies for the introduction of fluorine to molecules. The initial aim of this thesis is to investigate how the introduction of fluorine into known natural products affects the structure-activity relationships of these compounds. The initial model chosen to examine this was (*R*)-muscone **2.1**, the natural product responsible for the musk odour. Synthesis of a trifluoromethylated derivative (**2.40**) of (*R*)-muscone would allow for an investigation into how fluorine affects interactions with

human olfactory receptors. The synthesised molecule could be sent to collaborators in China, Dr. Wiehong Liu and Dr. Hanyi Zhuang, who are able to run a luciferase assay which can quantify the interactions between the odourant and the olfactory receptors. This work could then lead to development of further musk olfactory receptor agonists, which could allow for a wider study of how altering the structure of (*R*)-muscone affects interactions with human olfactory receptors.

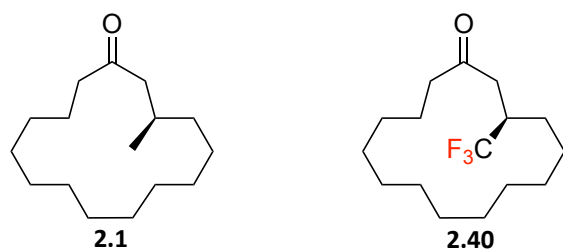


Figure 1.12 – The structure of (*R*)-muscone and a proposed trifluoromethylated derivative.

The introduction of fluorine into a known functional group could also allow for a study of how fluorine can be used to alter the properties of a molecule. One candidate for this could be the introduction of fluorine into the *tert*-butyl group. Introduction of fluorine is widely used within drug discovery to alter the lipophilicity, solubility and metabolism of drug candidates, and the development of a TFTB group could contribute to existing knowledge of the effects of fluorine on these properties. Fluorine is often used to alter these properties within molecules in drug discovery. Such a functional group could also be relevant within the PFAS discussion, as a TFTB group would not be considered a PFAS and as such could be a potential replacement for an existing PFAS.



Figure 1.13 – The structure of *tert*-butyl benzene and a proposed fluorinated derivative.

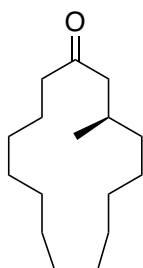
Chapter 2 - Synthesis of cyclic musks

Olfactory response assays were conducted by Dr. Weihong Liu and Dr. Hanyi Zhuang at Hanwang Technology Co. in Beijing, China. All other work within this chapter was completed by Luca Dobson.

2.1 Introduction

2.1.1 Muscone

Muscone **2.1** has a special place in the history of fragrances with a long folklore.⁷⁵ It is obtained from the musk pod of the male musk deer *Moschus moschiferus* and is found naturally as the (*R*)-(-)-enantiomer.⁷⁶ The (*R*)-enantiomer has a stronger musk odour than the (*S*)-enantiomer, with the odour of (*R*)-muscone being described as a “*very nice musky note, rich and powerful musk*” whereas the odour of (*S*)-muscone is described as “*poor (musky) and less strong*”.⁷⁷ However, obtaining naturally occurring (*R*)-muscone is a problem as it requires killing the musk deer to obtain the secretion. As a consequence, the musk deer is now an endangered animal, so it is desirable to find methods to synthesise (*R*)-muscone.



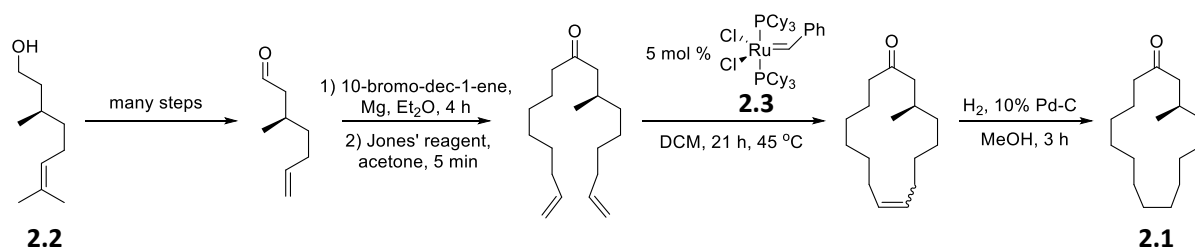
2.1

Figure 2.1 – Structure of (*R*)-muscone.

Muscone was first reported by Walbaum in 1906⁷⁸ and its structure was first determined by Laroslav Ruzicka in 1926. Ruzicka in Zurich then developed ‘the Ruzicka large-ring synthesis’, which for the first time allowed the synthesis of large macrocycles like muscone, albeit in low yields of around 5%.⁷⁹

A later and much more effective method for the synthesis of (*R*)-muscone was developed by Hagiwara *et al.*, who started from readily available (*R*)-citronellol **2.2**, as illustrated in Scheme 2.1.⁸⁰ The key to this synthesis involved the development of olefin-metathesis chemistry, using the Grubbs 1st generation ring-closing metathesis catalyst **2.3**.⁸¹ Metathesis

cyclisation followed by hydrogenation afforded (*R*)-muscone **2.1**. This has led to the expansion of synthetic muscone being used widely within the fragrance industry.



Scheme 2.1 – Hagiwara synthesis of (*R*)-muscone **2.1**.⁸⁰

2.1.2 Muscone and the mechanism of olfaction

There has been a debate over the olfaction mechanism of muscone, where some argued that the cause of the recognition of muscone was due to the shape and conformation adopted by the molecule, whereas others argued that it was due to the vibrational frequency of the C-H bonds within the molecule.⁸²

The shape and conformation of (*R*)-muscone interacting with, and then triggering olfactory receptors is generally considered to be the most likely mechanism responsible for its scent. This is known as the “lock and key” model⁸³, borrowed from Fischer’s analogy for enzymes, and involves a molecule of a specific shape or conformation interacting with the receptor. In the past, it has been difficult to determine the relevant shape and conformation of (*R*)-muscone. Some insights into ground-state conformations have come from X-ray crystallography, although it is a liquid at room temperature and not easily amenable to X-ray analysis. In 1982, Bernardinelli and Gerdill prepared the DNP derivative of (*R*)-muscone (muscone 2,4-dinitrophenylhydrazone).⁸⁴ X-ray analysis showed static disorder, with eight different possible conformers in the solid-state being found, as shown in Figure 2.2. This is consistent with (*R*)-muscone having a very flexible ring system, not unexpected for a 15-membered macrocycle.

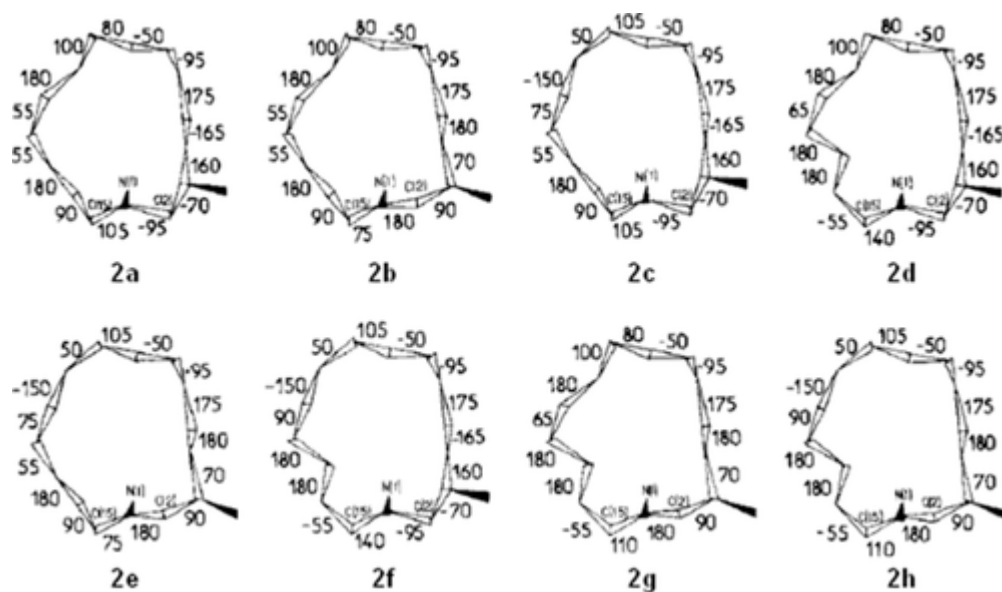


Figure 2.2 – Ring conformations of (*R*)-muscone **2.1** proposed by Bernardinelli and Gerdill.⁸⁴

O'Hagan *et al.* synthesised the Bernardinelli and Gerdill DNP **2.4** after preparing (*R*)-muscone **2.1** by the route developed by Hagiwara *et al.*⁸⁵ They were able to obtain a crystal structure, which did not match any of the eight possible structures originally proposed. They found that (*R*)-muscone adopts a pentagonal structure in the solid-state, with corners at the carbonyl carbon, the stereogenic carbon and at the C6, C9 and C13 positions, as shown in Figure 2.3. The C9 carbon was found to occupy a corner position in all eight structures deduced by Bernardinelli and Gerdill, and also in the structure obtained by O'Hagan *et al.* However, despite these studies, little work has been carried out to determine the conformations that contribute to the scent of (*R*)-muscone.⁸⁶

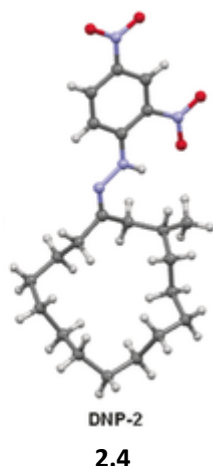


Figure 2.3 – X-ray structure of the DNP-hydrazine derivative of (*R*)-muscone (**2.4**) obtained by O’Hagan *et al.*⁸⁵

Meanwhile, discussions persisted that the scent of muscone is due to the vibrational frequency of the bonds within muscone. This mechanism of olfactory stimulus was initially proposed in 1938 by Dyson⁸⁷, who suggested that receptors could detect molecular vibrations. In 1977, this theory was further developed by Wright⁸⁸, who suggested that vibrations could only be detected by olfactory receptors at frequencies less than 500 cm^{-1} . However, this was considered unlikely as small molecules with strong odours such as ammonia and ozone have vibrational frequencies between 750 cm^{-1} and 3500 cm^{-1} .⁸⁹ It was later proposed by Turin that the vibrational origin of olfaction arises due to inelastic electron tunnelling.⁸⁹ Turin suggested that olfactory receptors act as tunnelling microscopes that are tuned to specific odorants, as shown by Turin in Figure 2.4.⁸⁹ Turin proposed that an olfactory receptor accepts electrons from a donor, likely NADPH, creating a filled energy level at the binding site. When a binding site is empty, electrons are unable to tunnel across the binding site to trigger a response from the receptor, as the energy gap to the lower energy levels across the binding site is too large for this to occur. When an odorant occupies the binding site of an olfactory receptor, an electron can lose energy by exciting its vibrational mode and can bridge the energy gap. The electron is able to tunnel across the binding site, activating that receptor. This effect can only take place if the energy of the vibrational mode is the same as the energy gap.

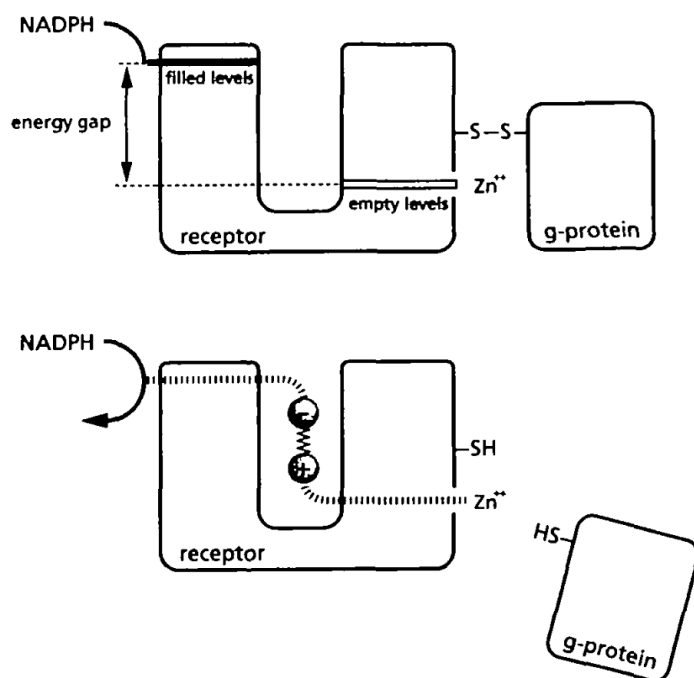


Figure 2.4 – Mechanism for electron tunnelling at the olfactory receptor binding site as proposed by Turin.⁸⁹

An approach to determine whether shape or bond vibrations are responsible for the odour involved isotopes, particularly experiments using perdeuterated (*R*)-muscone. Deuteration has no significant effect on ground state conformation, however, it has a large influence on the vibrational frequency of C-H/C-D bonds as a deuterium atom is double the mass of a hydrogen atom. Turin *et al.* tested this theory by per-deuterating acetophenone and cyclopentadecanone.⁹⁰ They conducted a double-blind study where samples of these deuterated and non-deuterated fragrances were provided to humans to smell and to assess if the samples smelt the same or differently. They concluded that there was no difference detected for the odour of deuterated and non-deuterated acetophenone, however, that there was in the case of cyclopentadecanone. On this basis, they proposed an electron transfer mechanism for olfaction, sensitive to partial charges.⁸³ As the C-H bond is only weakly polar, it would require a lot of C-H bonds to affect the electron transfer mechanism and be detectable by smell. They also suggested that molecules with 18 or more carbons tend to be odourless, which they believe suggests that a very small number of receptors are involved in sensing musk odour. This led them to propose that molecules must be large so

they activate the one or very few receptors responsible for sensing musk odour and that molecules must have intense IR bands in the 1380-1550 cm^{-1} range to be odorants.⁹⁰

It proved difficult to determine if either the shape or vibrational theory of olfaction was more correct because knowledge of the olfactory receptors was very limited. However, in 2014, Touhara *et al.* were able to identify both the mouse and human receptors that are responsible for the perception of muscone.⁹¹ Odorants are recognised by around 1000 olfactory receptors (ORs) within the nasal cavity.⁹² ORs are tuned to specific odorants and each odorant can usually be detected by multiple receptors.⁹³ These receptors are expressed on olfactory sensory neurons in the olfactory epithelium. The olfactory epithelium is the specialised tissue in the nasal cavity that is involved in smell. The neural inputs that are received by olfactory receptors are sent to the olfactory bulb (OB), which is located in the forebrain. Within the OB, the axons of the receptor cells that respond to a specific chemical all converge on one glomerulus.⁹⁴ Glomeruli are discrete spheres of nerve tissue that are located in the OB. The response patterns of the glomeruli that are stimulated by an odour are visualised to determine which ORs have responded to an odorant. Touhara *et al.* tested the ability of mouse olfactory receptors to bind to muscone. Of all the receptors, they found that MOR215-1 was the sole receptor that bound muscone and that it had a higher affinity for (*R*)-muscone over (*S*)-muscone, and also the racemate.⁹¹ The human OR with the highest similarity to MOR215-1 is OR5AN1 (68%). They found that the binding affinity of OR5AN1 to muscone was approximately ten times greater than that of MOR215-1. On assaying the binding of muscone to other similar ORs to MOR215-1 (OR5A1 and OR5A2), they found no binding affinity. Therefore, Touhara *et al.* were able to identify which specific OR responds to (*R*)-muscone.

It now became possible to explore more specifically whether shape or vibration is responsible for olfactory response. Accordingly, Block *et al.* assayed the response of OR5AN1 to muscone, acetophenone and their deuterated analogues.⁸² They found that all deuterated isotopomers of (*R*)-muscone gave highly similar responses, and very similar dose-response curves, as shown in Figure 2.5. Cyclopentadecanone and its per-deuterated isotopomer also gave very similar, albeit much smaller, dose-response curves than muscone and deuterated muscone.

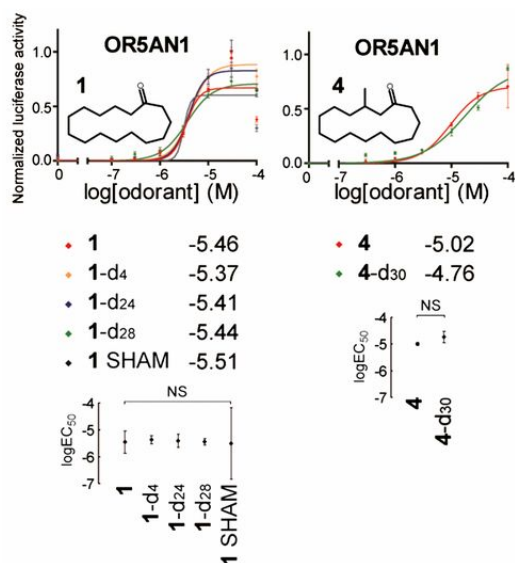


Figure 2.5 – Dose-response curves of OR5AN1 to cyclopentadecanone and muscone.⁸²

Furthermore, the IR absorption spectra of muscone and its perdeuterated isotopomer d₃₀-muscone are very different and that of perdeuterated d₃₀-muscone does not show any IR absorption in the 1380-1550 cm⁻¹ range, as shown in Figure 2.6.⁸² This is contrary to the specification postulated by Turin *et al.* for a musk odourant. Given that per-deuterated muscone elicits a very similar response to muscone when interacting with the OR5AN1 receptor, this made the vibrational theory of olfaction less plausible and lent greater support to the shape theory of olfaction.

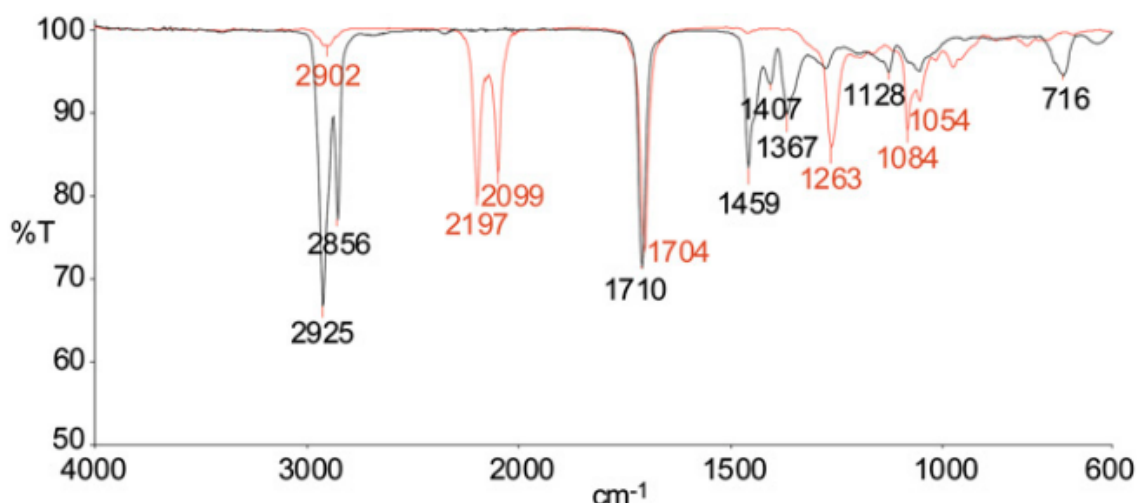


Figure 2.6 – Superimposed IR spectrum of muscone (black) and d₃₀-muscone (red).⁸²

2.1.3 Fluorine in muscone

Despite the increasing utility of fluorine and the continued growth of fluorine's use in medicinal chemistry, there has been little work done previously on the incorporation of fluorine into fragrance molecules. Furthermore, there are no known naturally occurring fragrances that contain fluorine.⁹⁵ Therefore, work on understanding the effect of fluorine on fragrance molecules is in its infancy.

O'Hagan *et al*, have assessed the effect of adding fluorine to macrocycles such as (*R*)-muscone investigating the effect of incorporating a CF₂ into the macrocycle.⁹⁶ For example, cyclododecane is a solid at room temperature and its crystal structure was determined in 1960 by Dunitz and Shearer, as shown in Figure 2.7.⁹⁷ It was found to have a [3333] square conformation in the solid-state however it has a conformational energy barrier of 7.3 kcal mol⁻¹ for interconversion to higher energy forms⁹⁸, a barrier lower than that of cyclohexane (10.5 kcal mol⁻¹), showing that cyclododecane is highly conformationally flexible.

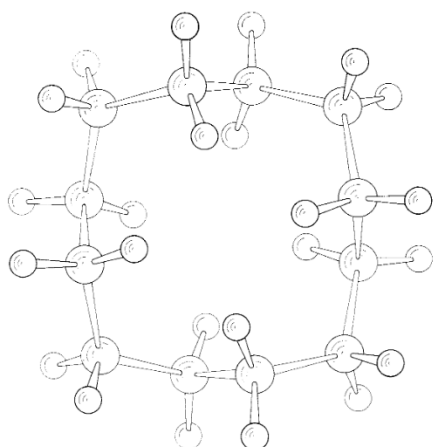


Figure 2.7 – The Dunitz and Shearer structure of cyclododecane.⁹⁷

This square structure has clearly defined edge and corner CH₂ groups and offered an ideal framework to examine if CF₂ groups might prefer to locate, either a corner or an edge, in such a macrocycle. Accordingly, 1,1,4,4- and 1,1,7,7- tetrafluorocyclododecanes **2.5** and **2.6** were synthesised where the CF₂ groups were incorporated on carbon atoms that were known to take corner positions on cyclododecane, as shown in Figure 2.8. It was found in both cases that the CF₂ groups adopted corner positions and that they stabilise the ground state structure. 1,1,4,4-Tetrafluorocyclododecanone was found to be 3.0 kcal mol⁻¹ more conformationally stable than cyclododecane and 1,1,7,7-tetrafluorocyclodecanone was

found to be 5.91 kcal mol⁻¹ more stable than cyclododecanone, showing that the CF₂ group has the effect of stabilising the ground state conformation of cyclododecane by securing corner locations. Furthermore, 1,1,6,6-tetrafluorocyclododecanone **2.7** was synthesised, with the incorporation of a CF₂ group at the C6 position of cyclododecane, which would hold an edge position in the Dunitz and Shearer square structure. However, the CF₂ group at C6 actually distorted the ring into a rectangular [4332] structure. This showed that the CF₂ group dictates a corner position, in order to avoid unfavourable 1,4-H,F transannular interactions that would occur if the CF₂ group held an edge position. This knowledge on the effect of the CF₂ group within macrocycles indicated that CF₂ might be used to stabilise ground state conformations of naturally occurring macrocyclic fragrance molecules.

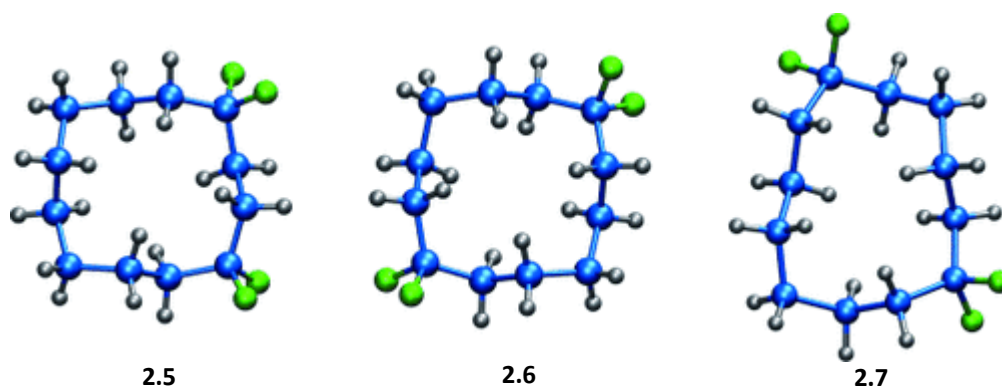


Figure 2.8 – Structures of CF₂-containing cyclododecanes **2.5-2.7**.⁹⁶

Accordingly, the CF₂ group was introduced separately into the C10 **2.8**, C9 **2.9**, C8 **2.10**, C7 **2.11** and C6 **2.12** positions, as illustrated in Figure 2.9.⁸⁵ These CF₂-containing muscones were synthesised by adapting the metathesis approach developed by Hagiwara *et al.*

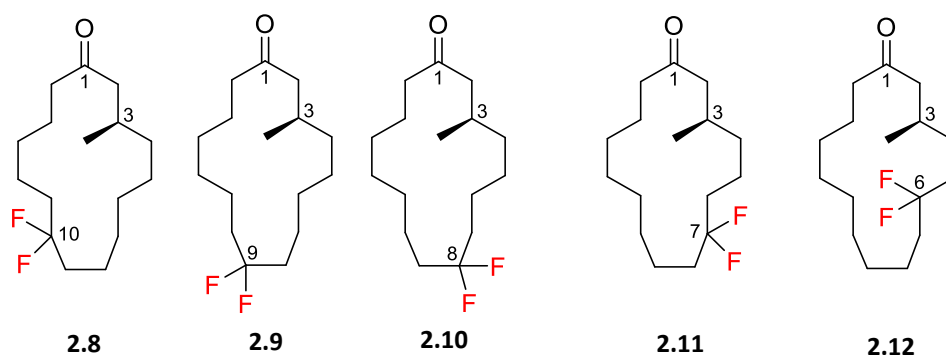


Figure 2.9 – CF₂-Containing derivatives of (*R*)-muscone synthesised by O'Hagan *et al.*⁸⁵

X-ray structures of the fluorinated derivatives of (*R*)-muscone revealed that the CF₂ groups preferentially adopt corner positions, with the C10 **2.8** and C7 **2.11** difluorinated muscone forming pseudo-rectangular structures, as shown in Figure 2.10. These both have weak musk odours. The C9 structure **2.9** adopts a square structure virtually identical to Bernardinelli's proposed structures shown in Figure 2.2, and also has a weak musk odour. The C8 difluorinated muscone **2.10** has a distorted rectangular conformation and is described as having a 'very good musk profile'. The C6 difluorinated muscone **2.12** was described as having 'a pleasant musky odour' like that of (*R*)-muscone. The general trend is that when the structures of the muscone derivatives deviate from rectangular conformations to square conformations, the strength of the musk odour is weakened. These results show that the incorporation of a CF₂ group in (*R*)-muscone influences the conformation of muscone due to its preference for adopting corner positions and this influences the odour of the muscone derivative.

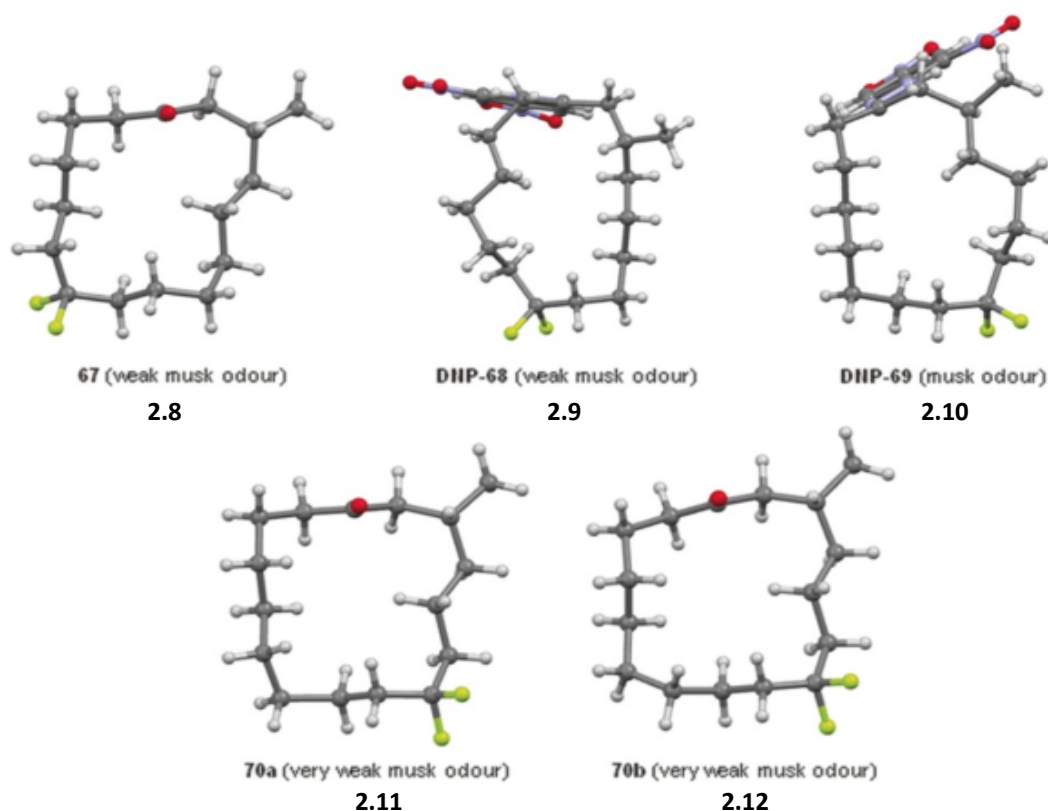


Figure 2.10 – X-ray structures of fluorinated derivatives of (*R*)-muscone.⁸⁵

With these fluorinated musk analogues in hand, their efficacy against the olfactory receptor OR5AN1 was explored. These assays were conducted via a luciferase coupled assay system,

which generates chemical luminescence when an odorant interacts with the receptor, and which can be quantified to measure the amount of luciferase produced.^{99 100} The greater the luciferase production, the greater the affinity to the OR5AN1 receptor. These results were plotted in a dose-response curve as shown in Figure 2.11. It was found that, while all of the analogues of (*R*)-muscone elicited a response the strength of the response was heavily influenced by the position of the CF₂ group on the molecule.¹⁰¹ The C8 substituted muscone **2.10** gave the best response, with very similar results to (*R*)-muscone, as shown in Figure 2.10. This was also consistent with the smell recorded in Figure 2.9.

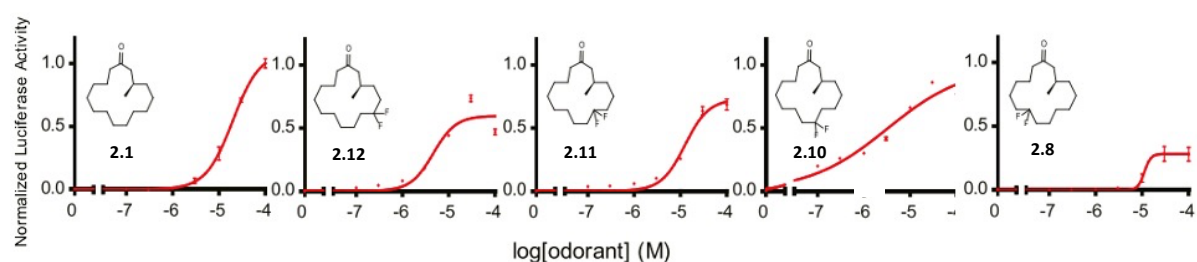


Figure 2.11 – Dose-response curves with OR5AN1 for CF₂- derivatives of (*R*)-muscone **2.8-2.12**.¹⁰¹

Interestingly, the best interaction was recorded with alkene **2.13**, which was found to be three orders of magnitude more potent than (*R*)-muscone in the OR5AN1 assay.¹⁰¹ This was most likely because the combination of a CF₂ group on the corner at C7 and the (*E*)-double bond had the combined effect of locking the molecule into a conformation that has a very strong affinity for interacting with OR5AN1, as shown in Figure 2.12.

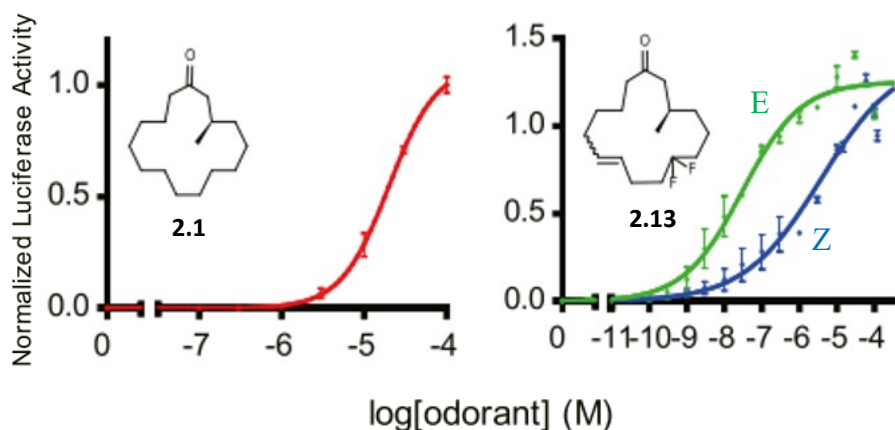
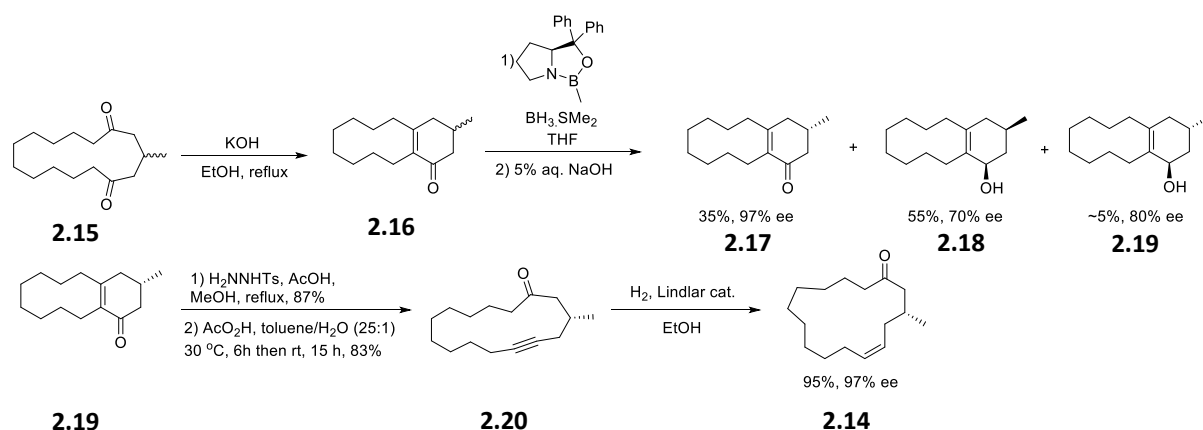


Figure 2.12 – Response of alkene **2.13** (right) compared to the dose-response curve of (*R*)-muscone (left).¹⁰¹

2.1.4 Recent cyclic musk developments

Work remains ongoing in the study of cyclic musk compounds inspired by the structure of (*R*)-muscone.¹⁰² In the development of a synthesis of (*R*)-muscone, 5-muscenone **2.14** was discovered. This compound is the precursor to (*R*)-muscone in a nitrous-oxide mediated synthesis of (*R*)-muscone and was found to be more potent than (*R*)-muscone itself.¹⁰³ A study of all possible stereoisomers of 5-muscenone by Fujimoto *et al.* found that the (*3R,5Z*)-isomer **2.14** was the most potent.¹⁰³ Fehr *et al.* later found that this isomer of muscenone is over ten times more potent than (*R*)-muscone.¹⁰⁴ They developed a synthesis of (*3R,5Z*)-muscenone, as shown in Scheme 2.2, which began with diketone **2.15**. This was reacted in a transannular aldol condensation to give enone **2.16**. The racemic product was then subject to a kinetic resolution via a CBS-mediated oxidation reaction, which gave *cis*- and *trans*-alcohols **2.17** and **2.18** and pure (*S*)-enone **2.19**. (*S*)-Enone **2.19** was then subjected to an Eschenmoser fragmentation to give macrocycle **2.20**. Partial reduction of the subsequent alkyne to an alkene using Lindlar catalyst gave the desired (*3R,5Z*)-muscenone **2.14**.



Scheme 2.2 – Synthesis of (*3R,5Z*)-muscenone **2.14** by Fehr *et al.*¹⁰⁴

A number of further molecules similar to (*R*)-muscone have been synthesised and characterised as potent musks, as illustrated in Figure 2.13.¹⁰² A common approach is the introduction of unsaturation to macrocyclic rings. Exaltenone **2.21**, like (*R*)-muscone, is a 15-membered heterocycle, but it contains a double bond at the 4 position. Cosmone **2.22** is a smaller heterocycle, with 14 carbon atoms. It contains a methyl group at C3 like muscone, however, introduces an alkene at C5. Nirvanolide **2.23** is a musk which also has ‘pleasant fruity notes’. This is a 15-membered lactone which necessarily has an oxygen in the ring. It

also has methyl group C13 and a (Z)-alkene at C10. Increasing the ring size to 16 leads to ‘warmer musk tones’. These molecules also tend to contain unsaturation, with Velvione **2.24**, Aurelione **2.25** and Globanone **2.26** containing alkenes at the C5, C7 and C8 respectively.

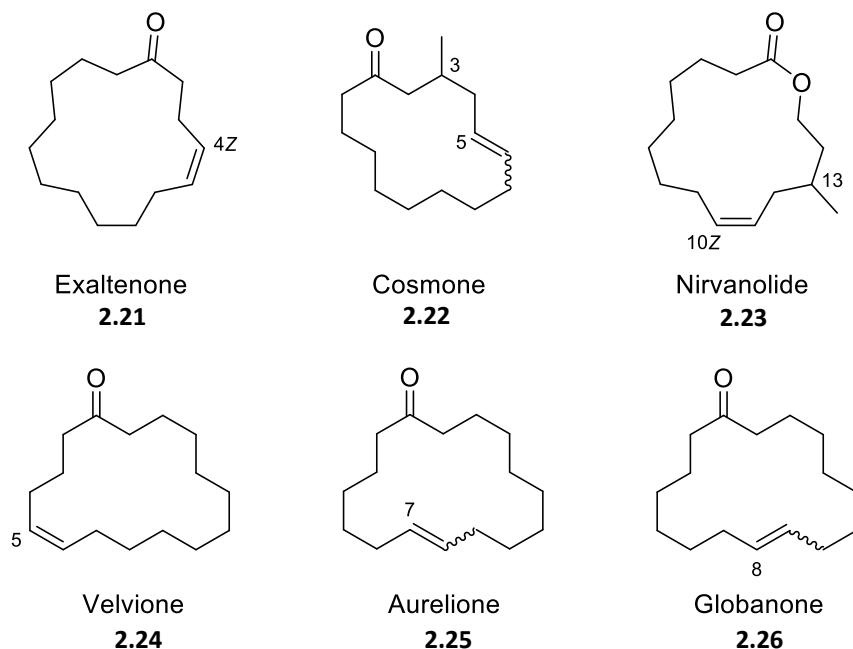


Figure 2.13 – Structures of cyclic musk compounds.

2.1.5 Olefin metathesis

Olefin metathesis is a reaction formally constituting the exchange of the two carbene fragments of an olefin, with those of another olefin, and leading to the formation of new olefins with different substituents.¹⁰⁵ It was first discovered during the development of the Ziegler-Natta polymerisation.¹⁰⁶ This can happen with chains or rings and consequently, there are different types of olefin metathesis reactions, such as cross metathesis, ring-opening and ring-closing metathesis, as illustrated in Figure 2.14.

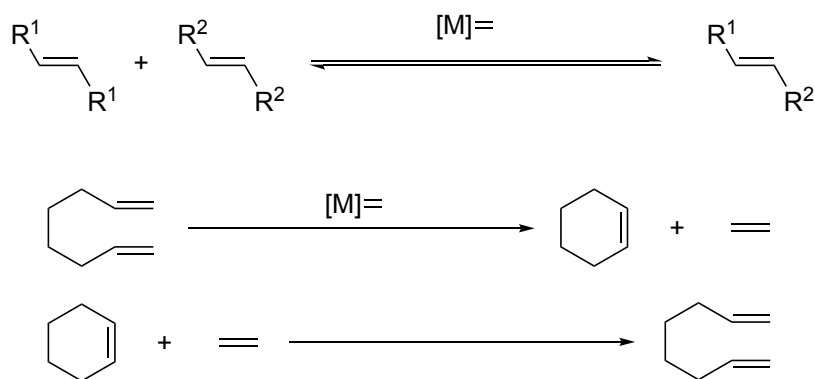


Figure 2.14 – General reactions of a cross-metathesis (top), ring-opening metathesis (middle) and ring-closing metathesis (bottom).

Olefin metathesis reactions typically use metal-carbene catalysts, as shown in Figure 2.15. The first of these was a tungsten-carbene catalyst synthesised by Casey in 1974.¹⁰⁷ Schrock *et al.* later followed this by developing molybdenum-carbene catalysts. Schrock's catalyst **2.27** exhibits high reactivity, however, it exhibited low functional group tolerance, incompatible with carboxylic acids, alcohols and aldehydes.¹⁰⁸ Grubbs *et al.* then followed with a first-generation catalyst **2.3** in 1995, which uses ruthenium as the metal instead of molybdenum.^{109, 110} Grubbs prepared this by reacting $\text{RuCl}_2(\text{PPh}_3)_3$ with phenyldiazomethane and tricyclohexylphosphine. This catalyst is much more tolerant of functional groups than Schrock's and generally requires less vigorous conditions.¹¹¹ Grubbs followed with the development of a second-generation catalyst **2.28**¹¹² which was found to exhibit higher activity while retaining air and water stability. The NHC-ruthenium catalytic centre has been found to have an increased binding affinity for π -acidic olefins relative to sigma-donating phosphines, promoting the metathesis reaction.¹¹³ The increased stability also allowed for lower loadings than the previous catalysts. Further developments came from Hoveyda *et al.*, with a first generation Hoveyda-Grubbs catalyst **2.29** in 1999.¹¹⁴ This catalyst introduced a chelating *ortho*-isopropoxy group in place of one of the phosphine ligands. A second-generation Hoveyda-Grubbs catalyst **2.30** swiftly followed in 2000, published almost simultaneously by Hoveyda and Blechert.¹¹⁵ This catalyst replaced the remaining cyclohexylphosphine ligand with an NHC ligand. With the addition of the NHC ligand, the second-generation Hoveyda-Grubbs catalyst exhibits improved thermal stability and increased air and moisture tolerance compared to the first-generation catalyst, but it also exhibits decreased activity.¹¹³

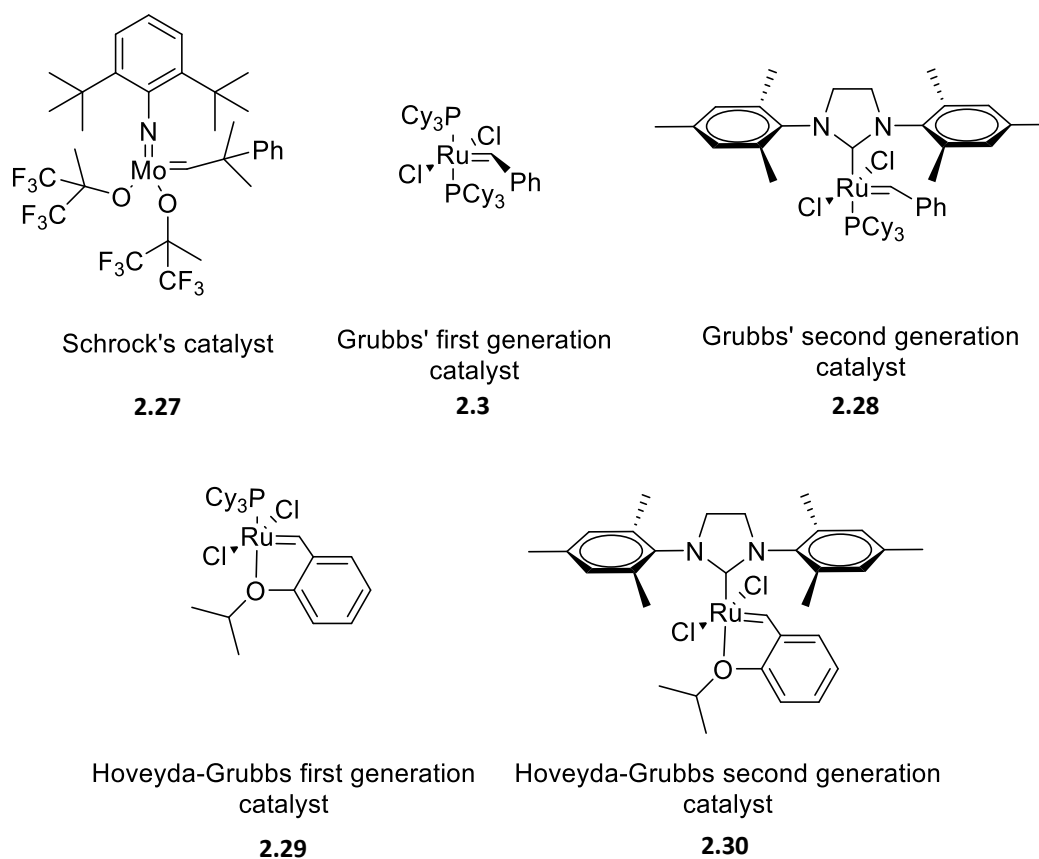
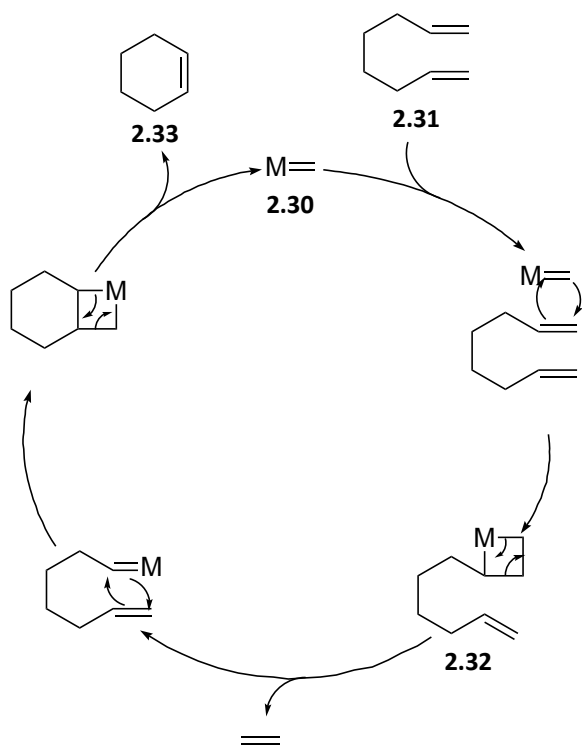


Figure 2.15 - Commonly used metathesis catalysts.

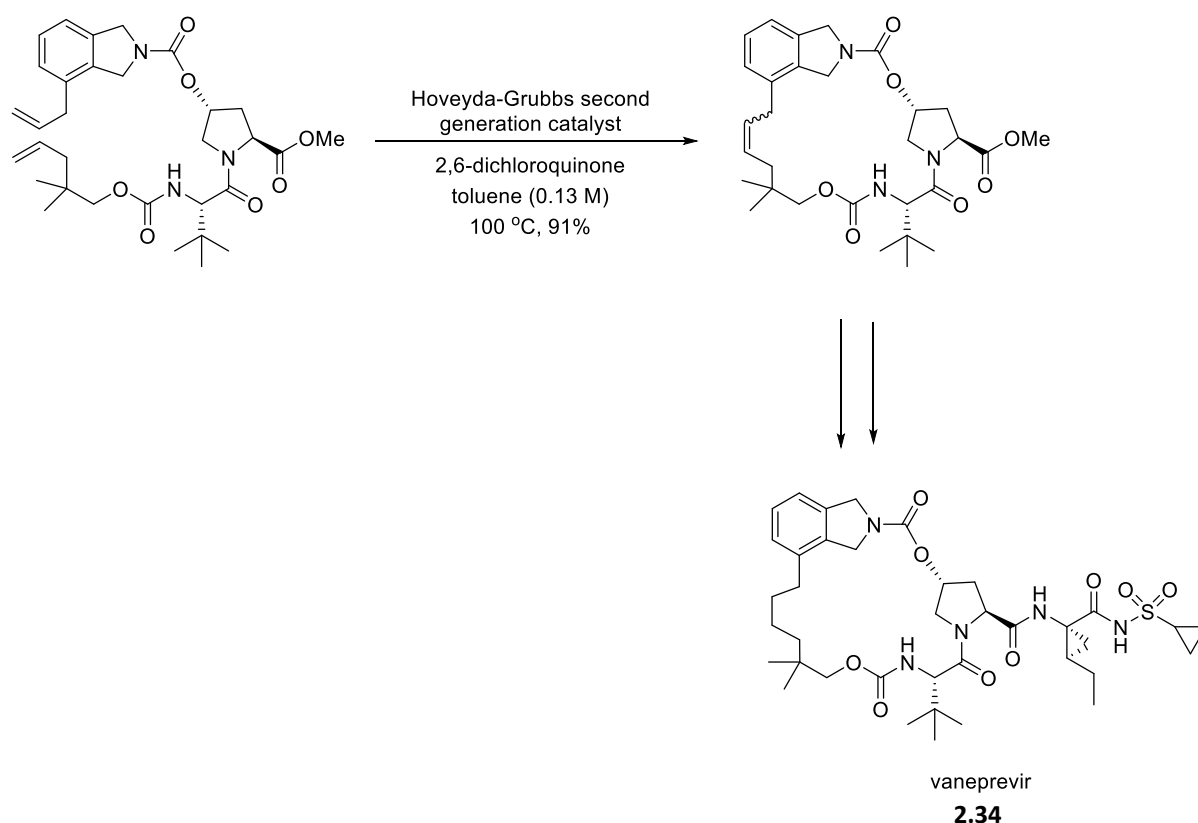
2.1.6 Ring-closing metathesis

The general mechanism for olefin metathesis was proposed by Chauvin in 1971, as illustrated in Scheme 2.3, who first identified the four-membered metallocycle intermediate **2.32**.¹¹⁶ This mechanism can be applied to ring-closing metathesis and involves a [2+2] cycloaddition of one of the alkenes of starting olefin **2.31** with the metal alkylidene. Cyclo-elimination of ethene then takes place. The terminal alkene of a second olefin substrate then undergoes an intramolecular [2+2] cycloaddition with the metal alkylidene **2.30**, followed by cyclo-elimination to give the ring-closed product **2.33** and a new metal alkylidene regenerating the active catalyst **2.30**.



Scheme 2.3 – Ring-closing metathesis mechanism.¹¹³

Ring-closing metathesis reactions are now widely used within synthetic chemistry. One example of this is in the synthesis of Vaniprevir **2.34**, a 20-membered heterocycle which acts as an inhibitor of the hepatitis C virus protease.¹¹⁷ A previous synthesis of Vaniprevir had 21 steps, however, Kong *et al.* were able to reduce this to nine linear steps by using a metathesis protocol, as shown in Scheme 2.4.¹¹⁸



Scheme 2.4 – RCM-mediated synthesis of Vaneprevir **2.34**.¹¹⁸

2.1.7 Sulfoxides and sulfones

Sulfoxides are mono-oxidised thio-ethers which contain a sulfinyl ($R_2S=O$) bond. Probably the most widely used sulfoxide is the solvent, dimethylsulfoxide (DMSO) **2.35**.¹¹⁹ The sulfoxide substituent is of interest structurally as the sulfur has a lone pair and this creates a configurationally stable stereogenic centre, with tetrahedral geometry at sulfur. The sulfoxide is often represented in one of two ways, either as a polarised sulfur-oxygen single bond, with formal charges on sulfur and oxygen, or as an $S=O$ double bond, as illustrated in Figure 2.16. This ambiguity conveys its double bond character while having tetrahedral geometry. The barrier to configurational inversion is high at between 35-45 kcal mol⁻¹, so sulfoxides are stable to configurational inversion at sulfur.¹²⁰ Further oxidation to sulfones **2.36** results in a tetrahedral geometry and the loss of stereochemistry at sulfur.¹²⁰

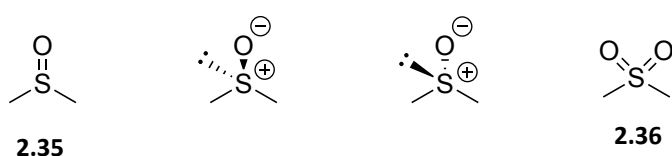


Figure 2.16 – Representations of the sulfoxide and structure of the sulfone.

Sulfoxides are typically prepared by the oxidation of thio-ethers using mild oxidising agents such as hydrogen peroxide or *m*CPBA, however, this must be done carefully to prevent over-oxidation to the sulfone.

Sulfoxide-containing molecules have been used in medicinal chemistry, as shown in Figure 2.17. One example is omeprazole **2.37**, which behaves as a proton pump inhibitor and is used in the treatment of gastroesophageal reflux disease and gastric ulcers.¹²¹

Esomeprazole **2.38** is an optically pure form of omeprazole, the (*S*)-isomer, and is sold as an over-the-counter drug under the name Nexium. Both enantiomers of omeprazole are potent, however, they differ in their pharmacokinetic profiles.¹²² It has been found that the (*S*)-isomer (esomeprazole) exhibits higher bioavailability and is more potent in inhibiting gastric acid secretion than the (*R*)-isomer.¹²¹ This shows that the chirality at the sulfoxide influences its potency. Armodafinil **2.39** is another example of a drug molecule containing a sulfoxide. It is used in the treatment of excessive daytime sleepiness. Armodafinil is the (*R*)-enantiomer of the racemic modafinil. This enantiomer has been found to have a longer half-life than the racemate. Therefore, the sulfoxide stereochemistry in armodafinil is also important in influencing potency.^{123, 124}

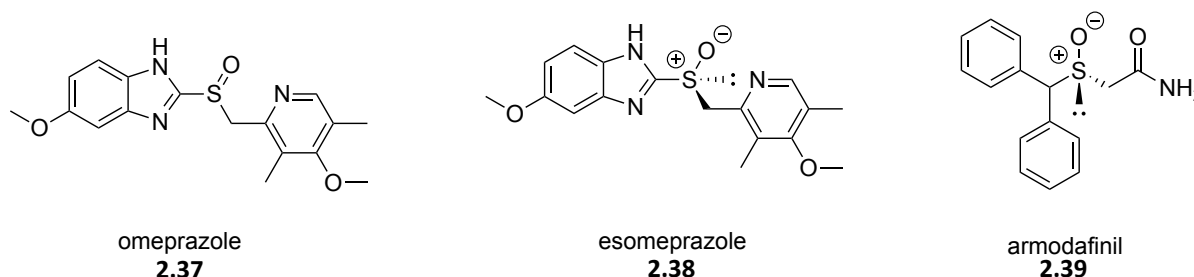


Figure 2.17 – Structures of omeprazole **2.37**, esomeprazole **2.38** and armodafinil **2.39**.

2.1.8 Aims and objectives

The overall aim of this Chapter is to build on the previous work from the St. Andrews group on understanding how the structure of (*R*)-muscone gives rise to its unique odour, and how conservatively altering the structure can alter the odour of (*R*)-muscone. Two synthetic targets were identified at the outset. The first was the trifluoromethylated-derivative of (*R*)-muscone **2.40**.

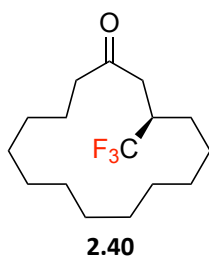


Figure 2.18 – CF_3 -(*R*)-muscone target.

Such a molecule would allow the unique properties of the trifluoromethyl group to be explored as a methyl mimetic in this sensitive bioactive system. The CF_3 is classically lipophilic which is consistent with the general nature of muscones.

The sulfoxide-diastereoisomers **2.41a** and **2.41b** offered a second target in which to explore pyramidal geometry relative to the trigonal planar geometry of the carbonyl in muscone. It was anticipated that it might be possible to separate the diastereoisomers to investigate the impact of chirality at the sulfur atom on the olfactory response.

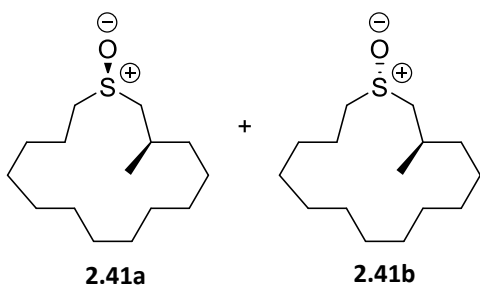


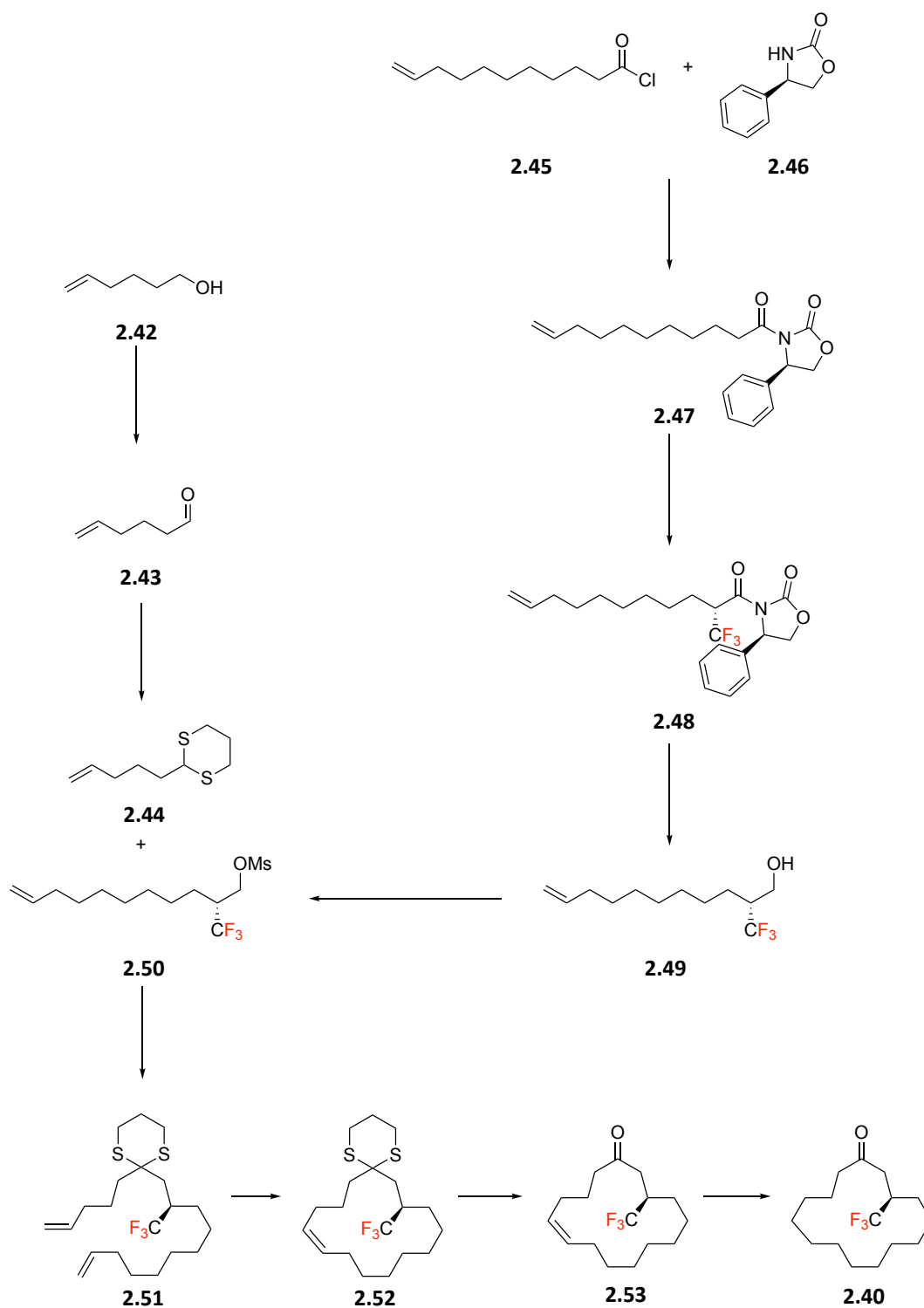
Figure 2.19 – Diastereoisomers of the sulfoxide derivative of (*R*)-muscone.

In a continuing collaboration, assays were carried out on the mouse and human olfactory receptors MOR215-1 and OR5AN-1 with Dr Hanyi Zhuang and Dr Weihong Liu at Hanwang Technology in Beijing, China.

2.2 Results and discussion

2.2.1 Synthesis of the CF₃ containing muscone

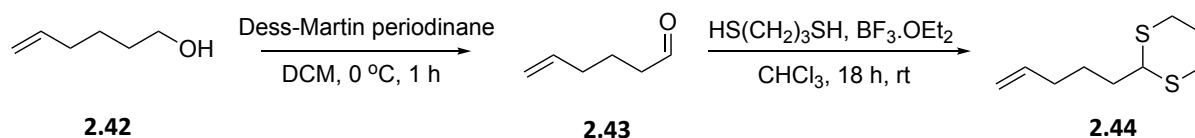
Initially, a synthesis route was developed for the preparation of the trifluoromethyl analogue of (*R*)-muscone **2.40**, as illustrated in Scheme 2.5.



Scheme 2.5 – Proposed synthesis of trifluoromethylated derivative of (*R*)-muscone **2.40**.

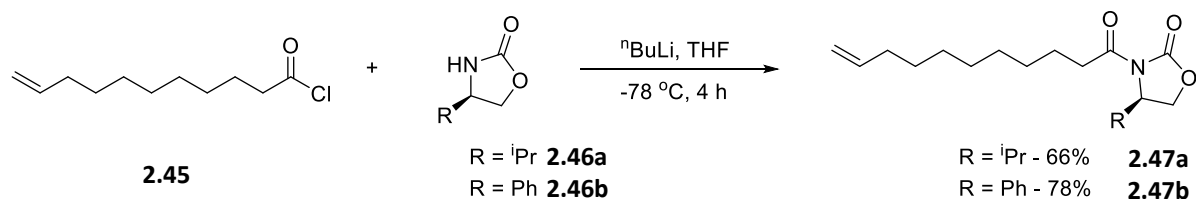
The initial plan involved a convergent synthesis. The first branch would start from 5-hexen-1-ol **2.42**, oxidising to 5-hexenal **2.43**, and then forming dithiane **2.44**. The second branch would start with the synthesis of oxazolidinone **2.47** from 11-undecenoyl chloride **2.45** and oxazolidinone **2.46**. This approach relies heavily on chiral auxiliary chemistry developed by Evans.¹²⁵ The stereogenic centre of the oxazolidinone is required to be of the (*R*)-configuration. Electrophilic addition of a trifluoromethyl group presented the greatest challenge of the synthesis and required an appropriate electrophilic trifluoromethylating agent. Reductive cleavage of **2.48** would follow, to give (*R*)-alcohol **2.49** which when activated with a good leaving group would complete the second branch of the synthesis. The reaction of **2.44** and activated alcohol **2.50** would then progress with a Corey-Seebach reaction, taking advantage of the “umpolung” reactivity of the dithiane to join the two branches together. Diene **2.51** would then undergo ring-closing metathesis⁸¹ to form heterocycle **2.52**. Hydrolysis of the dithiane of **2.52** to ketone **2.53** and then hydrogenation of the double bond should give target **2.54**.⁸⁰

The synthesis started with the development of the first branch, as shown in Scheme 2.6. 5-Hexen-1-ol **2.42** was smoothly (68% yield) oxidised to 5-hexenal **2.43** using Dess-Martin periodinane and then the aldehyde **2.43** was combined with propane-1,3-dithiol to generate dithiane **2.44**. Although the yield here was low (24%) this two-step protocol could be scaled and was not too limiting.



Scheme 2.6 – First branch of trifluoromethylated muscone synthesis.

The second branch began with the reaction of 10-undecenoyl chloride **2.45** with oxazolidinones **2.46a** and **2.46b** to form the oxazolidinones **2.47a** and **2.47b**, as illustrated in Scheme 2.7. Both the (*R*)-isopropyl **2.47a** and the (*R*)-phenyl **2.47b** auxiliaries were prepared in order to explore which would give the better diastereomeric excess when the trifluoromethylation reaction was attempted.

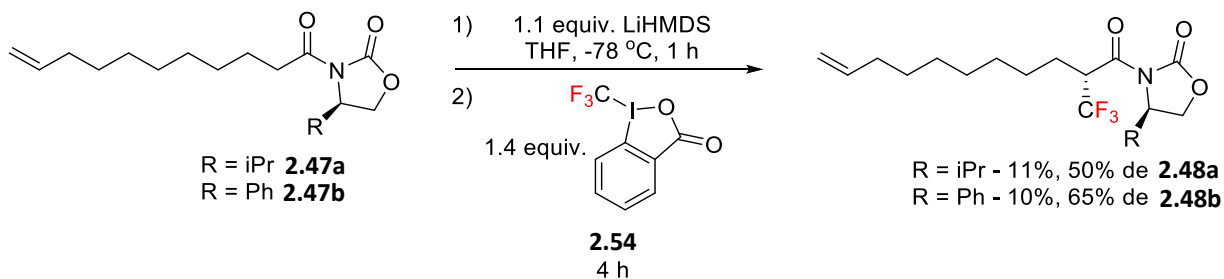


Scheme 2.7 – Synthesis of chiral auxiliaries 2.47a and 2.47b.

With the chiral auxiliaries in hand, the next step focused on trifluoromethylation. An electrophilic $-\text{CF}_3$ approach was more attractive than a radical $\cdot\text{CF}_3$ approach due to the terminal alkene, which could be susceptible to radical attack. It was decided to proceed with Togni's electrophilic fluorinating reagent **2.54** due to its availability and a relatively wide substrate scope had already been demonstrated.⁶⁵ However, it is worth noting that the reagent has not been explored previously with long-chain terminal alkenes.

In the event, there was a successful formation of the trifluoromethylated oxazolidinones **2.48a** and **2.48b**, as shown in Scheme 2.8. This was apparent by ^1H NMR. Taking the trifluoromethylation of the phenyl oxazolidinone as an example, the CH_2 peak adjacent to the carbonyl appears at 2.92 ppm, whereas in the trifluorinated oxazolidinone, the CH signal adjacent to the carbonyl, becomes a multiplet between 4.88-5.03 ppm along with the CH_2 alkene signal, as shown in Figure 2.20. The ^{19}F NMR signal was a singlet at -67.0 ppm, consistent with an installed CF_3 group.

However, the yields for this reaction were poor. Trifluoromethylation with **2.47a** generated **2.48a** in 11% and the reaction with **2.47b** gave **2.48b** in 10%. During purification, the products noticeably decomposed on silica gel. This could be due to the electron-withdrawing nature of $-\text{CF}_3$ rendering the exo-cyclic imide carbonyl susceptible to acid-catalysed hydrolysis during column chromatography. The reaction also gave lower diastereomeric excesses than desired, with a 50% de for **2.48a** and a 65% de for **2.48b** as judged by ^{19}F NMR.



Scheme 2.8 – Trifluoromethylation of chiral oxazolidinone using Togni's Reagent.

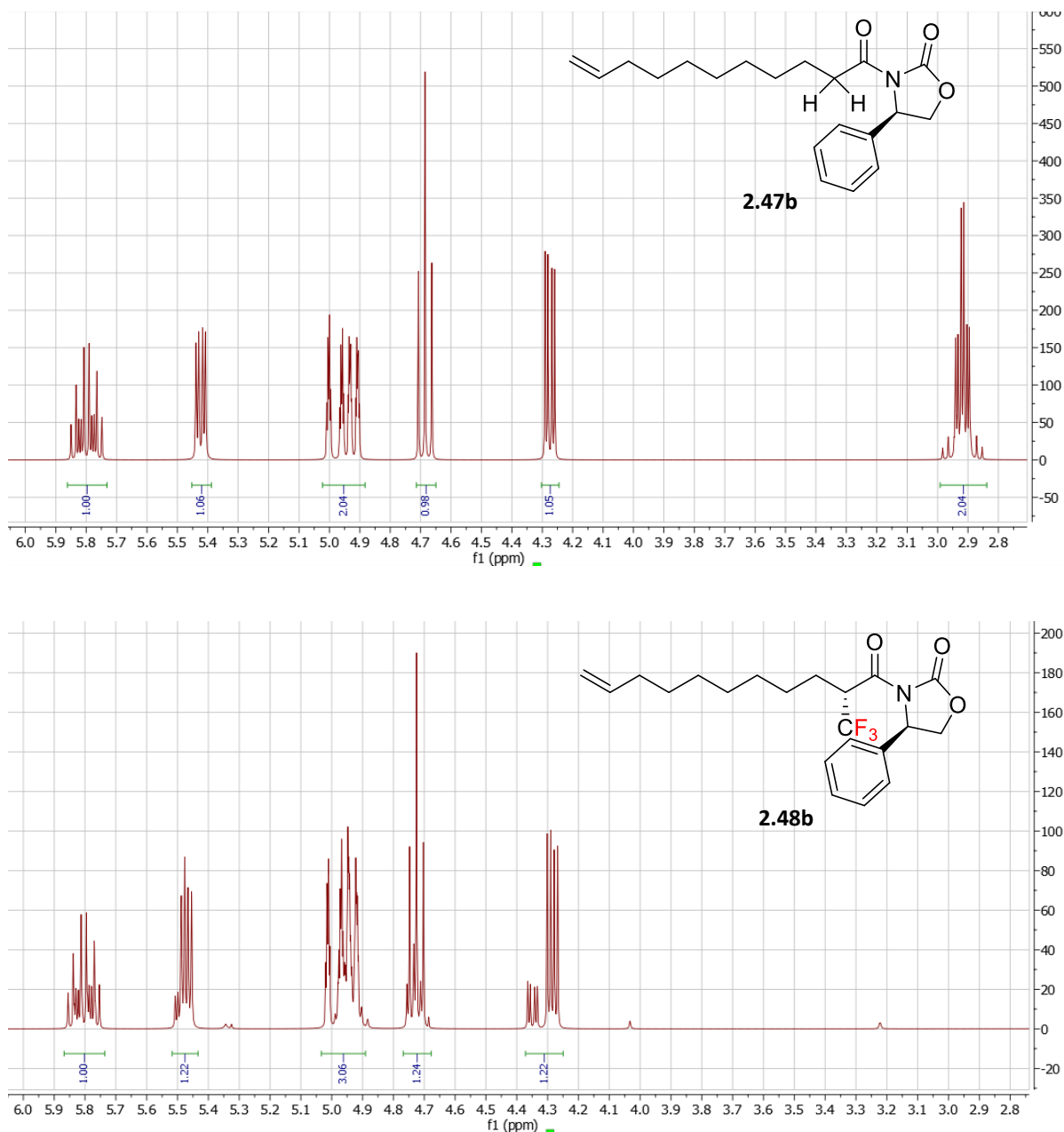
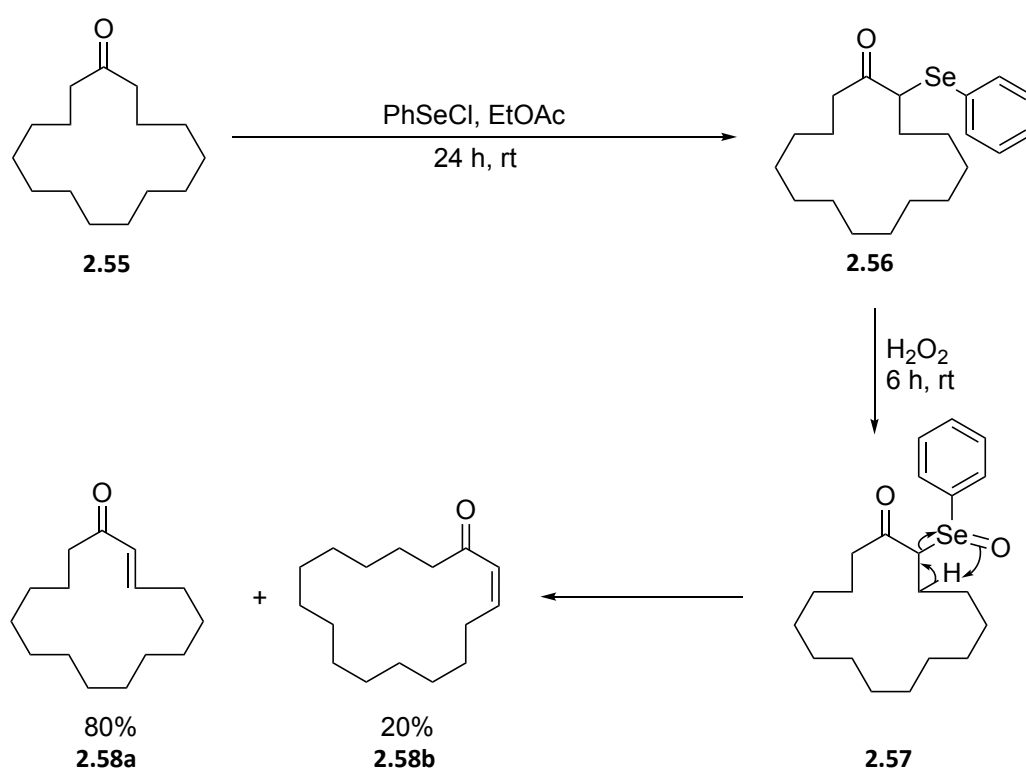


Figure 2.20 – Section of the ^1H NMR of phenyl oxazolidinone **2.47b** (starting material) and trifluoromethylated phenyl oxazolidinone **2.48b**. The minor signals indicate the minor diastereoisomer.

After several attempts, and primarily due to low yields, this approach was not pursued further. Alternatively, attention turned to exploring the 1,4-addition of nucleophiles to (*E*)-cyclopentadecenone. This would generate a racemate on introduction of the CF₃ group, and if successful separation of the enantiomers would be explored via a chiral resolution at a later stage.

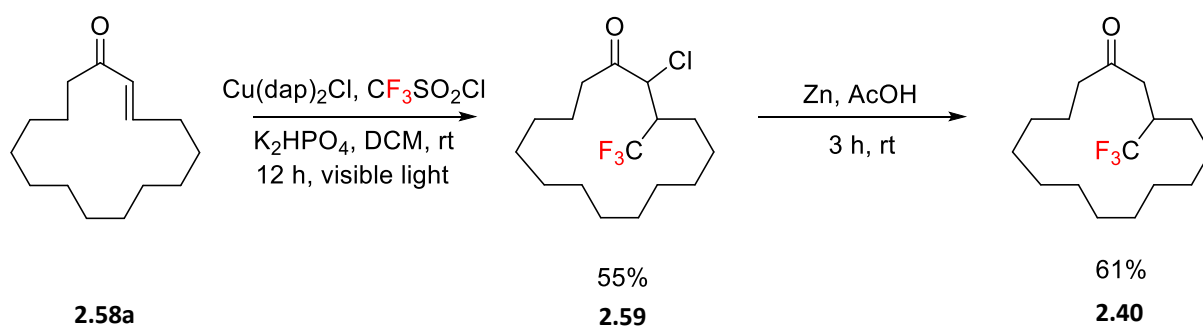
Starting from readily available cyclopentadecanone **2.55**, α,β -unsaturation was required to be introduced in order to conduct a 1,4-addition, as illustrated in Scheme 2.9. This was achieved *via* a selenoxide induced elimination reaction.¹²⁶ Initially, selenide **2.56** was synthesised by the reaction of cyclopentadecanone with phenylselenium chloride. Selenide **2.56** was then oxidised with hydrogen peroxide to give **2.57**. This led to an intramolecular *syn*-elimination to generate the desired cyclopentadecenone as a mixture of (*E*) and (*Z*) isomers **2.58a** and **2.58b** in a ratio of 4:1. The geometric isomers were readily separated by column chromatography in a yield of 73%.



Scheme 2.9 – Introduction of unsaturation into cyclopentadecanone using phenylselenium chloride.

From this point, it was possible to begin to explore the addition of substituents to the C3 position of **2.58a** via a conjugate addition. The first target was the -CF₃ muscone derivative

2.40. Addition of $-\text{CF}_3$ would again pose a challenge, this time because the CF_3 group is a hard nucleophile and generally adds to α,β -unsaturated ketones with a 1,2-preference. This was overcome by using a photo-redox method of CF_3 and chlorine addition to double bonds developed by Dolbier *et al.*⁷¹ Accordingly reaction of **2.58a** with copper photo-catalyst $\text{Cu}(\text{dap})_2\text{Cl}$ in the presence of trifluoromethylsulfonyl chloride and dipotassium phosphate in DCM at room temperature, induced by visible light, selectively and regioselectively added chlorine and a CF_3 group across the conjugated double bond to give intermediate **2.59**. Analysis of **2.59** via ^{19}F NMR shows four doublet peaks, as shown in Figure 2.21, showing coupling between the CF_3 fluorines and their neighbouring hydrogen atom. These peaks are in a ratio of 75:14:9:1, showing that there is one clear major diastereomeric product.



Scheme 2.10 – Synthesis of $-\text{CF}_3$ derivative **2.40** of muscone from (E)-cyclopentadecenone

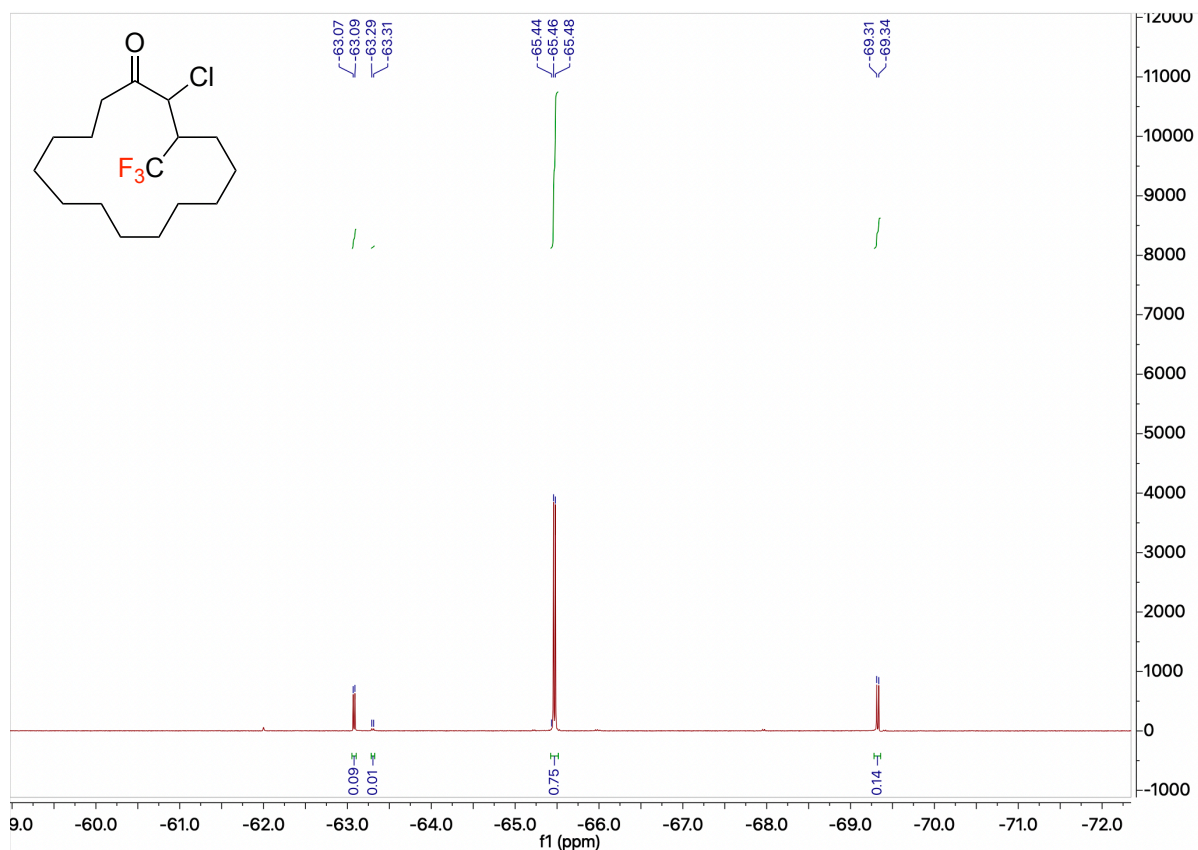
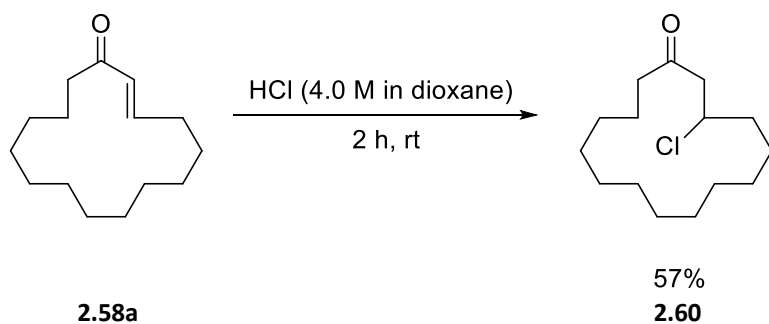


Figure 2.21 – ^{19}F NMR of **2.59** showing the peaks of the four diastereomers in a 75:14:9:1 ratio.

The initial photo-redox reaction was successful but the product proved difficult to purify, leading to a reduced yield. The chlorine atom was then reductively removed using zinc in acetic acid, and this gave muscone **2.40** in a 61% yield after purification. It was immediately noticeable that this product had a mild musk smell.

Attention then turned to other muscone derivatives that could be prepared by this conjugate addition approach. The first to be explored was the chloro derivative **2.60**. Chlorine is often considered to be a useful isostere for a methyl group, and this muscone analogue directly replaces chlorine for methyl. Accordingly (*E*)-cyclopentadecenone **2.58a** was treated with hydrochloric acid to give the desired product **2.60** in a 57% yield.

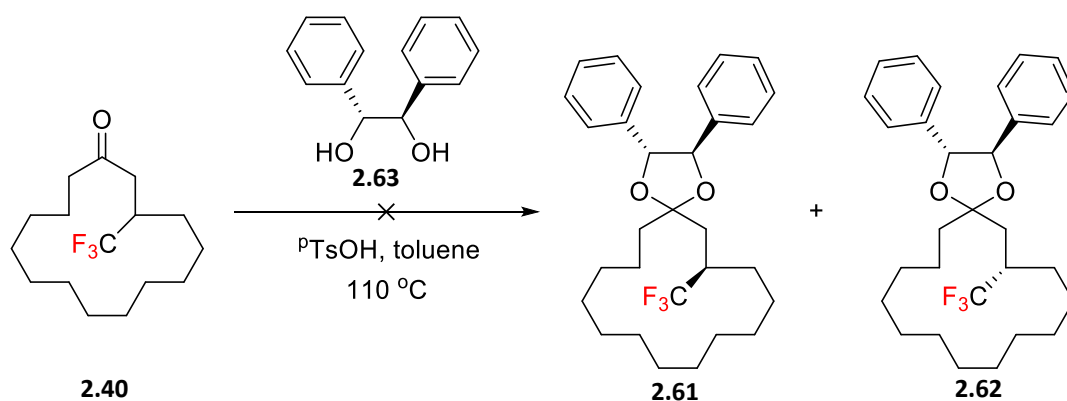


Scheme 2.11 – Synthesis of **2.60** from (*E*)-cyclopentadecenone.

Interestingly ketone **2.60** has a very strong musky smell consistent with the -Cl/Me bioisostere hypothesis. We hoped to be able to explore its efficacy against the olfactory receptors, however, after a few days at room temperature **2.60** decomposes with the release of HCl back to (*E*)-cyclopentadecenone **2.58a**. A preparation was carried out and sent immediately to China, however, the assay delay time was at least 10 days and the data received was poor. None-the-less the ‘muskiess’ of this compound was striking when immediately prepared.

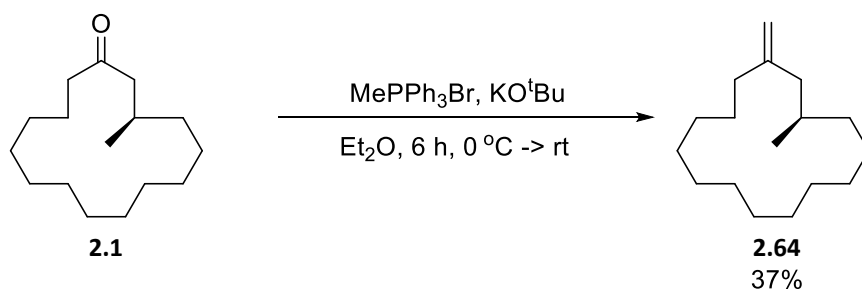
A chiral resolution of the CF₃- muscone derivative **2.40** was desirable. The approach taken envisaged the generation of diastereoisomers by reacting racemic **2.40** with an enantiopure 1,2-diol to form diastereoisomeric ketals **2.61** and **2.62**, as illustrated in Scheme 2.12. Separation of the diastereomers and then hydrolysis offered a strategy to the enantiomerically pure muscone derivatives.

(*R,R*)-(+)-Hydrobenzoin **2.63** was selected as a candidate chiral resolving agent. This was reacted with **2.40** in an attempt to form a mixture of diastereomeric ketals, however, no reaction occurred. With this challenge, it was decided to assay **2.40** as a racemate before investing a significant effort in the resolution. In the event, it was not active (see below) and this effort was not pursued.



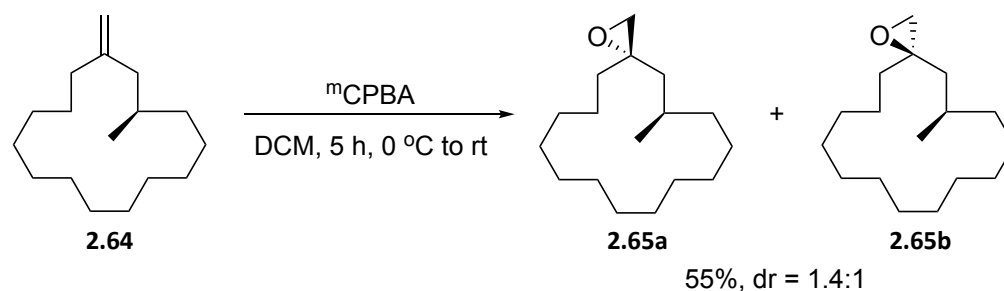
Scheme 2.12 – Failed attempt to synthesise chiral ketals of **2.40**.

Additional muscone derivatives were synthesised for olfactory receptor assay. Initially, (*R*)-muscone was converted to an exo-alkene **2.64** via a Wittig reaction, as shown in Scheme 2.13. This analogue removes the carbonyl oxygen but maintains sp^2 hybridisation at C-1.



Scheme 2.13 – Synthesis of terminal alkene derivative **2.64** of (*R*)-muscone.

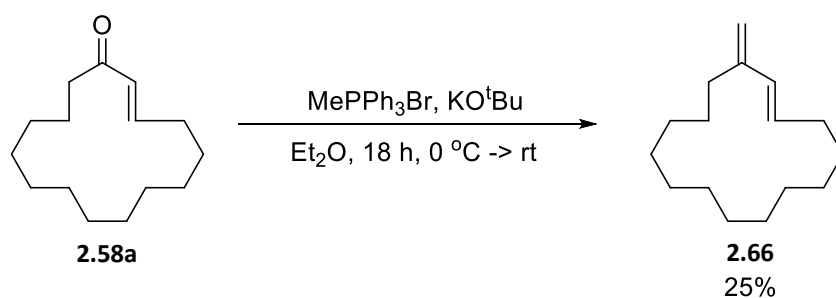
This proved relatively straightforward, and it was possible then to synthesise the corresponding exo-epoxide stereoisomers **2.65a** and **2.65b** after treatment of **2.64** with *m*CPBA. These epoxide diastereomers can probe the facial orientation of the carbonyl oxygen relative to the plane of the muscone molecule, and also the importance, or not, of maintaining sp^2 hybridisation at C-1.



Scheme 2.14 – Synthesis of an epoxide derivative **2.65a** and **2.65b** of (*R*)-muscone.

The epoxides were prepared as a mixture of diastereomers in a ratio of 1.4:1 per ^1H NMR, however it was not possible to determine which diastereomer was the major product. Also, the diastereomers could not be separated by column chromatography, despite considerable effort.

A Wittig reaction on (*E*)-cyclopentadecenone was carried out to generate conjugated diene **2.66**. This maintains the hybridisation of **2.58a**, which is a strong musk, but removes the carbonyl oxygen.



Scheme 2.15 – Synthesis of 2.66 from (E)-cyclopentadecenone.

This diene product **2.66** also had a faint musk aroma, but it was very weak, indicating the importance of the carbonyl group for a strong musk smell.

Prior to sending the samples for analysis descriptors of how the compounds smelt relative to (*R*)-muscone were recorded, as shown in Table 2.1. Several members of the O'Hagan group were asked to describe the smells of each compound, in order to build a consensus.

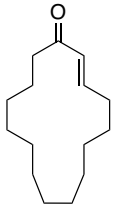
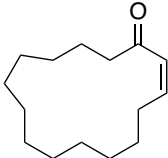
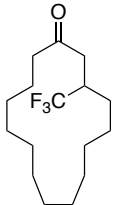
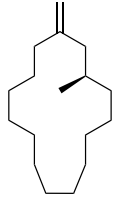
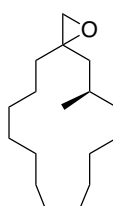
Muscone derivative	Smell
 <p>2.58a</p>	Musky, pine smell, pleasant.
 <p>2.58b</p>	Glue-like, chemical, burnt sugar, not musky.
 <p>2.40</p>	Sweet, leafy, camphor-like, weak musk.
 <p>2.64</p>	Rubbery smell, similar to balloons, very weak musk.
 <p>2.65a and 2.65b</p>	Chemical smell, similar to pool chlorine, not musky.

Table 2.1 – Consensus descriptions of the fragrances of the synthesised muscone derivatives.

It was concluded that the strongest musk was the (E)-unsaturated ketone **2.58a**, which had a very pleasant, musky smell. The (Z)-isomer **2.58b** had no musk odour at all, indicating that a change of shape is important. Otherwise, the greater the deviation from the structure of (R)-muscone, the weaker the compound smelled. Particularly weak were the epoxide diastereoisomers **2.65a** and **2.65b** suggesting that a change in hybridisation from sp^2 to sp^3 is detrimental.

Samples of these compounds were sent to China in order to be assayed against olfactory receptors OR5AN1 and OR1A1. It was found that only (E)-cyclopentadecenone **2.58a** triggered any response, as shown in Figure 2.22. Even this response was limited, and it was lower than the control, (R)-muscone. The (Z)-isomer **2.58b** did not show any response, again consistent with the importance of shape. Intriguingly the assays indicated that the (E)-cyclopentadecenone **2.58a**, -CF₃ muscone derivative **2.40**, the diene **2.66** and the epoxide **2.65** all caused cell death at high concentrations. These are all electrophiles in different ways and their reactivities may have been responsible for this effect.

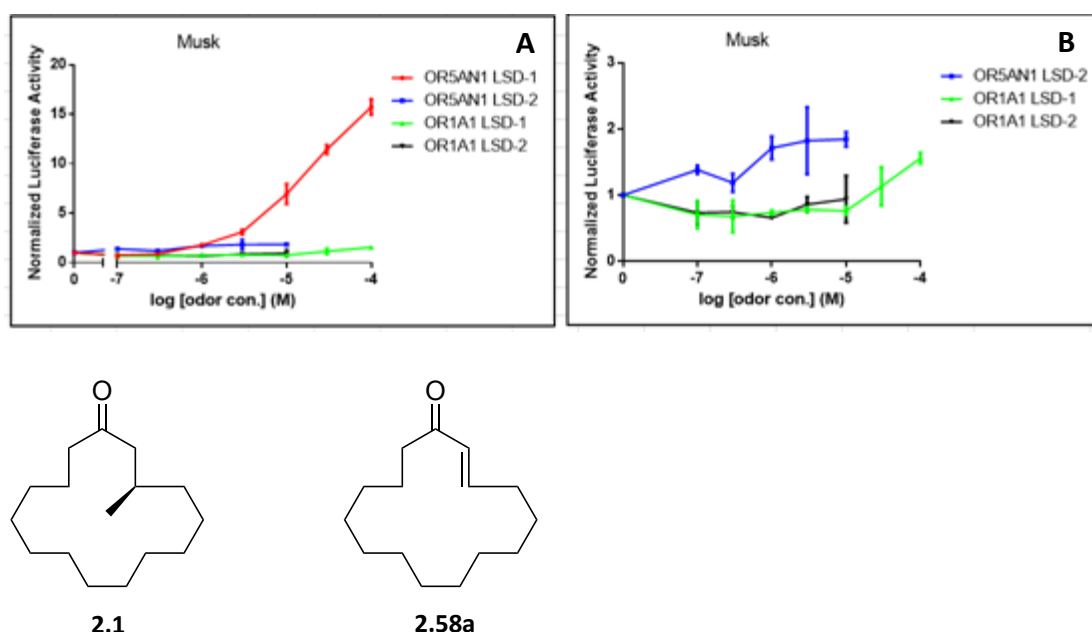
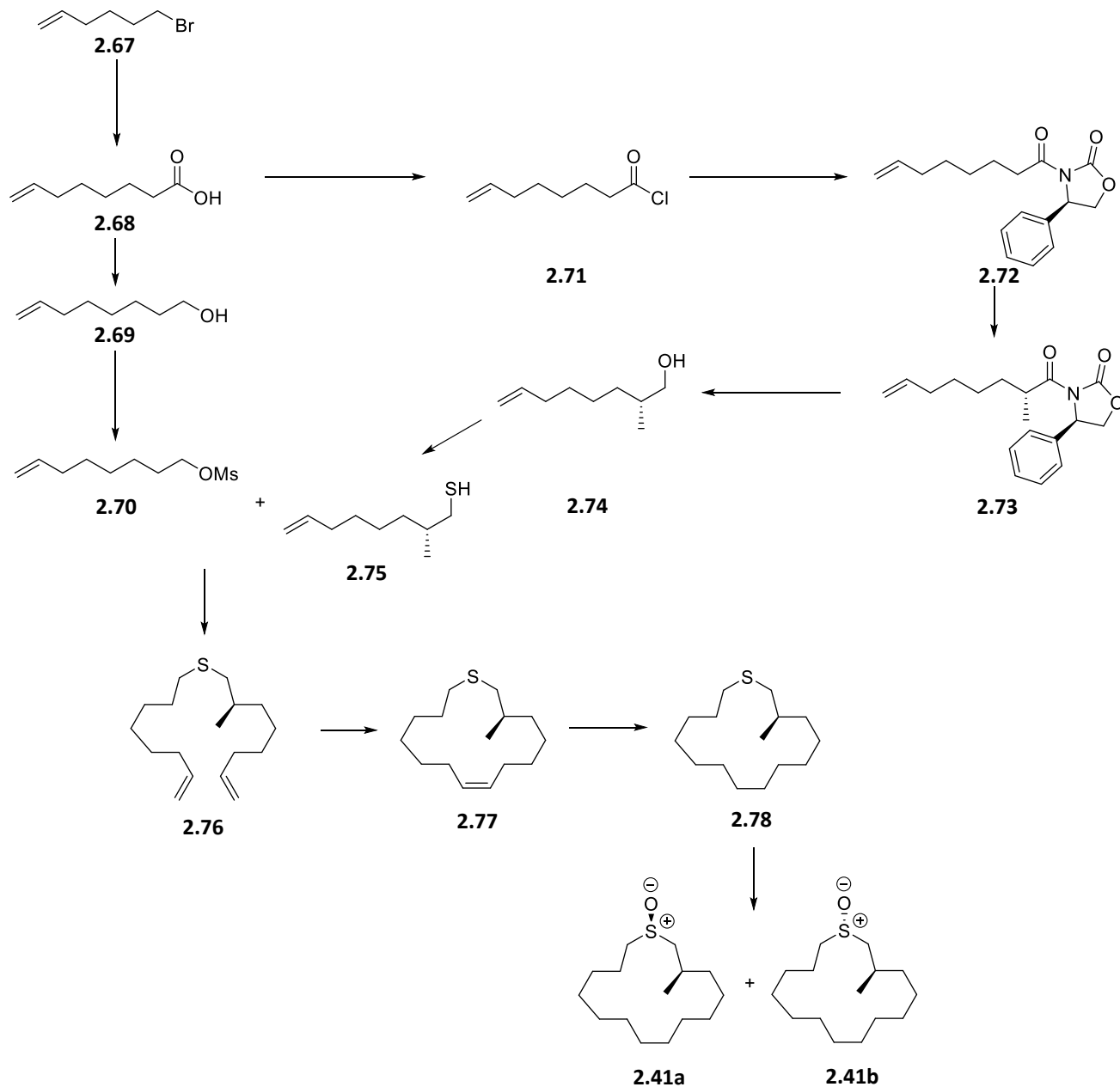


Figure 2.22 – Dose-response curves showing interactions between (R)-muscone **2.1** and (E)-cyclopentadecenone **2.58a** with olfactory receptors OR5AN1 and OR1A1. Graph A shows interactions of (R)-muscone with OR5AN1 (red line) and OR1A1 (green line) and (E)-cyclopentadecenone with OR5AN1 (blue line) and OR1A1 (black line). Graph B shows interactions of (R)-muscone with OR1A1 (green line) and interactions of (E)-cyclopentadecenone with OR5AN1 (blue line) and OR1A1 (black line).

2.2.2 Synthesis of a sulfoxide-derivative of (*R*)-muscone

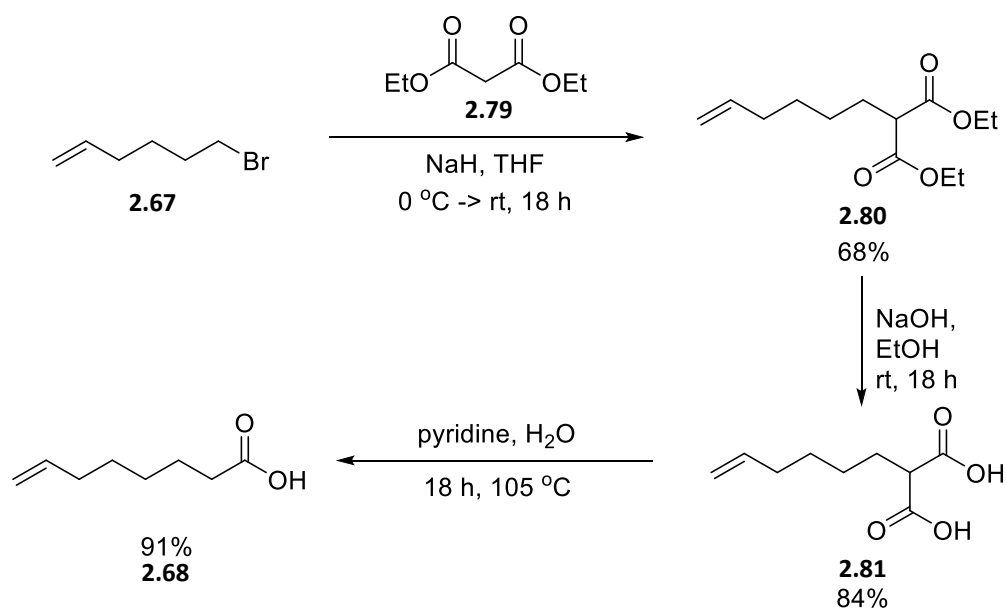
A synthesis was developed for the preparation of sulfoxide diastereoisomers **2.41a** and **2.41b** and the route is illustrated in Scheme 2.16.



Scheme 2.16 – Proposed synthetic pathway for the synthesis of sulfoxide **2.41a** and **2.41b**.

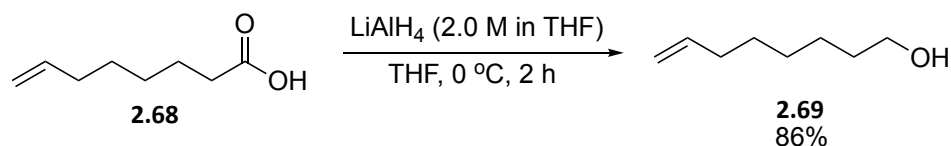
The approach started with 7-octenoic acid **2.68**. The initial synthesis of 7-octenoic acid **2.68** proceeded in three steps, as illustrated in Scheme 2.17. Firstly, 6-bromo-1-hexene **2.67** was reacted with diethyl malonate **2.79** using sodium hydride as the base to give malonic ester

2.80. Ester **2.80** was then hydrolysed using sodium hydroxide to form malonic acid **2.81**. This then underwent decarboxylation to the desired 7-octenoic acid **2.68**.



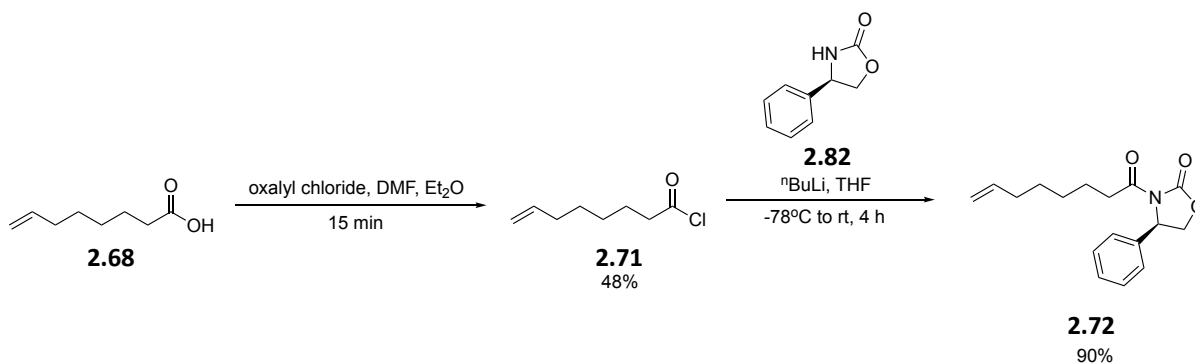
*Scheme 2.17 – Synthesis of 7-octenoic acid **2.68** from 6-bromo-hex-1-ene.*

The first branch of the pathway featured the smooth reduction of 7-octenoic acid **2.68** to 7-octen-1-ol **2.69** with lithium aluminium hydride (86% yield), as shown in Scheme 2.18. This alcohol was set aside to be activated when required.



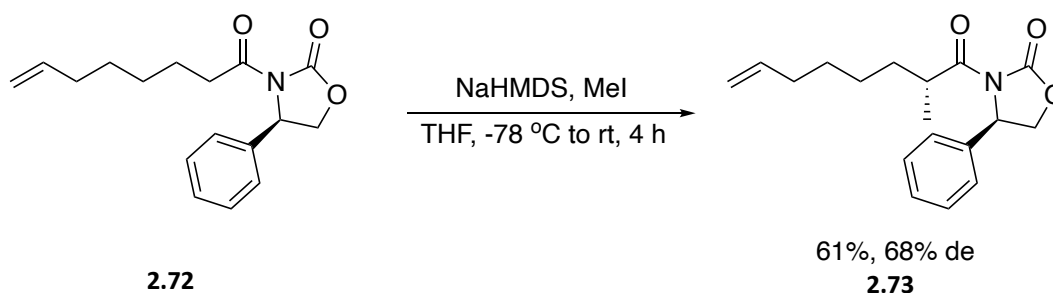
Scheme 2.18 – Reduction of 7-octenoic acid.

7-Octenoic acid **2.68** was also converted to 7-octenoyl chloride **2.71** using oxalyl chloride. The product was immediately reacted with (*R*)-4-phenyl-2-oxazolidinone **2.82** to give the desired chiral oxazolidinone **2.72** in a 90% yield, as shown in Scheme 2.19.



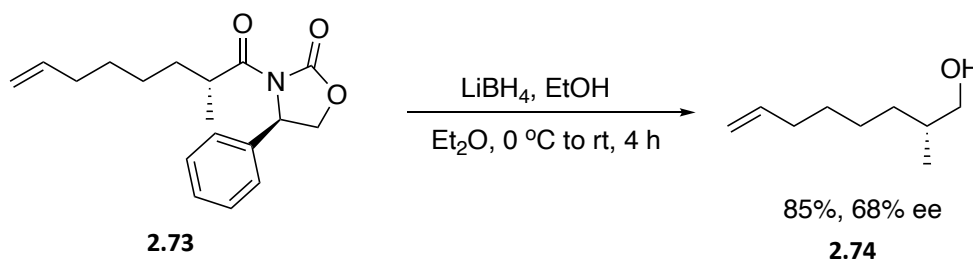
Scheme 2.19 – Synthesis of chiral Evans auxiliary **2.72**.

Oxazolidinone **2.72** was then alkylated to incorporate the necessary methyl group, creating the desired (*R*)-stereogenic centre, as illustrated in Scheme 2.20. This was achieved using sodium bis(trimethylsilyl)amide as the base, and methyl iodide as the alkylating agent, to give **2.73** in a 61% yield and a diastereomeric excess of 68% de.



Scheme 2.20 – Asymmetric methylation of oxazolidinone **2.58**.

Following this, acyl reduction of **2.73** was achieved with lithium borohydride to give alcohol **2.74** in an 85% yield (68% ee), as shown in Scheme 2.21.

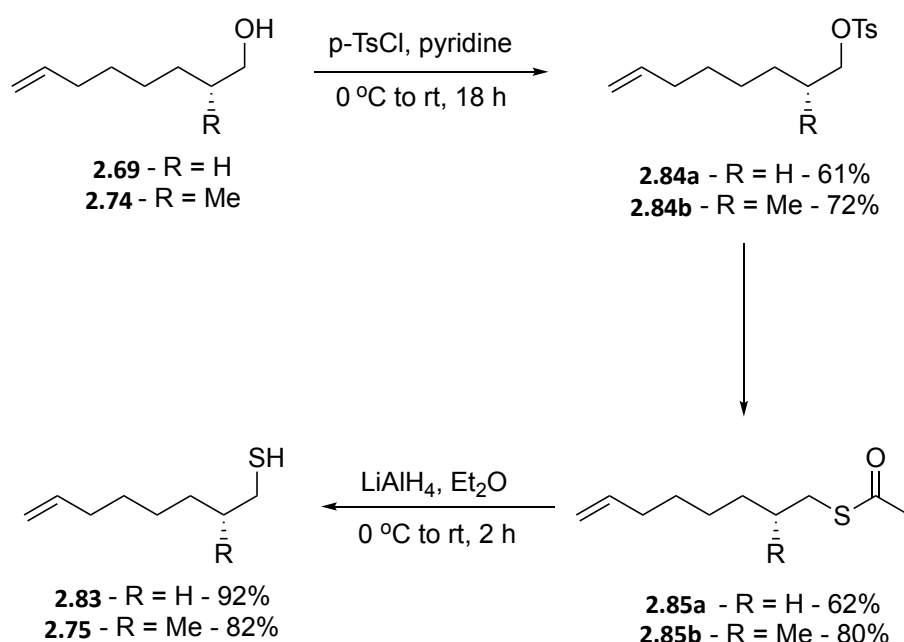


Scheme 2.21 – Reductive removal of the auxiliary from **2.73**.

Now having obtained both the (*R*)-alcohol **2.74** and alcohol **2.69**, it was then possible to address preparation of thioether **2.76**. While the original plan was to convert **2.74** into thiol **2.75**, the decision was made to instead convert alcohol **2.69** into its corresponding thiol **2.83**. There were concerns that the β -methyl group would render alcohol **2.74** a poorer

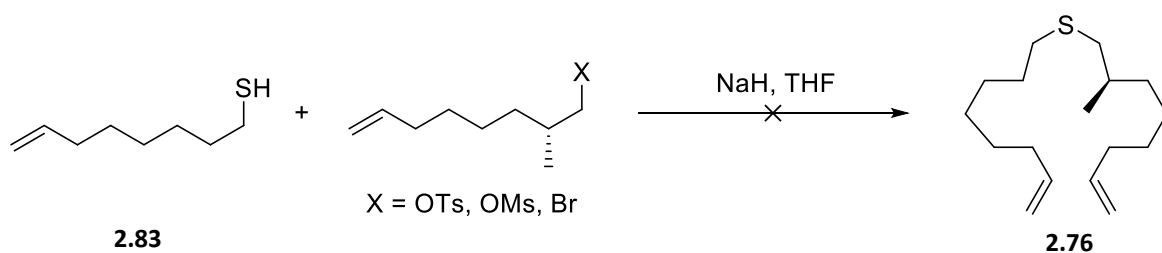
nucleophile due to possible steric hindrance. Also due to the larger number of steps required to make **2.74**, material was limited particularly to take it further to its corresponding thiol.

Accordingly, thiol **2.83** was prepared in three steps from alcohol **2.69** as illustrated in Scheme 2.22. Initially, 7-octen-1-ol **2.69** was activated to tosylate **2.84a**, which was then reacted with potassium thioacetate in DMF to give thioacetate **2.85a**. **2.85a** was then reduced with lithium aluminium hydride to generate the desired thiol **2.83**.



*Scheme 2.22 – Conversion of the alcohols **2.69** and **2.74** to thiols **2.83** and **2.75**.*

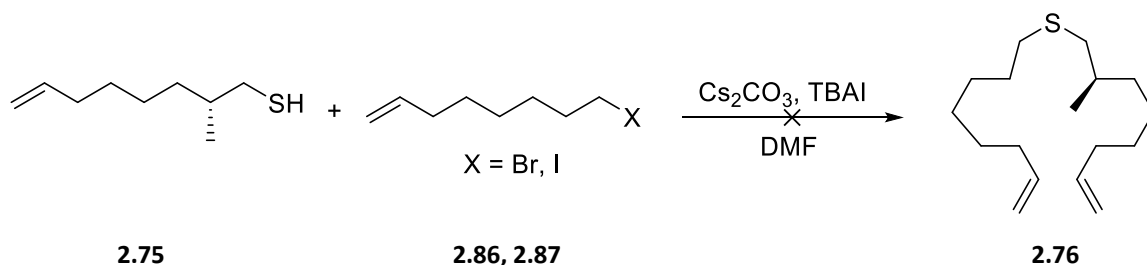
With the thiol in place, alcohol **2.74** was activated by conversion to tosylate **2.84b**. At this point, the thioether synthesis could be attempted and was carried out in the first case, by reaction with **2.83** using K_2CO_3 as the base. However, the reaction did not proceed, with the tosylate being cleanly recovered despite being the limiting reagent. Following this, other leaving groups and bases were attempted. The branched alcohol **2.74** was converted into a mesylate and reacted with **2.83** using sodium hydride as the base, however, this too did not give the desired thioether. Alcohol **2.74** was then converted to the corresponding bromide with an Appel protocol, however the attempted displacement by thiol **2.83** did not give any reaction.



Scheme 2.23 – Unsuccessful thioether reactions with 2.83.

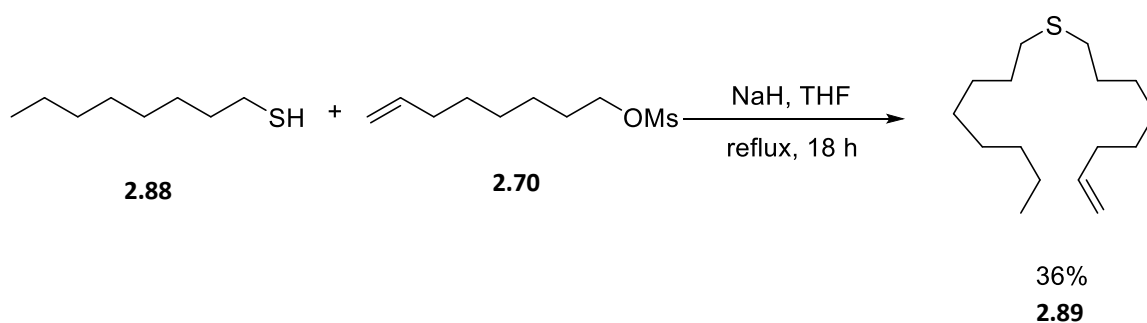
It was concluded that the β -methyl group was hindering these substitution reactions.

Therefore, a decision was taken to revert to converting alcohol **2.74** into thiol **2.75** and use this as the nucleophile. Thus, the route was reworked and progressed to thiol **2.75**. A first attempt at thioether formation was explored employing methodology developed by Salvatore *et al.*¹²⁷ This used caesium carbonate as a base, with the caesium cation acting as a shield after deprotonation of the sulfur, to prevent the formation of possible undesired side products such as disulfides by reaction of the resulting thiolate. Alcohol **2.60** was converted into the corresponding bromide **2.86** and iodide **2.87** in an attempt to offer good leaving groups to promote thioether formation. However, reactions with both of these alkylating reagents proved unsuccessful generating only an undesired (unknown) side product.



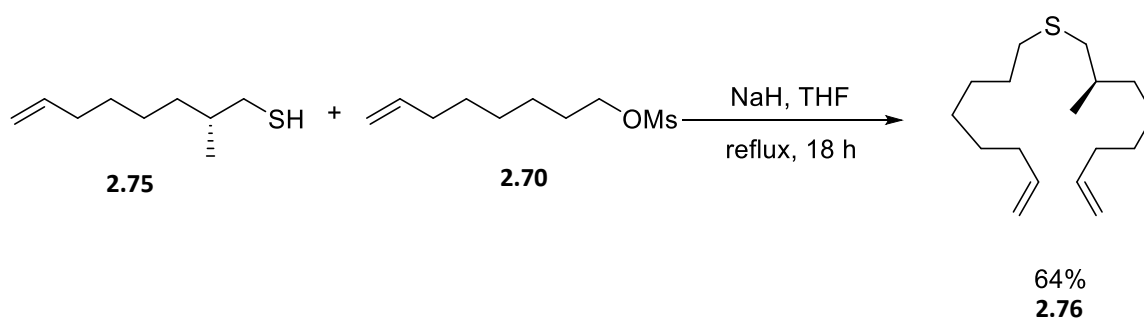
Scheme 2.24 – Attempted thioether formation using $\text{Ca}_2\text{CO}_3/\text{TBAI}$ in DMF.

In order to understand this reaction better, a trial thioether formation was explored using octane-1-thiol **2.88** and activated derivatives of the synthesised 7-octen-1-ol **2.69**. When the thioether reaction was attempted by reacting octane-1-thiol **2.88** with mesylate **2.70** with sodium hydride / THF at reflux, the reaction produced the desired thioether product **2.89**, albeit in a modest yield of 36%, as shown in Scheme 2.25. This gave reason to be optimistic.



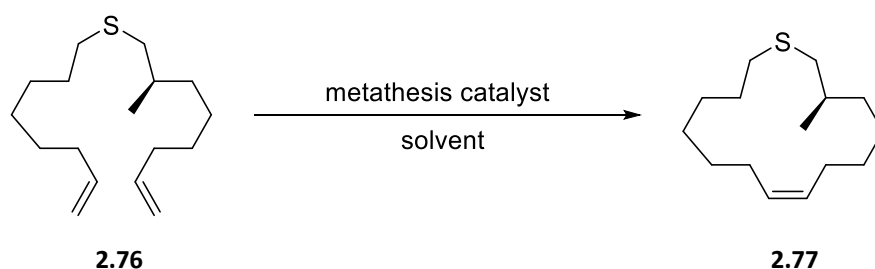
Scheme 2.25 – Successful trial thioether formation reaction.

Following this result and the further synthesis of thiol **2.75**, thioether **2.76** was successfully prepared under these reaction conditions and with a yield of 64%, as shown in Scheme 2.26.



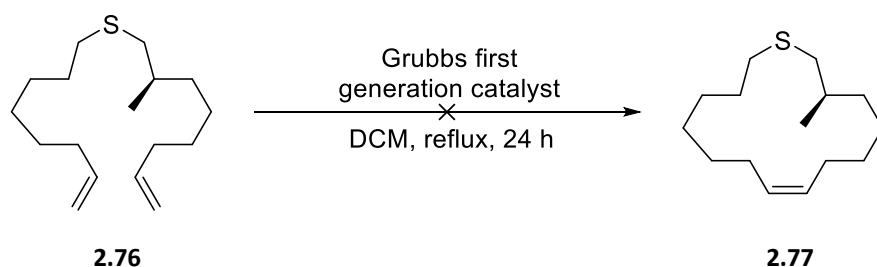
Scheme 2.26 – Successful formation of thioether 2.76.

With the thioether prepared, the next step to address was ring-closing metathesis to generate macrocycle **2.77**.



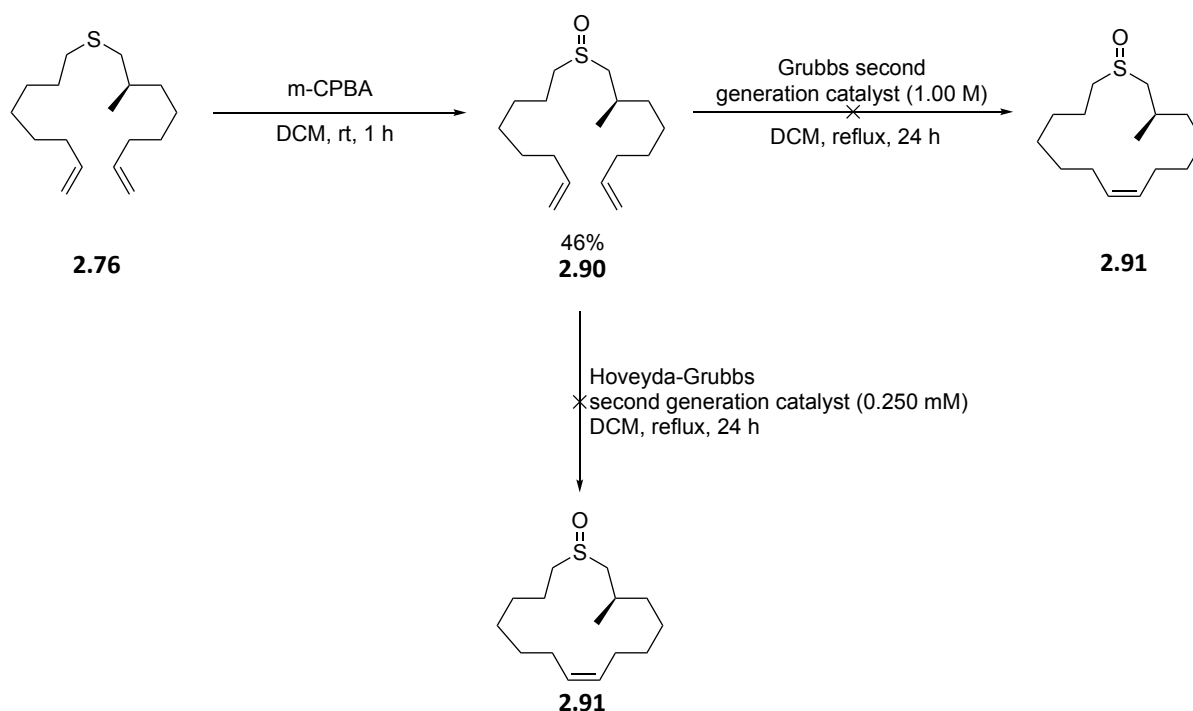
Scheme 2.27 – Proposed ring-closing metathesis step.

This step proved challenging, and a number of different metathesis catalysts and conditions had to be tested. Initial attempts used Grubbs' 1st generation catalyst **2.3** due to its relatively low cost and ready availability. However, reaction with this catalyst appeared to give an intermolecular product, rather than the desired ring-closed macrocycle **2.77**.



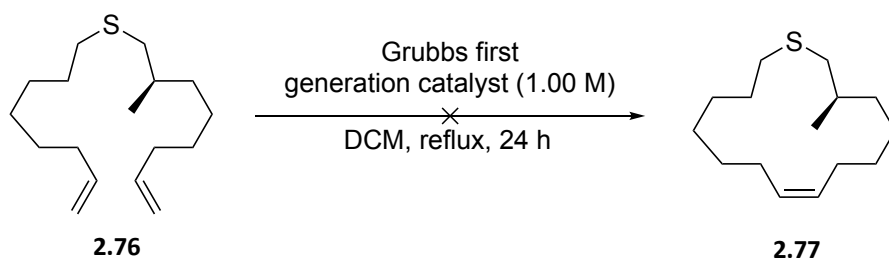
*Scheme 2.28 – Unsuccessful ring-closing metathesis to thioether **2.77**.*

Another approach taken was to first oxidise thioether **2.76** to sulfoxide **2.90**, then to attempt the ring-closing metathesis to give **2.91**, as illustrated in Scheme 2.29. Oxidation to sulfoxide **2.90** was achieved using 1.05 equivalents of *m*CPBA as the oxidising agent, controlling the stoichiometry to avoid over-oxidation to the sulfone. This proceeded reasonably well with a yield of 46%. With the thioether in hand, RCM was attempted using both Grubbs' 2nd generation catalyst **2.28** and with Hoveyda-Grubbs 2nd generation catalyst **2.30**. However, neither attempt was successful, with none of the desired ring-closed product observed and starting material **2.90** only recovered. This could be due to the sulfur or sulfoxide oxygen coordinating to the catalyst and hindering the reaction.



*Scheme 2.29 – Unsuccessful ring-closing metathesis of sulfoxide **2.90**.*

Attempted metathesis reactions of thioether **2.76** with Grubbs' 2nd-generation catalyst **2.28** gave a similarly unsuccessful result, with an intermolecular dimeric product again obtained. However, success was achieved using Hoveyda-Grubbs 2nd generation catalyst **2.30**, and this gave the desired unsaturated macrocycle **2.77** in a good 68% yield, as illustrated in Scheme 2.30. The reaction required an increased temperature (75 °C) to proceed to completion, so toluene was used as the solvent in place of DCM to facilitate this. The alkene peaks in the ¹H-NMR spectrum appeared as an overlapping multiplet, as shown in Figure 2.23, which made determination of the *cis* : *trans* ratio very difficult.



Scheme 2.30 – Successful ring-closing metathesis of thioether

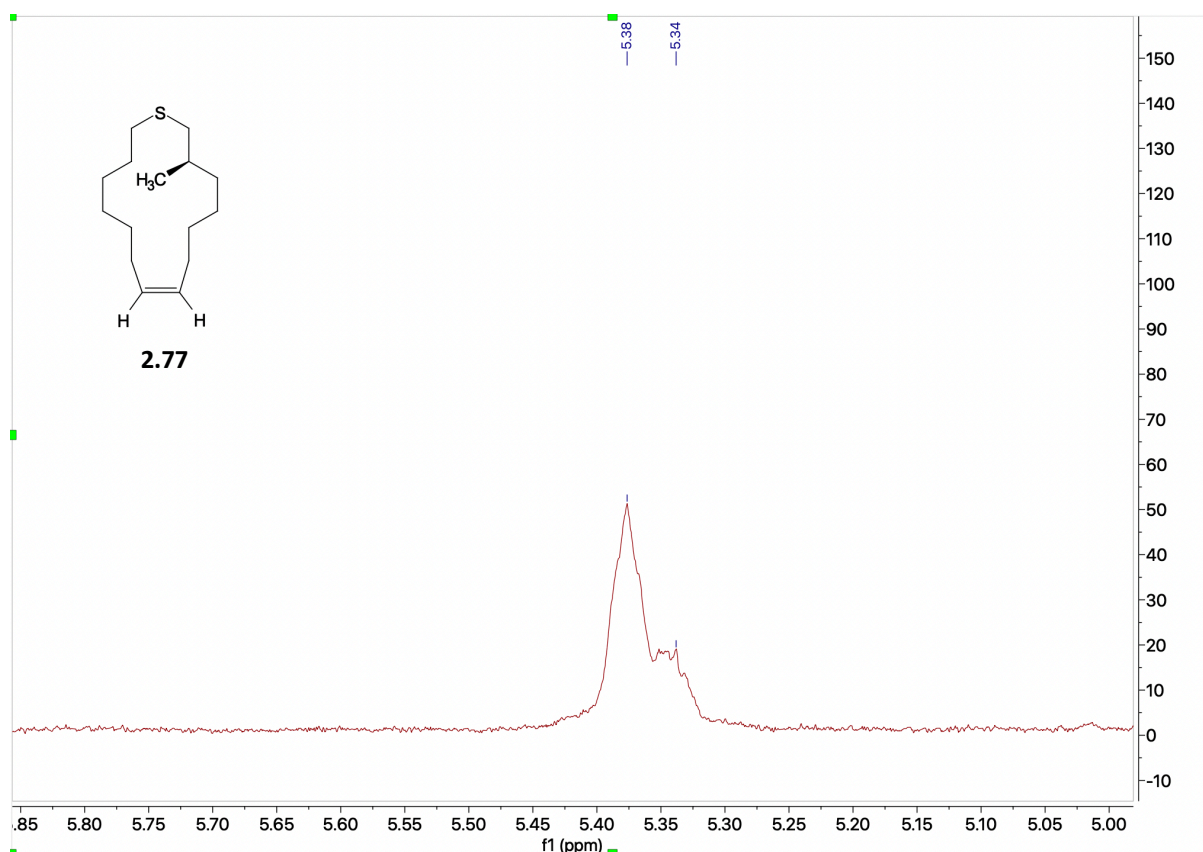
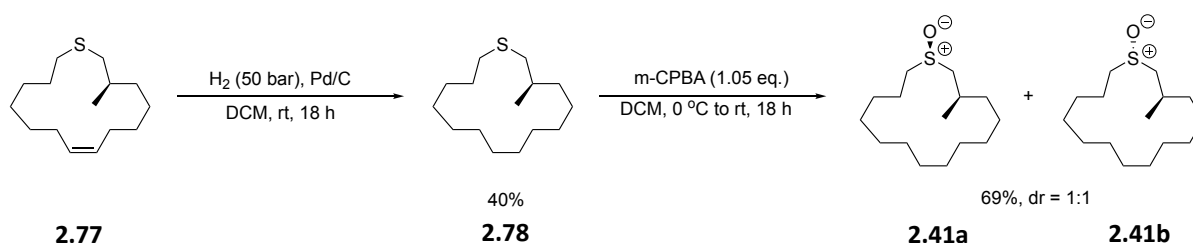


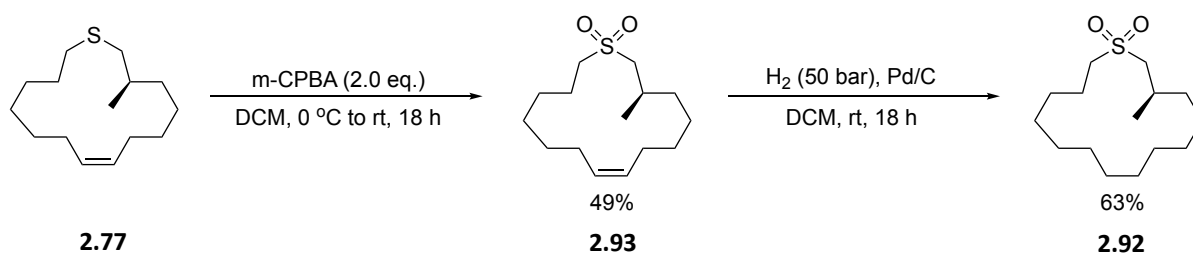
Figure 2.23 – Section of the ¹H-NMR spectrum of unsaturated macrocycle **2.77** showing overlapping alkene peaks.

At this stage, two options existed to complete the synthesis regarding the order of hydrogenation and sulfur oxidation. Hydrogenation of thioether **2.77** was explored first. Initial attempts used palladium on carbon with H₂ at atmospheric pressure, however, no reaction occurred and **2.77** was re-isolated. The pressure of the hydrogenation reaction of **2.77** was increased to 50 bar in an autoclave, and this proved successful, generating the saturated macrocycle **2.78** in a yield of 40%. Finally, **2.78** was oxidised using 1.05 equivalents of *m*CPBA to give desired sulfoxide diastereomers **2.41a** and **2.41b**, with an overall yield of 69%, as illustrated in Scheme 2.30.



Scheme 2.30 - Final steps in sulfoxide 2.41 synthesis

Meanwhile, sulfone derivative **2.92** was also synthesised, as illustrated in Scheme 2.31. This was achieved by treating unsaturated macrocyclic thioether **2.77** with 2 equivalents of *m*CPBA. Hydrogenation of the resulting sulfone **2.93** proceeded smoothly, using Pd/C with H₂ at atmospheric pressure to obtain macrocycle **2.92** in a 63% yield. This compound is assumed to be ~68% ee as the stereogenic centre is contributed from alcohol **2.74** which was prepared in 68% ee as described above.



Scheme 2.31 – Final steps in sulfone 2.92 synthesis

It was decided to send the mixture of sulfoxide diastereoisomers **2.41** for musk receptor assay rather than to attempt a separation at this stage. This was due to the low levels of isolated material after a long campaign (7.3 mg), as isomer separations would lead to further losses of valuable material.

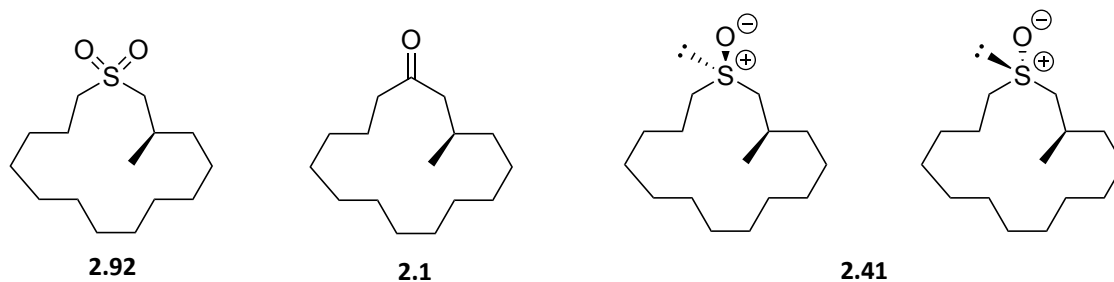
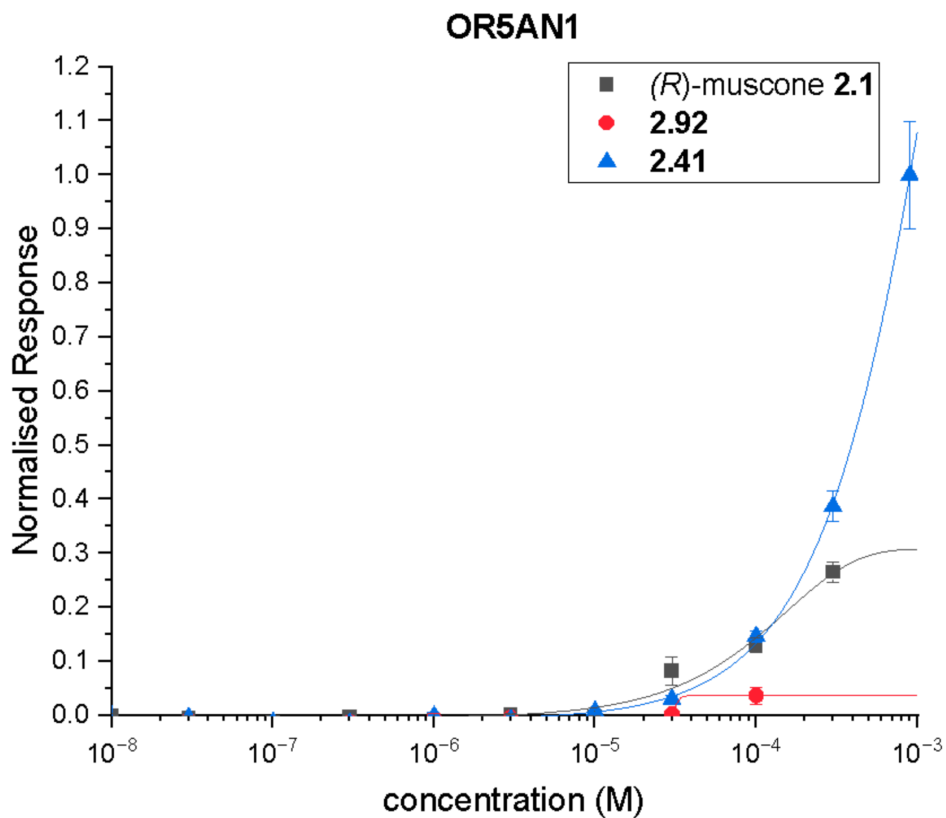


Figure 2.24 – Dose-response curve showing interactions of sulfoxide **2.41** and sulfone **2.92** with OR5AN1 olfactory receptor. Structures of compounds are shown in order from lowest relative activity (left) to highest relative activity (right).

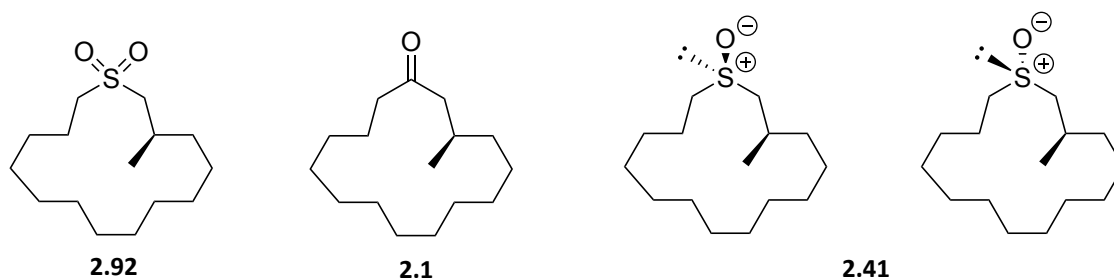
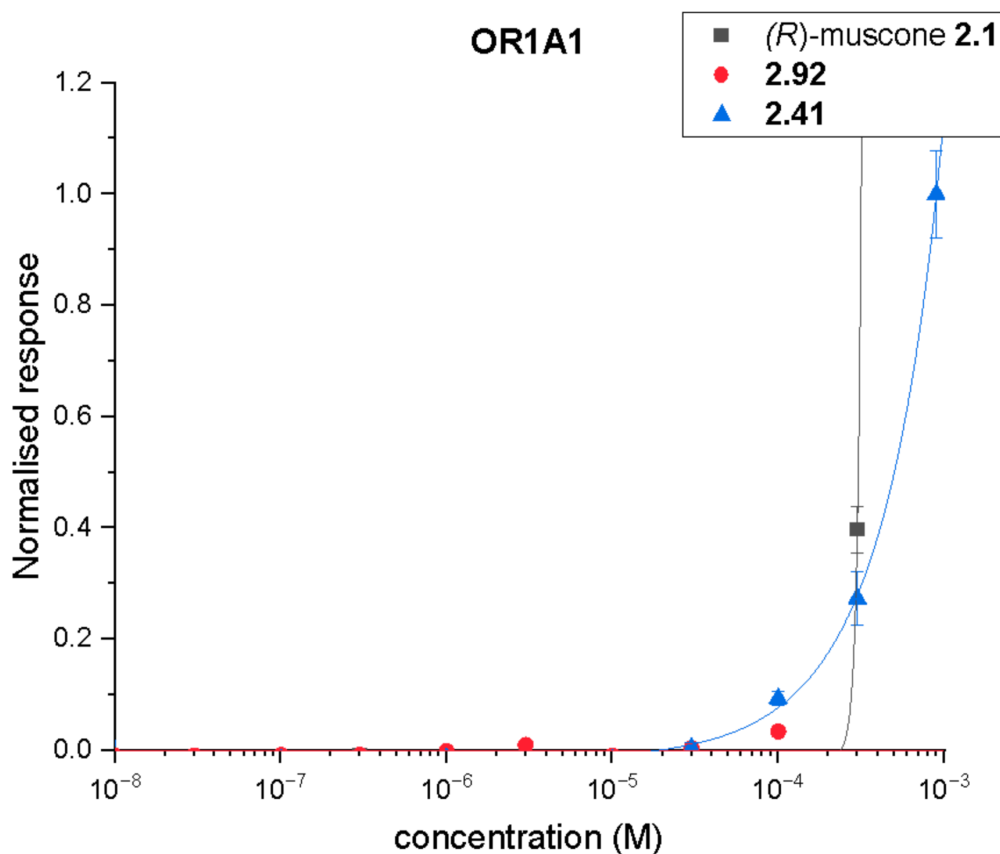


Figure 2.25 – Dose-response curves showing interactions of sulfoxide **2.41** and sulfone **2.92** with OR1A1 olfactory receptor. Structures of compounds are shown in order from lowest relative activity (left) to highest relative activity (right).

In the event, the sulfoxide diastereoisomers **2.41** showed very good activity, exhibiting strong interactions with OR5AN1, and requiring a similar concentration as (*R*)-muscone to trigger a response. Most notably the sulfoxides **2.41** triggered a more intense response at a similar concentration. When interacting with OR5AN1, sulfoxides **2.41** exhibited a relative EC₅₀ of 426.4 μM, while (*R*)-muscone **2.1** exhibited an EC₅₀ of 115.1 μM. This shows that the sulfoxide does require a relatively high concentration to achieve its maximum effect. Most notably the sulfoxide diastereoisomers triggered a much stronger response than that of (*R*)-

muscone **2.1** when assayed with the OR1A1 receptor, and they triggered at a lower concentration. Thus, these compounds seem to elicit a high level of response, albeit at high concentrations. It would make sense to assume that one stereoisomer isomer will be more active than the other, and perhaps substantially so, but this could not be determined, for the reasons articulated above, and remains an unanswered but intriguing question. It is important to note that introduction of the stereogenic centre as shown in Scheme 2.20 was achieved only with a 68% de, therefore within the mixture there will be a series of a minor diastereomers with the methyl group in an (*S*)- configuration, in addition to the major diastereomers with the methyl in the (*R*)- configuration. Formally this suggests four stereoisomers in a ratio of 42:42:8:8. It would therefore be interesting to see if these minor diastereomers have any effect on interactions with the olfactory receptors too.

It was notable too that sulfone **2.92** was almost inactive and triggered a very low response in the assays with both of the receptors. This further shows the sensitivity there is between receptor response and changes made around the muscone carbonyl binding site.

2.3 Conclusions

In this Chapter, the effect of altering the structure of (*R*)-muscone on interactions with olfactory receptors OR5AN1 and OR1A1 has been studied. The synthesis of a 3-CF₃-trifluoromethyl derivative **2.40** was successfully achieved in a racemic form, although this compound was a poor agonist when assayed against olfactory receptors OR5AN1 and OR1A1. Further derivatives were also prepared. The most fragrant compound synthesised was the 3-chlorinated derivative **2.60**, however, this was prone to ready decomposition by elimination of HCl and so could not be assayed.

A synthesis of a sulfoxide derivative **2.41** of (*R*)-muscone was completed as a mixture of diastereoisomers (**2.41a** and **2.41b**). This was achieved by a convergent multi-step synthesis which involved several challenging steps, particularly a ring-closing metathesis reaction and a hydrogenation. Assays against the OR5AN1 and OR1A1 receptors showed very good activity with a similar concentration efficacy to (*R*)-muscone itself, but the response was stronger. Also, the sulfoxide stereoisomers triggered a much stronger response than (*R*)-muscone with the OR1A1 receptor. It would clearly be of interest to separately assay the

four individual sulfoxide stereoisomers as one will almost certainly be more active than the others.

The work presented within this chapter represents a study of the effects of altering the structure of (*R*)-muscone at strategic positions within the molecule. The results of the assays show that replacement of the (*R*)-methyl group generally leads to a large decrease in the ability of the molecule to interact with known musk olfactory receptors. Altering the geometry at the sp^2 carbon also leads to a decrease in activity, with only the sulfoxide mixture (**2.41a** and **2.41b**) interacting with the receptors. This shows that the presence of a polarised sp^2 carbon is likely essential for interactions with the olfactory receptors. Future work on this project could involve the separation of the individual sulfoxide diastereomers, in order to determine which isomer is most responsible for interactions with the olfactory receptors.

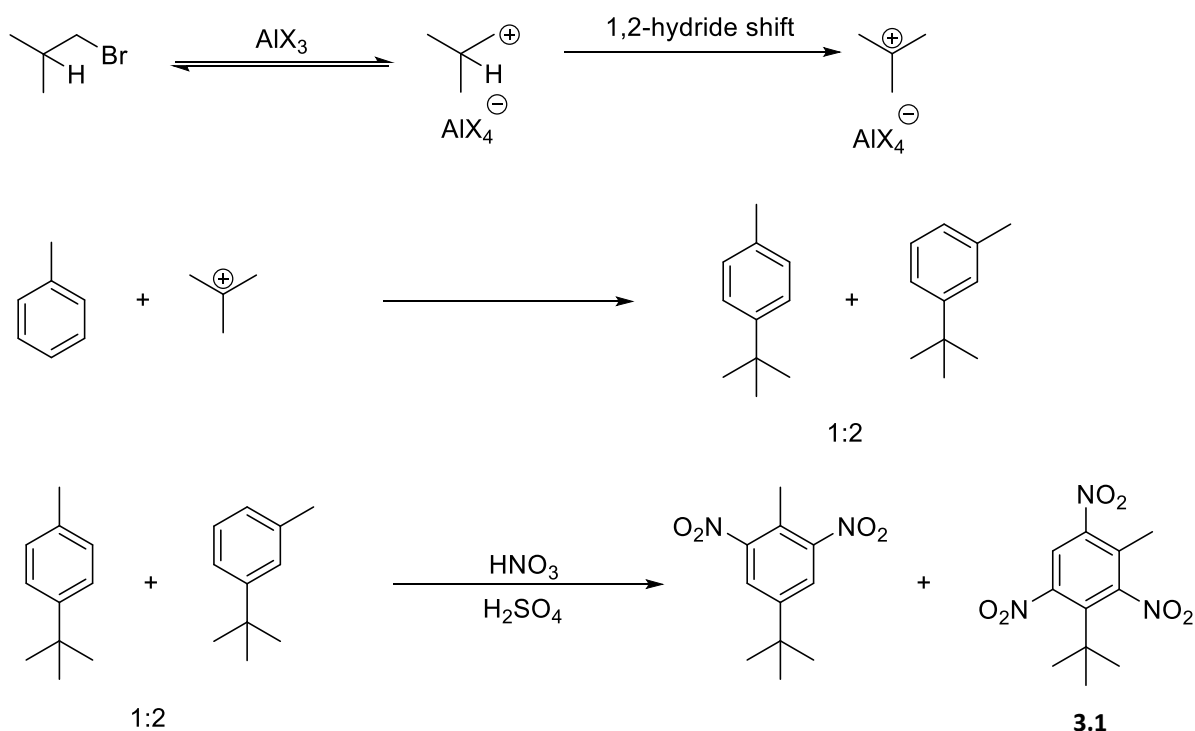
Chapter 3 – Synthesis of acetylene musks

Olfactory response assays were conducted by Dr. Weihong Liu and Dr. Hanyi Zhuang at Hanwang Technology Co. in Beijing, China. All other work within this chapter was completed by Luca Dobson.

3.1 Introduction to polycyclic musks

3.1.1 Nitromusks

While the musk odour is highly sought after for use within the fragrance industry, the only method to obtain naturally-occurring (*R*)-muscone is to kill the musk deer to obtain the musk gland.¹²⁸ Furthermore, naturally occurring musk is expensive and difficult to synthesise, so cheaper alternatives have been developed for the fragrance industry. Nitromusks usually consist of an aryl ring with alkyl substituents and at least two nitro groups.¹⁰¹ The first nitromusk was discovered by Baur in 1888 when he was working on developing derivatives of TNT. Baur isolated a nitroaromatic compound that he found to have a pleasant musky odour, and this compound became known as ‘musk Baur’ **3.1**.¹²⁹ The synthesis involved a Friedel-Crafts alkylation of toluene with isobutyl bromide, as illustrated in Scheme 3.1. Unbeknown to Baur, this gave a mixture of *para*- and *meta*-substituted *tert*-butyl-toluenes in a 1:2 ratio, whereas Baur believed he had synthesised only the *meta* isomer. Nitration of the mixture gave nitrated products which were separated by recrystallisation, resulting in ‘musk Baur’. Baur was quick to appreciate the commercial potential of his artificial musk, signing a deal in September 1891 for the production of ‘musk Baur’ for perfumers.¹³⁰



Scheme 3.1 – Synthesis of ‘musk Baur’ 3.1 as developed by Baur.

The five most notable nitromusks subsequently developed, were musk ketone **3.2**, musk xylene **3.3**, musk ambrette **3.4**, musk moskene **3.5** and musk tibetine **3.6**. Their structures are illustrated in Figure 3.1.¹³¹

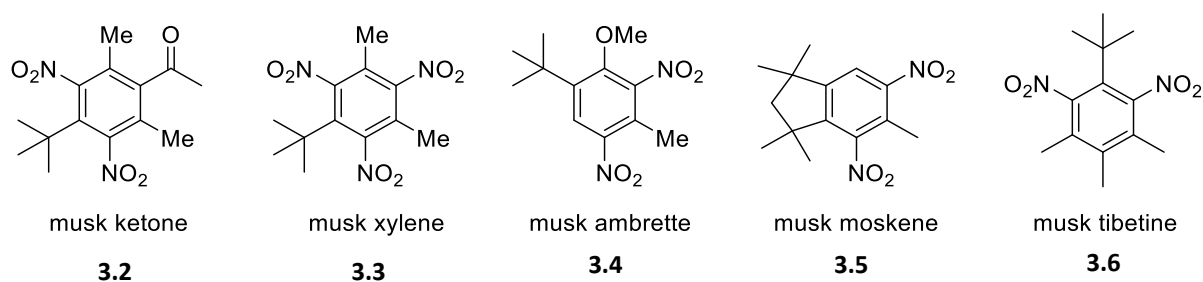
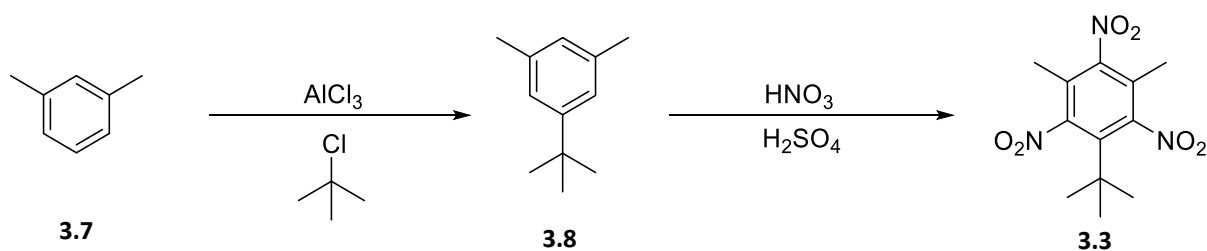


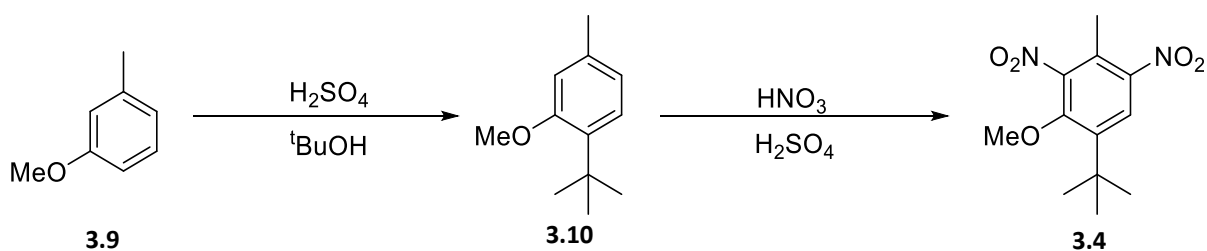
Figure 3.1 – Structures of notable nitromusks

Musk xylene **3.3** was developed by Emil Schnauffer and Heinrich Hupfeld in Frankfurt and prepared *via* a two-step synthesis, as shown in Scheme 3.2,¹³² shortly after the discovery of musk Baur. In this case, 1,3-dimethylbenzene **3.7** was subjected to a Friedel-Crafts alkylation reaction to give **3.8**, and this was followed by exhaustive nitration to give musk xylene **3.3**.



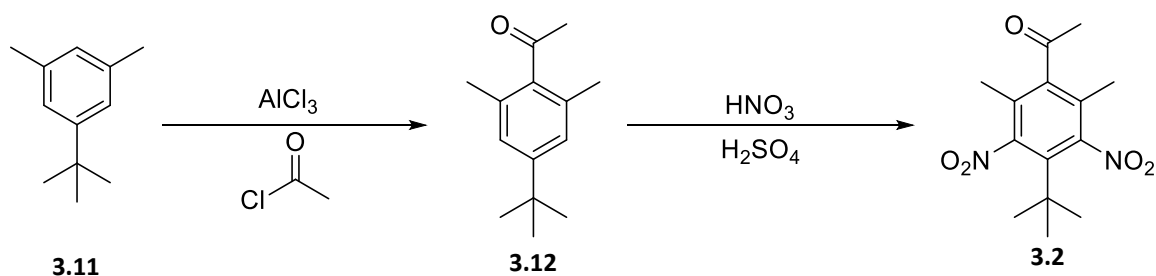
Scheme 3.2 – Synthesis of musk xylene by Schnauffer and Hupfeld⁶

Baur followed his discovery of musk Baur with the development of musk ambrette **3.4** in 1891.¹³³ This compound was prepared from *meta*-cresol **3.9**, which was alkylated to install a *tert*-butyl group to give **3.10**. **3.10** was then nitrated to give ‘musk ambrette’, as illustrated in Scheme 3.3. ‘Musk ambrette’ **3.4** was described as having “fine and distinctive floral undertones” and went on to feature in perfumes such as “L’air du temps” by Francis Fabron for Nina Ricci.¹³⁰



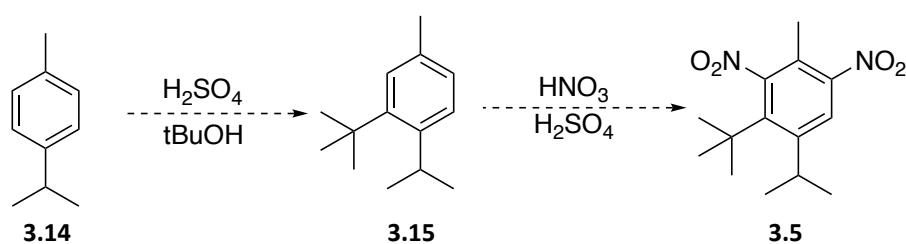
Scheme 3.3 – Synthesis of ‘musk ambrette’ by Baur.¹³³

Then, in 1894, a patent for musk ketone **3.2** was filed by William Mallmann.¹³⁴ Musk ketone has been described as having a “powdery-warm, slightly animalistic musk odour”.¹³⁵ It was synthesised beginning with **3.11**, as illustrated in Scheme 3.4. This was reacted in a Friedel-Crafts acylation to give intermediate **3.12**. Nitration of **3.12** gave musk ketone. Musk ketone, along with musk ambrette, was used as an ingredient in the perfume Chanel N°5.¹³⁰

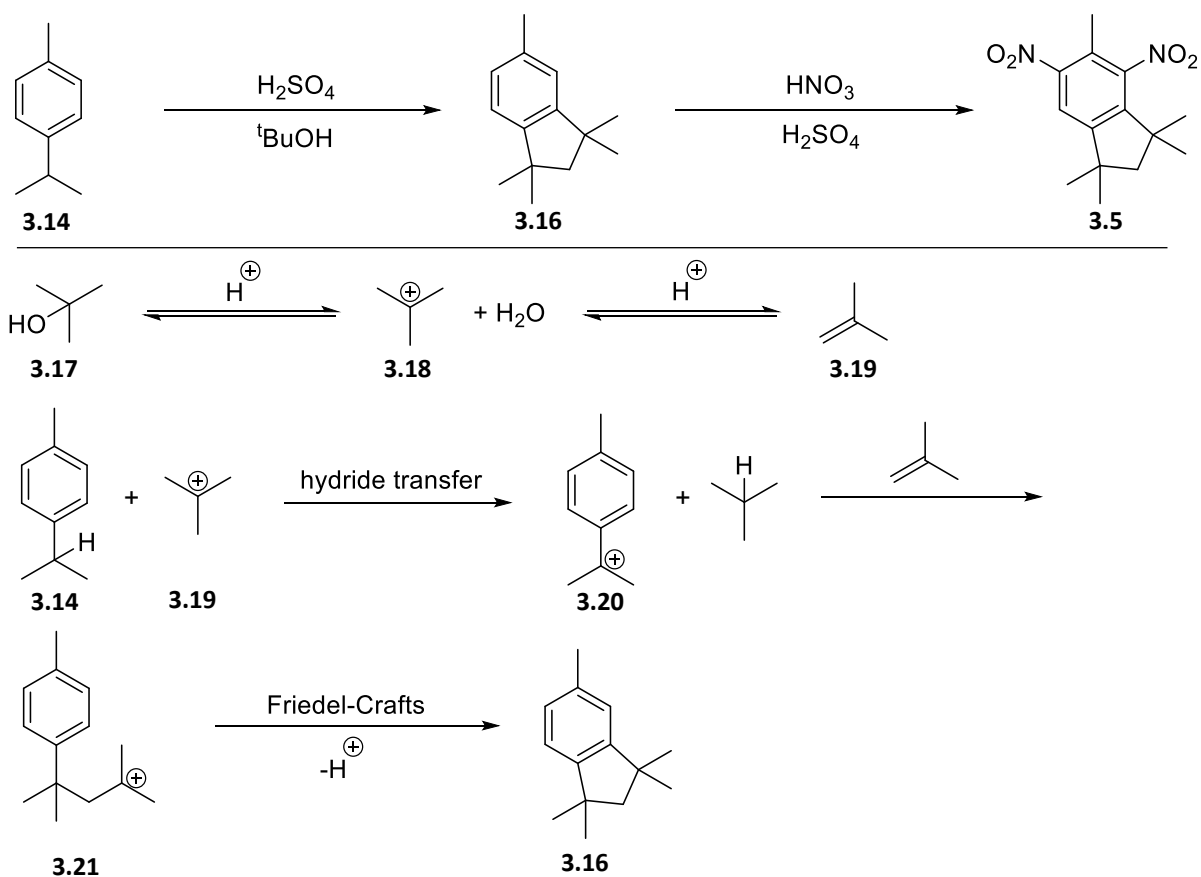


Scheme 3.4 – Synthesis of musk ketone by Baur.⁷

The next major nitromusk to be presented was ‘musk moskene’ **3.5**. ‘Musk moskene’ was an invention of Henri Barbier and a patent filed in 1930 was granted in 1932.¹³⁶ Initially, Barbier believed that ‘musk moskene’ was synthesised *via* a pathway beginning with cymene **3.14**, involving 1-methyl-4-(propan-2-yl)-5-*tert*-butylbenzene **3.15** as a key intermediate, as shown in Scheme 3.5. This led to an incorrect determination of the structure of ‘musk moskene’.¹³⁷ It wasn’t until 1955 that musk moskene was correctly structurally characterised, by a group of chemists from Givaudan based in New York and Geneva. They demonstrated that moskene possesses an indane structure.¹³⁸ Musk moskene was later synthesised by Givaudan beginning with cymene **3.14**, as illustrated in Scheme 3.6. The generation of isobutene **3.19** from *tert*-butanol **3.17** and then reaction with cymene **3.14** generates indane **3.16**. A possible mechanism is illustrated in Scheme 3.6. The product **3.16** is then nitrated to give ‘musk moskene’.

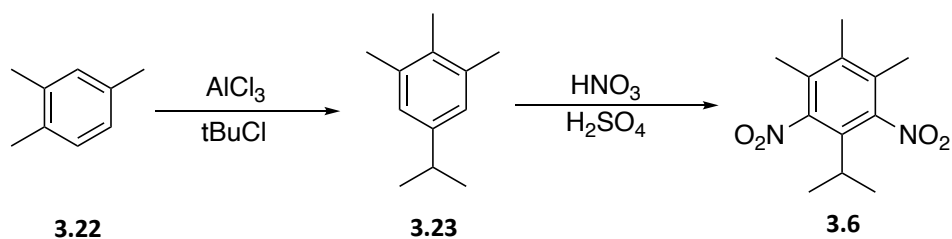


Scheme 3.5 – Barbier’s initial incorrect determination of the synthesis and structure of ‘musk moskene’ **3.5**.



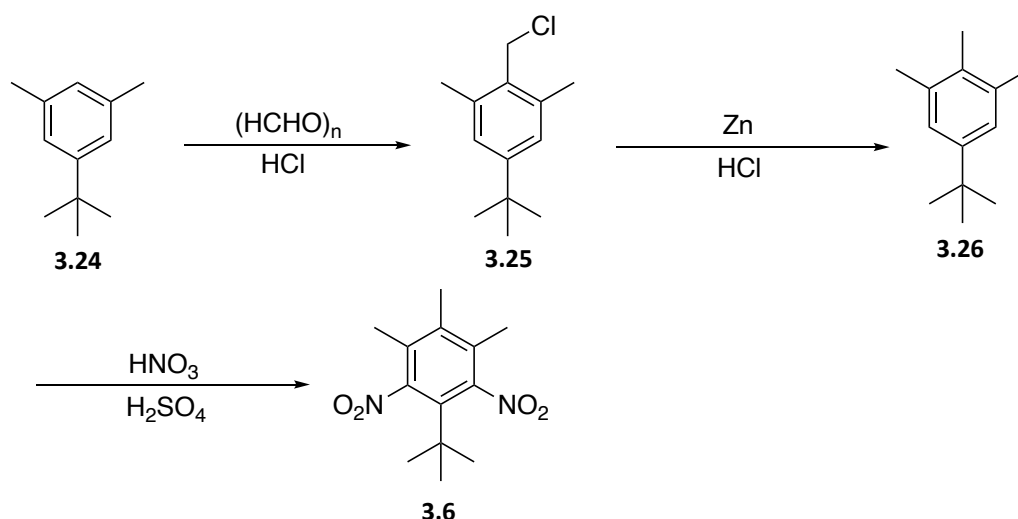
Scheme 3.6 – Synthesis of ‘musk moskene’ **3.5** as developed by Givaudin in 1955.¹³⁸

The last of the major nitromusks of that era was ‘musk tibetine’ **3.6**. Musk tibetine was first identified in 1935 by Marion Scott Carpenter, one of the fragrance chemists at Givaudan, who was studying potential nitromusks.¹³⁹ This synthesis of musk tibetine began with pseudo-cumene **3.22**, which was subjected to a Friedel-Crafts alkylation progressing through perhaps an unexpected rearrangement and forming product **3.23**, as illustrated in Scheme 3.7. Nitration of the alkylated product then gave ‘musk tibetine’ **3.6**.



Scheme 3.7 – Initial synthesis of ‘musk tibetine’ **3.6** developed by Carpenter.¹³⁹

Givaudan later developed an improved synthesis of ‘musk tibetine’ in 1947, as illustrated in Scheme 3.8.¹⁴⁰ This began with 1-(1,1-dimethylethyl)-3,5-dimethylbenzene **3.24**, which was alkylated using paraformaldehyde and hydrochloric acid to generate benzyl chloride **3.25**. Benzylic chloride chloride reduction using zinc in sodium hydroxide formed **3.26** followed by nitration to give musk tibetine **3.6**.



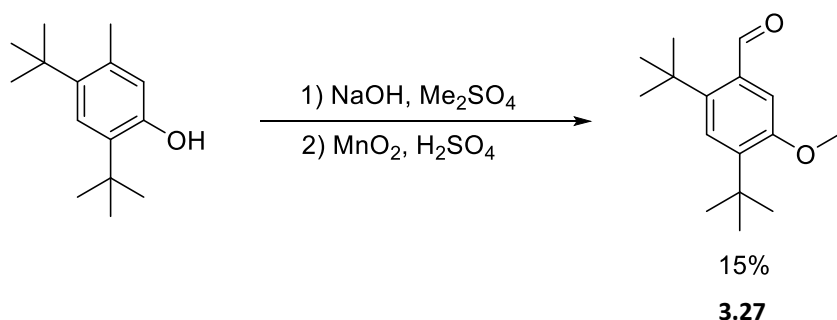
Scheme 3.8 – Improved synthesis of ‘musk tibetine’ **3.6** by Givaudan.¹⁴⁰

However, these musks have now fallen out of use.¹³¹ Musk ambrette was restricted in the 1980s as it was found to cause neuropathologic changes in the brain, spinal cord and damaged peripheral nerves in rats.¹⁴¹ ‘Musk xylene’ and ‘musk ketone’ are still being used, however, in the European Union use is strictly controlled as they are suspected carcinogens at high concentrations.^{142, 143} ‘Musk moskene’ and ‘musk tibetine’ are prohibited too due to the adverse effects of similar structures. A concern about nitromusks is that they have very long environmental half-lives and this leads to their bioaccumulation in human populations, for example transferring via breast milk and also during prenatal development.^{131, 144} The first evidence of the bioaccumulation of nitromusks came in 1981 in Japan, where Yamagishi *et al.*, analysed levels of ‘musk xylene’ and ‘musk ketone’ in freshwater fish in Tokyo Bay.¹⁴⁵ They found that 100% of sampled fish contained levels of ‘musk xylene’ and 80% contained levels of ‘musk ketone’. Also, nitromusks are unstable in alkaline media so their formulation in soaps and detergents is limited. Furthermore, nitromusks have been found to degrade in

sunlight when suspended in water.¹⁴⁶ As a result of all of these concerns, nitromusks have largely been replaced by polycyclic and macrocyclic musks, in fragrances, since the 1980s.

3.1.2 Polycyclic musks

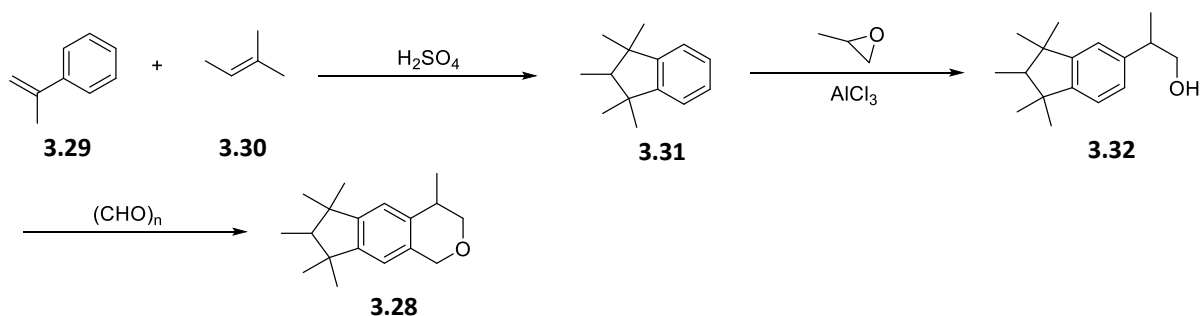
Nitro-free synthetic musks were reported in the late 1940s and the 1950s and are known as polycyclic musks. The first of these was Ambral **3.27** reported in 1947. Ambral was prepared by Carpenter *et al.*,¹⁴⁷ who were attempting to synthesise a number of derivatives of musk ambrette. It was initially an intermediate which was due to be nitrated in an attempt to prepare a nitro-musk however it had musk properties itself. In the event, Ambral never made it to market due to the inefficiency of its synthesis, with the final step being a low-yielding oxidation of a benzylic methyl group, as shown in Scheme 3.9. None-the-less the musky odour of Ambral was proof that problematic nitro groups were not necessary to generate a synthetic musk odour.



Scheme 3.9 – Final step in the synthesis of Ambral **3.27** by Carpenter *et al.*¹⁴⁷

The most successful of these musks in commercial terms was Galaxolide **3.28**, discovered in 1967.¹⁴⁸ It has an odour that has been described as a “*clean, sweet, floral, woody musk*”. Galaxolide was immediately successful, being used particularly in detergents and perfumes. The synthesis of Galaxolide was achieved in three steps, as shown in Scheme 3.10.¹⁴⁹ First, methyl styrene **3.29** was reacted with amylene **3.30** in a sulfuric acid-catalysed reaction to give pentamethyl indane **3.31**. This then underwent a Friedel-Crafts alkylation reaction with propylene oxide to form alcohol **3.32**. Cyclisation with paraformaldehyde then gave Galaxolide. This product is a highly viscous liquid which is diluted with a neutral odour liquid to be commercially useful. Galaxolide was initially synthesised as an isomeric mixture,

however, Fráter *et al.* were able to separate the four stereoisomers illustrated in Figure 3.2.¹⁴⁸ They found that two of these, the (4*S*, 7*R*) **3.33** and the (4*S*, 7*S*) **3.34**, were responsible for the odour. The odour of the (4*R*, 7*R*) stereoisomer **3.35** was considered very weak and that of the (4*R*, 7*S*) stereoisomer **3.36** was uncharacteristic of Galaxolide. Galaxolide has been used in a wide range of perfumes, including some by Yves Saint Laurent, Givenchy, Dior and Calvin Klein.¹⁵⁰



Scheme 3.10 – Synthesis of Galaxolide **3.28**.¹⁴⁹

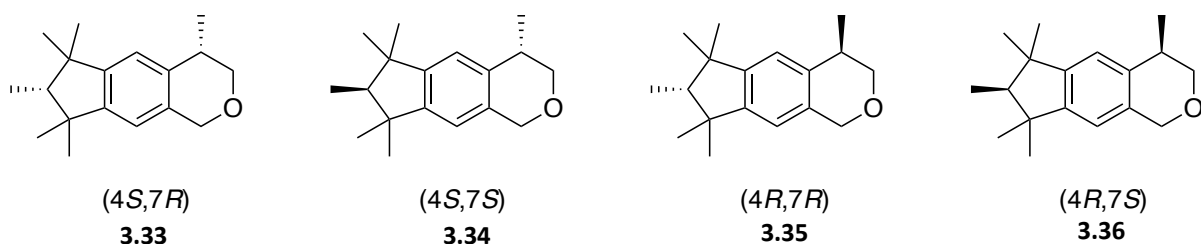
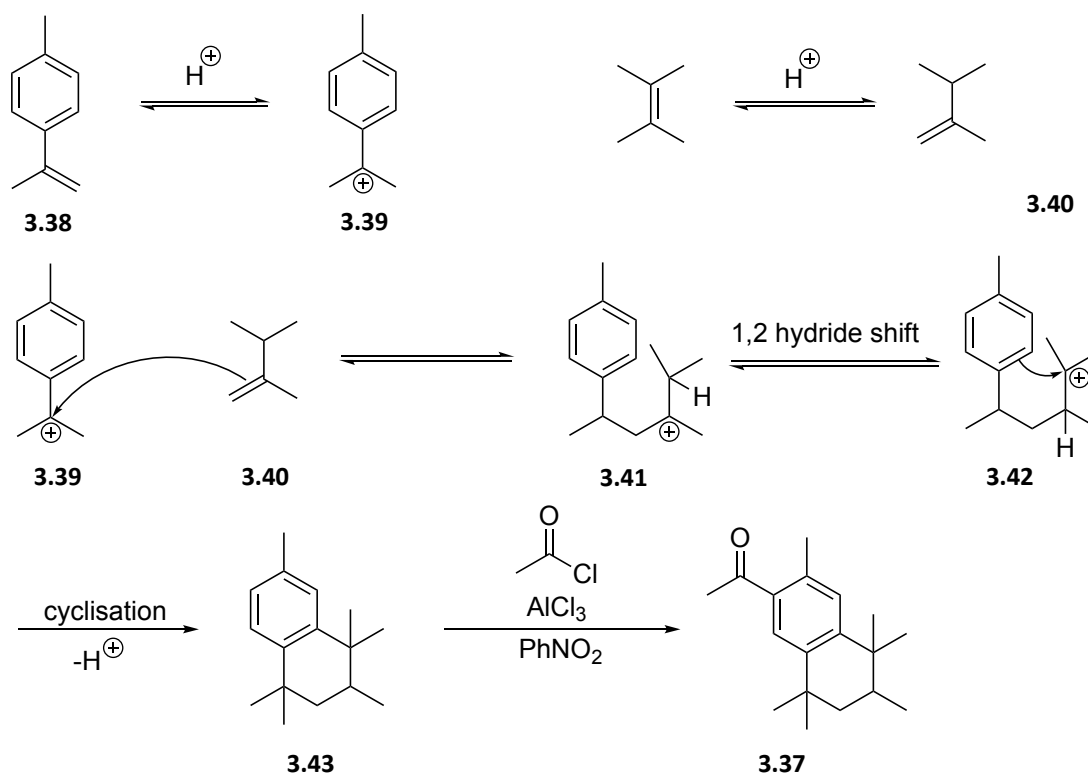


Figure 3.2 – Stereoisomers of Galaxolide separated by Fráter *et al.*¹⁴⁸

Another successful polycyclic musk is Tonalid **3.37**. Tonalid was synthesised beginning with the protonation of α -methylstyrene **3.38**, generating carbocation **3.39**. 2,3-Dimethyl-but-1-ene **3.40** then attacks this carbocation. The resulting carbocation intermediate **3.41** is then shifted down the carbon chain *via* a 1,2-hydride shift to form **3.42**. This then allows for ring-closure to form tetralin **3.43**.¹⁵¹ Friedel-Crafts acylation of **3.43** gave the final product, as illustrated in Scheme 3.11. This synthesis led to a mixture of isomers, however, later work carried out by the Sumitomo Chemical Company explored the individual enantiomers.¹⁵⁰ They determined that the (*S*)-isomer had a “*strongly-musky odour*” whereas the (*R*)-isomer merely possessed a “*light and sweet aromatic odour*”. This shows the crucial importance

that the overall shape plays in the interactions of a molecule with an olfactory receptor. Tonalid was used particularly within masculine toiletries and went on to become the second most commercially successful polycyclic musk, behind only Galaxolide.



Scheme 3.11 – Synthesis of Tonalid **3.37**.

In total, seven polycyclic aromatic musks were released to the market. However, environmental concerns have emerged here too, and it has been found that these musks exhibit poor biodegradability. Polycyclic musks have been found to accumulate and persist widely within aquatic environments. Heberer *et al.* conducted a study of the rivers, lakes and canals of Berlin in 1999.¹⁵² They found high concentrations of synthetic musks, particularly Galaxolide and Tonalid, with concentrations up to the low ng L⁻¹ level. Meanwhile, in a separate study, Galaxolide was found to accumulate at high concentrations in Canadian aquatic fauna, and the same study found that Galaxolide and Tonalid accumulate in high concentrations in aquatic fauna in Western Europe.¹⁵³ The polycyclic musks have also been found to accumulate in human and animal tissue.¹⁵⁴ Hutter *et al.* studied the accumulation of polycyclic musks within humans by taking blood samples from 114 students and analysing the samples for six polycyclic musks.¹⁵⁵ They found Galaxolide in

91% and Tonalid in 17%, of the samples taken. They found a median concentration of Galaxolide in the blood samples of 420 ng L⁻¹ and a maximum concentration of Galaxolide of 4100 ng L⁻¹. They also found a maximum concentration of Tonalid of 800 ng L⁻¹. This demonstrated the growing concern about the persistence of polycyclic musk molecules within the human body, and particularly for products directly applied.

3.1.3 Recent musk developments

As a result of the environmental concerns of the classical polycyclic musks, attention has turned to the development of more environmentally friendly alternatives to these compounds.¹⁰² This has led to the development of linear acyclic musks. The first of these was Helvetolide **3.44**, which can imitate the shape of a macrocycle due to its horseshoe shape.¹⁵⁶ It has gone on to be used in perfumes by Louis Vuitton and Lancome. Sereonlide **3.45** later followed and has been found to be three times more fragrant than Helvetolide.¹⁵⁷ The inclusion of the cyclopropyl ring stabilises the horseshoe shape and hence the pseudo-macrocyclic structure. A recent study found that the insertion of a methylene unit into Helvetolide and Sereonlide completely erases their musky odours, instead giving them a sweet aroma.¹⁵⁸ Sorbettolide **3.46** is considered to have a blackberry scent and is described as 'fruity and musky'.¹⁰² The stereochemistry around the epoxide group is important to the odour of Sorbettolide, with the *cis* isomer being described as having an unpleasant odour. Therefore, high *trans* selectivity is required for the synthesis of Sorbettolide **3.46**.¹⁰²

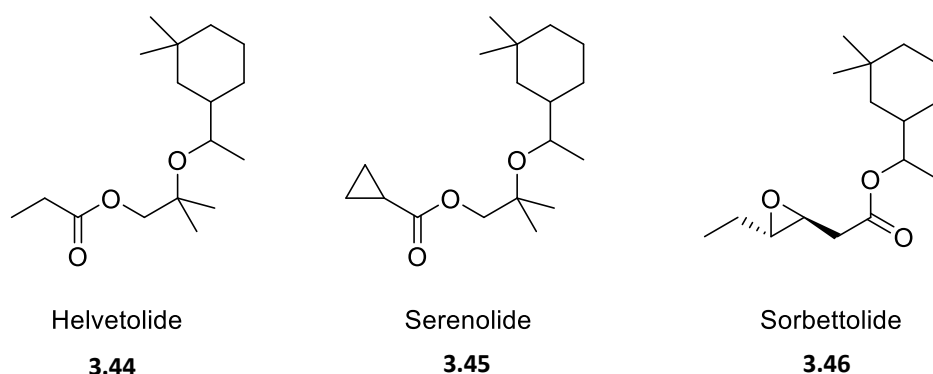


Figure 3.3 – Structures of linear acyclic musks Helvetolide **3.44**, Sereonlide **3.45** and Sorbettolide **3.46**.

Another group of recently disclosed musks are the dienones. These feature a ketone conjugated to a diene system, which has one or more bulky aliphatic groups, usually *tert*-butyl groups attached. The first of these to be discovered was **3.47**, followed by a more potent linear derivative **3.48**. The key to the odour in **3.48** appears to be the *tert*-butyl group, as lesser alkyl substituents lose their musky smell.¹⁵⁹ Di *tert*-butyl analogue **3.49** was found to have a more intense smell, albeit with more of a floral than a musky character. The most potent musk of this class is **3.50**, which contains a dimethylcyclopentene group and again features a *tert*-butyl group.¹⁶⁰

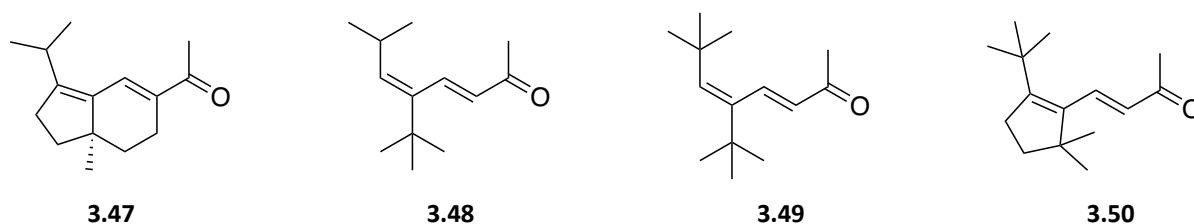


Figure 3.4 – Structures of dienone musk compounds.

New polycyclic systems have also been developed. One example of this is Cashmeran **3.51**, which features an α,β -unsaturated ketone system. However, this structure begins to move away from the typical musk odour, with more of a “musky-woody” odour being described.¹⁶¹ Interestingly the two Cashmeran enantiomers, when assessed separately have very similar fragrances and intensities. The hydroindenes enantiomers **3.52** and **3.53** were developed from Cashmeran and reintroduced the *tert*-butyl group.¹⁶² While both enantiomers are weaker musks than Cashmeran, it is interesting that only the (*R*)-enantiomer **3.52** has a similar odour to Cashmeran, whereas the (*S*)-enantiomer **3.53** had no similarity at all.

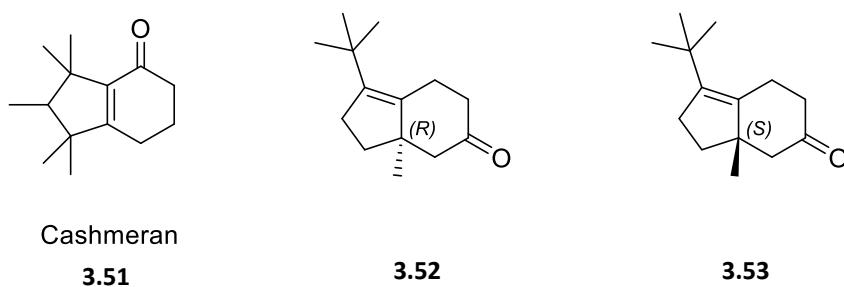
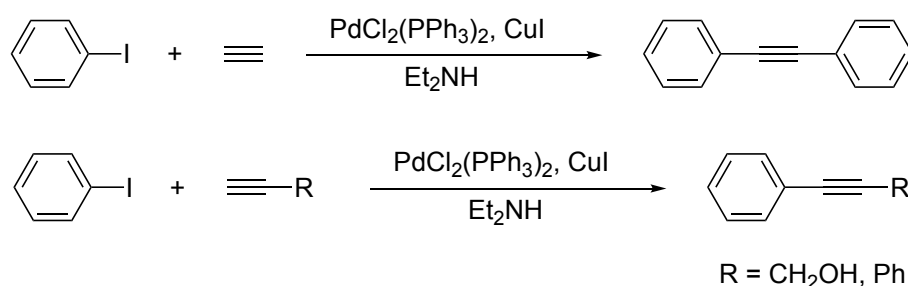


Figure 3.5 – Structures of Cashmeran **3.51** and hydroindene enantiomers **3.52** and **3.53**.

3.1.4 Sonogashira cross-coupling

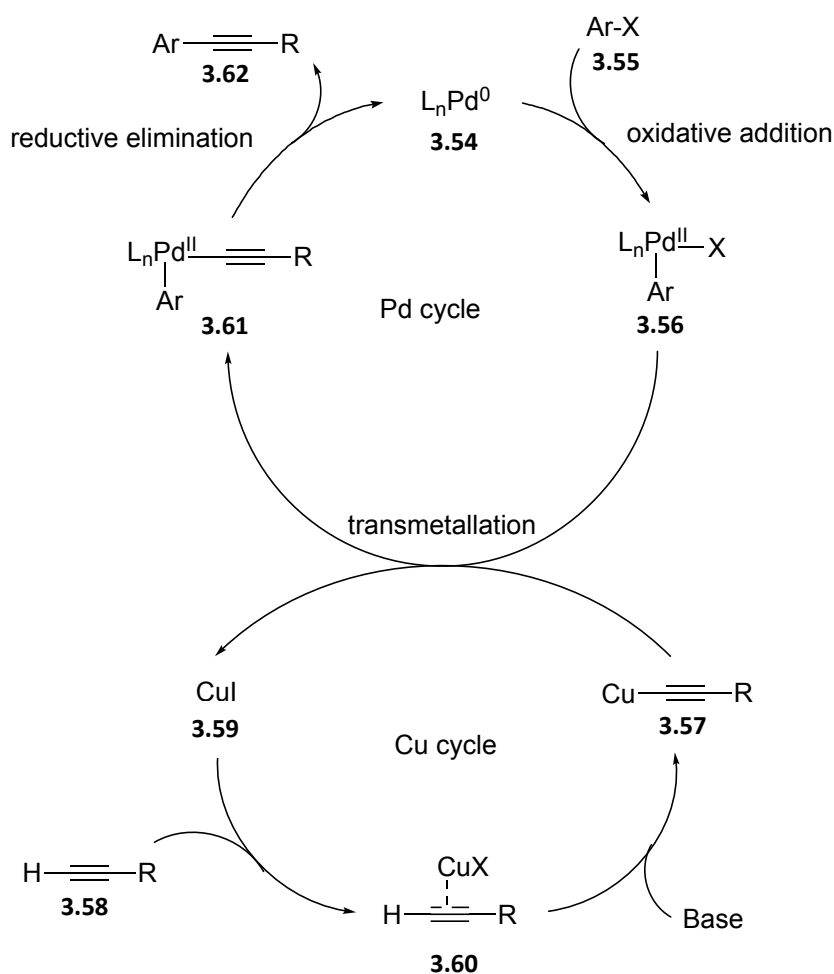
The Sonogashira reaction was first reported in 1975 and is a sp^2 - sp cross-coupling reaction, as illustrated in Scheme 3.12.¹⁶³ It involves a palladium-catalysed reaction between an aryl halide and an acetylene. The reaction also employs a Cu(I) co-catalyst and a base. Previously known couplings of aryl halides and acetylenes used much harsher conditions, such as the Castro-Stephens coupling.¹⁶⁴ This was a copper-catalysed reaction coupling an aryl halide with a pre-synthesised copper-acetylide complex, reacting in pyridine under reflux. The Sonogashira reaction achieved this same outcome under much milder conditions and without the need to pre-synthesise the copper-acetylide complex. The initial example provided by Sonogashira reacted iodobenzene with acetylene, using $\text{PdCl}_2(\text{PPh}_3)_2$ as the catalyst, Cu(I) iodide as co-catalyst and diethylamine as a base, forming a disubstituted acetylene product. Further examples of coupling reactions were disclosed with acetylene and mono-substituted acetylenes.



Scheme 3.12 – Initial Sonogashira reactions developed by Sonogashira.¹⁶³

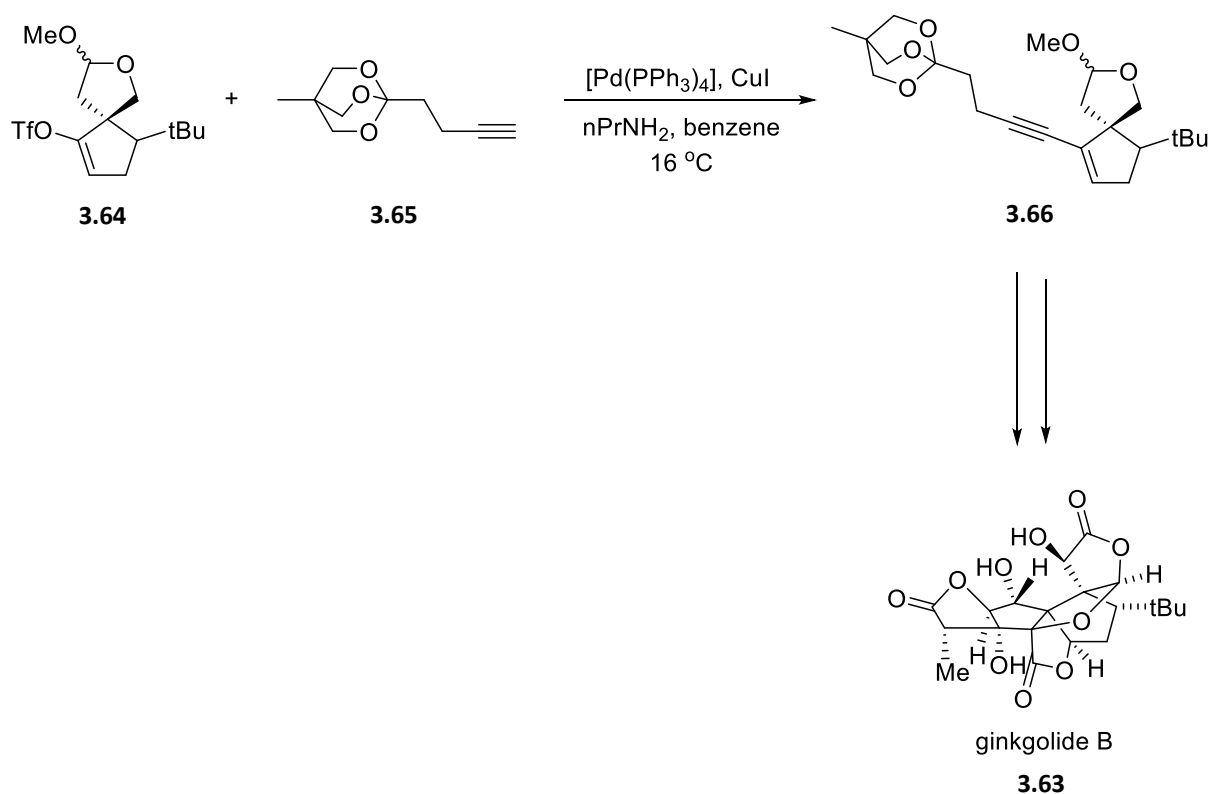
The mechanism of the Sonogashira reaction features a palladium cycle and a copper cycle, as illustrated in Scheme 3.13.¹⁶⁵ The palladium cycle begins with the formation of the catalyst. Commonly, a Pd(II) complex such as $\text{PdCl}_2(\text{PPh}_3)_2$ is used as a pre-catalyst, which is then reduced to form the active Pd(0) species **3.54**, although a Pd(0) complex such as $\text{Pd}(\text{PPh}_3)_4$ can also be used. Oxidative addition of the aryl halide **3.55** to the catalyst takes place, with Pd(0) being oxidised to Pd(II) **3.56**. Meanwhile, on the copper cycle, a copper acetylide complex **3.57** is formed via the reaction of acetylene **3.58** and copper iodide **3.59** to form Cu-alkyne π complex **3.60**. The base then facilitates the formation of the copper-acetylide complex. The two cycles converge at this point, with a trans-metallation step taking place, exchanging the halide ligand with the acetylene, forming species **3.61**.

Reductive elimination results in the aryl-acetylene product **3.62** and regenerates the Pd(0) catalyst **3.54** for another cycle.



Scheme 3.13 – Proposed mechanism of the Sonogashira cross-coupling reaction.¹⁶⁵

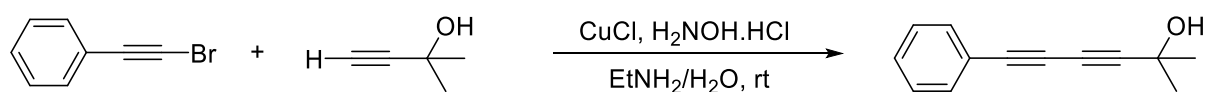
The Sonogashira reaction has gone on to be widely used within organic chemistry. One early illustrative example of this was in the synthesis of Ginkgolide B **3.63** by Corey *et al.* in 1988, as illustrated in Scheme 3.14.¹⁶⁶ In this synthesis, enol triflate **3.64** was coupled with alkyne **3.65** to give desired enyne product **3.66**. This was achieved using catalytic $Pd(PPh_3)_4$ (6 mol%) with a high catalyst loading of Cu(I) iodide (50 mol%) and *n*-propylamine as the base.



Scheme 3.14 – Sonogashira reaction in Corey's synthesis of ginkgolide B **3.63**.¹⁶⁶

3.1.5 Cadiot-Chodkiewicz cross-coupling

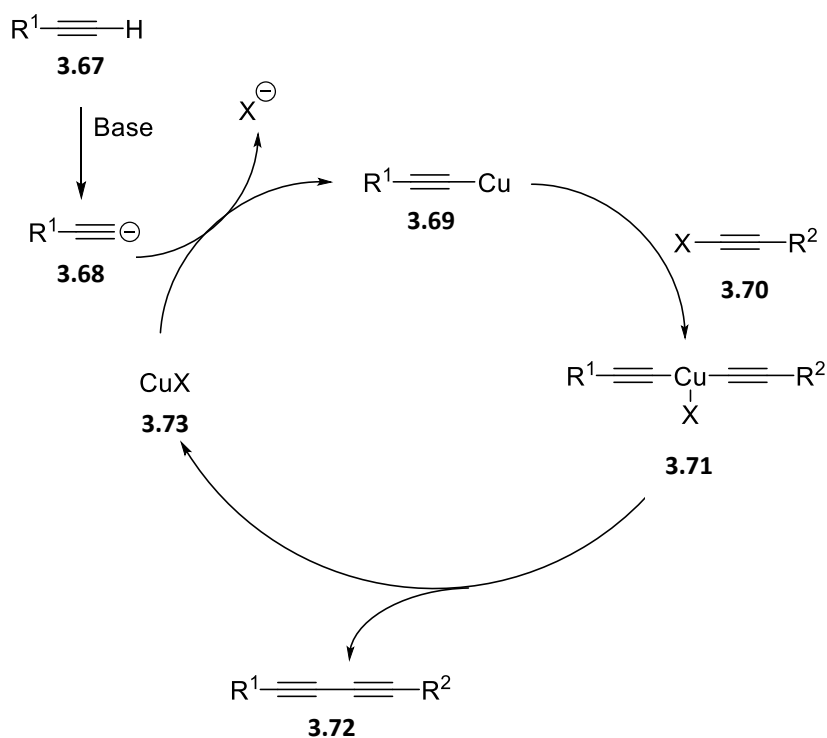
The Cadiot-Chodkiewicz cross-coupling reaction was first reported in 1955 involving the cross-coupling of a terminal alkyne and a haloalkyne (sp-sp coupling), as illustrated in Scheme 3.15.¹⁶⁷ This is a copper-catalysed process which also uses an amine base.



Scheme 3.15 – A Cadiot-Chodkiewicz cross-coupling reaction.¹⁶⁸

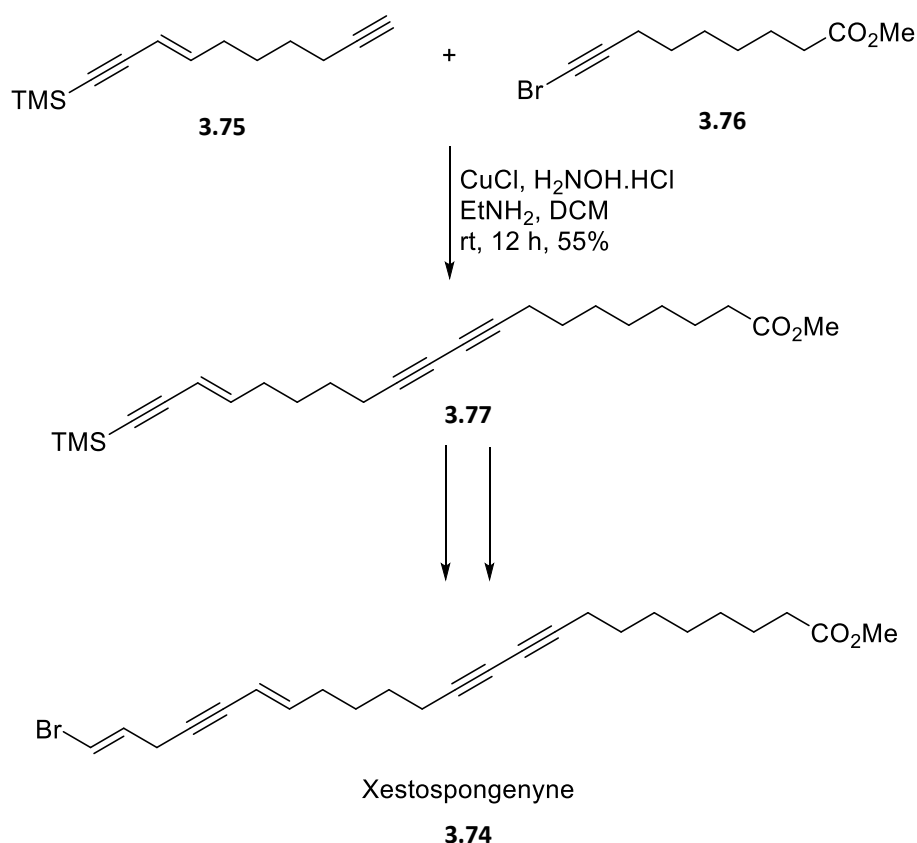
The catalytic cycle, as shown in Scheme 3.16, begins with deprotonation of the terminal alkyne **3.67** to give **3.68**.¹⁶⁸ A transmetalation step then follows, leading to the formation of a copper-acetylide complex **3.69**. Oxidative addition of the haloalkyne **3.70** to the copper complex then occurs, with concomitant oxidation of Cu(I) to Cu(III). Finally, reductive elimination of the *bis*-acetylene **3.72** generates product and with reduction back to Cu(I)

3.73, regenerating the active catalyst. One issue with the Cadiot-Chodkiewicz coupling reaction is that a homo-coupled side-product can be produced. This can be minimised by using an excess of the terminal alkyne. A hydroxylamine salt (eg H₂NOH.HCl) is usually added to reduce the presence of Cu(II) ions which are formed during the reaction.



Scheme 3.16 – Proposed mechanism of the Cadiot-Chodkiewicz reaction.¹⁶⁸

The Cadiot-Chodkiewicz reaction has had many applications in total synthesis.¹⁶⁹ One example is in the synthesis of xestosponginyne **3.74** by Guo *et al*, as illustrated in Scheme 3.17. They reacted diyne **3.75** and bromoalkyne ester **3.76**, forming a C-C (sp-sp) connection between the two units to give *bis*-acetylene **3.77**.¹⁷⁰ This reaction also demonstrates the tolerance of silyl protecting groups, which prevent the formation of undesired disubstituted alkyne side-products.



Scheme 3.17 – Cadiot-Chodkiewicz reaction in the synthesis of xestospongenyne **3.74** by Guo *et al.*¹⁷⁰

3.1.6 The *gauche* effect

The electronegativity of fluorine can lead to some unique effects on the conformation of molecules. In this context, the '*gauche* effect' is widely discussed. The '*gauche* effect' was first reported by Wolfe in 1970.¹⁷¹ It might be expected that the fluorine atoms on the vicinal carbons of 1,2-difluoroethane would prefer to be *anti* to each other, in order to minimise steric interactions and electrostatic repulsion between the fluorine atoms. However, the two C-F bonds unexpectedly prefer a *gauche* over an *anti* conformation by between 0.5-0.9 kcal mol⁻¹.⁶ This is because these repulsive effects are overcome by stability gained by hyperconjugation. In the *gauche* conformation, the C-F bonds each have an *anti*-periplanar C-H bond, whereas in the *anti* conformer, they are both *anti*-periplanar to the other C-F bond. Therefore, electron density is more easily transferred from the C-H σ orbital to the C-F σ^* *anti*-bonding orbital on the neighbouring carbon, as shown in Figure 3.6.⁶ This hyperconjugation adds stability to that conformer. Therefore, the *gauche* conformer is more

stable than the *anti*. By comparison, 1,2-dichloroethane, 1,2-dibromoethane and 1,2-diiodoethane have lower energy *anti* conformers as expected, as this minimises steric repulsion between these larger halogens, as illustrated in Figure 3.7.¹⁷²

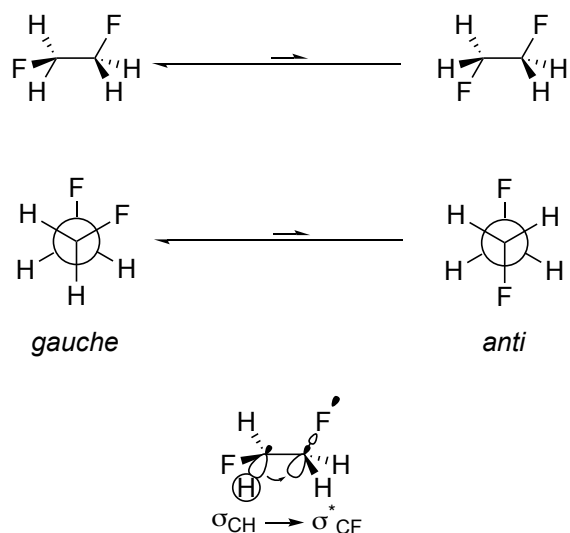


Figure 3.6 – Gauche effect in 1,2-difluoroethane. The lower structure illustrates key hyperconjugative interactions.¹⁷²

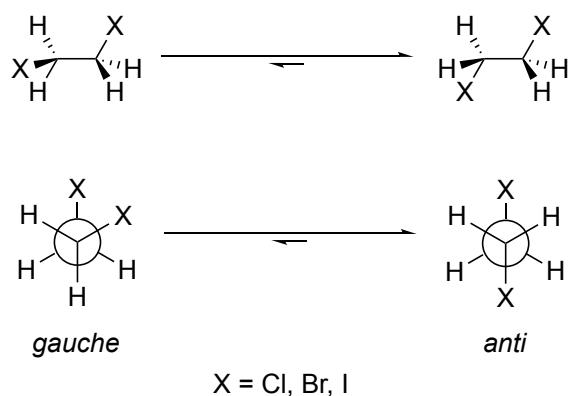


Figure 3.7 – Preference of *anti*-conformers of halogenated ethanes.¹⁷²

3.1.7 The anomeric effect

Another example of fluorine stereoelectronics influencing the conformation of molecules is in an anomeric effect. The anomeric effect recognises the preference of a heteroatom at the 2-position of a tetrahydropyran ring to prefer an axial over an equatorial conformation, as would normally be expected in a cyclohexane ring. This effect is also due to

hyperconjugation, with donation of a heteroatom lone pair into the C-X σ^* orbital of the exocyclic heteroatom. Such hyperconjugation lowers the overall energy level of the molecule. Classically, 2-methoxytetrahydropyran **3.78** favours the axial conformation by 0.7-0.9 kcal mol⁻¹. Replacing -OMe for -F at the 2-position increases this effect and 2-fluorotetrahydropyran **3.79** favours the axial conformation now by 2.8-2.9 kcal mol⁻¹, three times that observed in **3.78**.^{6,173}

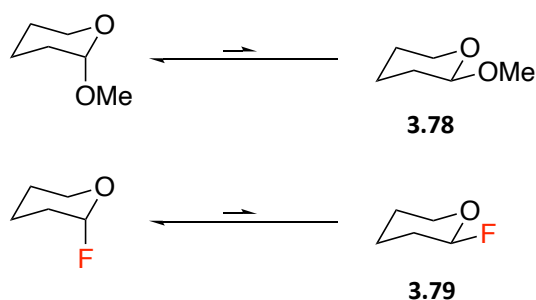


Figure 3.8 – The anomeric effect as shown in 2-methoxytetrahydropyran **3.78** and 2-fluorotetrahydropyran **3.79**.

3.1.8 Fluorine as a hydrogen bond acceptor

Fluorine is able to act as a hydrogen bond acceptor. However, while it might be expected that this would be a strong effect due to the highly polarising nature of fluorine, organofluorine compounds form weak hydrogen bonds.⁶ This has been supported by theory calculations, which suggest that the strength of a CF...HO hydrogen bond is at best up to half that of the O-H hydrogen bond, which typically has a bond strength of between 5 and 10 kcal mol⁻¹. In 1997, Dunitz and Taylor conducted a CSD search of compounds containing a C-F bond with at least one potential hydrogen bond donor group. They found that from 5947 C-F bonds in 1218 relevant CSD structures, only 37 (0.6%) of these are involved in hydrogen bonding.¹⁷⁴ Essentially the fluorine lone pairs are held closely to the nucleus and are less able to act as a hydrogen bond acceptor and they concluded that this low frequency arises as there are better alternatives for hydrogen bond donors. Therefore, for fluorine to act as a hydrogen bond acceptor, conditions for this to happen must be favourable with no competing options.

One example of a good C-F...H-O hydrogen bond is found in calcium bis[2-fluorobenzoate] dihydrate **3.80**, as shown in Figure 3.9.¹⁷⁴ Each hydrated water is bonded to a Ca²⁺ ion, which renders it more acidic than an isolated water molecule. Each water makes two hydrogen bonds, one to a carboxylate oxygen (H-O 1.77 Å) and the other to the fluorine atom (F-H 2.04 Å).¹⁷⁵ The fluorine is more electron-rich than normal due to it being part of an anion, and so is more able to accept a hydrogen bond. As a result, this creates favourable conditions for a fluorine hydrogen bond to be formed.

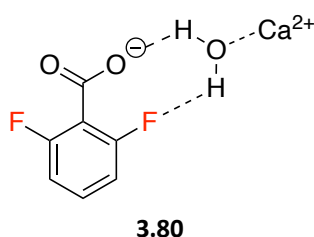


Figure 3.9 – Hydrogen bond to fluorine in calcium bis[2-fluorobenzoate] dihydrate **3.80**.

3.1.9 Influencing the conformation of an aryl-carbonyl group

A method used to influence the orientation of an aryl-bound carbonyl is to introduce an *ortho* fluorine atom into the aromatic ring. This effect was previously studied on 2'-fluoro-substituted acetophenone derivatives by Takahashi *et al.*, who measured the through-space spin-spin NMR couplings between the hydrogen atoms of an acetophenone group and the fluorine in the 2' position on the aromatic ring.¹⁷⁶ Initially, they synthesised malonitrile **3.81** and ethyl cyanoacetate **3.82** derivatives and measured the ⁵J_{HF} coupling constants of these molecules, as shown in Figure 3.10. These were determined to be 3.2 and 3.3 Hz respectively, much larger than a typical ⁵J_{HF} coupling constant of less than 1 Hz. This suggested a through-space coupling due to close contact between the fluorine and hydrogen atoms.

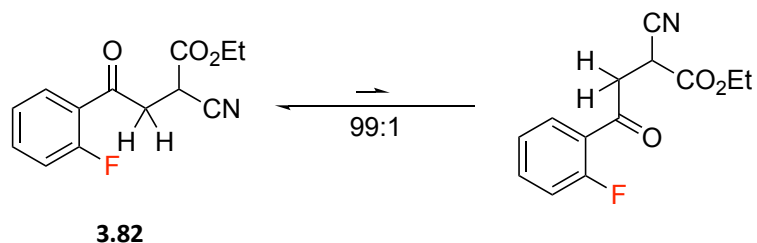
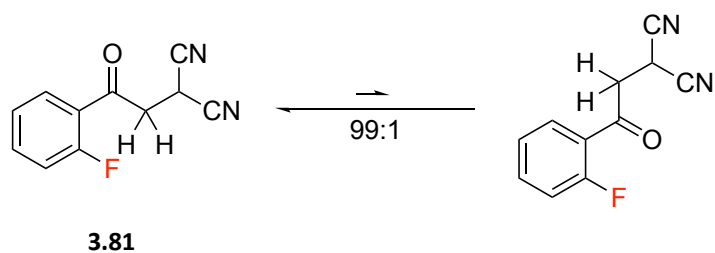
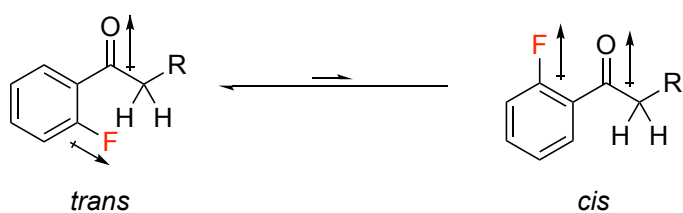


Figure 3.10 – Orientation of selectively fluorinated acetophenones **3.81** and **3.82** as shown by Takahashi et al.¹⁷⁶

A variety of 2'-fluoro-substituted acetophenone compounds shown in Figure 3.11 were prepared, all of which had $^5J_{\text{HF}}$ coupling constants of between 3.20-5.03 Hz. This suggests that these 2-fluoro-substituted acetophenones adopt a *trans*-conformation. DFT calculations also supported a strong bias for the *trans*- over the *cis*- conformer in all cases, some exhibiting a >99:1 bias. This arises due to a repulsion between the aryl fluorine and the carbonyl oxygen where the two dipoles move to oppose each other and minimise the overall molecular dipole.



R	$\Delta G_{\text{trans/cis}}$ (kcal mol ⁻¹)	Ratio (trans:cis)
CH(CN) ₂	2.57	99:1
CH(CN)(CO ₂ Et)	2.91	99:1
CH ₂ CH ₃	2.28	98:2
H	3.56	>99:1
Br	2.09	97:3
CH ₃	4.13	>99:1
CO ₂ CH ₂ CH ₃	2.67	99:1

Figure 3.11 – Energy difference and cis:trans ratios of selected fluorinated acetophenones as determined by Takahashi et al.¹⁷⁶

3.1.10 Aims and objectives

This chapter aims to build on the work as described in Chapter 2 on the synthesis of derivatives of (*R*)-muscone **2.1**. Whereas in Chapter 2 work was done to test cyclic musk structures similar in structure to (*R*)-muscone, in this Chapter the work takes inspiration from the work of Baur on nitromusks, and subsequent work on polycyclic musks such as Galaxolide. Similar to Chapter 2, the aim remains to test how making changes to the structure of a molecule affects the interaction of the molecule with known olfactory receptors.

Acetylene targets were identified to test interactions with olfactory receptors, in particular OR5AN1 and OR1A1. These targets were modelled to be similar to previously known and developed polycyclic musks such as Galaxolide **3.28** and Tonalid **3.37**. These targets would feature an acetophenone group linked to a *tert*-butyl group by an acetylene linker. The idea behind this was that these structures would be flat and rigid, with limited conformational flexibility and they should probe the spacial limitations of the receptors. The structures of

these molecules would allow for a number of effects to be tested, such as the positions of the aromatic and acetylene groups, and also to vary the number of acetylene linker groups.

Initial targets were the *para* and *meta* monoacetylenes **3.83-3.86**, as shown in Figure 3.12, which could be synthesised via cross-coupling reactions.

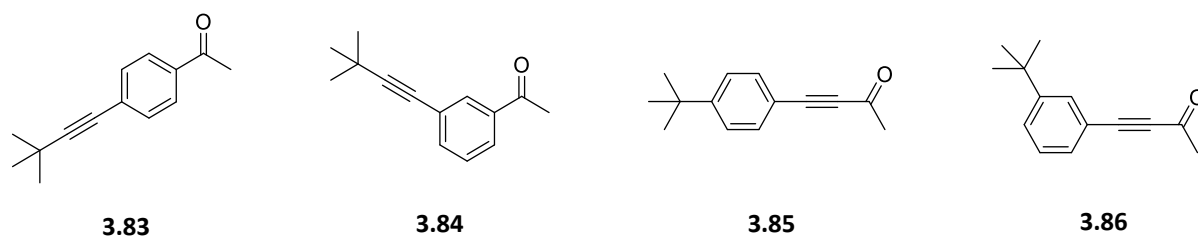
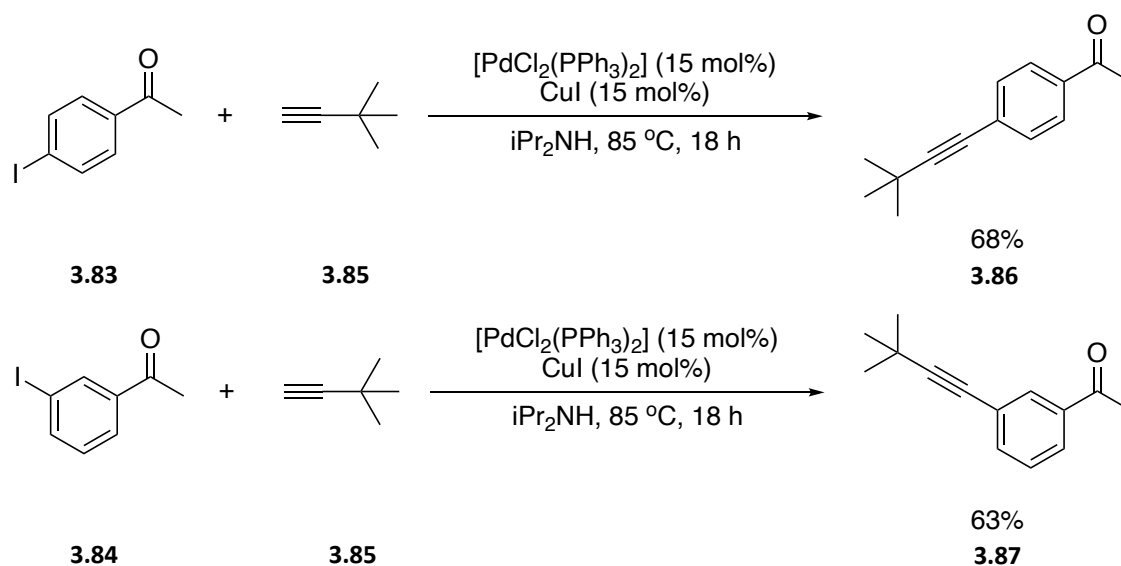


Figure 3.12 – Initial monoacetylene targets identified as potential musk odorants.

3.2 Synthesis of potential musks

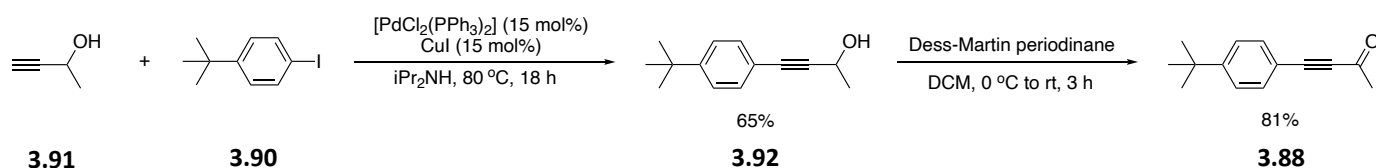
3.2.1 Synthesis of monoacetylenes

The monoacetylenes shown in Figure 3.12 were synthesised *via* Sonogashira cross-coupling reactions of iodoacetophenones **3.83** and **3.84** with *tert*-butyl acetylene **3.85**. The first targets were *para* and *meta* *tert*-butylacetylene acetophenones **3.86** and **3.87**, as shown in Scheme 3.18. These reactions proceeded smoothly, with *para* **3.86** being obtained in 68% yield and *meta* **3.87** in a yield of 63%.



Scheme 3.18 – Synthesis of *para* and *meta* monoacetylene compounds **3.86** and **3.87** via Sonogashira reactions.

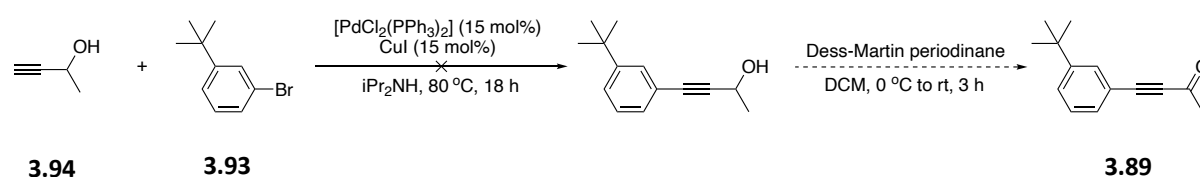
The isomeric compounds **3.88** and **3.89** were also identified as targets. These are structural isomers of **3.86** and **3.87**, where the ketone is bonded directly to the acetylene linker, which is then bonded to the aromatic ring. Target **3.88** was synthesised beginning with the Sonogashira cross-coupling reaction of 1-*tert*-butyl-4-iodobenzene **3.90** with 3-butyn-2-ol **3.91** to give monoacetylene alcohol **3.92**, as illustrated in Scheme 3.19. This was accomplished in a 65% yield. A sample of alcohol **3.92** was kept for assay, while the remaining alcohol was oxidised to the desired ketone **3.88** using Dess-Martin periodinane. This was an efficient reaction and gave the ketone with an 81% yield.



Scheme 3.19 – Synthesis of monoacetylene target **3.88**.

Preparation of *meta* *tert*-butyl acetylene **3.89** was attempted using the same approach, with a Sonogashira reaction between 1-bromo-3-*tert*-butylbenzene **3.93** with 3-butyn-2-ol **3.94**. However, this reaction was unsuccessful, and did not yield a product, as illustrated in Scheme 3.20. This could potentially have been achieved by using 1-iodo-3-*tert*-

butylbenzene, however, this starting material was expensive and it was decided to wait for the assay results of other monoacetylenes before pursuing this target.



Scheme 3.20 – Attempted synthesis of monoacetylene 3.89.

However, when monoacetylenes **3.86-3.88** were assayed, they triggered only a limited response with the OR5AN1 and OR1A1 receptors relative to (*R*)-muscone, as shown in Figures 3.12 and 3.13 respectively. Therefore, we looked to move on from the monoacetylene class to *bis*-acetylenes, in an attempt to find molecules that interact more strongly with these receptors.

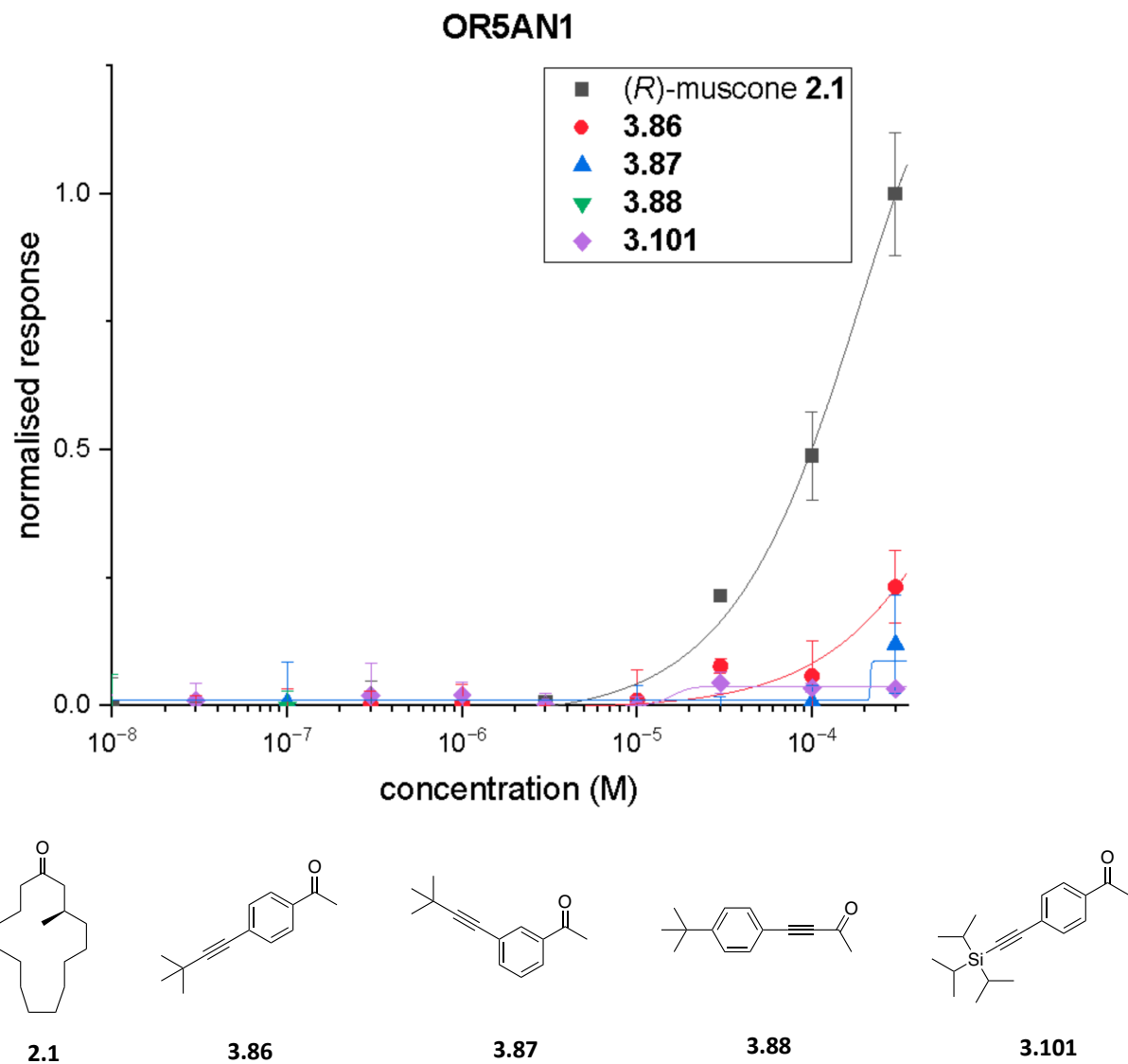


Figure 3.12 – Dose-response curve showing interactions of selected monoacetylenes with OR5AN1 olfactory receptor.

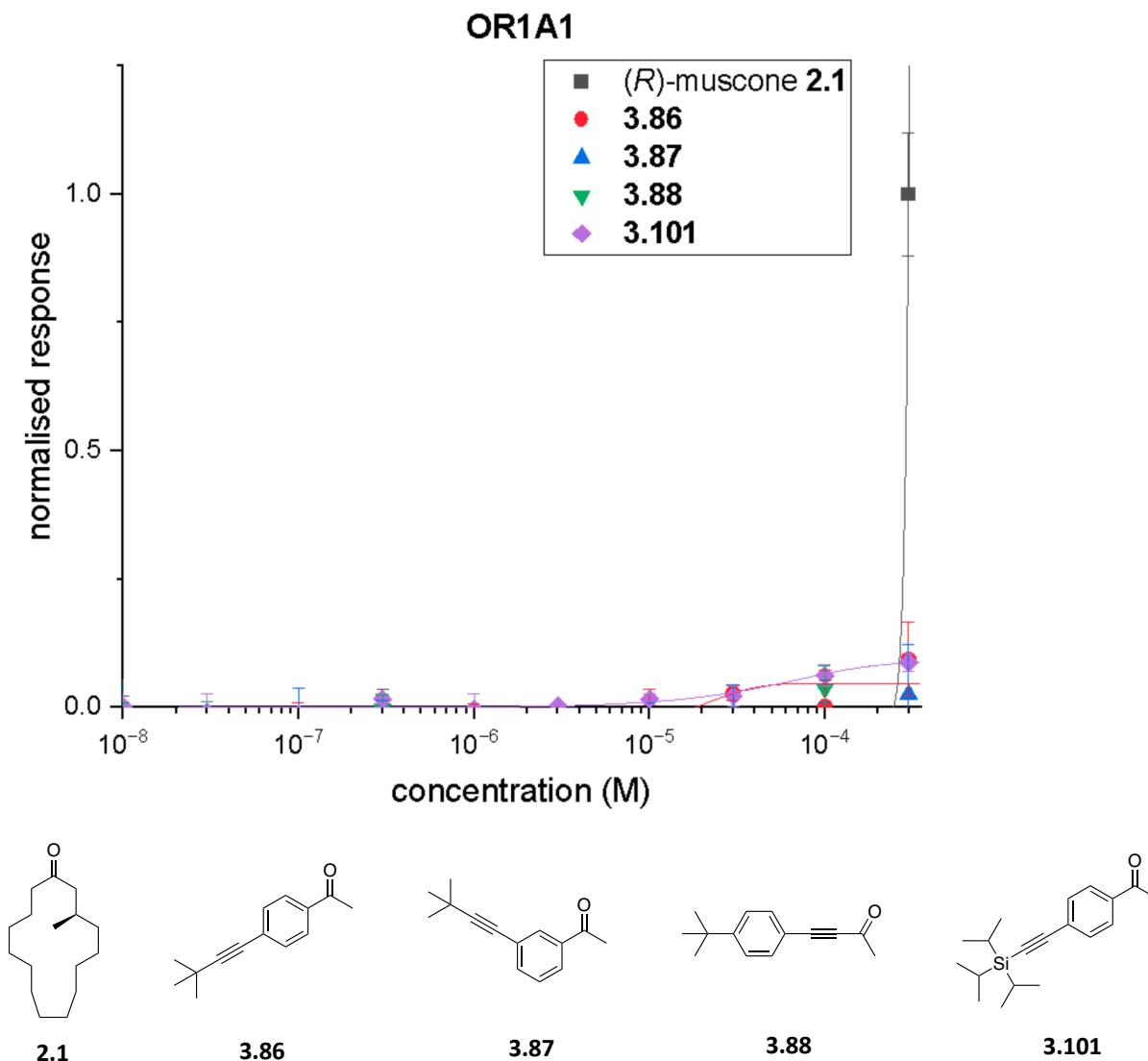


Figure 3.13 – Dose-response curve showing interactions of selected monoacetylenes with OR1A1 olfactory receptor.

3.2.2 Synthesis of initial *bis*-acetylene targets

Following this, the length and rigidity of these compounds was explored by introducing an additional acetylene spacer to test if this would lead to improved activity with the olfactory receptors. With this idea in mind, the selected *bis*-acetylene targets **3.95 – 3.98** were identified, as shown in Figure 3.14.

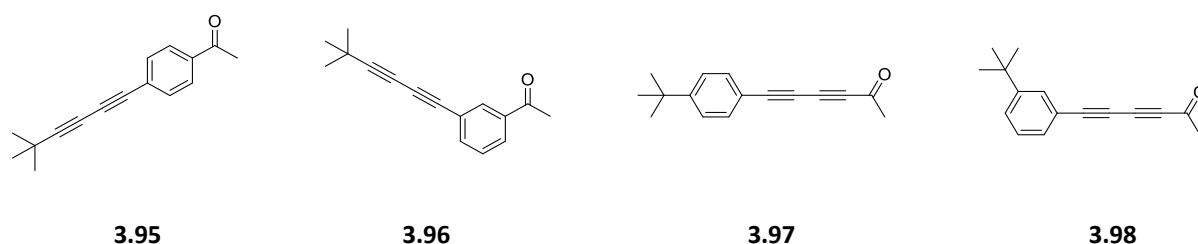
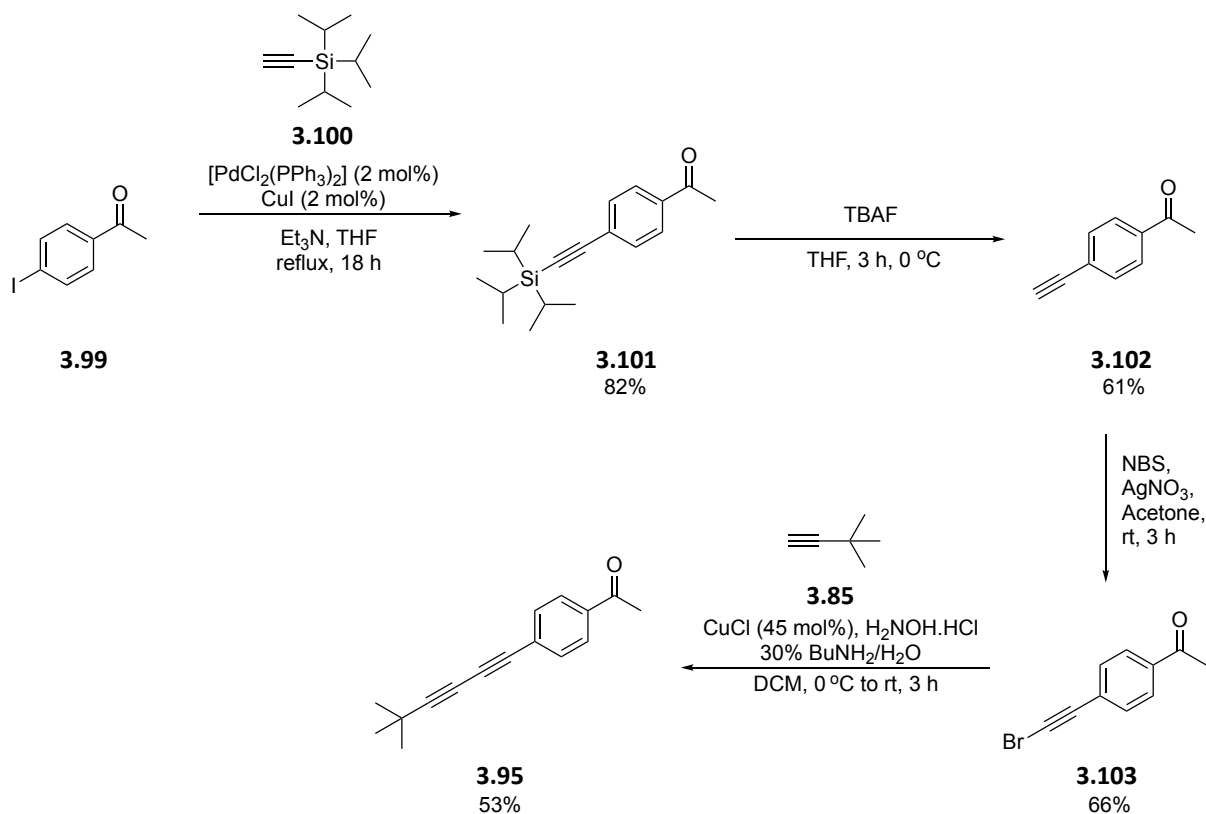


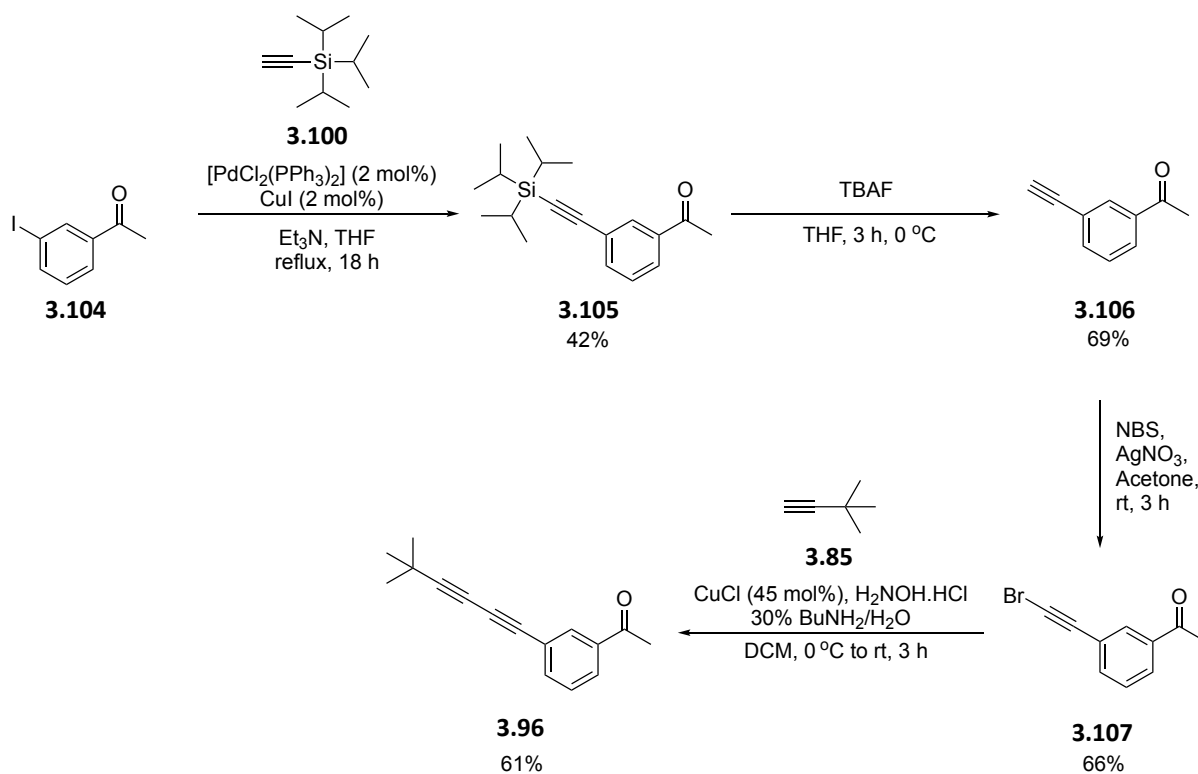
Figure 3.14 – Identified bis-acetylene targets.

Compounds **3.95** and **3.96** were synthesised in a four-step sequence. These targets were similar in structure to the acetophenones **3.86** and **3.87** respectively, however, they have an additional acetylene in the linker connecting the aryl ring to the *tert*-butyl group. The synthesis of **3.95** began with a Sonogashira cross-coupling between 4-iodoacetophenone **3.99** and triisopropylsilylacetylene **3.100** to insert the first acetylene group, producing silylacetylene **3.101** in good yield (82%). A sample of **3.101** was kept aside for testing, as it was similar in structure to monoacetylene target **3.86**. However, due to the hydrophobicity of the silyl group relative to a *tert*-butyl group, it would be more hydrophobic overall than monoacetylene **3.86**. It was of interest to test this more hydrophobic group to see how it effects interactions with the receptor relative to the *tert*-butyl group. However, like **3.86**, compound **3.101** failed to trigger a significant response when assayed against the receptors, as shown in Figure 3.12. Deprotection of acetylene **3.101** by removal of the silyl group using TBAF followed, with the desired product **3.102** obtained in a yield of 61%. The deprotected acetylene **3.102** was then brominated using *N*-bromosuccinimide and silver nitrate in acetone, to yield bromoacetylene **3.103** with a 66% yield. Finally, a Cadiot-Chodkiewicz coupling reaction of bromoacetylene **3.103** with *tert*-butyl acetylene **3.104** gave the desired product **3.95** in a moderate yield of 53%.



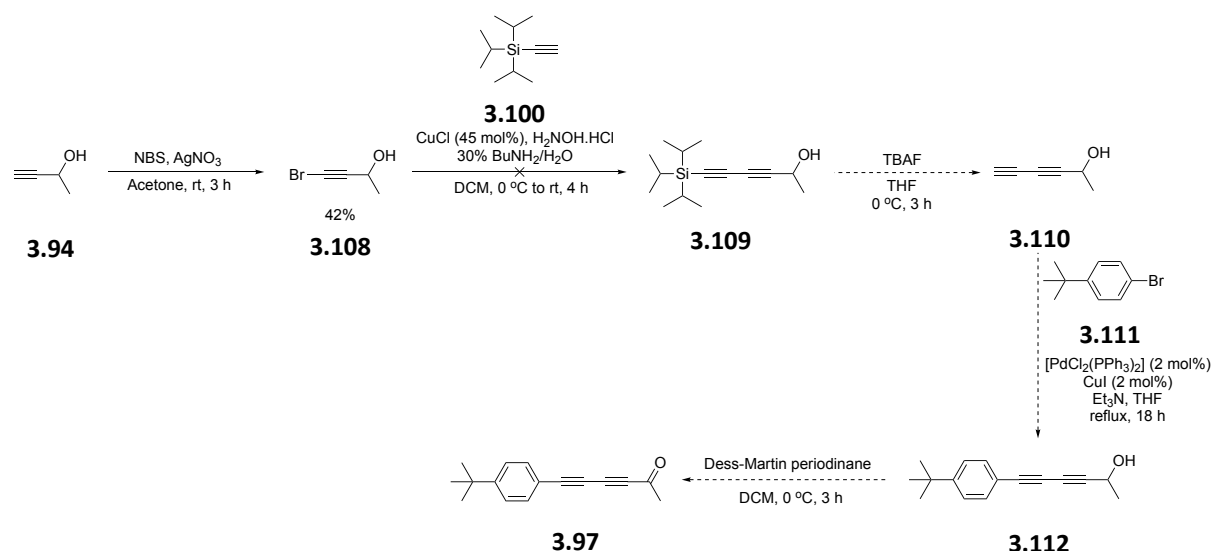
Scheme 3.21 – Synthesis of *para*-bis-acetylene target **3.95**.

Meta bis-acetylene **3.96** was prepared using the same approach, beginning instead with 3-bromoacetophenone **3.104**, as illustrated in Scheme 3.22. This was coupled with triisopropylsilylacetylene **3.100** in a Sonogashira reaction to generate protected *meta*-acetylene **3.105** although in only a modest yield of 42%. Deprotection with TBAF in THF gave the unprotected acetylene **3.106** (69% yield) and then bromination with NBS and silver nitrate generated **3.107** (66% yield) which was reacted in a Cadiot-Chodkiewicz cross-coupling reaction to give the desired product **3.96** in a yield of 61%.



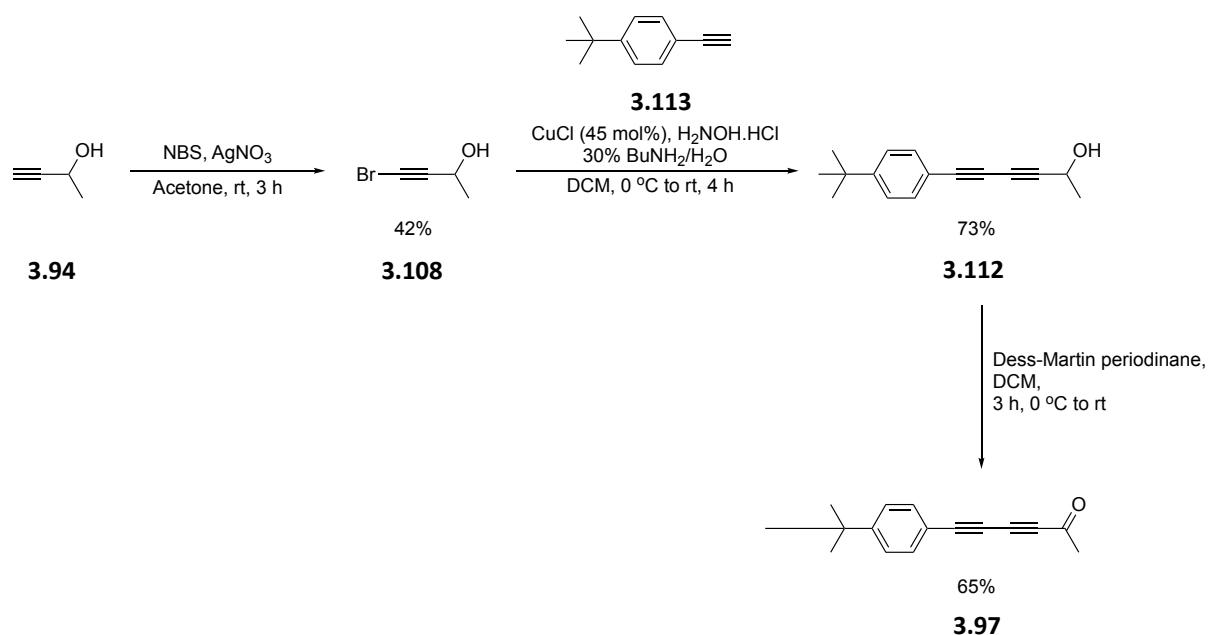
Scheme 3.22 – Synthesis of meta bis-acetylene target **3.96**.

Bis-acetylene **3.97** was also identified as a target. This is an isomer of **3.95** and **3.96**, but with the ketone now bonded directly to the *bis*-acetylene linker. Initial attempts to synthesise this target focused on first building the *bis*-acetylene linker, which would then be coupled to 1-bromo-3-(*tert*-butyl)benzene **3.111** to give the desired product. Accordingly, 3-butyne-2-ol **3.94** was first brominated (NBS/AgNO₃) to give **3.108** with a yield of 42%. This brominated acetylene was then subjected to the Cadiot-Chodkiewicz cross-coupling reaction with triisopropylsilylacetylene **3.100** to hopefully give the protected *bis*-acetylene alcohol **3.109**. However, this reaction was unsuccessful, with no product observed.



Scheme 3.23 – Attempted synthesis of bis-acetylene target **3.97**.

4-(*tert*-Butyl)phenylacetylene **3.113** became commercially available so an alternative three-step synthesis was developed, as illustrated in Scheme 3.24. The target **3.97** was synthesised by first brominating 3-butyn-1-ol **3.94** to give **3.108** in a modest yield of 42%. This was followed by a Cadiot-Chodkiewicz coupling reaction with 4-(*tert*-butyl)phenylacetylene **3.113**, yielding alcohol **3.112** in good yield (73%). A sample of secondary alcohol **3.112** was kept aside for assay, to determine how well the alcohol interacts with the olfactory receptors in comparison to the ketone in **3.97**. Some of alcohol **3.112** was then oxidised using the Dess-Martin periodinane to give the desired *bis*-acetylene ketone **3.97** (65% yield).



Scheme 3.24 – Improved synthesis of bis-acetylene target **3.97**

We then looked to apply the synthesis in Scheme 3.24 to that of *meta bis*-acetylene equivalent **3.98**. However, the corresponding starting material 3-(*tert*-butyl)phenylacetylene **3.114** was found to have limited availability commercially, and the only literature references found for the production of this compound are in patents. Accordingly, it was decided to wait for the assay results of the other targets in this series before considering an alternative synthesis approach.

The three ketones **3.95**, **3.96** and **3.97** along with alcohol **3.112** were sent to our collaborators in Beijing to be assayed against the OR5AN1 and OR1A1 olfactory receptors, as shown in Figures 3.15 and 3.16 respectively. *Meta bis*-acetylene **3.96** gave the strongest response of this series relative to (*R*)-muscone **2.1** when assayed against OR5AN1, triggering a response at a similar concentration to (*R*)-muscone and with a much stronger intensity of response. The compounds exhibited similar EC₅₀ values with OR5AN1, as **3.96** had an EC₅₀ of 26.3 μM whereas (*R*)-muscone **2.1** exhibited an EC₅₀ of 21.0 μM. **3.96** gave a strong response when assayed against OR1A1, with an EC₅₀ of 27.0 μM measured, much lower than that of (*R*)-muscone (248.1 μM). Product **3.95** also gave a promising result, triggering a response at a similar concentration to (*R*)-muscone but with slightly lower intensity, with an EC₅₀ of 12.1 μM when assayed with OR5AN1 and an EC₅₀ of 28.8 μM when assayed with

OR1A1. Interestingly, *meta* bis-acetylene **3.96** triggered a much stronger response than the *para* isomer **3.95**, with **3.96** giving a much greater intensity of response at a lower concentration when interacting with OR5AN1. *Meta* **3.96** also triggered a response from OR1A1 at a lower concentration than *para* **3.95**. This suggests that the *meta* geometry of this series of compounds is more optimal for the interactions with the olfactory receptors than the *para*. Ketone **3.97** however triggered a very limited response when interacting with both olfactory receptors. While alcohol **3.112** gave a weak response relative to (*R*)-muscone, **3.95** and **3.96** against OR5AN1, **3.112** interestingly gave a strong response when assayed against OR1A1, triggering an intense response at a much lower concentration than any other compounds tested in this series. The EC₅₀ of **3.112** with OR5AN1 was 167.8 μM whereas with OR1A1 it was measured as 12.6 μM, showing that **3.112** is significantly more active when assayed against OR1A1 than OR5AN1. This shows that OR1A1 has a stronger affinity for interacting with alcohols than ketones, presumably through a hydrogen bond.

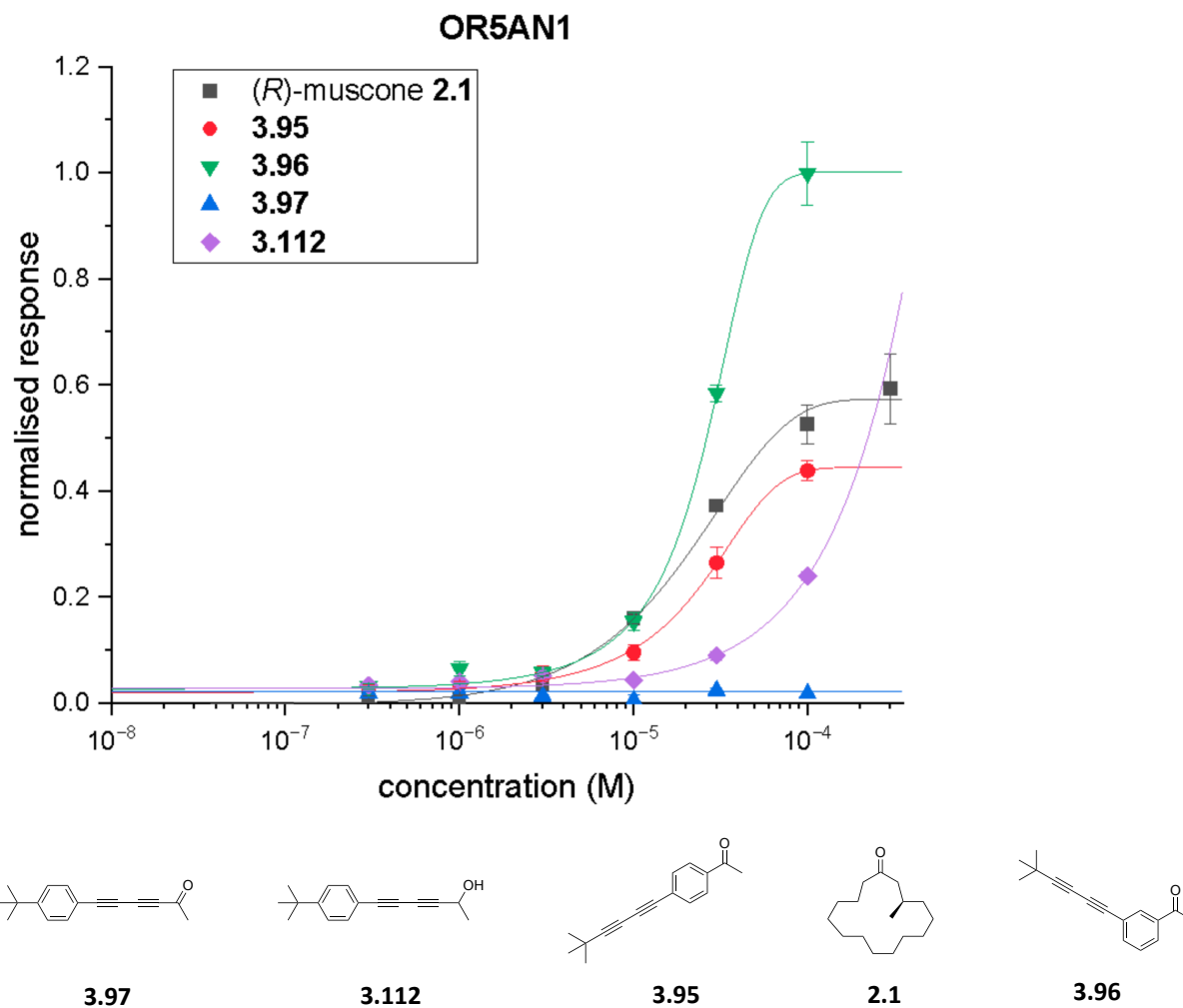


Figure 3.15 – Dose-response curve for interactions of synthesised bis-acetylenes with OR5AN1 receptor with compounds ordered from least (left) to most (right) active.

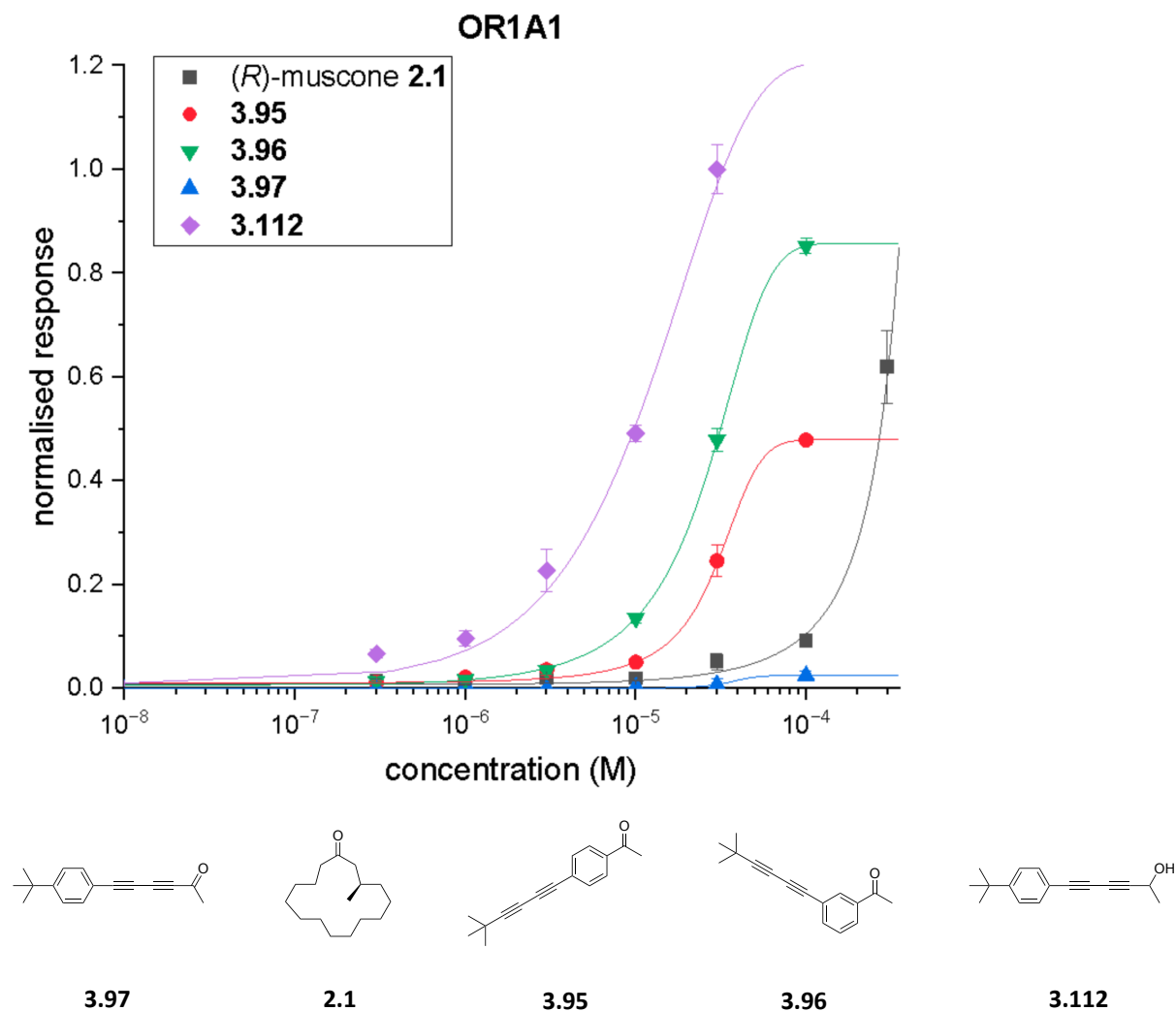


Figure 3.16 – Dose-response curves for interactions of synthesised bis-acetylenes with the OR1A1 receptor with compounds ordered from least (left) to most (right) active.

3.2.3 Synthesis of indanone acetylenes

The programme then looked at influencing the position of the carbonyl group by introducing some constraints. The *bis*-acetylenes introduced in section 3.2.2 are largely rigid, with rotational flexibility only around the acetyl group, which is free to rotate, as illustrated in Figure 3.17. Constraining the acetyl group would enable an exploration as to the optimal orientation of the carbonyl for triggering the olfactory receptors and may lead to enhanced activity if there was a bias towards an optimal conformation.

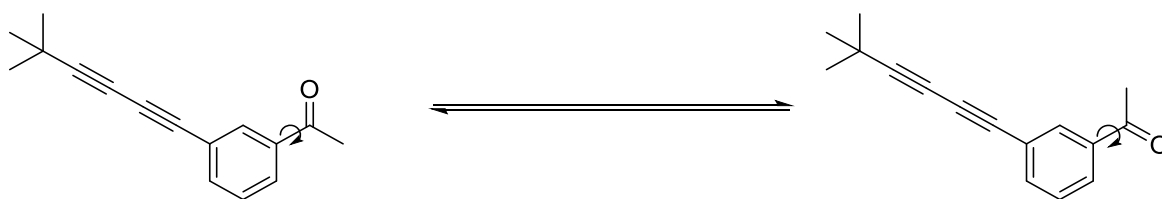


Figure 3.17 – Conformational flexibility within bis-acetylene **3.96**.

Therefore, *bis*-acetylenes **3.115** and **3.116** containing 5-membered rings in place of the free acetyl group became targets, as shown in Figure 3.18. These physically lock the carbonyl group into a fixed orientation and maintain a *meta* geometry, which appeared to be the optimal geometry for interaction with the receptors.

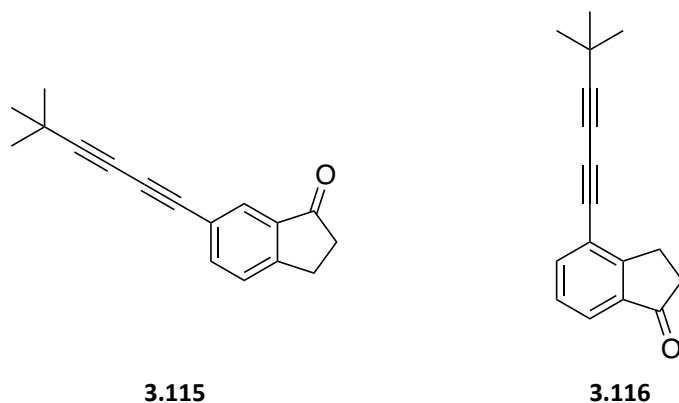
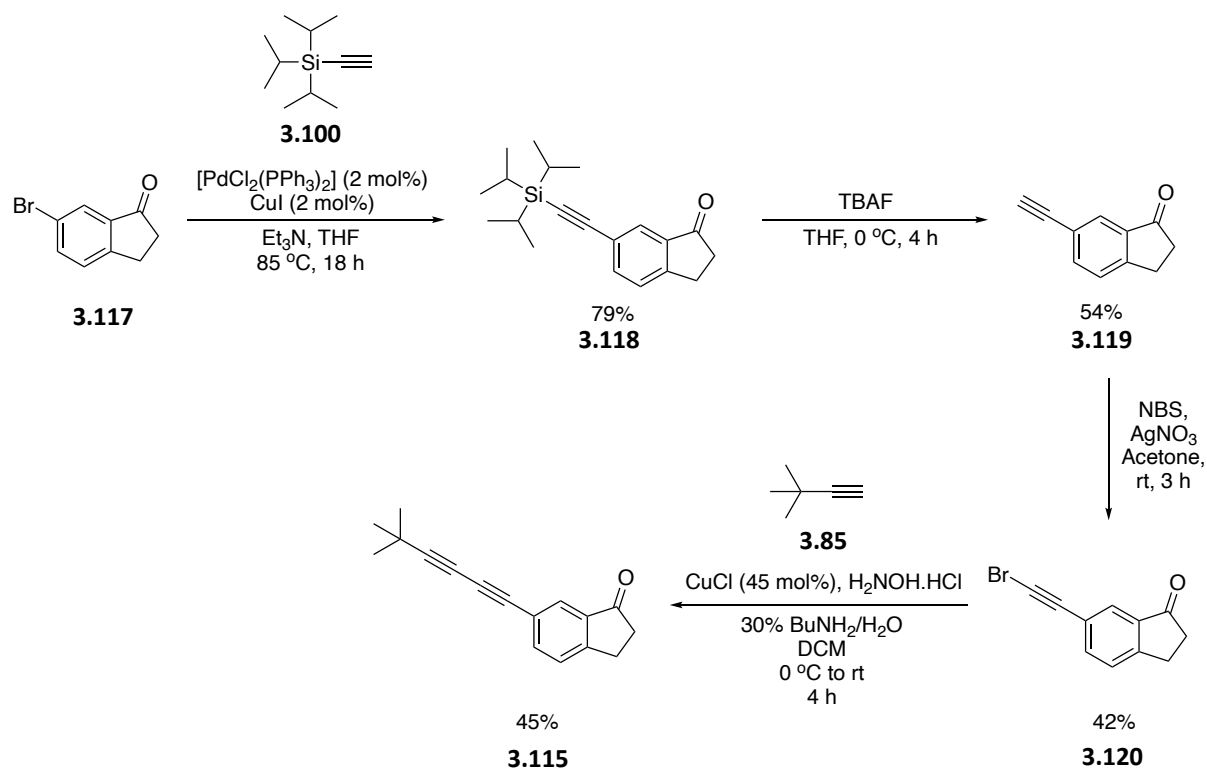


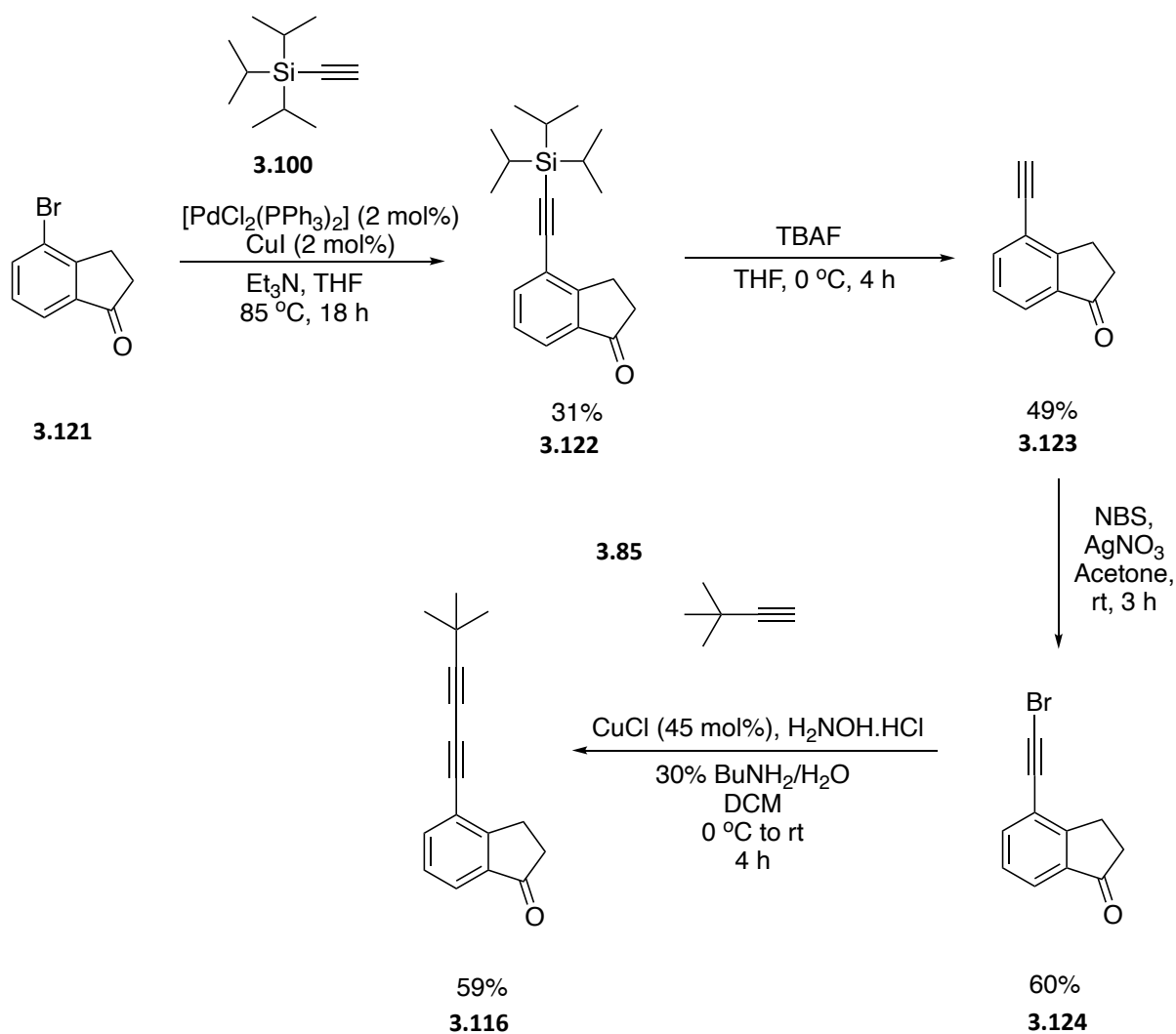
Figure 3.18 – Identified indanone bis-acetylene targets **3.115** and **3.116**.

These targets were synthesised using the general approach illustrated in Scheme 3.21. 6-Bromo-1-indanone **3.117** was first reacted in a Sonogashira reaction with tri(isopropylsilyl)acetylene **3.100** to install the first acetylene unit to give **3.118** (79% yield). This acetylene was then deprotected using TBAF in THF to give **3.119** in a moderate yield (54%). The deprotected acetylene was then brominated using N-bromosuccinimide and silver nitrate to give **3.120** (42% yield) which was then coupled with *tert*-butylacetylene **3.85** in a Cadiot-Chodkiewicz reaction to give the desired product, **3.115** in a yield of 45%.



Scheme 3.25 – Synthesis of indanone bis-acetylene **3.115**.

The same process was repeated with 4-bromo-1-indanone **3.121** to prepare isomer **3.116** as illustrated in Scheme 3.26. A Sonogashira cross-coupling of **3.121** with triisopropylsilylacetylene **3.100** gave the silyl-protected acetylene **3.122** in a modest yield (31%). Deprotection with TBAF in THF gave acetylene **3.123** (49% yield) which was brominated to generate **3.124** in a yield of 60%. This was followed by a Cadiot-Chodkiewicz cross-coupling of **3.124** with *tert*-butyl acetylene **3.85** to give the desired *bis*-acetylene target **3.116** in a yield of 59%.



Scheme 3.26 – Synthesis of indanone bis-acetylene **3.116**.

The assay outcomes of these indanone isomers **3.115** and **3.116** and the *bis*-acetylenes **3.96** and **3.112** with OR5AN1 and OR1A1 are shown below in Figures 3.19 and 3.20 respectively. The results showed that the indanone acetylene compounds are less good and require a much higher concentration than *meta* **3.96** to trigger a response from OR5AN1 and at a much higher concentration than **3.96** and alcohol **3.112** to trigger a response from OR1A1. **3.116** has an EC₅₀ value of 228.8 μM when assayed with OR5AN1, as determined from the dose-response curve. This is a much greater value than that of **3.96** measured from the same curve (39.9 μM). The EC₅₀ value for **3.116** when assayed with OR1A1 was 113.9 μM, much greater than that of alcohol **3.112** (9.82 μM) or of *meta* **3.96** (51.5 μM). This suggests that the indanone shape is less optimal than the linear *bis*-acetylene shape for triggering a response on the olfactory receptors. When comparing **3.115** and **3.116**, it appears that the

orientation of the carbonyl group is influential in determining the strength of interactions with the receptors, as **3.116** triggered a much greater response at a lower concentration than **3.115** against both OR5AN1 and OR1A1. The ‘downwards’ carbonyl in **3.116** appears to strengthen the interaction with the olfactory receptors relative to the ‘upwards’ orientation in **3.115**, although the ring carbons may also play a role in the relative activities.

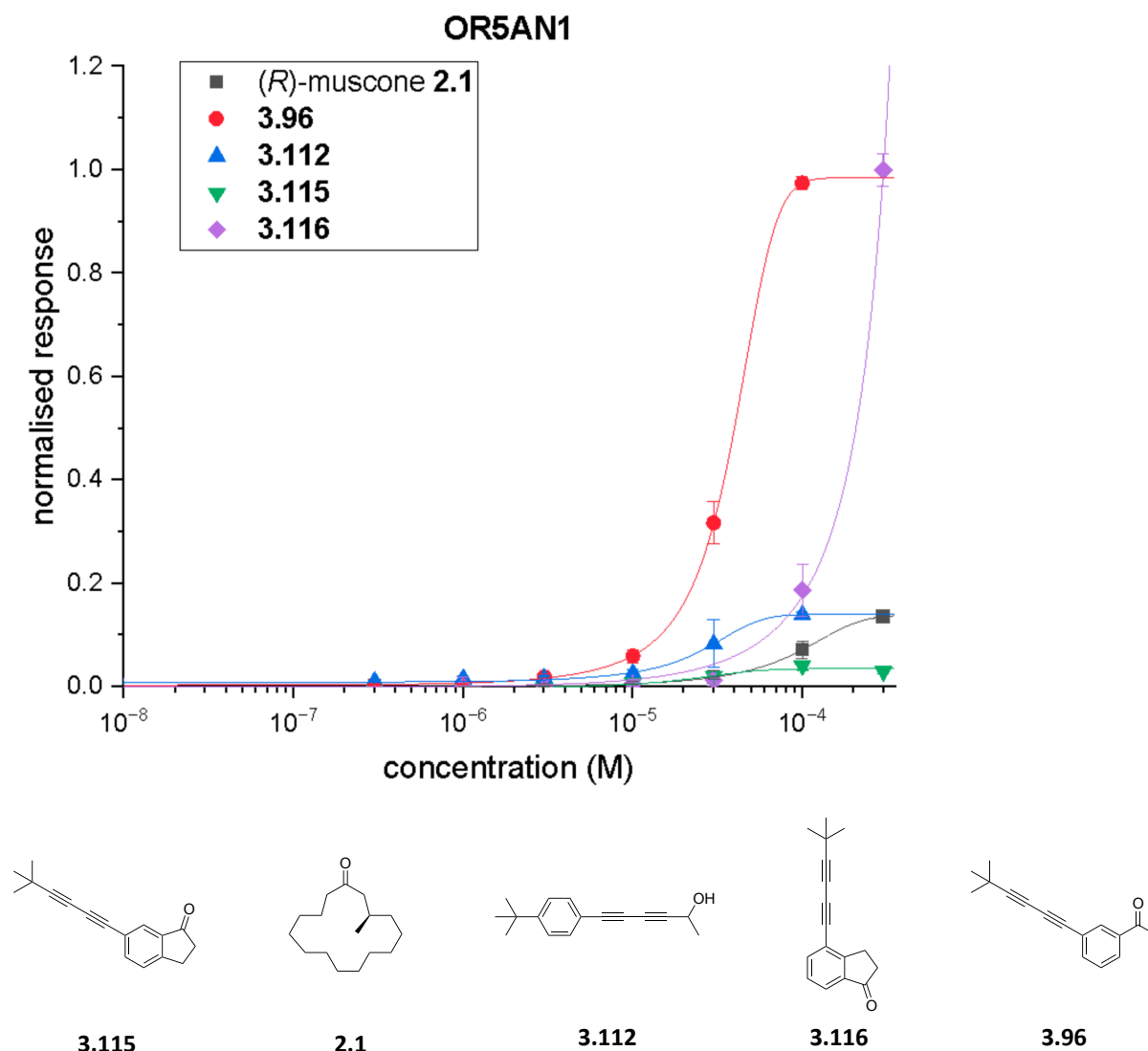


Figure 3.19 – Dose-response curve of interactions of indanone bis-acetylenes and linear bis-acetylenes **3.96** and **3.112** with OR5AN1 receptor, with compounds shown in order from least active (left) to most active (right).

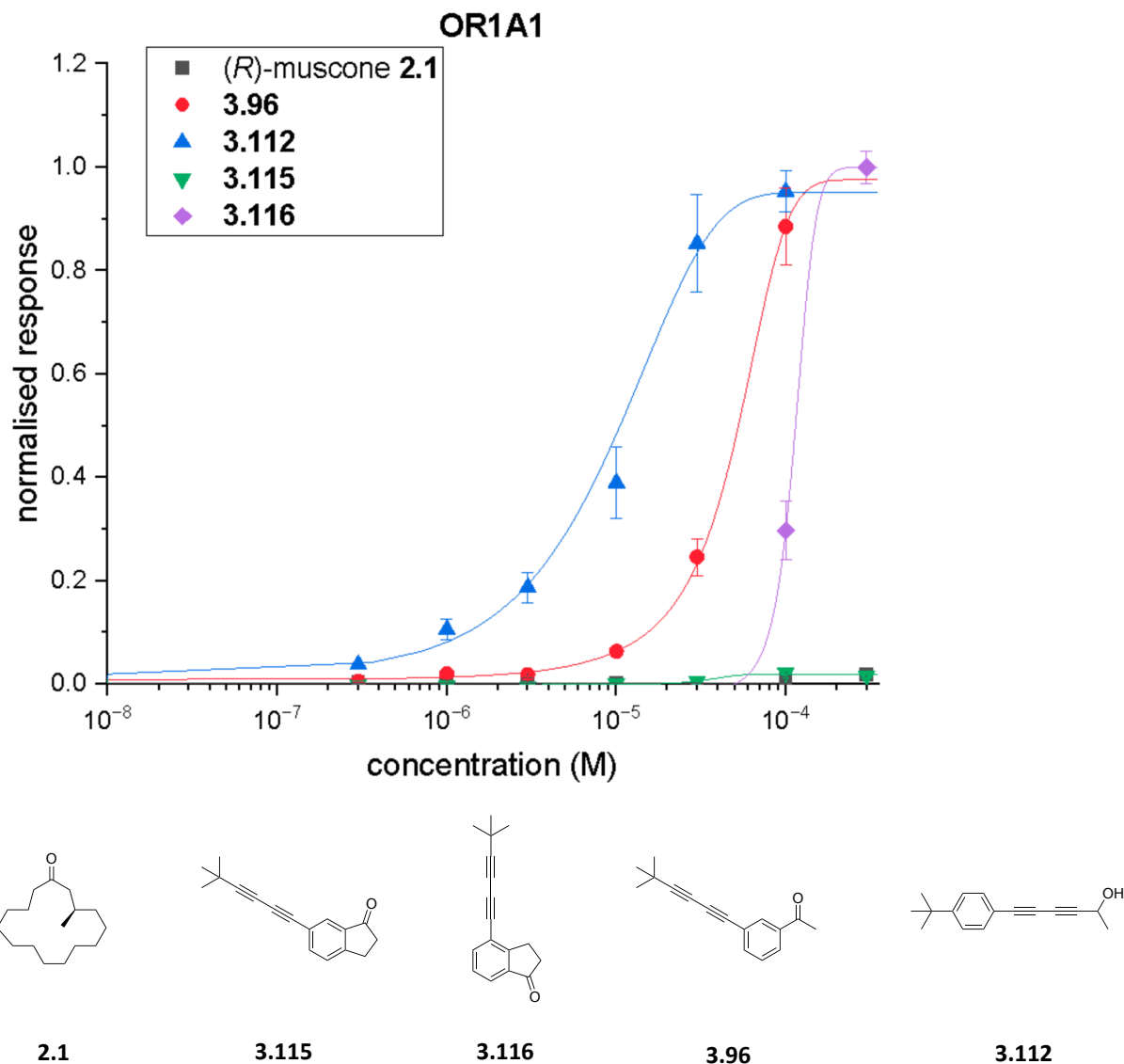


Figure 3.20 – Dose-response curves of interactions of indanone bis-acetylenes and linear bis-acetylenes **3.96** and **3.112** with OR1A1 receptor, with compounds shown in order from least (left) to most (right) active.

3.2.4 Synthesis of fluorinated *bis*-acetylenes

One aspect of the project aimed to introduce an electronic conformational bias into the *meta* bis-acetylenes. This was envisaged by strategically placing a fluorine onto the aromatic ring. The introduction of fluorine *ortho* to an acetyl group within acetophenone has been shown to bias the position of the carbonyl group so that the fluorine and the carbonyl are oriented away from each other.¹⁷⁶ This orientation is favoured as the carbonyl oxygen and

the fluorine repel each other and their *anti* orientation minimises the overall molecular dipole, as illustrated in Figure 3.21. Strategic replacements of aryl hydrogens for fluorine should test the effect of the orientation of the carbonyl group on the interactions of the molecule with the receptor, assuming the fluorine does not introduce a significant steric influence.

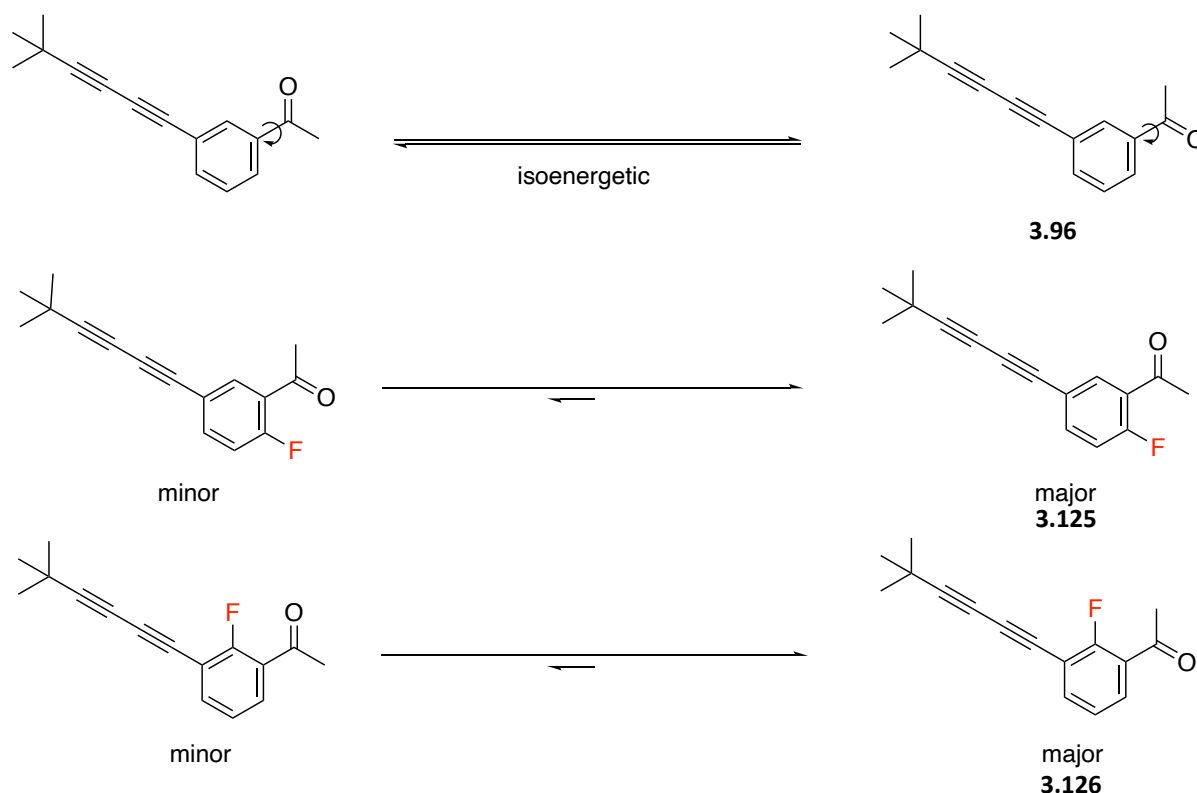
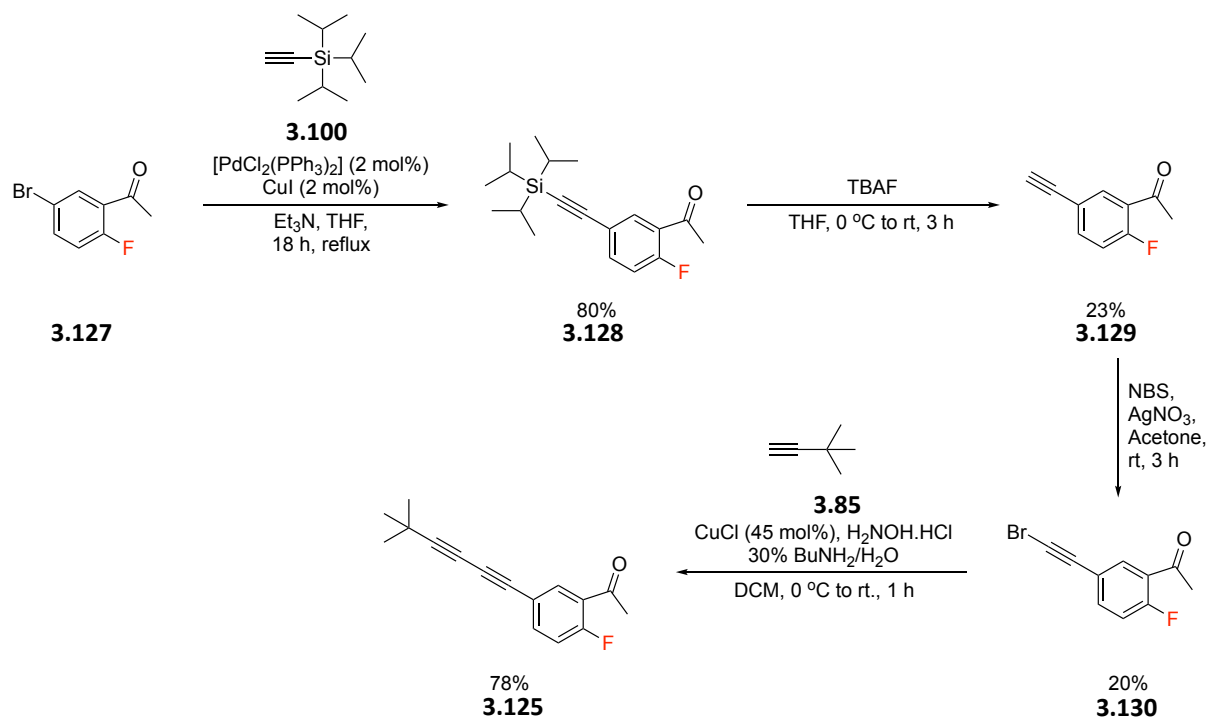


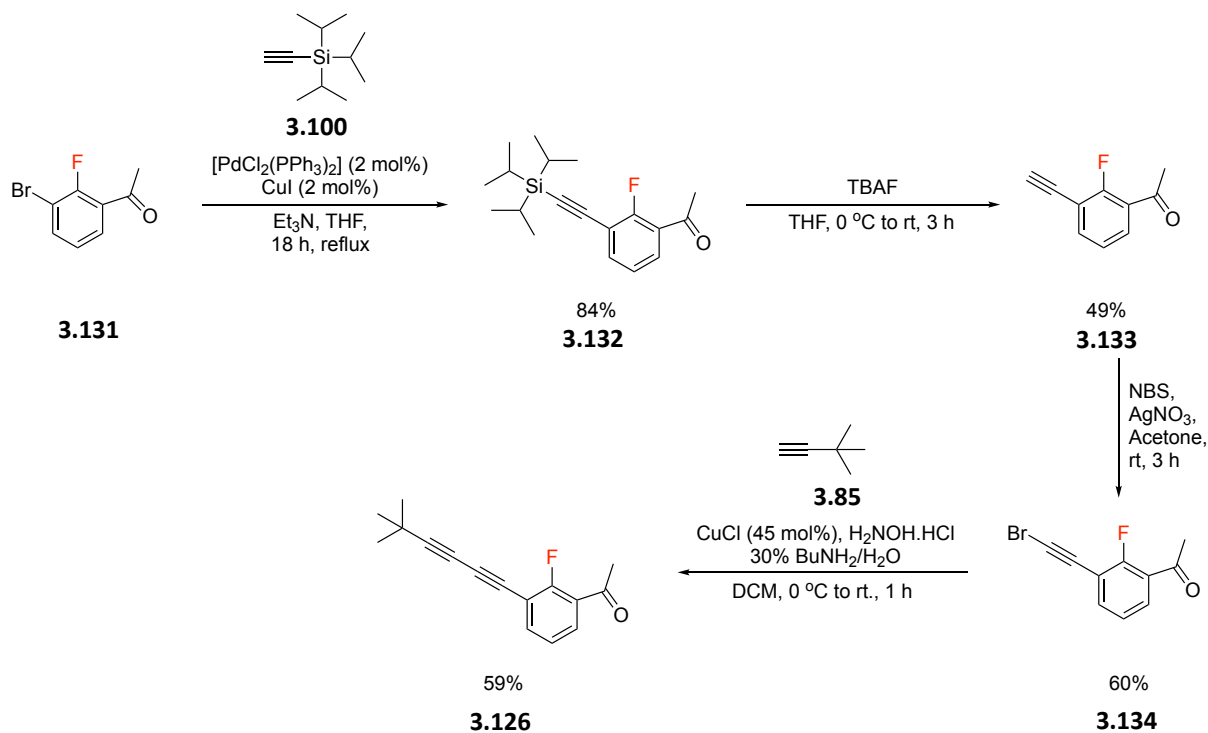
Figure 3.21 – Identified fluorinated bis-acetylene targets **3.125** and **3.126** and the predicted conformational bias of their carbonyl groups.

The fluorinated *bis*-acetylenes were synthesised by the approach shown in Scheme 3.21 but using the appropriate aryl fluorides as starting materials, as illustrated in Scheme 3.27. 1-(3-Bromo-2-fluorophenyl)-1-ethanone **3.127** underwent a Sonogashira reaction with tri(isopropylsilyl)acetylene **3.100** to install the first acetylene unit, giving **3.128** in an 80% yield. This acetylene was then deprotected (TBAF/THF) giving **3.129** (23%), which was then brominated to make **3.130** in a yield of 20%. The brominated acetylene was then coupled with *tert*-butylacetylene **3.85** in a Cadiot-Chodkiewicz reaction to give the desired product, **3.125** in an efficient last step (78% yield).



Scheme 3.27 – Synthesis of fluorinated meta bis-acetylene **3.125**.

The same process was repeated with 1-(5-bromo-2-fluorophenyl)-1-ethanone **3.131** to prepare **3.126** as summarised in Scheme 3.28.



Scheme 3.28 – Synthesis of fluorinated meta bis-acetylene **3.126**.

These two fluorinated derivatives were assayed against the olfactory receptors OR5AN1 and OR1A1, as shown in Figures 3.22 and 3.23 respectively. In each case it was found that **3.125** triggered a stronger response than **3.126**, requiring a lower concentration to do so. Thus, the data indicates that the carbonyl being oriented 'upwards' as drawn in **3.125**, interacts more strongly than the 'downwards' carbonyl in **3.126**. Interestingly, although **3.125** required a higher concentration than (*R*)-muscone **2.1** in order to trigger a response from OR5AN1, the overall response from **3.125** had a much higher intensity than (*R*)-muscone. With OR5AN1, **3.125** has an EC₅₀ of 133.1 μM and **3.126** has a much higher value of 258.0 μM, while (*R*)-muscone has a value of 37.7 μM. With OR1A1, **3.125** required a lower concentration to trigger a response than (*R*)-muscone **2.1** and again with a greater intensity, showing its potency. **3.125** had an EC₅₀ value of 117.8 μM, while (*R*)-muscone **2.1** had a value of 35.1 μM. The other isomer **3.126**, although less impressive overall still displayed some positive activity, particularly with the OR1A1 receptor, where it required a similar concentration as (*R*)-muscone to trigger a response by OR1A1. **3.126** had an EC₅₀ value of 216.3 μM with OR1A1, much larger than that of **3.125**. However, the response of **3.126** then became much greater than (*R*)-muscone with increasing concentration.

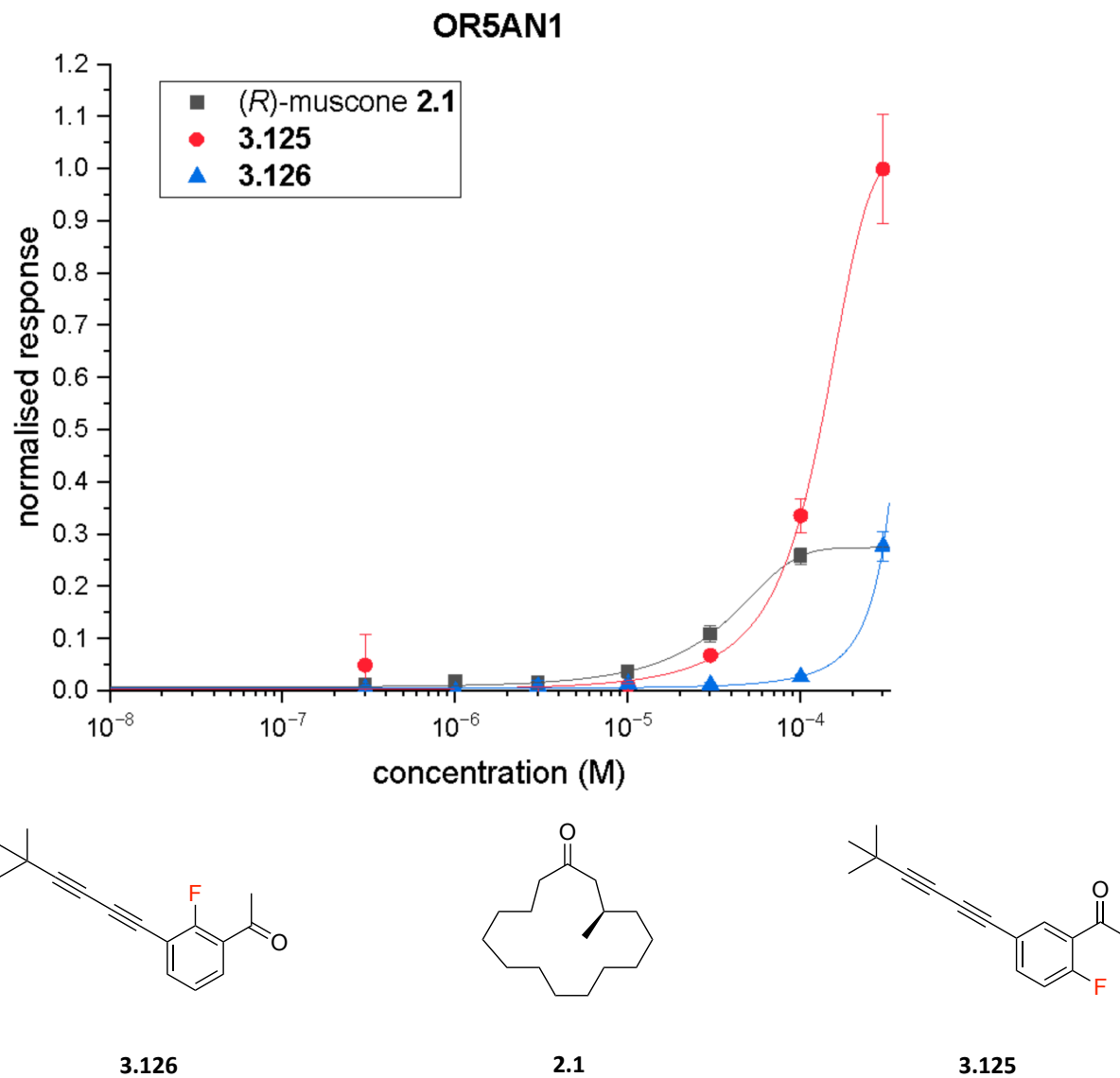
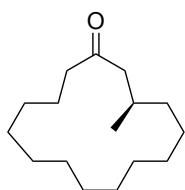
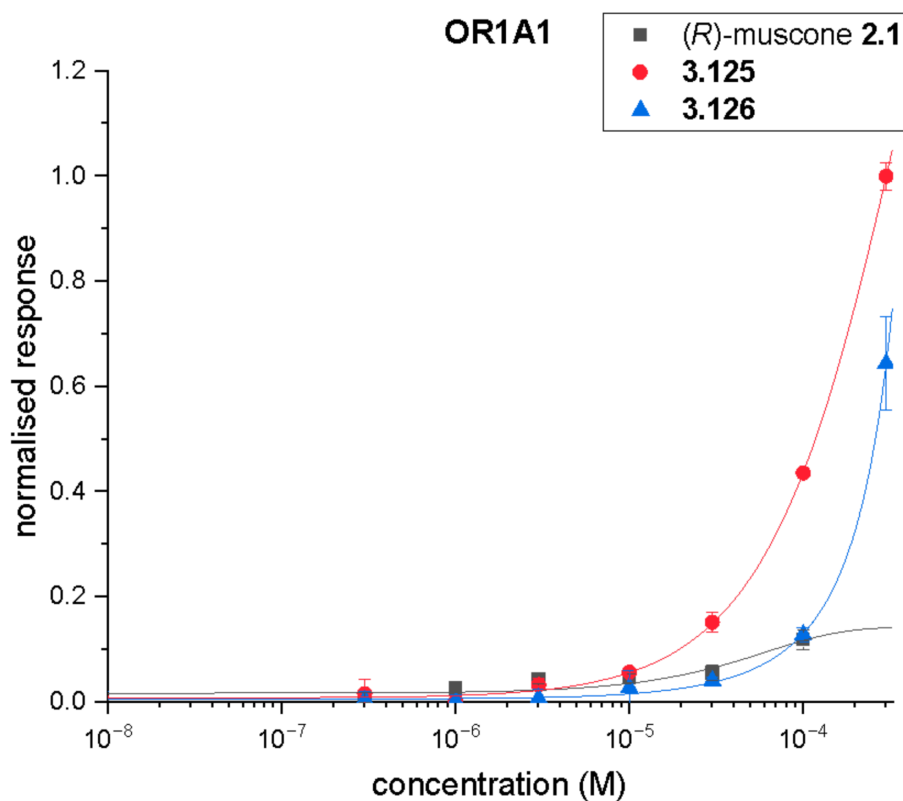
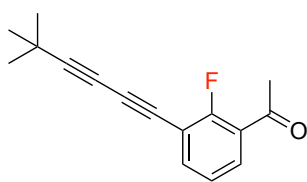


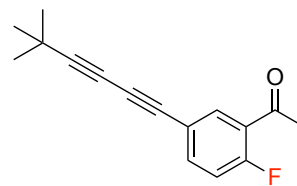
Figure 3.23 – Dose-response curves of the synthesised fluorinated meta bis-acetylenes and (R)-muscone with OR5AN1 receptor with compounds shown from least (left) to most (right) active.



2.1



3.126



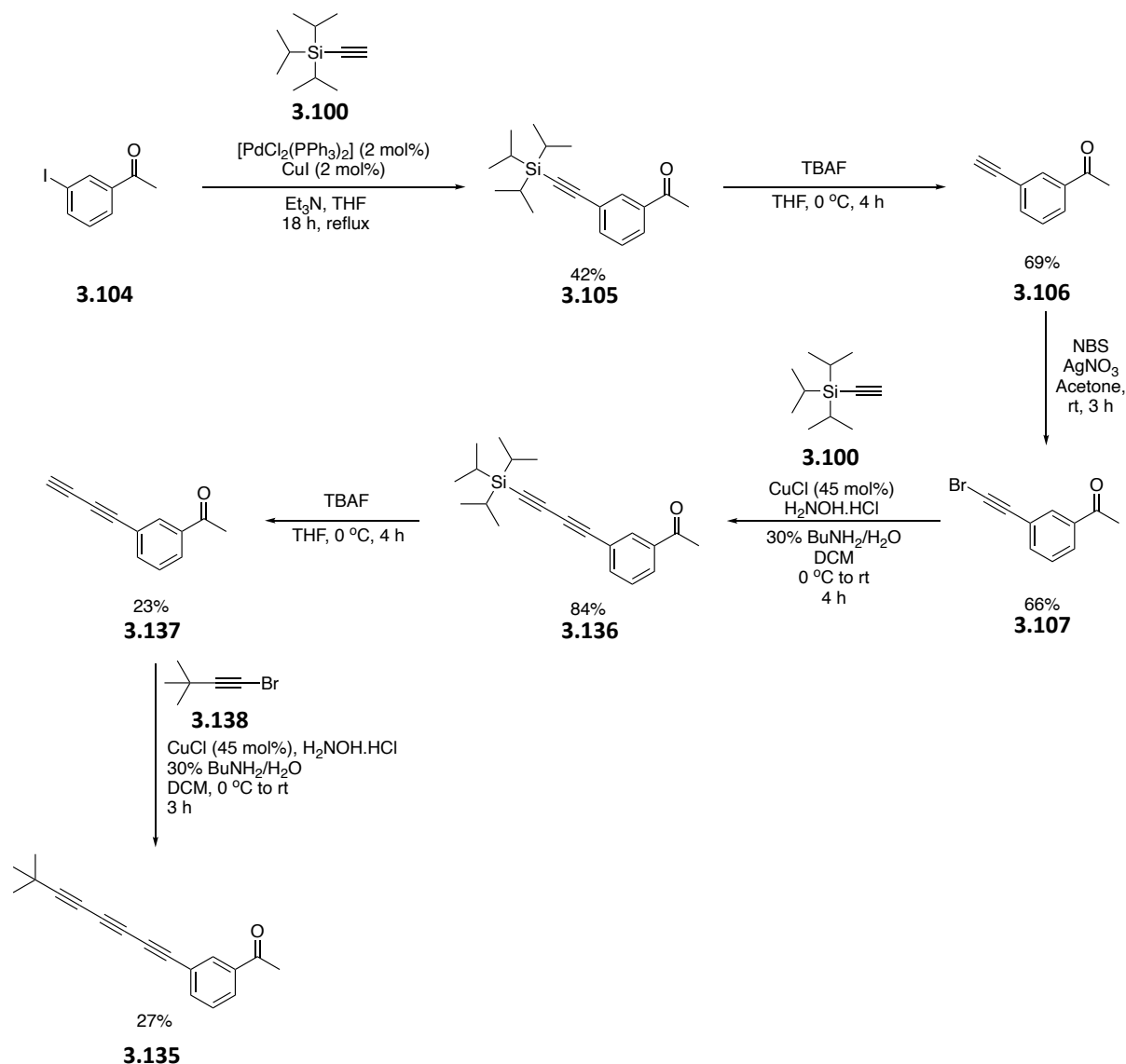
3.125

Figure 3.24 – Dose-response curves of the synthesised fluorinated meta bis-acetylenes and (*R*)-muscone with OR1A1 receptor, with compounds ordered from least (left) to most (right) active.

In terms of orienting the carbonyl geometry ‘upwards’ or ‘downwards’ for a maximum effect, the outcomes here for **3.125** and **3.126**, appear to give the opposite trend relative to the indanone derivatives **3.115** and **3.116** (Figure 3.20) discussed above. Thus, although carbonyl orientation had a clear effect within each series, no clear conclusion could be drawn *between* the molecular series. The introduction of the indanone ring in one case and the aryl fluorines in the other is clearly also influencing receptor activity.

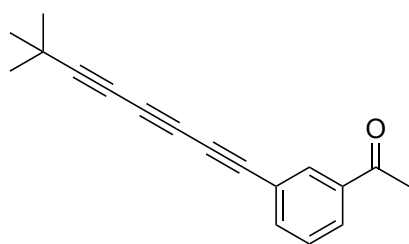
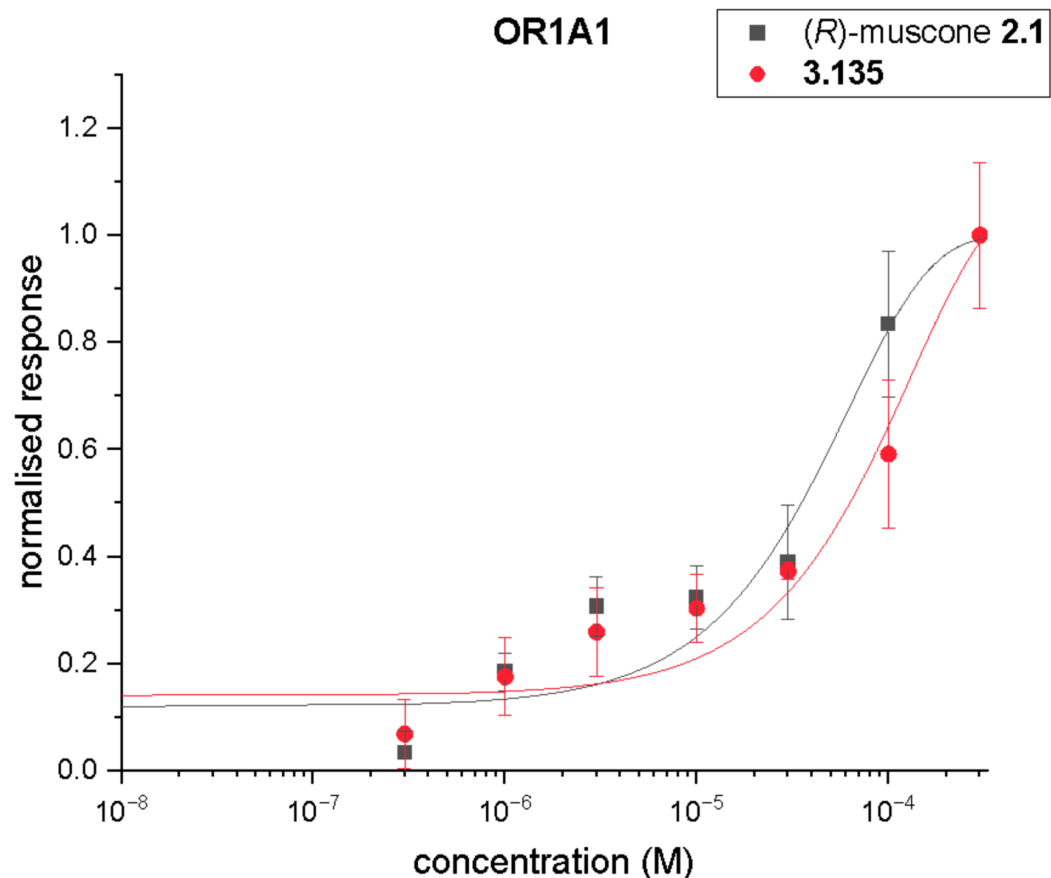
3.2.5 Synthesis of a *tris*-acetylene derivative

A synthesis of the *tris*-acetylene **3.135**, extending *meta bis*-acetylene **3.96** by an additional acetylene unit, was also developed to test the steric limit of the acetylene linker. This target would feature a *tris*-acetylene spacer attached *meta* to an acetophenone, and with a terminal *tert*-butyl group. This was prepared via a series of cross-coupling reactions similar to the synthesis first shown in Scheme 3.21. Accordingly, 3-iodoacetophenone **3.104** was first reacted with tri(isopropyl)silylacetylene **3.100** in a Sonogashira cross-coupling reaction to install the first acetylene unit, and giving **3.105**, which was isolated with a yield of 42%. Silyl deprotection with TBAF gave acetylene **3.106** (69% yield) which was then brominated to generate **3.107** in a yield of 66%. **3.107** was then coupled with tri(isopropylsilyl)acetylene **3.100** in a Cadiot-Chodkiewicz cross-coupling reaction to install the second acetylene unit, giving **3.136** in a remarkably good yield of 84%. Again, silyl deprotection generated *bis*-acetylene **3.137** (23% yield) which was combined with 1-bromo-3,3-dimethylbut-1-yne **3.138** in a final Cadiot-Chodkiewicz cross-coupling reaction. The yield was modest (27%) but the product was purified by chromatography and gave sufficient **3.135** (4.3 mg) for assay.

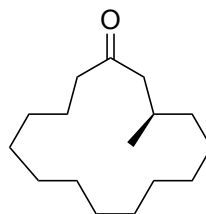


Scheme 3.29 – Synthesis of meta tris-acetylene **3.135**.

Tris-acetylene **3.135** was an active compound, particularly with the OR1A1 receptor, as shown in Figures 3.25 and 3.26. It required a higher concentration than (*R*)-muscone to trigger a response with OR5AN1 but a similar concentration with OR1A1, as shown in Figure 3.22. The EC₅₀ value for **3.135** with OR5AN1 was 190.6 μM, much higher than that of (*R*)-muscone **2.1** (38.1 μM). The EC₅₀ with OR1A1 is much lower than with OR5AN1 for **3.135**, with a value of 72.6 μM, although this is still greater than the value for (*R*)-muscone (35.1 μM). None the less it was less active than most of the *bis*-acetylenes discussed above. These outcomes indicate that increasing the acetylene linker units from two to three has a detrimental effect. Given also that the *bis*-acetylenes are more active than those with a



3.135



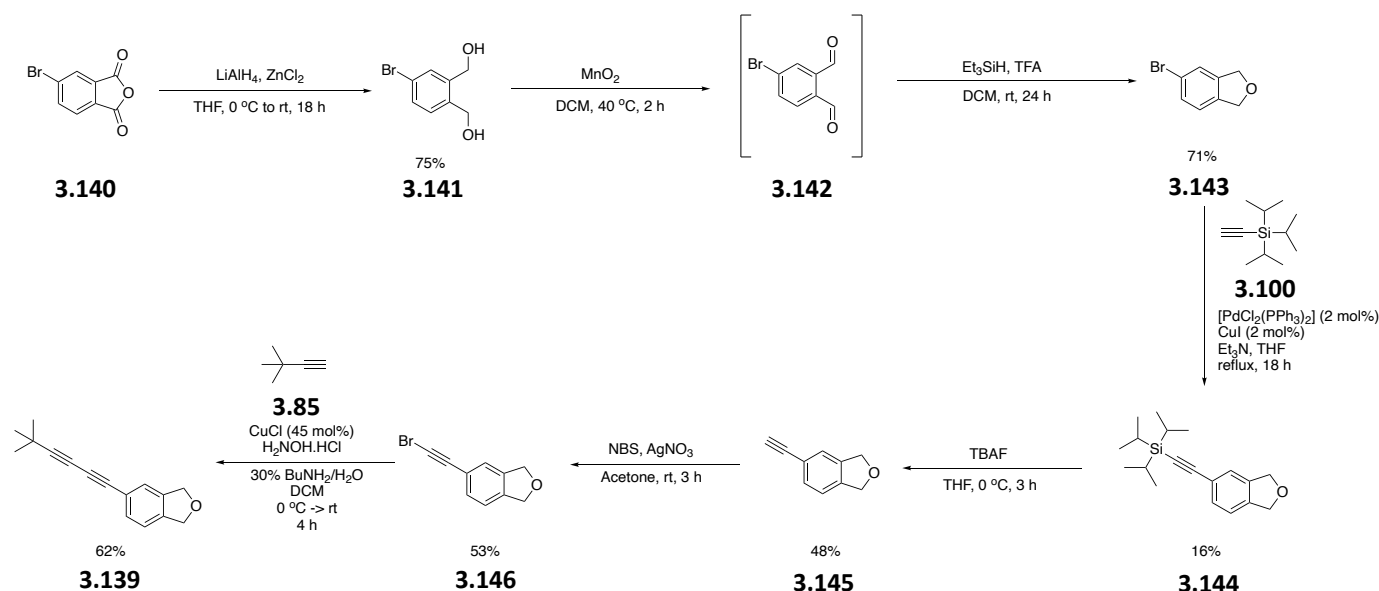
2.1

Figure 3.26 – Dose-response curve showing the interactions of meta tris-acetylene derivative **3.135** with OR1A1 relative to (*R*)-muscone **2.1**, with compounds shown from least (left) to most (right) active.

3.2.6 Synthesis of a dihydroisobenzylfuran *bis*-acetylene derivative

The combination of structure-activity relationships outlined above led to the synthesis of the dihydroisobenzylfuran *bis*-acetylene derivative **3.139**. This is a polycyclic target similar to the indanones, but with a *bis*-acetylene spacer again positioned in an attempt to mimic the more optimal *meta* geometry. This compound was synthesised in several steps as

summarised in Scheme 3.30. The commercially available cyclic anhydride **3.140** was ring opened by reduction to diol **3.141** using LiAlH₄ with zinc chloride. Cyclisation to form the dihydroisobenzylfuran **3.142** was achieved in a one-pot two-step reaction sequence where diol **3.141** was first oxidised to dialdehyde **3.143** using manganese dioxide (MnO₂) in DCM. Dialdehyde **3.143** was not isolated but instead, the unreacted MnO₂ was filtered off, and then cyclisation was achieved after the addition of triethylsilane and trifluoroacetic acid. This two-step process was quite efficient with an overall yield of 71%. Benzofuran **3.142** could then undergo a series of cross-coupling reactions through its aryl bromide. It was first coupled with tri(isopropyl)silylacetylene **3.100** in a Sonogashira cross-coupling reaction and then silyl deprotected to give acetylene **3.145**. This was then converted to bromo-acetylene **3.146** for a final Cadiot-Chodkiewicz reaction to generate the target product **3.139**.



Scheme 3.30 – Synthesis of dihydroisobenzylfuran bis-acetylene **3.139**.

When assayed against OR5AN1 and OR1A1, *bis*-acetylene **3.139** gave a strong response, as shown in Figure 3.27 and Figure 3.28 respectively. It can be compared to the fluorinated *bis*-acetylene **3.125**, where it required a slightly higher concentration to trigger a response, however, the intensity of response from **3.139** increased more rapidly. This response was especially strong when interacting with OR5AN1. **3.139** had an EC₅₀ value of 91.1 μM when interacting with OR5AN1, much lower than that of fluorinated **3.125** (427.4 μM). **3.139** also triggered a strong response with the OR1A1 receptor, requiring only a slightly higher

concentration than alcohol **3.112** to trigger a similar response and showing a greater increased intensity of response. **3.139** had an EC₅₀ value of 73.2 μM with OR1A1, similar to that of alcohol **3.112** (56.2 μM) and much lower than that of fluorinated **3.125** (323.3 μM).

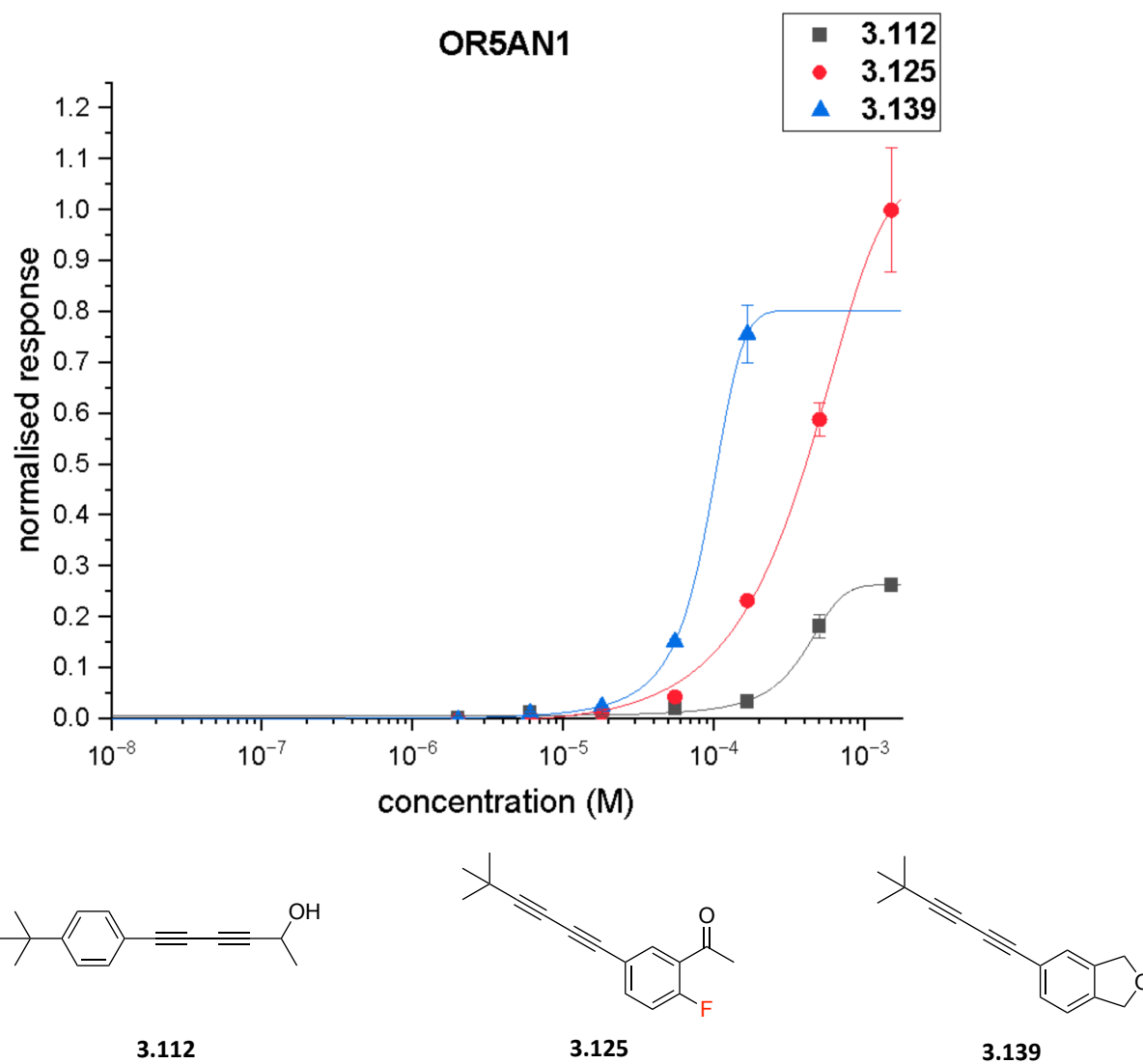


Figure 3.27 – Dose-response curves showing interactions of **3.139** relative to **3.112** and **3.125** with OR5AN1 olfactory receptor, with compounds ordered from least active (left) to most active (right).

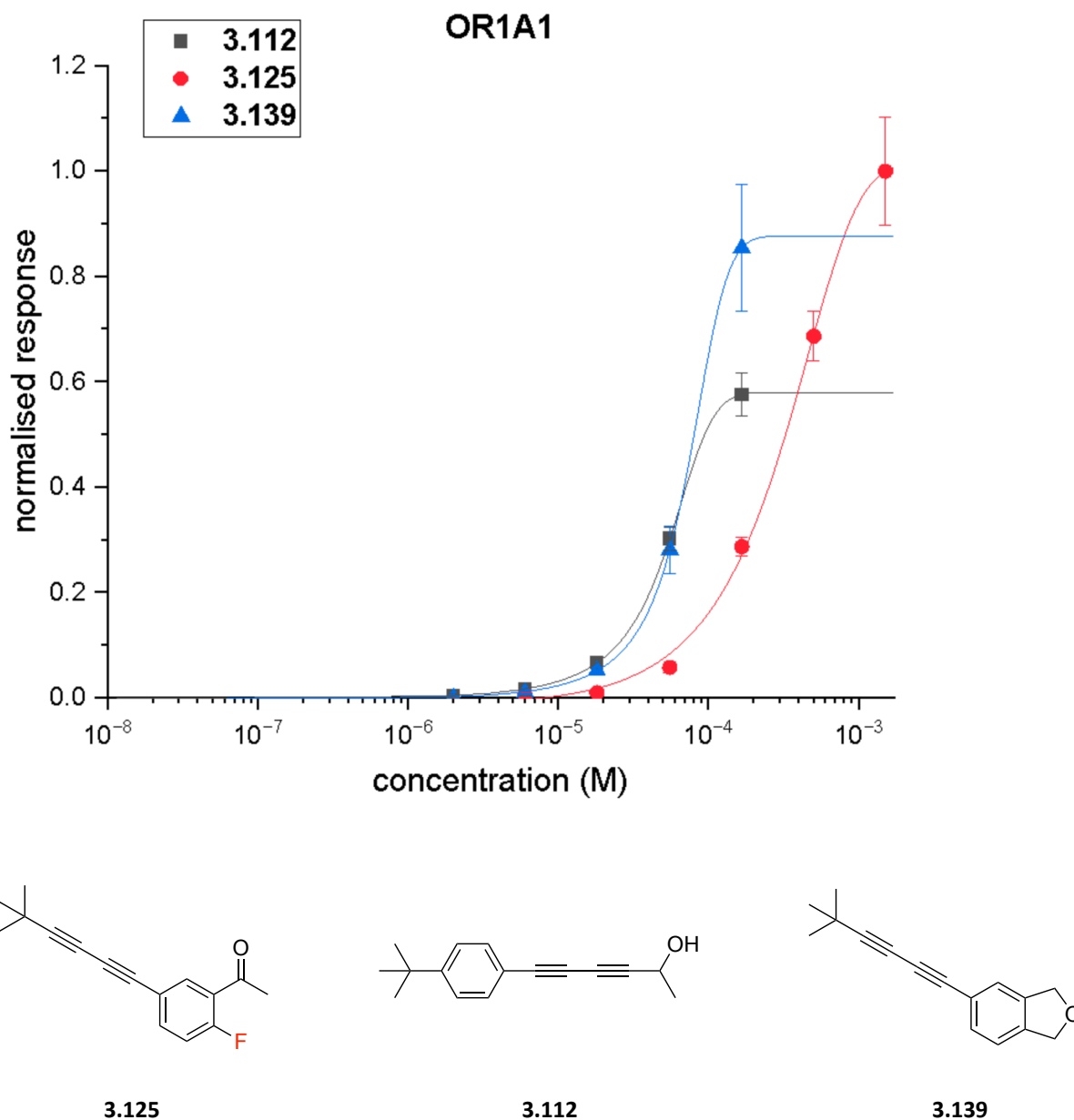


Figure 3.28 – Dose-response curves showing interactions of **3.139** relative to **3.112** and **3.125** with OR1A1 olfactory receptor, with compounds ordered from least active (left) to most active (right).

3.2.7 Synthesis of primary, tertiary and secondary alcohol *bis*-acetylenes

The programme also focused on investigating the earlier promising result with *bis*-acetylene alcohol **3.112**. This secondary alcohol showed strong interactions with the OR1A1 receptor (Figure 3.16). It is clearly structurally different from the compounds assayed so far as it offers the potential as a good hydrogen bonding donor. The role of the alcohol moiety was

further explored by preparing both primary **3.147** and tertiary alcohol **3.148** derivatives by either adding or subtracting a methyl group, the smallest alkyl group. Additionally, these derivatives are non-chiral, unlike **3.112**, and this removes an additional degree of complexity.

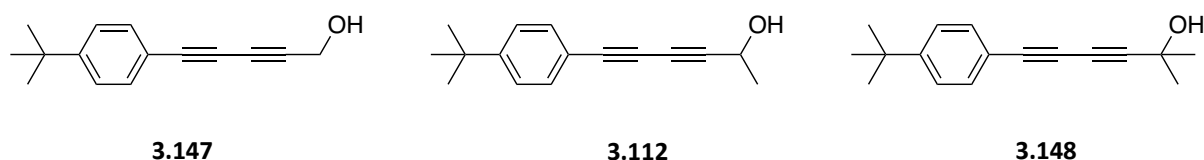
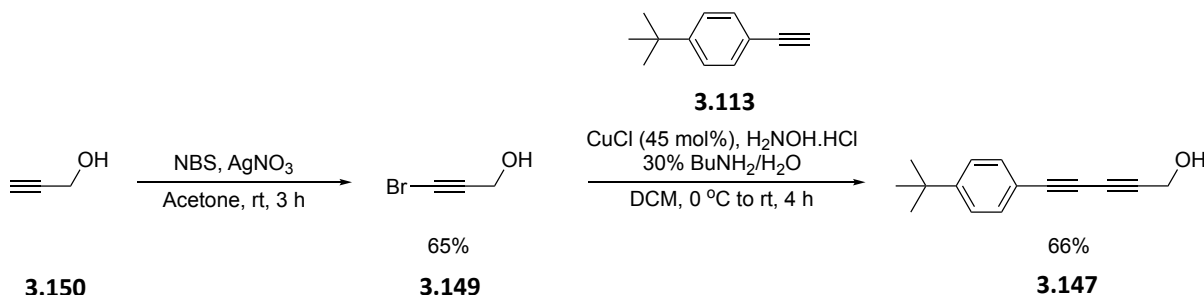


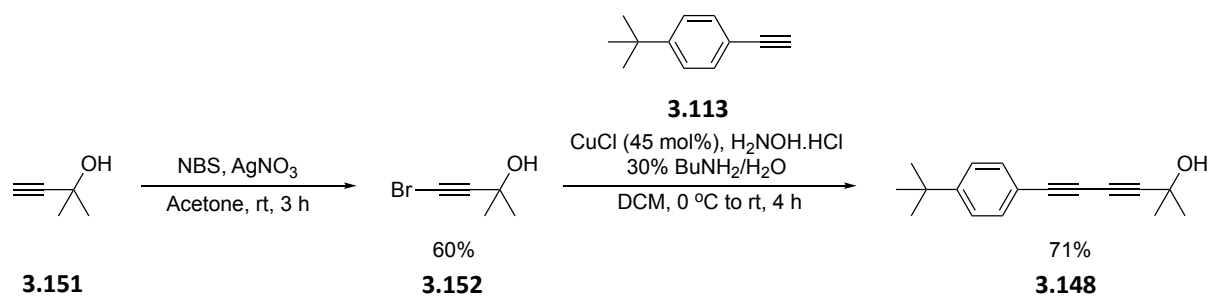
Figure 3.29 – Primary **3.147**, secondary **3.112** and tertiary **3.148** bis-acetylene targets

The alcohols **3.147** and **3.148** were synthesised as illustrated in Scheme 3.31. Brominated propargyl alcohol **3.149** was prepared by the reaction of prop-2-yn-1-ol **3.150** with NBS and silver nitrate, in a yield of 65%. It was then cross-coupled with *tert*-butylphenylacetylene **3.113** to give the desired primary alcohol **3.147** with a yield of 66%.



Scheme 3.31 – Synthesis route to the primary alcohol bis-acetylene target **3.147**.

Tertiary alcohol **3.148** was prepared using the same methodology but beginning with 2-methylbut-3-yn-2-ol **3.151**, as shown in Scheme 3.32. This propargyl alcohol was similarly brominated to give **3.152** in 60% yield. A Cadiot-Chodkiewicz cross-coupling then generated the desired tertiary alcohol **3.148** in an efficient transformation (71% yield).



*Scheme 3.32 – Synthesis of tertiary alcohol bis-acetylene target **3.148**.*

These alcohols were assayed. They were all active but they gave different relative activities on the two receptors, as shown in Figures 3.30 (OR5AN1) and 3.31 (OR1A1). Most notably, the primary alcohol **3.147** was similarly active in both assays, whereas the tertiary alcohol **3.148** was the most active compound on OR5AN1, but was the least active on OR1A1. The secondary alcohol (racemate) **3.112**, was best triggering OR1A1 but particularly poor triggering OR5AN1. The EC₅₀ values measured for the alcohols with OR5AN1 were all relatively high, with primary **3.147** having the lowest value of 238 μM, tertiary **3.148** having a value of 338 μM then finally secondary **3.112** with a value of 386 μM. With OR1A1, primary **3.147** had an EC₅₀ value of 44 μM, secondary **3.112** had a slightly higher value of 53 μM and tertiary **3.148** had a much higher value of 338 μM.

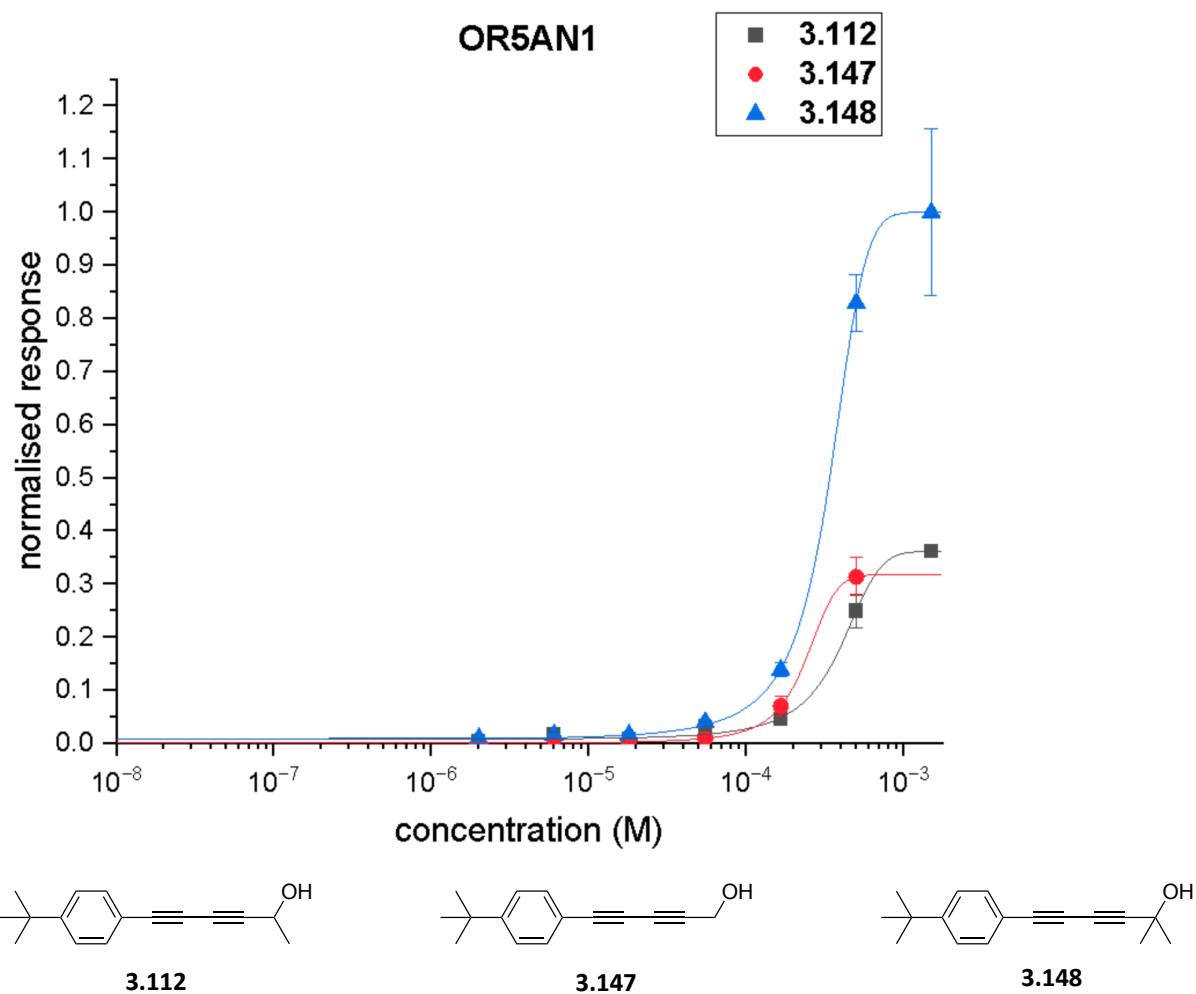


Figure 3.30 – Dose-response curves showing interactions of primary **3.147**, secondary **3.112** and tertiary **3.148** alcohol bis-acetylenes with the OR5AN1 receptor, with compounds ordered from least (left) to most (right) active.

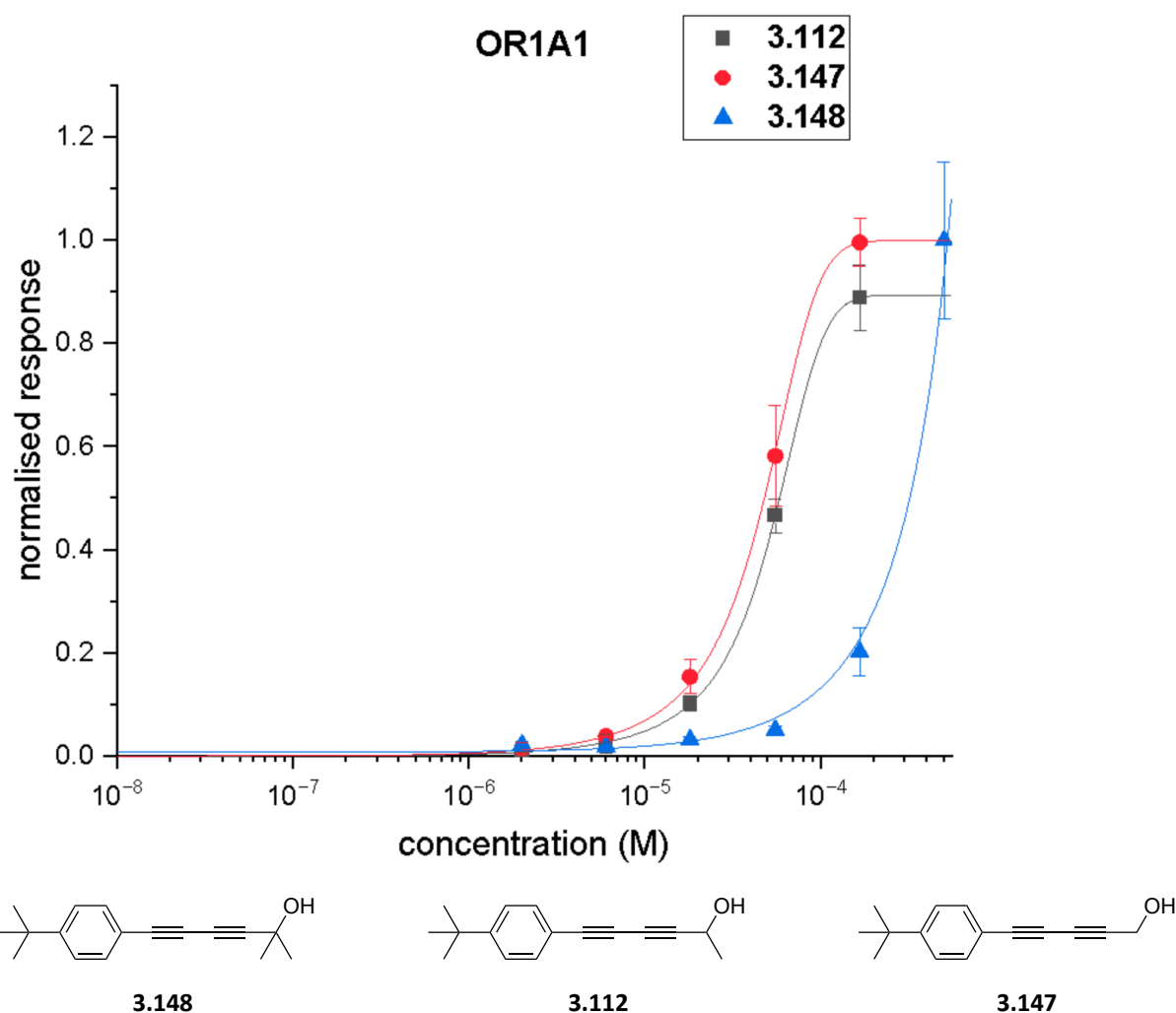
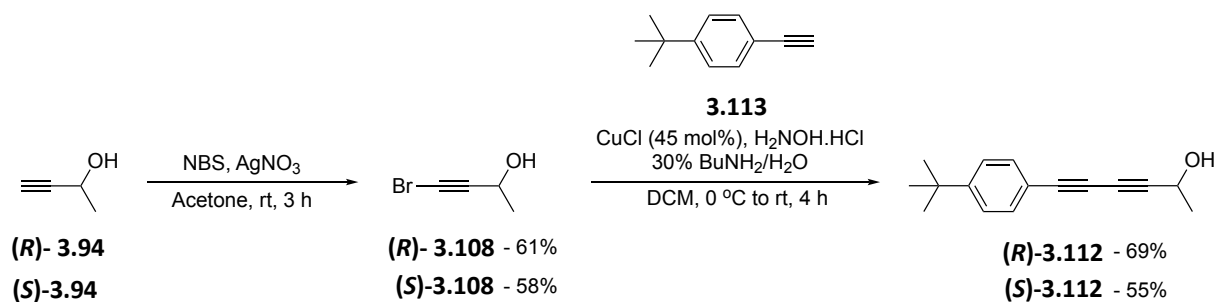


Figure 3.31 – Dose-response curves showing interactions of primary **3.147**, secondary **3.112** and tertiary **3.148** alcohol bis-acetylenes with the OR1A1 receptor, with compounds ordered from least (left) to most (right) active.

It became important to consider the individual isomers of secondary alcohol **3.112** as all assays on **3.112** had so far been carried out on the racemate. This was achieved starting from the individual (*R*)- **3.98** and (*S*)- **3.98** alcohol enantiomers which could be purchased in 99% ee. Accordingly (*R*)-alcohol *bis*-acetylene **3.112** was synthesised as illustrated in Scheme 3.33 following the two-step bromination ((*R*)- **3.108**, 61%), cross-coupling protocol to generate (*R*)- **3.112**. The (*S*)- enantiomer was similarly prepared as illustrated in Scheme 3.33.



Scheme 3.33 – Synthesis of enantiopure (R)- **3.112** and (S)- **3.112** alcohols.

These enantiopure alcohols were then sent to our collaborators in Beijing to be assayed, as shown in Figures 3.29 (OR5AN1) and 3.30 (OR1A1).

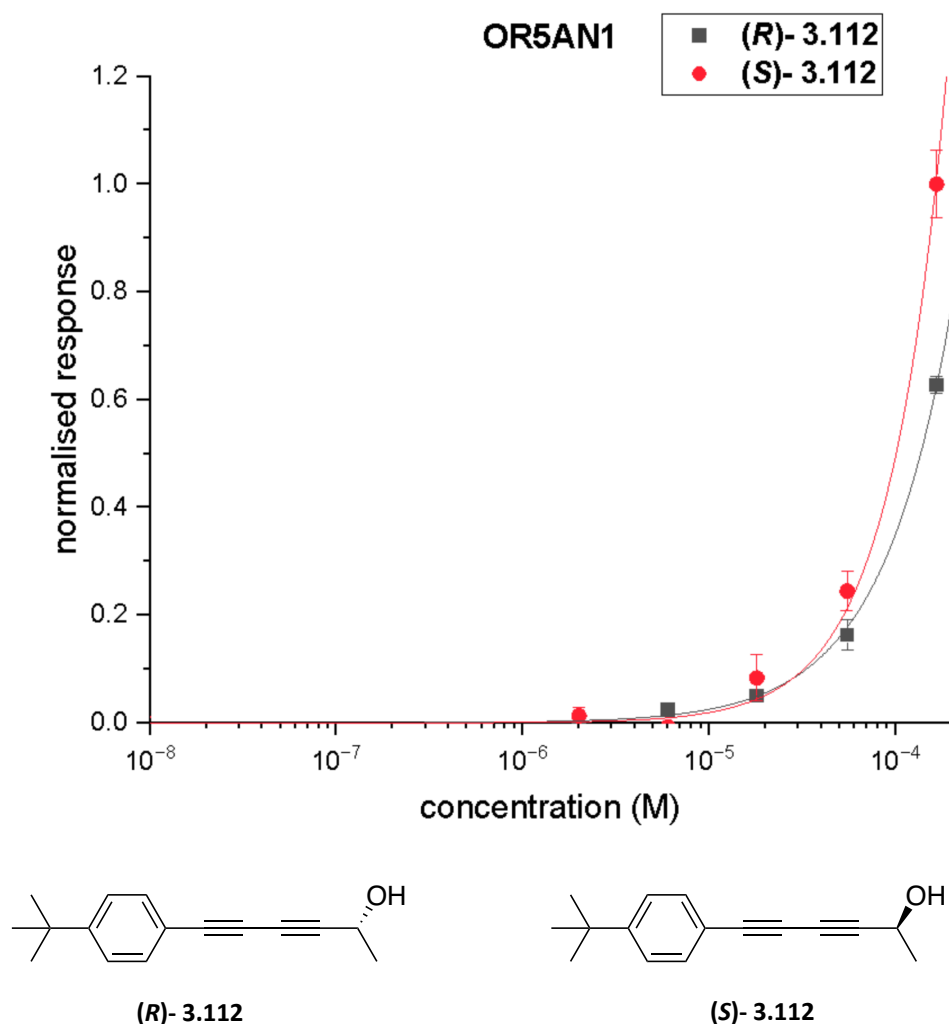


Figure 3.29 – Dose-response curves comparing (R)- **3.112** and (S)- **3.112** with the OR5AN1 receptor ordered from least active (left) to most active (right).

alcohols **3.147** and **3.148** respectively. The tertiary alcohol **3.148** was the poorest agonist for this receptor. This may suggest the importance of a hydrogen bonding donor effect in comparing these alcohols. Clearly, the tertiary alcohol **3.148** may find it most challenging to donate a hydrogen for steric reasons, and there is a clear difference between the secondary alcohol enantiomers, where presumably one is more optimally configured than the other to make a good hydrogen bond. Notably, the primary alcohol has good activity, and is similar to the (*R*)-**3.112** enantiomer indicating that it too can make a good hydrogen bond, consistent with a lack of steric congestion.

3.3 Conclusions

In this Chapter, the synthesis of novel musk receptor agonists has been detailed. This began with a series of monoacetylene products **3.86** - **3.88** (Figure 3.12), modelled on previously developed polycyclic musk odorants. However, when their interactions with the olfactory receptors were assayed, they triggered a limited response. Following this, a series of *bis*-acetylene compounds **3.95** - **3.97** were designed (Figure 3.13) with the *bis*-acetylene group acting as a rigid spacer, and these compounds were synthesised through a series of Sonogashira and Cadiot-Chodkiewicz cross-coupling reactions. Some gave promising results when they were assayed against the two olfactory receptors, with *meta bis*-acetylene **3.96** most notably triggering a strong response from OR5AN1 and racemic alcohol **3.112** triggering a strong response from OR1A1. An additional set of *bis*-acetylenes were then synthesised to explore structure-activity relationships further. Indanone *bis*-acetylenes **3.115** and **3.116** (Figure 3.15) were prepared in an attempt to fix the orientation of the carbonyl group via the use of a physical ring constraint. While these compounds required higher concentrations than *meta* **3.96** to trigger a response, the results of their assays showed a preference for the orientation of the carbonyl group to be 'downwards' rather than 'upwards'. Fluorinated derivatives of *meta bis*-acetylene **3.96** (Figure 3.18) were then synthesised in an attempt to bias the orientation of the carbonyl compound via repulsive electrostatic interactions. The results showed a clear 'upwards' carbonyl preference contrary to the indanone results. This could be due to several factors, such as introducing a ring into the molecule. *Meta tris*-acetylene **3.135** was also synthesised, showing weaker

activity with the receptors compared to the *meta bis*-acetylene **3.96**, suggesting that for this class of molecule the optimum number of spacer acetylenes for interacting with the olfactory receptors is two. Dihydroisobenzylfuran *bis*-acetylene **3.139** was also prepared and it triggered a strong response when assayed against both receptors but particularly with OR5AN1, although at a relatively high concentration.

Finally, the strong agonist activity of racemic alcohol **3.112** with OR1A1 was further investigated via the synthesis of primary and tertiary analogues and then individual enantiomers of **3.112** (Figure 3.20). It was found that primary alcohol *bis*-acetylene **3.147** gave the strongest response with this receptor, followed by the secondary **3.112** and then the tertiary **3.148** alcohols. It follows that the increasing steric impact around the alcohol group reduces the level of interaction (hydrogen bond donor ability) with the receptor. Finally, when the individual enantiomers of secondary alcohol **3.112** were tested, the (*R*)-alcohol **3.112** interacted much more strongly with the OR1A1 receptor than the (*S*)-alcohol **3.112**.

The work represented within this chapter details the discovery of a previously un-explored agonist of known human olfactory receptors responsible for detecting the musk odour. Taken collectively this study shows clear structure-activity relationships indicating the importance of functionality, shape and orientation in interactions with the olfactory receptors studied, similar to broader medicinal chemistry approaches. There is no particular basis to conclude other hypotheses operating that are particular to olfactory receptors over other classes of receptors.

Chapter 4 – The tri-fluoro *tert*-butyl (TFTB) group

Work reported in this chapter was done by:

Initial development of TFTB synthesis	Ben McKay
Synthesis of mono-fluorinated <i>tert</i> -butyl compound 4.70	Ben McKay
Synthesis of di-fluorinated <i>tert</i> -butyl compound 4.71	Dr. Qingzhi Zhang
LogP measurements	Dr. Qingzhi Zhang
NMR titrations	Luca Dobson
Cross-coupling reactions of the TFTB group	Luca Dobson
X-ray diffraction	Dr. David Cordes
Computational analysis	Bruno Piscelli and Dr. Rodrigo Cormanich at University of Campinas, Brazil
Solubility measurements	Luca Dobson
Synthesis of the aryl-TFTB pyridaben analogue	Luca Dobson
Other attempted reactions with the aryl-TFTB group	Luca Dobson
Metabolism study of the TFTB group with <i>Cunninghamella elegans</i>	Mohd Faheem Khan and Prof. Cormac Murphy at University College Dublin
Synthesis of putative metabolite	Luca Dobson

4.1 Introduction

4.1.1 Lipophilicity

Lipophilicity is the measure of a molecule's ability to partition between water and lipidic environments. It is widely used as a measure of a drug molecule's ability to cross membranes and bind to proteins.¹⁷⁷ Analytically this is measured as the ability of a molecule to pass between a non-polar organic phase (octanol) and water, which is quantified by measuring its logP, where P is a partition coefficient:

$$\log P = \log \left(\frac{[\text{molecule in octanol}]}{[\text{molecule in water}]} \right)$$

Molecules with higher logP are more hydrophobic and lipophilic. Those with lower logP are more polar and more hydrophilic.

LogP is a highly valued tool in medicinal chemistry, where it is often used as an indicator of whether a drug candidate can reach its intended target. Lipophilicity is one of the measures featured within Lipinski's rule of five. These are a list of criteria which apply to many effective drug molecules, as evaluated in a retrospective review of small molecule drugs that made it through clinical trials and were registered for clinical use. Lipinski *et al.*, determined that the logP of historically successful drugs generally did not exceed 5, their molecular masses were less than 500 Da, the number of hydrogen bond donors was generally less than 5 and the number of hydrogen bond acceptors less than 10.¹⁷⁸ Ghose *et al.* later refined this analysis, stating that the logP of a drug candidate should be within the range of -0.4 to +5.6.¹⁷⁹

4.1.2 Fluorine and lipophilicity

Fluorine has been shown to have a significant influence on the lipophilicity of molecules due to its unique properties. For aromatic compounds it is found that, as a general rule, the introduction of fluorine has the effect of increasing lipophilicity/logP¹⁸⁰ and thus reducing the molecule's ability to interact with water, as illustrated in Figure 4.1. Bohm *et al.* showed this by taking 293 different pairs of aromatic compounds from the Roche database that differ by one fluorine atom.¹⁸¹ They found that for the matched pairs, the introduction of just one fluorine atom increased the logP of the molecule by an average value of 0.25.

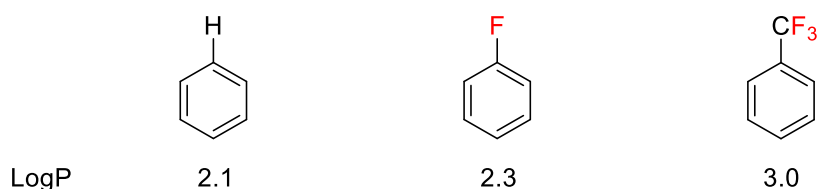


Figure 4.1 – LogP of fluorine substituted benzenes.

This effect is reversed for the partial fluorination of aliphatic molecules.¹⁸² As a general rule, as fluorination increases around a cyclohexane ring, there is a decrease in the logP as illustrated in Figure 4.2. This is again due to the unique properties of fluorine. When a

hydrogen is replaced with a fluorine on a CH₂ group, the highly electronegative fluorine atom has the effect of polarising its geminal hydrogen, making it more electropositive. This polarised hydrogen is then better able to interact with water and logP reduces. Relative stereochemistry impacts too. If the fluorine atoms on the cyclohexane ring are all located on the same face, this has a maximum effect on molecular polarity, creating two polarised faces, a negatively polarised fluorine face and a positively polarised hydrogen face.

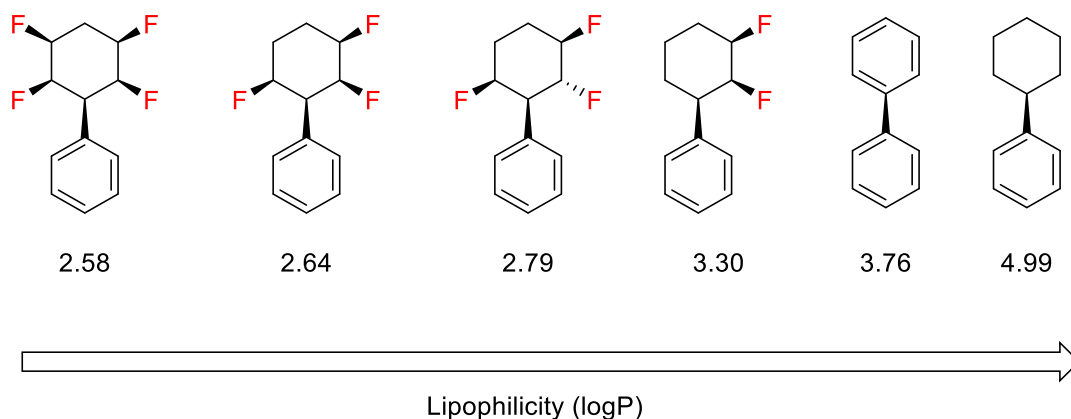


Figure 4.2 – Lipophilicity ($\log P$) of selectively fluorinated cyclohexanes¹⁸²

However, the introduction of heteroatoms into fluorinated molecules complicates the effect of fluorine on logP. In this case, the effect is determined by the distance between the heteroatom and the fluorine atom, with the logP only decreasing when the fluorine is remote from the heteroatom. One example of this is with trifluoromethylated alcohols, where the logP only decreases once the fluorine atoms are more than three C-C bonds remote from the alcohol moiety, as shown in Table 4.1.¹⁸⁰

Alcohol	logP	Δ logP
CH ₃ CH ₂ OH	-0.32	
CF ₃ CH ₂ OH	0.36	0.68
CH ₃ (CH ₂) ₂ OH	0.34	
CF ₃ (CH ₂) ₂ OH	0.39	0.05
CH ₃ (CH ₂) ₃ OH	0.88	
CF ₃ (CH ₂) ₃ OH	0.90	0.02
CH ₃ (CH ₂) ₄ OH	1.19	
CF ₃ (CH ₂) ₄ OH	1.14	-0.04

Table 4.1 – Lipophilicity of fluorinated alcohols.¹⁸⁰

Some work in St Andrews looked at the effect of the selective fluorination of cyclopropanes on lipophilicity.¹⁸³ This showed that sequentially attaching a fluorine to each carbon of the ring had the effect of decreasing logP as illustrated in Figure 4.3. This work again illustrated the influence of relative stereochemistry on the logP, with the molecule with the lowest logP (most polar) in the series being all-*cis* trifluorinated cyclopropane **4.1**. This molecule again has a maximum polarity and thus the lowest logP. The impact of facial polarisation is shown by **4.3**, which contains three fluorine atoms but only two on one face, having a higher logP than **4.1**. Also, **4.6** has four fluorine atoms, with two on the same carbon atom. The removal of a polarised geminal hydrogen increases logP.

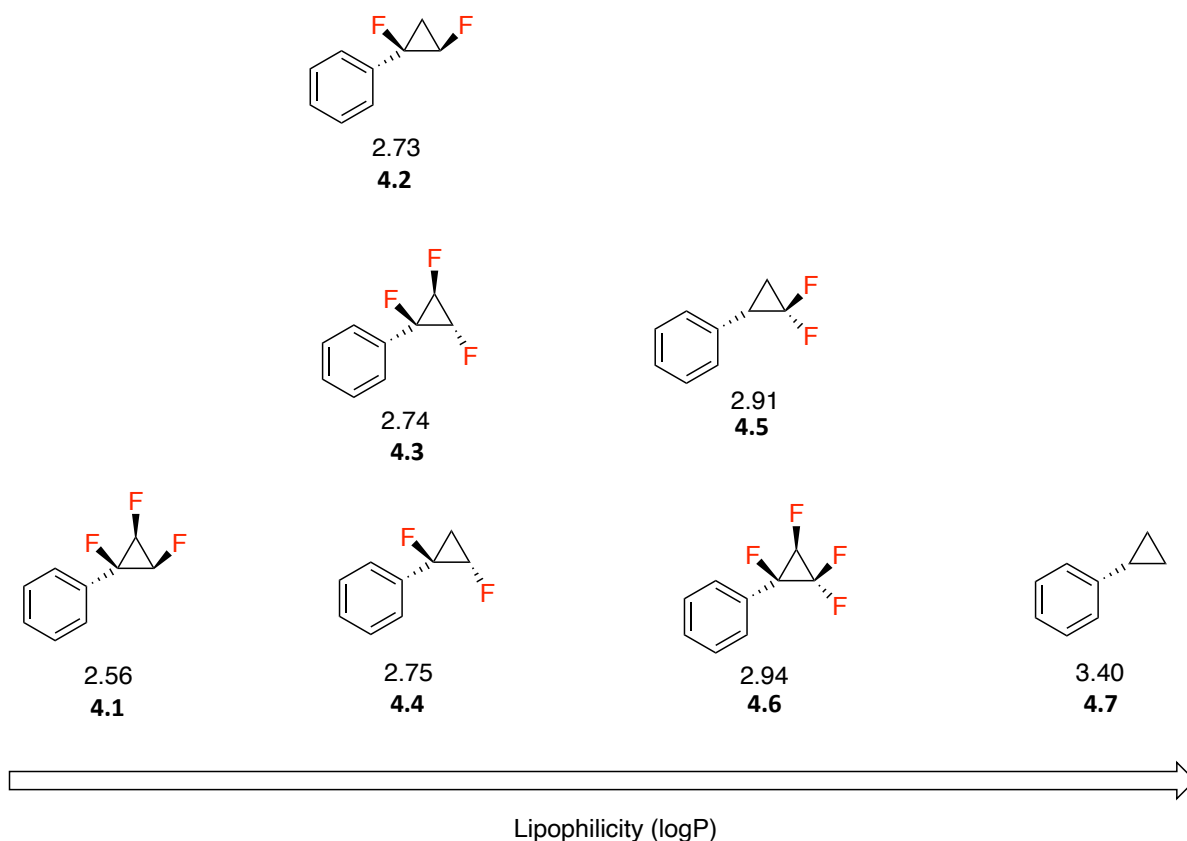


Figure 4.3 – Lipophilicity ($\log P$) of selectively fluorinated aryl cyclopropanes.¹⁸³

4.1.3 *tert*-Butyl group in nature and medicine

Natural products containing the *tert*-butyl group are uncommon.¹⁸⁴ One such group are the structurally complex polycyclic ginkgolides which contain a tetrahydrofuran ring, three lactones and a spiro[4,4]-nonane carbocyclic ring, as illustrated in Figure 4.4. The ginkgolides have been found to be antagonists of the platelet-activating factor receptor (PAF).¹⁸⁵ There are only five of this class of compounds that have been isolated, with the only difference between the five structures being the number and position of hydroxy groups. Corey and Rao developed a 21-step enantioselective total synthesis of an analogue of ginkgolide B **4.9** which contained a hydrogen in place of a *tert*-butyl group. They found that this analogue is approximately three orders of magnitude less active than ginkgolide B, showing that the *tert*-butyl group is key to its anti-PAF potency.¹⁸⁶

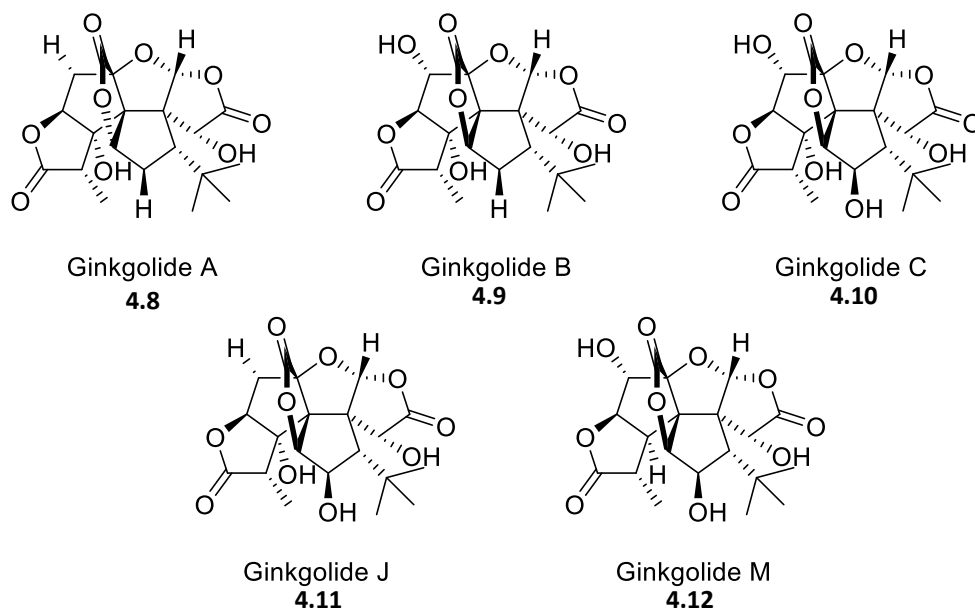


Figure 4.4 – Structures of ginkgolides.

One notable example of the rare group of *tert*-butyl natural products is butyrolactol A **4.13**. This is a polyketide that has been isolated from *Streptomyces rochei*.¹⁸⁷ It exhibits strong antifungal properties. Bilobalide **4.14** is a terpenoid which is found in Ginkgo leaves.¹⁸⁸ Bilobalide exhibits neuroprotective properties, and has also been found to induce the activity, protein and mRNA expression of the liver enzymes CYP3A1 and CYP1A2.^{189,190} 24-Methylene-25-methylcholesterol **4.15** is a sterol with a side chain containing a *tert*-butyl group. It was isolated from *Brassica juncea*, a species of mustard plant, and was then later found in a number of plants.¹⁹¹

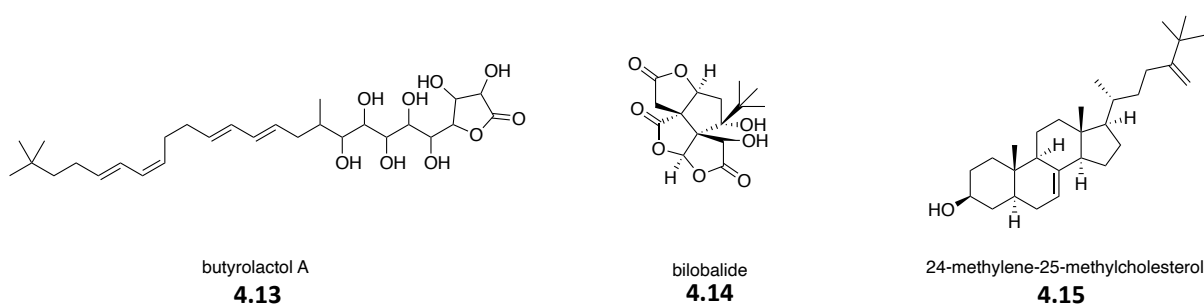


Figure 4.5 – Natural products containing a *tert*-butyl group.

The *tert*-butyl group is found in relatively few drugs due to its tendency to decrease the metabolic stability of a molecule through increased lipophilicity. However, within the top 200

selling drugs of 2021 there are representatives that contain a *tert*-butyl group, as shown in Figure 4.6. One example is Ivacaftor **4.16**, a component of the combination drug Trikafta (USA)/Kaftrio (EU), used in the treatment of cystic fibrosis.¹⁹² Salbutamol **4.17** is used to treat asthma and chronic obstructive pulmonary disease by relaxing the airway smooth muscle¹⁹³ and Glecaprevir **4.18** is used in the combination drug Mavyret with Pibrentasvir¹⁹⁴ for the treatment of Hepatitis C. The combination inhibits NS3/4A, which is a protease necessary for the replication of hepatitis C viral RNA. A relatively recently developed drug is nirmatrelvir **4.19**, which is used in combination with ritonavir in Paxlovid. Nirmatrelvir acts as an inhibitor of SARS-CoV-2 main protease, so is used with Paxlovid in the treatment of COVID-19.¹⁹⁵

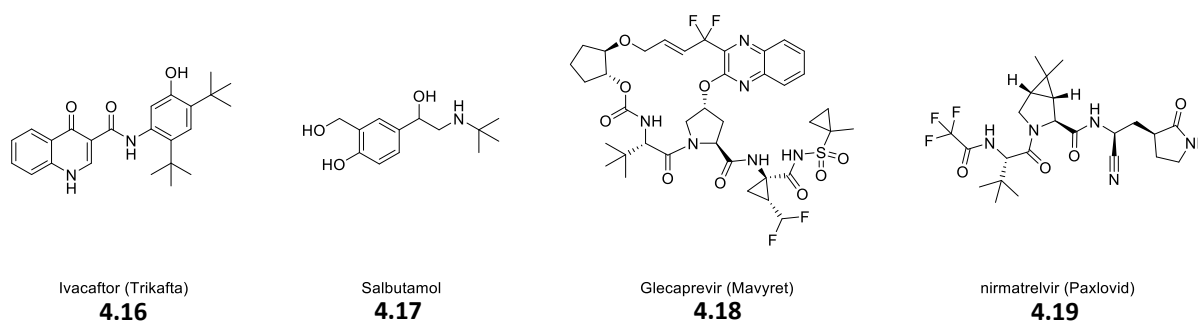
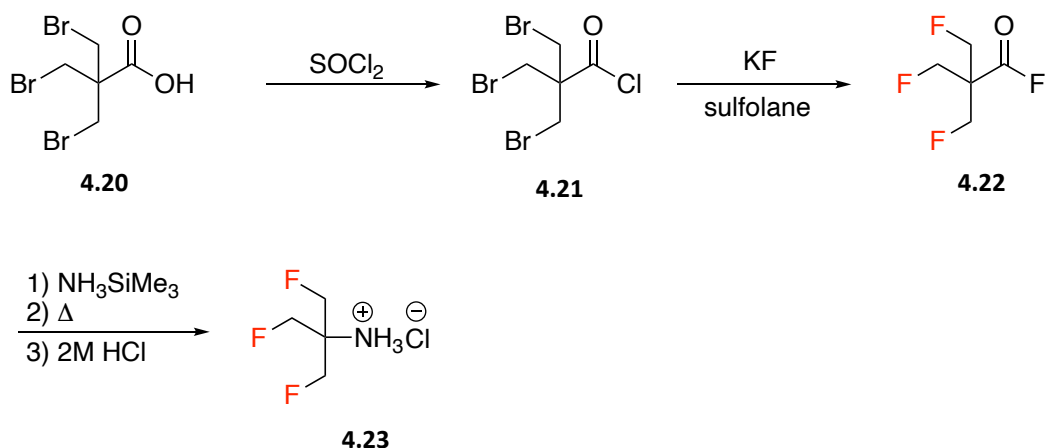


Figure 4.6 – FDA-approved drug molecules containing *tert*-butyl groups.

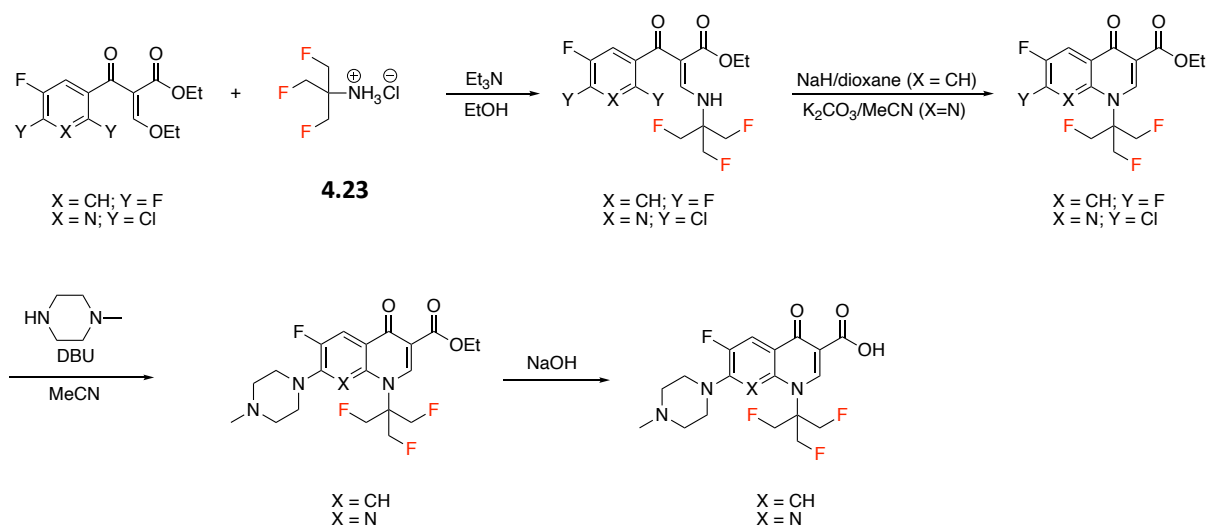
4.1.4 Tri-fluoro *tert*-butyl group

There are only two papers in the literature which report the synthesis of a $\beta,\beta'\beta''$ -tri-fluoro *tert*-butyl group with a fluorine on each of the three methyl groups. Both of these syntheses addressed only amine **4.23**. The first was reported in 1991 by Remuzon *et al.*, who were working on preparing fluoronaphthyridines and fluoroquinolones as antibacterial agents, and their route is summarised in Scheme 4.1.¹⁹⁶ It began with tribromopivalic acid **4.20**, converting it to 3-bromo-2,2-bis(bromomethyl)propanoyl chloride **4.21** using thionyl chloride, then to 3-fluoro-2,2-bis(fluoromethyl)propanoyl fluoride **4.22** using potassium fluoride in sulfolane, to introduce the tri-fluoro *tert*-butyl group. **4.22** was then converted to its hydrochloride salt **4.23** by reaction with sulfamic acid.



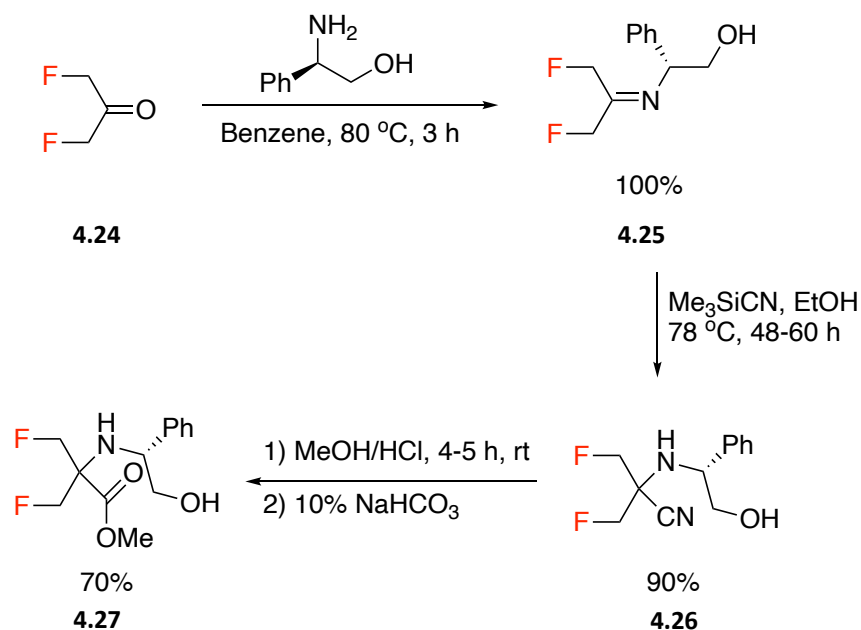
Scheme 4.1 – Synthesis of the tri-fluoro tert-butyl amine **4.23** by Remuzon et al.¹⁹⁶

Antibiotic targets were achieved from amine **4.23** as illustrated in Scheme 4.2.



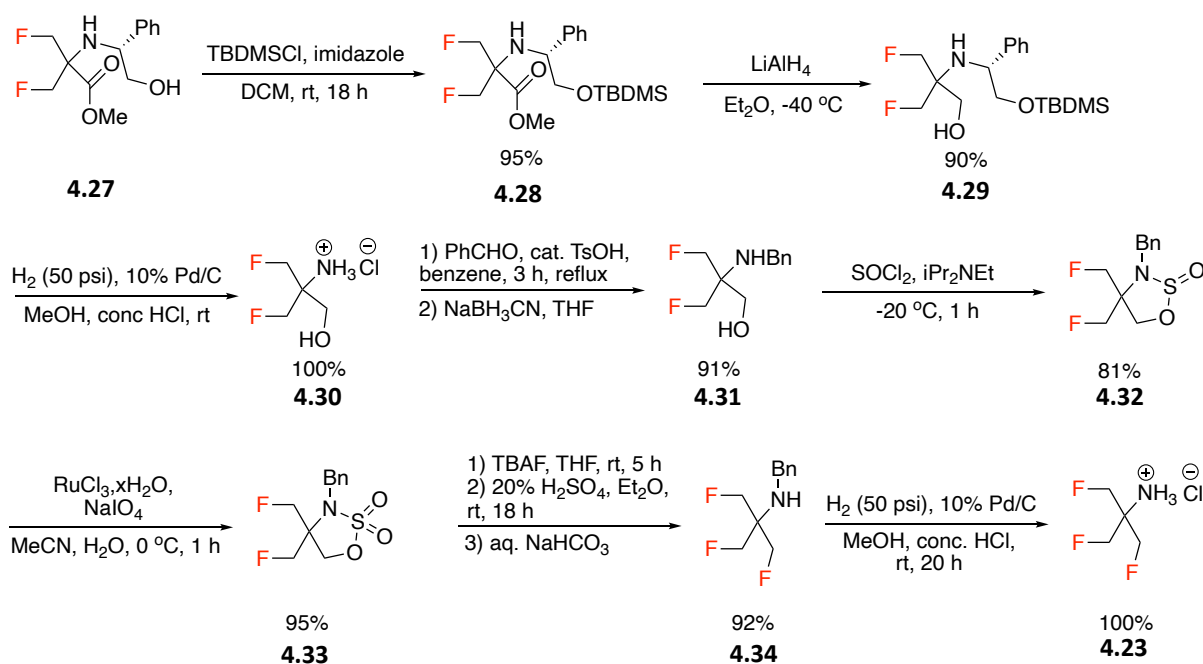
Scheme 4.2 – Fluoroquinoline antibiotic syntheses incorporating amine **4.23** by Remuzon et al.¹⁹⁶

Following this, Ok et al. developed another preparation of **4.23** in 1999.¹⁹⁷ This synthesis began from 1,3-difluoroacetone **4.24**, which was converted into ester **4.27** via a literature procedure as illustrated in Scheme 4.3.¹⁹⁸



Scheme 4.3 – First steps in the synthesis of **4.23** by Ok et al.¹⁹⁷

The synthesis progressed as illustrated in Scheme 4.4. Alcohol **4.27** was protected as TBDMS ether **4.28**, followed by reduction of the ester moiety using lithium aluminium hydride to give alcohol **4.29**. Amine **4.30** was then obtained by hydrogenolysis, followed by benzylation to give **4.31**. Cyclisation to sulfamidite **4.32** followed, then oxidation to sulfamidate **4.33** led to the fluorination using TBAF in 20% sulfuric acid, giving benzylamine **4.34** containing the tri-fluoro *tert*-butyl group. Finally, debenzylation gave the free amine **4.23**.

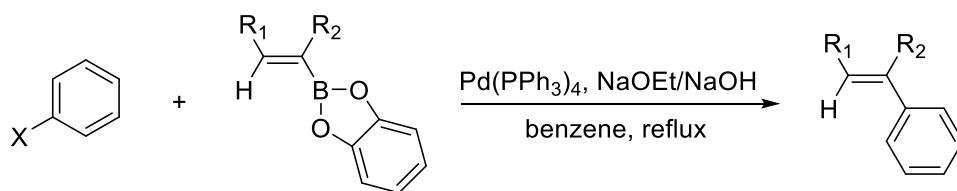


Scheme 4.4 – Synthesis of amine **4.23** by Ok et al.¹⁹⁷

There have been no further syntheses of any tri-fluoro *tert*-butyl containing molecules anywhere in the literature since 1999, and in these two cases, the core building block is amine **4.23** meaning that no other building blocks or constructs of the TFTB group have been developed. Therefore, there was scope to develop other constructs and the project focused on the aryl-TFTB, from which point the group could be incorporated into higher molecular architectures.

4.1.5 Suzuki cross-coupling reactions

The Suzuki cross-coupling reaction was first reported by Akira Suzuki in 1979. This involves the reaction of organohalides (aryl halides) with boronic acids.¹⁹⁹ Prior to this, there had been no previously reported coupling reactions using catalytic palladium with boron reagents. Heck had reported in 1975 the coupling of an alkene with an alkenyl boronic acid but that reaction required stoichiometric quantities of palladium to proceed.²⁰⁰ Suzuki initially took various aryl halides and reacted them with a series of alkenyl boranes in the presence of a Pd(PPh₃)₄ catalyst in refluxing benzene, as shown in Figure 4.7, although the reaction developed very widely, particularly to aryl boronic acids and esters.²⁰¹



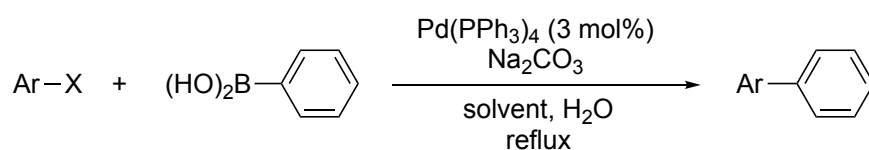
ArX	R ₁	R ₂	Catalyst (mol%)	Reaction time (h)	Yield (%)
PhI	<i>n</i> Bu	H	1	2	100
PhBr	<i>n</i> Bu	H	1	2	63
PhBr	<i>n</i> Bu	H	1	4	98
PhCl	<i>n</i> Bu	H	1	2	3
PhBr	<i>n</i> -hexyl	H	3	4	98
PhBr	Ph	H	5	4	50
PhBr	Ph	H	3	3	41
PhBr	Et	Et	3	4	87
<i>o</i> -MeC ₆ H ₄ Br	<i>n</i> Bu	H	3	4	93
<i>o</i> -MeOC ₆ H ₄ Br	<i>n</i> Bu	H	3	4	81
<i>p</i> -ClC ₆ H ₄ Br	<i>n</i> Bu	H	1	3	100
<i>o</i> -EtC ₆ H ₄ Br	<i>n</i> Bu	H	1	3	87
2-bromothiophene	<i>n</i> Bu	H	1	2	86
2-bromopyridine	<i>n</i> Bu	H	1	2	83

Figure 4.7 – Scope of Suzuki reaction of aryl halides and alkenyl bromides.¹⁹⁹

It was found that the reaction is robust for various aryl halides, with iodides giving the best results, followed by bromides. The reaction with phenyl chloride only gave a 3% yield. Various alkenyl boranes were tolerated, and the reaction was shown to work well using only 1 mol% of catalyst.

Suzuki then reported the coupling of aryl halides with phenylboronic acids to form biphenyls, as illustrated in Figure 4.8.²⁰² The reaction was shown to work well for aryl bromides and aryl iodides and with only 3 mol% of Pd(PPh₃)₄ catalyst, with sodium

carbonate as the base. A variety of aryl halides were shown to be well-tolerated, however, the reaction was slower when more sterically-hindered aryl bromides were used.

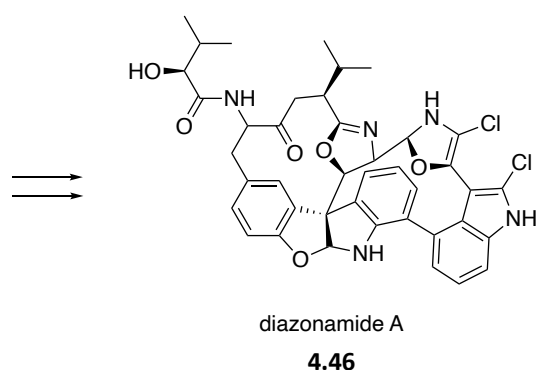
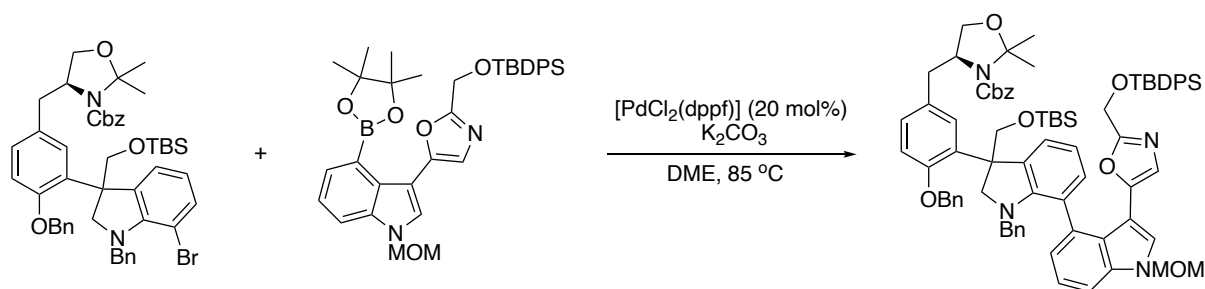


ArX	Solvent	Reaction time (h)	Yield (%)
<i>o</i> -MeC ₆ H ₄ Br	Benzene	6	94
<i>p</i> -MeC ₆ H ₄ Br	Benzene	6	88
<i>o</i> -MeOC ₆ H ₄ Br	Benzene	6	99
<i>p</i> -MeOC ₆ H ₄ Br	Benzene	6	66 (40)
<i>p</i> -ClC ₆ H ₄ Br	Benzene	6	89 (74)
<i>p</i> -MeO ₂ CC ₆ H ₄ Br	Benzene	6	(94)
Mesityl bromide	Toluene	17	(80)
1-Naphthyl bromide	Toluene	10	(49)
<i>p</i> -BrC ₆ H ₄ Br	Toluene	12	(40)

*Yields determined by GLC, yields in parentheses are isolated yields.

Figure 4.8 – Scope of Suzuki reaction of aryl halides and phenylboronic acid.²⁰²

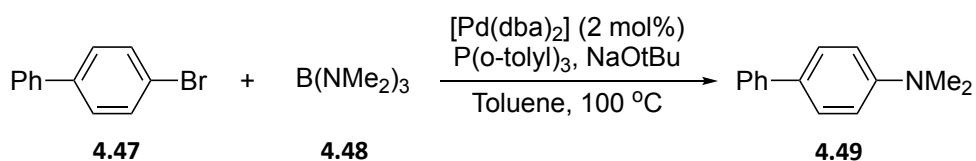
The mechanism of the Suzuki cross-coupling reaction is understood to begin with the generation of the Pd(0) catalyst **4.35** from the pre-catalyst, as shown in Scheme 4.5. The aryl bromide **4.36** then adds to Pd(0) via an oxidative addition, giving species **4.37**, with the Pd being oxidised to a +2 oxidation state. Reaction with base then takes place, with substitution of the bromide ligand by ethoxide to give **4.38**. Boronic acid **4.39** is activated by the base and a trans-metallation step follows, with the aromatic ring being transferred from boronic acid **4.40** to the palladium species **4.38**, forming **4.41**. Reductive elimination results in the release of biphenyl product **4.42** and regeneration of Pd(0) catalyst **4.35**.



Scheme 4.7 – Suzuki reaction in the synthesis of diazoniamide A **4.46**.²⁰⁵

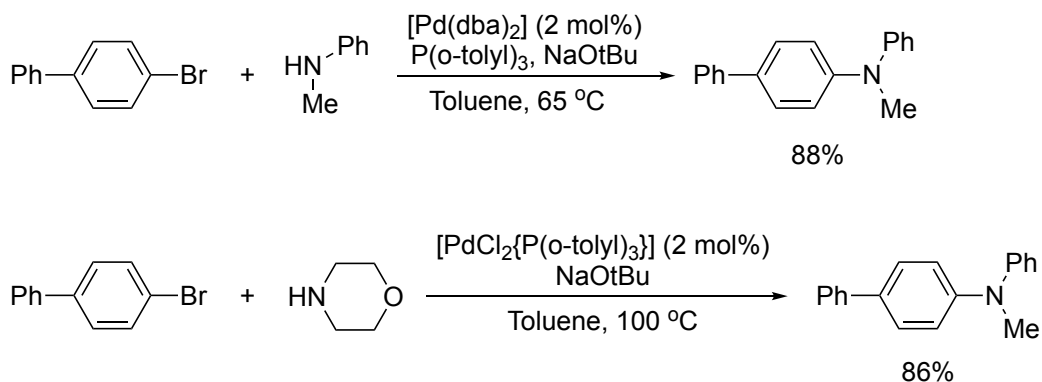
4.1.6 Buchwald-Hartwig cross-coupling reactions

The Buchwald-Hartwig reaction was developed in 1995 as a method to form C-N bonds. It is another example of a Pd-catalysed cross-coupling reaction. This reaction was developed independently by Buchwald and Hartwig in 1995. Initially, Buchwald *et al.*, took aryl bromide **4.47** with aminoborane **4.48** in the presence of a Pd catalyst and sodium *tert*-butoxide in toluene at 100 °C to form arylamine product **4.49**, as shown in Scheme 4.8.²⁰⁶



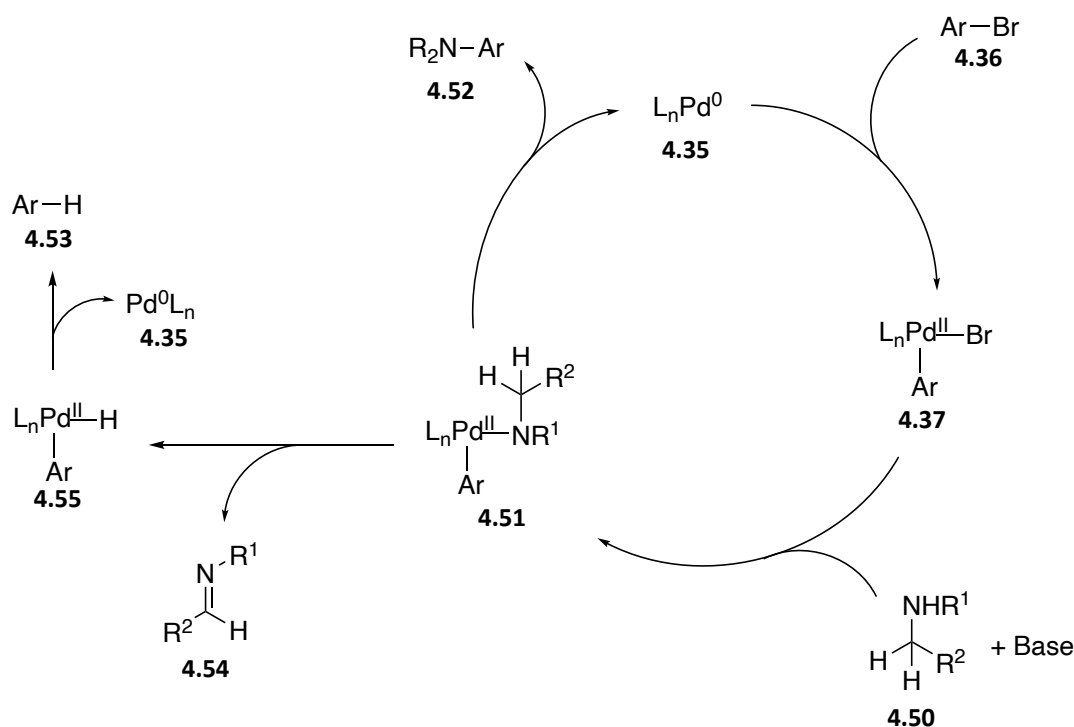
Scheme 4.8 – Buchwald-Hartwig cross-coupling of aryl bromide and aminoborane as developed by Buchwald.²⁰⁶

Buchwald found that a free amine could be coupled with an aryl bromide in the presence of a Pd catalyst and a base, as illustrated in Scheme 4.9. They found that the reaction tolerates aryl bromides with both electron-donating and electron-withdrawing substituents, as well as both primary and secondary amines.²⁰⁶



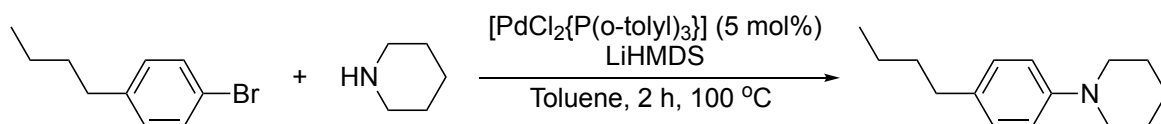
Scheme 4.9 – Examples of arylamine formation developed by Buchwald et al.²⁰⁶

Buchwald suggested a catalytic cycle for this reaction as illustrated in Scheme 4.10. The aryl bromide **4.36** first adds to the Pd(0) catalyst **4.35** via an oxidative addition step. After the substitution of the bromide ligand by amine **4.50**, a reductive elimination generates the desired aryl amine **4.52**, with Pd(0) catalyst **4.35** being regenerated. They also rationalised the formation of the reduced aryl bromide **4.53** as a side product, formed by the β -hydride elimination of the amine ligand from **4.51**, releasing imine **4.54**. This leaves species **4.55**, which can then undergo a reductive elimination to give the reduced aromatic side-product **4.53**.



Scheme 4.10 – Mechanism of Buchwald-Hartwig amination proposed by Buchwald *et al.*²⁰⁶

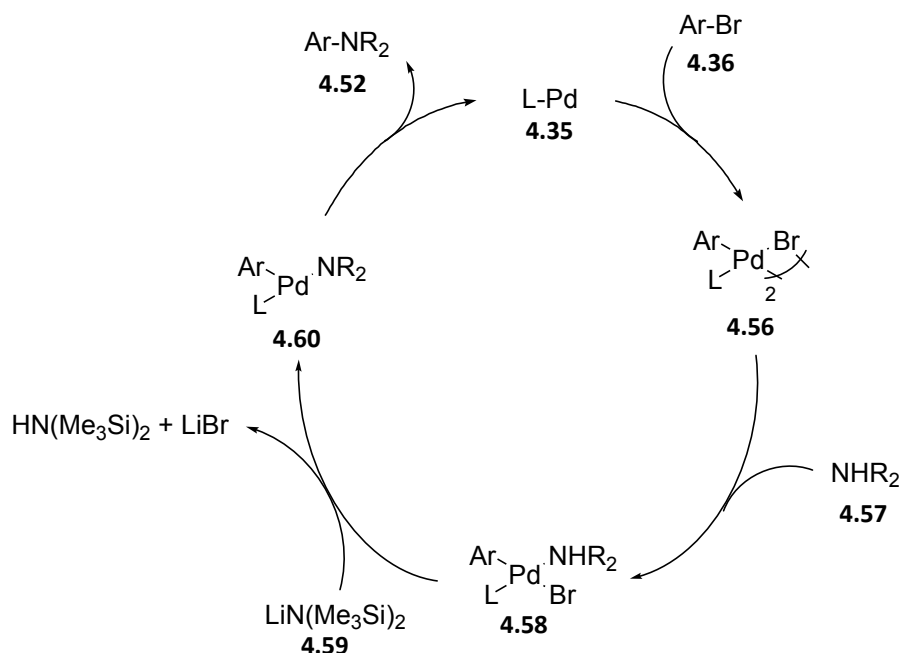
Meanwhile, Hartwig *et al.* independently reported a similar methodology for the coupling of aryl halides and amines to form aryl amines.²⁰⁷ Similarly, they used palladium catalysis, but in this case LiHMDS was primarily used as the base, as shown in the example in Scheme 4.11.



Scheme 4.11 – Example of an aryl amine formation developed by Hartwig *et al.*²⁰⁷

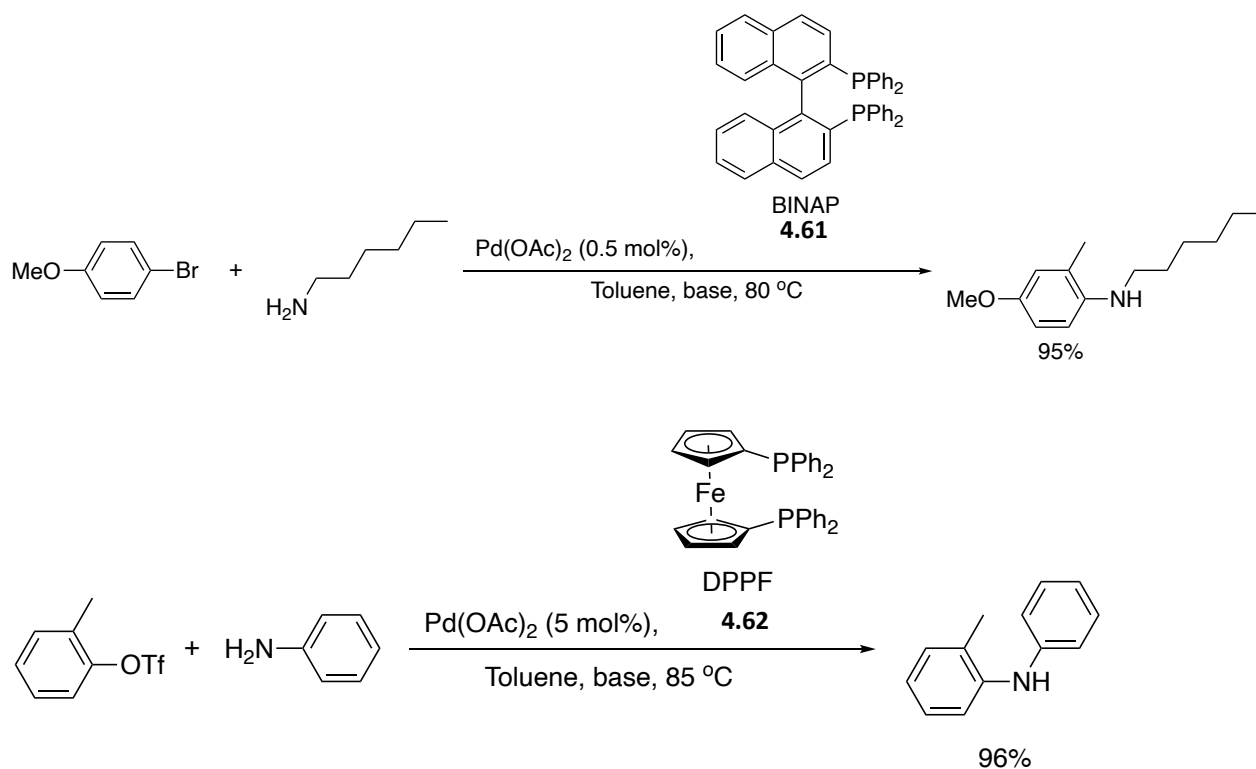
Hartwig *et al.*, also suggested a catalytic cycle for this reaction, in particular for the addition of aryl halides to tri *o*-tolylphosphinePd(0), where they suggested that a dimeric complex **4.56** forms when the aryl bromide **4.36** reacts with the catalyst **4.35**, rather than the monomeric complex **4.37** as suggested by Buchwald (Scheme 4.10). The dimeric complex **4.56** is then cleaved by the addition of amine **4.57** to give the reactive species. The subsequent amine **4.58** is then deprotonated by LiHMDS **4.59** due to the increased acidity of

the amine proton upon coordination. Reductive elimination from **4.60** then takes place to release arylamine **4.52**, with the regeneration of catalyst **4.35** as illustrated in Scheme 4.12.

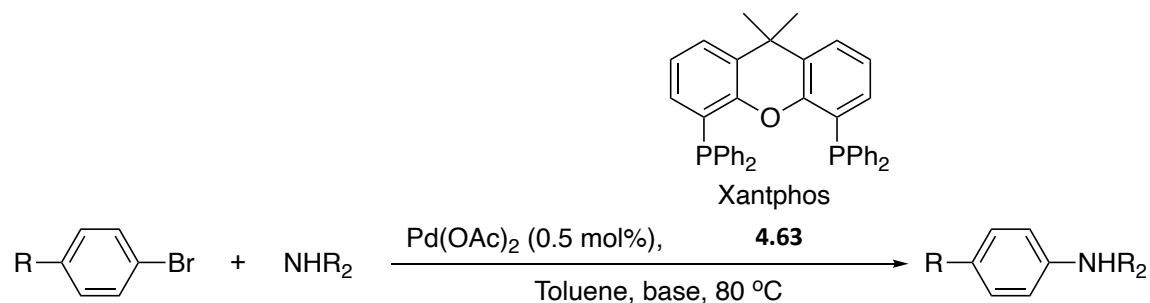


Scheme 4.12 – Catalytic cycle for the Buchwald-Hartwig cross-coupling reaction proposed by Hartwig et al.²⁰⁷

One further development in the methodology of these reactions involved the use of bidentate phosphine ligands to improve the overall yields, as shown in Schemes 4.13 and 4.14. The chelating effect of these ligands causes the reductive elimination of the desired product to be favoured, rather than the undesired competing β -hydride elimination as shown in the mechanism proposed by Buchwald (Scheme 4.12). Ligands such as BINAP **4.61**²⁰⁸, DPPF **4.62**²⁰⁹ and Xantphos **4.63**²¹⁰ were shown to be effective.



Scheme 4.13 – Buchwald-Hartwig reactions using bidentate phosphine ligands BINAP **4.61** and DPPF **4.62**.²¹¹

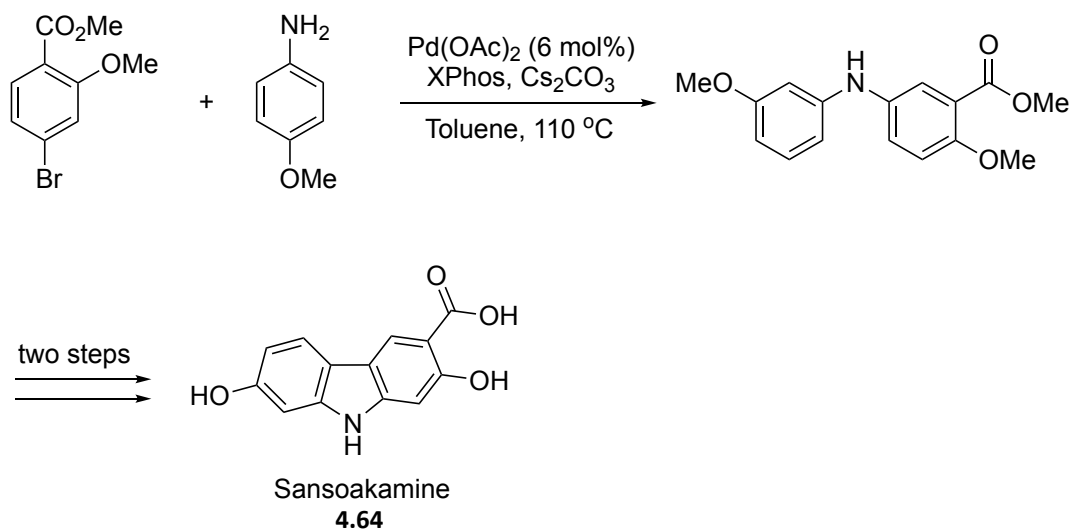


R	Amine	Time (h)	Yield (%)
CN	hexylamine	3	76
<i>t</i> Bu	<i>o</i> -anisidine	0.5	63
CN	<i>o</i> -anisidine	68	93
<i>t</i> Bu	hexylamine	3	66

Scheme 4.14 – Buchwald-Hartwig reactions using Xantphos **4.63** as a ligand.²¹⁰

The Buchwald-Hartwig reaction has gone on to be widely used across the synthesis community.²¹² One example is in work by Knökler *et al.*, who developed an improved

synthesis of sansoakamine **4.64**, as illustrated in Scheme 4.15.²¹³ Their original route gave the final product with an overall yield of 49%, however the improved synthesis, featuring the Buchwald-Hartwig reaction, led to an overall yield of 69%.



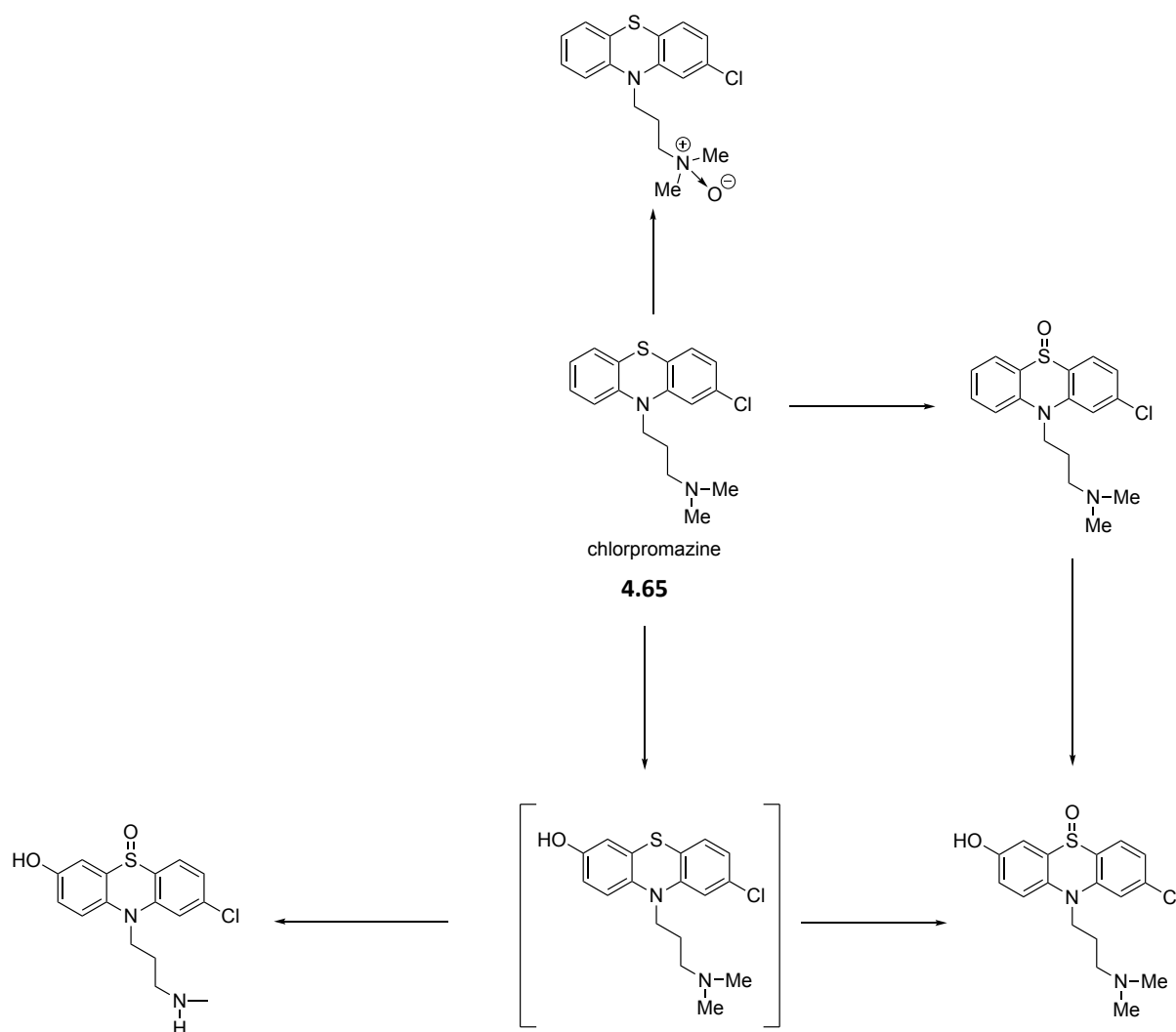
Scheme 4.15 – The Buchwald-Hartwig reaction in the synthesis of sansoakamine **4.64** by Knökler et al.²¹³

4.1.7 *Cunninghamella elegans*

Cunninghamella elegans (*C. elegans*) is a species of fungus which is found in soil and decaying plant matter. It is finding use as a model for mammalian liver metabolism due to the expression of a range of cytochrome P450 enzymes. It therefore generates oxidised metabolites similar to those found in mammalian metabolism when challenged with an exogenous organic compound (drug).^{214 215} This is explored by growing the fungus in culture and then adding the foreign compound at a mM concentration. The fungus then metabolises the compound and the resulting metabolites can be analysed.

One example of this process involved the metabolism of chlorpromazine **4.65** by *C. elegans*.²¹⁶ Chlorpromazine **4.65** is a phenothiazine which is used as an anti-psychotic drug in the treatment of illnesses such as schizophrenia.²¹⁷ Metabolites were generated by growing a culture of *C. elegans* then adding a dose of chlorpromazine to the culture and incubating for 96 h at 25 °C. The extracted metabolites were then separated by HPLC and

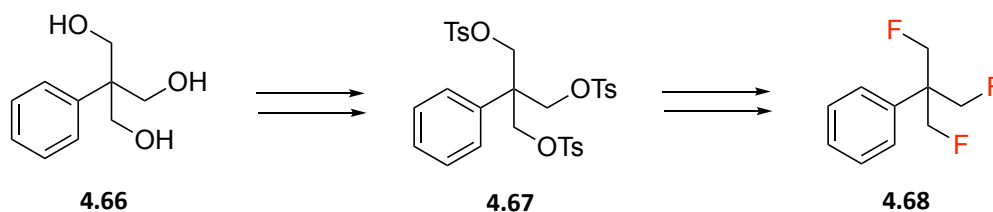
analysed by mass spectrometry and ^1H NMR. In this way, a metabolic pathway was evaluated as illustrated in Scheme 4.16.



Scheme 4.16 – Metabolic modifications of chlorpromazine **4.65** by *C. elegans* identified by Cerniglia et al.²¹⁶

4.1.8 Aims and objectives

This chapter reports the synthesis of the aryl tri-fluoro *tert*-butyl (TFTB) group for the first time. The approach envisaged starting from 2-(hydroxymethyl)-2-phenylpropane-1,3-diol **4.66**, where the triol could then be converted into the TFTB group directly attached to an aromatic ring. If successful, functionality on the aromatic ring would allow greater diversification in downstream reactions such as Pd cross-coupling reactions.



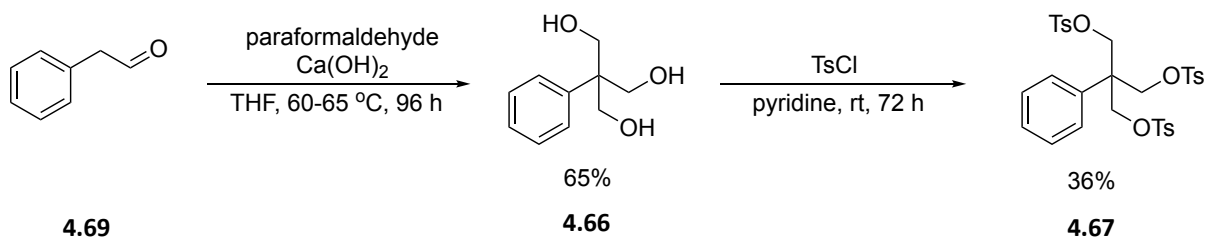
Scheme 4.17 – Envisaged approach to the aryl TFTB group 4.68.

It was of particular interest to evaluate the lipophilicity of these compounds, as the selective addition of fluorine to aliphatics influences their lipophilicities. It was also an objective to evaluate a crystalline derivative by X-ray structure analysis to explore the conformational arrangement of the fluorines on this moiety, and to support this by computational analysis.

4.2 Synthesis and properties of the tri-fluoro *tert*-butyl group

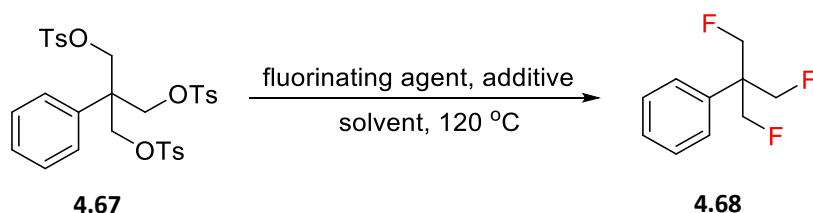
4.2.1 Development of a route to the aryl tri-fluoro *tert*-butyl group

The route to the aryl TFTB group developed here is illustrated in Scheme 4.18. The first run through of the synthesis was carried out by MChem project student Ben McKay and was then further developed. This route began by combining phenylacetaldehyde **4.69** with paraformaldehyde in the presence of calcium hydroxide in THF to generate triol **4.66** in a Cannizzaro-type reaction. Tosylation of the resultant triol **4.66** then proved straightforward to give the desired precursor tritosylate **4.67**. This synthesis to tritosylate **4.67** was previously described by Yulikov *et al.* and it offered a potential substrate to a direct fluorination reaction.²¹⁸



Scheme 4.18 – Initial steps in the developed synthesis of the aryl tri-fluoro tert-butyl (TFTB) group.²¹⁸

The fluorination reaction of **4.67** was developed first by Ben McKay, testing both cesium fluoride and potassium fluoride as fluorinating agents in a large excess (18 equiv.) and DMF and DMSO as solvents at 120 °C. The high temperature was found to be necessary in order to drive the reaction to full conversion within 24 h. The impact of adding catalytic TBAF was explored too, as was the addition of 18-crown-6 to complex the metal cations to generate a freer fluoride ion.



Reaction	Fluorinating agent	Solvent	Additive	Conversion after 24 h (%)
A	CsF	DMF	None	89
B	CsF	DMF	20% TBAF	99
C	CsF	DMSO	None	98
D	CsF	DMSO	20% TBAF	99
E	CsF	DMF	18-crown-6	89
F	CsF	DMSO	18-crown-6	95
G	KF	DMF	18-crown-6	1
H	KF	DMSO	18-crown-6	Trace

Figure 4.9 – Development of the trifluorination reaction (work done by Ben McKay).

Cesium fluoride in DMSO at 120 °C proved to offer the best conditions in the trial reactions as that gave **4.68** within 24 h. The use of KF gave very poor conversions, presumably due to its very poor solubility, even with additives such as TBAF and 18-crown-6, and there was no obvious advantage over the Cs/DMSO combination only, as conversions were already very high.

4.2.2 Spectroscopic properties and lipophilicity of the aryl tri-fluoro *tert*-butyl group

The ^1H NMR of the TFTB group in compound **4.68** shows a characteristic doublet of triplets centred around 4.81 ppm, with an overall integral of six, representing the CH_2 groups geminal to the fluorines, as shown in Figure 4.10. This features a $^2J_{\text{HF}}$ coupling of 46.9 Hz between the protons and their geminal fluorine, and also a long-range $^4J_{\text{HF}}$ coupling of 1.5 Hz, between the protons and the fluorines that are four bonds away.

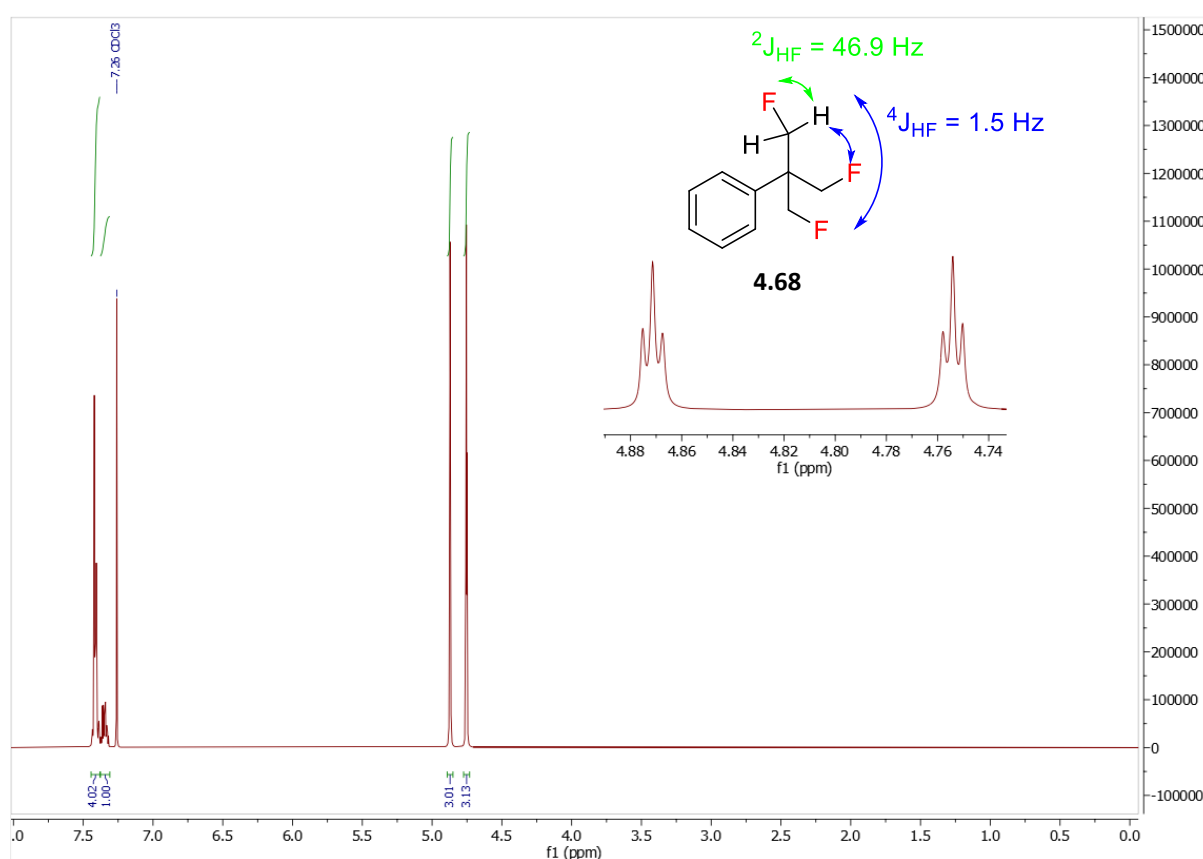


Figure 4.10 – ^1H NMR of the TFTB group in **4.68**.

The ^{19}F NMR signal is a triplet, with a reciprocal $^2J_{\text{HF}}$ value of 46.9 Hz as shown in Figure 4.11. The presence of a $^4J_{\text{HF}}$ coupling within the ^1H NMR spectrum suggests that there should also be a $^4J_{\text{FF}}$ coupling present, however this has not been resolved within ^{19}F or $^{19}\text{F}\{^1\text{H}\}$ NMR spectra.

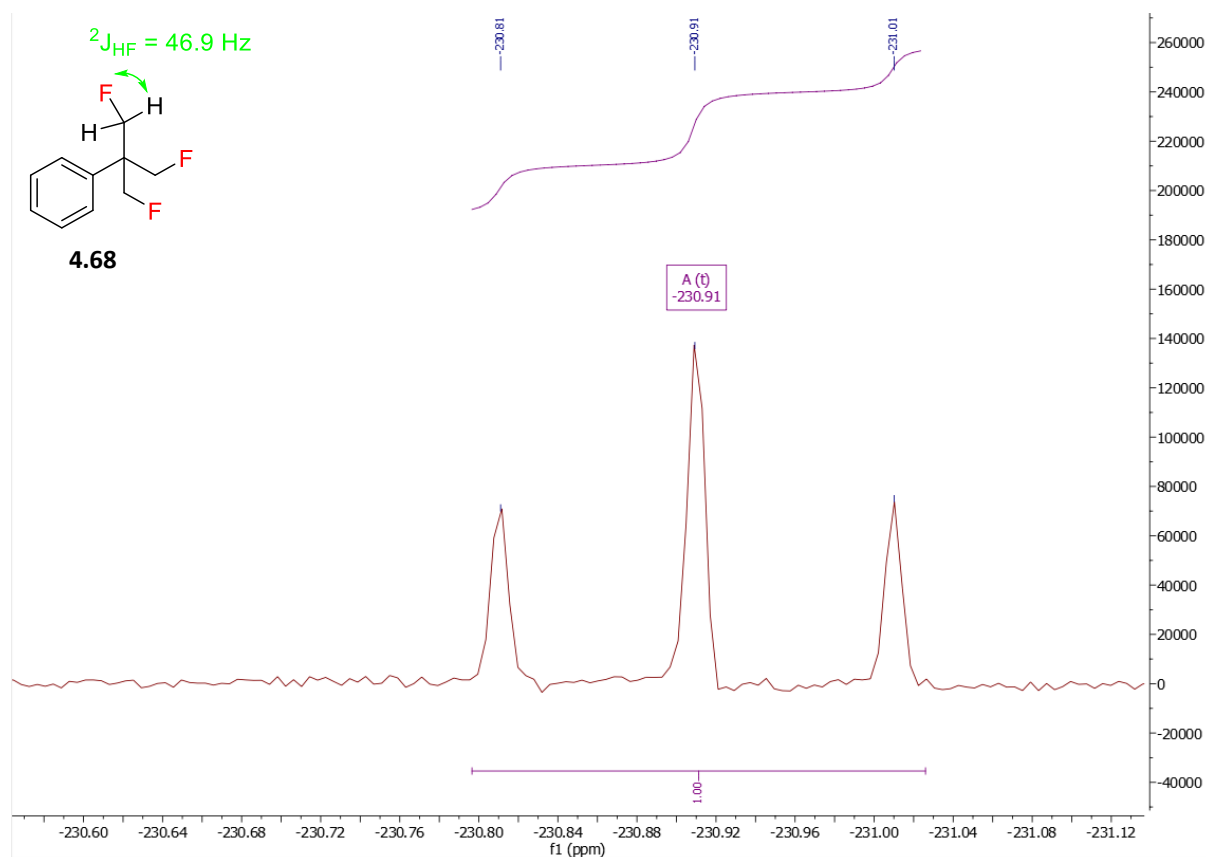


Figure 4.12 – ^{19}F NMR of the TFTB group in **4.68**.

The $^{13}\text{C}\{^1\text{H}\}$ NMR of the TFTB group also features a characteristic doublet of triplets representing the CH_2F group, as shown in Figure 4.13. There is a $^1J_{\text{CF}}$ coupling of 176.7 Hz between the CH_2F carbon and the fluorine. There is also a long-range $^3J_{\text{CF}}$ coupling of 5.9 Hz between the CH_2F carbon atom and the fluorines that are three bonds away.

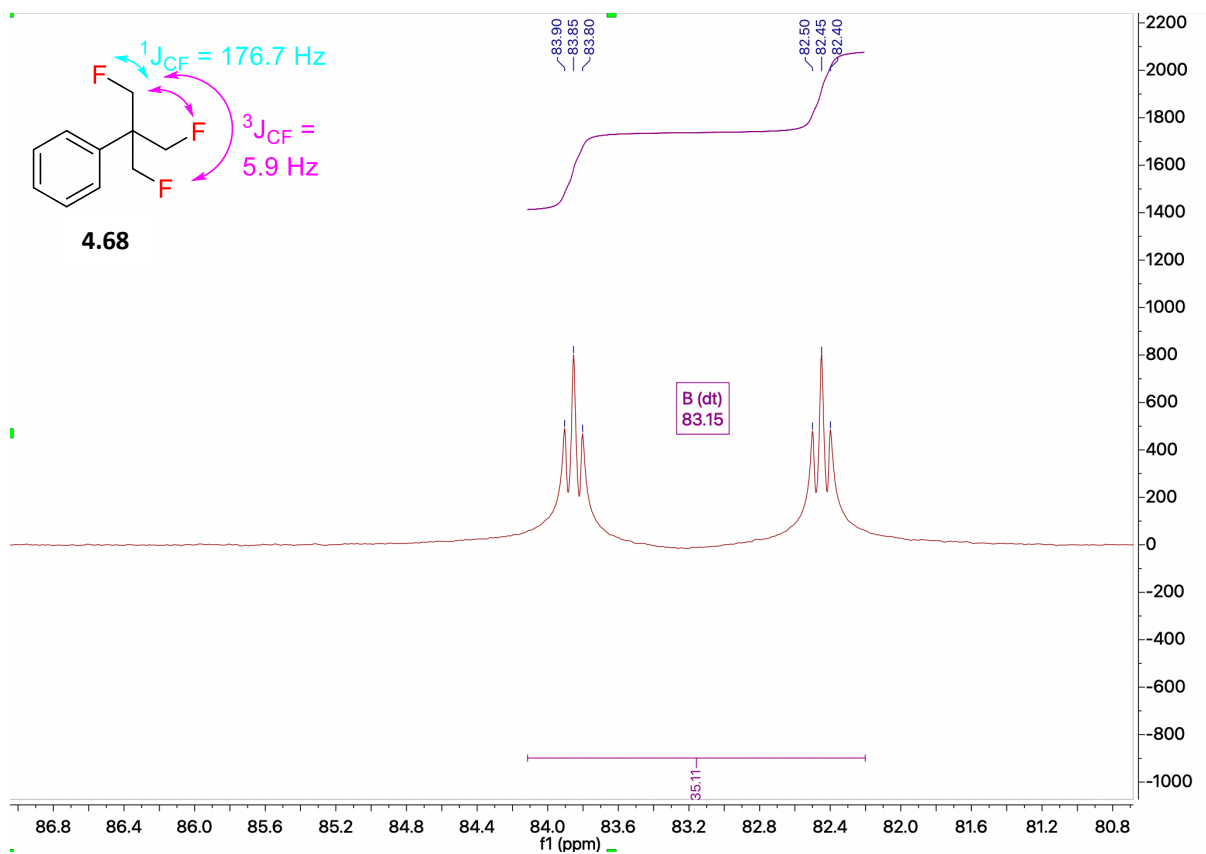


Figure 4.13 – CH_2F region in the $^{13}\text{C}\{^1\text{H}\}$ -NMR of the TFTB group in **4.68**.

The quaternary carbon ($\text{C}(\text{CH}_2\text{F})_3$) also exhibits a splitting in the $^{13}\text{C}\{^1\text{H}\}$ -NMR spectrum, as shown in Figure 4.14. This peak splits as a quadruplet, with the carbon coupling to the three fluorine atoms on the TFTB group. The coupling constant of this quartet is 16.8 Hz, representing a $^2J_{\text{CF}}$ coupling.

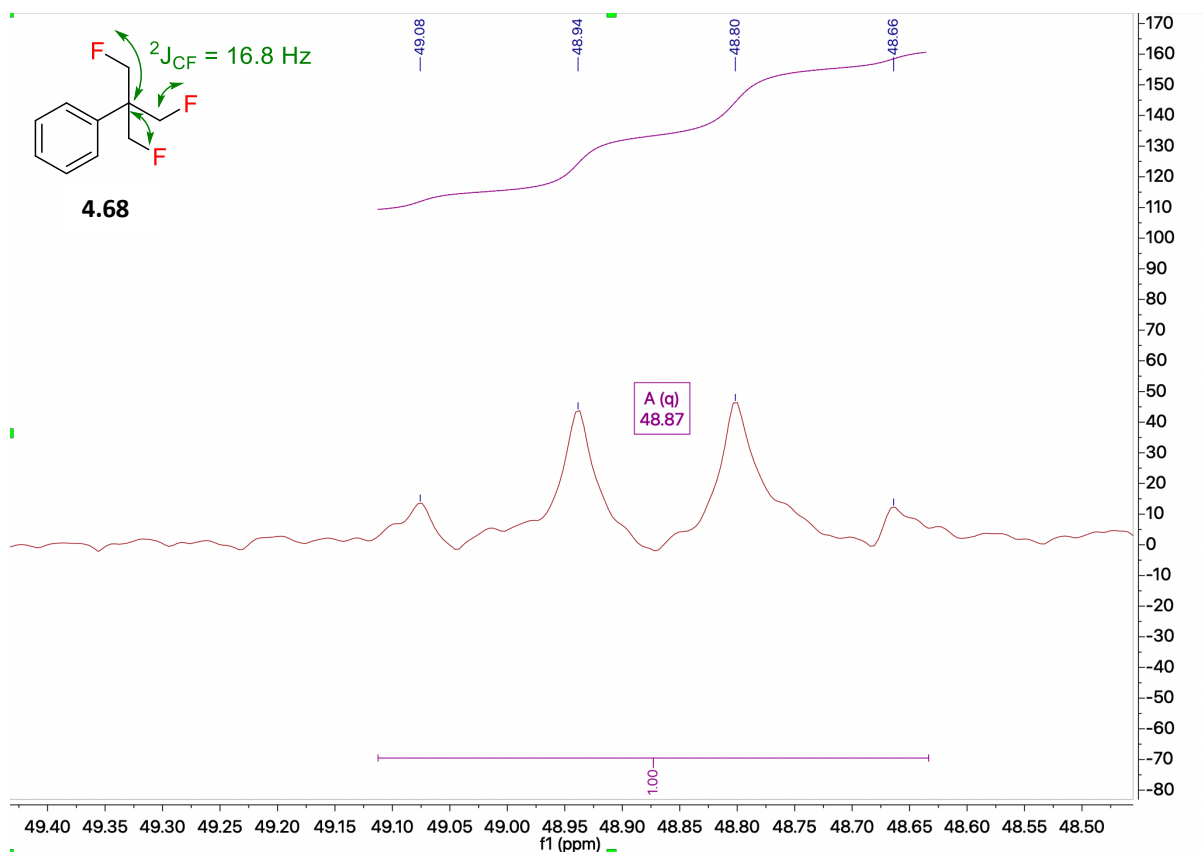


Figure 4.14 – $C(CH_2F)_3$ region in the $^{13}C\{^1H\}$ -NMR spectrum of the tri-fluoro *tert*-butyl group in **4.68**.

With the synthesis of the aryl-TFTB group developed, and with mono-, di- and tri-fluoro *tert*-butyl compounds synthesised, experiments were conducted to measure the logP of these substituents by reverse phase HPLC by Dr Qingzhi Zhang. Mono-fluorinated **4.70** was synthesised by Ben McKay and di-fluorinated **4.71** was synthesised by Dr Qingzhi Zhang. The reference compounds used in this experiment were phenol and toluene and the HPLC column used was a Phenomenex Luna C18 100A (250 × 4.60 mm) 5 μ . It was eluted with 60:40 acetonitrile:water supplemented with 0.05% TFA at a flow rate of 1 mL/min. The samples were injected onto the column (10 μ L of 0.5 mg/mL solution in MeCN) and the chromatograph shows the relative retention times of the samples on the column, as shown in Figure 4.15.

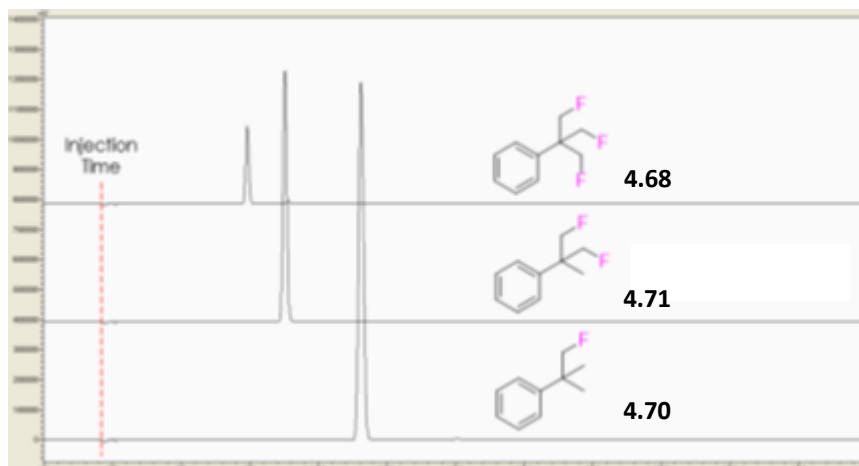


Figure 4.15 – HPLC chromatograph of the progressively fluorinated aryl *tert*-butyl groups obtained by Dr Qingzhi Zhang.

The chromatograph shows that with increasing fluorination of the *tert*-butyl group, the retention times decrease on reverse phase. This indicates an increase in polarity of the compound with increasing fluorination. Using these retention times against the reference compounds, the logPs of the variously fluorinated *tert*-butylbenzenes **4.68**, **4.70**, **4.71** and *tert*-butyl benzene **4.72** were determined and these are illustrated in Figure 4.16.

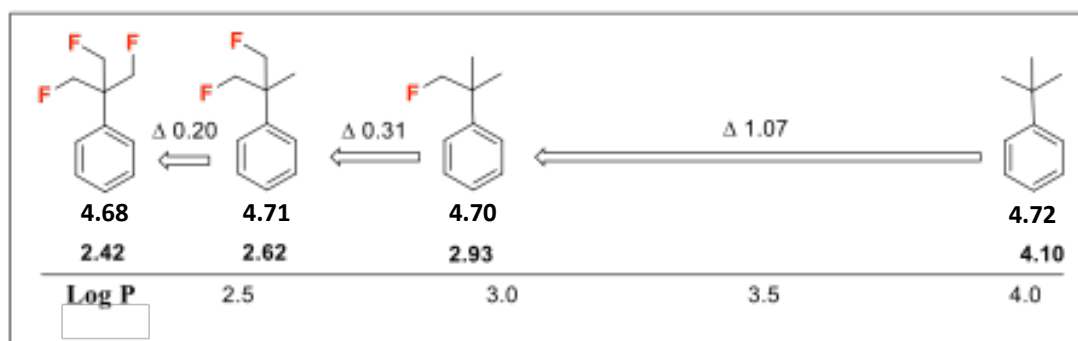


Figure 4.16 – Calculated logP values of the mono **4.70**, di **4.71** and tri-fluoro *tert*-butyl group **4.68**.

Consistent with the relative polarities by reverse phase HPLC, these values show a decrease in logP with increasing fluorination. Clearly, the lipophilicity of the aryl *tert*-butyl group decreases with increasing fluorination. It is interesting to note the diminishing size of the decrease in logP with progressively increasing levels of fluorination relative to the *tert*-butyl

group. The addition of one fluorine only lowers logP by an order of magnitude ($\Delta \log P = 1.07$). Adding a second fluorine lowers the logP by a smaller reduction of ($\Delta \log P = 0.31$), and a third fluorine lowers logP further but to a lesser extent again ($\Delta \log P = 0.2$). Overall, there is a very significant reduction in logP with the addition of three fluorines ($\Delta \log P = 1.58$) which offers an attractive profile for its inclusion in bioactives development relative to the *tert*-butyl group, at least on this parameter.

A calculation was also carried out by our collaborators, Bruno Piscelli and Dr Rodrigo Cormanich at State University Campinas in Brazil, to determine the molecular dipole moment of the tri-fluoro *tert*-butyl group in the model compound **4.68**, as molecular dipoles are also considered to be an important factor in assessing logP values.²¹⁹ These are shown in Figure 4.17.

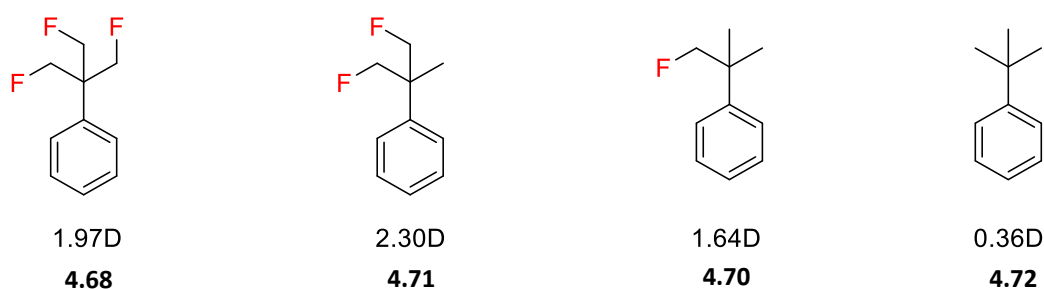


Figure 4.17 – Calculated molecular dipole values for **4.68**, **4.70**, **4.71** and **4.72** as determined by Bruno Piscelli and Dr Rodrigo Cormanich (University of Campinas, Brazil). Molecular dipole moments were calculated at the M06-2X/def2-TZVP level.

The addition of one fluorine atom to the *tert*-butyl group sees an increase in the molecular dipole moment from 0.36D to 1.64D, and thus an increase in polarity consistent with the large reduction in logP by over 1 log unit. When the second fluorine is added there is a smaller increase to 2.3D but the addition of the third fluorine atom results in a decrease in the molecular dipole moment. This is because the orientations of the three C-F bonds are partially cancelling their individual dipole moments. Despite this, there is still a decrease in logP with the third fluorine, presumably due to the increased number of polarised hydrogen atoms interacting with water molecules.

In order to further consider the polarity of the aryl-TFTB group, I began to explore the effect of changing the ^1H NMR solvent on the chemical shift of the CH_2F peak in NMR. This was done by recording ^1H NMR spectra of **4.73** in d_6 -acetone and d_8 -toluene and comparing the chemical shift of the fluoromethylene signal to that in d_1 -chloroform, as illustrated in Figure 4.18.

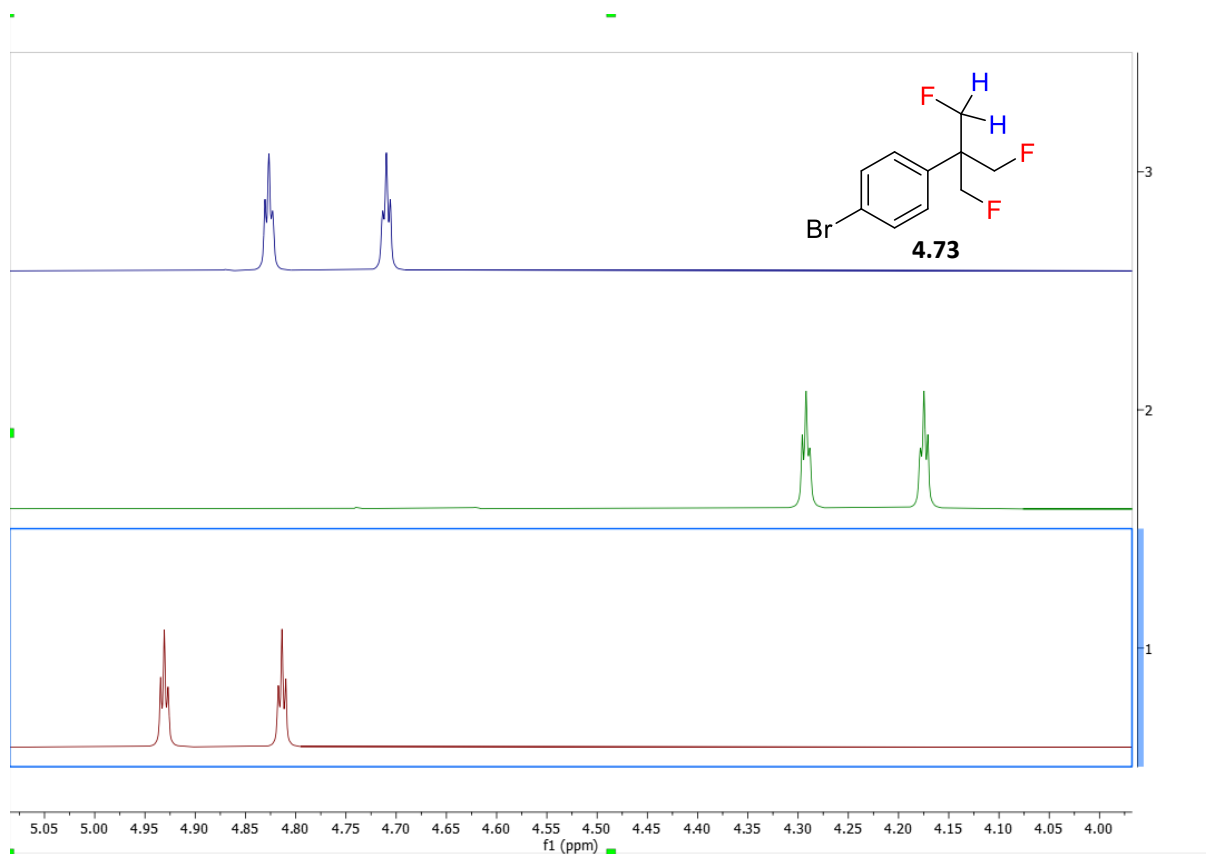


Figure 4.18 – ^1H NMR spectra of the CH_2F signal of **4.73** in d_1 -chloroform (top), d_8 -toluene (middle) and d_6 -acetone (bottom).

The ^1H NMR spectra of **4.73** show that the NMR solvent has a noticeable effect on the chemical shift of the CH_2F signals. In chloroform, the CH_2F signal comes at 4.77 ppm whereas recording the ^1H NMR in acetone causes the signal to shift downfield, to 4.87 ppm. This is consistent with the carbonyl oxygen of acetone interacting with the positively polarised CH_2F hydrogens through hydrogen bonding. Meanwhile, recording the ^1H NMR in toluene causes an upfield shift to 4.23 ppm. This is consistent with the aryl ring of toluene interacting with the electropositive hydrogens and being influenced by the ring current of the aryl ring (anisotropic effect), as illustrated in Figure 4.19.

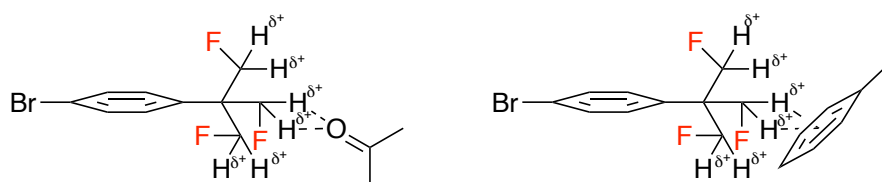


Figure 4.19 – An illustration of the interactions of **4.73** with the NMR solvents d^6 -acetone (left) and d^8 -toluene (right).

In order to explore electrostatic affinities further, interactions with chloride and bromide ions were monitored in a series of ^1H NMR titrations. When adding increasing amounts of a tetrabutylammonium halide salt to a fixed concentration of **4.73** in the NMR solvent, the affinity of the polarised hydrogens for the halogen ion can be visualised. This was explored in the first instance by titrating increasing concentrations of tetrabutylammonium bromide (TBAB) with *para*-bromo TFTB **4.73**, as shown in Figure 4.20.

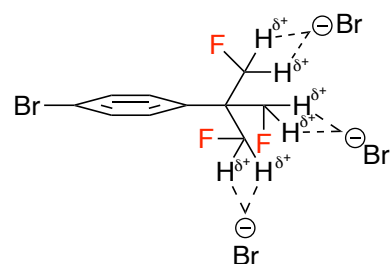
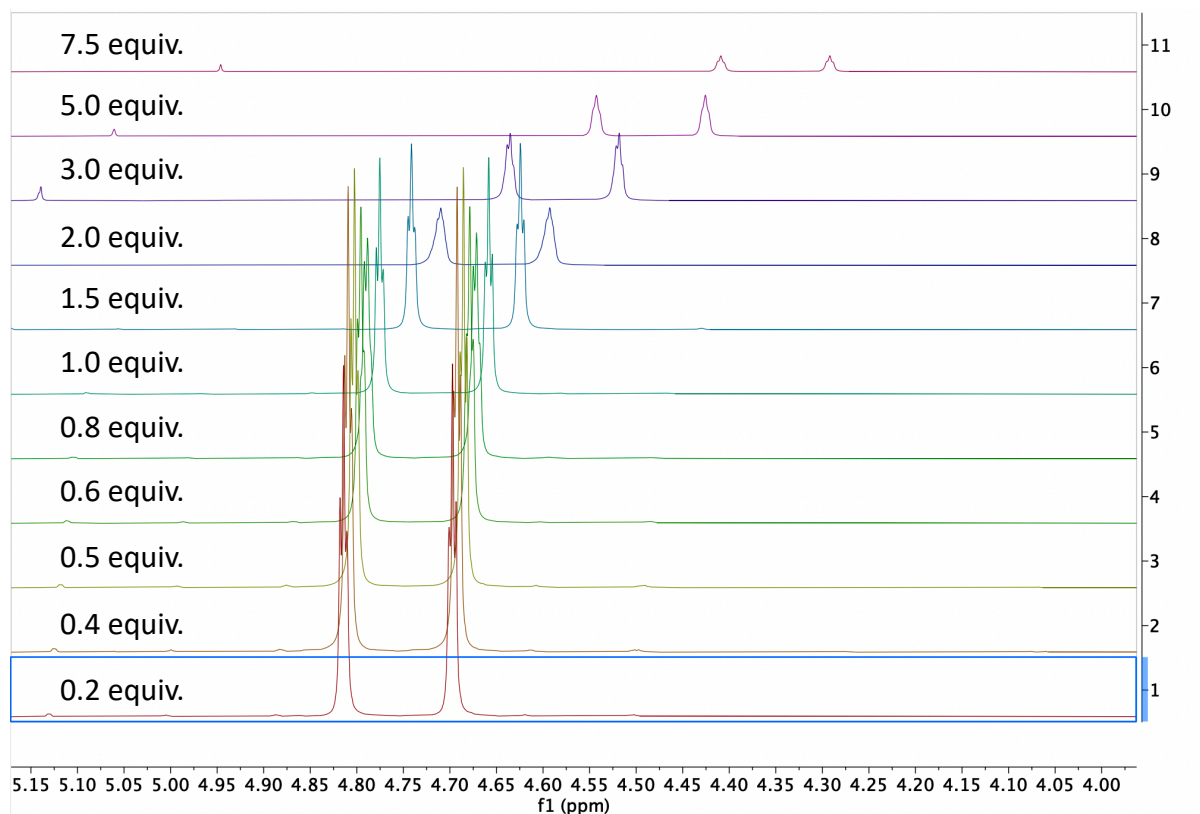


Figure 4.20 – $^1\text{H-NMR}$ titration of *para*-bromo TFTB **4.73** with increasing equivalents of tetrabutylammonium bromide, from 0.2 equiv. to 7.5 equiv., monitoring the $-\text{CH}_2\text{F}$ signal.

The $^1\text{H-NMR}$ spectra shows that the CH_2F peak shifts upfield with an increasing concentration of TBAB, consistent with an affinity between the $-\text{CH}_2\text{F}$ groups and the halide ion. The CH_2F peak shifted from 4.77 ppm (control) to 4.35 ppm at saturation with 7.5 equivalents of salt added, an upfield shift of 0.42 ppm. The experiment was also conducted with **4.73** and increasing amounts of tetrabutylammonium chloride (TBAC) as illustrated in Figure 4.21.

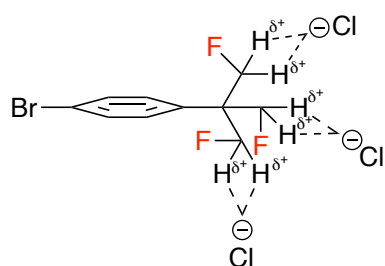
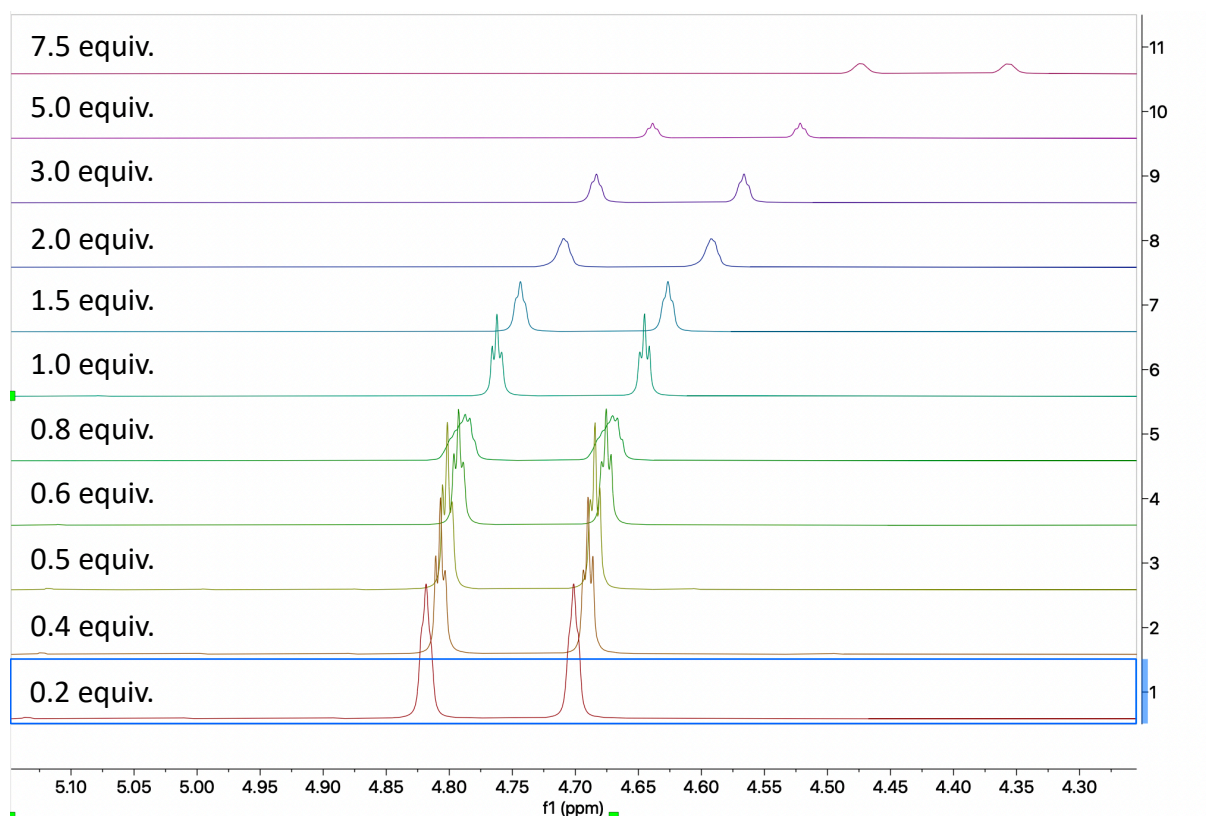


Figure 4.21 – ^1H -NMR titration of *para*-bromo TFTB **4.73** with increasing equivalents of tetrabutylammonium bromide, from 0.2 equiv. to 7.5 equiv., monitoring the $-\text{CH}_2\text{F}$ signal.

The ^1H NMR spectra again shows an upfield shift, with the CH_2F peak shifting from 4.77 ppm (control) to 4.41 ppm with 7.5 equiv of TBAC added, indicating a saturating effect. The magnitude of this shift at 0.36 ppm, is smaller than that with bromide ion suggesting a stronger affinity to bromide over chloride ion.

With this data in hand, it was possible to calculate an affinity constant in each case.²²⁰

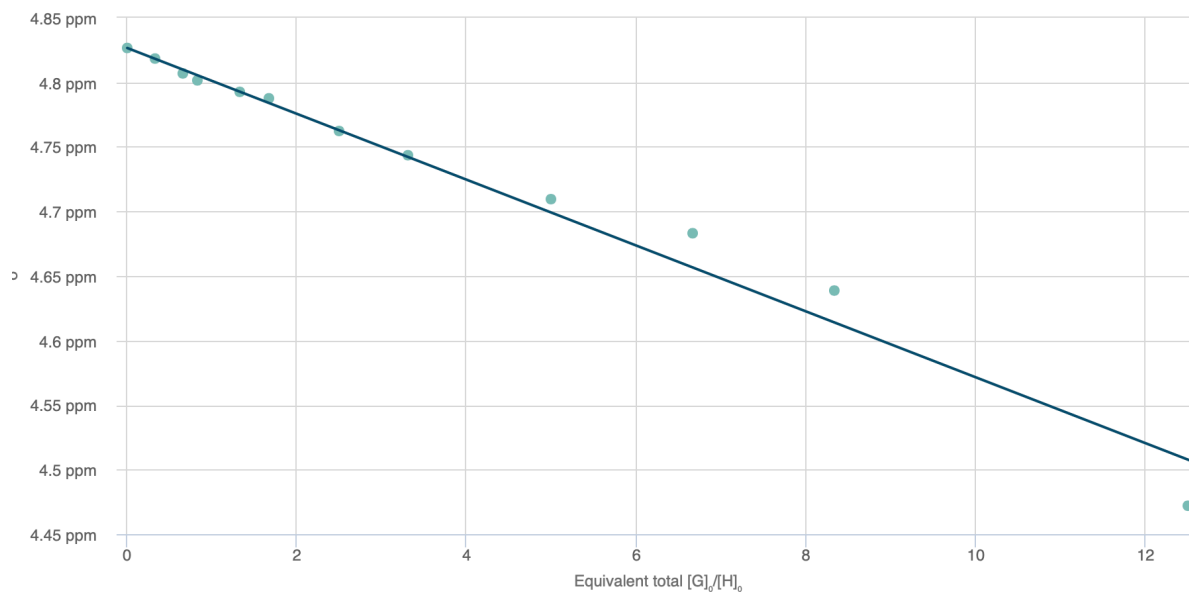


Figure 4.22 – Graph showing the binding fit of para-bromo TBTF **4.73** to chloride ion (TBAC) using the 1:1 host-guest binding model on <http://supramolecular.org>.²²¹

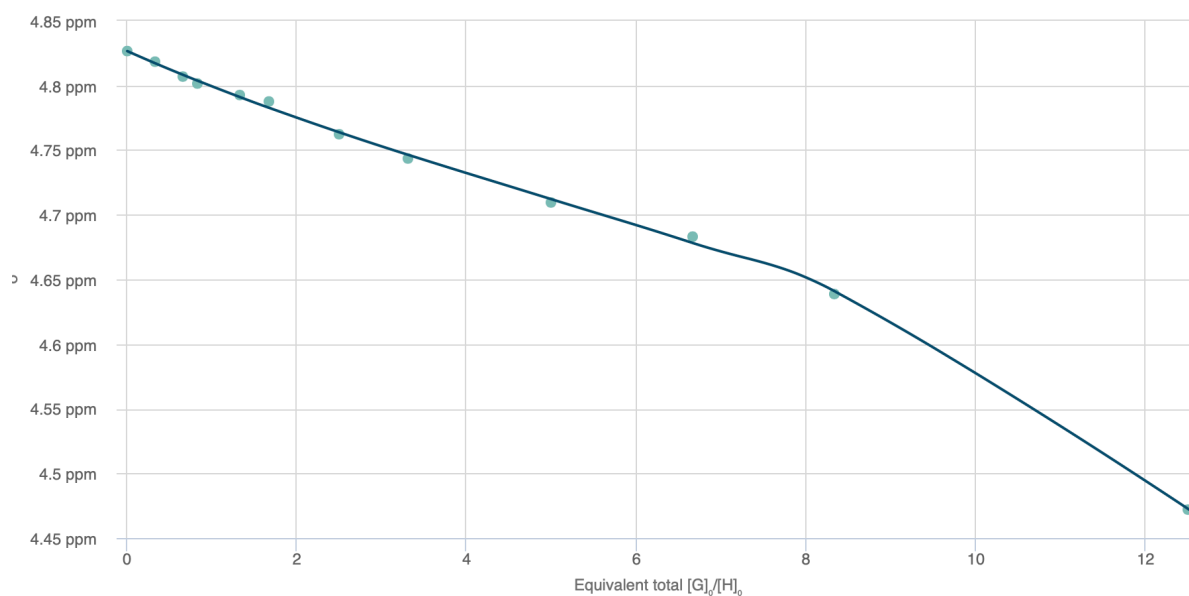


Figure 4.23 – Graph showing the binding fit of para-bromo TBTF **4.73** to chloride ion (TBAC) using the 1:2 host-guest binding model on <http://supramolecular.org>.²²¹

Association constants were determined by using the model developed by Thordarson at <http://supramolecular.org>.²²¹ Using the 1:1 host-guest binding model as shown in Figure 4.22, the association constant K for the binding of the TBTF moiety to chloride ion (TBAC) was calculated at $K = 1.83 \times 10^{-5} \text{ M}^{-1} \pm 3.30\%$, which is a very low value with a low margin of

error. Using the 1:2 host-guest binding model as shown in Figure 4.23, the value of the first association constant was determined as $K_1 = 1.20 \text{ M}^{-1} \pm 3.86\%$ and the value of the second was determined as $K_2 = -1.16 \text{ M}^{-1} \pm -3.19\%$. This value being negative shows that it is unlikely that the 1:2 host-guest binding model is the incorrect fit for this system. For bromide ion (TBAB), using the 1:1 host-guest binding model as shown in Figure 4.24, the value of the association constant was determined to be $K = 0.09 \text{ M}^{-1} \pm 2.81\%$, which is again a low value but with a low margin of error. Using the 1:2 host-guest binding model as shown in Figure 4.25, the value of the first association constant was determined as $K = 0.93 \text{ M}^{-1} \pm 13.2\%$ and the value of the second was determined as $K = 1.04 \text{ M}^{-1} \pm 19.2\%$. Although clearly observable by ^1H NMR, these values indicate rather weak interactions. These interactions would potentially better fit a 1:3 host-guest binding model, however such a model does not exist as of yet.

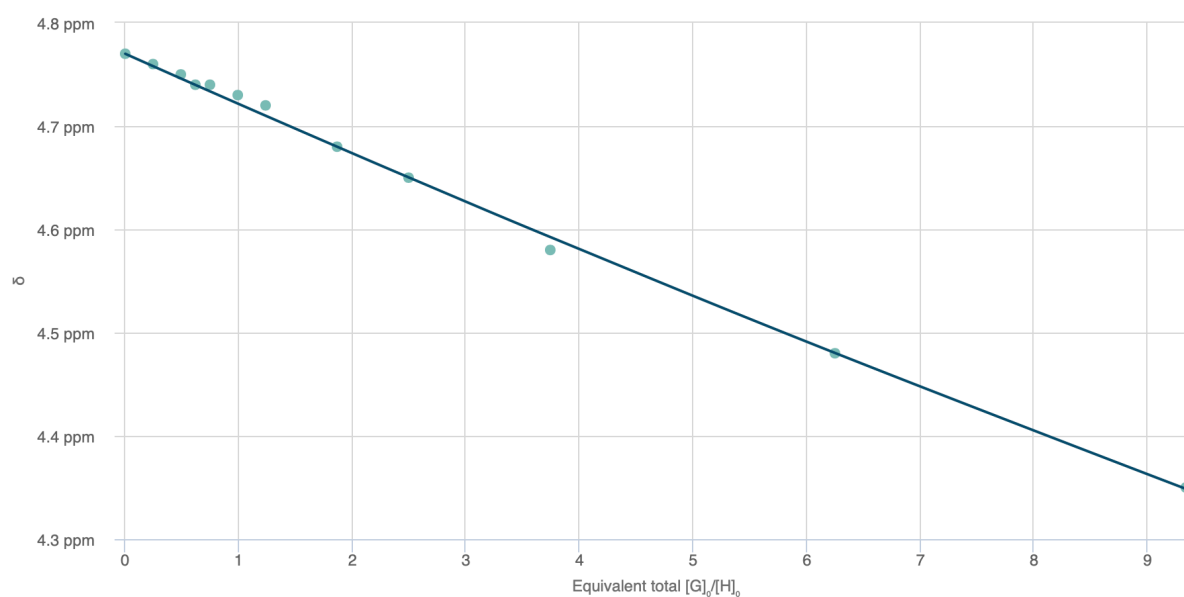


Figure 4.24 – Graph showing the binding fit of para-bromo TFTB **4.73** to bromide ion (TBAB) using the 1:1 host-guest binding model on <http://supramolecular.org>.²²¹

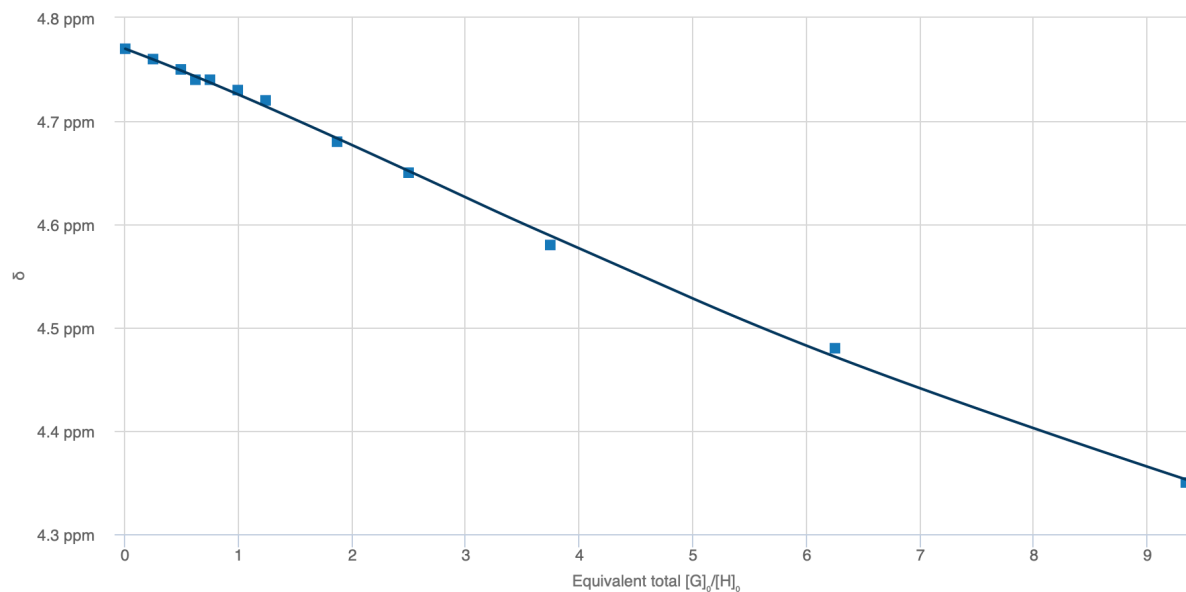
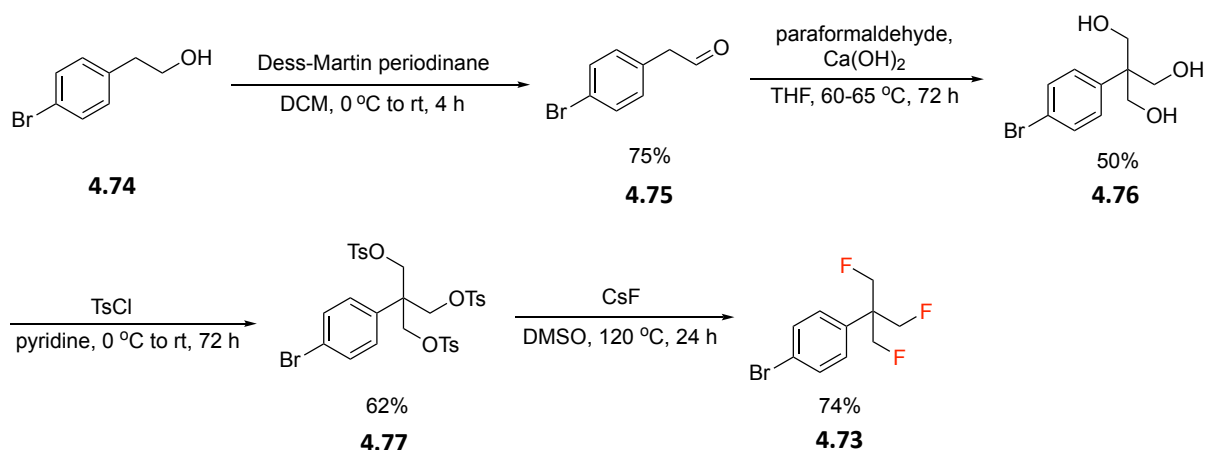


Figure 4.25 – Graph showing the binding fit of *para*-bromo TFTB **4.73** to bromide ion (TBAB) using the 1:2 host-guest binding model on <http://supramolecular.org>.²²¹

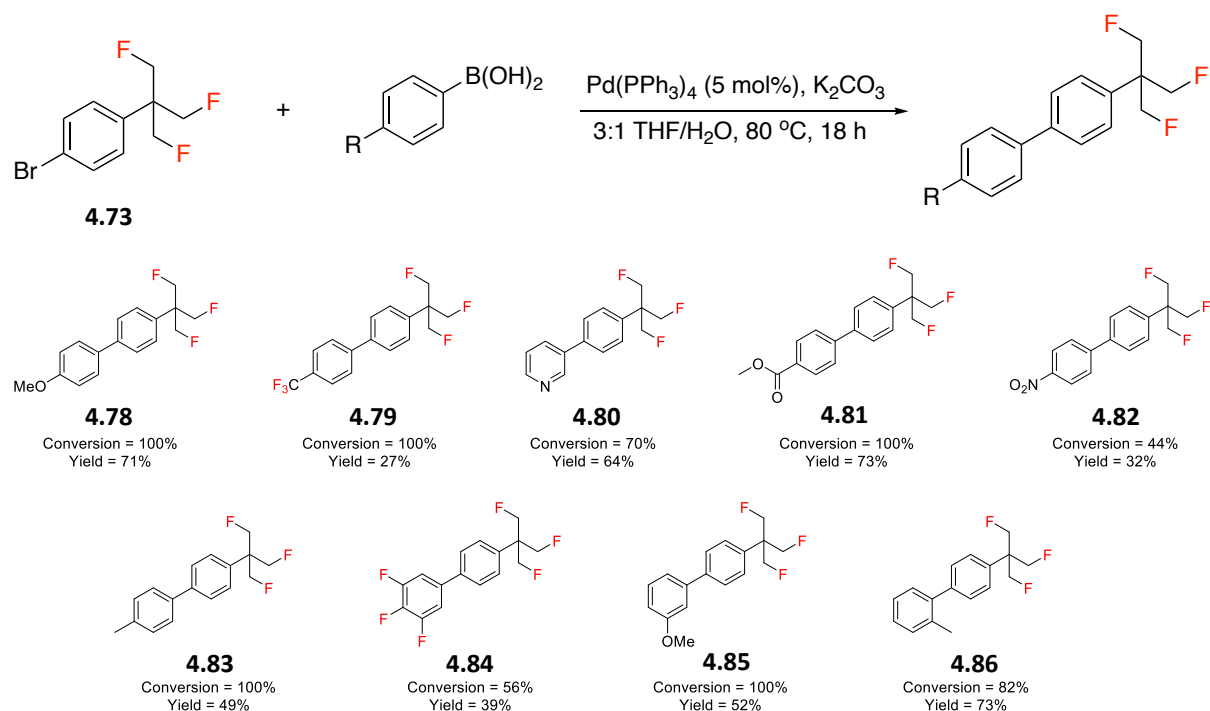
4.2.3 Cross-coupling reactions of the tri-fluoro *tert*-butyl group

With these results, a focus was placed on exploring the chemical properties of the aryl-TFTB moiety further. The *para*-bromo substituted TFTB product **4.73** was synthesised as a candidate substrate to explore cross-coupling reactions, as illustrated in Scheme 4.19. This was achieved starting with commercially available 2-(4-bromophenyl)ethanol **4.74**, which was oxidised using Dess-Martin periodinane to give 2-(4-bromophenyl)acetaldehyde **4.75**. The reaction was relatively efficient and the product was isolated in a 75% yield. Aldehyde **4.75** was then subjected to the three-step TFTB synthesis. The Cannizzaro reaction gave triol **4.76** in a 50% yield. This was then converted to the tritosylate **4.77** in 50%, and then fluorination with CsF gave the TFTB product **4.73** in a good conversion and it was isolated in 74% yield.



Scheme 4.19 – Synthesis of *para*-bromophenyl TFTB **4.73**.

Aryl bromide **4.73** was then explored as a substrate for Suzuki cross-coupling reactions, with a range of aryl boronic acids, and this generated the biphenyl products **4.78-4.86** as illustrated in Scheme 4.20.

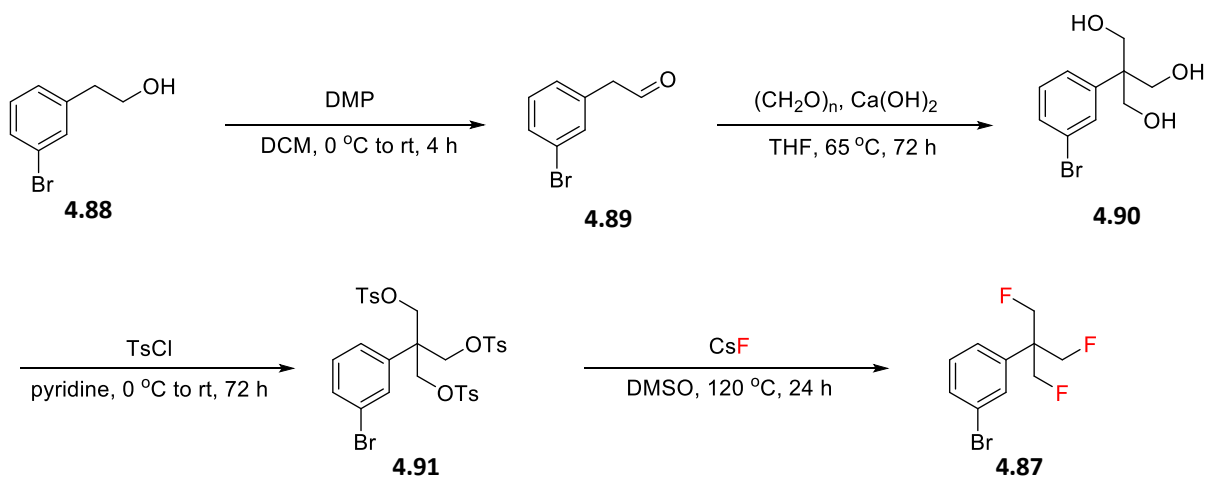


Scheme 4.20 – Products of the Suzuki cross-coupling reactions with **4.73**.

The Suzuki reactions proceed with conversions and yields dependent on the structure of the boronic acid used, showing the ability of this motif to be used in Pd(0)-catalysed cross-

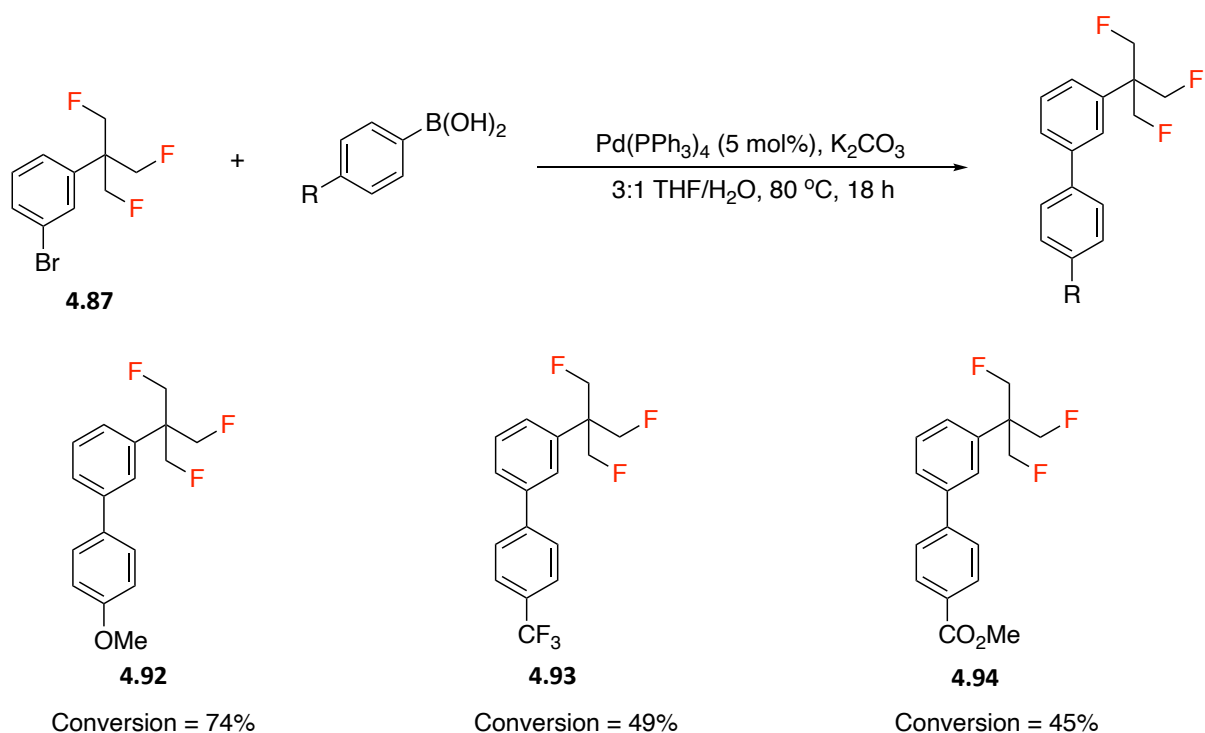
coupling reactions. The scope illustrated that the Suzuki reactions of the aryl-TFTB motif can be carried out with a wide range of substrates. Conversions and yields with boronic acids containing electron-donating groups were generally higher, for example in the case of **4.78** with a *para*-methoxyl group. However, yields and conversions with boronic acids containing electron-withdrawing groups generally dropped, as illustrated by the outcomes with **4.79** and **4.82** carrying *para*-CF₃ and *para*-NO₂ groups. The reaction was also shown to tolerate heterocyclic rings, as illustrated by pyridine **4.80**.

Following this, a synthesis of the *meta*-bromo substituent **4.87** was developed using the previously developed method, as illustrated in Scheme 4.21. The synthesis began with 2-(3-bromophenyl)ethanol **4.88** and involved an oxidation with Dess-Martin periodinane to give aldehyde **4.89**. The aldehyde was then reacted with paraformaldehyde and calcium hydroxide in THF in the Cannizzaro reaction to generate triol **4.90**. Purification of the triol here proved challenging by column chromatography due to the high polarity of the triol and attempts at recrystallisation were difficult due to the limited crystallinity of the product. None-the-less after chromatography and recrystallisation, the crude mixture was carried through to the next reaction. Reaction of triol **4.90** with tosyl chloride in pyridine gave tritosylate **4.91**. This again proved difficult to purify. Attempted purification by column chromatography failed to separate the desired product from the excess of tosyl chloride and attempts at recrystallisation also failed. Therefore, this material was carried through to the next reaction as an impure mixture. Trifluorination of the tosylate with CsF/DMSO gave the aryl-TFTB product **4.87**, again as an impure mixture, with ¹⁹F NMR analysis indicating a mixture of fluorinated products, likely mono, di and trifluoro compounds, which were not separated by column chromatography. Repeated attempts at fluorination for longer periods than 24 hours were unable to drive the reaction to completion.



Scheme 4.21 – Synthesis of meta-bromo aryl-TBTF **4.87**.

Arylbromide **4.87** was also explored in Suzuki cross-coupling reactions, as shown in Scheme 4.22.

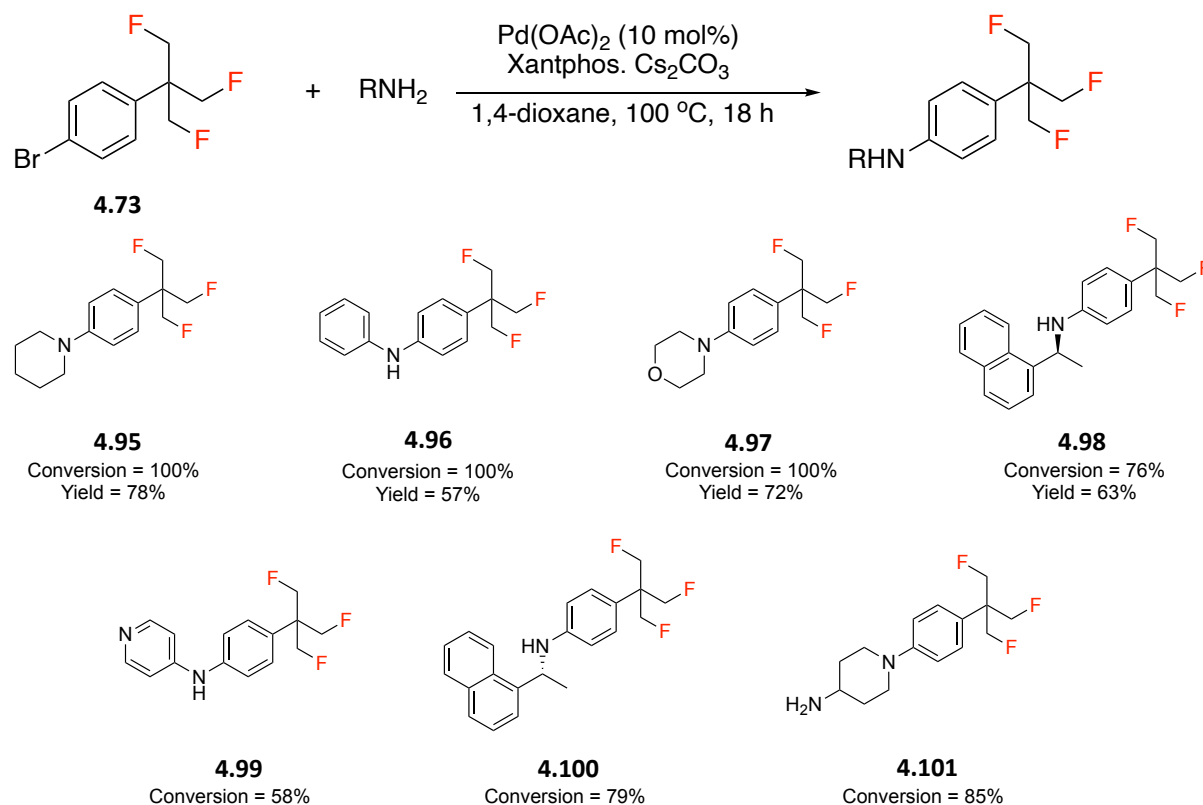


Scheme 4.22 – Suzuki cross-coupling products from meta-bromophenyl TFBT **4.87**.

While the reactions were conducted with good conversions, they were noticeably lower than those achieved with *para*-aryl bromide **4.73**. The three products of the *meta* motif also proved more difficult to purify by column chromatography yielding mixtures. Product **4.92** was isolated but was contaminated with boronic acid, which could not be separated after

multiple attempts at column chromatography. Products **4.93** and **4.94** were both isolated after column chromatography as mixtures of the desired product and starting material **4.87**.

Further cross-coupling reactions were explored using Buchwald-Hartwig reactions with **4.73** and a variety of amines. The products are illustrated in Scheme 4.23.



Scheme 4.23 – Buchwald-Hartwig cross-coupling reaction products **4.95-4.101** from **4.74**.

This reaction was shown to be robust, with good conversions achieved in general, and the TFTB aryl bromide **4.73** proved to be a good substrate with both primary and secondary amines. However, there were some issues with purification, with some of these compounds **4.99-4.101** undergoing decomposition when subjected to column chromatography, therefore only conversion values are presented in Scheme 4.23.

4.2.4 Conformational analysis of the aryl-TFTB group

These cross-coupling reactions generated a range of products and offered an opportunity to obtain a crystal structure. It was of interest to assess the conformation of the aryl-TFTB group, and particularly the disposition of the fluorine atoms relative to each other. *Meta*-methoxy biphenyl product **4.85** proved highly crystalline and emerged as a candidate for X-ray diffraction analysis. The structure is shown in Figure 4.27.

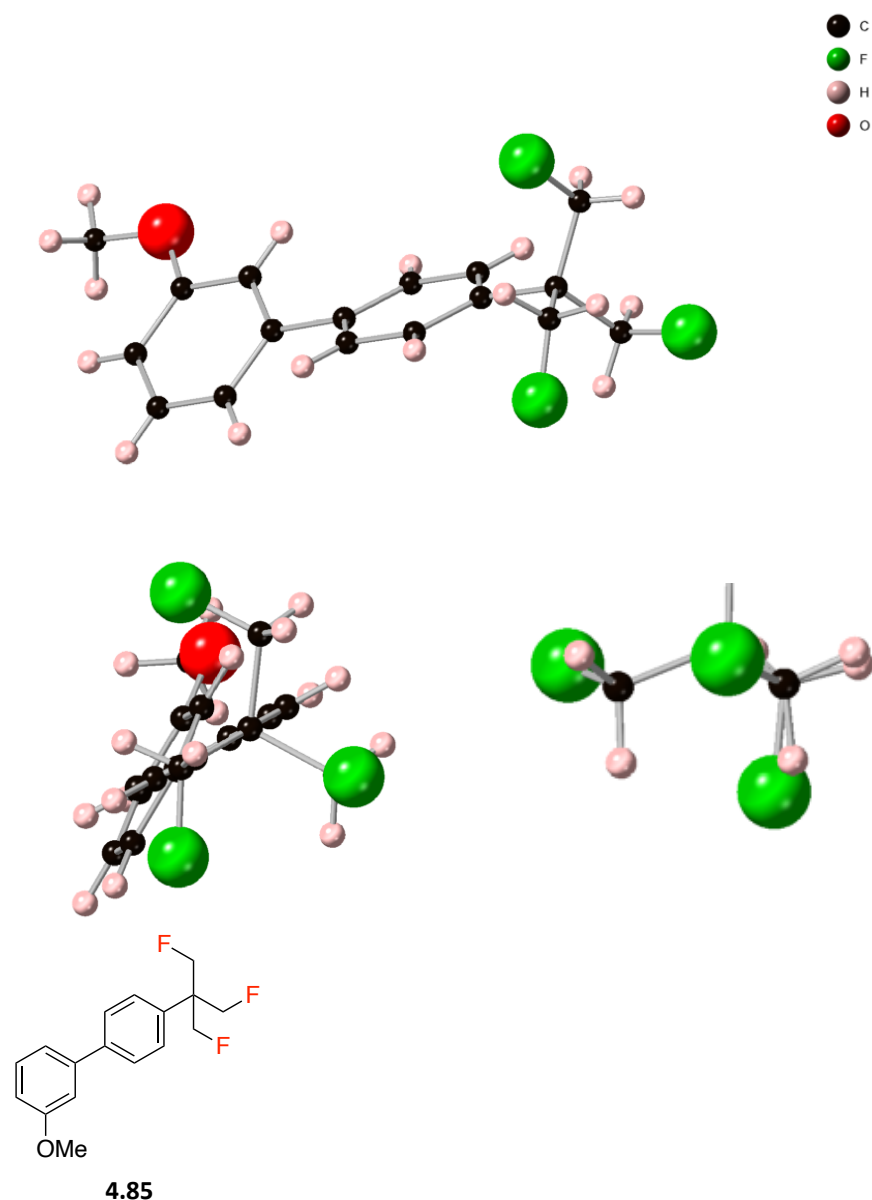


Figure 4.27 – Crystal structure of *meta*-methoxy TFTB **4.85**.

The resultant structure shows that the fluorine atoms orient away from each other, with the C-F bonds oriented along xyz axes. There are two interactions at play here. The primary interaction is that the fluorine atoms repel each other presumably to minimise electrostatic repulsion between the electronegative fluorine atoms. Also, there is a secondary interaction due to the electronegative fluorine atoms polarising their geminal hydrogen atoms. These positively polarised hydrogens then have an electrostatic attraction to the negatively polarised fluorine of a neighbouring fluoromethyl group, therefore creating an eclipsed conformation between neighbouring C-F and C-H bonds, as illustrated in Figure 4.28. Consistent with this, the HC...CF dihedral angle is almost planar ($\sim 11.0^\circ$).

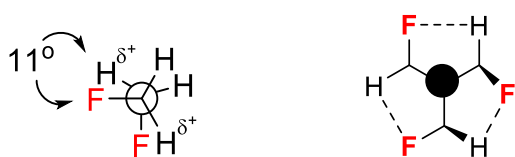


Figure 4.28 – Representation of the conformation of the aryl-TFTB group

This secondary interaction also offers a potential explanation for the non-linear drop in logP with increasing levels of fluorination as illustrated in Figure 4.16. With one fluoromethyl substituent, the polarised geminal hydrogens can interact directly with water resulting in the largest reduction in logP. However, when a second fluorine is added, the polarity of the geminal hydrogens is compensated by the electrostatic interaction with an adjacent fluorine, and their interactions with water are compromised to some extent. This effect increases again when the third fluorine is added.

These observations were confirmed in a computational analysis of the gas phase conformation of the aryl-TFTB moiety. In a collaboration with Dr Rodrigo Cormanich and Bruno Piscelli at the University of Campinas, Brazil, they used the X-ray data as the basis of a conformational analysis of aryl-TFTB **4.68**. In this study, they carried out a rotational energy map rotating around one of the fluoromethyl groups. In the study they identified three conformational minima and three transition states, and calculated their relative energy values in the gas phase, the results of which are summarised in Figure 4.29.

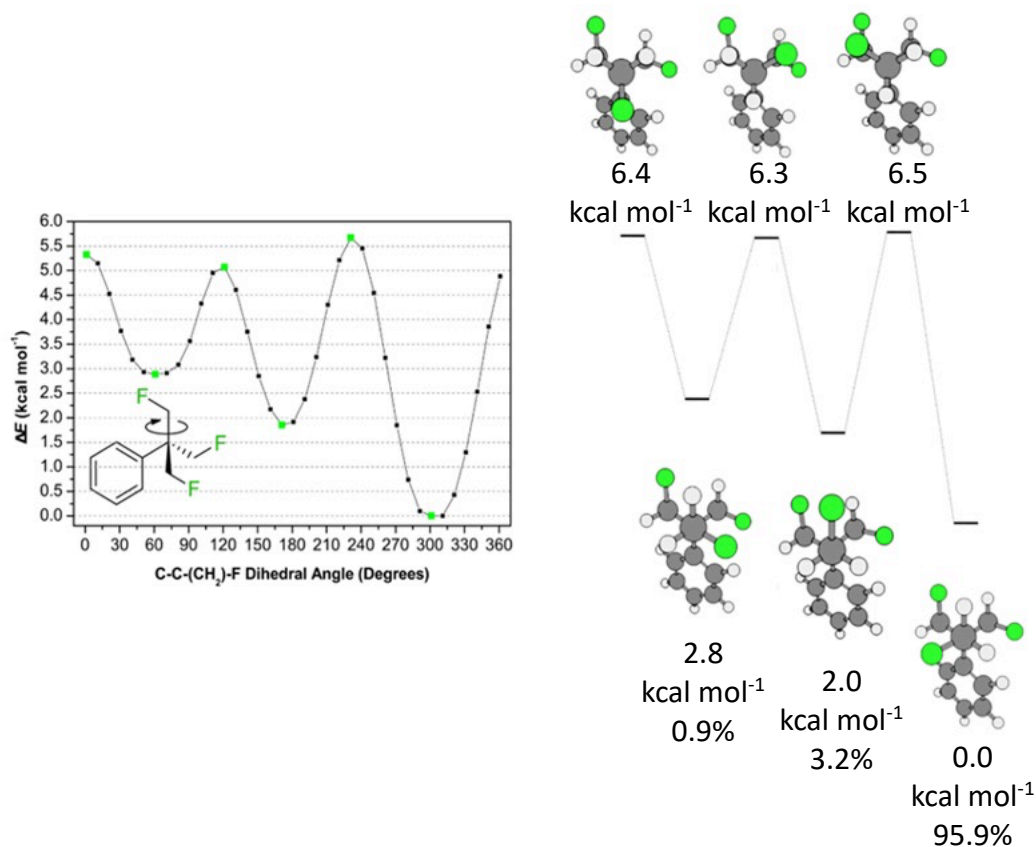


Figure 4.29 – Computational study: Rotational energy profile with three energy minima and three transition states and an overall conformational analysis of the TFTB group of compound **4.68**. The values below the structures show the Gibbs Free Energy (kcal mol⁻¹) of the conformation and the relative population of that conformation (%). (Conducted by Dr Rodrigo Cormanich and Bruno Piscelli at State University Campinas, Brazil.) The rotational energy profile was calculated at the M06-2X/def2-TZVP level.

The data revealed that the lowest energy conformation of the TFTB group was that observed in the X-ray derived structure of **4.85** (Figure 4.24), with a relative population of 95.9%. This analysis also confirmed the two stabilising effects as highlighted previously. Rotating one of the methyl groups 120° clockwise gives the next minimal energy conformation. The conformation features two of the fluorine atoms eclipsing each other and this generates an electrostatic repulsion, raising the energy of this conformer. This conformation was found to be 2.0 kcal mol⁻¹ higher in energy than the ground state energy conformation and had a relative population of only 3.2%. A further 120° clockwise rotation of the fluoromethyl group gives a final conformational minimum. This conformation also has two fluorine atoms eclipsing each other, however, it also features a steric interaction between a fluorine atom

and the aromatic ring which further raises the energy. Therefore, this conformer is 2.8 kcal mol⁻¹ higher in energy than the ground state conformation and has a relative population of only 0.9%.

Low temperature (-85 °C) ¹H NMR experiments were conducted on **4.73** to explore if the ground state conformer could be resolved, as shown in Figure 4.30. Toluene was chosen as the NMR solvent for this experiment due to its low melting point.

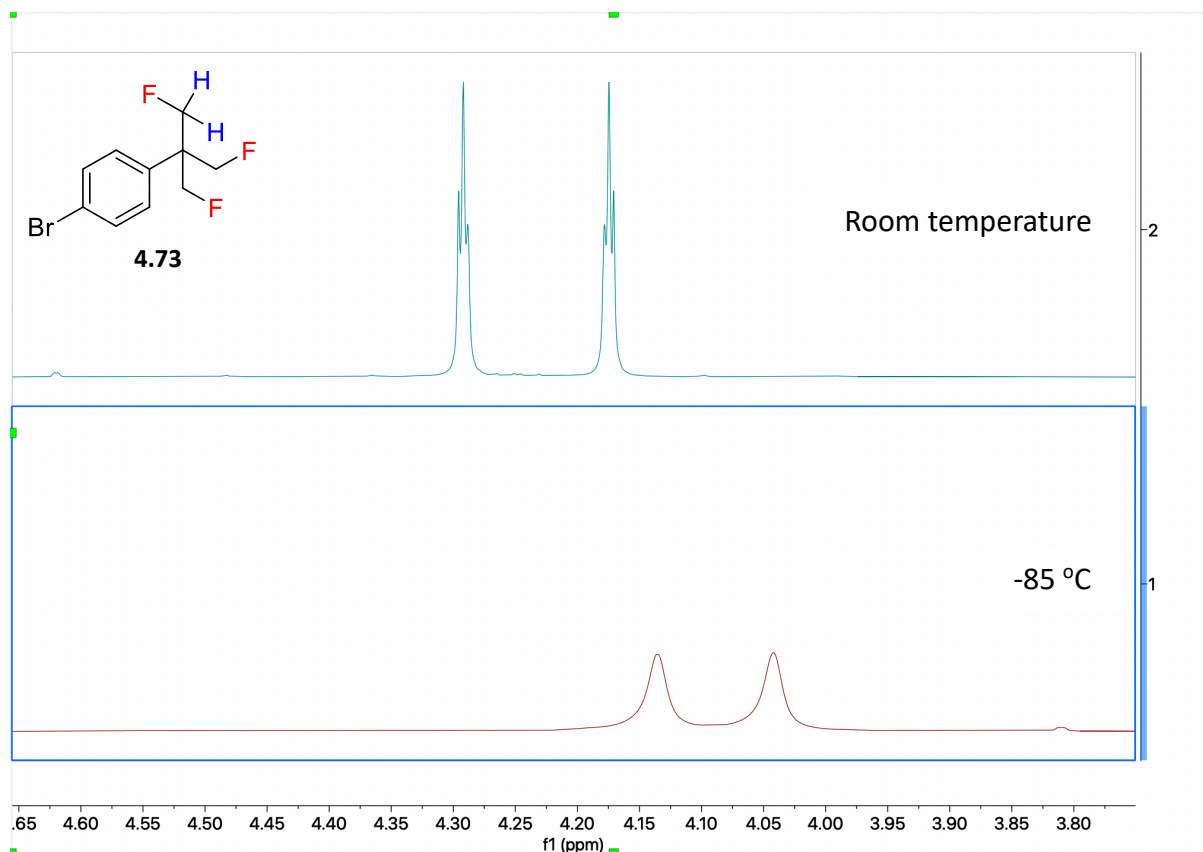
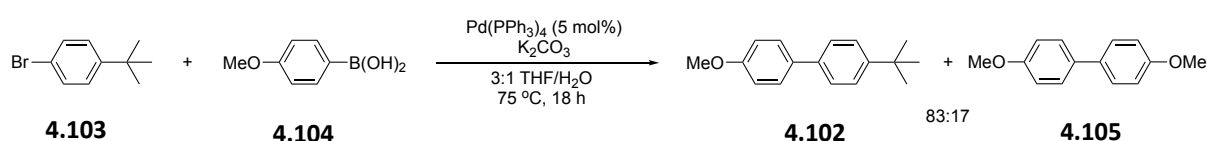


Figure 4.30 – CH₂F signal of **4.73** in the ¹H NMR experiment at -85 °C in toluene.

This ¹H-NMR experiment resulted only in a broadening of the CH₂F peak of **4.73**, such that the doublet of triplets was no longer resolved. There is also a small upfield shift associated with the CH₂F signal, shifting from 4.23 ppm at room temperature to 4.09 ppm at -85 °C. However, no resolution of the proton signals associated with different conformers of the aryl-TFTB moiety was observed, presumably as they are too close in energy.

4.2.5 Solubility of the aryl-TFTB group

Solubility is also an important metric in medicinal chemistry, and thus the solubility of one of the aryl-TFTB compounds was explored in water relative to its non-fluorinated analogue. *para*-Methoxy TFTB **4.78** was explored and the non-fluorinated *tert*-butyl analogue **4.102** was prepared via a Suzuki reaction between 1-bromo-4-*tert*-butylbenzene **4.103** and 4-methoxybenzoic acid **4.104**, as illustrated in Scheme 4.24. In this case, the final biphenyl product could not be completely separated from the homo-coupled side product **4.105**, leaving an 83:17 mixture of **4.102** and **4.105**.



Scheme 4.24 – Synthesis of **4.102** for use in solubility measurements.

Nevertheless, this mixture of non-fluorinated biphenyl compounds and the TFTB analogue were subjected to a solubility test. Around 20 mg of **4.78** and **4.102** were separately heated with water (1.5 mL) and each sample was boiled for 1 hour. The solutions were then cooled, and an accurate 1 mL sample of the water was taken, taking care to filter any remaining particulate. The samples were then freeze-dried and the mass of the remaining residue was measured to determine their solubilities per mL in water, which are shown in Figure 4.31.

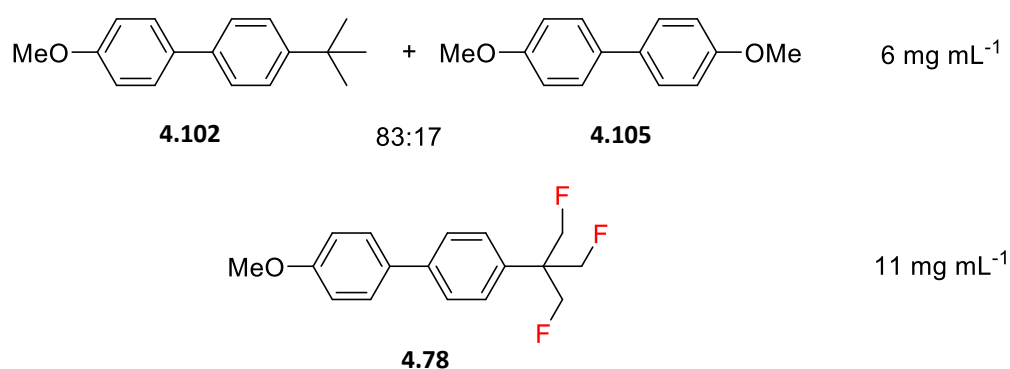


Figure 4.31 – Measured solubilities of *para*-methoxy TFTB **4.78** and **4.102** in water.

The measured solubility values show that the TFTB compound is measurably more soluble than the mixture of non-fluorinated biphenyls. Although a relatively limited study the outcome is consistent with the logP data and trends previously observed.

4.2.6 Synthesis of an aryl-TFTB analogue of pyridaben

Given that the aryl-TFTB group was a novel motif, it was of interest to incorporate it into an existing commercial product that contains a *tert*-butyl group. The model compound selected was pyridaben **4.106**. Pyridaben is an insecticide and acaricide which was developed in Japan.²²² It contains an aromatic *tert*-butyl group while also having an obvious disconnection at the C-S bond, making this an ideal candidate in which to incorporate an aryl-TFTB group.

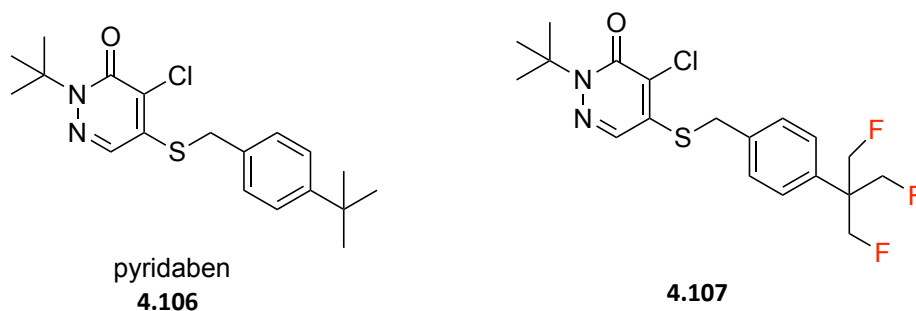
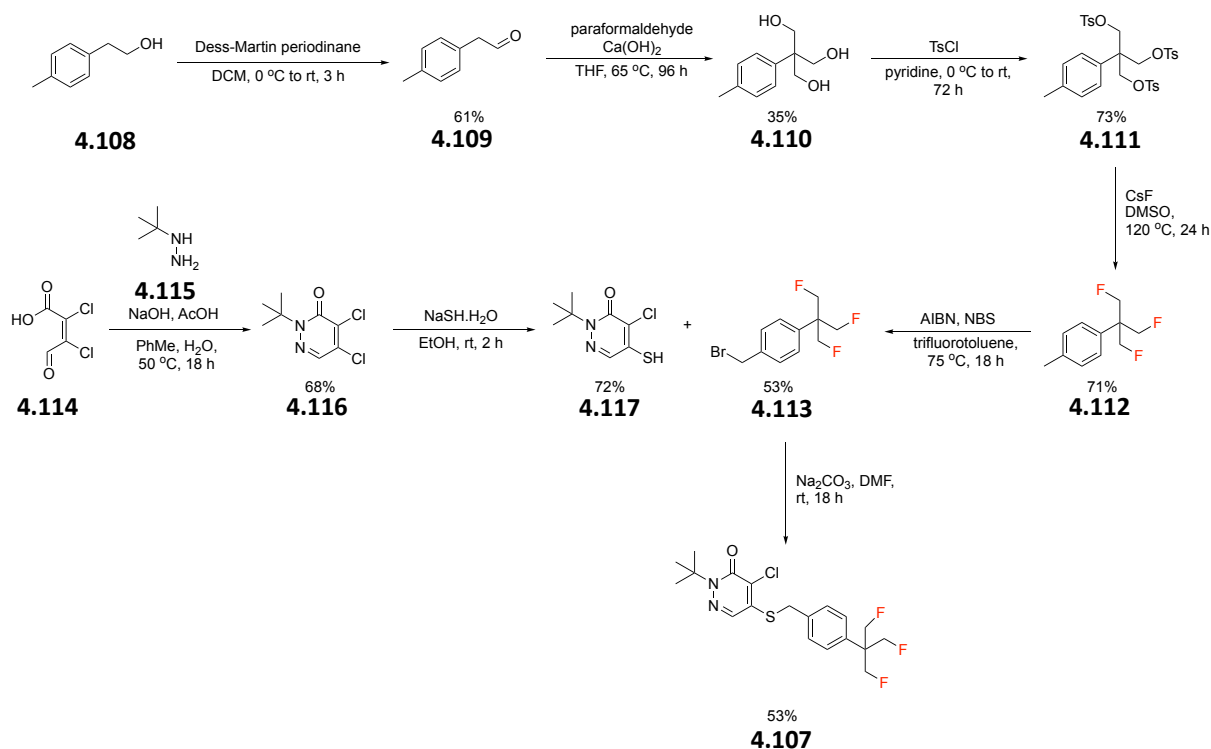


Figure 4.32 - Structures of pyridaben **4.106** and target aryl-TFTB-pyridaben derivative **4.107**.

In order to synthesise the appropriate electrophilic synthon, benzyl bromide **4.113**, triol **4.110** emerged as the obvious starting point. The already developed three-step aryl-TFTB synthesis could be initiated from aldehyde **4.108**. The aryl-methyl should be sufficiently reactive to bromination to install a good leaving group in **4.113**. Reaction then with thiolate **4.117** would generate the desired pyridaben derivative **4.107**. The synthesis proceeded as illustrated in Scheme 4.25.

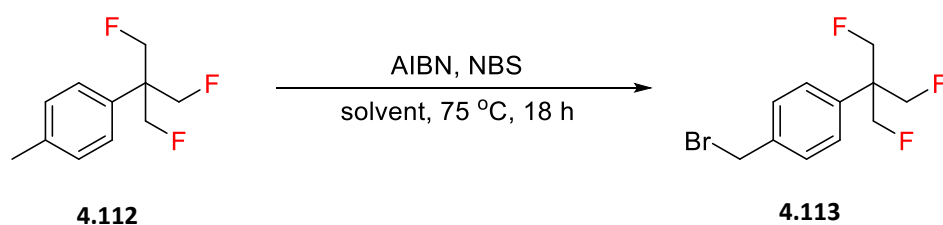


Scheme 4.25 – Synthesis of the aryl-TFTB-derivative of pyridaben **4.107**.

The route started with the oxidation of *p*-tolylethanol **4.108** using Dess-Martin periodinane to generate 2(*p*-tolyl)acetaldehyde **4.109** in a yield of 61%. The Cannizzaro reaction of aldehyde **4.109** with paraformaldehyde and calcium hydroxide generated triol **4.110** in a relatively modest yield of 35%. Tosylation of the triol generated **4.111** (73% yield) and finally, trifluorination with CsF/DMSO at 120 °C gave the desired TFTB substituted toluene **4.112** in a relatively good yield of 71%.

The next step involved benzylic bromination, however, this proved to be challenging. The basis for this bromination reaction was the Wohl-Ziegler reaction, which typically uses AIBN as a radical initiator, N-bromosuccinimide as the source of bromine, and carbon tetrachloride as the solvent, with heat to initiate the radical process. Acetonitrile was used initially as it is commonly used as a solvent in Wohl-Ziegler reactions. This was moderately successful, giving conversions of between 40% and 50% in multiple attempts. While it was possible to take this product and progress to the final pyridaben derivative, there was clear scope for improving the reaction, as shown in Figure 4.33. Several attempts were carried out with carbon tetrachloride, however, this actually proved less successful than acetonitrile,

where the best reaction gave only a 28% conversion. Finally, trifluorotoluene was explored as the solvent for this reaction, as reported by Golding *et al.*²²³ Reaction of **4.112** with AIBN, N-bromosuccinimide and trifluorotoluene, when heated to reflux, gave a full conversion to the desired benzyl bromide **4.113**, although the product could only be isolated in 53% yield after chromatography.



Solvent	Conversion ^a	Yield ^b
Acetonitrile	49%	37%
Carbon tetrachloride	28%	12%
Trifluorotoluene	100%	53%

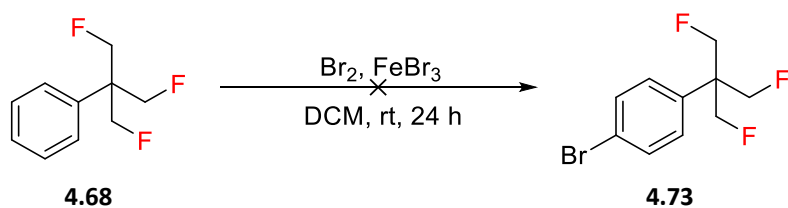
Figure 4.33 – Solvent screening of the Wohl-Ziegler reaction for the preparation of **4.113**.

^aConversions were monitored by ¹H NMR; ^b Yields after chromatography.

Meanwhile, mercaptopyridazinone **4.117** was synthesised following a literature procedure.²²⁴ This began with the combination of mucochloric acid **4.114** with *tert*-butylhydrazine **4.115** to generate dichloropyridazinone **4.116** in 68% yield. Selective nucleophilic thiolation of the *beta*-chlorine gave the desired thiol **4.117** in a 72% yield. Combination of the two building blocks **4.113** and **4.117** was conducted through a substitution reaction using sodium carbonate as the base, to give the desired TFTB pyridaben derivative **4.107** in a yield of 53%.

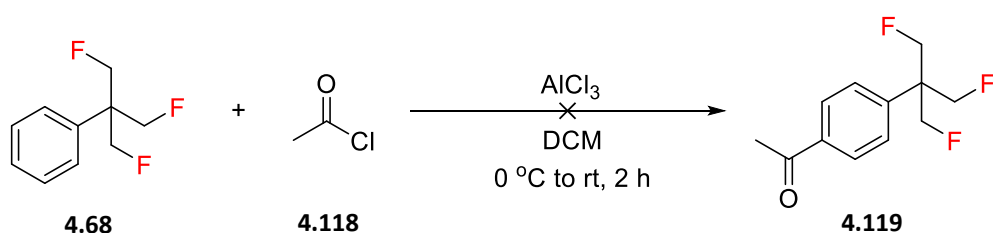
4.2.7 Other attempted reactions with the aryl trifluoro *tert*-butyl group

Several other reactions involving the para-bromoaryl-TFTB substrate were attempted that were unsuccessful. For example, attempts at electrophilic bromination of **4.68** using elemental bromine (Br₂) with FeBr₃ to give **4.73** were unsuccessful, as illustrated in Scheme 4.26, resulting in only starting material.



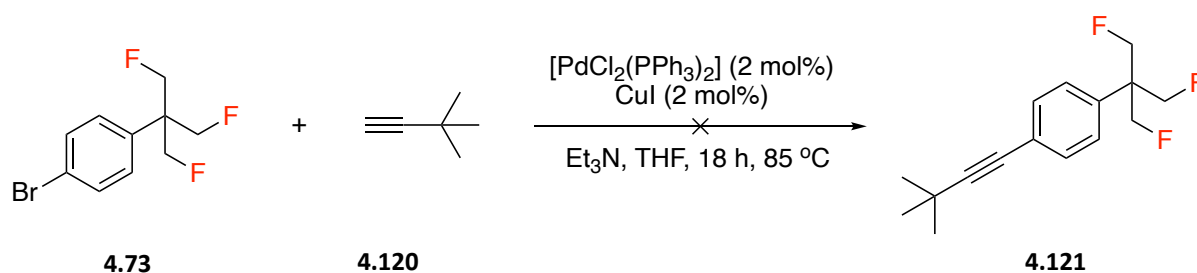
Scheme 4.26 – Attempted electrophilic bromination of phenyl TFTB compound **4.68**.

A Friedel-Crafts acylation was also attempted by reaction of **4.68** with acetyl chloride **4.118** to give **4.119**, as shown in Scheme 4.27. There was some evidence of product formation from the ^1H NMR, with peaks present potentially matching the TFTB CH_2F region and the acetyl CH_3 region. However, the product appeared to decompose during column chromatography. The origin of this instability was not clear, however it has been previously found that the reaction of fluorinated compounds with aluminium trichloride can lead to the exchange of halogen atoms between the organofluoride and aluminium chloride.²²⁵ Therefore, this could explain the inability of the TFTB group to undergo Friedel-Crafts acylation.



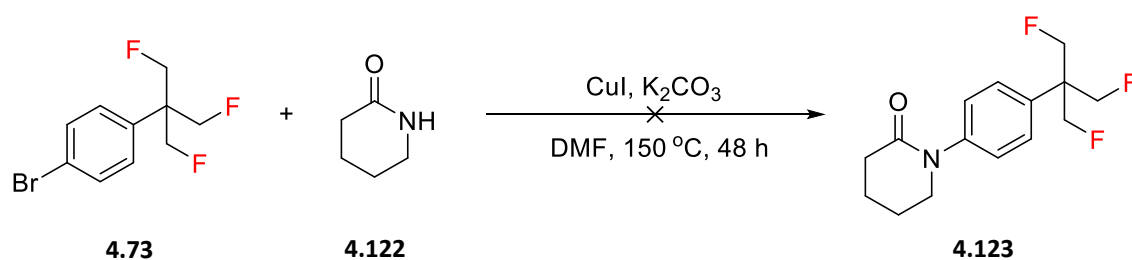
Scheme 4.27 – Unsuccessful Friedel-Crafts acylation of the phenyl TFTB **4.68** and **4.118**.

Sonogashira reactions were also attempted on a number of substrates including *para*-bromo TFTB **4.73** and 3,3-dimethylbut-1-yne **4.120**, to form acetylene **4.121** as shown in Scheme 4.28. However, these reactions were also unsuccessful, with only starting materials isolated.



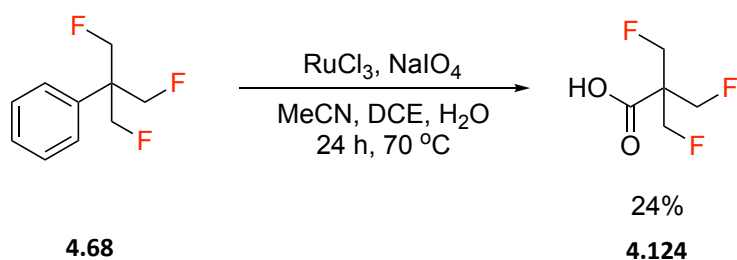
*Scheme 4.28 – Unsuccessful Sonogashira reaction of the para-bromophenyl TFTB **4.73** and 3,3-dimethylbut-1-yne **4.120**.*

Ullmann type N-arylation of *para*-bromo TFTB **4.73** with 2-piperidone **4.122**, and with catalytic Cu(I) / K_2CO_3 was also unsuccessful, giving only starting materials as shown in Scheme 4.29.



*Scheme 4.29 – Unsuccessful Ullmann type N-arylation of the para-bromophenyl TFTB **4.73** and 2-piperidone **4.122**.*

However, it was found to be possible to oxidise the aryl group of **4.68** to generate the corresponding carboxylic acid **4.124**, as shown in Scheme 4.30. This was achieved by reacting **4.68** with $Ru(III)Cl_3$ and $NaIO_4$ in an oxidation reaction following the biphasic protocols developed by Sharpless.²²⁶ This cleaved the aromatic ring to generate carboxylic acid **4.124**.



Scheme 4.30 – Ruthenium(III) chloride mediated oxidative cleavage of aromatic ring.

One challenge here involved the isolation of carboxylic acid **4.124**. The lack of a chromophore and the polarity of the carboxylic acid made chromatography challenging. This was solved by purifying **4.124** by titration, as unlike the starting material, the product was not soluble in hexane. In the event, the product was isolated in a yield of 24%. This reaction provides a new building block containing the TFTB motif and opens access to derivatives most obviously amides. However, exemplification was not pursued in this project due to the low recovery of carboxylic acid **4.124**, which is exacerbated by the large mass loss as a consequence of the aryl oxidation.

4.2.8 A study of the metabolism of the tri-fluoro *tert*-butyl group

With the introduction of the aryl-TFTB moiety as a potential motif for pharmaceutical and agrochemical products, work was initiated to explore its metabolism. This was approached using the fungus *Cunninghamella elegans*. This fungus is often used as a model for human metabolism as it is rich in cytochrome P450 enzymes. Therefore, exposing aryl-TFTB compounds to *C. elegans* should indicate to a first approximation what might happen within the human gut and liver. Accordingly, a sample of **4.68** was sent to collaborators at University College Dublin (Prof. Cormac D. Murphy and Mohd Faheem Khan), who work with *C. elegans* and they conducted a metabolism study. When **4.68** was exposed to the fungus in a 3 day (72 h) incubation, 55% was metabolised, leaving 45% of residual **4.68** as illustrated in the GC trace in Figure 4.34. The GC-MS analysis identified several metabolites, the most prominent of which was labelled as M4.

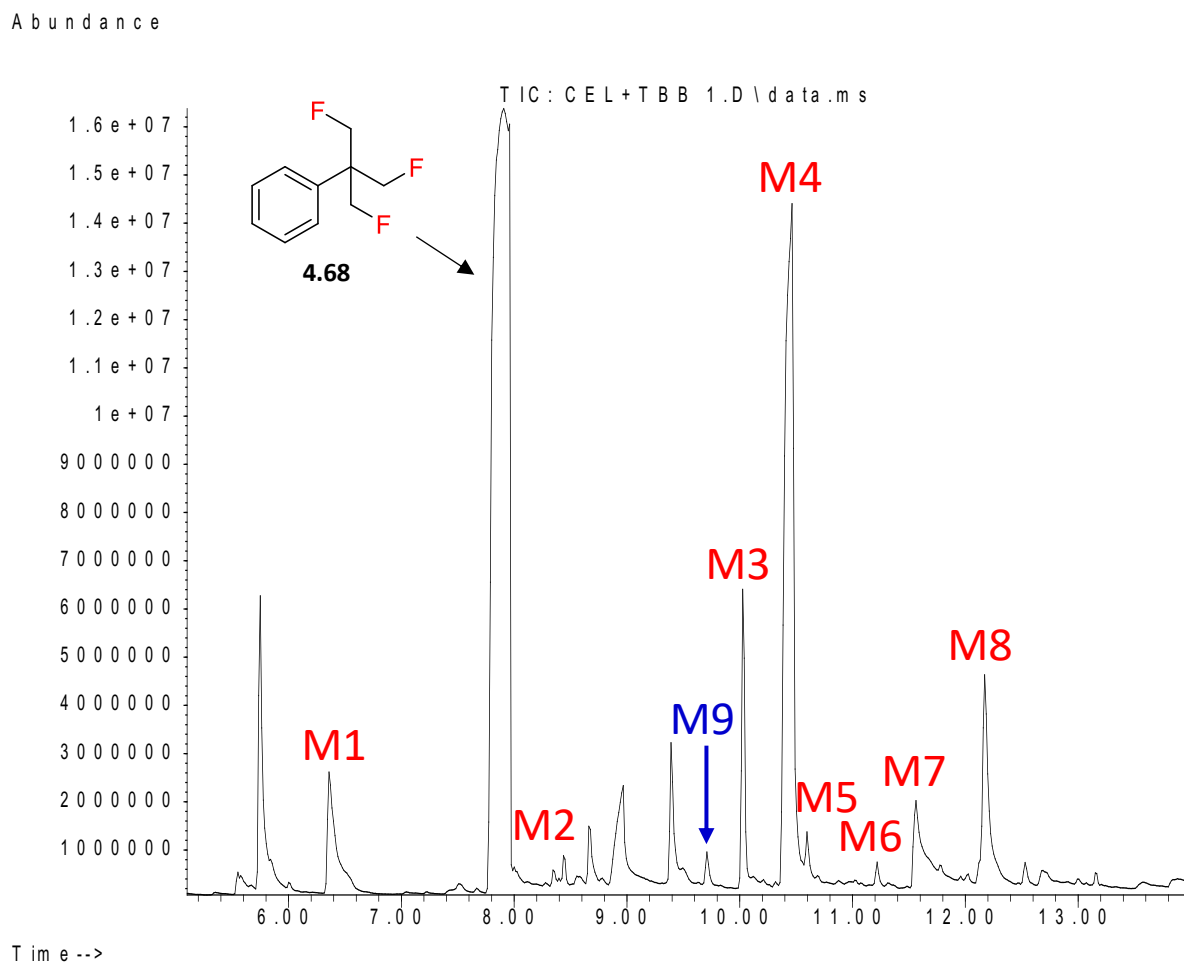


Figure 4.34 – GC trace of the extract after metabolism of **4.68** by *C. elegans* (obtained by Prof. Cormac D. Murphy and Mohd Faheem Khan at University College Dublin).

The metabolism of *tert*-butyl benzene **4.72** by *C. elegans* was also tested as a control, as shown in Figure 4.35, in order to provide a comparison of the rate of metabolism of the fluorinated and non-fluorinated *tert*-butylbenzenes.

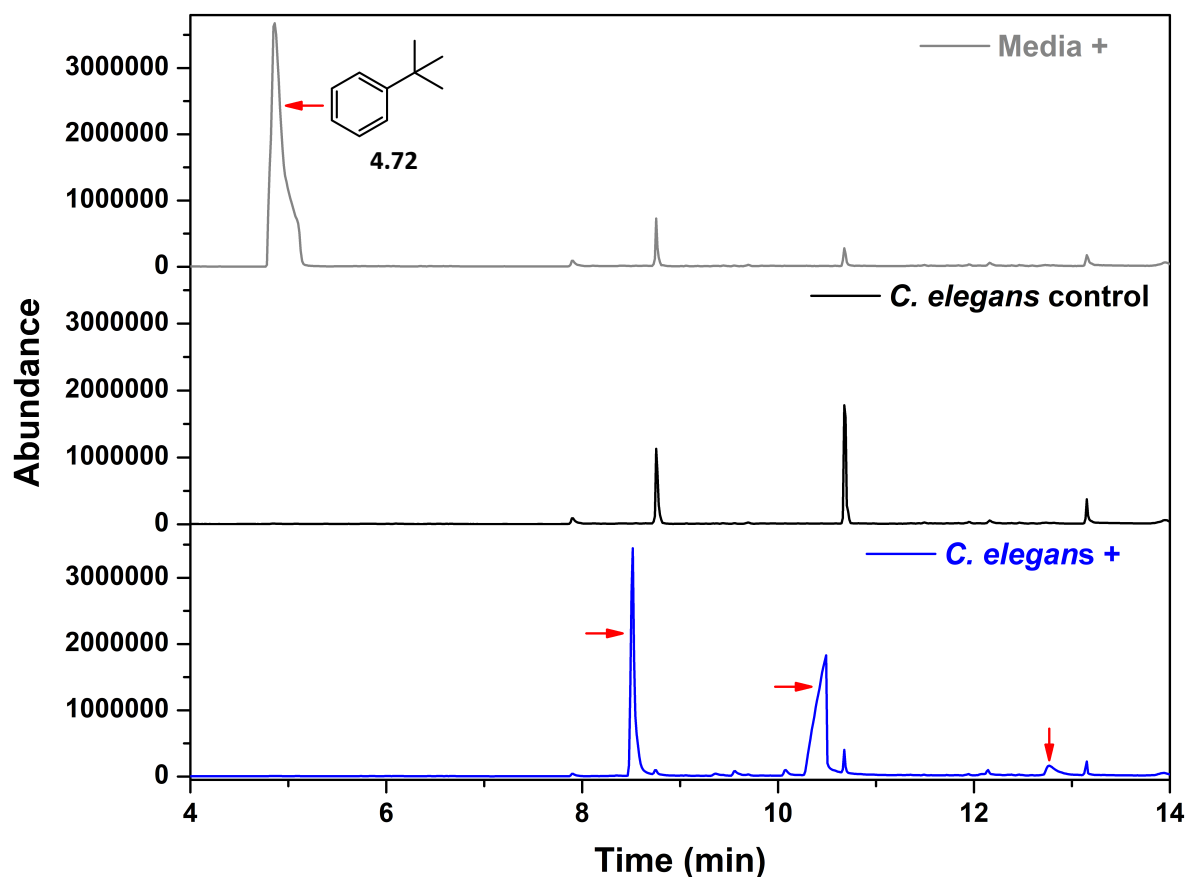
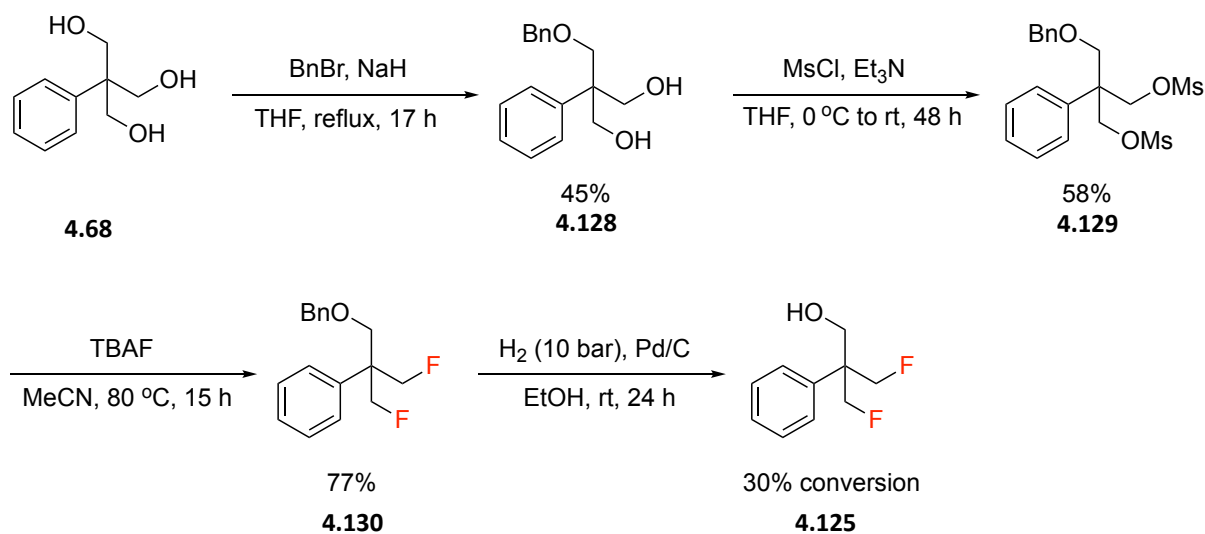


Figure 4.35 – GC-analysis after metabolism of tert-butyl benzene **4.72** with *C. elegans* (obtained by Prof. Cormac D. Murphy and Mohd Faheem Khan at University College Dublin).

In the event tert-butyl benzene **4.72** was fully metabolised by *C. elegans* after 72 hours, unlike the aryl-TFTB compound (55%), indicating a more rapid metabolism. Therefore, the three fluorine atoms slow the metabolism, indicating that the introduction of a TFTB group into a potential drug molecule could be used to modulate the rate of metabolism of that drug. It is important too to note in the context of the broader PFAS discussion that the TFTB group does metabolise, and that it is not a persistent fluorochemical motif.

GC-MS of the products of the metabolism of **4.68** suggested the presence of certain products and a potential degradation pathway, as illustrated in Scheme 4.30. The major metabolite M4 had a molecular mass consistent with alcohol **4.125**. This could arise by P-450 hydroxylation of one of the $-\text{CH}_2\text{F}$ groups to generate an intermediate fluorohydrin such as



Scheme 4.31 – Synthesis of putative metabolite M4 **4.125**.

The synthetic route to **4.125** as illustrated in Scheme 4.31 required an initial monobenylation reaction of **4.68** and was carried out using benzyl bromide (1.1 equiv.) and NaH (1 equiv.) to give the desired monobenzylated diol **4.128** in a 45% yield. Initial attempts to activate the unprotected alcohols as better leaving groups, by tosylation with tosyl chloride in pyridine, were unsuccessful. Although there was good evidence of monotosylation, the second tosylation would not take place. However, it was possible to activate both alcohols via mesylation using mesyl chloride and triethylamine, and this gave the desired product **4.129** in a 58% yield. Initial attempts to fluorinate the mesylate **4.129** using CsF gave a mixture of the desired product and a side-product that was inseparable by column chromatography. However, the use of TBAF in acetonitrile proved much more efficient and gave the difluorinated product **4.130** in 77% yield. For the final step, an attempted Pd/C/H₂ hydrogenation of **4.130** at atmospheric pressure did not give any reaction, and only starting materials were isolated. However, when the hydrogen pressure was increased (10 bar) there was some improvement with a 30% conversion to the desired product **4.125**. This gave enough product to determine whether **4.125** was also present in the metabolism extract.

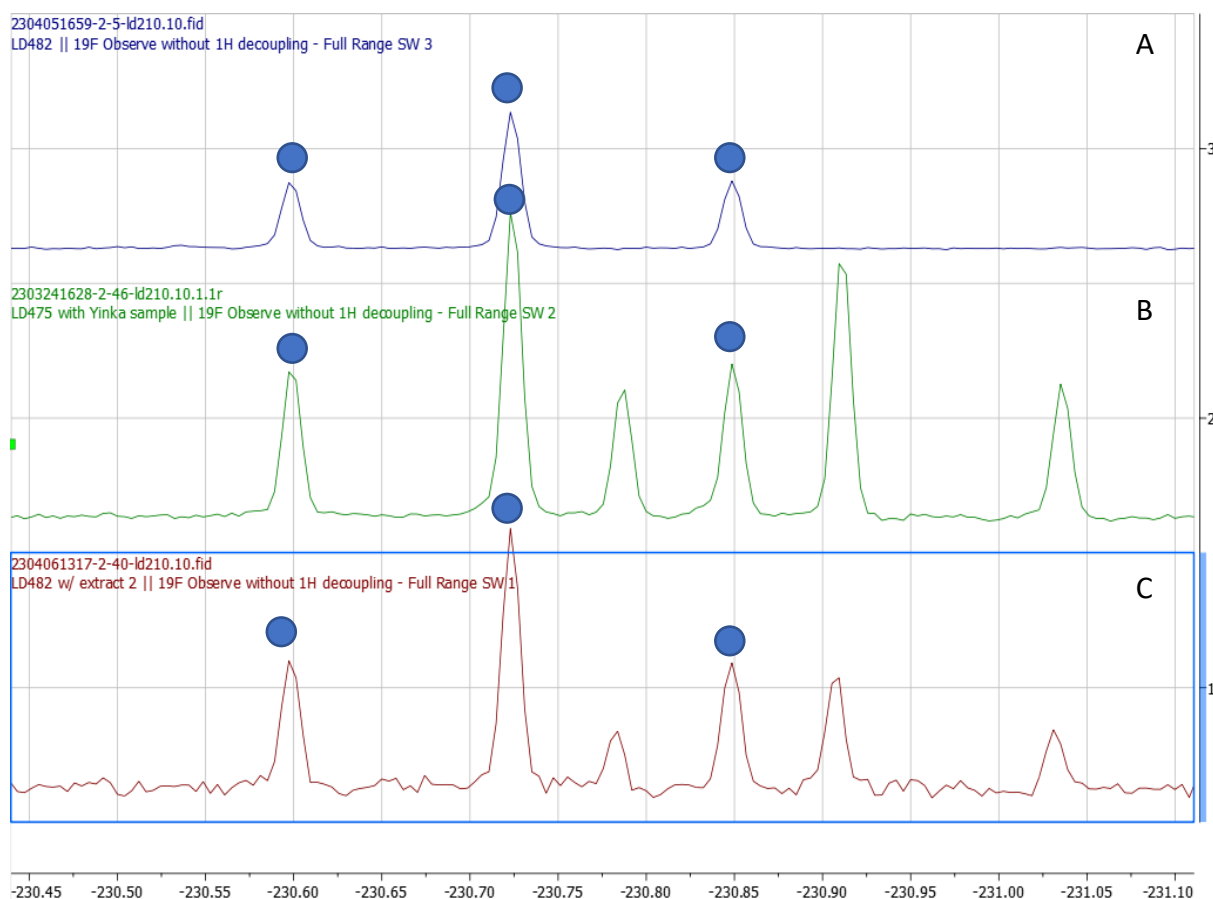


Figure 4.36 – ^{19}F NMR spectra of the co-addition of synthetic **4.125** and the metabolite extract from **4.68** in *C. elegans*. The blue dots indicate the synthetic reference. Spectrum A = ^{19}F NMR of synthetic **4.125**. B = ^{19}F NMR of the metabolite extract from **4.68** in *C. elegans*. C = ^{19}F NMR of a mixture of synthetic **4.125** and the metabolite extract from **4.68** in *C. elegans*.

The top ^{19}F NMR spectrum (A) in the stack in Figure 4.36 shows the spectrum for synthetic **4.125**. This appears as a triplet, with a $^2J_{\text{HF}}$ value of 47.2 Hz (blue dots). Spectrum (B) in the middle highlights the same area of the ^{19}F NMR spectrum of the extract from after *C. elegans* metabolism, clearly showing the same triplet with the same coupling constant ($^2J_{\text{HF}} = 47.2$ Hz). The bottom spectrum (C) shows a mixed ^{19}F -NMR sample with some of the synthesised product **4.125** co-added to the extract after *C. elegans* metabolism of **4.68**. There is an identical overlap which again shows the same triplet with a $^2J_{\text{HF}}$ value of 47.2 Hz. There are no new peaks but there is a clear increase in the intensity of the highlighted triplet compared to the neighbouring signal, which is the peak from the remaining unmetabolised

starting material **4.68** within the extract. This, along with the mass spec data, confirmed that the compounds are the same and that **4.125** is indeed the major metabolite of **4.68**.

4.3 Conclusions

In this Chapter, a robust synthesis of the aryl-TFTB group has been developed. It is the first introduction of this group. This then allowed a study of the chemistry and properties of this unexplored group. The lipophilicity of the TFTB group was measured and compared to the lipophilicities of non-fluorinated, mono-fluorinated and di-fluorinated analogues. While this showed a clear logP decrease with increasing fluorination, the trend was not linear, with the rate of logP decrease, decreasing with increasing fluorination. A series of cross-coupling reactions were carried out under standard conditions, which led to a variety of products. In one case the crystal structure of an aryl-TFTB group was solved. This structure showed that the fluorine atoms preferentially orient away from each other, along xyz axes. This also showed that the C-F bonds each eclipse a C-H bond from a neighbouring methyl group, due to electrostatic attractions. Computational studies were conducted, which determined that the aryl-TFTB group has a conformationally preferred ground state, which matched that shown in the crystal structure. This ground-state conformer has a relative population of 95.9% in the gas phase. The TFTB group was then incorporated as an analogue of the commercially significant insecticide pyridaben. Finally, a study of the metabolism of the TFTB group in *C. elegans* was conducted, finding that it metabolises readily, but more slowly than its non-fluorinated *tert*-butyl analogue. One metabolite was clearly identified as an alcohol, which could arise after P-450 hydroxylation, HF elimination and then biocatalytic reduction of the intermediate aldehyde. Synthesis of the synthetic alcohol allowed for confirmation of the identity of the major metabolite as the proposed alcohol. This work could further be explored by the development of the synthesis of an aliphatic TFTB group, which would allow for further exploration of the properties of this group.

Chapter 5 - Chiral *tert*-butyl group

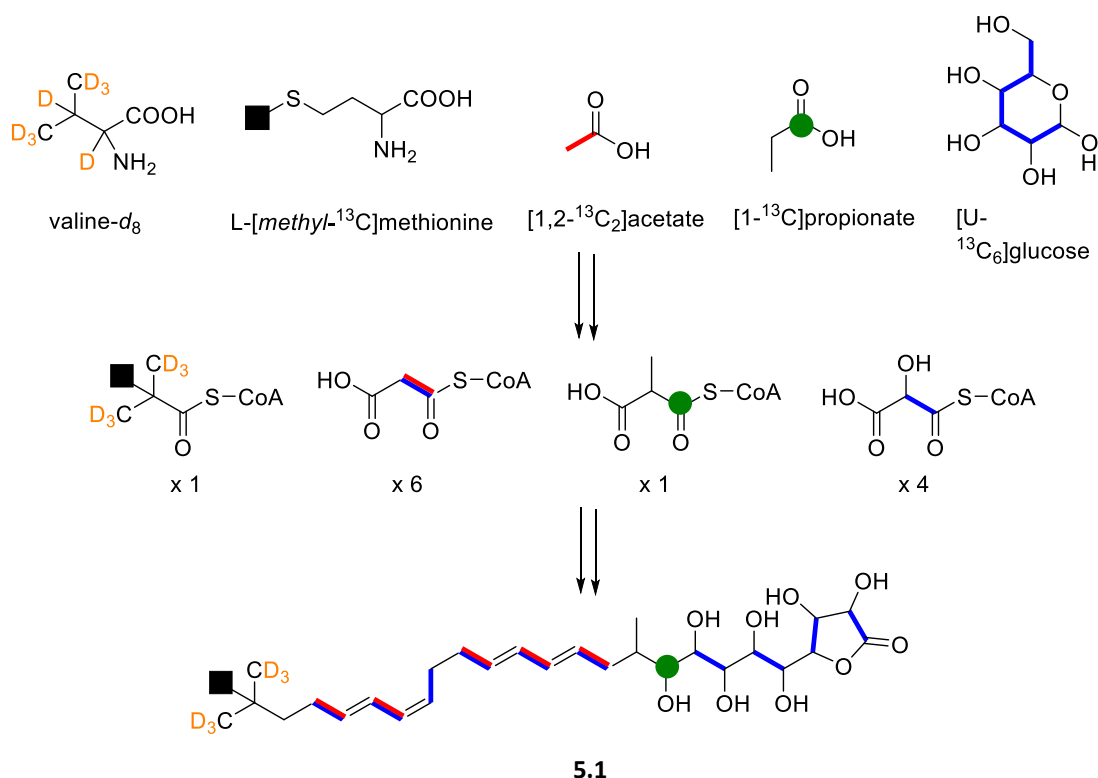
Work reported within this chapter was completed by:

Synthesis of anthracene derivatives	Luca Dobson
NMR assay	Luca Dobson
X-ray diffraction	Dr. David Cordes
Synthesis of deuterated oxazolidinones	J. L. Kellenberger and Prof. Duilio Arigoni at ETH Zurich

5.1 Introduction

5.1.1 Biosynthetic origin of the *tert*-butyl group

Butyrolactol A **5.1** is a polyketide that is a rare example of a natural product containing a *tert*-butyl group (Section 4.1.3). Butyrolactol A was first reported by Oki *et al.*, who isolated it from the culture broth of *Streptomyces rochei*.¹⁸⁷ They also found that butyrolactol A exhibited strong anti-fungal activity against strains of *Aspergillus fumigatus* and *T. mentagrophytes* and moderate activity against various yeasts. Igarashari *et al.* conducted a study to determine how the *tert*-butyl group is incorporated into butyrolactol A. They explored isotopic labelling experiments, incorporating candidate biosynthetic precursors into the structure of butyrolactol A to determine how the compound might be assembled, as illustrated in Scheme 5.1.²²⁷ It emerged that valine-d⁸ contributed two fully deuterated methyl groups of the *tert*-butyl group of butyrolactol A with the remaining methyl group originating from L-[*methyl*-¹³C]-methionine (SAM). This suggested that a C-methylation of the L-valine side group occurs, most likely involving the methyl transfer agent S-adenosyl-L-methionine (SAM).



Scheme 5.1 – Schematic of isotope incorporations from early metabolites during the biosynthesis of butyrolactol A 5.1.

5.1.2 The chiral methyl group

The *tert*-butyl group can be made chiral in principle, by differential isotope labelling of the methyl groups, (eg an enantiomer of $^{-13}\text{CH}_3$, $^{-\text{C}^2\text{H}_3}$, CH_3), however there are no examples of the synthesis of a chiral *tert*-butyl group reported in the literature. The closest reported analogue to a chiral *tert*-butyl group is the chiral methyl group using the three isotopes of hydrogen ($^{-\text{CH}_2^2\text{H}^3\text{H}} = \text{CHDT}$). The synthesis of individual enantiomers of this construct is challenging, as it requires sequential stereospecific introduction of the hydrogen isotopes. A straightforward NMR analysis of these products is also very challenging, as there are only tracer levels of the radioactive isotope tritium, and therefore a trace level of chiral molecules. This means that the enantiomers have to be determined through radioactivity after stereoselective enzymatic reactions.²²⁸

The chiral methyl group, illustrated in Figure 5.1 was first reported by Arigoni *et al.* in 1968.²²⁹

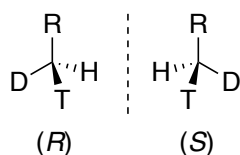
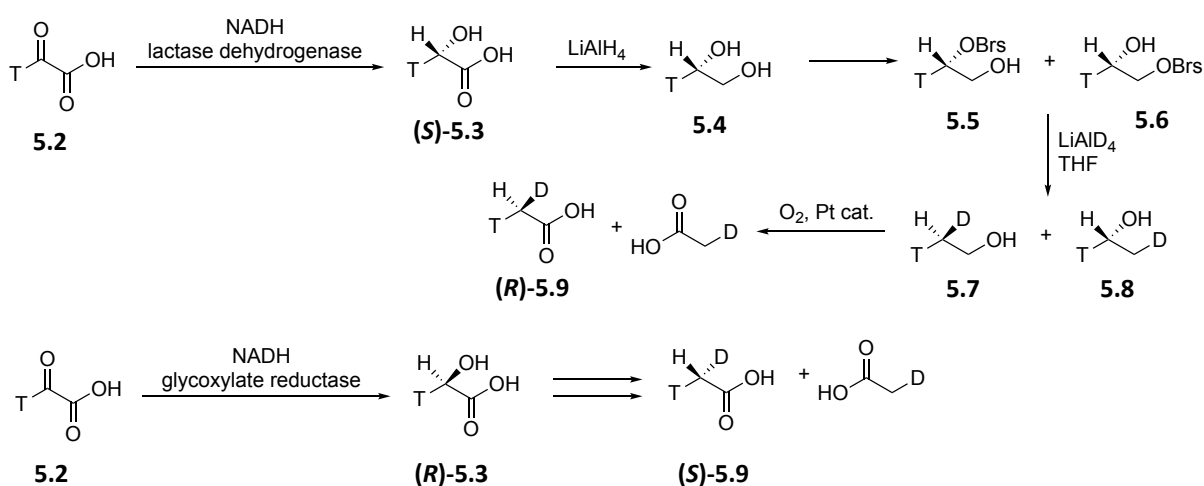


Figure 5.1 – The chiral methyl group.

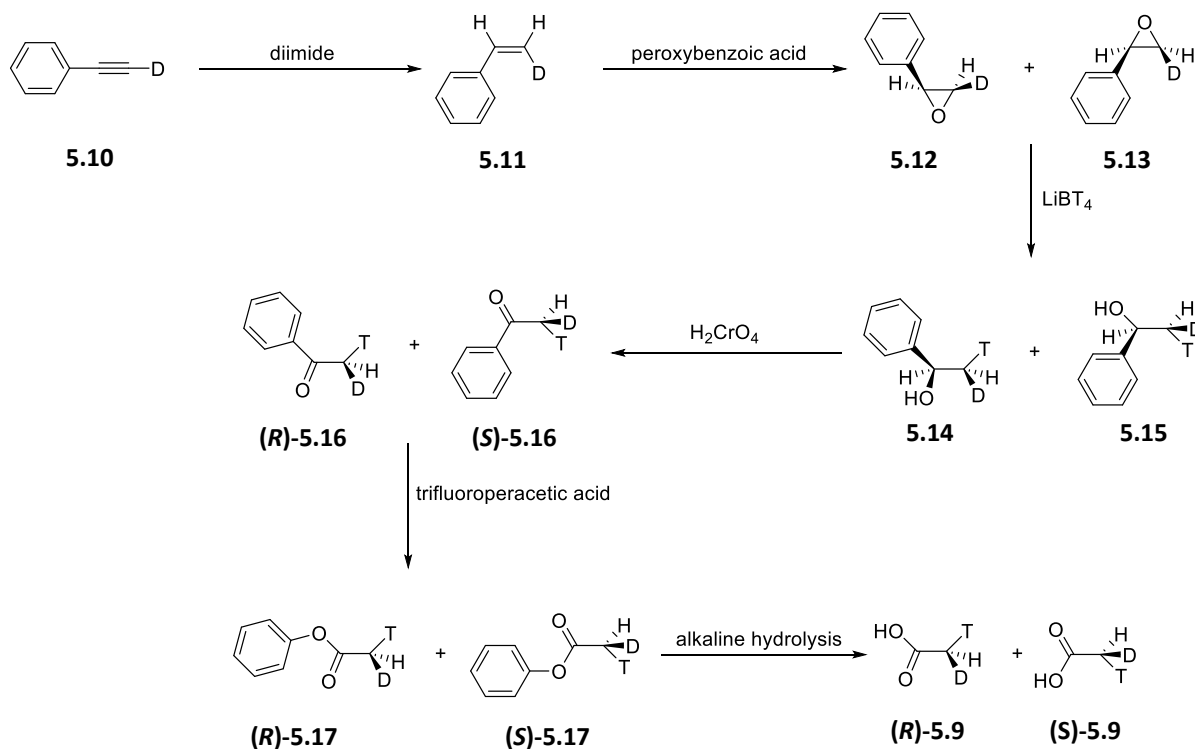
This was achieved by the synthesis shown in Scheme 5.2. 2- $^{3}\text{H}_1$ -Glyoxylate **5.2** was reduced using NADH in the presence of lactate dehydrogenase to give (2*S*)-2- $^{3}\text{H}_1$ -glycolic acid (**S**)-**5.3** as a single enantiomer. The corresponding methyl ester was chemically reduced with lithium aluminium hydride to generate (1*S*)-1- $^{3}\text{H}_1$ -ethylene glycol **5.4**. This was converted to a mixture of 1- $^{3}\text{H}_1$ - and 2- $^{3}\text{H}_1$ -monobrosylates **5.5** and **5.6**. Reaction of this mixture with deuterated lithium aluminium hydride gave a mixture of labelled ethanols **5.7** and **5.8**. The mixture was then oxidised using oxygen in the presence of a palladium catalyst to yield a mixture containing enantiomerically-pure (*R*)-acetic acid **5.9**. They also synthesised the (*S*)-acetic acid, as illustrated in Scheme 5.2. In that case 2- $^{3}\text{H}_1$ -glyoxylate **5.2** was reduced with glyoxylate reductase rather than lactate dehydrogenase to give the opposite enantiomer (2*R*)-2- $^{3}\text{H}_1$ -glycolic acid (**R**)-**5.3** which was then progressed in the same way to (*S*)-acetic acid (**S**)-**5.9**.



Scheme 5.2 – First synthesis of enantiomerically-pure (*R*)-acetic acid (**R**)-**5.9** and (*S*)-acetic acid (**S**)-**5.9** by Arigoni *et al.*²²⁹

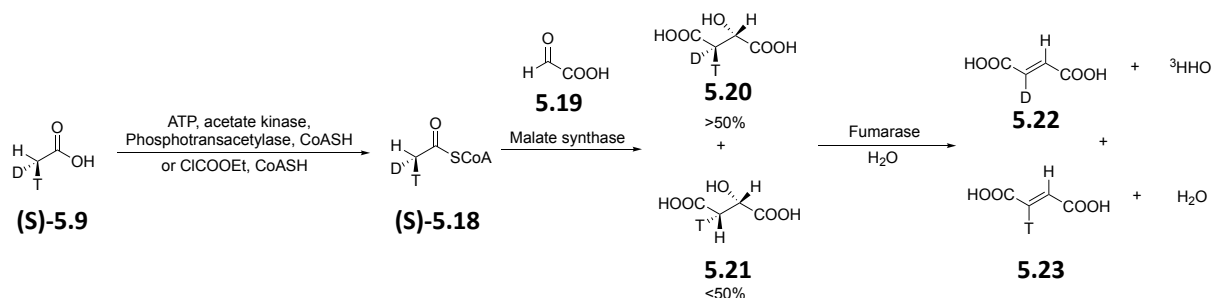
Meanwhile, Cornforth *et al.* were working on this same problem at the same time.²³⁰ They prepared (*R*)- and (*S*)- $^{2}\text{H}_1$, $^{3}\text{H}_1$ -acetic acids (**R**)-**5.9** and (**S**)-**5.9** beginning with deuterated phenylacetylene **5.10**, as illustrated in Scheme 5.3. In that case, the acetylene was reduced by diimide to *cis*- $^{2}\text{H}_1$ -1-phenylethylene **5.11**. Reaction with peroxybenzoic acid gave a

mixture of epoxides **5.12** and **5.13** and this mixture was then reduced using lithium borotritide to give 2-[²H₁,³H₁]-1-phenylethanol isomers **5.14** and **5.15**. Oxidation of the alcohol with chromic acid gave a mixture of acetophenones (**R**)-**5.16** and (**S**)-**5.16**. This mixture was then oxidised to give phenyl acetates (**R**)-**5.17** and (**S**)-**5.17** and then hydrolysis gave either (*R*) or (*S*)-[²H₁,³H₁]acetic acids (**R**)-**5.9** and (**S**)-**5.9**.



Scheme 5.3 – Synthesis of (*R*)- and (*S*)-acetic acids (**(R)-5.9** and (**(S)-5.9**) by Cornforth et al.²³⁰

With chiral methyl acetates in hand, it was then necessary to determine a method to distinguish between the two enantiomers. Both Cornforth and Arigoni approached this challenge similarly, using enzymatic reactions that exploited kinetic isotope effects, as illustrated in Scheme 5.4.^{228, 229, 230} Click or tap here to enter text. Both groups converted their chiral acetic acid enantiomers to their CoA esters. These were then condensed with glyoxylic acid **5.19** catalysed by malate synthase. This process has a kinetic deuterium isotope effect $k_{\text{H}}/k_{\text{D}}$ of 3.7, so an isotopic mixture of products **5.20** and **5.21** is obtained.²³¹ Incubation with fumarase led to the formation of alkenes **5.22** and **5.23**, with the release of water. When the original acetate had an (*S*)-configuration, 79% of the tritium was removed from the compound as water. When the original acetate has an (*R*)-configuration, 79% of the tritium remains bound to the compound. From these values, the enantiomeric excess can be calculated.



Scheme 5.4 – Malate/fumarase assay developed by Arigoni and Cornforth to determine the configuration of chiral acetic acids.²²⁸

Resolution of the chiral methyl group has since been assayed directly using ^3H NMR, as shown in Figure 5.2.²³² This was first achieved by Floss *et al.*, who synthesised (*R*)- and (*S*)-2-methylpiperidine derivatives of the chiral methyl group by reaction with an (*R*) chiral methyl group (86% enantiomeric excess). They found a difference of 4.4 Hz (0.014 ppm) between ^3H NMR peaks, with the tritium more shielded in (*2R,7S*) diastereomer **5.29** than in (*2S,7S*) diastereomer **5.27**, giving a clear diastereotopic resolution of the chiral methyl group.

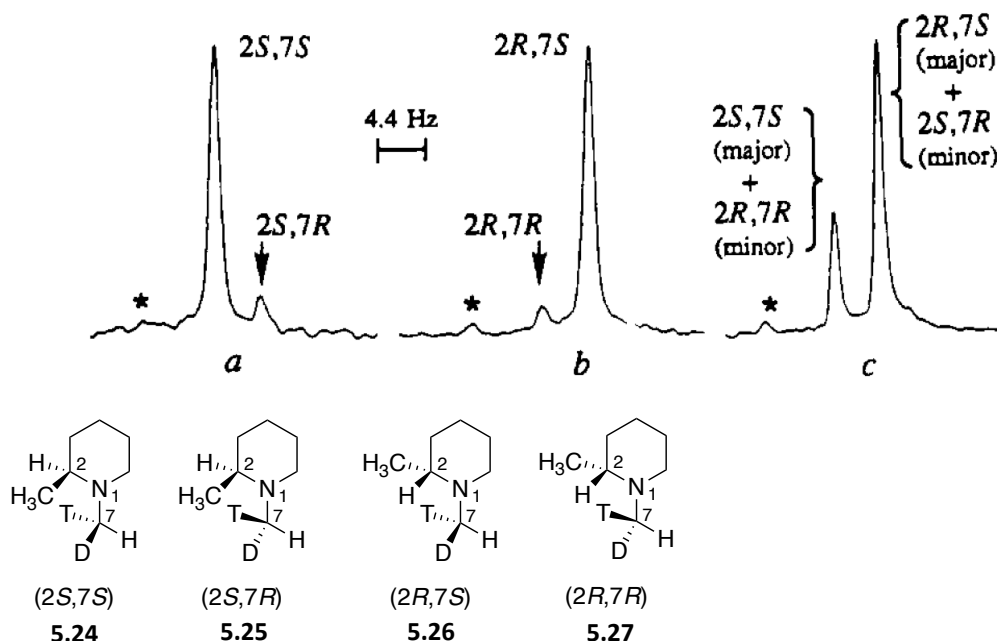
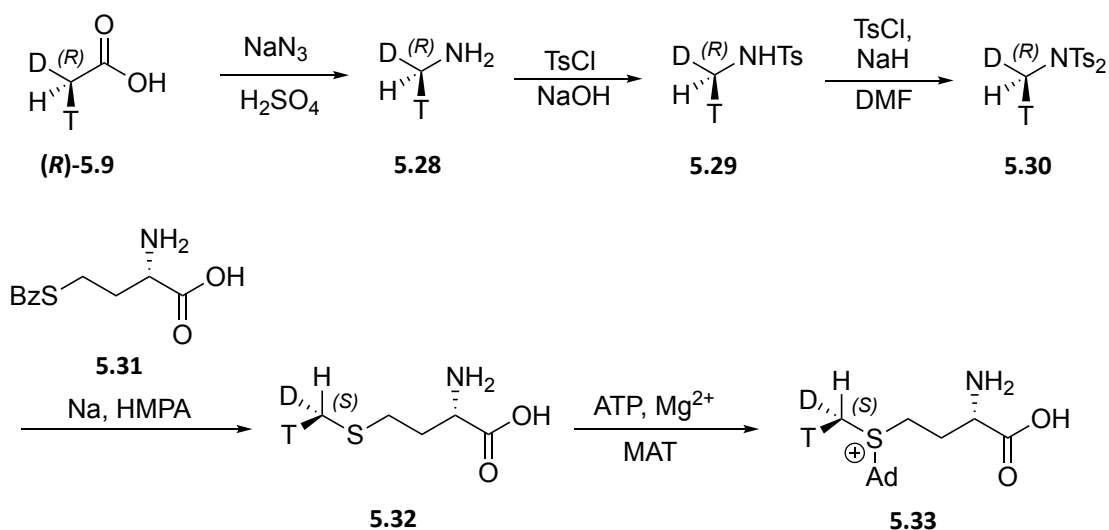


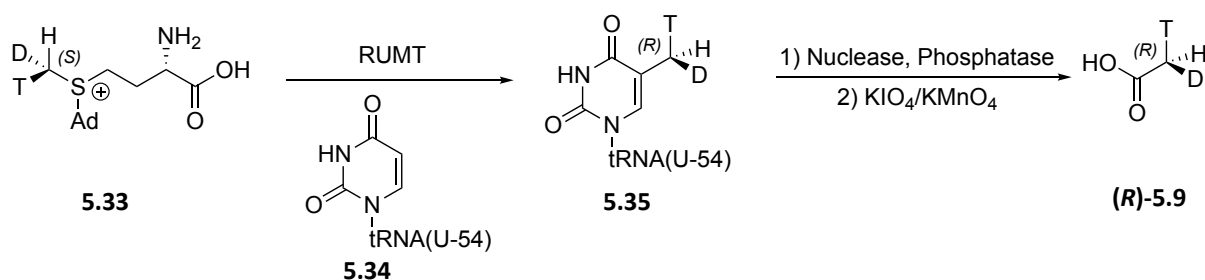
Figure 5.2 – ^3H NMR of 2-methylpiperidine derivatives of the chiral methyl group. NMR (a) shows (*2S,7S*) **5.24** and (*2S,7R*) **5.25**, NMR (b) shows (*2R,7S*) **5.26** and (*2R,7R*) **5.27**, and NMR (c) shows a mixture of the (a) and (b) samples in a 0.7:1 ratio. The small peaks labelled by asterisks are CH₂T groups in isotopic impurities.²³²

5.1.3 Applications of the chiral methyl group

The chiral methyl group has been used widely to probe the stereospecificity of enzymatic processes. One of these processes is the transfer of methyl groups by *S*-adenosylmethionine (SAM) to biological molecules. Floss *et al.* achieved this by synthesising SAM containing a chiral methyl group **5.33**, as illustrated in Scheme 5.5. They approached this by synthesising diastereomers of L-methionine **5.31** with the incorporation of the chiral methyl group, where the use of (*R*)-**5.9** incorporates the (*S*)-chiral methyl group within L-methionine.²³³ This was then enzymatically activated to give chiral SAM **5.33** containing an (*S*)-chiral methyl group. The chiral SAM **5.33** was then used as a methylating agent, followed by cleavage and recovery of the subsequent chiral methyl group, as shown by the example in Scheme 5.6.²³⁴ Analysis would then lead to the determination of the chirality of the methyl group and therefore the stereoselectivity of the methylation reaction. They determined that the transfer of a methyl group by SAM always occurs with an inversion of stereochemistry at the methyl group.²²⁸ This is shown by the example in Scheme 5.6, where the configuration of the methyl group inverts from (*S*)- to (*R*)- when methyl transfer takes place. This suggests that a single S_N2 -like transfer of a methyl group takes place. These results were corroborated by a parallel study by Arigoni, where he found that the transfer of methyl groups into the corrin ring of vitamin B₁₂ occurs with an inversion of configuration at all seven methyl groups.²³⁵

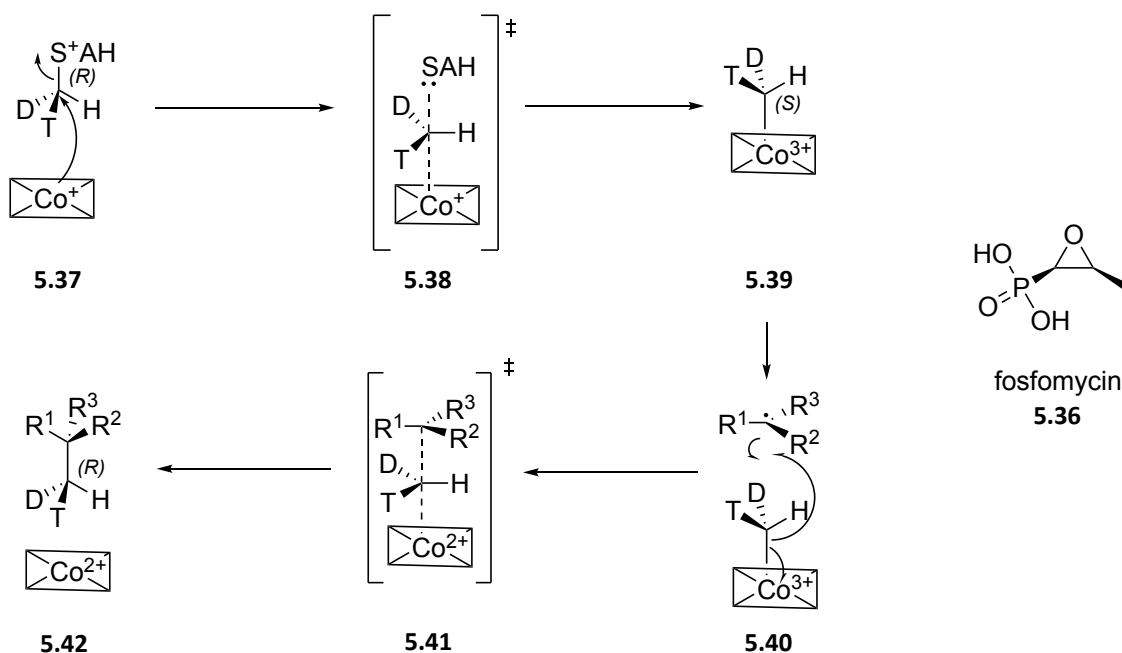


Scheme 5.5 – Synthesis of a chiral methyl group-containing SAM **5.33** by Floss *et al.*²³³



Scheme 5.6 - The use of the chiral methyl group within SAM to determine the stereochemical course of the methylation of a uracil residue in a tRNA.²³⁴

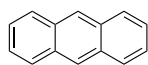
However, this methodology has since been used to probe the stereochemical process in examples where stereochemistry at the methyl group has been retained during the overall methyl transfer process. One example of this is in the cobalamin-dependent radical SAM methyl transfer in the biosynthesis of Fosfomycin **5.36**. Hammerschmidt *et al.* conducted feeding experiments, feeding chiral methyl SAM to *Streptomyces fradiae*, which produces Fosfomycin.²³⁶ By degradation of the subsequent Fosfomycin via a Kuhn-Roth oxidation, they could then conduct the malate/fumarase assay to determine the configuration at the chiral methyl group. They found that the methylation process occurs with overall retention of configuration at the methyl group, as illustrated in Scheme 5.7.²³⁷ They determined that SAM first reacts with cobalamin in an S_N2 -like methylation process, inverting the stereochemistry at the methyl centre. Radical transfer of the methyl group from methylcobalamin **5.37** to the substrate then occurs with a second inversion at the methyl group. This is a double-inversion process and leads to the overall retention of the stereochemistry at the methyl group.



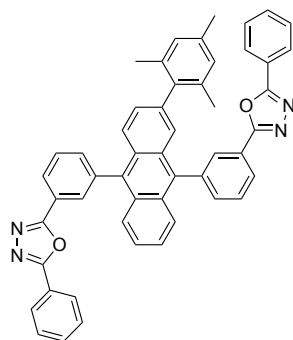
Scheme 5.7 – An illustration of the double-inversion methylation in the biosynthesis of Fosfomicin by chiral methylcobalamin as determined by Hammerschmidt et al.²³⁷

5.1.4 The anthracene group

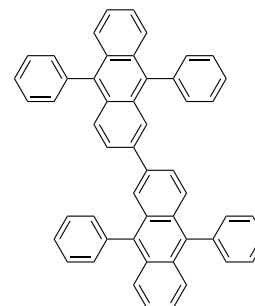
Anthracene **5.43** is a polycyclic aromatic compound consisting of three fused benzene rings, as shown in Figure 5.3.²³⁸ Due to its highly conjugated π -system, anthracene has a wide variety of uses across chemistry, as demonstrated in Figure 5.4. Anthracene derivative **5.44** is used in the manufacture of highly efficient blue organic light-emitting diodes (OLEDs).²³⁹ Derivative **5.45** is used in the manufacture of green OLEDs.²⁴⁰ **5.46** has been used as an organic semiconductor. Anthracene derivatives also have biological properties, with **5.47** being among a group of anthracenes extracted from the leaves of *Harungana madagascariensis* which exhibit antimicrobial properties.²⁴¹ **5.48** is an anthracene derivative of Mitoxantrone, which is a drug used in the treatment of multiple sclerosis. It has been shown to exhibit anti-inflammatory properties.²⁴²



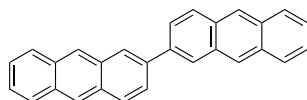
5.43



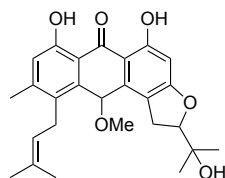
5.44



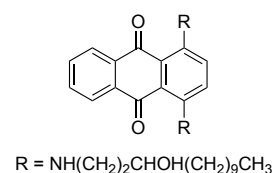
5.45



5.46



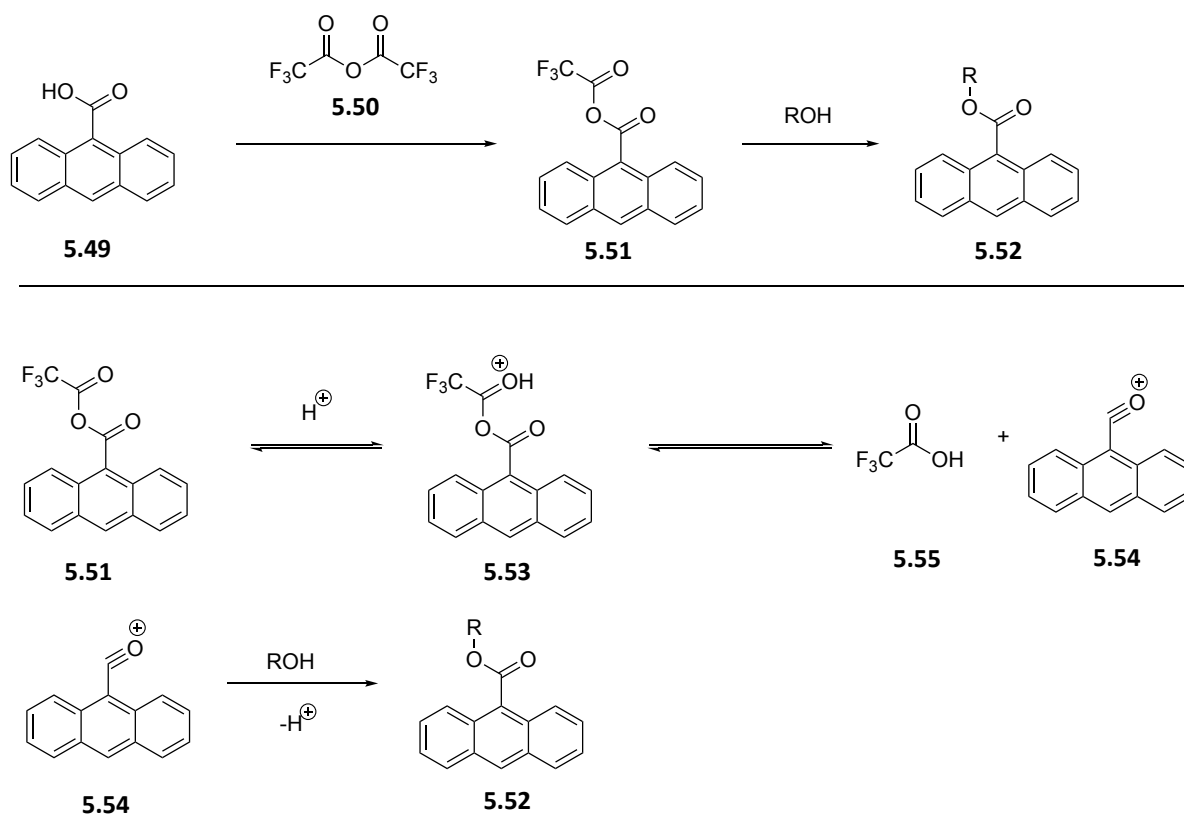
5.47



5.48

Figure 5.3 – Structures of anthracene **5.43** and derivatives **5.44-5.48** with uses in a variety of fields of chemistry.²³⁸

Synthesis of compounds containing the anthracene group is challenging due to the highly bulky nature of the group. This high level of steric hindrance renders classical esterification methods ineffective. A method for the esterification of sterically-hindered anthracene-9-carboxylic acid **5.49** was developed by Parish and Stock, as shown in Scheme 5.8.²⁴³ They treated **5.49** with trifluoroacetic anhydride **5.50**, synthesising anhydride intermediate **5.51**. They determined that the esterification reaction then occurs due to the formation of an oxo-carbenium ion **5.54** via the protonation of anhydride **5.51**, with the release of trifluoroacetic acid **5.55**. An alcohol can then react with **5.54** to form desired ester **5.52**.



Scheme 5.8 – Esterification of hindered anthracene-9-carboxylic acid **5.49** via a trifluoroacetic anhydride intermediate **5.51** with the course of reaction as determined by Parish and Stock.²⁴³

5.1.5 Aims and objectives

The previously discussed study by Igarashari *et al.* (Section 5.1.1) suggested that the biosynthesis of the *tert*-butyl group of butyrolactol A **5.1** involves a late-stage methylation. It follows that if this process is enzymatic, then it must also be stereoselective. Therefore, it would be interesting to probe the stereospecificity of the process. In order to do this, it would be advantageous to have reference compounds to explore subsequent chiral assay analysis for downstream biosynthetic experiments. Unlike the chiral methyl group which required radioactive tritium, this could be achieved most obviously with stable isotopes using $-\text{CH}_3$, $-\text{CD}_3$ and $^{-13}\text{CH}_3$, and then with NMR analysis. Also taking into account the 1% natural abundance of carbon-13, this would mean that a 'racemic' chiral *tert*-butyl group could be synthesised, but if constructed in a diastereotopic framework, then perhaps the ^{13}C -NMR signals may resolve in a 1:1 ratio? If successful, this would validate ^{13}C -NMR as a potential method for chiral *tert*-butyl assay. Accordingly, the compounds illustrated in

Figure 5.4 became synthetic targets as the two enantiomers in the ‘racemic’ chiral *tert*-butyl group are in diastereotopic environments.

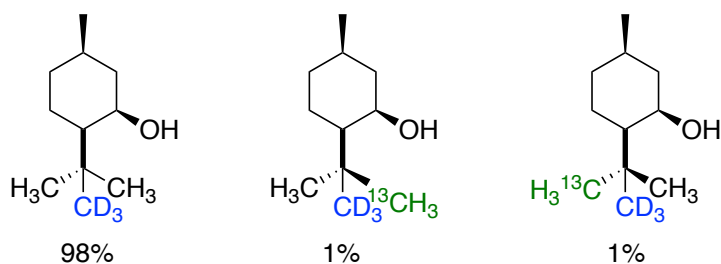


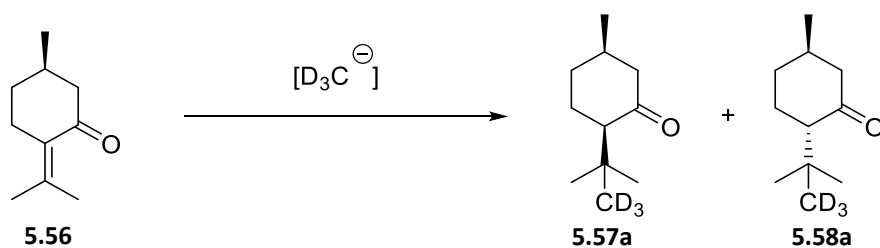
Figure 5.4 – ^{13}C -Isotope ratios of ‘racemic’ chiral *tert*-butyl group with each enantiomer in a diastereotopic environment.

If the ^{13}C -NMR resolution of the isotopically dictated diastereomers was successful, then this would inform a strategy for butyrolactol A analysis in biosynthetic experiments.

5.2 Synthesis and assay of the chiral *tert*-butyl group

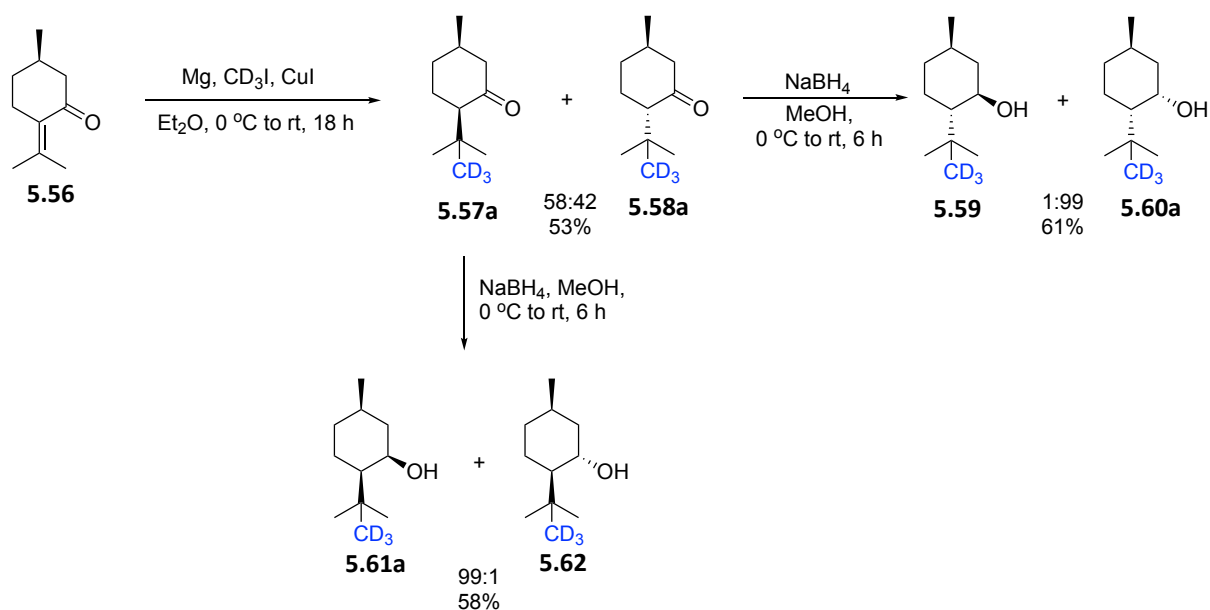
5.2.1 Construction of the chiral *tert*-butyl group via conjugate addition

This project began with the development of the synthesis of a diastereotopic *tert*-butyl group. The approach began with (*R*)-(+)-pulegone **5.56**. (*R*)-(+)-Pulegone is a natural product obtained from the essential oils of plants such as peppermint and catnip, with uses in fragrances.²⁴⁴ There are two advantages to using (*R*)-(+)-pulegone for this synthesis. (*R*)-(+)-Pulegone has a fully defined (*R*) stereogenic centre, meaning that the synthesis of two clearly defined diastereomers is assured. This should hopefully allow for the separation and isolation of diastereomers throughout the synthesis. The other advantage is the presence of an α,β -unsaturated ketone, with two methyl groups at the terminus of the alkene. This allows for a straightforward conjugate addition of an isotopically-enriched methyl group to access the diastereotopic *tert*-butyl groups **5.57a** and **5.58a**, as illustrated in Scheme 5.9.



Scheme 5.9 – Conjugate addition approach to construct the *tert*-butyl group.

Organocuprates are well known to promote conjugate additions to α,β -unsaturated ketones, and in this case, the appropriate organocuprate required to be prepared from [$^2\text{H}_3$]-methyl iodide as illustrated in Scheme 5.9. This was achieved in the first instance by generation of the Grignard reagent but with copper catalysis. In trial runs with unlabelled methyl iodide, the reaction gave a mixture of the diastereomers (*R,R*) **5.57** and (*R,S*) **5.58** in a ratio of 68:32 respectively in an overall yield of 51%. Importantly these isomers could be separated from each other by chromatography. The major isomer was then reduced to the corresponding alcohol, in this case with a very high diastereoselectivity (99:1) and this compound was isolated as a single isomer. This could be repeated now with [$^2\text{H}_3$]-methyl iodide as illustrated in Scheme 5.10. This began with the conjugate addition of deuterated methyl iodide in a copper-mediated Grignard reaction, yielding diastereoisomers (*R,R*) **5.57a** and (*R,S*) **5.58a**. The two diastereomers (*trans/cis* ratio of 68:32) were separated by chromatography and were then individually reduced to their corresponding alcohols using sodium borohydride, yielding alcohol stereoisomers **5.60a** and **5.61a**, again in very high stereoselectivity and in yields of 61% and 58% respectively.

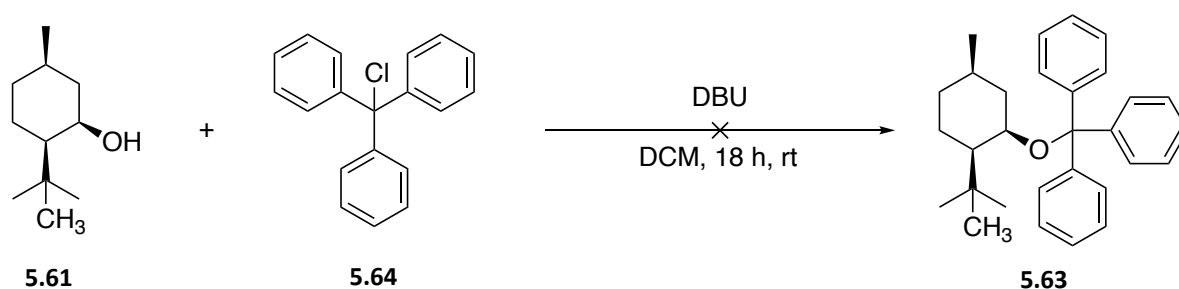


*Scheme 5.10 – Synthesis of deuterated tert-butyl pulegone alcohol derivatives **5.60a** and **5.61a**.*

The strategy now was to attach an aromatic group to the alcohol stereoisomers as an ether or as an ester, to induce NMR anisotropy close to the diastereotopic *tert*-butyl group. This was to try to maximise non-equivalence of the ^{13}C NMR signals of the two diastereotopic

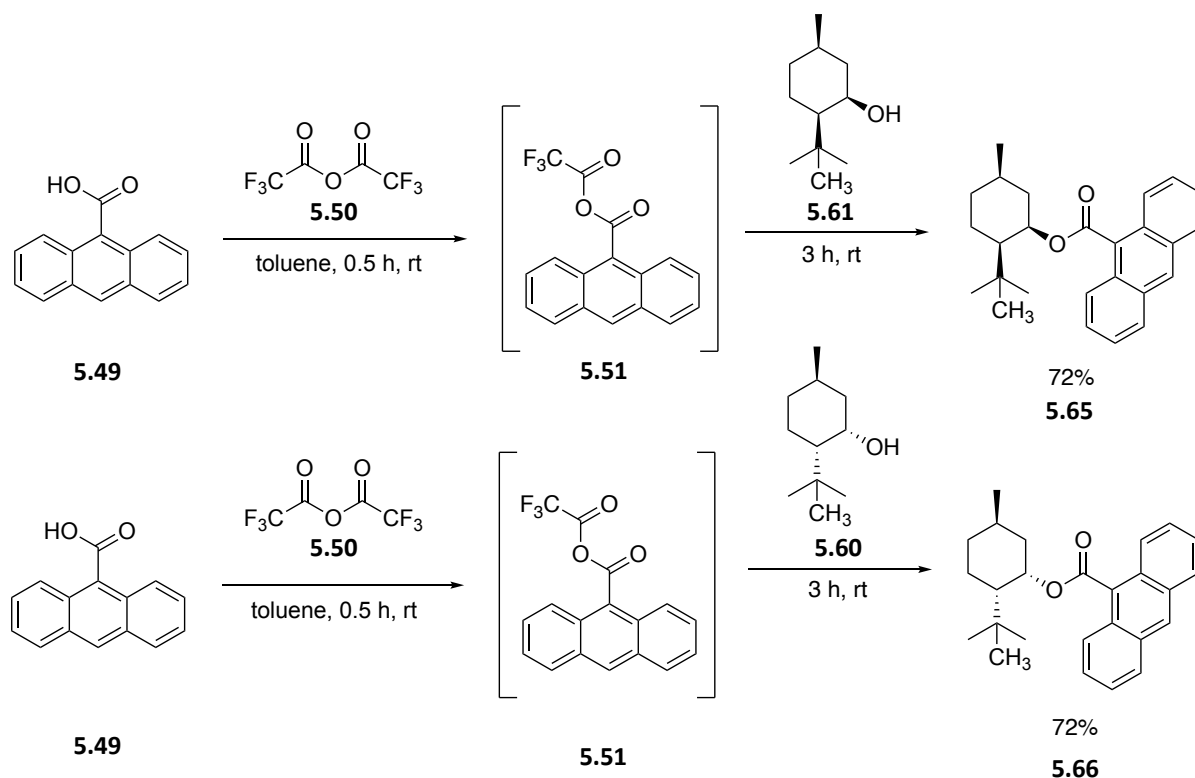
(unlabelled) methyl groups in the [C²H₃]-methyl containing *tert*-butyl group, to resolve them.

In a first attempt, a trityl ether of the pulegone derivative **5.61** became a target compound, as shown in Scheme 5.11. It was anticipated that the phenyl groups of the trityl group might induce this anisotropic effect on the *tert*-butyl methyl groups. However, reaction of each of the alcohol diastereoisomers **5.60** and **5.61** with trityl chloride **5.63** did not give any reaction and only starting materials were isolated. This could clearly be due to the steric challenge of combining a tertiary chloride with a secondary alcohol.



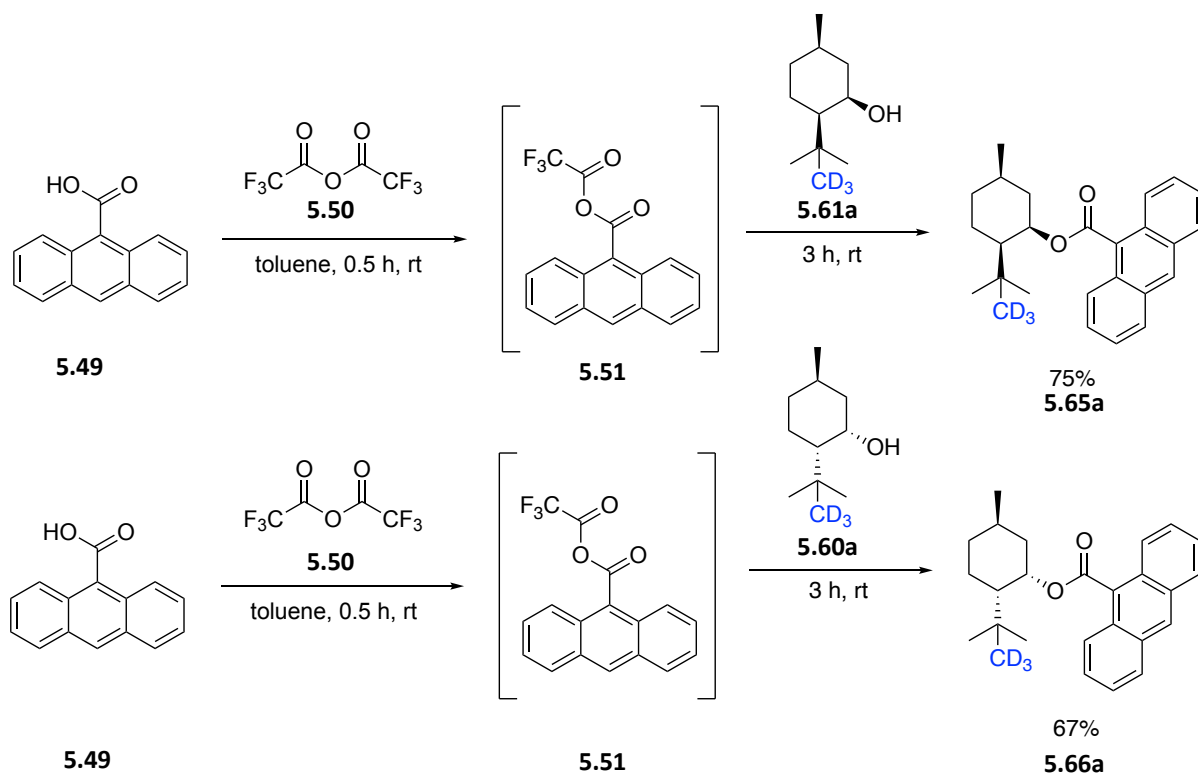
Scheme 5.11 – Unsuccessful formation of trityl ether derivative 5.63.

In light of a challenging ether synthesis, an anthracene ester derivative **5.65** was now explored, as shown in Scheme 5.12.²⁴⁵ This was achieved by first reacting 9-anthracenecarboxylic acid **5.49** with trifluoroacetic anhydride **5.50** in toluene to generate anthracene trifluoroacetic anhydride **5.51** *in situ*. Pulegone derivative **5.61** was then added to the reaction mixture, and this gave the desired anthracene ester derivative **5.66** in a relatively efficient transformation and with a yield of 72%. This synthesis was repeated using alcohol stereoisomer **5.60**, synthesising anthracene ester **5.66** with a yield of 72% as illustrated in Scheme 5.12.



*Scheme 5.12 – Synthesis of anthracene ester derivatives **5.65** and **5.66** from pulegol diastereomers **5.61** and **5.60**.*²⁴⁵

With the synthesis method established using non-labelled material, the protocol was now applied to the isotopically labelled alcohol stereoisomers **5.60a** and **5.61a**. This proved straightforward and gave the desired anthracene ester derivatives **5.65a** and **5.66b** in yields of 72% and 67% respectively, as illustrated in Scheme 5.13.



Scheme 5.13 – Synthesis of deuterated anthracene esters **5.65a** and **5.66a** from pulegol diastereomers **5.61a** and **5.60a**.

5.2.2 NMR assay and crystal structure

The two anthracene carboxylic acid ester stereoisomers **5.65a** and **5.66a** were isolated as crystalline solids and it was possible to obtain their X-ray derived structures, and this was used to confirm stereochemistry and establish also their absolute configurations. The crystal structure of diastereomer **5.66a** is shown in Figure 5.5.

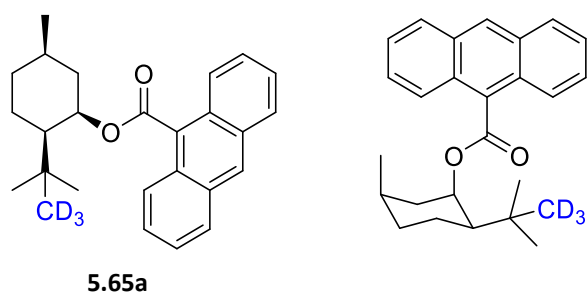
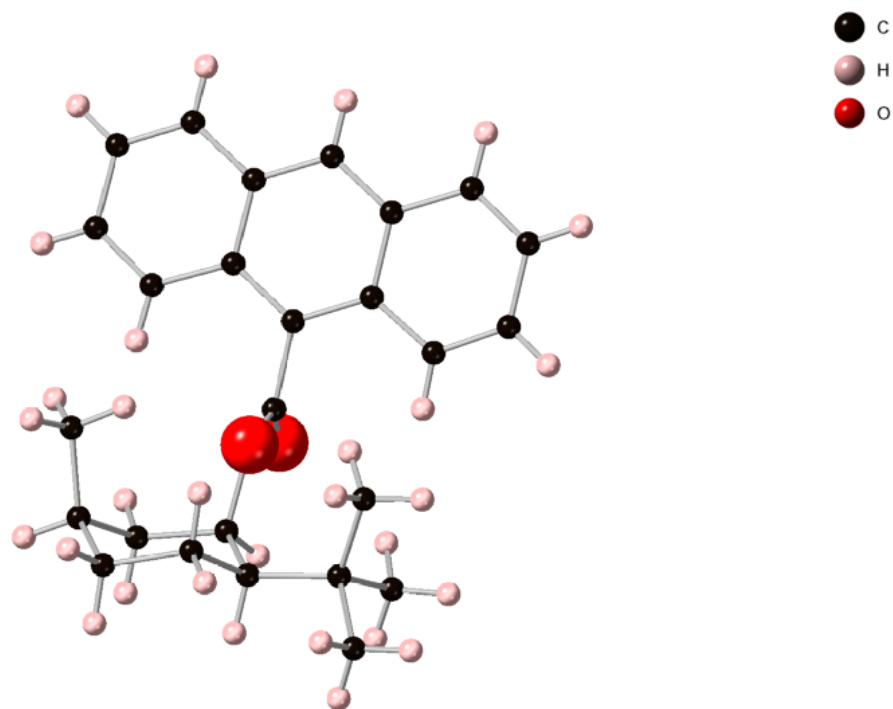


Figure 5.5 – Crystal structure and configuration of diastereomer **5.65a**.

The resultant structure shows that diastereomer **5.65a** is an all-*syn* product. As might be expected the large *tert*-butyl group orients equatorially in this chair structure which means both the methyl group and the anthracene ester moiety must adopt axial orientations. It is notable that the anthracene group is situated just above the *tert*-butyl group, a design feature that is required for a strong anisotropic influence for NMR.

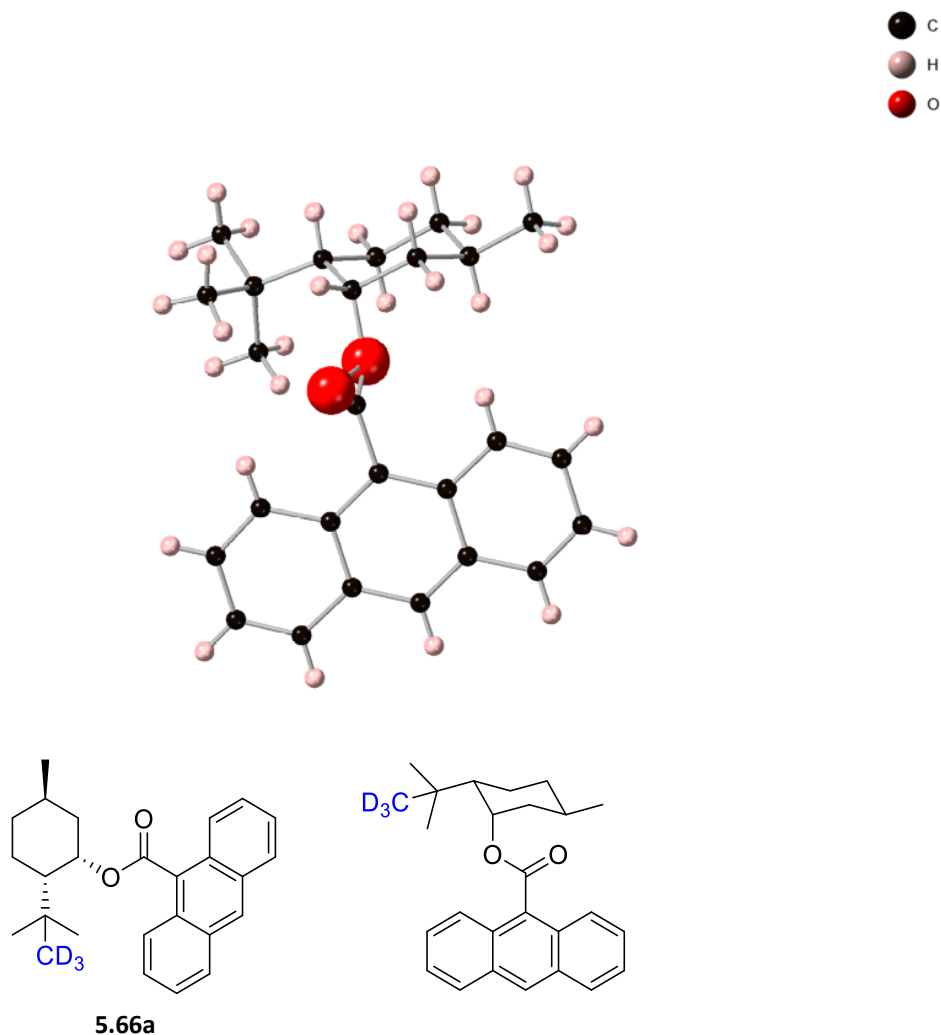


Figure 5.6 – Crystal structure and configuration of diastereomer **5.66a**.

The crystal structure of diastereomer **5.66a** was also obtained, and this confirmed a *syn-anti* configuration as shown in Figure 5.6. Again, the *tert*-butyl adopts an equatorial orientation in the chair structure placing the distal methyl group equatorial this time, but with the ester moiety again adopting an axial orientation. This structure also places the anthracene ring and the *tert*-butyl groups relatively close to each other with the possibility of the aromatic inducing the desired anisotropic effect of the methyl groups.

With the structure and stereochemistry of the anthracene carboxylic esters confirmed, each was now interrogated by NMR to determine if we could resolve the signals for the diastereotopic methyl groups in the [*methyl*-C²H₃]-labelled *tert*-butyl moieties. The *tert*-butyl methyl peaks in the ¹H NMR and ¹³C NMR of the (mono-methyl)deuterated and non-deuterated derivatives were compared. In the NMRs of the non-deuterated derivatives, all 9

(nine) protons will be in the same magnetic environment as expected. However, in the *tert*-butyl region of the ^1H NMR of diastereomer **5.65a** there is a clear splitting of the *tert*-butyl signal (0.97 ppm, 1.8 Hz), as shown in Figure 5.7.

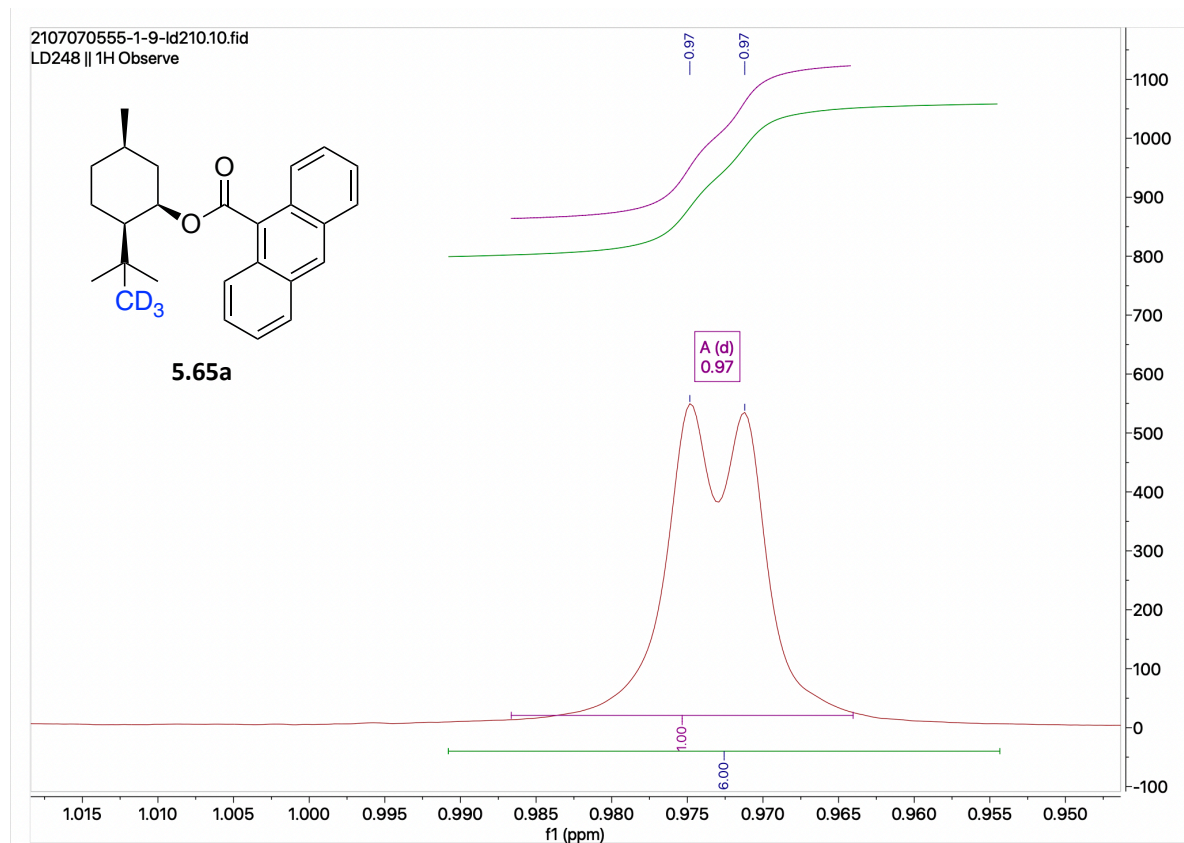


Figure 5.7 – *Tert*-butyl region of the ^1H NMR of diastereomer **5.65a** showing resolved signals at 0.91 ppm, with a separation between signals of 1.8 Hz.

The *tert*-butyl region of the ^1H NMR of diastereomer **5.66a** also shows a similar resolution of the *tert*-butyl peak (0.91 ppm, 1.5 Hz), as shown in Figure 5.8.

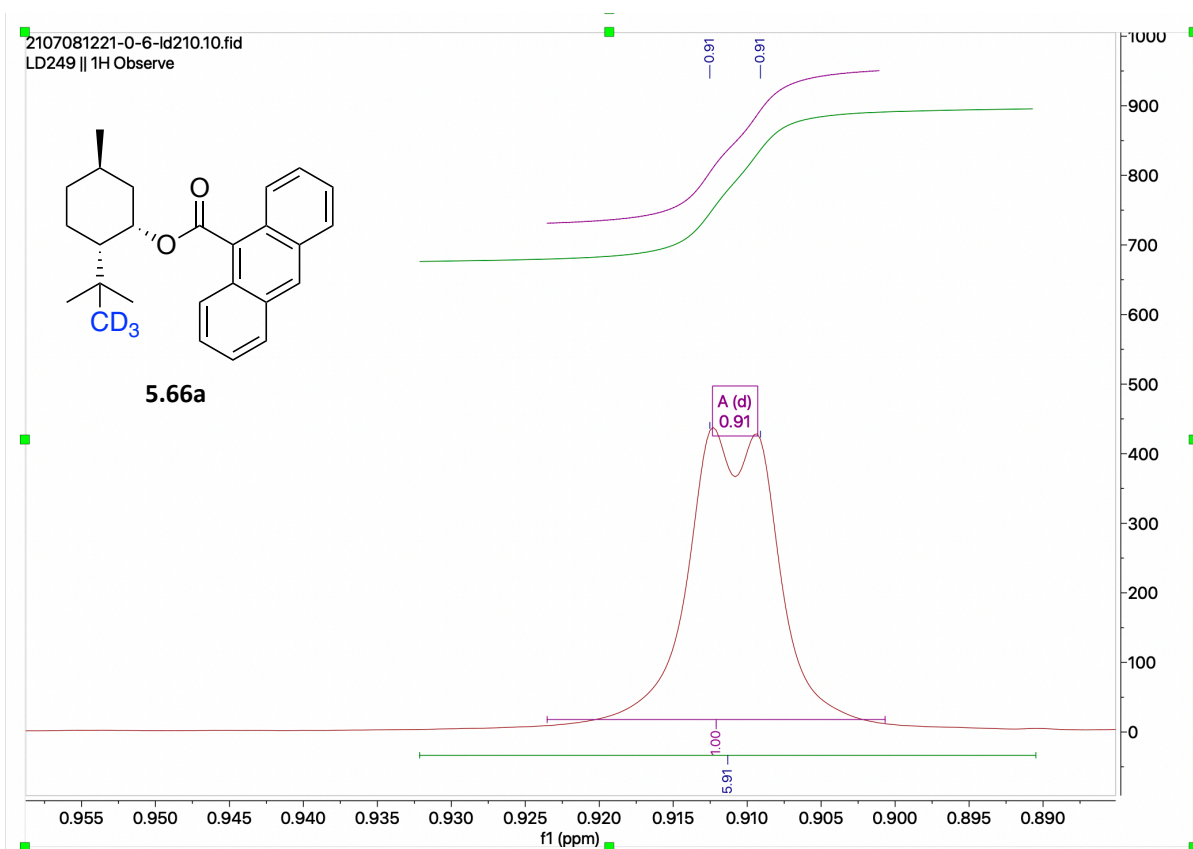


Figure 5.8 – *Tert*-butyl region of the ^1H NMR of diastereomer **5.66a** showing resolved signals at 0.91 ppm, with a separation between signals of 1.8 Hz.

It was necessary to establish that these resolved peaks in the *tert*-butyl region were two separate peaks associated with diastereotopic methyl groups, rather than a doublet, perhaps from some unexpected coupling in the NMR experiment. This was explored by conducting NMR experiments at different frequencies and measuring if there was a constant coupling constant (Hz) or if there was a change in chemical shift (Δ ppm) between the *tert*-butyl peaks in the different experiments, as couplings will remain constant but chemical shift differences will change at different frequencies. Therefore, ^1H NMR experiments were conducted for diastereomer **5.65a** on different NMR instruments at 400 MHz, 500 MHz and 700 MHz and the resultant spectra are summarised in Figure 5.9.

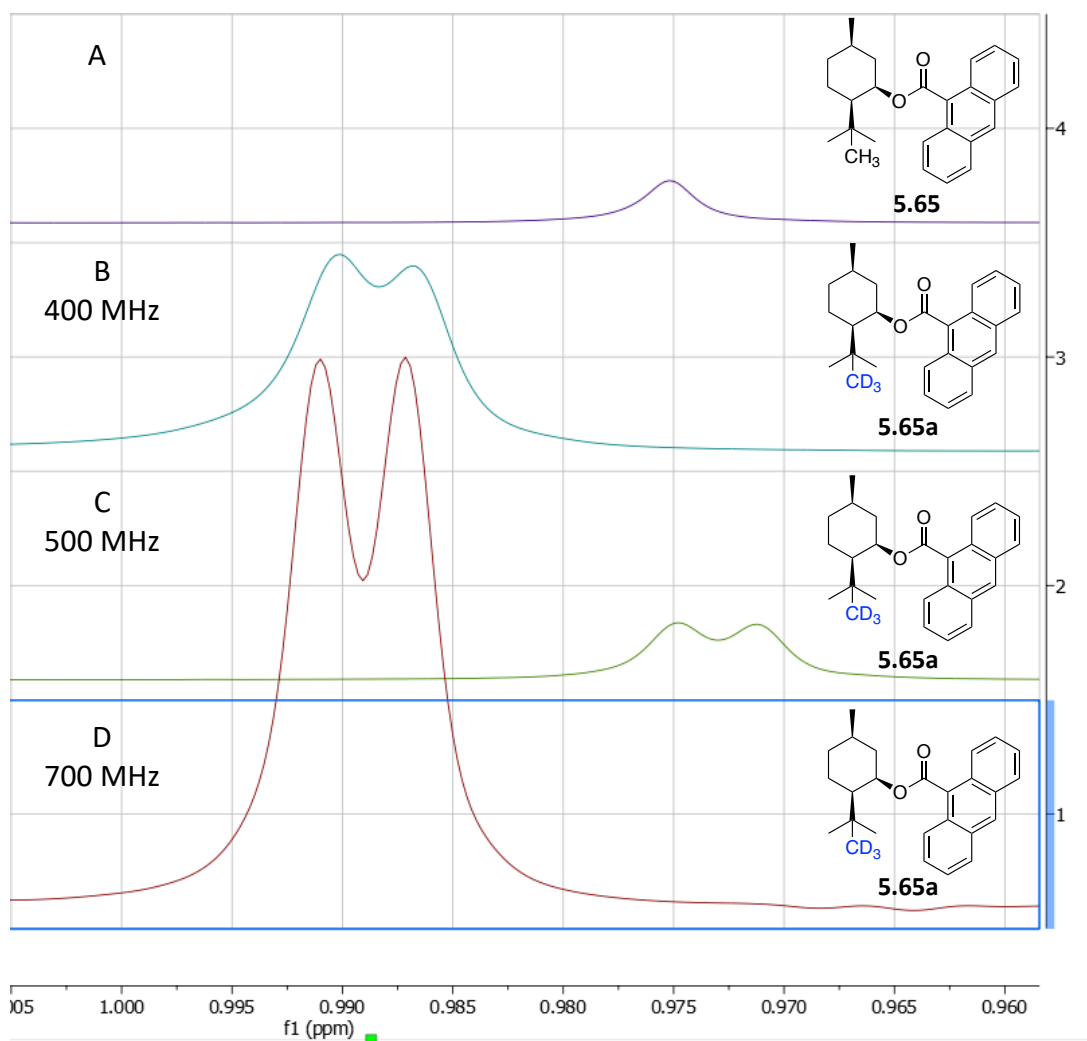


Figure 5.9 – ^1H NMR experiment showing the *tert*-butyl regions of non-deuterated **5.65** (spectrum A), deuterated **5.65a** at 400 MHz (spectrum B), deuterated **5.65a** at 500 MHz (spectrum C) and deuterated **5.65a** at 700 MHz (spectrum D).

The measured differences in Hz between the *tert*-butyl peaks for each ^1H NMR run are shown in Table 5.1.

NMR frequency	Difference (Hz) between peaks
400 MHz	1.3 Hz
500 MHz	1.8 Hz
700 MHz	2.7 Hz

Table 5.1 – Differences in Hz between the *tert*-butyl group peaks of diastereomer **5.65a**.

The ^1H NMR experiment shows an increasing difference (Hz) between the *tert*-butyl peaks with increasing magnetic field strength. This is inconsistent with an adventitious coupling and much more indicative of resolved diastereotopic methyl groups in the isotopically labelled *tert*-butyl moiety.

The same experiment was conducted with diastereomer **5.66a**, as shown in Figure 5.10.

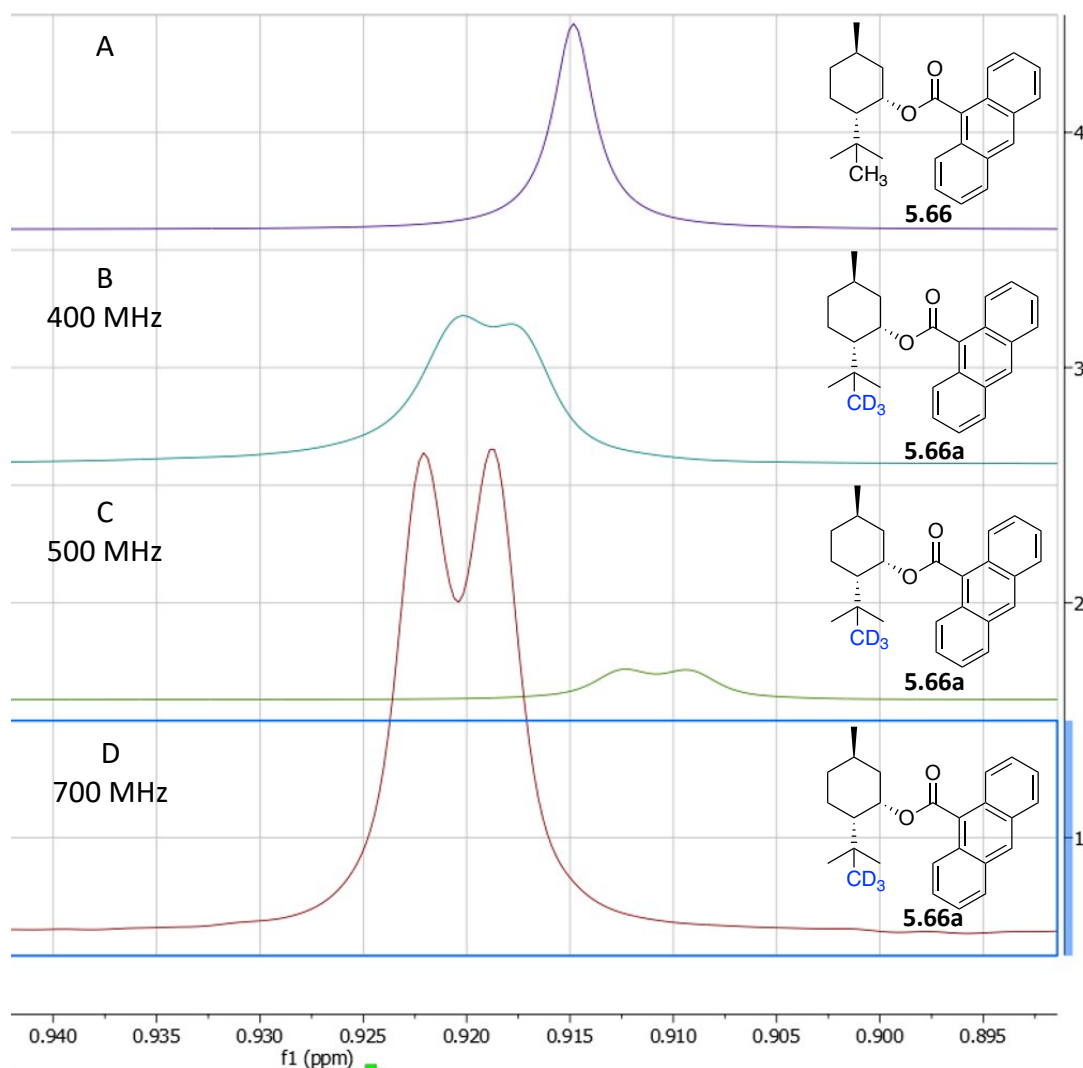


Figure 5.10 – ^1H NMR experiment showing the *tert*-butyl regions of non-deuterated **5.66** (spectrum A), deuterated **5.66a** at 400 MHz (spectrum B), deuterated **5.66a** at 500 MHz (spectrum C) and deuterated **5.66a** at 700 MHz (spectrum D).

The measured differences in Hz between the peaks were:

NMR frequency	Difference (Hz) between peaks
400 MHz	1.0 Hz
500 MHz	1.5 Hz
700 MHz	2.3 Hz

Table 5.2 – Difference in Hz between the *tert*-butyl peaks of diastereomer **5.66a**.

The results again show an increasing resolution between the peaks with increasing frequency, consistent with the diastereotopic resolution of the *tert*-butyl methyl groups in **5.66a**. It is interesting to note that the resolution achieved for diastereoisomer **5.66a** is smaller than that for diastereoisomer **5.66a** and is most likely due to a less strong anisotropic influence induced by the anthracene ring system.

In overview however, a system(s) was established where the diastereotopic non-labelled methyls of the *tert*-[methyl-²H₃]-butyl group have been resolved by NMR analysis.

Resolution by ¹³C NMR was also explored for each of these diastereoisomers, and the spectra are shown in Figures 5.11 and 5.12. However, in the event this proved too challenging, and no convincing resolutions could be determined, even when running at the highest available frequency for ¹³C NMR of 176 MHz (on a Bruker AVIII-HD 700 MHz instrument).

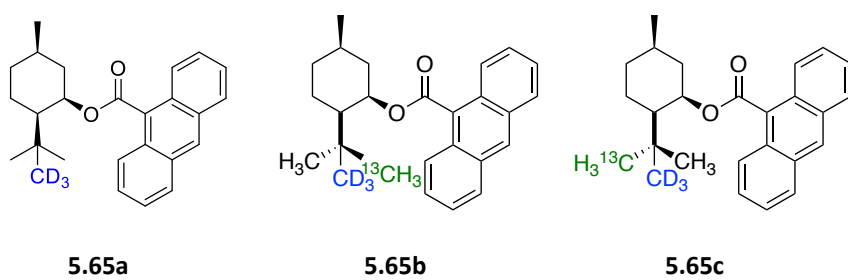
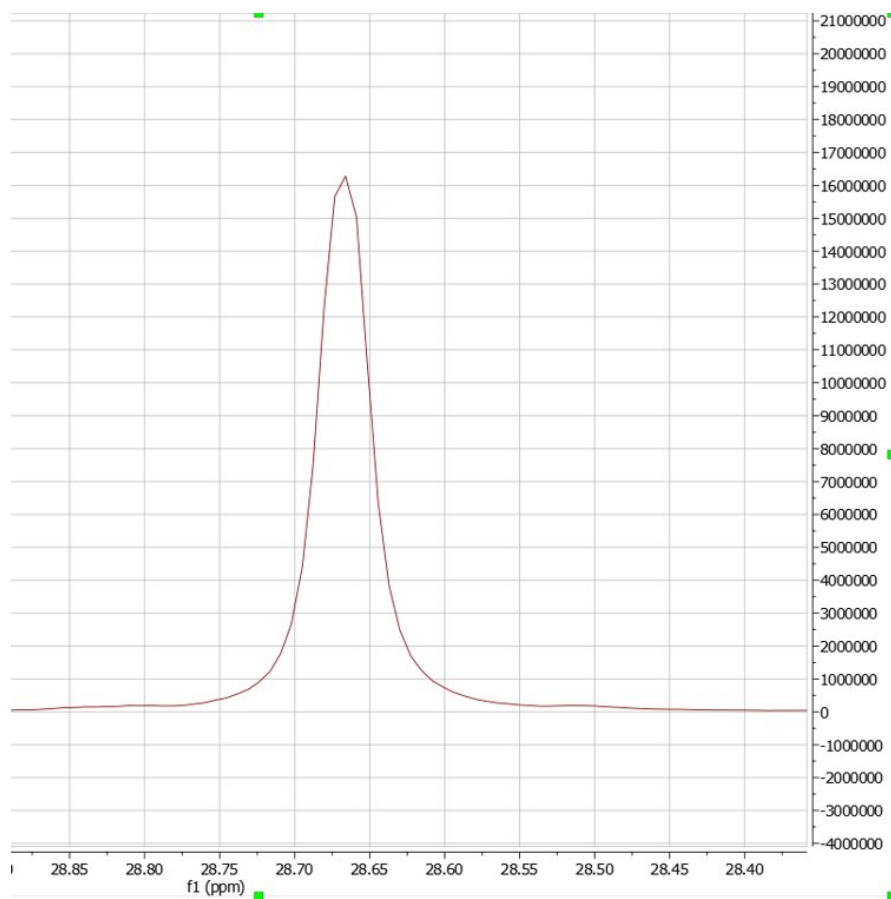


Figure 5.11 – Tert-butyl region of the ^{13}C NMR of diastereomer **5.65a** (^{13}C NMR performed in CDCl_3 at 176 MHz on a Bruker AVIII-HD 700 MHz instrument).

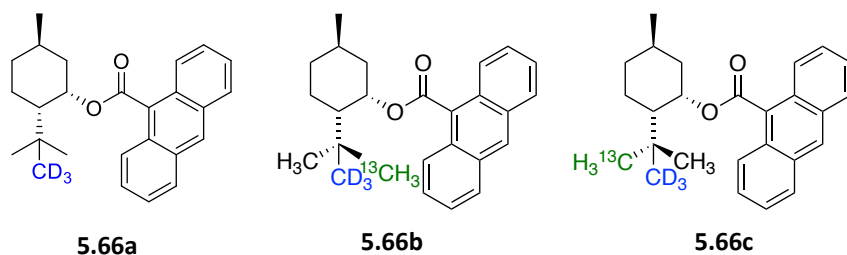
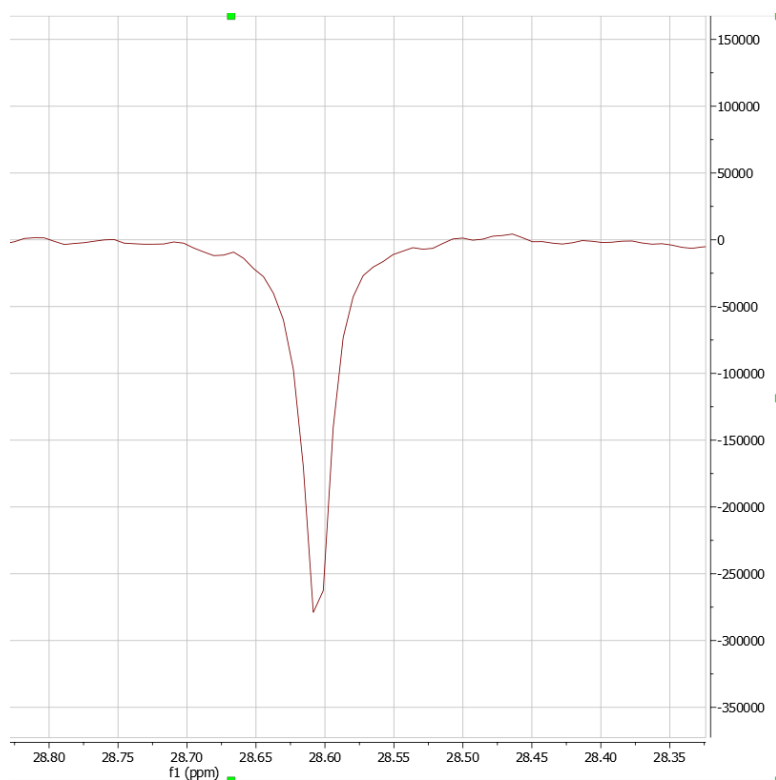
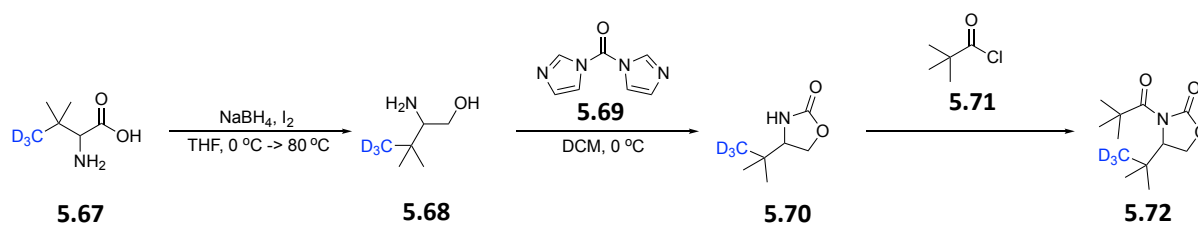


Figure 5.12 - *Tert-butyl region of the ^{13}C NMR of diastereomer 5.66a (^{13}C NMR performed in CDCl_3 at 176 MHz on a Bruker AVIII-HD 700 MHz instrument).*

In writing up this work we became aware of a Ph.D. thesis from 1997 by J. L. Kellenberger, who was a student of Prof. Dulio Arigoni at the ETH Zurich. They had also studied the problem of resolving the chiral *tert*-butyl group by NMR several years earlier, although they had never published the work in the literature.²⁴⁶ The thesis was obtained through inter library loan and a microfiche copy was sent to St Andrews. It emerged that they approached this problem by synthesising oxazolidinone **5.73**, as illustrated in Scheme 5.14.

Oxazolidinone **5.74** also has a *tert*-[*methyl*- $^2\text{H}_3$]-butyl group located in a chiral environment, and thus has two diastereotopic methyl groups, however it appears from the thesis that racemic starting material was used for the synthesis.



Scheme 5.13 – 1997 ETH Thesis. Arigoni and Kellenberger synthesis of deuterated oxazolidinone **5.72** (no stereochemistry at the chiral centre was indicated).²⁴⁶

The ^{13}C NMR spectra of oxazolidinones **5.70** and **5.72** each had resolved signals as shown in Figure 5.13.

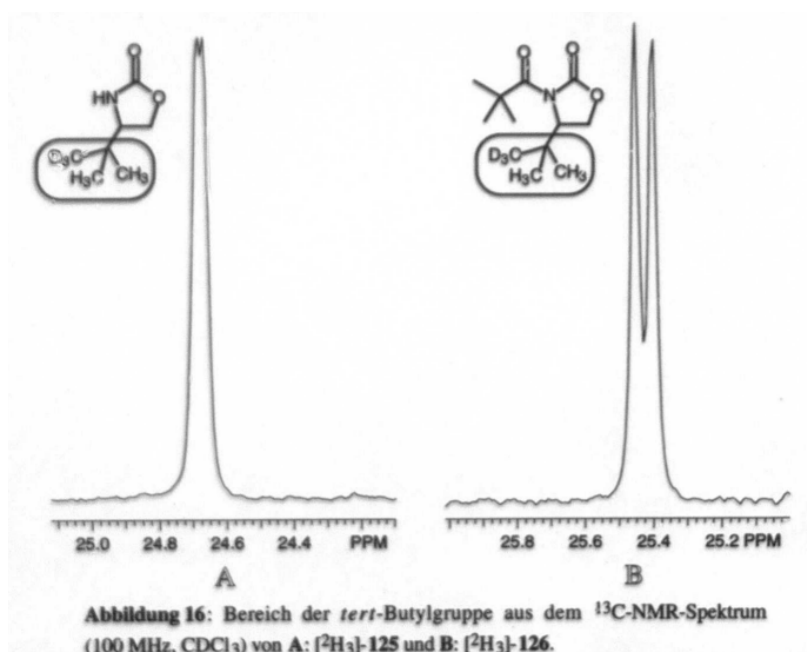


Figure 5.13 – *Tert*-butyl signal in the ^{13}C NMR spectra of *tert*-[methyl- $^2\text{H}_3$]-butyl derivatives **5.70** (left) and **5.72** (right). Reproduced from ETH thesis, J. L. Kellenberger, ETH Zürich, 1997.²⁴⁶

We have to ‘doff our caps’ and recognise that the unpublished ETH system demonstrates a better diastereotopic resolution of the chiral *tert*-butyl group than our system, but together they demonstrate the practicality of an NMR assay in future biosynthetic studies exploring *tert*-butyl assembly in natural products.

5.3 Conclusions

In this chapter, an NMR assay to resolve the chiral *tert*-butyl group has been outlined. Beginning with the natural product (*R*)-pulegone, diastereomers **5.60a** and **5.61a** were individually prepared. These could then be functionalised to introduce a group to induce an anisotropic effect, to maximise resolution of the diastereotopic methyl groups by NMR. Anthracene carboxylate esters **5.65a** and **5.66a** were successfully synthesised, and crystal structures confirmed their absolute and relative configurations, showing that **5.65a** has an all-*syn* configuration (Figure 5.5) and that **5.66a** has a *syn-anti* configuration (Figure 5.6). In the event, NMR assays proved successful, and experiments at different field strengths showed non-equivalent signals for the diastereotopic methyl groups in the labelled *tert*-butyl moiety by ^1H -NMR. However, resolutions could not be achieved by ^{13}C NMR, and may require higher field strengths than were available for success.

Chapter 6 – Conclusions and future work

Work within this thesis has largely focused on how altering the structure of a molecule can affect structure-activity relationships. This work began in Chapter 2, where the natural product (*R*)-muscone **2.1** was used as an initial model. Work began with the synthesis of trifluoromethylated (*R*)-muscone derivative **2.40**. It was hoped that the unique properties of the trifluoromethyl group as a methyl mimetic could alter the properties of (*R*)-muscone to impact the interactions of the odourant with musk olfactory receptors. However, luciferase assay results determined that synthesised **2.40** did not interact with the musk olfactory receptors OR5AN1 and OR1A1. This led to the synthesis of further derivatives of (*R*)-muscone, such as alkenes **2.64** and **2.66**, and epoxide diastereomers **2.65a** and **2.65b**. However, the luciferase assay again determined that these molecules did not interact with the olfactory receptor. This suggests that altering the structure of the molecule to remove the polarised sp^2 carbon of (*R*)-muscone greatly reduces the ability of the molecule to interact with olfactory receptors. Meanwhile, sulfoxide diastereomer derivatives **2.41a** and **2.41b** of (*R*)-muscone were also identified as targets, due to the unique chirality at the sulfoxide bond. A mixture of diastereomers was synthesised, and assay results showed a similar concentration efficacy to (*R*)-muscone, but with a stronger response. Sulfone derivative **2.92** was also synthesised, however only exhibited limited interactions with the olfactory receptors. Future work could look at isolating the individual sulfoxide diastereomers, to determine how chirality at the sulfur affects interactions with the olfactory receptors.

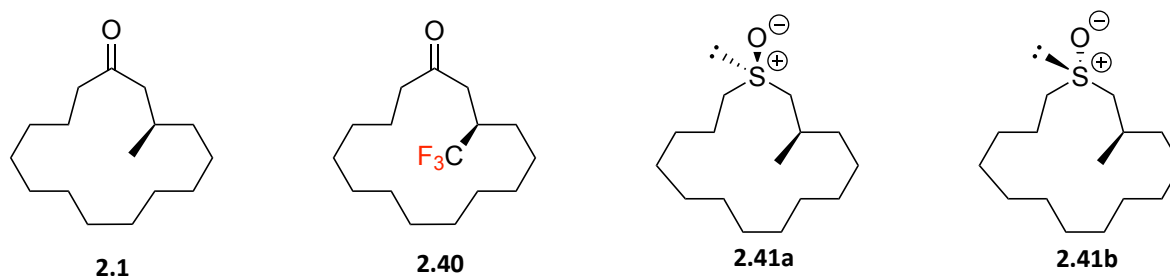


Figure 6.1 – Structures of (*R*)-muscone and synthesised derivatives of (*R*)-muscone,

Work then proceeded in Chapter 3 to the development of a new class of potential musk receptor agonist molecule. The acetylenes were developed to be structurally similar to

previously developed nitromusks and polycyclic musks. Initially synthesised *mono*-acetylenes showed limited interactions with olfactory receptors when assayed. However, synthesised *bis*-acetylene molecules showed a strong ability to interact with olfactory receptors, with *meta* *bis*-acetylene ketone **3.96** exhibiting particularly strong interactions with OR5AN1 and *para* *bis*-acetylene alcohol **3.112** exhibiting particularly strong interactions with OR1A1. Subsequent targets looked at how altering the structure of these *bis*-acetylenes affects interactions with the olfactory receptors. Synthesis of indanone and fluorinated *bis*-acetylene ketones showed that the orientation of the carbonyl group greatly influences the interactions with the olfactory receptors. Synthesis of *meta* *tris*-acetylene **3.135** showed that the strength of interactions with olfactory receptors decreases when increasing the number of acetylene groups from two to three, suggesting that two is the optimum number of acetylene groups for this class of molecule. The effect of altering the alcohol group of **3.112** was also studied, with assay results showing that primary alcohol **3.147** requires a much higher concentration to interact with OR1A1, compared to secondary alcohol **3.112** and tertiary alcohol **3.147**. Changing the chirality of secondary alcohol group also influences the interactions with OR1A1, with (*R*)-**3.112** requiring a significantly lower concentration than (*S*)-**3.112** to trigger a response. These results represent the first reporting of these *bis*-acetylene compounds as agonists of the musk olfactory receptors, and also show that the structure of an odourant strongly influences how the molecule interacts with olfactory receptors, supporting the 'lock and key model' of interaction.



Figure 6.2 – Structures of *bis*-acetylenes **3.96** and **3.112**, which strongly interacted with OR5AN1 and OR1A1 olfactory receptors respectively.

Work then returned in Chapter 4 to investigating how fluorine can influence structure-activity relationships via the development of the aryl tri-fluoro *tert*-butyl (TFTB) group. The synthesis of the group was previously developed by MChem project student Ben McKay, who

along with Dr. Qingzhi Zhang, investigated how progressive fluorination affects the lipophilicity of the *tert*-butyl group. They determined that increasing fluorination leads to decreasing logP of the molecule, consistent with previous studies showing that fluorination of an aliphatic group leads to a decrease in logP. However, it was found that the size of the decrease in logP of the molecule decreases with increasing fluorination. Our collaborators, Bruno Piscelli and Dr. Rodrigo Cormanich at University of Campinas, Brazil, ran computational analysis which determined that the polarity of the molecule increases up to the addition of two fluorines to the *tert*-butyl group, however upon the third fluorination, the polarity of the *tert*-butyl group decreases. This is likely due to the three fluorine atoms orienting away from each other, partially cancelling their individual dipole moments. Cross-coupling reactions with the aryl-TFTB group led to a crystal structure of the TFTB group being obtained. This structure showed that the three fluorine atoms orient away from each other along xyz axes, in order to minimise electrostatic repulsion between the electronegative fluorine atoms. It was also found that the TFTB group holds an eclipsed conformation between C-F and C-H bonds in neighbouring methyl groups. Computational analysis by Bruno Piscelli and Dr. Rodrigo Cormanich showed that the lowest energy conformation of the TFTB group was that shown in the crystal structure, with this conformation having a relative population of 95.9%. Metabolism studies of the aryl TFTB group with *Cunninghamella elegans* were conducted with Mohd Faheem Khan and Prof. Cormac Murphy at University College Dublin. It was found that 55% of compound **4.68** was metabolised by *C. elegans* within 72 hours, whereas *tert*-butyl benzene **4.72** was fully metabolised within the same time period. This shows that introduction of fluorine into the *tert*-butyl group delays its metabolism, meaning that introduction of the TFTB group into a drug molecule could be used to delay its metabolism. The study also shows that the group does metabolise, therefore it is not a persistent fluorochemical motif similar to a PFAS. A metabolism pathway was determined as suggested by GC-MS analysis. Proposed major metabolite **4.125** was synthesised in order to provide some support to the proposed pathway. Subsequent ¹⁹F NMR analysis found that the synthesised compound and the extract were found to give identical ¹⁹F NMR signals, with matching chemical shift and coupling constants. This confirmed that the compounds were the same and that **4.125** is the major metabolite of **4.68**. Future work could focus on further developing the TFTB moiety

with the synthesis of an aliphatic TFTB compound. This could lead to a further study of the properties of the TFTB group and incorporation within existing compounds.

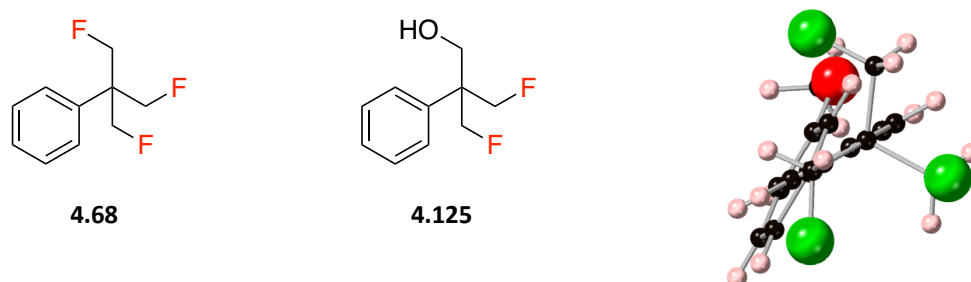


Figure 6.3 – Structures of the aryl TFTB group, the major metabolite of the TFTB group and crystal structure showing the orientation of the TFTB group.

The *tert*-butyl group was also of interest in the synthesis of a chiral *tert*-butyl group in Chapter 5. Inspired by the work of Prof. Duilio Arigoni, who worked on the synthesis of the chiral methyl group. Work began on the synthesis of a ‘racemic’ *tert*-butyl group using -CH₃ and -CD₃. The 1% natural abundance of carbon-13 would mean the chiral *tert*-butyl group would be present within this system. The chiral *tert*-butyl groups could then potentially be resolved at a 1:1 ratio within a diastereotopic environment. Alcohol diastereomers **5.59** and **5.62** were synthesised, followed the synthesis of anthracene derivatives **5.66a** and **5.69a** to introduce NMR anisotropy close to the diastereotopic *tert*-butyl group, Subsequent ¹H NMR assay showed a successful resolution of the chiral *tert*-butyl group. However, resolution by ¹³C NMR was unsuccessful. At this stage, discovery of a previously unpublished PhD thesis by J. L. Kellenberger, a student of Prof. Arigoni at ETH Zürich, found that they had been able to successfully develop a system where a successful ¹³C NMR resolution of the chiral *tert*-butyl group was observed. Our efforts to develop a ¹³C NMR resolution then came to an end. Subsequent work would have led to the use of the chiral *tert*-butyl group within a biosynthetic study of the biosynthesis of butyrolactol A **5.1**, in order to determine the directionality of the enzymatic incorporation of the *tert*-butyl group within butyrolactol A.

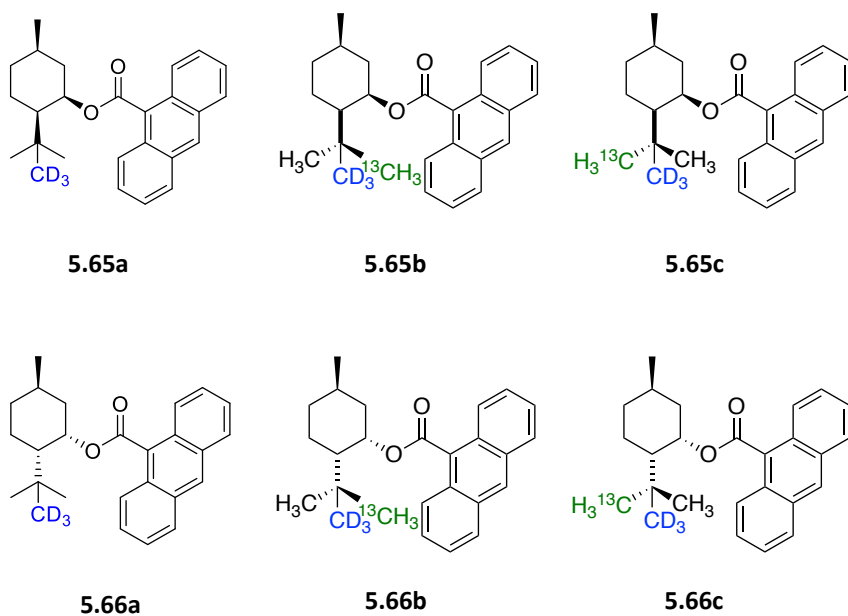


Figure 6.4 – Structures of synthesised anthracene diastereomers containing the chiral tert-butyl group taking into account the 1% natural abundance of carbon-13.

Chapter 7 - Experimental

7.1 General experimental

All reactions were carried out under argon or nitrogen atmosphere with standard Schlenk techniques unless otherwise specified. The reaction glassware was flame dried or oven dried overnight and cooled under vacuum. Commercially available chemicals were purchased from Acros, Alfa Aesar, Apollo Scientific, Fisher Scientific, Fluorochem, Manchester Organics, Sigma Aldrich, and TCI (UK) and used as received unless otherwise stated. Anhydrous solvents such as DCM, diethyl ether, THF, toluene and hexane were dried in a solvent purification system (Mbraun MB SPS-200). Anhydrous acetonitrile, DMF, methanol and pentane were purchased as dry solvent and used as received. Room temperature refers to the temperature range 15-27 °C. The heating temperatures are measured as the temperature of an oil bath or Drysyn heating block. *In vacuo* refers to the use of a rotary evaporator with a membrane pump at 30-50 mbar at 40 °C unless otherwise stated.

¹H, ¹³C and ¹⁹F NMR spectra were recorded on a Bruker AVIII-HD 700 MHz with CryoProbe Prodigy TCI (¹H, 700 MHz, ¹³C, 176 MHz, ¹⁹F, 659 MHz), a Bruker AVIII 500 MHz with CryoProbe Prodigy BBO, or a Bruker AVIII-HD 500 MHz with SmartProbe BBFO+ (500 MHz ¹H, 126 MHz ¹³C, and 470 MHz for ¹⁹F) or Bruker AV 400 MHz with BBFO probe (400 MHz ¹H, 100 MHz ¹³C, and 376 MHz for ¹⁹F). NMR analyses were carried out at room temperature in indicated deuterated solvents unless otherwise noted. Chemical shift data were reported as δ units of ppm corrected by the solvent residue peak and coupling constants, *J*, are reported in Hz. Multiplicities are indicated by: s for singlet, d for doublet, t for triplet, q for quartet and m for multiplet and br. for broad band. Analytical thin layer chromatography was carried out on aluminium backed Merck TLC silica gel 60 F254 plates. These plates were visualised using UV light at 254 nm wavelength, dyed by potassium permanganate or phosphomolybdic acid followed by heating. Flush column chromatography was performed with Sigma-Aldrich silica gel, 60 Å pore size and 230-400 mesh, 40-63 μ m particle size under 5 psi compressed air. Melting points were measured on an Electrothermal 9100 melting point apparatus, a Griffin electric thermal melting point apparatus with thermometer or hot stage microscopy with thermometer reading uncorrected.

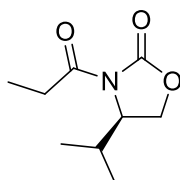
Mass spectra measurements were carried at either the University of St Andrews Mass Spectrometer Facility or University of Edinburgh Mass Spectrometer Facility using given methods.

7.2 Chapter 2

Synthesis of oxazolidinones (General procedure A)

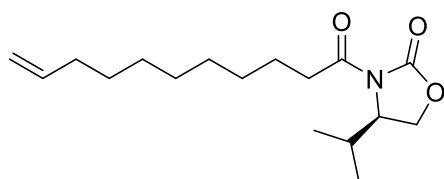
Oxazolidinone (1 equiv.) and dry THF were added to a flask in an inert Ar atmosphere. To this, *n*-butyllithium (1.6 M in hexanes, 1.1 equiv.) was added at -78 °C and stirred for 10 minutes. Acyl chloride (1.2 equiv.) was added at -78 °C and the reaction was warmed to room temperature and monitored by TLC (3:1 hexane/ethyl acetate). On completion, the reaction was quenched with addition of ammonium chloride to the reaction mixture. The mixture was extracted 8 times with DCM, dried over magnesium sulfate, filtered and the filtrate concentrated under reduced pressure to give the crude product. The crude was purified by column chromatography (hexane/ethyl acetate).

(*R*)-4-Isopropyl-3-propionyloxazolidin-2-one



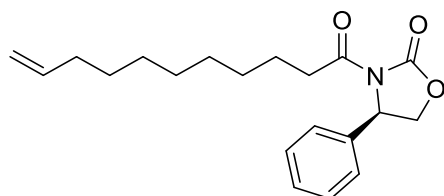
The title compound was prepared according to General Procedure A from (*R*)-4-isopropyl-2-oxazolidinone (1 g, 7.74 mmol), propionyl chloride (0.812 mL, 9.29 mmol) and *n*-butyllithium (1.6 M in hexanes, 5.33 mL, 8.52 mmol) and purified by column chromatography over silica gel (0-20% hexanes/ethyl acetate) to give a colourless liquid (1.15 g, 80.2 %). ¹H NMR (500 MHz, CDCl₃) δ_H 4.43 (1H, ddd, *J* = 8.2, 3.9, 3.1 Hz, CH₂OCO), 4.27 (1H, dd, *J* = 9.1, 8.2 Hz, CH₂OCO), 4.21 (1H, dd, *J* = 9.1, 3.1 Hz, CHCH(CH₃)₂), 3.14-2.79 (2H, m, CH₃CH₂CO), 2.38 (1H, m, CH(CH₃)₂), 1.16 (3H, t, *J* = 7.4 Hz, CH₃CH₂CO), 0.91 (3H, d, 7.0 Hz, (CH₃)₂CH), 0.87 (3H, d, *J* = 7.0 Hz, (CH₃)₂CH). Data is in agreement with that reported in the literature.²⁴⁷

(R)-4-Isopropyl-3-(undec-10-enoyl)oxazolidin-2-one (2.47a)



The title compound was prepared according to General Procedure A from (*R*)-4-isopropyl-2-oxazolidinone (1 g, 7.74 mmol), 10-undecenoyl chloride (2.00 mL, 9.29 mmol) and *n*-butyllithium (1.6 M in hexanes, 5.33 mL, 8.52 mmol) and purified by column chromatography over silica gel (0-20% hexanes/ethyl acetate) to give the purified product as a colourless liquid (1.51 g, 66.0 %). IR $\nu_{\max}/\text{cm}^{-1}$ 2926 (C-H), 2854 (C-H), 1778 (C=O), 1701 (C=O), 1385 (C-N), 1204 (C-O). ^1H NMR (500 MHz, CDCl_3) δ_{H} 5.80 (1H, ddt, $J = 23.6, 10.3, 6.6$ Hz, $\text{CH}_2=\text{CH}$), 4.99 (1H, dq, $J = 17.1, 1.7$ Hz, $\text{CH}_2=\text{CH}$), 4.92 (1H, ddt, $J = 10.3, 2.4, 1.2$ Hz, $\text{CH}_2=\text{CH}$), 4.43 (1H, ddd, $J = 11.3, 6.9, 3.0$ Hz, CH_2OCO), 4.26 (1H, t, $J = 8.5$ Hz, CH_2OCO), 4.20 (1H, dd, $J = 9.1, 3.0$ Hz, $\text{CHCH}(\text{CH}_3)_2$), 2.98 (1H, ddd, $J = 16.6, 8.5, 6.6$ Hz, CH_2CO), 2.85 (1H, ddd, $J = 16.6, 8.5, 6.6$ Hz, CH_2CO), 2.32-2.42 (1H, m, $(\text{CH}_3)_2\text{CH}$), 2.00-2.06 (2H, m, $\text{CH}_2=\text{CHCH}_2$), 1.61-1.69 (2H, m, $\text{CH}_2\text{CH}_2\text{CO}$), 1.26-1.40 (11H, m, CH_2), 0.91 (3H, d, $J = 7.0$ Hz, $(\text{CH}_3)_2\text{CH}$), 0.87 (3H, d, $J = 7.0$ Hz, $(\text{CH}_3)_2\text{CH}$). ^{13}C NMR (126 MHz, CDCl_3) δ_{C} 173.5 (CH_2CON), 154.1 (NCOO), 139.3 ($\text{CH}_2=\text{CH}$), 114.2 ($\text{CH}_2=\text{CH}$), 63.3 ($\text{CHCH}(\text{CH}_3)_2$), 58.4 (CH_2OCO), 35.5, 33.8, 29.3, 29.1, 29.1, 28.9, 28.4, 24.5, 18.0 ($(\text{CH}_3)_2\text{CH}$), 14.7 ($(\text{CH}_3)_2\text{CH}$). HRMS (ESI⁺): Exact mass calculated for $\text{C}_{17}\text{H}_{30}\text{O}_3\text{N}$ $[\text{M}+\text{H}]^+$: 296.2226, found: 296.2212. $[\alpha]_{\text{D}}^{25} = -46.9^\circ$ ($c = 1$, CHCl_3).

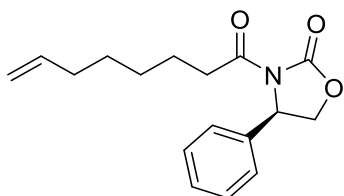
(R)-4-Phenyl-3-(undec-10-enoyl)oxazolidin-2-one (2.47)



The title compound was prepared according to General Procedure A from (*R*)-4-phenyl-2-oxazolidinone (1.00 g, 6.13 mmol), 10-undecenoyl chloride (1.58 mL, 7.35 mmol) and *n*-butyllithium (1.6 M in hexanes, 4.21 mL, 6.74 mmol) and purified by column chromatography over silica gel (0-20% hexanes/ethyl acetate) to give the purified product as a white solid (1.57 g, 77.9 %). m.p. 33-35 °C. IR $\nu_{\max}/\text{cm}^{-1}$ 2924 (C-H), 2853 (C-H), 1786 (C=O),

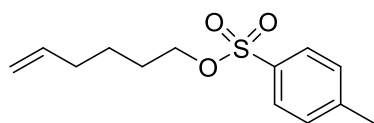
1697 (C=O), 1327 (C-N), 1200 (C-O), 1065 (C-O), 758 (C-H), 702 (C-H). ^1H NMR (500 MHz, CDCl_3) δ_{H} 7.42-7.27 (5H, m, ArH), 5.80 (1H, ddt, $J = 17.1, 10.2, 6.7$ Hz, $\text{CH}_2=\text{CH}$), 5.42 (1H, dd, $J = 8.7, 3.7$ Hz, ArCH), 4.98 (1H, ddt, $J = 17.1, 2.2, 1.6$ Hz, $\text{CH}_2=\text{CH}$), 4.92 (1H, ddt, $J = 10.2, 2.3, 1.2$ Hz, $\text{CH}_2=\text{CH}$), 4.69 (1H, t, $J = 8.8$ Hz, CHCH_2OCO), 4.27 (1H, dd, $J = 8.8, 3.7$ Hz, CHCH_2OCO), 2.92 (2H, td, $J = 7.3, 3.1$ Hz, CH_2CON), 1.98-2.06 (2H, m, $\text{CH}_2=\text{CHCH}_2$), 1.54-1.64 (2H, m, $\text{CH}_2\text{CH}_2\text{CON}$), 1.21-1.39 (10H, m, CH_2). ^{13}C NMR (126 MHz, CDCl_3) δ_{C} 172.9 (CH_2CON), 153.8 (NCOO), 139.2 ($\text{CH}_2=\text{CH}$), 129.2 (2C, ArC), 128.7 (ArC), 125.9 (2C, ArC), 114.2 ($\text{CH}_2=\text{CH}$), 70.0 (ArCH), 57.6 (CH_2OCON), 35.6, 33.8, 29.3 (3C), 29.1, 29.0 (2C), 28.9, 24.1. HRMS (ESI⁺): Exact mass calculated for $\text{C}_{20}\text{H}_{27}\text{O}_3\text{NNa}^+$ $[\text{M}+\text{Na}]^+$: 352.1883, found: 352.1878. $[\alpha]_{\text{D}}^{25} = -42.5^\circ$ ($c = 1, \text{CHCl}_3$).

(R)-3-(Oct-7-enoyl)-4-phenyloxazolidin-2-one (2.72)



The title compound was prepared according to General Procedure A from (*R*)-4-phenyl-2-oxazolidinone (3.29 g, 20.2 mmol), 7-octenoyl chloride (3.87 g, 24.2 mmol) and *n*-butyllithium (1.6 M in hexanes, 13.9 mL, 22.2 mmol) and purified by column chromatography over silica gel (0-20% hexanes/ethyl acetate) to give the purified product as a white solid (1.57 g, 90.0 %). m.p. 33-35 °C. IR $\nu_{\text{max}}/\text{cm}^{-1}$ 2932 (C-H), 1778 (C=O), 1697 (C=O), 1385 (C-N), 1327 (C-N), 1200 (C-O), 700 (C-H). ^1H NMR (500 MHz, CDCl_3) δ_{H} 7.41-7.27 (5H, m, ArH), 5.77 (1H, ddt, $J = 17.0, 10.2, 6.7$ Hz, $\text{CH}_2=\text{CH}$), 5.42 (1H, dd, $J = 8.8, 3.6$ Hz, ArCH), 4.97 (1H, ddt, $J = 17.0, 2.3, 1.4$ Hz, $\text{CH}_2=\text{CH}$), 4.92 (1H, ddt, $J = 10.2, 2.3, 1.4$ Hz, $\text{CH}_2=\text{CH}$), 4.69 (1H, t, $J = 8.8$ Hz, CHCH_2OCO), 4.28 (1H, dd, $J = 8.8, 3.6$ Hz, CHCH_2OCO), 2.93 (2H, td, $J = 7.4, 2.3$ Hz, CH_2CON), 1.98-2.04 (2H, m, $\text{CH}_2=\text{CHCH}_2$), 1.61 (2H, p, $J = 7.4$ Hz, $\text{CH}_2\text{CH}_2\text{CON}$), 1.42-1.24 (6H, m, CH_2). ^{13}C NMR (126 MHz, CDCl_3) δ_{C} 172.8 (CH_2CON), 153.8 (NCOO), 138.9 ($\text{CH}_2=\text{CH}$), 129.2 (2C, ArCH), 128.7 (CCHN), 125.9 (2C, ArCH), 114.4 ($\text{CH}_2=\text{CH}$), 70.0 (CH_2OCO), 57.6 (CNCO), 35.5 (CH_2CON), 33.6 ($\text{CH}_2=\text{CHCH}_2$), 28.6, 28.5, 28.4, 24.0. HRMS (ESI⁺): Exact mass calculated for $\text{C}_{17}\text{H}_{22}\text{O}_3\text{N}^+$ $[\text{M}+\text{H}]^+$: 288.1600, found: 288.1589. $[\alpha]_{\text{D}}^{25} = -44.6^\circ$ ($c = 1, \text{CHCl}_3$).

Hex-5-en-1-yl 4-methylbenzenesulfonate

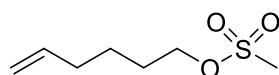


5-Hexene-1-ol (5.92 mL, 49.9 mmol) and p-toluenesulfonyl chloride (11.4 g, 59.8 mmol) were dissolved in dichloromethane (50 mL) at room temperature. To this, triethylamine was added (8.36 mL, 59.9 mmol) and the mixture is stirred at room temperature and the reaction monitored by TLC (hexane/ethyl acetate 4:1). Once completed the mixture was filtered through celite, the filtrate collected and the solvent removed to obtain the crude product. The crude product was purified by column chromatography over silica gel (hexane/ethyl acetate) to give the purified product as a colourless liquid (7.74 g, 61%). ¹H NMR (400 MHz, CDCl₃) δ_H 7.79 (2H, d, *J* = 8.2 Hz, ArH), 7.34 (2H, d, *J* = 8.2 Hz, ArH), 5.66-5.77 (1H, ddt, *J* = 16.9, 10.2, 6.6 Hz, CH₂=CH), 4.91-4.99 (2H, m, CH₂=CH), 4.03 (2H, t, *J* = 6.6 Hz, CH₂OSO₂Ar) 2.45 (3H, s, ArCH₃), 1.96-2.03 (2H, m, CH₂=CHCH₂), 1.61-1.69 (2H, m, CH₂), 1.36-1.45 (2H, m, CH₂). Data is in agreement with that reported in the literature.²⁴⁸

Synthesis of mesylates (General procedure B)

Alcohol (1 equiv.) and triethylamine (1.2 equiv.) were stirred in DCM at 0 °C. To this, methanesulfonyl chloride (1.01 equiv.) was added dropwise. The reaction was warmed to room temperature and monitored by TLC (hexane/ethyl acetate 7:3). On completion, the reaction was quenched by adding saturated aqueous ammonium chloride solution and the organic phase was separated. The aqueous layer was extracted with DCM (3x) and the combined organic layers were washed with brine. The organic layer was dried over magnesium sulfate, filtered and the solution concentrated under vacuum to give the crude product.

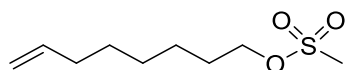
Hex-5-en-1-yl methanesulfonate



The title compound was prepared according to General Procedure B from 5-hexene-1-ol (1.20 mL, 9.98 mmol), triethylamine (1.67 mL, 12.0 mmol) and methanesulfonyl chloride (0.780 mL, 10.1 mmol). The crude product was used without further purification (1.77 g,

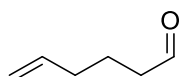
99%). ^1H NMR (400 MHz, CDCl_3) δ_{H} 5.78 (1H, ddt, $J = 23.7, 10.2, 6.7$ Hz, $\text{CH}_2=\text{CH}$), 4.94-5.09 (2H, m, $\text{CH}_2=\text{CH}$), 4.23 (2H, t, $J = 6.7$ Hz, $\text{CH}_2\text{OSO}_2\text{CH}_3$), 3.00 (3H, s, SO_2CH_3), 2.06-2.14 (2H, m, $\text{CH}_2=\text{CHCH}_2$), 1.72-1.81 (2H, m, CH_2), 1.47-1.56 (2H, m, CH_2). Data is in agreement with that reported in the literature.²⁴⁹

Oct-7-en-1-yl methanesulfonate (2.70)



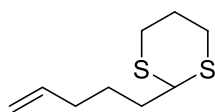
The title compound was prepared according to General Procedure B from 7-octene-1-ol (0.588 mL, 3.90 mmol), triethylamine (0.652 mL, 4.68 mmol) and methanesulfonyl chloride (0.305 mL, 3.94 mmol). The crude product was purified by column chromatography over silica gel (petroleum ether/ethyl acetate) to give the purified product as a colourless liquid (657 mg, 82%). ^1H NMR (400 MHz, CDCl_3) δ_{H} 5.79 (1H, ddt, $J = 17.0, 10.2, 6.6$ Hz, $\text{CH}_2=\text{CH}$), 5.00 (1H, dq, $J = 17.0, 1.7$ Hz, $\text{CH}_2=\text{CH}$), 4.94 (1H, ddt, $J = 10.2, 2.3, 1.2$ Hz, $\text{CH}_2=\text{CH}$), 4.22 (2H, t, $J = 6.7$ Hz, CH_2OSO_2), 3.00 (3H, s, SO_2CH_3), 2.08–2.02 (2H, m, $\text{CH}_2=\text{CHCH}_2$), 1.74 (2H, dt, $J = 8.5, 6.6$ Hz, $\text{CH}_2\text{CH}_2\text{SO}_2$), 1.45–1.30 (6H, m, CH_2). ^{13}C NMR (126 MHz, CDCl_3) δ_{C} 138.8 ($\text{CH}_2=\text{CH}$), 114.5 ($\text{CH}_2=\text{CH}$), 70.1 (CH_2OSO_2), 37.4 ($\text{CH}_2=\text{CHCH}_2$), 29.1, 29.0, 28.7, 28.5, 25.3. HRMS (ESI⁺): Exact mass calculated for $\text{C}_9\text{H}_{18}\text{O}_3\text{S}^+$ [$\text{M}+\text{H}$]⁺: 229.0874, found: 229.0872.

Hex-5-enal (2.43)



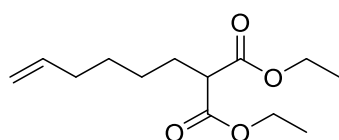
Dess-Martin periodinane (3.18 g, 7.5 mmol) is dissolved in dry dichloromethane (5 mL) and cooled to 0 °C. 5-hexen-1-ol (0.600 mL, 5 mmol) was added and the reaction stirred at 0 °C for 1 hour. The reaction is then warmed to room temperature and stirred for a further hour. The white solid is filtered off and the solvent is removed under reduced pressure. The residue is dissolved in diethyl ether and extracted with sodium bicarbonate solution. The organic layer is dried over magnesium sulfate, filtered and the solvent removed to give a colourless oil which was used without further purification (332 mg, 68%). ^1H NMR (400 MHz, CDCl_3) δ_{H} 9.78 (1H, t, $J = 1.7$ Hz, CHO), 5.71-5.85 (1H, m, $\text{CH}_2=\text{CH}$), 4.92-5.07 (2H, m, $\text{CH}_2=\text{CH}$), 2.45 (2H, td, $J = 7.3, 1.7$ Hz, CH_2CHO), 2.08 (2H, m, $\text{CH}_2=\text{CHCH}_2$), 1.74 (2H, p, $J = 7.3$ Hz, $\text{CH}_2\text{CH}_2\text{CHO}$). Data is in agreement with that reported in the literature.²⁵⁰

2-(Pent-4-en-1-yl)-1,3-dithiane (2.44)



Propane-1,3-dithiol (0.558 mL, 5.57 mmol) was added to a solution of hex-5-enal (547 mg, 5.57 mmol) in chloroform (10 mL) and stirred for 1 hour, then cooled to -10 °C. Boron trifluoride etherate (0.688 mL, 5.57 mmol) was then added dropwise. The solution was allowed to warm to room temperature and was stirred for 17 hours. The mixture was washed with water (3 x 25 mL), 10% sodium hydroxide solution (25 mL) and water, dried over magnesium sulfate, filtered and concentrated in vacuo. The crude product was purified by column chromatography over silica gel (hexane/ethyl acetate, 0 to 10% ethyl acetate) to give the purified product as a yellow oil (152 mg, 24%). $^1\text{H NMR}$ (400 MHz, CDCl_3) δ_{H} 5.79 (1H, ddt, $J = 17.0, 10.2, 6.7$ Hz, $\text{CH}_2=\text{CH}$), 5.02 (1H, ddt, $J = 17.0, 2.1, 1.4$ Hz, $\text{CH}_2=\text{CH}$), 4.97 (1H, ddt, $J = 10.2, 2.1, 1.4$ Hz, $\text{CH}_2=\text{CH}$), 4.05 (1H, t, $J = 6.9$ Hz, SCHS), 2.78-2.90 (4H, m, $\text{CH}_2\text{S} \times 2$) 2.04-2.15 (2H, m, $\text{CH}_2=\text{CHCH}_2$), 1.80-1.92 (2H, m, CH_2CHS), 1.73-1.80 (2H, m, $\text{CH}_2\text{CH}_2\text{S}$), 1.55-1.63 (2H, m, $\text{CH}_2\text{CH}_2\text{CH}=\text{CH}_2$). Data is in agreement with that reported in the literature.²⁵⁰

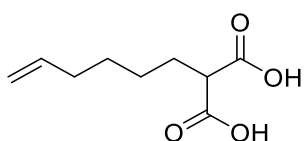
Diethyl 2-(hex-5-en-1-yl)malonate (2.80)



Diethyl malonate (10.24 mL, 61.3 mmol) was added slowly to a stirred solution of sodium hydride (60% dispersion in mineral oil, 2.70 g, 67.5 mmol) in tetrahydrofuran (280 mL) at 0 °C. The resulting solution was stirred at 0 °C for 15 minutes, then at room temperature for 30 minutes before being cooled again to 0 °C. A solution of 6-bromo-1-hexene (8.20 mL, 61.3 mmol) in THF (160 mL) was then added slowly and the reaction was heated to reflux overnight. After cooling to room temperature, the reaction was quenched by addition of water (40 mL). Ethyl acetate (80 mL) and water (160 mL) were added and the layers separated. The aqueous layer was extracted with ethyl acetate (3 x 160 mL). The combined organic layers were washed with brine (160 mL), dried over magnesium sulfate and the solvent removed under vacuum to give the crude product. The crude product was purified

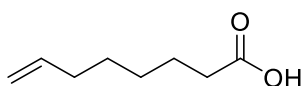
by column chromatography over silica gel (petroleum ether/ethyl acetate, 0% to 20% ethyl acetate) to give the purified product as a yellow liquid (10.1 g, 68%). $^1\text{H NMR}$ (500 MHz, CDCl_3) δ_{H} 5.78 (1H, ddt, $J = 17.0, 10.2, 6.6$ Hz, $\text{CH}=\text{CH}_2$), 4.96-5.02 (1H, m, $\text{CH}=\text{CH}_2$), 4.91-4.96 (1H, m, $\text{CH}=\text{CH}_2$), 4.19 (4H, qd, $J = 7.2, 0.9$ Hz, OCH_2CH_3), 3.33 (1H, t, $J = 7.6$ Hz, $\text{CH}(\text{COOEt})_2$), 2.05 (2H, m, $\text{CH}_2=\text{CHCH}_2$), 1.96–1.88 (2H, m, $\text{CH}_2\text{CH}(\text{COOEt})_2$), 1.30-1.46 (4H, m), 1.26 (6H, t, $J = 7.2$ Hz, 2 x OCH_2CH_3). Data is in agreement with that reported in the literature.²⁵¹

2-(Hex-5-en-1-yl)malonic acid (2.81)



An aqueous solution of sodium hydroxide (2 M, 200 mL, 0.400 mol) was added to a stirring solution of diethyl 2-(hex-5-en-1-yl)malonate (29.9 g, 0.123 mol) in ethanol (200 mL) and the solution was stirred overnight at room temperature and monitored by TLC. On completion, the solution was concentrated under vacuum. Water (300 mL) was added and the aqueous layer was extracted with diethyl ether (3 x 200 mL). The aqueous layer was acidified to $\text{pH} < 1$ with hydrochloric acid solution (3 M). The acidified solution was extracted with diethyl ether (3 x 200 mL). The organic layers were combined, dried over sodium sulfate and the solvent removed under vacuum to give the crude product as a white solid (19.2 g, 84%). The crude product was used without further purification. $^1\text{H NMR}$ (400 MHz, CDCl_3) δ_{H} 5.79 (1H, ddt, $J = 16.9, 10.2, 6.7$ Hz, $\text{CH}_2=\text{CH}$), 5.06–4.90 (2H, m, $\text{CH}_2=\text{CH}$), 3.44 (1H, t, $J = 7.5$ Hz, $\text{CH}(\text{COOH})_2$), 2.11–2.02 (2H, m, $\text{CH}_2=\text{CHCH}_2$), 1.96 (2H, q, $J = 7.5$ Hz, $\text{CH}_2\text{CH}(\text{COOH})_2$), 1.36-1.49 (4H, m, CH_2). Data is in agreement with that reported in the literature.²⁵²

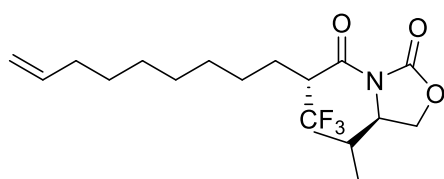
7-Octenoic acid (2.68)



2-(Hex-5-en-1-yl)malonic acid (11.0 g, 59.3 mmol) was dissolved in pyridine (24.5 mL) and water (1.23 mL). The mixture was heated to reflux and the reaction was monitored by TLC. On completion, the reaction was cooled to room temperature and the reaction mixture was concentrated under reduced pressure. The residue was dissolved in water (80 mL) and acidified to $\text{pH} < 1$ with concentrated hydrochloric acid solution (5 M). The aqueous layer was

extracted with DCM (3 x 160 mL), dried over sodium sulfate, filtered and concentrated under reduced pressure to give the crude product as a colourless liquid (7.67 g, 91%). The crude product was used without further purification. ¹H NMR (400 MHz, CDCl₃) δ_H 5.80 (1H, ddt, *J* = 16.9, 10.2, 6.7 Hz, CH₂=CH), 5.03–4.97 (1H, m, CH₂=CH), 4.94 (1H, ddt, *J* = 10.2, 2.2, 1.3 Hz, CH₂=CH), 2.36 (2H, t, *J* = 7.5 Hz, CH₂COOH), 2.05 (2H, tdd, *J* = 6.7, 5.3, 1.3 Hz, CH₂=CHCH₂), 1.65 (2H, p, *J* = 7.5 Hz, CH₂CH₂COOH), 1.31–1.46 (4H, m, 2 x CH₂). Data is in agreement with that reported in the literature.²⁵³

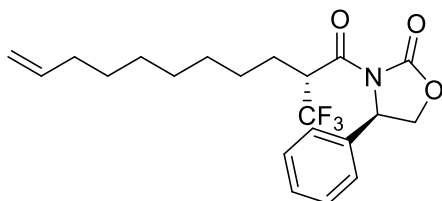
(*R*)-4-Isopropyl-3-((*R*)-2-(trifluoromethyl)undec-10-enoyl)oxazolidin-2-one (2.48a)



(*R*)-4-Isopropyl-3-(undec-10-enoyl)oxazolidin-2-one (500 mg, 1.69 mmol) was dissolved under argon in dry THF (6.25 mL) and cooled to -78 °C. Lithium bis(trimethylsilylamide) (1 M solution in THF, 1.86 mL, 1.86 mmol) was slowly introduced with vigorous stirring. After 30 minutes Togni's Reagent II (contains 60% Diatomaceous earth, 749 mg, 2.37 mmol) was added as a solid in one portion. The reaction was warmed to room temperature over a period of four hours. On completion, the reaction was quenched by addition of saturated sodium bicarbonate solution and diluted with water. The aqueous layer was extracted with ethyl acetate (3 x 40 mL) and the combined organic layers were washed with sodium bicarbonate, phosphate buffer pH = 4, water and brine. The organic layer was dried over sodium sulfate and the solvent was removed under vacuum to obtain the crude product. The crude product was purified by column chromatography over silica gel (hexane/ethyl acetate) to give the purified product as a colourless oil (68.0 mg, 11%). ¹H NMR (500 MHz, CDCl₃) δ_H 5.74–5.86 (1H, m, CH=CH₂), 4.90–5.02 (3H, m, CH₂=CH, CHCF₃), 4.50–4.55 (1H, m, CH(CH₃)₂), 4.28–4.33 (1H, m, CH₂OCON), 4.24 (1H, dd, *J* = 9.2, 3.3 Hz, CH₂OCON), 2.39 (1H, pd, *J* = 7.1, 3.9 Hz, CHCH(CH₃)₂), 2.00–2.06 (2H, m, CH₂=CHCH₂), 1.92–1.99 (1H, m, CH₂CHCF₃), 1.74–1.89 (1H, m, CH₂CHCF₃), 1.22–1.43 (10H, m), 0.85–0.96 (6H, m, (CH₃)₂CH). ¹³C NMR (126 MHz, CDCl₃) δ_C 167.7 (CF₃CHCON), 153.7 (CONCOO), 139.3 (CH₂=CH), 124.9 (q, *J* = 281.8 Hz, CF₃), 114.3 (CH₂=CH), 63.3 (CHCH₂OCON), 58.8 ((CH₃)₂CH), 46.7 (q, *J* = 26.7 Hz, CHCF₃), 33.9

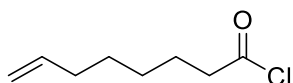
(CH₂=CHCH₂), 29.4, 29.3, 29.1, 28.9, 28.8, 28.1 ((CH₃)₂CHCH), 26.7, 26.3, 17.9 ((CH₃)₂), 14.3 ((CH₃)₂). ¹⁹F NMR (470 MHz, CDCl₃) δ_F -67.1 (3F, d, *J* = 8.2 Hz, CF₃).

(*R*)-4-Phenyl-3-((*R*)-2-(trifluoromethyl)undec-10-enoyl)oxazolidin-2-one (2.48b)



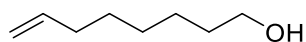
(*R*)-3-((*R*)-2-Methylundec-10-enoyl)-4-phenyloxazolidin-2-one (65.0 mg, 0.197 mmol) was dissolved under argon in dry THF (1 mL) and cooled to -78 °C. Lithium bis(trimethylsilylamide) (1 M solution in toluene, 0.217 mL, 0.217 mmol) was slowly introduced with vigorous stirring. After 30 minutes Togni's Reagent II (contains 60% Diatomaceous earth, 228 mg, 0.276 mmol) was added as a solid in one portion. The reaction was warmed to room temperature over a period of four hours. On completion, the reaction was quenched by addition of saturated sodium bicarbonate solution and diluted with water. The aqueous layer was extracted with ethyl acetate (3 x 4 mL) and the combined organic layers were washed with sodium bicarbonate, phosphate buffer pH = 4, water and brine. The organic layer was dried over sodium sulfate and the solvent was removed under vacuum to obtain the crude product. The crude product was purified by column chromatography over silica gel (hexane/ethyl acetate, 0 to 20% ethyl acetate) to give the purified product as a colourless oil (7.16 mg, 10%). IR ν_{max}/cm⁻¹ 2924 (C-H), 2359, 1778 (C=O), 1717 (C=O), 1387 (C-N), 1250 (C-O), 1198 (C-O), 1043 (C-F), 734 (C-H). ¹H NMR (500 MHz, CDCl₃) δ_H 7.27-7.42 (5H, m, ArH), 5.74-5.86 (1H, m, CH=CH₂), 5.48 (1H, td, *J* = 8.9, 8.2, 4.0 Hz, ArCH), 4.90-5.03 (3H, m, CH₂=CH, CHCF₃), 4.72 (1H, t, *J* = 8.9 Hz, CHCH₂OCO), 4.28 (1H, dd, *J* = 9.0, 4.5 Hz, CH₂OCON), 2.00-2.07 (2H, m, CH₂=CHCH₂), 1.90-1.98 (1H, m, CH₂CHCF₃), 1.71-1.82 (1H, m, CH₂CHCF₃), 1.22-1.43 (10H, m). ¹⁹F NMR (470 MHz, CDCl₃) δ_F -67.0 (3F, d, *J* = 8.2 Hz, CF₃). HRMS (EI): Exact mass calculated for C₂₁H₂₆F₃NO₃: 397.1859, found: 397.1864. [α]_D²⁰ = -35.1° (c = 0.0410, CHCl₃).

7-Octenoyl chloride (2.71)



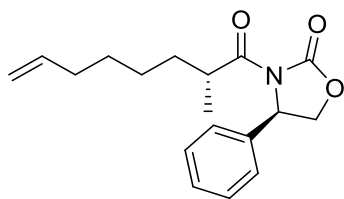
A CH_2Cl_2 solution of oxalyl chloride (2 M, 9.17 mL, 15.7 mmol) was added to a mixture of 7-octenoic acid (1.71 g, 12.1 mmol) and DMF (a few drops) and the resulting mixture was stirred at room temperature for 15 minutes. Diethyl ether was added, and the resulting mixture was filtered and concentrated under reduced pressure to give the crude product as a yellow liquid (1.68 g, 87%). The crude product was used immediately in the next step without further purification. ^1H NMR (500 MHz, CDCl_3) δ_{H} 5.78 (1H, ddt, $J = 17.0, 10.2, 6.8$ Hz, $\text{CH}_2=\text{CH}$), 4.92-5.04 (2H, m, $\text{CH}_2=\text{CH}$), 2.89 (2H, t, $J = 7.3$ Hz, CH_2COCl), 2.01-2.10 (2H, m, $\text{CH}_2=\text{CHCH}_2$), 1.68-1.76 (2H, m, $\text{CH}_2\text{CH}_2\text{COCl}$), 1.31-1.46 (4H, m, CH_2). Data is in agreement with that reported in the literature.²⁵⁴

7-Octen-1-ol (2.69)



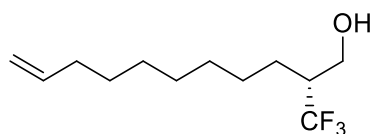
7-Octenoic acid (0.216 mL, 1.41 mmol) was dissolved in tetrahydrofuran (5 mL) and lithium aluminium hydride (2.0 M in THF, 1.48 mL, 2.95 mmol) was added portionwise at 0 °C. The reaction was stirred at 0 °C for 2 hours and monitored by TLC (4:1 petroleum ether/ethyl acetate). On completion, the reaction was quenched by addition of 2M NaOH solution and filtered through celite. The organic layer was extracted three times with diethyl ether. The combined organic layers were dried over magnesium sulfate and the filtrate was concentrated under vacuum to give the crude product as a colourless liquid (159.1 mg, 86%). The crude product was used without further purification. ^1H NMR (500 MHz, CDCl_3) δ_{H} 5.81 (1H, ddt, $J = 17.0, 10.1, 6.6$ Hz, $\text{CH}_2=\text{CH}$), 4.99 (1H, dq, $J = 17.0, 1.7$ Hz, $\text{CH}_2=\text{CH}$), 4.93 (1H, ddt, $J = 10.2, 2.3, 1.2$ Hz, $\text{CH}_2=\text{CH}$), 3.64 (2H, t, $J = 6.6$ Hz, CH_2OH), 2.00-2.09 (2H, m, $\text{CH}_2=\text{CHCH}_2$), 1.52-1.67 (4H, m, $\text{CH}_2\text{CH}_2\text{OH}$, $\text{CH}_2=\text{CHCH}_2\text{CH}_2$), 1.30-1.44 (4H, m, CH_2). Data is in agreement with that reported in the literature.²⁵⁵

(R)-3-((R)-2-Methyloct-7-enoyl)-4-phenyloxazolidin-2-one (2.73)



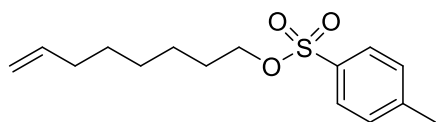
Sodium bis(trimethylsilyl)amide (1.0 M in THF, 33.9 mL, 33.9 mmol) was added to a solution of (R)-3-(oct-7-enoyl)-4-phenyloxazolidin-2-one (8.86 g, 30.8 mmol) in dry tetrahydrofuran (96 mL) under argon at -78 °C and stirred at -78 °C for 1 hour. Methyl iodide (9.60 mL, 154.2 mmol) was added and the reaction was stirred at -78 °C for 1 hour, then warmed to room temperature and stirred for a further hour. On completion, the reaction was quenched with saturated ammonium chloride solution (65 mL) and the organic layer was extracted three times with ethyl acetate (65 mL). The combined organic layers were washed with saturated sodium bicarbonate solution (65 mL), saturated ammonium chloride solution (65 mL) and brine (65 mL). The organic layer was dried over sodium sulfate and the solvent removed under vacuum to give the crude product. The crude product was purified by column chromatography over silica gel (0-20% petroleum ether/ethyl acetate) to give the purified product as a white solid (5.64 g, 61%). m.p. 44-46 °C. IR $\nu_{\max}/\text{cm}^{-1}$ 2932 (C-H), 1778 (C=O), 1697 (C=O), 1385 (C-N), 1327 (C-N), 1200 (C-O), 700 (C-H). ^1H NMR (500 MHz, CDCl_3) δ_{H} 7.41–7.27 (5H, m, ArH), 5.79 (1H, ddt, $J = 17.0, 10.2, 6.7$ Hz, $\text{CH}_2=\text{CH}$), 5.43 (1H, dd, $J = 8.8, 3.8$ Hz, ArCH), 4.98 (1H, dq, $J = 17.1, 1.6$ Hz, $\text{CH}_2=\text{CH}$), 4.92 (1H, ddd, $J = 10.2, 2.2, 1.1$ Hz, $\text{CH}_2=\text{CH}$), 4.69 (1H, t, $J = 8.8$ Hz, CHCH_2OCO), 4.25 (1H, dd, $J = 8.8, 3.8$ Hz, CHCH_2OCO), 3.73 (1H, q, $J = 6.7$ Hz, CH_3CHCO), 2.03 (2H, m, $\text{CH}_2=\text{CHCH}_2$), 1.66-1.76 (2H, m, CH_2CHCON), 1.42–1.25 (4H, m, CH_2), 1.10 (3H, d, $J = 6.7$ Hz, CH_3). ^{13}C NMR (126 MHz, CDCl_3) δ_{C} 176.7 (CHCON), 153.5 (NCOO), 139.4 (CCHCH₂OCO), 139.0 ($\text{CH}_2=\text{CH}$), 129.4 (2C, ArC), 128.8 (ArC), 125.9 (2C, ArC), 114.5 ($\text{CH}_2=\text{CH}$), 69.9 (CH_2OCON), 57.9 (CHCH₂OCO), 37.9 (CH_3CHCO), 33.8 ($\text{CH}_2=\text{CHCH}_2$), 33.0 (CH_2CHCON), 29.0, 26.9, 17.5 (CH_3). HRMS (ESI⁺): Exact mass calculated for $\text{C}_{18}\text{H}_{23}\text{O}_3\text{NNa}^+$ $[\text{M}+\text{Na}]^+$: 324.1576, found: 324.1562. $[\alpha]_{\text{D}}^{25} = -88.5^\circ$ ($c = 1, \text{CHCl}_3$).

(R)-2-(Trifluoromethyl)undec-10-en-1-ol (2.49)



(*R*)-4-Isopropyl-3-((*R*)-2-(trifluoromethyl)undec-10-enoyl)oxazolidin-2-one (68.0 mg, 0.212 mmol) was treated at 0 °C in a 3:1 THF/H₂O mixture (1 mL) with sodium borohydride (32.0 mg, 0.846 mmol) and monitored by TLC (4:1 petroleum ether/ethyl acetate). On completion, the reaction was quenched by addition of saturated ammonium chloride solution until effervescence ceased. The organic layer was extracted with three times with ethyl acetate and the combined organic layers were washed with saturated sodium bicarbonate solution, brine and dried over sodium sulfate. The solvent was removed under vacuum to give the crude product. The crude product was purified using column chromatography over silica gel (0-20% petroleum ether/ethyl acetate) to give the purified product as a colourless oil (41.0 mg, 81%). IR $\nu_{\max}/\text{cm}^{-1}$ 2918 (C-H), 1674 (C=C), 1425 (O-H), 1356 (C-F), 1283 (C-O), 799 (C-H), 681 (C-H). ¹H NMR (500 MHz, CDCl₃) δ_{H} 5.81 (1H, ddt, $J = 17.0, 10.1, 6.7$ Hz, CH₂=CH), 4.99 (1H, dq, $J = 17.0, 1.7$ Hz, CH₂=CH), 4.93 (1H, ddt, $J = 10.1, 2.3, 1.2$ Hz, CH₂=CH), 3.74-3.86 (2H, m, CH₂OH), 2.16-2.27 (1H, m, CF₃CH), 2.00-2.06 (2H, m, CH₂=CHCH₂), 1.74 (1H, dq, $J = 13.5, 6.7$ Hz, CH₂CHCF₃), 1.50-1.56 (5H, m, CH₂CHCF₃, CH₂), 1.29-1.40 (6H, m, CH₂). ¹³C NMR (126 MHz, CDCl₃) δ_{C} 143.5 (CH₂=CH), 118.4 (CH₂=CH), 46.5, 41.0, 33.9, 33.8, 29.3, 24.0, 20.9, 17.4, 14.8. ¹⁹F NMR (470 MHz, CDCl₃) δ_{F} -69.1 (d, $J = 10.0$ Hz, CF₃). HRMS (ESI⁺): Exact mass calculated for C₁₂H₂₂F₃O⁺ [M+H]⁺: 239.1617, found: 239.1617. $[\alpha]_{\text{D}}^{20} = -13.0^{\circ}$ (c = 0.0460, CHCl₃).

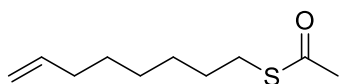
Oct-7-en-1-yl 4-methylbenzenesulfonate (2.84a)



7-Octen-1-ol (0.807 g, 6.29 mmol) and triethylamine (1.05 mL, 7.55 mmol) were stirred in dichloromethane (10 mL) at 0 °C. To this, p-toluenesulfonyl chloride (1.21 g, 6.36 mmol) was added and the reaction warmed to room temperature. The reaction was quenched by addition of saturated ammonium chloride solution and the aqueous layer was extracted with dichloromethane (3 x 6 mL). The combined organic layers were washed with brine (25

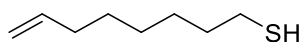
mL), dried over magnesium sulfate and concentrated under reduced pressure to give the crude product. The crude product was purified by column chromatography over silica gel (0-10% petroleum ether/diethyl ether) to give the purified product as a colourless liquid (1.08 g, 61%). $^1\text{H NMR}$ (500 MHz, CDCl_3) δ_{H} 7.79 (2H, d, $J = 8.2$ Hz, $\text{SO}_2\text{C}(\text{CH}_3)_2$), 7.34 (2H, d, $J = 8.2$ Hz, $\text{CH}_3\text{C}(\text{CH}_3)_2$), 5.76 (1H, ddt, $J = 16.9, 10.2, 6.7$ Hz, $\text{CH}_2=\text{CH}$), 4.97 (1H, dq, $J = 16.9, 1.7$ Hz, $\text{CH}_2=\text{CH}$), 4.92 (1H, ddt, $J = 10.2, 2.3, 1.2$ Hz, $\text{CH}_2=\text{CH}$), 4.02 (2H, t, $J = 6.5$ Hz, CH_2OSO_2), 2.45 (3H, s, CH_3), 1.99 (2H, q, $J = 7.3$ Hz, $\text{CH}_2=\text{CHCH}_2$), 1.59-1.67 (2H, m, $\text{CH}_2\text{CH}_2\text{OSO}_2$), 1.20-1.37 (6H, m, CH_2). Data is in agreement with that reported in the literature.²⁵⁶

S-(Oct-7-en-1-yl)ethanethioate (2.85a)



Oct-7-en-1-yl 4-methylbenzenesulfonate (1.22 g, 4.32 mmol) was dissolved in *N,N*-dimethylformamide (12 mL) and potassium thioacetate (1.48 g, 13.0 mmol) was added. The solution was stirred at 85 °C for 2 hours and monitored by TLC (9:1 pentane/diethyl ether). On completion, the reaction mixture was diluted with diethyl ether (15 mL). The organic layer was washed with brine (10 mL), dried over sodium sulfate and concentrated under reduced pressure to give the crude product. The crude product was purified by column chromatography over silica gel (0-10% pentane/diethyl ether) to give the purified product as a pale yellow liquid (551 mg, 62%). $^1\text{H NMR}$ (500 MHz, CDCl_3) δ_{H} 5.80 (1H, ddt, $J = 17.1, 10.2, 6.7$ Hz, $\text{CH}_2=\text{CH}$), 4.99 (1H, ddt, $J = 17.1, 2.1, 1.6$ Hz, $\text{CH}_2=\text{CH}$), 4.93 (1H, ddt, $J = 10.2, 2.3, 1.2$ Hz, $\text{CH}_2=\text{CH}$), 2.86 (2H, t, $J = 7.4$ Hz, CH_2S), 2.32 (3H, s, CH_3), 2.03 (2H, q, $J = 6.8$ Hz, $\text{CH}_2=\text{CHCH}_2$), 1.52-1.61 (2H, m, $\text{CH}_2\text{CH}_2\text{S}$), 1.23-1.44 (6H, m, CH_2). Data is in agreement with that reported in the literature.²⁵⁷

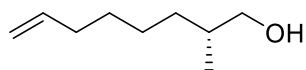
7-Octene-1-thiol (2.83)



S-(Oct-7-en-1-yl) ethanethioate (418 mg, 2.24 mmol) was dissolved in dry diethyl ether (17 mL) and cooled to 0 °C. Lithium aluminium hydride (4.0 M in Et_2O , 1.12 mL, 4.48 mmol) was slowly added and the reaction was stirred for 2 hours at room temperature and monitored by TLC (9:1 pentane/diethyl ether). On completion, the reaction was cooled to 0 °C and dry diethyl ether (17 mL), saturated ammonium chloride solution (12 mL) and 1 M HCl solution

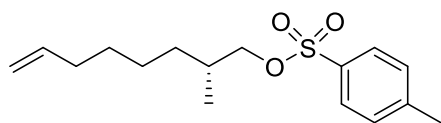
(25 mL) were added. The organic layer was extracted twice with diethyl ether (16 mL) and the combined organic layers were washed twice with saturated sodium bicarbonate solution (16 mL) then dried over sodium sulfate. The solvent was removed to give the crude product as a colourless liquid (325 mg, 92%). The crude product was used without further purification. ^1H NMR (500 MHz, CDCl_3) δ_{H} 5.80 (1H, ddt, $J = 17.0, 10.2, 6.7$ Hz, $\text{CH}_2=\text{CH}$), 4.99 (1H, ddt, $J = 17.0, 1.7$ Hz, $\text{CH}_2=\text{CH}$), 4.93 (1H, ddt, $J = 10.2, 2.3, 1.3$ Hz, $\text{CH}_2=\text{CH}$), 2.52 (2H, q, $J = 7.5$ Hz, CH_2SH), 2.01-2.08 (2H, m, $\text{CH}_2=\text{CHCH}_2$), 1.58-1.65 (2H, m, $\text{CH}_2\text{CH}_2\text{SH}$), 1.28-1.43 (6H, m, CH_2). ^{13}C NMR (126 MHz, CDCl_3) δ_{C} 139.0 ($\text{CH}_2=\text{CH}$), 114.3 ($\text{CH}_2=\text{CH}$), 34.0 ($\text{CH}_2=\text{CHCH}_2$), 33.7 ($\text{CH}_2\text{CH}_2\text{SH}$), 29.7, 29.2, 28.9, 24.6 (CH_2SH). HRMS (ESI⁺): Exact mass calculated for $\text{C}_8\text{H}_{17}\text{S}^+$ [$\text{M}+\text{H}$]⁺: 145.1051, found: 145.1040.

(R)-2-Methyloct-7-en-1-ol (2.74)



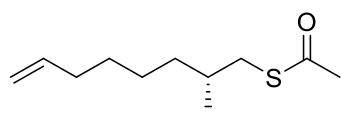
Lithium aluminium hydride (4.0 M in Et_2O , 1.08 mL, 4.33 mmol) was added to a solution of (*R*)-3-((*R*)-2-methyloct-7-enoyl)-4-phenyloxazolidin-2-one (435 mg, 1.44 mmol) in diethyl ether (13 mL) at 0 °C. The reaction was monitored by TLC (4:1 petroleum ether/ethyl acetate). On completion, the reaction was quenched by dropwise addition of saturated ammonium chloride solution and the organic layer was extracted with diethyl ether (3 x 13 mL). The combined organic layers were dried over sodium sulfate and the solvent removed under vacuum to give the crude product as a colourless liquid. The crude product was purified by column chromatography over silica gel (0-20% petroleum ether/ethyl acetate) to give the purified product as a colourless liquid (174 mg, 85% yield). ^1H NMR (500 MHz, CDCl_3) δ_{H} 5.81 (1H, ddt, $J = 17.0, 10.2, 6.7$ Hz, $\text{CH}_2=\text{CH}$), 4.96-5.03 (1H, m, $\text{CH}_2=\text{CH}$), 4.93 (1H, ddt, $J = 10.2, 2.3, 1.2$ Hz, $\text{CH}_2=\text{CH}$), 3.51 (1H, dd, $J = 10.5, 5.8$ Hz, CH_2OH), 3.42 (1H, dd, $J = 10.5, 6.2$ Hz, CH_2OH), 2.02-2.09 (2H, m, $\text{CH}_2=\text{CHCH}_2$), 1.57-1.66 (1H, m, CHCH_2OH), 1.22-1.44 (9H, m, CH_2). $[\alpha]_{\text{D}}^{20} = +9.4^\circ$ ($c = 0.0081$, CHCl_3). Data is in agreement with that reported in the literature.²⁵⁸

(*R*)-2-Methyloct-7-en-1-yl 4-methylbenzenesulfonate (2.84b)



p-Toluenesulfonyl chloride (626 mg, 1.81 mmol) was dissolved in pyridine (1 mL) and the solution was cooled to 0 °C. (*R*)-2-Methyloct-7-en-1-ol (258 mg, 1.81 mmol) was added dropwise and the reaction was warmed to room temperature and monitored by TLC (19:1 petroleum ether/diethyl ether). On completion, the reaction was quenched by consecutive addition of icy water (6 mL) and concentrated hydrochloric acid (5 M, 2.5 mL) and the mixture was extracted with diethyl ether (3 x 12 mL). The combined organic layers were dried over magnesium sulfate and concentrated under vacuum to give the crude product. The crude product was purified by column chromatography over silica gel (0-10% petroleum ether/diethyl ether) to give the purified product as a colourless liquid (385 mg, 72%). IR $\nu_{\text{max}}/\text{cm}^{-1}$ 2972 (C-H), 2929 (C-H), 1360 (S=O), 1175 (C-O), 962 (C=C), 812 (C-H). ^1H NMR (500 MHz, CDCl_3) δ_{H} 7.76-7.82 (2H, m, ArH), 7.32-7.36 (2H, m, ArH), 5.77 (1H, ddt, $J = 17.1, 10.2, 6.7$ Hz, $\text{CH}_2=\text{CH}$), 4.97 (1H, dq, $J = 17.1, 1.7$ Hz, $\text{CH}_2=\text{CH}$), 4.93 (1H, ddt, $J = 10.2, 2.2, 1.7$ Hz, $\text{CH}_2=\text{CH}$), 3.88 (1H, dd, $J = 9.4, 5.8$ Hz, CH_2OSO_2), 3.81 (1H, dd, $J = 9.4, 6.4$ Hz, CH_2OSO_2), 2.45 (3H, s, ArCH₃), 1.96-2.03 (2H, m, $\text{CH}_2=\text{CHCH}_2$), 1.71-1.88 (1H, m, $\text{CH}_3\text{CHCH}_2\text{O}$), 1.24-1.37 (6H, m, CH_2), 0.88 (3H, d, $J = 6.7$ Hz, $\text{CH}_3\text{CHCH}_2\text{O}$). ^{13}C NMR (126 MHz, CDCl_3) δ_{C} 144.8 (SO_2C), 138.9 ($\text{CH}_2=\text{CH}$), 133.4 (CH_3C), 129.9 (2C, ArC), 128.1 (2C, ArC), 114.5 ($\text{CH}_2=\text{CH}$), 75.2 (CH_2OSO_2), 33.7 ($\text{CH}_2=\text{CHCH}_2$), 32.9 ($\text{CH}_3\text{CHCH}_2\text{OSO}_2$), 32.6 ($\text{CH}_2\text{CHCH}_2\text{OSO}_2$), 29.0, 26.2, 21.8 (CH_3C), 16.6 (CH_3CH). HRMS (ESI⁺): Exact mass calculated for $\text{C}_{16}\text{H}_{25}\text{O}_3\text{S}^+$ $[\text{M}+\text{H}]^+$: 297.1524, found: 297.1514. $[\alpha]_{\text{D}}^{20} = -3.6^\circ$ ($c = 0.0093$, CHCl_3).

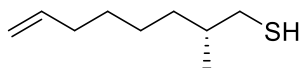
(*R*)-S-(2-Methyloct-7-en-1-yl) ethanethioate (2.85b)



(*R*)-2-Methyloct-7-en-1-yl 4-methylbenzenesulfonate (2.64 g, 8.91 mmol) was dissolved in *N,N*-dimethylformamide (21 mL) and potassium thioacetate (3.05 g, 26.7 mmol) was added. The solution was stirred at 85 °C for two hours and the reaction was monitored by TLC (9:1 pentane/diethyl ether). On completion, the reaction mixture was diluted with diethyl ether

(27 mL). The organic layer was washed with brine (27 mL), dried over sodium sulfate and concentrated under reduced pressure to give the crude product. The crude product was purified by column chromatography over silica gel (0-10% pentane/diethyl ether) to give the purified product as a yellow liquid (1.42 g, 80%). ^1H NMR (500 MHz, CDCl_3) δ_{H} 5.75-5.86 (1H, m, $\text{CH}_2=\text{CH}$), 4.99 (1H, d, $J = 17.2$ Hz, $\text{CH}_2=\text{CH}$), 4.93 (1H, d, $J = 10.2$ Hz, $\text{CH}_2=\text{CH}$), 2.92 (1H, dd, $J = 13.3, 5.7$ Hz, CH_2SCO), 2.74 (1H, dd, $J = 13.3, 7.3$ Hz, CH_2SCO), 2.33 (3H, s, SCOCH_3), 2.05 (2H, q, $J = 6.9$ Hz, $\text{CH}_2=\text{CHCH}_2$), 1.60-1.70 (1H, m, CH_3CH), 1.23-1.42 (5H, m, $\text{CH}_2\text{CHCH}_2\text{S}$, CH_2), 1.12-1.22 (1H, m, $\text{CH}_2\text{CHCH}_2\text{S}$), 0.93 (3H, d, $J = 6.7$ Hz, CH_3CH). ^{13}C NMR (126 MHz, CDCl_3) δ_{C} 196.1 ($\text{C}=\text{O}$), 139.1 ($\text{CH}_2=\text{CH}$), 114.4 ($\text{CH}_2=\text{CH}$), 36.2 (CH_2SCO), 36.0 ($\text{CH}_2\text{CHCH}_2\text{SCO}$), 33.8 ($\text{CH}_2=\text{CHCH}_2$), 33.4 (CH_3CH), 31.1 (SCOCH_3), 29.1, 26.5, 19.3 (CH_3CH). HRMS (ESI $^+$): Exact mass calculated for $\text{C}_{11}\text{H}_{21}\text{OS}^+$ [$\text{M}+\text{H}$] $^+$: 201.1313, found: 201.1308. $[\alpha]_{\text{D}}^{20} = -8.6^\circ$ ($c = 0.0067$, CHCl_3).

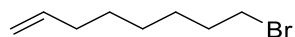
(R)-2-Methyloct-7-ene-1-thiol (2.75)



(R)-S-(2-Methyloct-7-en-1-yl)ethanethioate (1.42 g, 7.10 mmol) was dissolved in dry diethyl ether (59 mL) and cooled to 0 °C. Lithium aluminium hydride (1.0 M in Et_2O , 14.2 mL, 14.2 mmol) was added slowly and the reaction was warmed to room temperature and monitored by TLC (9:1 pentane/diethyl ether). On completion, saturated ammonium chloride solution (59 mL) and hydrochloric acid (2 M, 59 mL) were added and the aqueous layer was extracted with diethyl ether (3 x 59 mL). The combined organic layers were washed with saturated sodium bicarbonate solution (2 x 59 mL), dried over sodium sulfate and the solvent removed under vacuum to give the crude product as a pale yellow liquid. The crude product was used without further purification (916 mg, 82%). IR $\nu_{\text{max}}/\text{cm}^{-1}$ 2926, 2855, 2361, 1456. ^1H NMR (500 MHz, CDCl_3) δ_{H} 5.80 (1H, ddt, $J = 17.0, 10.2, 6.7$ Hz, $\text{CH}_2=\text{CH}$), 5.00 (1H, ddt, $J = 17.0, 2.2, 1.5$ Hz, $\text{CH}_2=\text{CH}$), 4.94 (1H, ddt, $J = 10.2, 2.2, 1.2$ Hz, $\text{CH}_2=\text{CH}$), 2.52 (1H, ddd, $J = 13.5, 8.2, 5.4$ Hz, CH_2SH), 2.40 (1H, ddd, $J = 13.1, 8.2, 6.8$ Hz, CH_2SH), 2.01-2.09 (2H, m, $\text{CH}_2=\text{CHCH}_2$), 1.55-1.65 (1H, m, CH_3CH), 1.21-1.47 (5H, m, $\text{CH}_2\text{CHCH}_2\text{SH}$, CH_2), 1.13-1.20 (1H, m, $\text{CH}_2\text{CHCH}_2\text{SH}$), 0.96 (3H, d, $J = 6.8$ Hz, CH_3). ^{13}C NMR (126 MHz, CDCl_3) δ_{C} 139.1 ($\text{CH}_2=\text{CH}$), 114.5 ($\text{CH}_2=\text{CH}$), 36.1 ($\text{CH}_3\text{CHCH}_2\text{SH}$), 35.2 ($\text{CH}_2\text{CHCH}_2\text{SH}$), 33.9 ($\text{CH}_2=\text{CHCH}_2$), 31.7

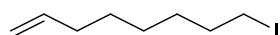
(CH₂SH), 29.2, 26.5, 18.8 (CH₃). HRMS (ESI⁻): Exact mass calculated for C₉H₁₇S⁻ [M-H]⁻: 157.1057, found: 157.1230. [α]_D²⁰ = -7.1° (c = 0.0024, CHCl₃).

8-Bromooct-1-ene (2.86)



A solution of triphenylphosphine (614 mg, 2.34 mmol) in dichloromethane (1.4 mL) was added at 0 °C to a mixture containing dichloromethane (4.40 mL), 7-octen-1-ol (200 mg, 1.56 mmol) and tetrabromomethane (621 mg, 1.87 mmol). The resulting solution was stirred at 0 °C and monitored by TLC (pentane/diethyl ether 9:1). On completion, the solvent was removed by vacuum to give the crude product. The crude product was purified by column chromatography over silica gel (pentane) to give the purified product as a colourless liquid (372 mg, 83%). ¹H NMR (500 MHz, CDCl₃) δ_H 5.80 (1H, ddt, *J* = 16.9, 10.1, 6.9 Hz, CH₂=CH), 5.00 (1H, ddt, *J* = 17.1, 2.2, 1.6 Hz, CH₂=CH), 4.94 (1H, ddt, *J* = 10.1, 2.2, 1.2 Hz, CH₂=CH), 3.41 (2H, t, *J* = 6.9 Hz, CH₂Br), 2.01-2.09 (2H, m, CH₂=CHCH₂), 1.81-1.90 (2H, m, CH₂CH₂Br), 1.24-1.47 (6H, m, CH₂). Data is in agreement with that reported in the literature.²⁵⁹

8-Iodoct-1-ene (2.87)



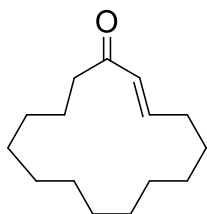
A flame-dried round-bottomed flask was charged with 7-octen-1-ol (300 mg, 2.34 mmol) and tetrahydrofuran (0.5 mL). The flask was cooled to 0 °C. Imidazole (239 mg, 3.51 mmol), triphenylphosphine (614 mg, 2.34 mmol) and iodine (891 mg, 3.51 mmol) were added sequentially and the reaction was monitored by TLC (4:1 petroleum ether/ethyl acetate). On completion, the reaction was quenched with saturated sodium thiosulfate solution. The organic layer was separated, and the aqueous layer was washed three times with diethyl ether. The combined organic layers were dried with sodium sulfate and concentrated under reduced pressure to give the crude product. The crude product was purified by column chromatography over silica gel (0-5% petroleum ether/ethyl acetate) to give the purified product as a colourless liquid (383 mg, 69% yield). ¹H NMR (500 MHz, CDCl₃) δ_H 5.80 (1H, ddt, *J* = 17.0, 10.2, 6.7 Hz, CH₂=CH), 5.00 (1H, dq, *J* = 17.0, 1.8 Hz, CH₂=CH), 4.94 (1H, ddt, *J* = 10.2, 2.4, 1.8 Hz, CH₂=CH), 3.19 (2H, t, *J* = 7.0 Hz, CH₂I), 2.01-2.09 (2H, m, CH₂=CHCH₂), 1.83

(2H, p, $J = 7.0$ Hz, CH_2CH_2), 1.36-1.44 (4H, m, CH_2), 1.30-1.36 (2H, m, CH_2). Data is in agreement with that reported in the literature.²⁶⁰

Cyclopentadec-2-en-1-one

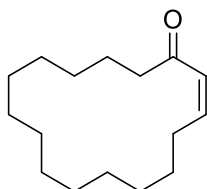
To a solution of cyclopentadecanone (200 mg, 0.891 mmol) in ethyl acetate (8 mL) was added phenylselenenyl chloride (207 mg, 1.08 mmol) and the resulting red-orange solution was stirred until it turned pale yellow. Water (15 mL) was added to the stirred reaction mixture. After the aqueous phase had been drawn off, THF (55 mL) was added and 30% hydrogen peroxide (0.220 mL) was added dropwise. Stirring was continued for 4 hours. The reaction mixture was washed with water and saturated sodium carbonate solution, dried and concentrated to give the crude product as a mixture of (E) and (Z) isomers. The crude product was purified by column chromatography over silica gel to give the separated (E) and (Z) isomers (145.5 mg, 73.4% yield, 78:22 ratio, (E) major).

(E)-Cyclopentadec-2-en-1-one (2.58a)



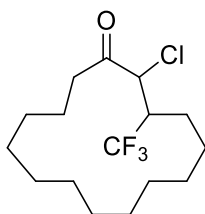
^1H NMR (500 MHz, CDCl_3) δ_{H} 6.82 (1H, dt, $J = 15.7, 7.4$ Hz, $\text{CH}=\text{CHCO}$), 6.19 (1H, dt, $J = 15.7, 1.4$ Hz, $\text{CH}=\text{CHCO}$), 2.50 (2H, t, $J = 6.6$ Hz, CH_2CO), 2.23-2.31 (2H, m, $\text{CH}_2\text{CH}=\text{CHCO}$), 1.63-1.73 (2H, m, $\text{CH}_2\text{CH}_2\text{CO}$), 1.49-1.58 (2H, m, $\text{CH}_2\text{CH}_2\text{CH}=\text{CH}$), 1.16-1.38 (16H, m, CH_2). Data is in agreement with that reported in the literature.²⁶¹

(Z)-Cyclopentadec-2-en-1-one (2.58b)



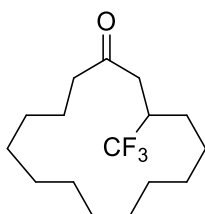
^1H NMR (500 MHz, CDCl_3) δ_{H} 6.71 (1H, dt, $J = 16.0, 7.1$ Hz, $\text{CH}=\text{CHCO}$), 6.28 (1H, dt, $J = 16.0, 1.4$ Hz, $\text{CH}=\text{CHCO}$), 2.26-2.34 (2H, m, CH_2CO), 1.48-1.61 (2H, m, $\text{CH}_2\text{CH}_2\text{CH}=\text{CH}$), 1.25-1.40 (16H, m, CH_2). Data is in agreement with that reported in the literature.²⁶²

2-Chloro-3-(trifluoromethyl)cyclopentadecan-1-one (2.59)



To a flame-dried round-bottomed flask in an argon atmosphere, (*E*)-cyclopentadec-2-en-1-one (100 mg, 0.450 mmol), Cu(dap)₂Cl (19.9 mg, 0.5 mol%) and dipotassium phosphate (15.7 mg, 20 mol%) were added. Dichloromethane (2 mL) and trifluoromethanesulfonyl chloride (95.7 μL, 0.899 mmol) were then added in subsequence. The reaction was then stirred while being irradiated with a fluorescent light bulb. On completion, the dichloromethane was removed under vacuum to give the crude product. The crude product was purified using column chromatography over silica gel (0-25% hexane/ethyl acetate) to give the purified product as a colourless liquid (80.4 mg, 55% yield). IR $\nu_{\max}/\text{cm}^{-1}$ 2931 (C-H), 1734 (C=O), 1717 (C=O), 1157 (C-F), 1120 (C-F), 1036 (C-F). ¹H NMR (500 MHz, CDCl₃) δ_{H} 4.34 (1H, d, *J* = 7.9 Hz, CHCl), 2.94-3.07 (1H, m, CHCF₃), 2.58-2.79 (2H, m, CH₂CO), 1.75-1.88 (1H, m, CH₂CHCF₃), 1.57-1.69 (3H, m, CH₂CHCF₃, CH₂CH₂CO), 1.19-1.54 (m, CH₂). ¹³C NMR (126 MHz, CDCl₃) δ_{C} 202.2 (C=O), 125.2 (CF₃), 58.5 (CCl), 44.6 (q, *J* = 25.8 Hz, CCF₃), 38.8 (CH₂CO), 27.3, 26.8, 26.5, 26.3, 26.3, 26.2, 26.2, 26.0, 25.9, 25.1, 22.5 (CH₂CCF₃). ¹⁹F NMR (470 MHz, CDCl₃) δ_{F} -69.3 (3F, d, *J* = 9.1 Hz, CF₃, 14%), -65.5 (3F, d, *J* = 8.6 Hz, CF₃, 75%), -63.3 (3F, d, *J* = 8.8 Hz, CF₃, 1%), -63.1 (3F, d, *J* = 7.8 Hz, CF₃, 9%). HRMS (ESI⁺): Exact mass calculated for C₁₆H₂₆O³⁵ClF₃Na⁺ [M+Na]⁺: 349.1522, found: 349.1512.

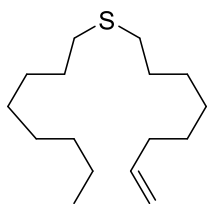
3-(Trifluoromethyl)cyclopentadecan-1-one (2.40)



A mixture of zinc metal (192 mg, 2.94 mmol) and 2-chloro-3-(trifluoromethyl)cyclopentadecan-1-one (80 mg, 0.245 mmol) in acetic acid (1.3 mL) was stirred at room temperature in an argon atmosphere at room temperature for three hours. The solution was filtered and diethyl ether (10 mL) was added. The resulting solution was

washed with water and brine, dried over sodium sulfate and the solvent was removed under vacuum to give the crude product. The crude product was purified by column chromatography over silica gel to give the purified product as a colourless liquid (43.5 mg, 61% yield). ^1H NMR (500 MHz, CDCl_3) δ_{H} 2.83-2.95 (1H, m, CHCF_3), 2.55-2.68 (2H, m, CH_2CO), 2.50-2.55 (1H, m, $\text{CF}_3\text{CHCH}_2\text{CO}$), 2.41 (1H, dd, $J = 7.4, 4.7$ Hz, $\text{CF}_3\text{CHCH}_2\text{CO}$), 1.81-1.90 (1H, m, $\text{CH}_2\text{C}(\text{CF}_3)\text{CH}_2\text{CO}$), 1.64-1.75 (2H, m, $\text{CH}_2\text{CH}_2\text{CO}$), 1.46-1.54 (1H, m, $\text{CH}_2\text{C}(\text{CF}_3)\text{CH}_2\text{CO}$), 1.17-1.43 (18H, m, CH_2). ^{13}C NMR (126 MHz, CDCl_3) δ_{C} 207.6 (C=O), 129.5 (t, $J = 279.4$ Hz, CF_3), 42.1 (CHCH_2CO), 41.5 ($\text{CH}_2\text{CH}_2\text{CO}$), 37.5 (q, $J = 26.0$ Hz, CF_3CH), 28.4 ($\text{CH}_2\text{CH}_2\text{CO}$), 27.6, 27.4, 26.9, 26.6, 26.5, 26.5, 26.3, 25.9, 22.9 ($\text{CH}_2\text{C}(\text{CF}_3)\text{CH}_2\text{CO}$). ^{19}F NMR (470 MHz, CDCl_3) δ_{F} -71.6 (3F, d, $J = 9.7$ Hz, CF_3). HRMS (ESI $^+$): Exact mass calculated for $\text{C}_{16}\text{H}_{27}\text{OF}_3\text{Na}^+$ [M+Na] $^+$: 315.1912, found: 315.1911.

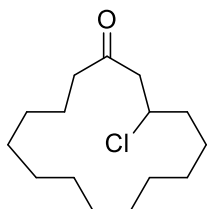
Oct-7-en-1-yl(octyl)sulfane (2.89)



In a flame-dried round-bottomed flask under argon, 1-octanethiol (0.119 mL, 0.684 mmol) was dissolved in dry tetrahydrofuran (8 mL) and cooled to 0 °C. Sodium hydride (60% dispersion in mineral oil, 30.1 mg, 1.25 mmol) was added portionwise and the mixture was stirred for 15 minutes. Oct-7-en-1-yl methanesulfonate (138 mg, 0.718 mmol) was then added and the reaction was heated to reflux and monitored by TLC (petroleum ether). On completion, the reaction mixture was cooled to room temperature and diluted with water (16 mL). The aqueous phase was extracted with ethyl acetate (3 x 16 mL). The combined organic layers were washed with 10% sodium hydroxide solution and brine, dried over sodium sulfate and concentrated under vacuum to give the crude product. The crude product was purified by column chromatography over silica gel (petroleum ether) to give the purified product as a yellow liquid (64.0 mg, 36% yield). ^1H NMR (500 MHz, CDCl_3) δ_{H} 5.80 (1H, ddt, $J = 16.9, 10.2, 6.7$ Hz, $\text{CH}_2=\text{CH}$), 4.99 (1H, dq, $J = 17.2, 1.7$ Hz, $\text{CH}_2=\text{CH}$), 4.93 (1H, ddt, $J = 10.2, 2.3, 1.2$ Hz, $\text{CH}_2=\text{CH}$), 2.50 (4H, ddd, $J = 7.6, 6.8, 1.0$ Hz, CH_2S), 2.00-2.09 (2H, m, $\text{CH}_2=\text{CHCH}_2$), 1.52-1.62 (4H, m, $\text{CH}_2\text{CH}_2\text{S}$), 1.21-1.43 (16H, m, CH_2), 0.81-0.91 (3H, m, CH_3). ^{13}C NMR (126 MHz, CDCl_3) δ_{C} 139.2 ($\text{CH}_2=\text{CH}$), 114.4 ($\text{CH}_2=\text{CH}$), 33.9 ($\text{CH}_2=\text{CHCH}_2$), 32.4

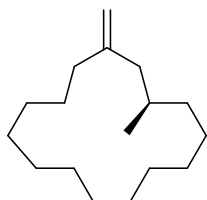
(CH₂S), 32.4 (CH₂S), 32.0, 29.9 (CH₂CH₂S), 29.9 (CH₂CH₂S), 29.4, 29.4, 29.1, 29.0, 28.9, 28.9, 22.8 (CH₂CH₃), 14.2 (CH₃). HRMS (ESI⁺): Exact mass calculated for C₁₆H₃₃S⁺ [M+H]⁺: 257.2303, found: 257.2300.

3-Chlorocyclopentadecan-1-one (2.60)



Hydrochloric acid (4.0 M, in dioxane, 1.0 mL, 4.00 mmol) was added to (*E*)-cyclopentadec-2-en-1-one (200 mg, 0.900 mmol) and the reaction was stirred at room temperature and monitored by TLC (10% pentane/diethyl ether). After three hours, the solvent was removed under vacuum to give the crude product. The crude product was purified by column chromatography over silica gel (0-5% pentane/diethyl ether) to give the purified product as a yellow liquid (133.1 mg, 57% yield). ¹H NMR (500 MHz, CDCl₃) δ_H 4.42-4.48 (1H, m, CHCl), 3.02 (1H, dd, *J* = 16.6, 9.2 Hz, CHClCH₂CO), 2.86 (1H, dd, *J* = 16.6, 4.8 Hz, CHClCH₂CO), 2.50 (1H, ddd, *J* = 15.9, 8.4, 4.8 Hz, CH₂CH₂CO), 2.34-2.42 (1H, m, CH₂CH₂CO), 1.71-1.86 (3H, m, CH₂CHClCH₂CO, CH₂CH₂CO), 1.51-1.60 (1H, m, CH₂CH₂CO), 1.14-1.48 (18H, m, CH₂). ¹³C NMR (126 MHz, CDCl₃) δ_C 208.4 (C=O), 56.7 (CHCl), 51.1 (CHClCH₂CO), 42.4 (CH₂CH₂CO), 36.9 (CH₂CHClCH₂CO), 27.8, 26.9, 26.8, 26.6, 26.6, 26.6, 26.3, 26.1, 23.8, 23.2 (CH₂CH₂CO). HRMS (ESI⁺): Exact mass calculated for C₁₅H₂₇O³⁵ClNa⁺ [M+Na]⁺: 281.1648, found: 281.1646.

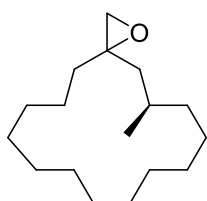
(*R*)-1-Methyl-3-methylenecyclopentadecane (2.64)



To a round-bottomed flask in argon was added methyltriphenylphosphonium bromide (359.6 mg, 1.01 mmol), potassium tert-butoxide (113.0 mg, 1.01 mmol) and diethyl ether (3 mL). The mixture was cooled to 0 °C. (*R*)-Muscone (0.217 mL, 0.839 mmol) was added dropwise to the mixture. The flask was warmed to room temperature and the reaction was monitored by TLC (4:1 petroleum ether/ethyl acetate). After six hours the mixture was

diluted with pentane (6 mL) and the mixture was filtered through alumina. The filtrate was concentrated under vacuum to give the crude product. The crude product was purified by column chromatography over silica gel (0-10% petroleum ether/ethyl acetate) to give the purified product as a colourless liquid (73.8 mg, 37% yield). ^1H NMR (500 MHz, CDCl_3) δ_{H} 4.73-4.75 (1H, m, $\text{CH}_2=\text{C}$), 4.67-4.70 (1H, m, $\text{CH}_2=\text{C}$), 2.09 (1H, ddd, $J = 13.5, 6.0, 1.2$ Hz, CHCH_2C), 1.99-2.03 (1H, m, $\text{CH}_2\text{CH}_2\text{C}$), 1.96 (1H, ddd, $J = 14.5, 9.3, 5.1$ Hz, $\text{CH}_2\text{CH}_2\text{C}$), 1.75 (1H, ddd, $J = 13.6, 7.9, 1.0$ Hz, CHCH_2C), 1.62 (1H, ddd, $J = 13.6, 7.7, 6.3$ Hz, CHCH_3), 1.46-1.53 (1H, m, $\text{CH}_2\text{CH}_2\text{CO}$), 1.19-1.44 (20H, m, CH_2 , $\text{CH}_2\text{CH}(\text{CH}_3)\text{CH}_2\text{CO}$, $\text{CH}_2\text{CH}_2\text{CO}$), 1.08-1.14 (1H, m, $\text{CH}_2\text{CH}(\text{CH}_3)\text{CH}_2\text{CO}$), 0.84 (3H, d, $J = 6.3$ Hz, CH_3). ^{13}C NMR (126 MHz, CDCl_3) δ_{C} 149.4 ($\text{CH}_2=\text{C}$), 110.9 ($\text{CH}_2=\text{C}$), 44.3 (CHCH_2C), 35.5 ($\text{CH}_2\text{CH}(\text{CH}_3)\text{CH}_2\text{CO}$), 35.2 ($\text{CH}_2\text{CH}_2\text{C}$), 29.5 (CHCH_3), 27.7, 27.2, 27.0, 26.9, 26.8, 26.8 (3C), 26.6, 20.4 (CH_3).

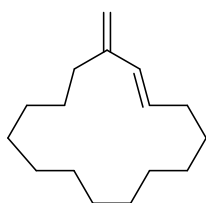
(5R)-5-Methyl-1-oxaspiro[2.14]heptadecane (2.65)



Meta-chloroperbenzoic acid (39.4 mg, 0.228 mmol) was added slowly to a stirring solution of (*R*)-1-methyl-3-methylenecyclopentadecane (45 mg, 0.190 mmol) in dichloromethane (0.5 mL) at 0 °C. The resulting solution was stirred at room temperature and monitored by TLC (9:1 petroleum ether/diethyl ether). After five hours, saturated sodium thiosulfate solution was added and the reaction mixture was stirred for an additional hour before filtering through celite. The aqueous phase was extracted with dichloromethane (3 x 1 mL). The combined organic layers were washed with saturated sodium bicarbonate solution (3 x 1 mL), dried with magnesium sulfate and concentrated under vacuum to give the crude product. The crude product was purified by column chromatography over silica gel (0-5% pentane/diethyl ether) to give the purified product as a mixture of diastereomers as a colourless oil (26.6 mg, 55%). ^1H NMR (500 MHz, CDCl_3) δ_{H} 2.60 (2H, dd, $J = 6.4, 5.7$ Hz, CH_2O (major)), 2.54 (1H, d, $J = 4.9$ Hz, CH_2O (minor)), 2.46 (1H, dd, $J = 4.9, 1.4$ Hz, CH_2O (minor)), 2.09 (1H, dd, $J = 14.0, 4.5$ Hz, CHCH_2CO), 1.87-1.94 (1H, m, $\text{CH}_2\text{CH}_2\text{CO}$), 1.84 (1H, t, $J = 5.5$ Hz, CHCH_2CO (minor)), 1.71-1.79 (1H, m, CH_3CH (minor)), 1.60-1.70 (1H, m, CH_3CH (major)), 1.23-1.53 (2H, m, CH_2), 1.12-1.23 (1H, m, $\text{CH}_2\text{CH}_2\text{CO}$), 1.07 (1H, dd, $J = 14.0, 8.5$ Hz, CHCH_2CO

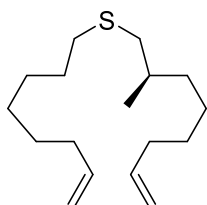
(minor)), 0.96 (3H, d, $J = 6.5$ Hz, CH_3 (minor)), 0.90 (3H, d, $J = 6.6$ Hz, CH_3 (major)), 0.79 (1H, dd, $J = 14.0, 9.9$ Hz, CHCH_2CO (major)). ^{13}C NMR (126 MHz, CDCl_3) δ_{C} 59.1 (CO), 54.8 (CH_2O (major)), 53.0 (CH_2O (minor)), 41.7 (CHCH_2CO (minor)), 41.4 (CHCH_2CO (major)), 36.3 ($\text{CH}_2\text{CHCH}_2\text{CO}$ (major)), 35.8 ($\text{CH}_2\text{CHCH}_2\text{CO}$ (minor)), 33.9 ($\text{CH}_2\text{CH}_2\text{CO}$ minor), 33.8 ($\text{CH}_2\text{CH}_2\text{CO}$ (major)), 28.7 (CH_3CH (major)), 28.3 (CH_3CH (minor)), 27.7 (major), 27.6 (minor), 27.2, 27.0, 26.9, 26.9, 26.8, 26.7, 26.6, 26.6, 26.4, 25.3, 25.1, 24.0, 23.0, 20.8 (CH_3 (minor)), 20.4 (CH_3 (major)). HRMS (ESI⁺): Exact mass calculated for $\text{C}_{17}\text{H}_{33}\text{O}^+$ [M+H]⁺: 253.2531, found: 253.2526.

(E)-3-Methylenecyclopentadec-1-ene (2.66)



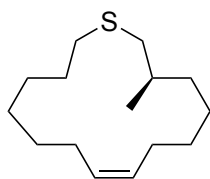
To a round-bottomed flask in argon was added methyltriphenylphosphonium bromide (385.5 mg, 1.08 mmol), potassium *tert*-butoxide (121.1 mg, 1.08 mmol) and diethyl ether (3 mL). The mixture was cooled to 0 °C. (E)-Cyclopentadec-2-en-1-one (200 mg, 0.899 mmol) in diethyl ether (1 mL) was then added to the mixture. The flask was warmed to room temperature and the reaction was monitored by TLC (4:1 petroleum ether/ethyl acetate). After six hours the mixture was diluted with pentane (8 mL) and the mixture was filtered through alumina. The filtrate was concentrated under vacuum to give the crude product. The crude product was purified by column chromatography over silica gel (0-10% petroleum ether/ethyl acetate) to give the purified product as a colourless oil (49.1 mg, 25% yield). IR $\nu_{\text{max}}/\text{cm}^{-1}$ 2924 (C-H), 2358, 1716 (C=C), 1701 (C=C), 1066, 1059. ^1H NMR (500 MHz, CDCl_3) δ_{H} 6.03 (1H, d, $J = 15.8$ Hz, $\text{CH}=\text{CHC}$), 5.71 (1H, dt, $J = 15.1, 7.2$ Hz, $\text{CH}=\text{CHC}$), 4.87 (1H, s, $\text{CH}_2=\text{C}$), 4.81 (1H, s, $\text{CH}_2=\text{C}$), 2.23 (2H, t, $J = 7.2$ Hz, CH_2CO), 2.16 (2H, q, $J = 6.6$ Hz, $\text{CH}_2\text{CH}=\text{CH}$), 1.40-1.52 (4H, m, $\text{CH}_2\text{CH}_2\text{CH}=\text{CH}$, $\text{CH}_2\text{CH}_2\text{CO}$), 1.25-1.41 (14H, m, CH_2), 1.22 (2H, q, $J = 7.3$ Hz, CH_2). ^{13}C NMR (126 MHz, CDCl_3) δ_{C} 150.0 ($\text{CH}_2=\text{C}$), 132.3 ($\text{CH}=\text{CHC}$), 131.2 ($\text{CH}=\text{CHC}$), 113.5 ($\text{CH}_2=\text{C}$), 33.2 (CH_2CO), 32.0 ($\text{CH}_2\text{CH}=\text{CH}$), 28.5 ($\text{CH}_2\text{CH}_2\text{CO}$), 28.1 ($\text{CH}_2\text{CH}_2\text{CH}=\text{CH}$), 27.3, 27.2, 27.1, 27.0, 26.8, 26.6, 26.6, 25.4. HRMS (ESI⁺): Exact mass calculated for $\text{C}_{18}\text{H}_{29}^+$ [M+H]⁺: 221.2269, found: 221.2261.

(R)-(2-Methyloct-7-en-1-yl)(oct-7-en-1-yl)sulfane (2.76)



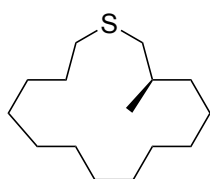
In a flame-dried round-bottomed flask under argon, (*R*)-2-methyloct-7-ene-1-thiol (100 mg, 0.632 mmol) was dissolved in dry tetrahydrofuran (8 mL) and cooled to 0 °C. Sodium hydride (60% dispersion in mineral oil, 27.8 mg, 1.16 mmol) was added portionwise and the mixture was stirred for 15 minutes. Oct-7-en-1-yl methanesulfonate (136.8 mg, 0.663 mmol) was then added and the reaction was heated to reflux and monitored by TLC (petroleum ether). On completion, the reaction mixture was cooled to room temperature and diluted with water (16 mL). The aqueous phase was extracted with ethyl acetate (3 x 16 mL). The combined organic layers were washed with 10% sodium hydroxide solution and brine, dried over sodium sulfate and concentrated under vacuum to give the crude product. The crude product was purified by column chromatography over silica gel (petroleum ether) to give the purified product as a yellow oil (109 mg, 64% yield). IR $\nu_{\text{max}}/\text{cm}^{-1}$ 2974 (C-H), 2922 (C-H), 1786, 1697, 1327 (S=O), 1211 (S=O), 1200 (S=O), 1065 (S=O), 758, 702. ^1H NMR (500 MHz, CDCl_3) δ_{H} 5.76-5.85 (2H, m, $\text{CH}_2=\text{CH}$), 4.99 (2H, ddt, $J = 17.1, 3.7, 1.5$ Hz, $\text{CH}_2=\text{CH}$), 4.93 (2H, ddq, $J = 10.2, 2.1, 1.1$ Hz, $\text{CH}_2=\text{CH}$), 2.49 (1H, dd, $J = 12.5, 5.8$ Hz, SCH_2CH), 2.48 (2H, t, $J = 7.5$ Hz, $\text{CH}_2\text{CH}_2\text{S}$), 2.34 (1H, dd, $J = 12.5, 7.5$ Hz, SCH_2CH), 2.01-2.08 (4H, m, $\text{CH}_2=\text{CHCH}_2$), 1.60-1.68 (1H, m, CHCH_3), 1.54-1.59 (2H, m, $\text{CH}_2\text{CH}_2\text{S}$), 1.23-1.50 (11H, m, $\text{CH}_2, \text{CH}_2\text{CH}(\text{CH}_3)$), 1.13-1.21 (1H, m, $\text{CH}_2\text{CH}(\text{CH}_3)$), 0.97 (3H, d, $J = 6.6$ Hz, CH_3). ^{13}C NMR (126 MHz, CDCl_3) δ_{C} 139.2 (2C, $\text{CH}_2=\text{CH}$), 114.4 (2C, $\text{CH}_2=\text{CH}$), 40.1 (SCH_2CH), 36.2 ($\text{CH}_2\text{CH}(\text{CH}_3)$), 33.9 ($\text{CH}_2=\text{CHCH}_2$), 33.9 ($\text{CH}_2=\text{CHCH}_2$), 33.5 (CH_3CH), 33.0 ($\text{CH}_2\text{CH}_2\text{S}$), 29.9 ($\text{CH}_2\text{CH}_2\text{SH}$), 29.2, 28.9, 28.9, 28.7, 26.6, 19.6 (CH_3). HRMS (ESI⁺): Exact mass calculated for $\text{C}_{17}\text{H}_{33}\text{S}^+$ [$\text{M}+\text{H}$]⁺: 269.2303, found: 269.2298. $[\alpha]_{\text{D}}^{20} = -18.9^\circ$ ($c = 0.0053, \text{CHCl}_3$).

(R,Z)-3-Methylthiacyclopentadec-8-ene (2.77)



In a foil-covered round-bottomed flask, Hoveyda-Grubbs second generation catalyst (23.6 mg, 10 mol%) was added to a solution of (*R*)-(2-methyloct-7-en-1-yl)(oct-7-en-1-yl)sulfane (100 mg, 0.376 mmol) in toluene (150 mL). The reaction was heated to 70 °C and stirred for 24 hours. The reaction was cooled to room temperature and the solvent was removed to give the crude product. The crude product was purified by column chromatography over silica gel (petroleum ether) to give the purified product as a yellow oil (61.5 mg, 68%). IR $\nu_{\max}/\text{cm}^{-1}$ 2924 (C-H), 2853 (C-H), 1456 (C-H), 1067, 966. 908. ^1H NMR (500 MHz, CDCl_3) δ_{H} 5.31-5.44 (2H, m, HC=CH), 2.40-2.54 (3H, m, SCH_2CH , $\text{CH}_2\text{CH}_2\text{S}$), 2.30-2.38 (1H, m, SCH_2CH), 1.92-2.10 (4H, m, $\text{CH}_2\text{CH}=\text{CH}$), 1.53-1.70 (3H, m, $\text{CH}_2\text{CH}_2\text{S}$, CHCH_3), 1.23-1.48 (11H, m, CH_2), 1.12-1.21 (1H, m, $\text{CH}_2\text{CH}(\text{CH}_3)$), 0.95-1.00 (3H, m, CH_3). ^{13}C NMR (126 MHz, CDCl_3) δ_{C} 131.4 (C=C), 131.3 (C=C), 40.0 (SCH_2CH), 36.0 ($\text{CH}_2\text{CH}(\text{CH}_3)$), 35.7, 35.5, 33.5 (CHCH_3), 32.6 ($\text{CH}_2\text{CH}_2\text{S}$), 32.5 ($\text{CH}_2\text{CH}=\text{CH}$), 32.2 ($\text{CH}_2\text{CH}=\text{CH}$), 29.6 ($\text{CH}_2\text{CH}_2\text{SH}$), 28.5, 27.5, 27.2, 19.6 (CH_3). HRMS (EI): Exact mass calculated for $\text{C}_{15}\text{H}_{28}\text{S}$: 240.1906, found: 240.1911. $[\alpha]_{\text{D}}^{20} = -7.1^\circ$ ($c = 0.0084$, CHCl_3).

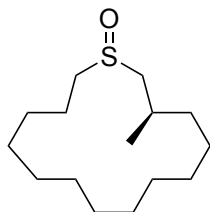
(R)-3-Methylthiacyclopentadecane (2.78)



10% Palladium on carbon (25.0 mg) was added to a solution of (*R,Z*)-3-methylthiacyclopentadec-8-ene (25.0 mg, 0.104 mmol) in DCM in a sealed autoclave filled with hydrogen (50 bar). The reaction was stirred under pressure for 18 hours. The autoclave was then depressurised, and the solution filtered to remove the palladium on carbon. The filtrate was concentrated under reduced pressure to give the crude product. The crude was purified by column chromatography over silica gel (hexane) to give the purified product as a colourless oil (10.0 mg, 0.0412 mmol). ^1H NMR (400 MHz, CDCl_3) δ_{H} 2.42-2.56 (3H, m, CH_2S , CHCH_2S), 2.29-2.41 (1H, m, CHCH_2S), 1.52-1.68 (5H, m, $\text{CH}_2\text{CH}_2\text{S}$, CHCH_2S , CH_2CHCH_3), 1.21-

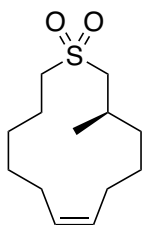
1.44 (18H, m, CH₂), 0.97 (3H, d, *J* = 6.6 Hz, CH₃). HRMS (ESI⁺): Exact mass calculated for C₁₅H₃₁S⁺ [M+H]⁺: 242.2068, found: 242.2016.

(3R)-3-Methylthiacyclopentadecane 1-oxide (2.41)



Meta-perchlorobenzoic acid (77%, 9.71 mg, 0.0433 mmol) was added to a solution of (*R*)-3-methylthiacyclopentadecane (10.0 mg, 0.0412 mmol) in DCM (0.5 mL) at 0 °C and the reaction was stirred for 30 minutes. The reaction was then warmed to room temperature and stirred for 18 hours. The reaction was quenched with saturated sodium bicarbonate solution and the aqueous layer was extracted three times with DCM. The combined organic layers were washed with brine, dried over sodium sulfate and concentrated under reduced pressure to give the product as a white solid (7.3 mg, 69%). m.p. 51-53 °C. IR ν_{max} /cm⁻¹ 2943 (C-H), 2866 (C-H), 1709, 1487 (C-H), 1271, 1217 (S=O), 895, 793. ¹H NMR (500 MHz, CDCl₃) δ_{H} 2.90-2.97 (3H, m, CH₂S), 2.73-2.80 (1H, m, CH₂S), 2.18-2.25 (1H, m, CHCH₃), 1.70-1.87 (4H, m, CH₂CH₂S, CHCH₂S), 1.54-1.60 (1H, m, CH₂CHCH₃), 1.20-1.50 (19H, m, CH₂), 1.13 (3H, d, *J* = 6.7 Hz, CH₃). ¹³C NMR (126 MHz, CDCl₃) δ_{C} 58.9 (CH₂S), 54.3 (CH₂S), 37.1, 35.8, 32.0, 29.8, 29.7, 29.5, 29.4, 28.1 (CHCH₃), 26.6, 22.8, 22.7, 22.1, 20.2 (CH₃). HRMS (ESI⁺): Exact mass calculated for C₁₅H₃₁OS⁺ [M+H]⁺: 259.2096, found: 259.2088. [α]_D²⁰ = -15.0° (c = 0.002, CHCl₃).

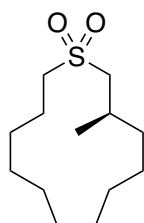
(*R,Z*)-3-Methylthiacyclotridec-7-ene 1,1-dioxide (2.93)



Meta-perchlorobenzoic acid (77%, 37.7 mg, 0.168 mmol) was added to a solution of (*R,Z*)-3-methylthiacyclopentadec-8-ene (20.2 mg, 0.0840 mmol) in DCM (0.5 mL) at 0 °C and the reaction was stirred for 30 minutes. The reaction was then warmed to room temperature

and stirred for 18 hours. The reaction was quenched with saturated sodium bicarbonate solution and the aqueous layer was extracted three times with DCM. The combined organic layers were washed with brine, dried over sodium sulfate and concentrated under reduced pressure to give the product as a white solid (11.1 mg, 49%). m.p. 62-64 °C. ^1H NMR (500 MHz, CDCl_3) δ_{H} 5.26-5.48 (2H, m, $\text{HC}=\text{CH}$), 2.84-3.21 (3H, m, $\text{CH}_2\text{CH}_2\text{SO}_2$, CHCH_2SO_2), 2.50-2.63 (1H, m, CHCH_2SO_2), 2.00-2.21 (4H, m), 1.86-1.99 (2H, m), 1.63-1.74 (1H, m), 1.13-1.49 (12H, m, CH_2), 1.17 (3H, d, $J = 6.7$ Hz, CH_3). ^{13}C NMR (126 MHz, CDCl_3) δ_{C} 131.5 (alkene CH), 131.3 (alkene CH), 57.7 (CHCH_2SO_2), 52.2 ($\text{CH}_2\text{CH}_2\text{SO}_2$), 36.7, 32.3, 31.9, 30.3 (CHCH_3), 28.7, 27.8, 27.2, 26.6, 26.4, 23.0, 22.4 (CH_3). HRMS (ESI^+): Exact mass calculated for $\text{C}_{15}\text{H}_{28}\text{O}_2\text{SNa}^+$ $[\text{M}+\text{Na}]^+$: 295.1702, found: 295.1692. $[\alpha]_{\text{D}}^{20} = -12.1^\circ$ ($c = 0.005$, CHCl_3).

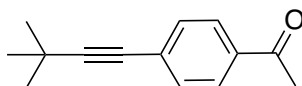
(R)-3-Methylthiacyclotridecane 1,1-dioxide (2.92)



Hydrogen gas was added to a solution of (*R,Z*)-3-Methylthiacyclotridec-7-ene 1,1-dioxide (11.1 mg, 0.0407 mmol) and palladium on carbon (10 wt. %, 2.04 mg) in methanol (0.2 mL) in an inert Ar atmosphere and the reaction was stirred for 18 h. On completion, the methanol was removed and the residue was re-dissolved in ethyl acetate. The solution was filtered through celite and the solvent was removed under reduced pressure to give the crude product. The crude was purified by column chromatography over silica gel (pentane/ethyl acetate 2:1) to give the product as a colourless oil (7.0 mg, 63%). ^1H NMR (500 MHz, CDCl_3) δ_{H} 3.00-3.14 (2H, m), 2.84-2.91 (1H, m, CH_2SO_2), 2.64-2.72 (1H, ddd, $J = 15.0, 8.0, 1.5$ Hz), 1.98-2.09 (1H, m), 1.71-1.94 (2H, m), 1.21-1.58 (20H, m, CH_2), 1.15 (3H, d, $J = 6.6$ Hz, CH_3). HRMS (ESI^+): Exact mass calculated for $\text{C}_{15}\text{H}_{30}\text{O}_2\text{SNa}^+$ $[\text{M}+\text{Na}]^+$: 297.1859, found: 297.1848. $[\alpha]_{\text{D}}^{20} = -11.3^\circ$ ($c = 0.004$, CHCl_3).

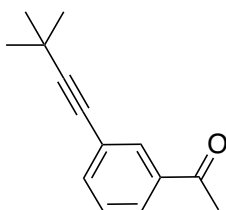
7.3 Chapter 3

1-(4-(3,3-Dimethylbut-1-yn-1-yl)phenyl)ethan-1-one (3.83)



Bis(triphenylphosphine)palladium(II)dichloride (15 mol%, 85.6 mg, 0.122 mmol) was added to a solution of 4'-iodoacetophenone (200 mg, 0.813 mmol), 3,3-dimethyl-1-butyne (0.120 mL, 0.975 mmol), copper (I) iodide (15 mol%, 23.2 mg, 0.122 mmol) in diisopropylamine (7 mL). The reaction mixture was heated to 80 °C and stirred for 24 h. The reaction was then cooled to room temperature and was passed through a pad of silica gel with an elution of ethyl acetate. The solvent was removed under reduced pressure to give the crude product. The crude was purified by column chromatography over silica gel (0-20% petroleum ether/ethyl acetate) to give the product as a red solid (110.7 mg, 68%). ¹H NMR (400 MHz, CDCl₃) δ_H 7.84-7.90 (2H, m, ArH), 7.43-7.48 (2H, m, ArH), 2.59 (3H, s, CH₃), 1.33 (9H, s, (CH₃)₃). Data is in agreement with that reported in the literature.²⁶³

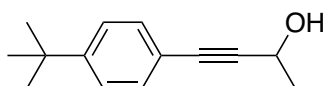
1-(3-(3,3-Dimethylbut-1-yn-1-yl)phenyl)ethan-1-one (3.84)



Bis(triphenylphosphine)palladium(II)dichloride (15 mol%, 85.6 mg, 0.122 mmol) was added to a solution of 3'-iodoacetophenone (200 mg, 0.813 mmol), 3,3-dimethyl-1-butyne (0.120 mL, 0.975 mmol), copper (I) iodide (15 mol%, 23.2 mg, 0.122 mmol) in diisopropylamine (7 mL). The reaction mixture was heated to 80 °C and stirred for 24 h. The reaction was then cooled to room temperature and was passed through a pad of silica gel with an elution of ethyl acetate. The solvent was removed under reduced pressure to give the crude product. The crude was purified by column chromatography over silica gel (0-20% petroleum ether/ethyl acetate) to give the purified product as an orange oil (102.6 mg, 63%). IR ν_{max}/cm⁻¹ 2963 (C-H), 2866 (C-H), 1686 (C=O), 1231, 681. ¹H NMR (500 MHz, CDCl₃) δ_H 7.96 (1H, td, *J* = 1.8, 0.6 Hz, CCHC), 7.84 (1H, ddd, *J* = 7.7, 1.8, 1.3 Hz, COCCCHC), 7.56 (1H, dt, *J* =

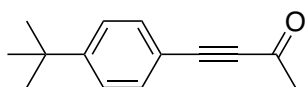
7.7, 1.3 Hz, CCHCH), 7.37 (1H, dt, $J = 7.7, 0.6$ Hz, COCCCHCH), 2.60 (3H, s, CH₃), 1.33 (9H, s, (CH₃)₃). ¹³C NMR (126 MHz, CDCl₃) δ_c 197.8 (C=O), 137.1 (COC), 136.1 (CCHCH), 131.7 (CCHC), 128.6 (COCCCHCH), 127.2 (COCCCHCH), 124.8 ((CH₃)₃CCCC), 99.9 ((CH₃)₃CC), 78.3 ((CH₃)₃CCC), 31.1 ((CH₃)₃), 26.8 (CH₃). HRMS (ESI⁺): Exact mass calculated for C₁₄H₁₇O⁺ [M+H]⁺: 201.1279, found: 201.1270.

4-(4-(*Tert*-butyl)phenyl)but-3-yn-2-ol (3.92)



Bis(triphenylphosphine)palladium(II)dichloride (15 mol%, 81.0 mg, 0.115 mmol) was added to a solution of 1-*tert*-butyl-4-iodobenzene (0.136 mL, 0.769 mmol), 3-butyn-2-ol (72.3 μ L, 0.923 mmol), copper (I) iodide (15 mol%, 21.9 mg, 0.115 mmol) in diisopropylamine (7 mL). The reaction mixture was heated to 80 °C and stirred for 24 h. The reaction was then cooled to room temperature and was passed through a pad of silica gel with an elution of ethyl acetate. The solvent was removed under reduced pressure to give the crude product. The crude was purified by column chromatography over silica gel (0-20% petroleum ether/ethyl acetate) to give the purified product as a pale yellow oil (101.1 mg, 65%). ¹H NMR (500 MHz, CDCl₃) δ_H 7.30-7.39 (4H, m, ArH), 4.76 (1H, q, $J = 6.6$ Hz, CHOH), 1.55 (3H, d, $J = 6.6$ Hz, CH₃), 1.30 (9H, s, (CH₃)₃). Data is in agreement with that reported in the literature.²⁶⁴

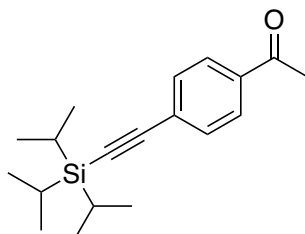
4-(4-(*Tert*-butyl)phenyl)but-3-yn-2-one (3.88)



Dess-Martin periodinane (115.3 mg, 0.272 mmol) was added to a solution of 4-(4-(*tert*-butyl)phenyl)but-3-yn-2-ol (50.0 mg, 0.247 mmol) in DCM (1.24 mL) and the reaction was allowed to warm to room temperature and stirred for 3 hours. On completion, the reaction was quenched by addition of 1 M sodium hydroxide solution. The layers were separated and the aqueous layer was extracted three times with DCM. The combined organic layers were dried over sodium sulfate, filtered and concentrated under reduced pressure to give the crude product. The crude was purified by column chromatography over silica gel (20% ethyl acetate/petroleum ether) to give the purified product as a yellow solid (40.3 mg, 81%). ¹H

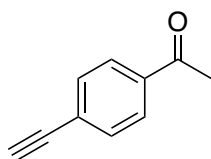
NMR (500 MHz, CDCl₃) δ_H 7.49-7.54 (2H, m, ArH), 7.37-7.43 (2H, m, ArH), 2.45 (3H, s, CH₃), 1.32 (9H, s, (CH₃)₃). Data is in agreement with that reported in the literature.²⁶⁵

1-(4-((Triisopropylsilyl)ethynyl)phenyl)ethan-1-one (3.101)



Bis(triphenylphosphine)palladium(II)dichloride (2 mol%, 28.5 mg, 0.0410 mmol) was added to a solution of 4'-iodoacetophenone (500 mg, 2.03 mmol), tri(isopropylsilyl)acetylene (0.729 mL, 3.25 mmol), copper (I) iodide (2 mol%, 28.5 mg, 0.0410 mmol) and triethylamine (5 mL) in THF (5 mL). The reaction mixture was heated to 80 °C and stirred for 24 h. The reaction was then cooled to room temperature and was passed through a pad of silica gel with an elution of ethyl acetate. The solvent was removed under reduced pressure to give the crude product. The crude was purified by column chromatography over silica gel (0-20% petroleum ether/ethyl acetate) to give the purified product as a colourless oil (500.2 mg, 82%). ¹H NMR (400 MHz, CDCl₃) δ_H 7.87-7.92 (2H, m, ArH), 7.52-7.57 (2H, m, ArH), 2.60 (3H, s, CH₃), 1.12-1.15 (21H, m, SiCH, SiCH(CH₃)₂). Data is in agreement with that reported in the literature.²⁶⁶

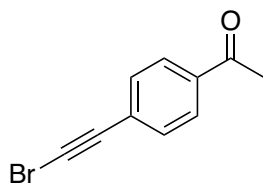
1-(4-Ethynylphenyl)ethan-1-one (3.102)



TBAF (1.0 M in THF, 0.429 mL, 0.429 mmol) was added to a solution of 1-(4-((triisopropylsilyl)ethynyl)phenyl)ethan-1-one (100 mg, 0.328 mmol) in THF (0.8 mL) at 0 °C and the reaction was stirred for 3 hours. The reaction was quenched with water and warmed to room temperature. The aqueous layer was extracted three times with DCM. The combined organic layers were dried over sodium sulfate, filtered and concentrated under vacuum to give the crude product. The crude product was purified by column chromatography over silica gel (0-20% petroleum ether/ethyl acetate) to give the purified

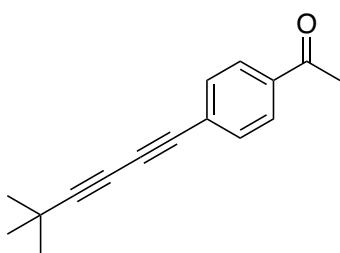
product as a white solid (28.8 mg, 61%). $^1\text{H NMR}$ (400 MHz, CDCl_3) δ_{H} 7.90-7.93 (2H, m, ArH), 7.56-7.59 (2H, m, ArH), 3.25 (1H, s, CH), 2.61 (3H, s, CH_3). Data is in agreement with that reported in the literature.²⁶⁷

1-(4-(Bromoethynyl)phenyl)ethan-1-one (3.103)



1-(4-Ethynylphenyl)ethan-1-one (93.5 mg, 0.649 mmol) was added to a solution of N-bromosuccinimide (112.2 mg, 0.778 mmol) and silver nitrate (11.0 mg, 10 mol%) in acetone (1 mL) and the solution was stirred at room temperature for 3 hours. On completion, the solvent was removed under reduced pressure. The resulting residue was dissolved in water (3 mL) and the aqueous layer was extracted with diethyl ether (3 x 3 mL). The combined organic layers were washed with brine (5 mL), dried over magnesium sulfate, filtered and concentrated under reduced pressure. The crude was purified by column chromatography over silica gel (20% ethyl acetate in petroleum ether) to give the purified product as a white solid (44.4 mg, 31%). $^1\text{H NMR}$ (400 MHz, CDCl_3) δ_{H} 7.88-7.92 (2H, m, ArH), 7.51-7.56 (2H, m, ArH), 2.60 (3H, s, CH_3). Data is in agreement with that reported in the literature.²⁶⁸

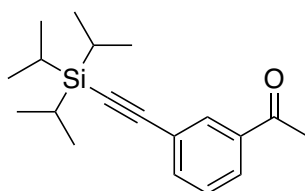
1-(4-(5,5-Dimethylhexa-1,3-diyn-1-yl)phenyl)ethan-1-one (3.95)



A 30% butylamine/water solution (0.5 mL) was added to an RBF containing copper(I) chloride (4.93 mg, 0.0498 mmol) at 0 °C. A pinch of hydroxylamine hydrochloride was added until the blue colour disappeared. A solution of 3,3-dimethyl-1-butyne (20.4 μL , 0.166 mmol) in DCM (0.1 mL) was added, quickly followed by a solution of 1-(4-(Bromoethynyl)phenyl)ethan-1-one (44.4 mg, 0.199 mmol) in DCM (0.1 mL). The reaction was warmed to room temperature and stirred for 3 hours. On completion, the aqueous

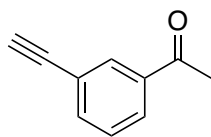
layer was extracted with DCM. The organic layer was dried over sodium sulfate, filtered and concentrated under vacuum to give the crude product. The crude was purified by column chromatography over silica gel (0 to 20% petroleum ether/ethyl acetate) to give the purified product as a yellow solid (25.3 mg, 53%). m.p. 173-175 °C. IR $\nu_{\text{max}}/\text{cm}^{-1}$ 2970 (C-H), 1670 (C=O), 1358, 1260, 1179, 833. ^1H NMR (500 MHz, CDCl_3) δ_{H} 7.87-7.90 (2H, m, CHCCO), 7.52-7.55 (2H, m, CHCHCCO), 2.59 (3H, s, CH_3), 1.29 (9H, s, $(\text{CH}_3)_3$). ^{13}C NMR (126 MHz, CDCl_3) δ_{C} 197.3 (C=O), 136.6 (CCO), 132.6, 128.3, 127.2 (CHCCCC), 94.3 ($\text{CC}(\text{CH}_3)_3$), 77.5 (alkyne C), 75.1 (CHCCCC), 63.7 (alkyne C), 30.6 ($(\text{CH}_3)_3$), 26.8 (CH_3). HRMS (ESI⁺): Exact mass calculated for $\text{C}_{16}\text{H}_{17}\text{O}^+$ [M+H]⁺: 225.1274, found: 225.1272.

1-(3-((Triisopropylsilyl)ethynyl)phenyl)ethan-1-one (3.105)



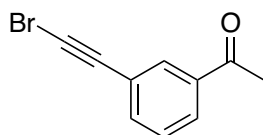
Bis(triphenylphosphine)palladium(II)dichloride (2 mol%, 28.5 mg, 0.0410 mmol) was added to a solution of 3'-iodoacetophenone (500 mg, 2.03 mmol), tri(isopropylsilyl)acetylene (0.729 mL, 3.25 mmol), copper (I) iodide (2 mol%, 28.5 mg, 0.0410 mmol) and triethylamine (5 mL) in THF (5 mL). The reaction mixture was heated to 80 °C and stirred for 24 h. The reaction was then cooled to room temperature and was passed through a pad of silica gel with an elution of ethyl acetate. The solvent was removed under reduced pressure to give the crude product. The crude was purified by column chromatography over silica gel (0-25% petroleum ether/ethyl acetate) to give the purified product as a colourless oil (274.6 mg, 42%). ^1H NMR (400 MHz, CDCl_3) δ_{H} 8.03 (1H, td, $J = 1.8, 0.5$ Hz, ArH), 7.89 (1H, ddd, $J = 7.8, 1.8, 1.3$ Hz, ArH), 7.66 (1H, dt, $J = 7.8, 1.3$ Hz, ArH), 7.41 (1H, td, $J = 7.8, 0.5$ Hz, ArH), 2.61 (3H, s, CH_3), 1.14 (21H, m, SiCH, SiCH(CH_3)₂). Data is in agreement with that reported in the literature.²⁶⁹

1-(3-Ethynylphenyl)ethan-1-one (3.106)



TBAF (1.0 M in THF, 0.844 mL, 0.844 mmol) was added to a solution of 1-(3-((triisopropylsilyl)ethynyl)phenyl)ethan-1-one (195.0 mg, 0.914 mmol) in THF (1.5 mL) at 0 °C and the reaction was stirred for 3 hours. The reaction was quenched with water and warmed to room temperature. The aqueous layer was extracted with DCM (3x). The combined organic layers were dried over sodium sulfate, filtered and concentrated under vacuum to give the crude product. The crude product was purified by column chromatography over silica gel (0-20% petroleum ether/ethyl acetate) to give the purified product as a white solid (64.8 mg, 69%). ¹H NMR (400 MHz, CDCl₃) δ_H 8.07 (1H, t, *J* = 1.7 Hz, ArH), 7.94 (1H, dt, *J* = 7.8, 1.4 Hz, ArH), 7.68 (1H, dt, *J* = 7.8, 1.4 Hz, ArH), 7.44 (1H, td, *J* = 7.8, 0.6 Hz, ArH), 3.14 (1H, s, CH), 2.61 (3H, s, CH₃). Data is in agreement with that reported in the literature.²⁷⁰

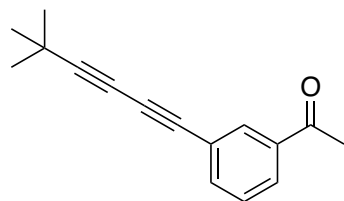
1-(3-(Bromoethynyl)phenyl)ethan-1-one (3.107)



1-(3-Ethynylphenyl)ethan-1-one (64.8 mg, 0.449 mmol) was added to a solution of N-bromosuccinimide (96.0 mg, 0.539 mmol) and silver nitrate (7.63 mg, 0.0449 mmol) in acetone (1 mL) and the solution was stirred at room temperature for 3 hours. On completion, the solvent was removed under reduced pressure. The resulting residue was dissolved in water (3 mL) and the aqueous layer was extracted with diethyl ether (3 x 3 mL). The combined organic layers were washed with brine (5 mL), dried over magnesium sulfate, filtered and concentrated under reduced pressure. The crude was purified by column chromatography over silica gel (20% ethyl acetate in petroleum ether) to give the purified product as a white solid (66.6 mg, 66%). m.p. 61-63 °C. IR ν_{max}/cm⁻¹ 2913 (C-H), 1660 (C=O), 1445, 1380, 1302, 805. ¹H NMR (500 MHz, CDCl₃) δ_H 8.03 (1H, t, *J* = 1.8 Hz, BrCCCCHCO), 7.93 (1H, dt, *J* = 7.9, 1.5 Hz, CHCHCCO), 7.63 (1H, dt, *J* = 7.7, 1.5 Hz, BrCCCCHCH), 7.43 (1H, t, *J* = 7.9 Hz, BrCCCCHCH), 2.60 (3H, s, CH₃). ¹³C NMR (126 MHz, CDCl₃) δ_C 137.4 (CCO), 136.3

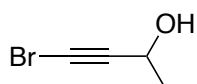
(BrCCCCHCH), 132.2 (BrCCCCHCO), 128.9 (COCCHCH), 128.4 (COCCHCH), 123.5 (BrCCC), 79.2 (alkyne C), 51.5 (alkyne C), 26.8 (CH₃). HRMS (ESI⁺): Exact mass calculated for C₁₀H₈⁷⁹BrO⁺ [M+H]⁺: 222.9753, found: 222.9749.

1-(3-(5,5-Dimethylhexa-1,3-diyne-1-yl)phenyl)ethan-1-one (3.96)



A 30% butylamine/water solution (0.844 mL) was added to an RBF containing copper(I) chloride (7.40 mg, 0.0747 mmol) at 0 °C. A pinch of hydroxylamine hydrochloride was added until the blue colour disappeared. A solution of 3,3-dimethyl-1-butyne (30.6 μL, 0.166 mmol) in DCM (0.15 mL) was added, quickly followed by a solution of 1-(3-(bromoethynyl)phenyl)ethan-1-one (66.6 mg, 0.299 mmol) in DCM (0.15 mL). The reaction was warmed to room temperature and stirred for 3 hours. On completion, the aqueous layer was extracted with DCM. The organic layer was dried over sodium sulfate, filtered and concentrated under vacuum to give the crude product. The crude was purified by column chromatography over silica gel (0 to 20% petroleum ether/ethyl acetate) to give the purified product as a yellow solid (41.1 mg, 61%). m.p. 121-123 °C. ¹H NMR (500 MHz, CDCl₃) δ_H 8.03 (1H, t, *J* = 1.7 Hz, CCHCCO), 7.91 (1H, dd, *J* = 7.9, 1.7, 1.3 Hz, CHCHCCO), 7.63 (1H, dt, *J* = 7.7, 1.3 Hz, CCCHCH), 7.41 (1H, t, *J* = 7.9 Hz, COCCHCHCH), 2.58 (3H, s, CH₃), 1.29 (9H, s, (CH₃)₃). ¹³C NMR (126 MHz, CDCl₃) δ_C 197.3 (C=O), 137.3 (CCO), 136.6 (CCCHCH), 132.6 (CCHCCO), 128.9 (COCCHCH), 128.4 (CHCHCCO), 123.0 (BrCCC), 93.2, 75.3 (alkyne C), 74.9, 63.6 (alkyne C), 30.6 ((CH₃)₃), 26.8 (CH₃). HRMS (ESI⁺): Exact mass calculated for C₁₆H₁₇O⁺ [M+H]⁺: 225.1279, found: 225.1271.

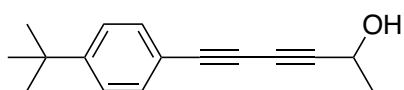
4-Bromobut-3-yn-2-ol (3.108)



3-Butyn-2-ol (0.559 mL, 7.13 mmol) was added to a solution of N-bromosuccinimide (1.40 g, 7.85 mmol) and silver nitrate (121.2 mg, 0.713 mmol) in acetone (12 mL) and the solution was stirred at room temperature for 3 hours. On completion, the solvent was removed

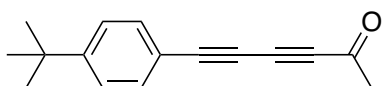
under reduced pressure. The resulting residue was dissolved in water (3 mL) and the aqueous layer was extracted with diethyl ether (3 x 3 mL). The combined organic layers were washed with brine (5 mL), dried over magnesium sulfate, filtered and concentrated under reduced pressure. The crude was purified by column chromatography over silica gel (20% ethyl acetate in petroleum ether) to give the purified product as a white solid (445.1 mg, 42%). $^1\text{H NMR}$ (400 MHz, CDCl_3) δ_{H} 4.55 (1H, q, $J = 6.6$ Hz, CHOH), 1.46 (3H, d, $J = 6.6$ Hz, CH_3). Data is in agreement with that reported in the literature.²⁷¹

6-(4-(*tert*-Butyl)phenyl)hexa-3,5-diyne-2-ol (3.112)



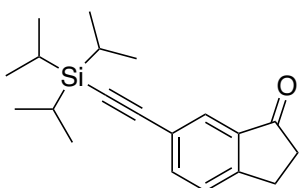
A 30% butylamine/water solution (2.16 mL) was added to an RBF containing copper(I) chloride (18.8 mg, 0.190 mmol) at 0 °C. A pinch of hydroxylamine hydrochloride was added until the blue colour disappeared. A solution of 4-(*tert*-butyl)phenylacetylene (0.112 mL, 0.632 mmol) in DCM (0.82 mL) was added, quickly followed by a solution of 4-bromobut-3-yn-2-ol (113.0 mg, 0.758 mmol) in DCM (0.82 mL). The reaction was warmed to room temperature and stirred for 3 hours. On completion, the aqueous layer was extracted with DCM. The organic layer was dried over sodium sulfate, filtered and concentrated under vacuum to give the crude product. The crude was purified by column chromatography over silica gel (0 to 20% petroleum ether/ethyl acetate) to give the purified product as a white solid (196.0 mg, 73%). m.p. 77-79 °C. IR $\nu_{\text{max}}/\text{cm}^{-1}$ 3302 (O-H), 2957 (C-H), 1367 (O-H), 1074 (O-H), 1067 (O-H), 836. $^1\text{H NMR}$ (500 MHz, CDCl_3) δ_{H} 7.41-7.44 (2H, m, $(\text{CH}_3)_3\text{CCCHCH}$), 7.32-7.36 (2H, m, $(\text{CH}_3)_3\text{CCCHCH}$), 4.66 (1H, q, $J = 6.6$ Hz, CHOH), 1.52 (3H, d, $J = 6.6$ Hz, CH_3), 1.30 (9H, s, $(\text{CH}_3)_3$). $^{13}\text{C NMR}$ (126 MHz, CDCl_3) δ_{C} 153.0 ($(\text{CH}_3)_3\text{CC}$), 132.5 (2C, $(\text{CH}_3)_3\text{CCCHCH}$), 125.6 (2C, $(\text{CH}_3)_3\text{CCCHCH}$), 118.5 (CHOHCCCC), 83.7 (CCHOH), 79.2 (CHCCC), 72.6 (alkyne C), 69.2 (alkyne C), 59.1 (CHOH), 35.1 ($(\text{CH}_3)_3\text{C}$), 31.3 (3C, $(\text{CH}_3)_3$), 24.2 (CH_3). HRMS (ESI⁺): Exact mass calculated for $\text{C}_{16}\text{H}_{18}\text{ONa}^+$ $[\text{M}+\text{Na}]^+$: 249.1250, found: 249.1250.

6-(4-(*tert*-Butyl)phenyl)hexa-3,5-diyne-2-one (3.97)



Dess-Martin periodinane (206.1 mg, 0.486 mmol) was added to a solution of 6-(4-(*tert*-butyl)phenyl)hexa-3,5-diyne-2-ol (100.0 mg, 0.442 mmol) in DCM (2.22 mL) and the reaction was allowed to warm to room temperature and stirred for 3 hours. On completion, the reaction was quenched by addition of 1 M sodium hydroxide solution. The layers were separated and the aqueous layer was extracted three times with DCM. The combined organic layers were dried over sodium sulfate, filtered and concentrated under reduced pressure to give the crude product. The crude was purified by column chromatography over silica gel (20% ethyl acetate/petroleum ether) to give the purified product as an orange solid (64.4 mg, 65%). m.p. 141-143 °C. IR $\nu_{\max}/\text{cm}^{-1}$ 2961 (C-H), 2203 (C-C alkyne), 1672 (C=O), 1603 (C=O), 1362, 1267, 1107, 908, 835. ^1H NMR (500 MHz, CDCl_3) δ_{H} 7.47-7.50 (2H, m, $(\text{CH}_3)_3\text{CCCH}$), 7.37-7.40 (2H, m, $(\text{CH}_3)_3\text{CCCHCH}$), 2.41 (3H, s, CH_3), 1.32 (9H, s, $(\text{CH}_3)_3$). ^{13}C NMR (126 MHz, CDCl_3) δ_{C} 183.6 (C=O), 154.4 ($(\text{CH}_3)_3\text{CC}$), 133.0 (2C, $(\text{CH}_3)_3\text{CCCH}$), 125.9 (2C, $(\text{CH}_3)_3\text{CCCHCH}$), 117.2 (CHCCCCCO), 87.2 (CHCC), 78.8 (CCO), 75.7 (alkyne C), 71.8 (alkyne C), 35.2 ($\text{C}(\text{CH}_3)_3$), 32.8 (CH_3), 31.2 (3C, $(\text{CH}_3)_3$). HRMS (ESI⁺): Exact mass calculated for $\text{C}_{16}\text{H}_{16}\text{ONa}^+$ [M+Na]⁺: 247.1093, found: 247.1087.

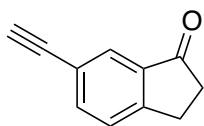
6-((Triisopropylsilyl)ethynyl)-2,3-dihydro-1H-inden-1-one (3.118)



Bis(triphenylphosphine)palladium(II)dichloride (2 mol%, 33.3 mg, 0.0474 mmol) was added to a solution of 6-bromo-1-indanone (500 mg, 2.37 mmol), tri(isopropylsilyl)acetylene (0.850 mL, 3.79 mmol), copper (I) iodide (2 mol%, 9.03 mg, 0.0474 mmol) and triethylamine (5.84 mL) in THF (5.84 mL). The reaction mixture was heated to 80 °C and stirred for 24 h. The reaction was then cooled to room temperature and was passed through a pad of silica gel with an elution of ethyl acetate. The solvent was removed under reduced pressure to give the crude product. The crude was purified by column chromatography over silica gel (0-25%

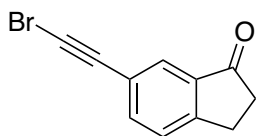
petroleum ether/ethyl acetate) to give the purified product as a colourless oil (585.1 mg, 79%). m.p. 84-86 °C. IR $\nu_{\max}/\text{cm}^{-1}$ 2940 (C-H), 2862 (C-H), 2156 (C-C alkyne), 1711 (C=O), 1287, 881, 839, 662. ^1H NMR (500 MHz, CDCl_3) δ_{H} 7.86 (1H, dd, $J = 1.6, 0.9$ Hz, CHCCO), 7.67 (1H, dd, $J = 7.9, 1.6$ Hz, CHCCHCCO), 7.42 (1H, dd, $J = 7.9, 0.9$ Hz, $\text{CHCCH}_2\text{CH}_2$), 3.12-3.17 (2H, m, $\text{CH}_2\text{CH}_2\text{CO}$), 2.69-2.74 (2H, m, CH_2O), 1.11-1.15 (21H, s, SiCH , $\text{SiCH}(\text{CH}_3)_2$). ^{13}C NMR (126 MHz, CDCl_3) δ_{C} 206.6 (C=O), 155.0, 138.0, 137.2, 127.5, 126.7, 105.9 (alkyne C), 91.8 (alkyne C), 36.5 ($\text{CH}_2\text{CH}_2\text{CO}$), 26.0 (CH_2CO), 18.8 (3C, CH), 11.4 (3C, $(\text{CH}_3)_3$). HRMS (ESI⁺): Exact mass calculated for $\text{C}_{20}\text{H}_{28}\text{OSiNa}^+$ $[\text{M}+\text{Na}]^+$: 335.1087, found: 335.1802.

6-Ethynyl-2,3-dihydro-1H-inden-1-one (3.119)



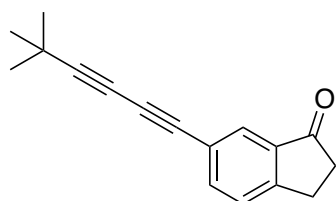
TBAF (1.0 M in THF, 0.876 mL, 0.876 mmol) was added to a solution of 6-((triisopropylsilyl)ethynyl)-2,3-dihydro-1H-inden-1-one (247.3 mg, 0.791 mmol) in THF (1.92 mL) at 0 °C and the reaction was stirred for 3 hours. The reaction was quenched with water and warmed to room temperature. The aqueous layer was extracted three times with DCM. The combined organic layers were dried over sodium sulfate, filtered and concentrated under vacuum to give the crude product. The crude product was purified by column chromatography over silica gel (0-20% petroleum ether/ethyl acetate) to give the purified product as a yellow oil (66.3 mg, 54%). IR $\nu_{\max}/\text{cm}^{-1}$ 2361, 2342, 1559 (C=O), 1541 (C=O). ^1H NMR (400 MHz, CDCl_3) δ_{H} 7.87 (1H, s, ArH), 7.68 (1H, dd, $J = 7.9, 1.6$ Hz, CHCCHCCO), 7.44 (1H, dp, $J = 7.9, 0.9$ Hz, $\text{CHCCH}_2\text{CH}_2$), 3.13-3.19 (2H, m, $\text{CH}_2\text{CH}_2\text{CO}$), 3.10 (1H, s, alkyne-H), 2.69-2.74 (2H, m, CH_2O). ^{13}C NMR (126 MHz, CDCl_3) δ_{C} 206.6 (C=O), 163.4, 138.1, 135.3, 127.6, 126.9, 82.5 (alkyne C), 78.1 (alkyne C), 36.5 ($\text{CH}_2\text{CH}_2\text{CO}$), 26.0 (CH_2CO). HRMS (EI): Exact mass calculated for $\text{C}_{11}\text{H}_8\text{O}$: 156.0570, found: 155.0566.

6-(Bromoethynyl)-2,3-dihydro-1H-inden-1-one (3.120)



6-Ethynyl-2,3-dihydro-1H-inden-1-one (66.3 mg, 0.425 mmol) was added to a solution of N-bromosuccinimide (90.7 mg, 0.509 mmol) and silver nitrate (7.22 mg, 0.0425 mmol) in acetone (1 mL) and the solution was stirred at room temperature for 3 hours. On completion, the solvent was removed under reduced pressure. The resulting residue was dissolved in water (1 mL) and the aqueous layer was extracted with diethyl ether (3 x 1 mL). The combined organic layers were washed with brine (5 mL), dried over magnesium sulfate, filtered and concentrated under reduced pressure. The crude was purified by column chromatography over silica gel (20% ethyl acetate in petroleum ether) to give the purified product as a colourless oil (41.6 mg, 42%). IR $\nu_{\max}/\text{cm}^{-1}$ 2922 (C-H), 2864 (C-H), 2361, 1686 (C=O), 1231, 679 (C-Br). ^1H NMR (400 MHz, CDCl_3) δ_{H} 7.83 (1H, s, ArH), 7.64 (1H, dd, $J = 7.9$, 1.6 Hz, CHCCHCCO), 7.44 (1H, d, $J = 7.9$ Hz, CHCCH₂CH₂), 3.11-3.17 (2H, m, CH₂CH₂CO), 2.68-2.75 (2H, m, CH₂O). ^{13}C NMR (126 MHz, CDCl_3) δ_{C} 205.8 (C=O), 154.3, 135.7, 134.4, 127.5, 126.9, 84.5 (alkyne C), 83.5 (alkyne C), 36.5 (CH₂CH₂CO), 26.0 (CH₂CO). HRMS (EI): Exact mass calculated for $\text{C}_{11}\text{H}_7\text{O}^{79}\text{Br}$: 233.9675, found: 233.9677.

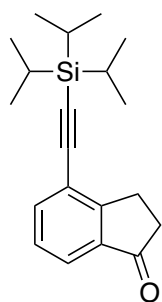
6-(5,5-Dimethylhexa-1,3-diyne-1-yl)-2,3-dihydro-1H-inden-1-one (3.115)



A 30% butylamine/water solution (0.5 mL) was added to an RBF containing copper(I) chloride (4.37 mg, 0.177 mmol) at 0 °C. A pinch of hydroxylamine hydrochloride was added until the blue colour disappeared. A solution of 3,3-dimethylbut-1-yne (18.2 μL , 0.147 mmol) in DCM (0.2 mL) was added, quickly followed by a solution of 6-(bromoethynyl)-2,3-dihydro-1H-inden-1-one (41.6 mg, 0.177 mmol) in DCM (0.2 mL). The reaction was warmed to room temperature and stirred for 3 hours. On completion, the aqueous layer was extracted with DCM. The organic layer was dried over sodium sulfate, filtered and

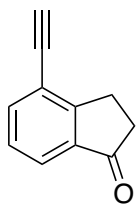
concentrated under vacuum to give the crude product. The crude was purified by column chromatography over silica gel (0 to 20% petroleum ether/ethyl acetate) to give the purified product as a yellow solid (18.8 mg, 45%). m.p. 135-137 °C. IR $\nu_{\text{max}}/\text{cm}^{-1}$ 2922 (C-H), 2361 (alkyne C-C), 1653 (C=O), 1558, 1506, 1456, 1057. ^1H NMR (500 MHz, CDCl_3) δ_{H} 7.83 (1H, dd, $J = 1.6, 0.8$ Hz, CCHCCO), 7.65 (1H, dd, $J = 7.9, 1.6$ Hz, CHCCHCCO), 7.42 (1H, dq, $J = 7.9, 0.8$ Hz, CHCCH₂CH₂), 3.11-3.18 (2H, m, CH₂CH₂CO), 2.67-2.74 (2H, m, CH₂CO), 1.29 (9H, s, (CH₃)₃). ^{13}C NMR (126 MHz, CDCl_3) δ_{C} 206.0 (C=O), 155.5 (CCH₂CH₂), 138.3 (CHCCHCCO), 137.4 (CCO), 127.8 (CCHCCO), 127.0 (CHCCH₂CH₂), 121.8 (CCCCCH), 93.0 ((CH₃)₃CC), 75.0 (alkyne C), 74.9 (alkyne C), 63.7 ((CH₃)₃CCC), 36.5 (CH₂CO), 30.6 (3C, (CH₃)₃), 29.8 (C(CH₃)₃), 26.1 (CH₂CH₂CO). HRMS (ESI⁺): Exact mass calculated for C₁₇H₁₇O [M+H]⁺: 237.1279, found: 237.1267.

4-((Triisopropylsilyl)ethynyl)-2,3-dihydro-1H-inden-1-one (3.122)



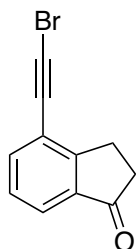
Bis(triphenylphosphine)palladium(II)dichloride (2 mol%, 33.3 mg, 0.0474 mmol) was added to a solution of 4-bromo-1-indanone (500 mg, 2.37 mmol), tri(isopropylsilyl)acetylene (0.850 mL, 3.79 mmol), copper (I) iodide (2 mol%, 9.03 mg, 0.0474 mmol) and triethylamine (5.84 mL) in THF (5.84 mL). The reaction mixture was heated to 80 °C and stirred for 24 h. The reaction was then cooled to room temperature and was passed through a pad of silica gel with an elution of ethyl acetate. The solvent was removed under reduced pressure to give the crude product. The crude was purified by column chromatography over silica gel (0-25% petroleum ether/ethyl acetate) to give the purified product as a colourless oil (228.0 mg, 31%). ^1H NMR (400 MHz, CDCl_3) δ_{H} 7.67-7.73 (2H, m, ArH), 7.31-7.37 (1H, m, ArH), 3.17-3.23 (2H, m, CH₂CH₂CO), 2.70-2.75 (2H, m, CH₂CO), 1.13-1.19 (21H, m, SiCH, SiCH(CH₃)₂). Data is in agreement with that reported in the literature.²⁷²

4-Ethynyl-2,3-dihydro-1H-inden-1-one (3.123)



TBAF (1.0 M in THF, 0.948 mL, 0.948 mmol) was added to a solution of 4-((triisopropylsilyl)ethynyl)-2,3-dihydro-1H-inden-1-one (228.0 mg, 0.730 mmol) in THF (1.78 mL) at 0 °C and the reaction was stirred for 3 hours. The reaction was quenched with water and warmed to room temperature. The aqueous layer was extracted with DCM (3x). The combined organic layers were dried over sodium sulfate, filtered and concentrated under vacuum to give the crude product. The crude product was purified by column chromatography over silica gel (0-20% petroleum ether/ethyl acetate) to give the purified product as a yellow solid (56.1 mg, 49%). m.p. 150-152 °C. IR $\nu_{\max}/\text{cm}^{-1}$ 2972 (C-H), 2922 (C-H), 2361 (alkyne C-C), 1786 (C=O), 1697 (C=O), 1327, 1200, 1065, 702. ^1H NMR (400 MHz, CDCl_3) δ_{H} 7.74 (1H, dd, $J = 7.5, 1.1$ Hz, ArH), 7.70 (1H, dd, $J = 7.5, 1.1$ Hz, ArH), 7.36 (1H, tt, $J = 7.5, 1.1$ Hz, ArH), 3.36 (1H, s, alkyne H), 3.16-3.23 (2H, m, $\text{CH}_2\text{CH}_2\text{CO}$), 2.60-2.76 (2H, m, $\text{CH}_2\text{CH}_2\text{CO}$). ^{13}C NMR (126 MHz, CDCl_3) δ_{C} 206.6 (C=O), 157.8, 137.8, 137.3, 127.7, 124.2, 121.2, 82.6 (alkyne C), 80.1 (alkyne CH), 36.2, 25.6. HRMS (ESI⁺): Exact mass calculated for $\text{C}_{11}\text{H}_8\text{ONa}^+$ [M+Na]⁺: 179.0473, found: 179.0467.

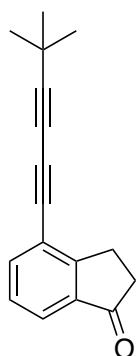
4-(Bromoethynyl)-2,3-dihydro-1H-inden-1-one (3.124)



4-Ethynyl-2,3-dihydro-1H-inden-1-one (56.1 mg, 0.359 mmol) was added to a solution of N-bromosuccinimide (76.7 mg, 0.431 mmol) and silver nitrate (6.10 mg, 0.0359 mmol) in acetone (1 mL) and the solution was stirred at room temperature for 3 hours. On completion, the solvent was removed under reduced pressure. The resulting residue was dissolved in water (1 mL) and the aqueous layer was extracted with diethyl ether (3 x 1 mL).

The combined organic layers were washed with brine (5 mL), dried over magnesium sulfate, filtered and concentrated under reduced pressure. The crude was purified by column chromatography over silica gel (20% ethyl acetate in petroleum ether) to give the purified product as a yellow solid (50.3 mg, 60%). m.p. 168-170 °C. IR $\nu_{\text{max}}/\text{cm}^{-1}$ 2361 (alkyne C-C), 2342 (alkyne C-C), 1653 (C=O), 1558 (C=O), 1506. ^1H NMR (400 MHz, CDCl_3) δ_{H} 7.73 (1H, dd, $J = 7.6, 1.0$ Hz, ArH), 7.70 (1H, dd, $J = 7.6, 1.0$ Hz, ArH), 7.35 (1H, tt, $J = 7.6, 1.0$ Hz, ArH), 3.15-3.22 (2H, m, $\text{CH}_2\text{CH}_2\text{CO}$), 2.68-2.74 (2H, m, $\text{CH}_2\text{CH}_2\text{CO}$). ^{13}C NMR (126 MHz, CDCl_3) δ_{C} 206.5 (C=O), 159.3, 137.7, 137.5, 127.7, 124.1, 123.8, 77.3, 55.4 (alkyne C), 36.2, 25.6. HRMS (ESI⁺): Exact mass calculated for $\text{C}_{11}\text{H}_7^{79}\text{BrONa}^+$ $[\text{M}+\text{Na}]^+$: 256.9578, found: 256.9573.

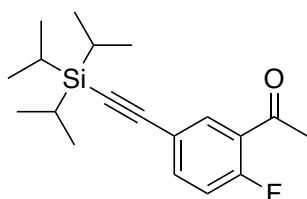
4-(5,5-Dimethylhexa-1,3-diyne-1-yl)-2,3-dihydro-1H-inden-1-one (3.116)



A 30% butylamine/water solution (0.6 mL) was added to an RBF containing copper(I) chloride (2.11 mg, 0.0214 mmol) at 0 °C. A pinch of hydroxylamine hydrochloride was added until the blue colour disappeared. A solution of 3,3-dimethylbut-1-yne (22.0 μL , 0.178 mmol) in DCM (0.2 mL) was added, quickly followed by a solution of 4-(bromoethynyl)-2,3-dihydro-1H-inden-1-one (50.3 mg, 0.214 mmol) in DCM (0.2 mL). The reaction was warmed to room temperature and stirred for 3 hours. On completion, the aqueous layer was extracted with DCM. The organic layer was dried over sodium sulfate, filtered and concentrated under vacuum to give the crude product. The crude was purified by column chromatography over silica gel (0 to 20% petroleum ether/ethyl acetate) to give the purified product as a yellow solid (18.9 mg, 59%). m.p. 78-80 °C. IR $\nu_{\text{max}}/\text{cm}^{-1}$ 2965 (C-H), 2924 (C-H), 2231 (alkyne C-C), 1708 (C=O), 1558 (C=O), 1325, 1260, 1032, 781. ^1H NMR (500 MHz, CDCl_3) δ_{H} 7.72 (1H, dd, $J = 7.6, 1.1$ Hz, CHCCO), 7.68 (1H, dd, $J = 7.6, 1.1$ Hz, $(\text{CH}_3)_3\text{CCCCCCH}$), 7.34 (1H, tt, $J = 7.6, 1.1$ Hz, CHCHCCO), 3.18-3.23 (2H, m, $\text{CH}_2\text{CH}_2\text{CO}$), 2.69-2.73 (2H, m, $\text{CH}_2\text{CH}_2\text{CO}$), 1.31 (9H, s, $(\text{CH}_3)_3$). ^{13}C NMR (126 MHz, CDCl_3) δ_{C} 206.5 (C=O), 158.4 (CCO),

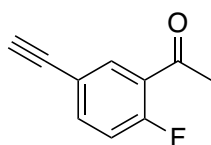
138.1 ((CH₃)₃CCCCCCH), 137.5 ((CH₃)₃CCCCC), 127.7 (CHCHCCO), 124.0 (CHCCO), 121.4 (CCH₂CH₂CO), 94.1 ((CH₃)₃CC), 79.4 (alkyne C), 72.3 ((CH₃)₃CCCC), 63.7 (alkyne C), 36.1 (CH₂CH₂CO), 30.6 ((CH₃)₃), 28.5 ((CH₃)₃C), 25.7 (CH₂CH₂CO). HRMS (ESI⁺): Exact mass calculated for C₁₇H₁₇O⁺ [M+H]⁺: 237.1279, found: 237.1268.

1-(2-Fluoro-5-((triisopropylsilyl)ethynyl)phenyl)ethan-1-one (3.128)



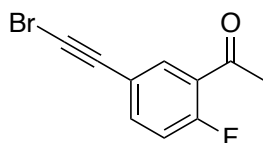
Bis(triphenylphosphine)palladium(II)dichloride (2 mol%, 32.3 mg, 0.0460 mmol) was added to a solution of 1-(5-bromo-2-fluorophenyl)-1-ethanone (0.326 mL, 2.30 mmol), tri(isopropylsilyl)acetylene (0.826 mL, 3.68 mmol), copper (I) iodide (2 mol%, 8.76 mg, 0.0460 mmol) and triethylamine (5.67 mL) in THF (5.67 mL). The reaction mixture was heated to 80 °C and stirred for 24 h. The reaction was then cooled to room temperature and was passed through a pad of silica gel with an elution of ethyl acetate. The solvent was removed under reduced pressure to give the crude product. The crude was purified by column chromatography over silica gel (0-25% petroleum ether/ethyl acetate) to give the purified product as a yellow solid (586.5 mg, 80%). m.p. 37-39 °C. IR $\nu_{\max}/\text{cm}^{-1}$ 2943 (C-H), 2866 (C-H), 1686 (C=O), 1485 (C-H), 1217 (C-F), 783. ¹H NMR (500 MHz, CDCl₃) δ_{H} 7.96 (1H, dd, $J = 7.0, 2.3$ Hz, CHCCO), 7.60 (1H, ddd, $J = 8.5, 4.7, 2.3$ Hz, CHCHCF), 7.08 (1H, dd, $J = 10.8, 8.5$ Hz, CHCF), 2.64 (3H, d, $J = 4.7$ Hz, CH₃), 1.11-1.13 (21H, m, SiCH, SiCH(CH₃)₂). ¹³C NMR (126 MHz, CDCl₃) δ_{C} 195.4 (C=O), 160.7 (CF), 138.1 (1C, d, $J = 9.5$ Hz, CHCHCF), 134.5 (1H, d, $J = 2.6$ Hz, CHCCO), 125.9 (CH₃COC), 120.5 (SiCCC), 117.0 (1C, d, $J = 24.9$ Hz, CHCF), 104.8 (SiCC), 91.7 (SiC), 31.5 (1C, d, $J = 7.2$ Hz, CH₃), 18.8 (6C, CH(CH₃)₂), 11.4 (3C, SiCH). ¹⁹F{¹H} NMR (470 MHz, CDCl₃) δ_{F} -108.2. HRMS (ESI⁺): Exact mass calculated for C₁₉H₂₈OFSi⁺ [M+H]⁺: 319.1893, found: 319.1884.

1-(5-Ethynyl-2-fluorophenyl)ethan-1-one (3.129)



TBAF (1.0 M in THF, 2.04 mL, 2.04 mmol) was added to a solution of 1-(2-fluoro-5-((triisopropylsilyl)ethynyl)phenyl)ethan-1-one (500 mg, 1.57 mmol) in THF (3.83 mL) at 0 °C and the reaction was stirred for 3 hours. The reaction was quenched with water and warmed to room temperature. The aqueous layer was extracted three times with DCM. The combined organic layers were dried over sodium sulfate, filtered and concentrated under vacuum to give the crude product. The crude product was purified by column chromatography over silica gel (0-20% petroleum ether/ethyl acetate) to give the purified product as a yellow solid (59.2 mg, 23%). m.p. 116-118 °C. IR $\nu_{\max}/\text{cm}^{-1}$ 3285 (C-H alkyne), 3262 (C-H alkyne), 1654 (C=O), 1568, 1483, 868. ^1H NMR (500 MHz, CDCl_3) δ_{H} 8.00 (1H, dd, $J = 7.0, 2.3$ Hz, CHCCO), 7.62 (1H, ddd, $J = 8.5, 4.7, 2.3$ Hz, CHCHCF), 7.11 (1H, dd, $J = 10.6, 8.5$ Hz, CHCF), 3.08 (1H, s, alkyne CH), 2.64 (3H, d, $J = 4.7$ Hz, CH_3). $^{19}\text{F}\{^1\text{H}\}$ NMR (470 MHz, CDCl_3) δ_{F} -107.5. ^{13}C NMR (126 MHz, CDCl_3) δ_{C} 195.4 (C=O), 160.7 (CF), 138.1 (1C, d, $J = 9.5$ Hz, CHCHCF), 134.5 (1H, d, $J = 2.4$ Hz, CHCCO), 125.9 (CH_3COC), 120.5 (SiCCC), 117.0 (1C, d, $J = 24.9$ Hz, CHCF), 104.8 (SiCC), 91.7 (SiC), 31.5 (1C, d, $J = 7.2$ Hz, CH_3). HRMS (ESI⁺): Exact mass calculated for $\text{C}_{10}\text{H}_8\text{OF}^+$ [$\text{M}+\text{H}$]⁺: 163.0554, found: 163.0552.

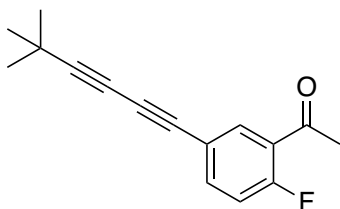
1-(5-(Bromoethynyl)-2-fluorophenyl)ethan-1-one (3.130)



1-(5-Ethynyl-2-fluorophenyl)ethan-1-one (59.2 mg, 0.365 mmol) was added to a solution of N-bromosuccinimide (78.0 mg, 0.438 mmol) and silver nitrate (6.20 mg, 0.0365 mmol) in acetone (1 mL) and the solution was stirred at room temperature for 3 hours. On completion, the solvent was removed under reduced pressure. The resulting residue was dissolved in water (1 mL) and the aqueous layer was extracted with diethyl ether (3 x 1 mL). The combined organic layers were washed with brine (5 mL), dried over magnesium sulfate, filtered and concentrated under reduced pressure. The crude was purified over silica gel

(20% ethyl acetate in petroleum ether) to give the purified product as a yellow solid (17.9 mg, 20%). m.p. 102-104 °C. IR $\nu_{\text{max}}/\text{cm}^{-1}$ 1668 (C=O), 1481, 1215 (C-F), 837. ^1H NMR (500 MHz, CDCl_3) δ_{H} 7.96 (1H, dd, $J = 7.0, 2.3$ Hz, CHCCO), 7.57 (1H, ddd, $J = 8.6, 4.7, 2.3$ Hz, CHCHCF), 7.10 (1H, dd, $J = 10.6, 8.6$ Hz, CHCF), 2.63 (3H, d, $J = 4.7$ Hz, CH_3). ^{13}C NMR (126 MHz, CDCl_3) δ_{C} 194.9 (C=O), 163.0 (CF), 137.9 (1C, d, $J = 9.5$ Hz, CHCHCF), 134.7 (1H, d, $J = 3.0$ Hz, CHCCO), 126.1 (CH_3COC), 119.1 (SiCCC), 117.3 (1C, d, $J = 25.1$ Hz, CHCF), 104.8 (SiCC), 91.7 (SiC), 31.5 (1C, d, $J = 7.2$ Hz, CH_3). $^{19}\text{F}\{^1\text{H}\}$ NMR (470 MHz, CDCl_3) δ_{F} -107.4. HRMS (ESI⁺): Exact mass calculated for $\text{C}_{10}\text{H}_6^{79}\text{BrOFNa}^+$ $[\text{M}+\text{Na}]^+$: 262.9484, found: 262.9478.

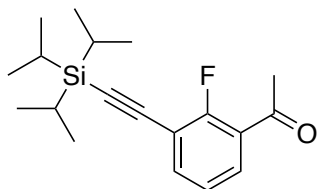
1-(5-(5,5-Dimethylhexa-1,3-diy-1-yl)-2-fluorophenyl)ethan-1-one (3.125)



A 30% butylamine/water solution (0.21 mL) was added to an RBF containing copper(I) chloride (1.84 mg, 0.0190 mmol) at 0 °C. A pinch of hydroxylamine hydrochloride was added until the blue colour disappeared. A solution of 3,3-dimethylbut-1-yne (7.62 μL , 0.062 mmol) in DCM (0.1 mL) was added, quickly followed by a solution of 1-(5-(bromoethynyl)-2-fluorophenyl)ethan-1-one (17.9 mg, 0.074 mmol) in DCM (0.1 mL). The reaction was warmed to room temperature and stirred for 3 hours. On completion, the aqueous layer was extracted with DCM. The organic layer was dried over sodium sulfate, filtered and concentrated under vacuum to give the crude product. The crude was purified by column chromatography over silica gel (0 to 20% petroleum ether/ethyl acetate) to give the purified product as a yellow solid (17.8 mg, 78%). m.p. 50-52 °C. IR $\nu_{\text{max}}/\text{cm}^{-1}$ 2920 (C-H), 2361, 1670 (C=O), 1599 (C=O), 1485, 1261 (C-F), 1213 (C-F), 827. ^1H NMR (500 MHz, CDCl_3) δ_{H} 7.97 (1H, dd, $J = 7.1, 2.3$ Hz, CHCCO), 7.58 (1H, ddd, $J = 8.6, 4.7, 2.3$ Hz, CHCHCF), 7.09 (1H, dd, $J = 10.6, 8.6$ Hz, CHCF), 2.62 (3H, d, $J = 4.7$ Hz, CH_3). ^{13}C NMR (126 MHz, CDCl_3) δ_{C} 196.7 (C=O), 163.0 (CF), 138.3 (1C, d, $J = 9.4$ Hz, CHCHCF), 135.1 (1H, d, $J = 3.0$ Hz, CHCCO), 126.0 (CH_3COC), 122.1 ($(\text{CH}_3)_3\text{CCCC}$), 117.4 (1C, d, $J = 25.0$ Hz, CHCF), 105.1 (alkyne C), 93.0 (alkyne C), 73.9 (alkyne C), 63.5 (alkyne C), 31.5 (1C, d, $J = 7.2$ Hz, CH_3), 30.6 (3C, $(\text{CH}_3)_3$), 29.9 ($(\text{CH}_3)_3\text{C}$).

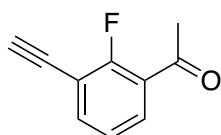
$^{19}\text{F}\{^1\text{H}\}$ NMR (470 MHz, CDCl_3) δ_{F} -107.1. HRMS (ESI⁺): Exact mass calculated for $\text{C}_{16}\text{H}_{16}\text{OF}^+$ $[\text{M}+\text{H}]^+$: 243.1185, found: 243.1173.

1-(2-Fluoro-3-((triisopropylsilyl)ethynyl)phenyl)ethan-1-one (3.132)



Bis(triphenylphosphine)palladium(II)dichloride (2 mol%, 32.3 mg, 0.0460 mmol) was added to a solution of 1-(3-bromo-2-fluorophenyl)-1-ethanone (0.326 mL, 2.30 mmol), tri(isopropylsilyl)acetylene (0.826 mL, 3.68 mmol), copper (I) iodide (2 mol%, 8.76 mg, 0.0460 mmol) and triethylamine (5.67 mL) in THF (5.67 mL). The reaction mixture was heated to 80 °C and stirred for 24 h. The reaction was then cooled to room temperature and was passed through a pad of silica gel with an elution of ethyl acetate. The solvent was removed under reduced pressure to give the crude product. The crude was purified by column chromatography over silica gel (0-25% petroleum ether/ethyl acetate) to give the purified product as a yellow oil (614.0 mg, 84%). IR $\nu_{\text{max}}/\text{cm}^{-1}$ 2943 (C-H), 2866 (C-H), 1612 (C=O), 1445, 1273 (C-F), 991, 696. ^1H NMR (400 MHz, CDCl_3) δ_{H} 7.80 (1H, dd, J = 7.7, 6.7, 1.9 Hz, CHCCO), 7.63 (1H, ddd, J = 7.7, 6.7, 1.9 Hz, CFCH), 7.16 (1H, t, J = 7.7 Hz, CHCHCCO), 2.66 (3H, d, J = 5.0 Hz, CH_3), 1.13-1.16 (21H, m, SiCH, SiCH(CH_3)₂). ^{13}C NMR (126 MHz, CDCl_3) δ_{C} 195.7 (C=O), 163.8 (CF), 138.4 (CFCH), 130.6 (CHCCO), 126.0 (d, J = 12.9 Hz, CCO), 124.1 (d, J = 4.2 Hz, CHCHCCO), 113.7 (d, J = 18.3 Hz, SiCCC), 98.9 (SiCC), 98.3 (SiCC), 31.7 (1C, d, J = 7.4 Hz, CH_3), 18.8 (6C, CH(CH_3)₂), 11.4 (3C, SiCH). $^{19}\text{F}\{^1\text{H}\}$ NMR (470 MHz, CDCl_3) δ_{F} -106.5. HRMS (ESI⁺): Exact mass calculated for $\text{C}_{19}\text{H}_{27}\text{OFSiNa}^+$ $[\text{M}+\text{Na}]^+$: 341.1713, found: 341.1704.

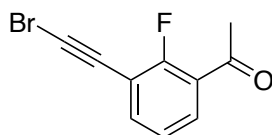
1-(3-Ethynyl-2-fluorophenyl)ethan-1-one (3.133)



TBAF (1.0 M in THF, 2.04 mL, 2.04 mmol) was added to a solution of 1-(2-fluoro-5-((triisopropylsilyl)ethynyl)phenyl)ethan-1-one (500 mg, 1.57 mmol) in THF (3.83 mL) at 0 °C and the reaction was stirred for 3 hours. The reaction was quenched with water and

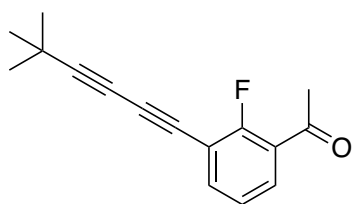
warmed to room temperature. The aqueous layer was extracted three times with DCM. The combined organic layers were dried over sodium sulfate, filtered and concentrated under vacuum to give the crude product. The crude product was purified by column chromatography over silica gel (0-20% petroleum ether/ethyl acetate) to give the purified product as a yellow solid (114 mg, 49%). IR $\nu_{\max}/\text{cm}^{-1}$ 2988 (C-H), 2901 (C-H), 2361, 1558 (C=O), 1506 (C=O), 1057 (C-F). ^1H NMR (400 MHz, CDCl_3) δ_{H} 7.86 (1H, dd, $J = 7.8, 6.7, 1.9$ Hz, CHCCO), 7.66 (1H, ddd, $J = 7.8, 6.7, 1.9$ Hz, CFCCH), 7.20 (1H, t, $J = 7.8$ Hz, CHCHCCO), 3.36 (1H, s, alkyne CH), 2.66 (3H, d, $J = 5.1$ Hz, CH_3). $^{19}\text{F}\{^1\text{H}\}$ NMR (470 MHz, CDCl_3) δ_{F} -107.0. HRMS (ESI⁺): Exact mass calculated for $\text{C}_{10}\text{H}_8\text{FO}^+$ [M+H]⁺: 163.0559, found: 163.0552.

1-(3-(Bromoethynyl)-2-fluorophenyl)ethan-1-one (3.134)



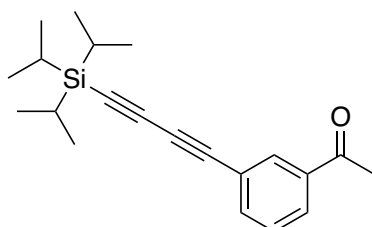
1-(3-Ethynyl-2-fluorophenyl)ethan-1-one (114.0 mg, 0.703 mmol) was added to a solution of N-bromosuccinimide (150.1 mg, 0.844 mmol) and silver nitrate (11.9 mg, 0.0703 mmol) in acetone (1.57 mL) and the solution was stirred at room temperature for 3 hours. On completion, the solvent was removed under reduced pressure. The resulting residue was dissolved in water (2 mL) and the aqueous layer was extracted with diethyl ether (3 x 2 mL). The combined organic layers were washed with brine (5 mL), dried over magnesium sulfate, filtered and concentrated under reduced pressure. The crude was purified by column chromatography over silica gel (20% ethyl acetate in petroleum ether) to give the purified product as a yellow solid (17.9 mg, 20%). ^1H NMR (400 MHz, CDCl_3) δ_{H} 7.84 (1H, dd, $J = 7.8, 6.7, 1.9$ Hz, CHCCO), 7.62 (1H, ddd, $J = 7.8, 6.7, 1.9$ Hz, CFCCH), 7.18 (1H, t, $J = 7.8$ Hz, CHCHCCO), 2.65 (3H, d, $J = 5.2$ Hz, CH_3). $^{19}\text{F}\{^1\text{H}\}$ NMR (470 MHz, CDCl_3) δ_{F} -107.1. HRMS (ESI⁺): Exact mass calculated for $\text{C}_{10}\text{H}_6^{79}\text{BrOFNa}^+$ [M+Na]⁺: 262.9484, found: 262.9478.

1-(3-(5,5-Dimethylhexa-1,3-diyne-1-yl)-2-fluorophenyl)ethan-1-one (3.126)



A 30% butylamine/water solution (0.186 mL) was added to an RBF containing copper(I) chloride (1.63 mg, 0.017 mmol) at 0 °C. A pinch of hydroxylamine hydrochloride was added until the blue colour disappeared. A solution of 3,3-dimethylbut-1-yne (6.8 μ L, 0.055 mmol) in DCM (0.1 mL) was added, quickly followed by a solution of 1-(3-(bromoethynyl)-2-fluorophenyl)ethan-1-one (16.0 mg, 0.066 mmol) in DCM (0.1 mL). The reaction was warmed to room temperature and stirred for 3 hours. On completion, the aqueous layer was extracted with DCM. The organic layer was dried over sodium sulfate, filtered and concentrated under vacuum to give the crude product. The crude was purified by column chromatography over silica gel (0 to 20% petroleum ether/ethyl acetate) to give the purified product as a yellow solid (7.86 mg, 59%). m.p. 61-63 °C. IR $\nu_{\text{max}}/\text{cm}^{-1}$ 2947 (C-H), 2926 (C-H), 2359, 1709 (C=O), 1215 (C-F). ^1H NMR (500 MHz, CDCl_3) δ_{H} 7.82 (1H, dd, $J = 7.7, 6.7, 1.9$ Hz, CHCCO), 7.62 (1H, ddd, $J = 7.7, 6.7, 1.9$ Hz, CFCCH), 7.17 (1H, t, $J = 7.7$ Hz, CHCHCCO), 2.65 (3H, d, $J = 5.2$ Hz, CH_3). ^{13}C NMR (126 MHz, CDCl_3) δ_{C} 196.8 (C=O), 163.3 (ArCF), 138.7 (ArCH), 137.4 (ArC), 131.7 (ArCH), 124.4 (ArCH), 108.3 (ArC), 90.1 (alkyne C), 85.6 (alkyne C), 67.5 (alkyne C), 60.6 (alkyne C), 31.7 (CH_3), 30.5 (3C, $(\text{CH}_3)_3$), 27.7 ($\text{C}(\text{CH}_3)_3$). $^{19}\text{F}\{^1\text{H}\}$ NMR (470 MHz, CDCl_3) δ_{F} -106.2. HRMS (ESI $^+$): Exact mass calculated for $\text{C}_{16}\text{H}_{16}\text{FO}^+$ [M+H] $^+$: 243.1185, found: 243.1172.

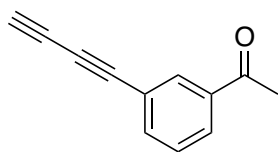
1-(3-((Triisopropylsilyl)buta-1,3-diyne-1-yl)phenyl)ethan-1-one (3.136)



A 30% butylamine/water solution (2.52 mL) was added to an RBF containing copper(I) chloride (22.2 mg, 0.224 mmol) at 0 °C. A pinch of hydroxylamine hydrochloride was added until the blue colour disappeared. A solution of tri(isopropylsilyl)acetylene (0.167 mL, 0.747

mmol) in DCM (2 mL) was added, quickly followed by a solution of 1-(3-(bromoethynyl)phenyl)ethan-1-one (200 mg, 0.897 mmol) in DCM (2 mL). The reaction was warmed to room temperature and stirred for 3 hours. On completion, the aqueous layer was extracted with DCM. The organic layer was dried over sodium sulfate, filtered and concentrated under vacuum to give the crude product. The crude was purified by column chromatography over silica gel (0 to 20% petroleum ether/ethyl acetate) to give the purified product as a yellow solid (203.7 mg, 84%). m.p. 82-84 °C. IR $\nu_{\max}/\text{cm}^{-1}$ 2943 (C-H), 2864 (C-H), 1686 (C=O), 1360, 1231, 883, 804, 679. ^1H NMR (500 MHz, CDCl_3) δ_{H} 8.08 (1H, t, $J = 1.7$ Hz, CCHCCO), 7.94 (1H, dt, $J = 7.8, 1.4$ Hz, CHCHCCO), 7.68 (1H, dt, $J = 7.8, 1.4$ Hz, CHCHCHCCO), 7.43 (1H, t, $J = 7.8$ Hz, CHCHCCO), 2.59 (3H, s, CH_3), 1.10-1.14 (21H, m, SiCH, SiCH(CH_3)₂). ^{13}C NMR (126 MHz, CDCl_3) δ_{C} 197.1 (C=O), 137.4 (CCO), 136.9 (CHCHCHCCO), 132.9 (CCHCCO), 129.0 (CHCHCCO), 128.8 (CHCHCCO), 122.4 (SiCCCCC), 89.2 (alkyne C), 89.1 (alkyne C), 75.8 (alkyne C), 74.5 (SiCCCC), 26.8 (CH_3), 18.7 (6C, (CH_3)₂), 11.4 (3C, CH(CH_3)₂). HRMS (ESI⁺): Exact mass calculated for $\text{C}_{21}\text{H}_{29}\text{OSi}^+$ $[\text{M}+\text{H}]^+$: 325.1988, found: 325.1973.

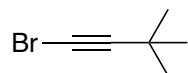
1-(3-(Buta-1,3-diyne-1-yl)phenyl)ethan-1-one (3.137)



TBAF (1.0 M in THF, 0.329 mL, 0.329 mmol) was added to a solution of 1-(3-((triisopropylsilyl)buta-1,3-diyne-1-yl)phenyl)ethan-1-one (82.0 mg, 0.253 mmol) in THF (0.62 mL) at 0 °C and the reaction was stirred for 3 hours. The reaction was quenched with water and warmed to room temperature. The aqueous layer was extracted three times with DCM. The combined organic layers were dried over sodium sulfate, filtered and concentrated under vacuum to give the crude product. The crude product was purified by column chromatography over silica gel (0-20% petroleum ether/ethyl acetate) to give the purified product as a yellow solid (10.0 mg, 23%). m.p. 141-143 °C. IR $\nu_{\max}/\text{cm}^{-1}$ 2963 (C-H), 2916 (C-H), 1684 (C=O), 1260, 1016, 795. ^1H NMR (500 MHz, CDCl_3) δ_{H} 8.09 (1H, t, $J = 1.6$ Hz, CCHCCO), 7.96 (1H, dt, $J = 7.8, 1.6$ Hz, CHCHCCO), 7.69 (1H, dt, $J = 7.8, 1.6$ Hz, CHCHCHCCO), 7.45 (1H, t, $J = 7.8$ Hz, CHCHCCO), 2.60 (3H, s, CH_3), 2.51 (1H, s, alkyne CH). ^{13}C NMR (126 MHz, CDCl_3) δ_{C} 197.1 (C=O), 137.4 (CCO), 137.0 (CHCHCHCCO), 132.9 (CCHCCO), 129.2 (CHCHCCO), 129.0 (CHCHCCO), 121.9 (SiCCCCC), 89.1 (alkyne C), 75.8 (alkyne C), 74.3 (alkyne

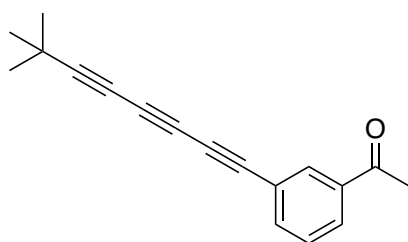
C), 72.1 (alkyne C), 26.8 (CH₃). HRMS (ESI⁺): Exact mass calculated for C₁₂H₉O⁺ [M+H]⁺: 169.0648, found: 169.0644.

1-Bromo-3,3-dimethylbut-1-yne (3.138)



3,3-Dimethylbut-1-yne (1.5 mL, 12.2 mmol) was added to a solution of N-bromosuccinimide (2.38 g, 13.4 mmol) and silver nitrate (207.2 mg, 1.22 mmol) in acetone (60 mL) and the solution was stirred at room temperature for 3 hours. On completion, the solvent was removed under reduced pressure. The resulting residue was dissolved in water (35 mL) and the aqueous layer was extracted with diethyl ether (3 x 35 mL). The combined organic layers were washed with brine (90 mL), dried over magnesium sulfate, filtered and concentrated under reduced pressure. The crude was purified by column chromatography over silica gel (20% ethyl acetate in petroleum ether) to give the purified product as a colourless liquid (216.4 mg, 11%). ¹H NMR (500 MHz, CDCl₃) δ_H 1.23 (9H, s, (CH₃)₃). ¹³C NMR (126 MHz, CDCl₃) δ_C 88.4 (alkyne C), 37.2 (alkyne C), 30.8 ((CH₃)₃), 27.8 ((CH₃)₃C). Data is in agreement with that reported in the literature.²⁷³

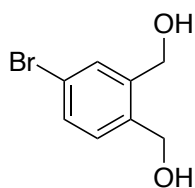
1-(3-(7,7-Dimethylocta-1,3,5-triyn-1-yl)phenyl)ethan-1-one (3.135)



A 30% butylamine/water solution (0.2 mL) was added to an RBF containing copper(I) chloride (1.76 mg, 0.0178 mmol) at 0 °C. A pinch of hydroxylamine hydrochloride was added until the blue colour disappeared. A solution of 1-(3-(buta-1,3-diyne-1-yl)phenyl)ethan-1-one (10.0 mg, 0.0592 mmol) in DCM (0.1 mL) was added, quickly followed by a solution of 1-bromo-3,3-dimethylbut-1-yne (11.4 mg, 0.0710 mmol) in DCM (0.1 mL). The reaction was warmed to room temperature and stirred for 3 hours. On completion, the aqueous layer was extracted with DCM. The organic layer was dried over sodium sulfate, filtered and concentrated under vacuum to give the crude product. The crude was purified by column

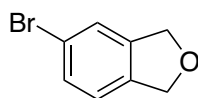
chromatography over silica gel (0 to 20% petroleum ether/ethyl acetate) to give the purified product as a yellow solid (4.0 mg, 27%). m.p. 102-104 °C. ¹H NMR (500 MHz, CDCl₃) δ_H 8.07 (1H, td, *J* = 1.8, 0.5 Hz, CCHCCO), 7.95 (1H, dt, *J* = 7.8, 1.8, 1.3 Hz, CHCHCCO), 7.68 (1H, dt, *J* = 7.8, 1.3 Hz, CHCHCHCCO), 7.45 (1H, td, *J* = 7.8, 0.5 Hz, CHCHCCO), 2.60 (3H, s, CH₃), 1.28 (9H, s, (CH₃)₃). ¹³C NMR (126 MHz, CDCl₃) δ_C 197.1 (C=O), 137.2, 133.0, 129.0, 121.9, 90.5, 83.8, 71.5, 66.7, 64.5, 60.6, 30.4 ((CH₃)₃), 28.6 ((CH₃)₃C), 26.8 (CH₃). HRMS (ESI⁺): Exact mass calculated for C₁₈H₁₇O⁺ [M+H]⁺: 249.1279, found: 249.1267.

(4-Bromo-1,2-phenylene)dimethanol (3.141)



Zinc chloride (880 mg, 6.50 mmol) was added to a suspension of lithium aluminium hydride (2.0 M in THF, 12.8 mL, 25.8 mmol) in dry THF (80 mL) at 0 °C. A solution of 4-bromophthalic anhydride (2.5 g, 10.8 mmol) in dry THF (12.5 mL) was added and the reaction was warmed to room temperature and stirred for 18 hours. The reaction was cooled to 0 °C. Water (25 mL) and 10% hydrochloric acid solution (75 mL) were added and the aqueous phase was extracted with ethyl acetate (3 x 50 mL). The combined organic layers were washed with brine, dried over magnesium sulfate, filtered and concentrated in vacuo to give the crude product. The crude was purified by column chromatography over silica gel (1:1 petroleum ether/ethyl acetate to 100% ethyl acetate) to give the purified product as a white solid (1.76 g, 75%). ¹H NMR (400 MHz, CDCl₃) δ_H 7.50 (1H, d, *J* = 2.1 Hz, CHCHCCH₂OH), 7.43 (1H, dd, *J* = 8.0, 2.1 Hz, BrCCHCCH₂OH), 7.21 (1H, d, *J* = 8.0 Hz, CHCHCCH₂OH), 4.66 (2H, s, CH₂OH), 4.65 (2H, s, CH₂OH), 3.12 (1H, s, OH), 3.06 (1H, s, OH). Data is in agreement with that reported in the literature.²⁷⁴

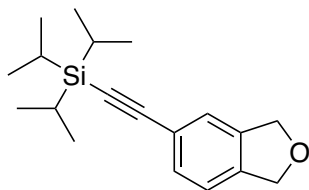
5-Bromo-1,3-dihydroisobenzofuran (3.143)



Manganese dioxide (1.08 g, 12.4 mmol) was added to a solution of (4-bromo-1,2-phenylene)dimethanol (538.3 mg, 2.48 mmol) in DCM (43 mL). The reaction was stirred at

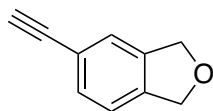
40 °C for 2 hours. Additional manganese dioxide (1.08 g, 12.4 mmol) was added and the mixture was stirred at 40 °C for a further 40 minutes. The mixture was then filtered through celite. Triethylsilane (1.19 mL, 7.44 mmol) was added dropwise and the mixture was stirred for 30 minutes, followed by the addition of trifluoroacetic acid (0.949 mL, 12.4 mmol). The reaction mixture was stirred for 24 hours. The reaction mixture was concentrated under vacuum to give the crude product. The crude was purified by column chromatography over silica gel (hexane/ethyl acetate, 0% to 20% ethyl acetate) to give the purified product as a white solid (349.8 mg, 71%). ¹H NMR (400 MHz, CDCl₃) δ_H 7.37-7.41 (2H, m, ArH), 7.11 (1H, dt, *J* = 8.5 Hz, ArH), 5.07-5.09 (2H, m, CH₂), 5.04-5.06 (2H, m, CH₂). Data is in agreement with that reported in the literature.²⁷⁵

((1,3-Dihydroisobenzofuran-5-yl)ethynyl)triisopropylsilane (3.144)



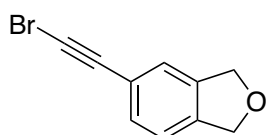
Bis(triphenylphosphine)palladium(II)dichloride (2 mol%, 24.7 mg, 0.0352 mmol) was added to a solution of 5-bromo-1,3-dihydroisobenzofuran (349.8 mg, 1.76 mmol), tri(isopropylsilyl)acetylene (0.632 mL, 2.82 mmol), copper (I) iodide (2 mol%, 6.70 mg, 0.0352 mmol) and triethylamine (4.35 mL) in THF (4.35 mL). The reaction mixture was heated to 80 °C and stirred for 24 h. The reaction was then cooled to room temperature and was passed through a pad of silica gel with an elution of ethyl acetate. The solvent was removed under reduced pressure to give the crude product. The crude was purified by column chromatography over silica gel (0-25% petroleum ether/ethyl acetate) to give the product as a yellow oil (86.9 mg, 16%). IR $\nu_{\text{max}}/\text{cm}^{-1}$ 2941 (C-H), 2862 (C-H), 1047 (C-O), 808. ¹H NMR (500 MHz, CDCl₃) δ_H 7.39 (1H, d, *J* = 7.8 Hz, ArH), 7.36 (1H, s, CCHC), 7.17 (1H, d, *J* = 7.8 Hz, ArH), 5.09 (2H, d, *J* = 1.6 Hz, CH₂), 5.08 (2H, d, *J* = 1.6 Hz, CH₂). ¹³C NMR (126 MHz, CDCl₃) δ_C 139.5, 139.4, 131.4, 124.7, 122.7, 121.0, 107.1 (SiCCC), 90.4 (SiCCC), 73.7 (CH₂), 73.4 (CH₂), 18.8 (6C, (CH₃)₂C), 11.4 (3C, (CH₃)₂C). HRMS (ESI⁺): Exact mass calculated for C₁₉H₂₉OSi⁺ [M+H]⁺: 301.1988, found: 301.1972.

5-Ethynyl-1,3-dihydroisobenzofuran (3.145)



TBAF (1.0 M in THF, 0.376 mL, 0.376 mmol) was added to a solution of ((1,3-dihydroisobenzofuran-5-yl)ethynyl)triisopropylsilane (86.7 mg, 0.289 mmol) in THF (0.7 mL) at 0 °C and the reaction was stirred for 3 hours. The reaction was quenched with water and warmed to room temperature. The aqueous layer was extracted three times with DCM. The combined organic layers were dried over sodium sulfate, filtered and concentrated under vacuum to give the crude product. The crude product was purified by column chromatography over silica gel (0-20% petroleum ether/ethyl acetate) to give the purified product as a yellow oil (20.1 mg, 48%). IR $\nu_{\text{max}}/\text{cm}^{-1}$ 2862 (C-H), 1771, 1045 (C-O), 808. ^1H NMR (500 MHz, CDCl_3) δ_{H} 7.40 (1H, d, $J = 7.8$ Hz, ArH), 7.36 (1H, s, CCHC), 7.19 (1H, d, $J = 7.8$ Hz, ArH), 5.10 (2H, d, $J = 2.4$ Hz, CH_2), 5.09 (2H, d, $J = 2.4$ Hz, CH_2), 3.06 (1H, s, alkyne H). ^{13}C NMR (126 MHz, CDCl_3) δ_{C} 140.1, 139.6, 131.6, 124.8, 121.3, 121.1, 83.7 (alkyne CH), 77.1 (alkyne C), 73.6 (CH_2), 73.4 (CH_2). HRMS (ESI⁺): Exact mass calculated for $\text{C}_{10}\text{H}_8\text{ONH}_4^+$ $[\text{M}+\text{NH}_4]^+$: 162.0913, found: 162.0912.

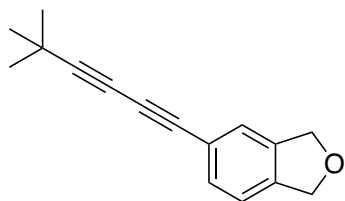
5-(Bromoethynyl)-1,3-dihydroisobenzofuran (3.146)



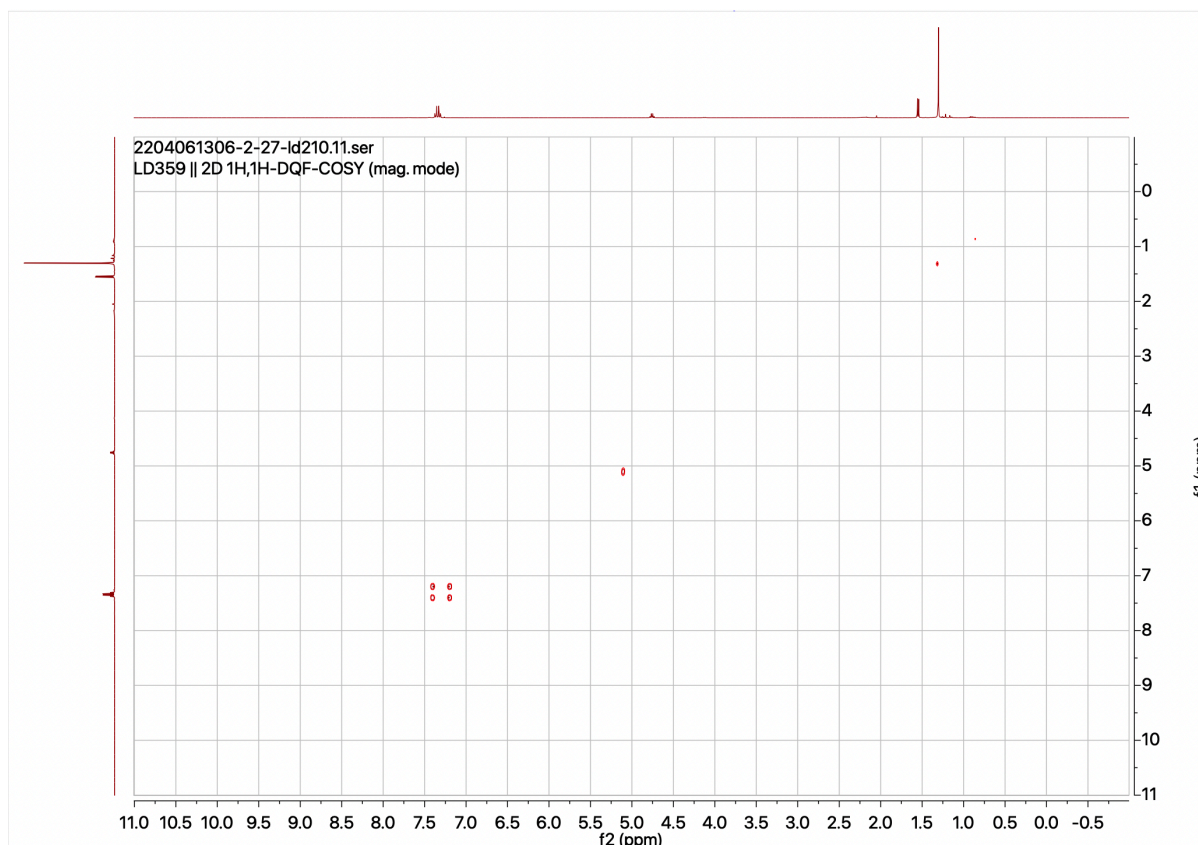
5-Ethynyl-1,3-dihydroisobenzofuran (20.0 mg, 0.139 mmol) was added to a solution of N-bromosuccinimide (29.6 mg, 0.167 mmol) and silver nitrate (2.36 mg, 0.0139 mmol) in acetone (0.404 mL) and the solution was stirred at room temperature for 3 hours. On completion, the solvent was removed under reduced pressure. The resulting residue was dissolved in water and the aqueous layer was extracted with diethyl ether (3 x). The combined organic layers were washed with brine, dried over magnesium sulfate, filtered and concentrated under reduced pressure. The crude was purified by column chromatography over silica gel (20% ethyl acetate in petroleum ether) to give the purified product as a yellow oil (16.4 mg, 53%). IR $\nu_{\text{max}}/\text{cm}^{-1}$ 2916 (C-H), 2849 (C-H), 1037 (C-O), 815. ^1H NMR (500 MHz, CDCl_3) δ_{H} 7.36 (1H, d, $J = 7.8$ Hz, ArH), 7.32 (1H, s, CCHC), 7.18 (1H, d, $J =$

7.8 Hz, ArH), 5.06-5.11 (4H, m, CH₂). ¹³C NMR (126 MHz, CDCl₃) δ_C 140.0, 139.6, 131.4, 124.7, 121.9, 121.2, 80.0 (alkyne C), 73.6 (CH₂), 73.4 (CH₂), 49.7 (CBr). HRMS (EI): Exact mass calculated for C₁₀H₇⁷⁹BrO: 221.9675, found: 221.9679.

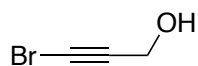
5-(5,5-Dimethylhexa-1,3-diyne-1-yl)-1,3-dihydroisobenzofuran (3.139)



A 30% butylamine/water solution (0.21 mL) was added to an RBF containing copper(I) chloride (1.78 mg, 0.0180 mmol) at 0 °C. A pinch of hydroxylamine hydrochloride was added until the blue colour disappeared. A solution of 5-(bromoethynyl)-1,3-dihydroisobenzofuran (16.3 mg, 0.0731 mmol) in DCM (0.1 mL) was added, quickly followed by a solution of 3,3-dimethylbut-1-yne (7.50 μL, 0.0601 mmol) in DCM (0.1 mL). The reaction was warmed to room temperature and stirred for 3 hours. On completion, the aqueous layer was extracted with DCM. The organic layer was dried over sodium sulfate, filtered and concentrated under vacuum to give the crude product. The crude was purified by column chromatography over silica gel (0 to 20% petroleum ether/ethyl acetate) to give the desired product as a yellow solid (8.4 mg, 65%). m.p. 41-43 °C. IR ν_{max}/cm⁻¹ 2964 (C-H), 2922 (C-H), 2862 (C-H), 1047 (C-O), 820. ¹H NMR (500 MHz, CDCl₃) δ_H 7.36-7.39 (1H, m, ArH), 7.31-7.34 (1H, s, CCHC), 7.17 (1H, d, *J* = 7.9 Hz, ArH), 5.08-5.10 (2H, m, CH₂), 5.06-5.08 (2H, m, CH₂), 1.29 (9H, s, (CH₃)₃). HRMS (ESI⁺): Exact mass calculated for C₁₆H₁₇O⁺ [M+H]⁺: 225.1279, found: 225.1276.

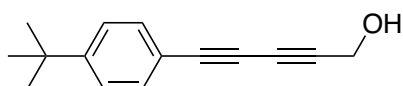


3-Bromoprop-2-yn-1-ol (3.149)



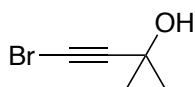
Propargyl alcohol (1.04 mL, 17.8 mmol) was added to a solution of N-bromosuccinimide (3.49 g, 19.6 mmol) and silver nitrate (302 mg, 1.78 mmol) in acetone (30 mL) and the solution was stirred at room temperature for 3 hours. On completion, the solvent was removed under reduced pressure. The resulting residue was dissolved in water and the aqueous layer was extracted three times with diethyl ether. The combined organic layers were washed with brine, dried over magnesium sulfate, filtered and concentrated under reduced pressure. The crude was purified by column chromatography over silica gel (20% ethyl acetate in petroleum ether) to give the purified product as a yellow oil (16.4 mg, 53%). ^1H NMR (500 MHz, CDCl_3) δ_{H} 4.30 (2H, d, $J = 6.0$ Hz, CH_2), 1.65-1.89 (1H, broad m, OH). Data is in agreement with that reported in the literature.²⁷⁶

5-(4-(*Tert*-butyl)phenyl)penta-2,4-diyne-1-ol (3.147)



A 30% butylamine/water solution (2.16 mL) was added to an RBF containing copper(I) chloride (18.8 mg, 0.190 mmol) at 0 °C. A pinch of hydroxylamine hydrochloride was added until the blue colour disappeared. A solution of 4-(*tert*-butyl)phenylacetylene (0.112 mL, 0.632 mmol) in DCM (0.82 mL) was added, quickly followed by a solution of 3-bromoprop-2-yn-1-ol (102.4 mg, 0.758 mmol) in DCM (0.82 mL). The reaction was warmed to room temperature and stirred for 3 hours. On completion, the aqueous layer was extracted with DCM. The organic layer was dried over sodium sulfate, filtered and concentrated under vacuum to give the crude product. The crude was purified by column chromatography over silica gel (0 to 20% petroleum ether/ethyl acetate) to give the purified product as a white solid (88.3 mg, 66%). m.p. 104-106 °C. IR $\nu_{\text{max}}/\text{cm}^{-1}$ 2947 (C-H), 1325 (O-H), 1117 (O-H), 1016 (O-H), 1009, 825. ^1H NMR (500 MHz, CDCl_3) δ_{H} 7.41-7.45 (2H, m, $(\text{CH}_3)_3\text{CCCHCH}$), 7.33-7.36 (2H, m, $(\text{CH}_3)_3\text{CCCHCH}$), 4.42 (1H, s, CHOH), 1.30 (9H, s, $(\text{CH}_3)_3$). ^{13}C NMR (126 MHz, CDCl_3) δ_{C} 153.0 ($(\text{CH}_3)_3\text{CC}$), 132.5 (2C, $(\text{CH}_3)_3\text{CCCHCH}$), 125.6 (2C, $(\text{CH}_3)_3\text{CCCHCH}$), 118.4 (CHOHCCCCC), 80.2 (CCHOH), 79.1 (CHCCC), 72.7 (alkyne C), 70.8 (alkyne C), 51.9 (CH_2OH), 35.1 ($(\text{CH}_3)_3\text{C}$), 31.2 (3C, $(\text{CH}_3)_3$). HRMS (ESI⁺): Exact mass calculated for $\text{C}_{15}\text{H}_{16}\text{ONa}^+$ $[\text{M}+\text{Na}]^+$: 235.1099, found: 235.1093.

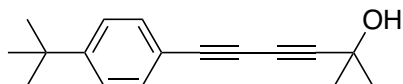
4-Bromo-2-methylbut-3-yn-2-ol (3.152)



2-Methylbut-3-yn-2-ol (1.15 mL, 11.9 mmol) was added to a solution of N-bromosuccinimide (2.33 g, 13.1 mmol) and silver nitrate (202.1 mg, 1.19 mmol) in acetone (20 mL) and the solution was stirred at room temperature for 3 hours. On completion, the solvent was removed under reduced pressure. The resulting residue was dissolved in water and the aqueous layer was extracted three times with diethyl ether. The combined organic layers were washed with brine, dried over magnesium sulfate, filtered and concentrated under reduced pressure. The crude was purified by column chromatography over silica gel (20% ethyl acetate in petroleum ether) to give the purified product as a colourless oil (1.38

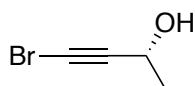
g, 60%). ^1H NMR (500 MHz, CDCl_3) δ_{H} 2.06 (1H, broad s, OH), 1.65-1.89 (6H, s, CH_3). Data is in agreement with that reported in the literature.²⁷⁷

6-(4-(*Tert*-butyl)phenyl)-2-methylhexa-3,5-diyne-2-ol (3.148)



A 30% butylamine/water solution (2.16 mL) was added to an RBF containing copper(I) chloride (18.8 mg, 0.190 mmol) at 0 °C. A pinch of hydroxylamine hydrochloride was added until the blue colour disappeared. A solution of 4-(*tert*-butyl)phenylacetylene (0.112 mL, 0.632 mmol) in DCM (0.82 mL) was added, quickly followed by a solution of 4-bromo-2-methylbut-3-yn-2-ol (123.6 mg, 0.758 mmol) in DCM (0.82 mL). The reaction was warmed to room temperature and stirred for 3 hours. On completion, the aqueous layer was extracted with DCM. The organic layer was dried over sodium sulfate, filtered and concentrated under vacuum to give the crude product. The crude was purified by column chromatography over silica gel (0 to 20% petroleum ether/ethyl acetate) to give the purified product as a white solid (107.8 mg, 71%). m.p. 110-112 °C. IR $\nu_{\text{max}}/\text{cm}^{-1}$ 2970 (C-H), 2901 (C-H), 2361, 1363 (O-H), 1066 (O-H), 839. ^1H NMR (500 MHz, CDCl_3) δ_{H} 7.40-7.44 (2H, m, $(\text{CH}_3)_3\text{CCCHCH}$), 7.32-7.35 (2H, m, $(\text{CH}_3)_3\text{CCCHCH}$), 1.94 (1H, s, OH), 1.58 (6H, s, $(\text{CH}_3)_2$), 1.31 (9H, s, $(\text{CH}_3)_3$). ^{13}C NMR (126 MHz, CDCl_3) δ_{C} 152.9 ($(\text{CH}_3)_3\text{CC}$), 132.5 (2C, $(\text{CH}_3)_3\text{CCCHCH}$), 125.6 (2C, $(\text{CH}_3)_3\text{CCCHCH}$), 118.6 (CHOHCCCC), 86.4 (CCOH), 79.3 (CHCCC), 72.7 (CCCCOH), 67.4 (CCCCOH), 51.9 (CH_2OH), 35.1 ($(\text{CH}_3)_3\text{C}$), 31.3 (2C, $\text{C}(\text{CH}_3)_2$), 31.3 (3C, $(\text{CH}_3)_3$). HRMS (ESI⁺): Exact mass calculated for $\text{C}_{17}\text{H}_{20}\text{ONa}^+$ $[\text{M}+\text{Na}]^+$: 263.1412, found: 263.1406.

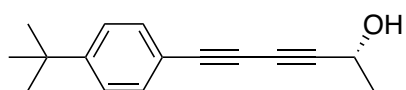
(*R*)-4-Bromobut-3-yn-2-ol ((*R*)-3.108)



(*R*)-(-)-3-Butyn-2-ol (0.559 mL, 7.13 mmol) was added to a solution of N-bromosuccinimide (1.40 g, 7.85 mmol) and silver nitrate (121.2 mg, 0.713 mmol) in acetone (12 mL) and the solution was stirred at room temperature for 3 hours. On completion, the solvent was removed under reduced pressure. The resulting residue was dissolved in water (3 mL) and the aqueous layer was extracted with diethyl ether (3 x 3 mL). The combined organic layers were washed with brine (5 mL), dried over magnesium sulfate, filtered and concentrated

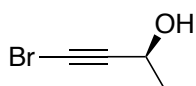
under reduced pressure. The crude was purified by column chromatography over silica gel (20% ethyl acetate in petroleum ether) to give the purified product as a yellow liquid (734.4 mg, 69%). IR $\nu_{\max}/\text{cm}^{-1}$ 2984 (C-H), 1373 (O-H), 1265, 1119 (C-O), 1043 (C-O). ^1H NMR (400 MHz, CDCl_3) δ_{H} 4.55 (1H, qd, $J = 6.6, 5.4$ Hz, CHOH), 1.46 (3H, dd, $J = 6.6$ Hz, CH_3). ^{13}C NMR (126 MHz, CDCl_3) δ_{C} 81.8 (alkyne **C**), 59.3 (CHOH), 44.6 (CBr), 24.1 (CH_3). HRMS (ESI^+): Exact mass calculated for $\text{C}_4\text{H}_6^{79}\text{BrO}^+$: 148.9597, found: 148.9590. $[\alpha]_{\text{D}}^{20} = +23.1^\circ$ ($c = 0.0167$, CHCl_3).

(R)-6-(4-(Tert-butyl)phenyl)hexa-3,5-diyn-2-ol ((R)-3.112)



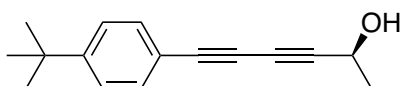
A 30% butylamine/water solution (2.16 mL) was added to an RBF containing copper(I) chloride (18.8 mg, 0.190 mmol) at 0 °C. A pinch of hydroxylamine hydrochloride was added until the blue colour disappeared. A solution of 4-(*tert*-butyl)phenylacetylene (0.112 mL, 0.632 mmol) in DCM (0.82 mL) was added, quickly followed by a solution of (*S*)-4-bromobut-3-yn-2-ol (113.0 mg, 0.758 mmol) in DCM (0.82 mL). The reaction was warmed to room temperature and stirred for 3 hours. On completion, the aqueous layer was extracted with DCM. The organic layer was dried over sodium sulfate, filtered and concentrated under vacuum to give the crude product. The crude was purified by column chromatography over silica gel (0 to 20% petroleum ether/ethyl acetate) to give the purified product as a white solid (98.4 mg, 69%). m.p. 81-83 °C. IR $\nu_{\max}/\text{cm}^{-1}$ 3297, 2957 (C-H), 1069 (O-H), 837. ^1H NMR (500 MHz, CDCl_3) δ_{H} 7.41-7.45 (2H, m, $(\text{CH}_3)_3\text{CCCHCH}$), 7.32-7.36 (2H, m, $(\text{CH}_3)_3\text{CCCHCH}$), 4.63-4.70 (1H, m, CHOH), 1.52 (3H, d, $J = 6.6$ Hz, CH_3), 1.30 (9H, s, $(\text{CH}_3)_3$). ^{13}C NMR (126 MHz, CDCl_3) δ_{C} 153.0 ($(\text{CH}_3)_3\text{CC}$), 132.5 (2C, $(\text{CH}_3)_3\text{CCCHCH}$), 125.6 (2C, $(\text{CH}_3)_3\text{CCCHCH}$), 118.5 (CHOHCCCCC), 83.7 (CCHOH), 79.2 (CHCCC), 72.6 (alkyne C), 69.2 (alkyne C), 59.1 (CHOH), 34.9 ($(\text{CH}_3)_3\text{C}$), 31.2 (3C, $(\text{CH}_3)_3$), 24.2 (CH_3). HRMS (ESI^+): Exact mass calculated for $\text{C}_{16}\text{H}_{18}\text{ONa}^+$ [$\text{M}+\text{Na}$] $^+$: 249.1250, found: 249.1250. $[\alpha]_{\text{D}}^{20} = +15.9^\circ$ ($c = 0.0076$, CHCl_3).

(S)-4-Bromobut-3-yn-2-ol ((S)-3.108)



(S)-(-)-3-Butyn-2-ol (0.559 mL, 7.13 mmol) was added to a solution of N-bromosuccinimide (1.40 g, 7.85 mmol) and silver nitrate (121.2 mg, 0.713 mmol) in acetone (12 mL) and the solution was stirred at room temperature for 3 hours. On completion, the solvent was removed under reduced pressure. The resulting residue was dissolved in water (3 mL) and the aqueous layer was extracted with diethyl ether (3 x 3 mL). The combined organic layers were washed with brine (5 mL), dried over magnesium sulfate, filtered and concentrated under reduced pressure. The crude was purified by column chromatography over silica gel (20% ethyl acetate in petroleum ether) to give the purified product as a yellow liquid (616.7 mg, 58%). IR $\nu_{\max}/\text{cm}^{-1}$ 2981 (C-H), 1371 (O-H), 1234, 1128 (C-O), 1069 (C-O). ^1H NMR (500 MHz, CDCl_3) δ_{H} 4.41-4.51 (1H, m, CHOH), 1.40 (3H, dd, $J = 6.6, 2.5$ Hz, CH_3). ^{13}C NMR (126 MHz, CDCl_3) δ_{C} 81.8 (alkyne C), 59.3 (CHOH), 44.6 (alkyne CBr), 24.1 (CH_3). HRMS (ESI⁺): Exact mass calculated for $\text{C}_4\text{H}_6^{79}\text{BrO}^+$: 148.9597, found: 148.9598. $[\alpha]_{\text{D}}^{20} = -24.1^\circ$ ($c = 0.0975$, CHCl_3).

(S)-6-(4-(*Tert*-butyl)phenyl)hexa-3,5-diyne-2-ol ((S)-3.112)

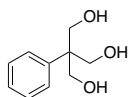


A 30% butylamine/water solution (2.16 mL) was added to an RBF containing copper(I) chloride (18.8 mg, 0.190 mmol) at 0 °C. A pinch of hydroxylamine hydrochloride was added until the blue colour disappeared. A solution of 4-(*tert*-butyl)phenylacetylene (0.112 mL, 0.632 mmol) in DCM (0.82 mL) was added, quickly followed by a solution of (S)-4-bromobut-3-yn-2-ol (113.0 mg, 0.758 mmol) in DCM (0.82 mL). The reaction was warmed to room temperature and stirred for 3 hours. On completion, the aqueous layer was extracted with DCM. The organic layer was dried over sodium sulfate, filtered and concentrated under vacuum to give the crude product. The crude was purified by column chromatography over silica gel (0 to 20% petroleum ether/ethyl acetate) to give the purified product as a white solid (196.0 mg, 73%). m.p. 78-80 °C. IR $\nu_{\max}/\text{cm}^{-1}$ 2963 (C-H), 1363, 1267 (O-H), 1132 (O-H), 1016 (O-H), 835. ^1H NMR (500 MHz, CDCl_3) δ_{H} 7.41-7.44 (2H, m, $(\text{CH}_3)_3\text{CCCH}$), 7.33-7.36

(2H, m, (CH₃)₃CCCHCH), 4.66 (1H, q, *J* = 6.5 Hz, CHOH), 1.52 (3H, d, *J* = 6.5 Hz, CH₃), 1.30 (9H, s, (CH₃)₃). ¹³C NMR (126 MHz, CDCl₃) δ_c 153.0 ((CH₃)₃CC), 132.5 (2C, (CH₃)₃CCCHCH), 125.6 (2C, (CH₃)₃CCCHCH), 118.5 (CHOHCCCC), 83.7 (CCHOH), 79.2 (CHCCC), 72.6 (alkyne C), 69.2 (alkyne C), 59.1 (CHOH), 35.1 ((CH₃)₃C), 31.3 (3C, (CH₃)₃), 24.2 (CH₃). HRMS (ESI⁺): Exact mass calculated for C₁₆H₁₈ONa⁺ [M+Na]⁺: 249.1250, found: 249.1250. [α]²⁰_D = -7.6° (c = 0.05, CHCl₃).

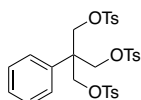
7.4 Chapter 4

2-(Hydroxymethyl)-2-phenylpropane-1,3-diol (4.66)



Phenylacetaldehyde (5.0 mL, 8.57 mmol) and calcium hydroxide (12.7 g, 42.9 mmol) were added to a suspension of paraformaldehyde (5.15 g, 171.5 mmol) in THF (65 mL). The reaction mixture was stirred at 60-65 °C for four days. After cooling to room temperature, the reaction mixture was filtered through celite and the celite was rinsed with DCM (50 mL). The filtrate was concentrated under reduced pressure to give the crude product. The crude product was purified by column chromatography over silica gel (1:1 hexane/ethyl acetate to 100% ethyl acetate) to give the desired product as a white solid (1.02 g, 65.3%). ¹H NMR (400 MHz, d⁶-DMSO) δ 7.39-7.43 (2H, m, CHC), 7.23-7.28 (2H, m, CHCHC), 7.12-7.17 (1H, m, CHCHCHC), 4.41 (3H, t, *J* = 5.2 Hz, OH), 3.71 (6H, d, *J* = 5.2 Hz, CH₂). Data is in agreement with that reported in the literature.¹

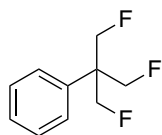
2-Phenyl-2-((tosyloxy)methyl)propane-1,3-diyl bis(4-methylbenzenesulfonate) (4.67)



p-Toluenesulfonyl chloride (11.0 g, 57.8 mmol) was added slowly to a solution of 2-(hydroxymethyl)-2-phenylpropane-1,3-diol (2.23 g, 12.3 mmol) in pyridine (25.3 mL) at 0 °C and the reaction was warmed to room temperature and stirred for three days. On completion, the reaction mixture was concentrated under reduced pressure. The resulting residue was dissolved in DCM (250 mL) and the suspension was filtered. The filtrate was

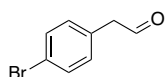
washed with water (250 mL). The organic phase was separated, and the aqueous phase was extracted with DCM (3 x 75 mL). The combined organic phases were washed with brine (125 mL), dried over magnesium sulfate, filtered, and concentrated under vacuum to give the crude product. The crude product was suspended in ethanol (37 mL) and the suspension was stirred vigorously and heated to 92 °C. The suspension was filtered to give the desired product as a white solid (2.81 g, 35.5%). ¹H NMR (500 MHz, CDCl₃) δ 7.62-7.66 (6H, m, ArH), 7.31-7.34 (6H, m, ArH), 7.15-7.22 (3H, m, ArH), 6.93-6.98 (2H, m, ArH), 4.20 (6H, s, CH₂), 2.48 (9H, s, CH₃). Data is in agreement with that reported in the literature.¹

(1,3-Difluoro-2-(fluoromethyl)propan-2-yl)benzene (4.68)



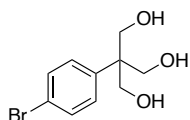
Cesium fluoride (8.48 g, 55.8 mmol) was added to a solution of 2-phenyl-2-((tosyloxy)methyl)propane-1,3-diyl bis(4-methylbenzenesulfonate) (2.00 g, 3.10 mmol) in DMSO (68 mL) and the reaction was heated to 120 °C and stirred for 24 h. On completion, the reaction mixture was diluted with water and the aqueous layer was extracted three times with diethyl ether. The combined organic layer was washed with water, dried over magnesium sulfate, filtered and concentrated under vacuum to give the crude product. The crude product was purified by column chromatography over silica gel (hexane/ethyl acetate, gradient from 0 to 10% ethyl acetate) to give the purified product as a yellow oil (417.8 mg, 71.4%). IR $\nu_{\max}/\text{cm}^{-1}$ 2970 (C-H), 2922 (C-H), 2361, 1717, 1028 (C-F), 1005 (C-F), 698. ¹H NMR (400 MHz, CDCl₃) δ 7.38-7.44 (4H, m, ArH), 7.31-7.37 (1H, m, ArH), 4.81 (6H, dt, *J* = 46.9, 1.5 Hz, CH₂F). ¹³C NMR (101 MHz, CDCl₃) δ 136.3 (CCCH₂), 129.1, 128.2, 127.0, 83.3 (3C, dt, *J* = 176.2, 5.9 Hz, CH₂F), 48.9 (apparent q, *J* = 17.1 Hz, CCH₂F). ¹⁹F NMR (376 MHz, CDCl₃), δ -230.9 (3F, t, *J* = 46.9 Hz, CH₂F). HRMS (EI): exact mass calculated for C₁₀H₁₁F₃, 188.0807; found 188.0807. Data is in agreement with that reported in the literature.¹

2-(4-Bromophenyl)acetaldehyde (4.75)



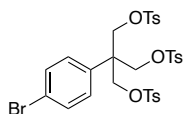
Dess-Martin periodinane (12.6 g, 30.3 mmol) was added to a stirred solution of 2-(4-bromophenyl)ethanol (3.86 mL, 27.5 mmol) in DCM (275 mL) and the reaction was stirred for 3 hours. The reaction was quenched by addition of sat. aq. sodium thiosulfate and sat. aq. sodium hydrogen carbonate. The aqueous layer was extracted with DCM (3x). The combined organic layers were washed with NaHCO₃ and brine, dried over sodium sulfate, filtered and concentrated to give the crude product. The crude product was dissolved in 9:1 hexane/ethyl acetate solution and filtered. The filtrate was concentrated under reduced pressure to give the purified product as a colourless liquid (4.53 g, 75.1%). ¹H NMR (400 MHz, CDCl₃) δ 9.74 (1H, t, *J* = 1.9 Hz, CHO), 7.47-7.52 (2H, m, ArH), 7.09 (2H, d, *J* = 8.9 Hz, CHCHCBr), 3.69 (2H, d, *J* = 1.9 Hz, CH₂). Data is in agreement with that reported in the literature.²

2-(4-Bromophenyl)-2-(hydroxymethyl)propane-1,3-diol (4.76)



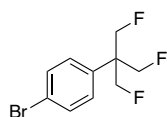
2-(4-Bromophenyl)acetaldehyde (4.53 g, 22.8 mmol) and calcium hydroxide (6.75 g, 94.0 mmol) were added to a suspension of paraformaldehyde (2.73 g, 91.0 mmol) in THF (35 mL). The reaction mixture was stirred at 60-65 °C for four days. After cooling to room temperature, the reaction mixture was filtered through celite and the celite was rinsed with DCM (50 mL). The filtrate was concentrated under reduced pressure to give the crude product. The crude product was purified by column chromatography over silica gel (1:1 hexane/ethyl acetate gradient to 100% ethyl acetate) to give the purified product as a white solid (2.99 g, 50%). m.p. 117-119 °C. IR $\nu_{\text{max}}/\text{cm}^{-1}$ 2868 (C-H), 1767 (C-H), 1580, 1454 (O-H), 1361 (O-H), 1132 (C-O), 1042 (C-O), 775, 750 (C-Br). ¹H NMR (400 MHz, d⁶-DMSO) δ 7.42-7.46 (2H, m, ArH), 7.35-7.39 (2H, m, ArH), 4.46 (3H, t, *J* = 5.2 Hz, OH), 3.67 (6H, d, *J* = 5.2 Hz, CH₂). HRMS (ESI⁺) exact mass calculated for C₁₀H₁₃O₃⁷⁹BrNa⁺ [M+Na]⁺: 282.9940; found 282.9938. Data is in agreement with that reported in the literature.³

**2-(4-Bromophenyl)-2-((tosyloxy)methyl)propane-1,3-diyl bis(4-methylbenzenesulfonate)
(4.77)**



p-Toluenesulfonyl chloride (9.47 g, 49.7 mmol) was added slowly to a solution of 2-(4-bromophenyl)-2-(hydroxymethyl)propane-1,3-diol (2.99 g, 10.6 mmol) in pyridine (21.9 mL) at 0 °C and the reaction was warmed to room temperature and stirred for three days. On completion, the reaction mixture was concentrated under reduced pressure. The resulting residue was dissolved in DCM (220 mL) and the suspension was filtered. The filtrate was washed with water (220 mL). The organic phase was separated, and the aqueous phase was extracted with DCM (3 x 65 mL). The combined organic phases were washed with brine (110 mL), dried over magnesium sulfate, filtered and concentrated under vacuum to give the crude product. The crude product was suspended in ethanol (30 mL) and the suspension was stirred vigorously and heated to 92 °C. The suspension was filtered to give the purified product as a white solid (4.78 g, 62%). m.p. 134-136 °C. IR $\nu_{\text{max}}/\text{cm}^{-1}$ 1356 (S=O), 1171 (C-O), 989, 968, 820, 667, 548. ^1H NMR (400 MHz, CDCl_3) δ 7.59-7.62 (6H, m, ArH), 7.30-7.33 (6H, m, ArH), 7.22-7.25 (2H, m, ArH), 6.76-6.79 (2H, m, ArH), 4.15 (6H, s, CH_2O), 2.47 (9H, s, CH_3). ^{13}C NMR (126 MHz, CDCl_3) δ 145.6 (ArC), 133.9 (ArC), 131.9 (ArC), 131.6 (ArC), 130.1 (ArC), 127.9 (ArC), 127.9 (ArC), 122.4 (ArC), 68.5 (CH_2O), 46.0 (CCH_2O), 21.8 (Ar CH_3). HRMS (ESI⁺) exact mass calculated for $\text{C}_{31}\text{H}_{31}\text{O}_9^{79}\text{BrS}_3\text{Na}^+$ [M+Na]⁺: 745.0182; found 745.0199.

1-Bromo-4-(1,3-difluoro-2-(fluoromethyl)propan-2-yl)benzene (4.78)



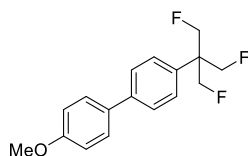
Cesium fluoride (1.89 g, 12.4 mmol) was added to a solution of 2-phenyl-2-((tosyloxy)methyl)propane-1,3-diyl bis(4-methylbenzenesulfonate) (500 mg, 0.691 mmol) in DMSO (15 mL) and the reaction was heated to 120 °C and stirred for 24 h. On completion, the reaction mixture was diluted with water and the aqueous layer was extracted three times with diethyl ether. The combined organic layer was washed with water, dried over magnesium sulfate, filtered and concentrated under vacuum to give the crude product. The

crude product was purified by column chromatography over silica gel (hexane/ethyl acetate, gradient from 0 to 10% ethyl acetate) to give the purified product as a yellow oil (136.2 mg, 74%). IR $\nu_{\max}/\text{cm}^{-1}$ 2972, 2916 (C-H), 1497, 1072 (C-F), 1028 (C-F), 1003 (C-F), 818 (C-Br). ^1H NMR (400 MHz, CDCl_3) δ 7.51-7.56 (2H, m, ArH), 7.28-7.32 (2H, m, ArH), 4.77 (6H, dt, $J = 47.0$, 1.6 Hz, CH_2F). ^{13}C NMR (126 MHz, CDCl_3) δ 135.4 (ArC), 132.2 (ArC), 128.8 (ArC), 122.4 (ArC), 82.9 (3C, dt, $J = 177.1$, 5.9 Hz, CH_2F), 41.1 (CCH_2F). ^{19}F NMR (376 MHz, CDCl_3) δ -231.0 (3F, t, $J = 47.0$ Hz, CH_2F). HRMS (EI) exact mass calculated for $\text{C}_{10}\text{H}_{10}^{79}\text{BrF}_3$: 265.9913; found 265.9914.

General procedure for Suzuki cross-coupling reactions (General Method A)

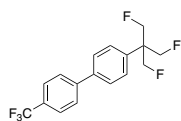
Tetrakis(triphenylphosphine)palladium(0) (5 mol%) was added to a solution of 1-bromo-4-(1,3-difluoro-2-(fluoromethyl)propan-2-yl)benzene (1 equiv.), boronic acid (1.2 equiv.) and potassium carbonate (2 equiv.) in 3:1 THF/water solution (0.2 M) and the reaction was heated to reflux and stirred for 18 h. Subsequently, the reaction was cooled to room temperature and diluted with water. The aqueous layer was extracted three times with DCM. The combined organic layers were washed with brine, dried over sodium sulfate, filtered and concentrated under vacuum to give the crude product. The crude was purified by column chromatography over silica gel (hexane/DCM 7:3).

4-(1,3-Difluoro-2-(fluoromethyl)propan-2-yl)-4'-methoxy-1,1'-biphenyl (4.78)



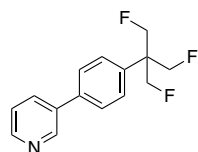
This compound was prepared according to General Procedure A. The compound was isolated as a white solid (31.9 mg, 90%). m.p. 118-120 °C. IR $\nu_{\max}/\text{cm}^{-1}$ 2920, 2853 (C-H), 1604, 1501, 1253, 1186, 1028, 1003, 821, 810. ^1H NMR (500 MHz, CDCl_3) δ 7.57-7.61 (2H, m, ArH), 7.51-7.54 (2H, m, ArH), 7.45-7.48 (2H, m, ArH), 6.97-7.00 (2H, m, ArH), 4.84 (6H, dt, $J = 47.0$, 1.5 Hz, CH_2), 3.86 (3H, s, CH_3). ^{13}C NMR (126 MHz, CDCl_3) δ 140.5 (ArC), 134.4 (ArC), 132.8 (ArC), 128.1 (ArC), 127.3 (ArC), 127.2 (ArC), 114.3 (ArC), 83.2 (3C, dt, $J = 176.7$, 5.9 Hz, CH_2F), 55.4 (apparent q, $J = 16.5$ Hz, CCH_2F), 29.7 (CH_3). ^{19}F NMR (377 MHz, CDCl_3) δ -230.8 (3F, t, $J = 47.0$ Hz, CH_2F). HRMS (ESI $^+$) exact mass calculated for $\text{C}_{17}\text{H}_{17}\text{OF}_3\text{Na}^+ [\text{M}+\text{Na}]^+$: 317.1129; found 317.1125.

Methyl 4'-(1,3-difluoro-2-(fluoromethyl)propan-2-yl)-[1,1'-biphenyl]-4-carboxylate (4.79)



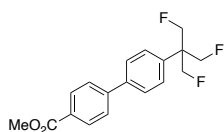
This compound was prepared according to General Procedure A. The compound was isolated as a white solid (12.3 mg, 27%). m.p. 72-74 °C. IR $\nu_{\max}/\text{cm}^{-1}$ 2961, 2916 (C-H), 1616 (C=C), 1325 (C-F), 1165, 1138, 1126, 1109, 1066, 1016, 1004, 822. ^1H NMR (500 MHz, CDCl_3) δ 7.66-7.73 (4H, m, ArH), 7.62-7.66 (2H, m, ArH), 7.51-7.56 (2H, m, ArH), 4.85 (6H, dt, $J = 47.0, 1.5$ Hz, CH_2). ^{13}C NMR (126 MHz, CDCl_3) δ 143.8 (ArC), 139.4 (ArC), 129.6 (q, $J = 32.6$ Hz, CF_3), 127.8 (ArC), 127.6 (ArC), 127.4 (ArC), 125.8 (q, $J = 3.7$ Hz, CCF_3), 83.0 (3C, dt, $J = 176.2, 5.9$ Hz, CH_2F), 48.8 (q, $J = 16.8$ Hz, CCH_2F). ^{19}F NMR (376 MHz, CDCl_3) δ -62.4 (3F, s, CF_3), -230.9 (3F, t, $J = 47.0$ Hz, CF_2H). HRMS (ESI⁺) exact mass calculated for $\text{C}_{17}\text{H}_{14}\text{F}_6\text{Na}^+$ $[\text{M}+\text{Na}]^+$: 355.0897; found 355.0892.

3-(4-(1,3-Difluoro-2-(fluoromethyl)propan-2-yl)phenyl)pyridine (4.80)



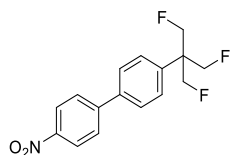
This compound was prepared according to General Procedure A. The compound was isolated as a white solid (43.1 mg, 64%). m.p. 95-97 °C. IR $\nu_{\max}/\text{cm}^{-1}$ 2972, 2911, 1474, 1437, 1186, 1119, 1026, 1001, 802, 719, 711. ^1H NMR (500 MHz, CDCl_3) δ 8.85 (1H, m, ArH), 8.61 (1H, m, ArH), 7.87 (1H, dt, $J = 7.9, 2.1$ Hz, ArH), 7.63 (2H, dt, $J = 8.7, 2.1$ Hz, ArH), 7.55 (2H, dt, $J = 8.3, 2.1$ Hz, ArH), 7.36-7.41 (1H, m, ArH), 4.85 (6H, dt, $J = 46.9, 1.5$ Hz, CH_2F). ^{13}C NMR (126 MHz, CDCl_3) δ 148.9 (ArC), 148.4 (ArC), 137.7 (ArC), 136.3 (ArC), 136.0 (ArC), 134.5 (ArC), 132.3 (ArC), 132.2 (ArC), 127.8 (ArC), 127.8 (ArC), 123.8 (ArC), 83.2 (3C, dt, $J = 176.6, 5.9$ Hz, CH_2F). $^{19}\text{F}\{^1\text{H}\}$ NMR (470 MHz, CDCl_3) δ -231.0 (3F, s, CH_2F). HRMS (ESI⁺) exact mass calculated for $\text{C}_{15}\text{H}_{14}\text{F}_3\text{NNa}^+$ $[\text{M}+\text{Na}]^+$: 288.0976; found 288.0971.

4-(1,3-Difluoro-2-(fluoromethyl)propan-2-yl)-4'-methoxy-1,1'-biphenyl (4.81)



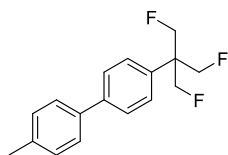
This compound was prepared according to General Procedure A. The compound was isolated as a white solid (39.3 mg, 73%). m.p. 92-94 °C. IR $\nu_{\max}/\text{cm}^{-1}$ 2956, 2922, 2853 (C-H), 1714 (C=O), 1436 (C-H), 1280 (C-F), 1101 (C-O). ^1H NMR (500 MHz, CDCl_3) δ 8.10-8.13 (2H, m, ArH), 7.64-7.68 (4H, m, ArH), 7.51-7.54 (2H, m, ArH), 4.84 (6H, dt, $J = 46.9, 1.6$ Hz, CH_2), 3.94 (3H, s, CH_3). ^{13}C NMR (126 MHz, CDCl_3) δ 166.9 (C=O), 144.7 (ArC), 139.7 (ArC), 136.1 (ArC), 130.2 (ArC), 129.2 (ArC), 127.7 (ArC), 127.5 (ArC), 127.0 (ArC), 83.0 (dt, $J = 176.2, 5.4$ Hz, CH_2F), 52.2 (CH_3), 48.7 (apparent q, $J = 16.9$ Hz, CCH_2F). $^{19}\text{F}\{^1\text{H}\}$ NMR (376 MHz, CDCl_3) δ -230.9 (3F, s, CH_2F). HRMS (ESI⁺) exact mass calculated for $\text{C}_{18}\text{H}_{18}\text{F}_3\text{O}_2^+[\text{M}+\text{H}]^+$: 323.1259; found 323.1250.

4-(1,3-Difluoro-2-(fluoromethyl)propan-2-yl)-4'-nitro-1,1'-biphenyl (4.82)



This compound was prepared according to General Procedure A. The compound was isolated as a white solid (16.4 mg, 32%). m.p. 114-116 °C. IR $\nu_{\max}/\text{cm}^{-1}$ 2972 (C-H), 2920 (C-H), 1514 (N-O), 1341 (N-O), 1018 (C-N), 825 (C=C). ^1H NMR (400 MHz, CDCl_3) δ 8.29-8.33 (2H, m, ArH), 7.72-7.76 (2H, m, ArH), 7.65-7.69 (2H, m, ArH), 7.54-7.59 (2H, m, ArH), 4.85 (6H, dt, $J = 46.8, 1.5$ Hz, CH_2F). ^{13}C NMR (126 MHz, CDCl_3) δ 147.4 (ArC), 146.8 (ArC), 138.6 (ArC), 137.2 (ArC), 128.5 (ArC), 127.9 (ArC), 124.5 (ArC), 124.3 (ArC), 83.1 (3C, dt, $J = 176.7, 5.9$ Hz, CH_2F), 49.0 (apparent q, $J = 16.7$ Hz, CCH_2F). $^{19}\text{F}\{^1\text{H}\}$ NMR (376 MHz, CDCl_3) δ -231.0 (3F, s, CH_2F). HRMS (ESI⁺) exact mass calculated for $\text{C}_{16}\text{H}_{14}\text{F}_3\text{NO}_2\text{Na}^+[\text{M}+\text{Na}]^+$: 332.0874; found 332.0869.

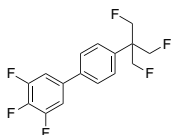
4-(1,3-Difluoro-2-(fluoromethyl)propan-2-yl)-4'-methyl-1,1'-biphenyl (4.83)



This compound was prepared according to General Procedure A.

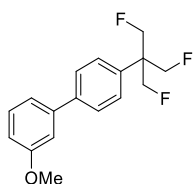
Tetrakis(triphenylphosphine)palladium(0) (14.6 mg, 5 mol%) was added to a solution of 1-bromo-4-(1,3-difluoro-2-(fluoromethyl)propan-2-yl)benzene (67.4 mg, 0.252 mmol), 4-tolylboronic acid (41.1 mg, 0.302 mmol) and potassium carbonate (69.7 mg, 0.504 mmol) in 3:1 THF/water solution (1.25 mL) and the reaction was heated to reflux and stirred for 18 h. Subsequently, the reaction was cooled to room temperature and diluted with water. The aqueous layer was extracted three times with DCM. The combined organic layers were washed with brine, dried over sodium sulfate, filtered and concentrated under vacuum to give the crude product. The crude was purified by column chromatography over silica gel (hexane/DCM 7:3). The compound was isolated as a white solid (34.6 mg, 49%). m.p. 98-100 °C. IR $\nu_{\text{max}}/\text{cm}^{-1}$ 2972, 2918 (C-H), 1501 (C=C), 1028, 991, 810. ^1H NMR (500 MHz, CDCl_3) δ 7.60-7.64 (2H, m, ArH), 7.46-7.53 (4H, m, ArH), 7.25-7.29 (2H, m, ArH), 4.85 (6H, dt, $J = 47.0$, 1.5 Hz, CH_2), 2.41 (3H, s, CH_3). ^{13}C NMR (126 MHz, CDCl_3) δ 140.8 (ArC), 137.4 (ArC), 134.8 (ArC), 129.6 (ArC), 127.4 (ArC), 127.3 (ArC), 126.9 (ArC), 83.1 (3C, dt, $J = 176.8$, 5.8 Hz, CH_2F), 48.6 (q, $J = 17.1$ Hz, CCH_2), 21.2 (CH_3). $^{19}\text{F}\{^1\text{H}\}$ NMR (376 MHz, CDCl_3) δ -230.8 (3F, s, CH_2F). HRMS (ESI⁺) exact mass calculated for $\text{C}_{17}\text{H}_{17}\text{F}_3\text{Na}^+$: 301.1175; found 301.1169.

4'-(1,3-Difluoro-2-(fluoromethyl)propan-2-yl)-3,4,5-trifluoro-1,1'-biphenyl (4.84)



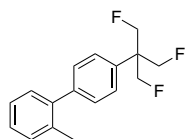
This compound was prepared according to General Procedure A. The compound was isolated as a yellow oil (10.1 mg, 39.2%). ^1H NMR (400 MHz, CDCl_3) δ 7.49-7.56 (4H, m, ArH), 7.15-7.21 (2H, m, ArH), 4.83 (6H, dt, $J = 46.8$, 1.5 Hz, CH_2F). $^{19}\text{F}\{^1\text{H}\}$ NMR (376 MHz, CDCl_3) δ -231.0 (3F, s, CH_2F), -162.1 (1F, t, $J = 20.2$ Hz, CF), -133.8 (2F, d, $J = 20.2$ Hz, CHCF). HRMS (ESI⁺) exact mass calculated for $\text{C}_{16}\text{H}_{12}\text{F}_6\text{Na}^+$ [M+Na]⁺: 341.0741; found 341.0735.

4'-(1,3-Difluoro-2-(fluoromethyl)propan-2-yl)-3-methoxy-1,1'-biphenyl (4.85)



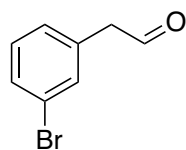
This compound was prepared according to General Procedure A. The compound was isolated as a white solid (22.8 mg, 52%). m.p. 70-72 °C. IR $\nu_{\text{max}}/\text{cm}^{-1}$ 2955 (C-H), 1172 (C-F), 1024 (C-F), 999, 787. ^1H NMR (500 MHz, CDCl_3) δ 7.61-7.65 (2H, m, ArH), 7.48-7.53 (2H, m, ArH), 7.34-7.40 (1H, m, ArH), 7.16-7.20 (1H, m, ArH), 7.11-7.14 (1H, m, ArH), 6.90-6.94 (1H, m, ArH), 4.85 (6H, dt, $J = 46.8, 1.6$ Hz, CH_2), 3.87 (3H, s, CH_3). ^{13}C NMR (126 MHz, CDCl_3) δ 160.1 (ArC), 141.9 (ArC), 140.9 (ArC), 135.4 (ArC), 130.0 (ArC), 127.8 (ArC), 127.4 (ArC), 119.7 (ArC), 113.0 (ArC), 83.2 (3C, dt, $J = 176.2, 5.9$ Hz, CH_2F), 55.4 (CH_3), 48.8 (q, $J = 17.3$ Hz, CCH_2F). $^{19}\text{F}\{^1\text{H}\}$ NMR (376 MHz, CDCl_3) δ -230.8 (3F, s, CH_2F). HRMS (ESI) exact mass calculated for $\text{C}_{17}\text{H}_{17}\text{F}_3\text{ONa}^+ [\text{M}+\text{Na}]^+$: 317.1129; found 317.1124.

4'-(1,3-Difluoro-2-(fluoromethyl)propan-2-yl)-2-methyl-1,1'-biphenyl (4.86)



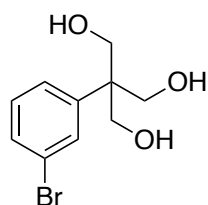
This compound was prepared according to General Procedure A. The compound was isolated as a white solid (33.6 mg, 73.6%). m.p. 66-68 °C. IR $\nu_{\text{max}}/\text{cm}^{-1}$ 2970 (C-H), 2901 (C-H), 2361, 1485, 1015 (C-F), 997, 982, 633. ^1H NMR (500 MHz, CDCl_3) δ 7.44-7.48 (2H, m, ArH), 7.35-7.39 (2H, m, ArH), 7.20-7.30 (4H, m, ArH), 4.86 (6H, dt, $J = 46.9, 1.5$ Hz, CH_2), 2.28 (3H, s, CH_3). ^{13}C NMR (126 MHz, CDCl_3) δ 141.8 (ArC), 141.2 (ArC), 135.5 (ArC), 134.7 (ArC), 130.5 (ArC), 129.8 (ArC), 127.6 (ArC), 126.7 (ArC), 126.0 (ArC), 83.3 (3C, dt, $J = 176.7, 5.9$ Hz, CH_2F), 48.8 (apparent q, $J = 16.8$ Hz, CCH_2F), 20.6 (CH_3). $^{19}\text{F}\{^1\text{H}\}$ NMR (376 MHz, CDCl_3) δ -230.8 (3F, s, CH_2F). HRMS (ESI $^+$) exact mass calculated for $\text{C}_{17}\text{H}_{17}\text{F}_3\text{Na}^+$: 301.1180; found 301.1175.

2-(3-Bromophenyl)acetaldehyde (4.89)



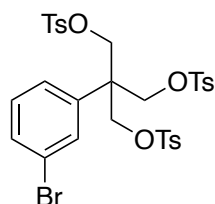
Dess-Martin periodinane (5.62 g, 13.2 mmol) was added to a stirred solution of 3-bromophenethyl alcohol (1.64 mL, 12.0 mmol) in DCM (120 mL) and the reaction was stirred for 3 hours. The reaction was quenched by addition of sat. aq. sodium thiosulfate and sat. aq. sodium hydrogen carbonate. The aqueous layer was extracted with DCM (3x). The combined organic layers were washed with NaHCO₃ and brine, dried over sodium sulfate, filtered and concentrated to give the crude product. The crude product was dissolved in 9:1 hexane/ethyl acetate solution and filtered. The filtrate was concentrated under reduced pressure to give the purified product as a colourless liquid (703 mg, 29%). ¹H NMR (400 MHz, CDCl₃) δ 9.75 (1H, td, *J* = 2.4, 1.0 Hz, CHO), 7.42-7.47 (1H, m, ArH), 7.39 (1H, t, *J* = 2.0 Hz, ArH), 7.24 (1H, t, *J* = 7.7 Hz, ArH), 7.15 (1H, d, *J* = 7.7 Hz, ArH), 3.68 (2H, d, *J* = 2.0 Hz, CH₂). Data is in agreement with that reported in the literature.²⁷⁸

2-(3-Bromophenyl)-2-(hydroxymethyl)propane-1,3-diol (4.90)



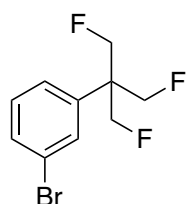
2-(3-Bromophenyl)acetaldehyde (703 mg, 3.53 mmol) and calcium hydroxide (1.08 g, 14.1 mmol) were added to a suspension of paraformaldehyde (423 mg, 14.1 mmol) in THF (5.43 mL). The reaction mixture was stirred at 60-65 °C for four days. After cooling to room temperature, the reaction mixture was filtered through celite and the celite was rinsed with DCM (50 mL). The filtrate was concentrated under reduced pressure to give the crude product. The crude product was purified by column chromatography over silica gel (1:1 hexane/ethyl acetate gradient to 100% ethyl acetate) to give the desired product as an impure white solid (440.5 mg, 48%). ¹H NMR (400 MHz, d⁶-DMSO) δ 7.59 (1H, t, *J* = 1.9 Hz, ArH), 7.18-7.44 (3H, m, ArH), 4.46-4.54 (3H, m, OH), 3.66 (6H, d, *J* = 3.8 Hz, CH₂).

2-(3-Bromophenyl)-2-((tosyloxy)methyl)propane-1,3-diyl bis(4-methylbenzenesulfonate)
(4.91)



p-Toluenesulfonyl chloride (3.06 g, 16.0 mmol) was added slowly to a solution of 2-(3-bromophenyl)-2-(hydroxymethyl)propane-1,3-diol (891 mg, 3.41 mmol) in pyridine (7.08 mL) at 0 °C and the reaction was warmed to room temperature and stirred for three days. On completion, the reaction mixture was concentrated under reduced pressure. The resulting residue was dissolved in DCM (70 mL) and the suspension was filtered. The filtrate was washed with water (70 mL). The organic phase was separated, and the aqueous phase was extracted with DCM (3 x 21 mL). The combined organic phases were washed with brine (35 mL), dried over magnesium sulfate, filtered and concentrated under vacuum to give the crude product. The crude product was suspended in ethanol and the suspension was stirred vigorously and heated to 92 °C. The suspension was filtered to give the desired product as an impure white solid (2.12 g, 65%). ¹H NMR (400 MHz, CDCl₃) δ 7.59-7.64 (6H, m, ArH), 7.29-7.34 (6H, m, ArH), 7.03-7.10 (2H, m, ArH), 6.89-6.93 (2H, m, ArH), 4.14 (6H, s, CH₂O), 2.46 (9H, s, 3 x CH₃). HRMS (ESI⁺) exact mass calculated for C₃₂H₃₄O₉S₃Na⁺ [M+Na]⁺: 681.1263; found 681.1257.

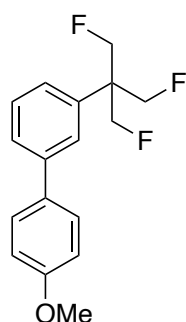
1-Bromo-3-(1,3-difluoro-2-(fluoromethyl)propan-2-yl)benzene (4.87)



Cesium fluoride (1.02 g, 6.70 mmol) was added to a solution of 2-(p-tolyl)-2-((tosyloxy)methyl)propane-1,3-diyl bis(4-methylbenzenesulfonate) (245.2 mg, 0.372 mmol) in DMSO (8.15 mL) and the reaction was heated to 120 °C and stirred for 24 h. On completion, the reaction mixture was diluted with water and the aqueous layer was extracted three times with diethyl ether. The combined organic layer was washed with

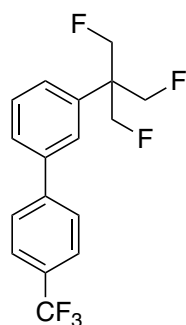
water, dried over magnesium sulfate, filtered and concentrated under vacuum to give the crude product. The crude product was purified by column chromatography over silica gel (hexane/ethyl acetate, gradient from 0 to 10% ethyl acetate) to give the desired product as an impure yellow oil (53.0 mg, 71%). ^1H NMR (400 MHz, CDCl_3) δ 7.56 (1H, t, $J = 1.9$ Hz, ArH), 7.48 (1H, ddd, $J = 7.9, 1.9, 1.1$ Hz, ArH), 7.34-7.38 (1H, m, ArH), 7.27-7.30 (1H, m, ArH), 4.77 (6H, dt, $J = 46.8, 1.5$ Hz, CH_2F). $^{19}\text{F}\{^1\text{H}\}$ NMR (376 MHz, CDCl_3) δ -231.0 (3F, s, CH_2F).

3-(1,3-Difluoro-2-(fluoromethyl)propan-2-yl)-4'-methoxy-1,1'-biphenyl (4.92)



This compound was prepared according to General Procedure A. The compound was isolated as an impure yellow solid (74% conversion by ^{19}F NMR). ^1H NMR (400 MHz, CDCl_3) δ 7.56-7.59 (1H, m, ArH), 7.49-7.52 (4H, m, ArH), 7.33-7.37 (1H, m, ArH), 6.97-7.01 (2H, m, ArH), 4.85 (6H, dt, $J = 46.9, 1.5$ Hz, CH_2F), 3.86 (3H, s, CH_3). $^{19}\text{F}\{^1\text{H}\}$ NMR (376 MHz, CDCl_3) δ -230.7 (3F, s, CH_2F). HRMS (ESI $^+$) exact mass calculated for $\text{C}_{17}\text{H}_{17}\text{F}_3\text{ONa}^+$ [$\text{M}+\text{Na}$] $^+$: 317.1124; found 317.1124.

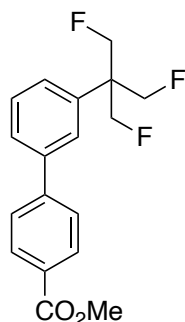
3-(1,3-Difluoro-2-(fluoromethyl)propan-2-yl)-4'-(trifluoromethyl)-1,1'-biphenyl (4.93)



This compound was prepared according to General Procedure A. The compound was isolated as an impure yellow solid (49% conversion by ^{19}F NMR). ^1H NMR (400 MHz, CDCl_3) δ 7.66-7.73 (4H, m, ArH), 7.61-7.64 (1H, m, ArH), 7.44-7.50 (2H, m, ArH), 7.27-7.31 (1H, m,

ArH), 4.86 (6H, dt, $J = 46.9, 1.5$ Hz, CH_2F). $^{19}\text{F}\{^1\text{H}\}$ NMR (376 MHz, CDCl_3) δ -62.4 (3F, s, CF_3), -230.8 (3F, s, CH_2F). HRMS (EI) exact mass calculated for $\text{C}_{17}\text{H}_{14}\text{F}_6$: 332.0994; found 332.0995.

Methyl 3'-(1,3-difluoro-2-(fluoromethyl)propan-2-yl)-[1,1'-biphenyl]-4-carboxylate (4.94)

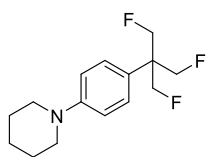


This compound was prepared according to General Procedure A. The compound was isolated as an impure yellow solid (45% conversion by ^{19}F NMR). ^1H NMR (400 MHz, CDCl_3) δ 8.09-8.14 (2H, m, ArH), 7.62-7.71 (4H, m, ArH), 7.27-7.31 (2H, m, ArH), 4.85 (6H, dt, $J = 46.9, 1.5$ Hz, CH_2F), 3.95 (3H, s, CH_3). $^{19}\text{F}\{^1\text{H}\}$ NMR (376 MHz, CDCl_3) δ -230.8 (3F, s, CH_2F). HRMS (ESI^+) exact mass calculated for $\text{C}_{17}\text{H}_{17}\text{F}_3\text{ONa}^+ [\text{M}+\text{Na}]^+$: 345.1073; found 345.1073.

General procedure for Buchwald-Hartwig cross-coupling reactions (General Method B)

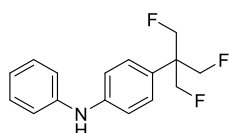
1-bromo-4-(1,3-difluoro-2-(fluoromethyl)propan-2-yl)benzene (1.0 equiv.), amine (1.2 equiv.), palladium(II) acetate (10 mol%), Xantphos (10 mol%) and cesium carbonate (2.0 equiv.) were dissolved in 1,4-dioxane (0.187 M) under nitrogen. The reaction was heated to 100 °C and stirred overnight. On completion, the reaction was cooled to room temperature and the mixture was filtered through celite, eluting with ethyl acetate. The filtrate was washed with saturated aqueous ammonium chloride and brine, dried over magnesium sulfate, filtered and concentrated under vacuum to give the crude product. The crude was purified by column chromatography over silica gel (hexane/ethyl acetate, gradient 0 to 100% ethyl acetate).

1-(4-(1,3-Difluoro-2-(fluoromethyl)propan-2-yl)phenyl)piperidine (4.95)



This compound was prepared according to General Procedure B. 1-bromo-4-(1,3-difluoro-2-(fluoromethyl)propan-2-yl)benzene (50.0 mg, 0.187 mmol), piperidine (22.2 mL, 0.225 mmol), palladium(II) acetate (4.20 mg, 10 mol%), Xantphos (10.8 mg, 10 mol%) and cesium carbonate (121.9 mg, 0.374 mmol) were dissolved in 1,4-dioxane (1.0 mL) under nitrogen. The reaction was heated to 100 °C and stirred overnight. On completion, the reaction was cooled to room temperature and the mixture was filtered through celite, eluting with ethyl acetate. The filtrate was washed with saturated aqueous ammonium chloride and brine, dried over magnesium sulfate, filtered and concentrated under vacuum to give the crude product. The crude was purified by column chromatography over silica gel (hexane/ethyl acetate, gradient 0 to 100% ethyl acetate). The compound was isolated as a yellow oil (39.7 mg, 78%). IR $\nu_{\max}/\text{cm}^{-1}$ 2931 (C-H), 1612, 1520, 1240 (C-N), 1024 (C-F), 993, 819. ^1H NMR (500 MHz, CDCl_3) δ 7.25-7.30 (2H, m, ArH), 6.91-6.96 (2H, m, ArH), 4.76 (6H, dt, $J = 47.0, 1.5$ Hz, CH_2F), 3.15-3.19 (4H, m, CH_2N), 1.67-1.73 (4H, m, $\text{CH}_2\text{CH}_2\text{N}$), 1.55-1.61 (2H, m, $\text{CH}_2\text{CH}_2\text{CH}_2\text{N}$). ^{13}C NMR (126 MHz, CDCl_3) δ 151.5 (ArC), 127.6 (ArC), 125.8 (ArC), 116.4 (ArC), 83.5 (3C, dt, $J = 176.2, 5.9$ Hz, CH_2F), 50.2 (2C, CH_2N), 48.1 (q, $J = 17.3$ Hz, CCH_2F), 25.8 (2C, $\text{CH}_2\text{CH}_2\text{N}$), 24.4 ($\text{CH}_2\text{CH}_2\text{CH}_2\text{N}$). $^{19}\text{F}\{^1\text{H}\}$ NMR (376 MHz, CDCl_3) δ -230.5 (3F, s, CH_2F). HRMS (EI) exact mass calculated for $\text{C}_{15}\text{H}_{20}\text{F}_3\text{N}$: 271.1542; found 271.1550.

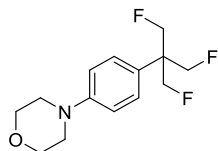
4-(1,3-Difluoro-2-(fluoromethyl)propan-2-yl)-N-phenylaniline (4.96)



This compound was prepared according to General Procedure B. The compound was isolated as a yellow oil (21.0 mg, 57%). IR $\nu_{\max}/\text{cm}^{-1}$ 2361, 1595 (N-H), 1520, 1497, 1316 (C-N), 1016 (C-N), 995, 750. ^1H NMR (500 MHz, CDCl_3) δ 7.28-7.32 (4H, m, ArH), 7.06-7.12 (4H, m, ArH), 6.97 (1H, tt, $J = 7.3, 1.1$ Hz, ArH), 5.75 (1H, s, NH), 4.78 (6H, dt, $J = 47.0, 1.5$ Hz, CH_2F). ^{13}C NMR (126 MHz, Acetone- d_6) δ 130.0 (ArC), 128.7 (ArC), 121.3 (ArC), 118.5 (ArC),

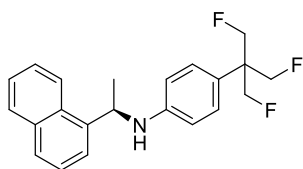
117.7 (ArC), 84.1 (3C, dt, $J = 173.9$, 5.4 Hz, CH₂F), 41.3 (CCH₂F). ¹⁹F{¹H} NMR (376 MHz, CDCl₃) δ -230.5 (3F, s, CH₂F). HRMS (EI) exact mass calculated for C₁₆H₁₆F₃N: 279.1229; found 279.1238.

4-(4-(1,3-Difluoro-2-(fluoromethyl)propan-2-yl)phenyl)morpholine (4.97)



This compound was prepared according to General Procedure B. The compound was isolated as a yellow oil (36.1 mg, 72%). IR $\nu_{\max}/\text{cm}^{-1}$ 1519, 1236 (C-N), 1119 (C-O), 1022 (C-F), 1011 (C-O), 993, 932. ¹H NMR (500 MHz, CDCl₃) δ 7.30-7.34 (2H, m, ArH), 6.90-6.95 (2H, m, ArH), 4.77 (6H, dt, $J = 47.0$, 1.5 Hz, CH₂F), 3.83-3.88 (4H, m, OCH₂), 3.15-3.20 (4H, m, NCH₂). ¹³C NMR (126 MHz, CDCl₃) δ 127.9 (ArC), 115.7 (ArC), 83.4 (3C, dt, $J = 176.2$, 5.6 Hz, CH₂F), 67.0 (2C, CH₂O), 49.0 (2C, CH₂N). ¹⁹F{¹H} NMR (376 MHz, CDCl₃) δ -230.6 (3F, s, CH₂F). HRMS (EI) exact mass calculated for C₁₄H₁₈F₃NO: 273.1335; found 273.1339.

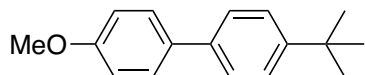
(R)-4-(1,3-Difluoro-2-(fluoromethyl)propan-2-yl)-N-(1-(naphthalen-1-yl)ethyl)aniline (4.98)



This compound was prepared according to General Procedure B. The compound was isolated as a yellow oil (38.0 mg, 63%). IR $\nu_{\max}/\text{cm}^{-1}$ 2968, 2361 (C-H), 1614, 1512, 1508, 1026 (C-F), 999, 799, 775. ¹H NMR (500 MHz, CDCl₃) δ 8.15 (1H, d, $J = 8.2$ Hz, ArH), 7.90-7.93 (1H, m, ArH), 7.76 (1H, d, $J = 8.2$ Hz, ArH), 7.64 (1H, d, $J = 7.3$ Hz, ArH), 7.50-7.59 (2H, m, ArH), 7.42 (1H, dd, $J = 8.0$, 7.3 Hz, ArH), 7.07-7.11 (2H, m, ArH), 6.46-6.52 (2H, m, ArH), 5.27 (1H, q, $J = 6.7$ Hz, CHCH₃), 4.69 (6H, dt, $J = 47.1$, 1.5 Hz, CH₂F), 1.66 (3H, d, $J = 6.7$ Hz, CH₃). ¹³C NMR (126 MHz, CDCl₃) δ 146.8 (ArC), 139.8 (ArC), 134.3 (ArC), 130.7 (ArC), 129.3 (ArC), 127.8 (ArC), 127.7 (ArC), 126.3 (ArC), 126.0 (ArC), 125.7 (ArC), 124.2 (ArC), 122.6 (ArC), 122.4 (ArC), 113.5 (ArC), 83.5 (3C, dt, $J = 176.1$, 6.0 Hz, CH₂F), 49.6 (NCCH₃), 48.7 (CCH₂F), 23.7 (CH₃). ¹⁹F{¹H} NMR (376 MHz, CDCl₃) δ -230.4 (3F, s, CH₂F). HRMS (ESI⁺) exact mass

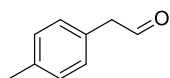
calculated for $C_{22}H_{22}F_3NNa^+ [M+Na]^+$: 380.1602; found 380.1597. $[\alpha]_D^{20} = +25.5^\circ$ ($c = 0.0167$, $CHCl_3$).

4-(*tert*-Butyl)-4'-methoxy-1,1'-biphenyl (4.102)



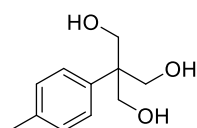
This compound was prepared according to General Procedure A. The compound was isolated as a white solid (163.2 mg, 72%). 1H NMR (400 MHz, $CDCl_3$) δ 7.48-7.57 (4H, m, ArH), 7.43-7.46 (2H, m, ArH), 6.95-6.98 (2H, m, ArH), 3.85 (3H, s, CH_3), 1.36 (9H, s, $(CH_3)_3$). Data is in agreement with that reported in the literature.²⁷⁹

2-(*p*-Tolyl)acetaldehyde (4.109)



Dess-Martin periodinane (8.56 g, 20.2 mmol) was added to a stirred solution of 2-(*p*-tolyl)ethan-1-ol (2.53 mL, 18.4 mmol) in DCM (184 mL) and the reaction was stirred for 3 hours. The reaction was quenched by addition of sat. aq. sodium thiosulfate and sat. aq. sodium hydrogen carbonate. The aqueous layer was extracted with DCM (3x). The combined organic layers were washed with $NaHCO_3$ and brine, dried over sodium sulfate, filtered and concentrated to give the crude product. The crude product was dissolved in 9:1 hexane/ethyl acetate solution and filtered. The filtrate was concentrated under reduced pressure to give the purified product as a colourless liquid (1.55 g, 63%). 1H NMR (400 MHz, $CDCl_3$) δ 9.73 (1H, t, $J = 2.4$ Hz, CHO), 7.18 (2H, d, $J = 7.9$ Hz, ArH), 7.12 (2H, d, $J = 7.9$ Hz, ArH), 3.65 (2H, d, $J = 2.4$ Hz, CH_2), 2.35 (3H, s, CH_3). Data is in agreement with that reported in the literature.⁴

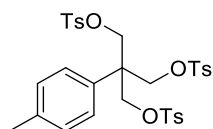
2-(Hydroxymethyl)-2-(*p*-tolyl)propane-1,3-diol (4.110)



2-(*p*-Tolyl)acetaldehyde (1.72 g, 12.8 mmol) and calcium hydroxide (3.80 g, 51.3 mmol) were added to a suspension of paraformaldehyde (1.54 g, 51.3 mmol) in THF (19.2 mL). The

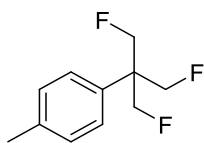
reaction mixture was stirred at 60–65 °C for four days. After cooling to room temperature, the reaction mixture was filtered through celite and the celite was rinsed with DCM (50 mL). The filtrate was concentrated under reduced pressure to give the crude product. The crude product was purified by column chromatography over silica gel (1:1 hexane/ethyl acetate gradient to 100% ethyl acetate) to give the purified product as a white solid (1.47 g, 58%). IR $\nu_{\max}/\text{cm}^{-1}$ 3333 (O-H), 2920 (C-H), 2878 (C-H), 1516, 1115 (C-O), 1065 (C-O), 1013, 812. ^1H NMR (500 MHz, d^6 -DMSO) δ 7.27–7.30 (2H, m, ArH), 7.04–7.08 (2H, m, ArH), 4.38 (6H, t, J = 5.2 Hz, CH_2), 3.68 (3H, t, J = 5.2 Hz, OH), 3.35 (3H, s, CH_3). ^{13}C NMR (126 MHz, d^6 -DMSO) δ 139.9 (ArC), 134.3 (ArC), 128.2 (ArC), 127.5 (ArC), 63.5 (3C, CH_2), 48.7 (CCH_2), 20.6 (CH_3). HRMS (EI) exact mass calculated for $\text{C}_{11}\text{H}_{16}\text{O}_3$: 196.1094; found 196.1095.

2-(*p*-Tolyl)-2-((tosyloxy)methyl)propane-1,3-diyl bis(4-methylbenzenesulfonate) (4.111)



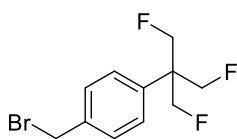
p-Toluenesulfonyl chloride (4.43 g, 23.2 mmol) was added slowly to a solution of 2-(hydroxymethyl)-2-(*p*-tolyl)propane-1,3-diol (1.29 g, 4.94 mmol) in pyridine (10.2 mL) at 0 °C and the reaction was warmed to room temperature and stirred for three days. On completion, the reaction mixture was concentrated under reduced pressure. The resulting residue was dissolved in DCM (100 mL) and the suspension was filtered. The filtrate was washed with water (100 mL). The organic phase was separated, and the aqueous phase was extracted with DCM (3 x 30 mL). The combined organic phases were washed with brine (50 mL), dried over magnesium sulfate, filtered and concentrated under vacuum to give the crude product. The crude product was suspended in ethanol and the suspension was stirred vigorously and heated to 92 °C. The suspension was filtered to give the purified product as a white solid (2.12 g, 65%). m.p. 136–138 °C. IR $\nu_{\max}/\text{cm}^{-1}$ 2988 (C-H), 2901 (C-H), 2361, 1362 (S=O), 1173 (C-O), 1076 (C-O), 1067 (C-O), 970, 827, 802. ^1H NMR (500 MHz, CDCl_3) δ 7.60–7.64 (6H, m, ArH), 7.29–7.33 (6H, m, ArH), 6.95–6.98 (2H, m, ArH), 6.79–6.83 (2H, m, ArH), 4.16 (6H, s, CH_2O), 2.46 (9H, s, CH_3), 2.29 (3H, s, CH_3). ^{13}C NMR (126 MHz, CDCl_3) δ 145.4 (ArC), 138.0 (ArC), 131.9 (ArC), 131.8 (ArC), 130.1 (ArC), 129.6 (ArC), 128.1 (ArC), 126.2 (ArC), 69.1 (3C, CH_2O), 45.9 (CCH_2), 21.9 (3C, 3 x SO_2ArCH_3), 21.1 (Ar CH_3). HRMS (ESI $^+$) exact mass calculated for $\text{C}_{32}\text{H}_{34}\text{O}_9\text{S}_3\text{Na}^+$ [$\text{M}+\text{Na}$] $^+$: 681.1263; found 681.1257.

1-(1,3-Difluoro-2-(fluoromethyl)propan-2-yl)-4-methylbenzene (4.112)



Cesium fluoride (1.02 g, 6.70 mmol) was added to a solution of 2-(p-tolyl)-2-((tosyloxy)methyl)propane-1,3-diyl bis(4-methylbenzenesulfonate) (245.2 mg, 0.372 mmol) in DMSO (8.15 mL) and the reaction was heated to 120 °C and stirred for 24 h. On completion, the reaction mixture was diluted with water and the aqueous layer was extracted three times with diethyl ether. The combined organic layer was washed with water, dried over magnesium sulfate, filtered and concentrated under vacuum to give the crude product. The crude product was purified by column chromatography over silica gel (hexane/ethyl acetate, gradient from 0 to 10% ethyl acetate) to give the purified product as a yellow oil (53.0 mg, 71%). IR $\nu_{\max}/\text{cm}^{-1}$ 2970 (C-H), 2924 (C-H), 2361, 1518, 1030 (C-F), 1003 (C-F), 814. ^1H NMR (500 MHz, CDCl_3) δ 7.30 (2H, d, $J = 8.0$ Hz, ArH), 7.22 (2H, d, $J = 8.0$ Hz, ArH), 4.79 (6H, dt, $J = 47.0, 1.6$ Hz, CH_2F), 2.35 (3H, s, CH_3). ^{13}C NMR (126 MHz, CDCl_3) δ 138.0 (ArC), 133.2 (ArC), 129.8 (ArC), 126.8 (ArC), 83.3 (3C, dt, $J = 176.6, 5.8$ Hz, CH_2F), 21.1 (CH_3). $^{19}\text{F}\{^1\text{H}\}$ NMR (376 MHz, CDCl_3) δ -230.8 (3F, s, CH_2F). HRMS (ESI⁺) calculated for $\text{C}_{11}\text{H}_{13}\text{F}_3\text{Na}^+$ [M+Na]⁺: 225.0867; found 225.0862.

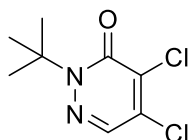
1-(Bromomethyl)-4-(1,3-difluoro-2-(fluoromethyl)propan-2-yl)benzene (4.113)



1-(1,3-Difluoro-2-(fluoromethyl)propan-2-yl)-4-methylbenzene (38.8 mg, 0.192 mmol) was added to a solution of N-bromosuccinimide (61.5 mg, 0.0384 mmol) in trifluorotoluene (1.0 mL). The reaction was heated to reflux and stirred for 18 hours. On completion, the reaction was cooled to room temperature, hexane was added to the mixture and the mixture was filtered. The solvent was removed under reduced pressure to give the crude product. The crude product was purified by column chromatography over silica gel (100:1 hexane/ethyl acetate) to give the purified product as a yellow oil (28.7 mg, 53%). IR $\nu_{\max}/\text{cm}^{-1}$ 2972 (C-H), 1024 (C-F), 1001 (C-F), 642 (C-Br), 624 (C-Br). ^1H NMR (400 MHz, CDCl_3) δ 7.38-7.45 (4H, m,

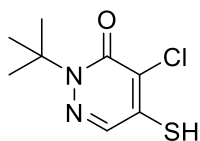
ArH), 4.79 (6H, (dq, $J = 46.9, 1.6$ Hz, CH_2F), 4.48 (2H, s, CH_2Br). ^{13}C NMR (126 MHz, CDCl_3) δ 137.7 (ArC), 136.6 (ArC), 129.6 (ArC), 127.5 (ArC), 83.1 (3C, dt, $J = 175.9, 6.7$ Hz, CH_2F), 40.2 ($\text{C}(\text{CH}_2\text{F})_3$), 32.7 (CH_2Br). $^{19}\text{F}\{^1\text{H}\}$ NMR (470 MHz, CDCl_3) δ -231.0 (3F, s, CH_2F). HRMS (EI) exact mass calculated for $\text{C}_{11}\text{H}_{12}^{79}\text{BrF}_3$: 280.0069; found 280.0060.

2-(*tert*-Butyl)-4,5-dichloropyridazin-3(2H)-one (4.116)



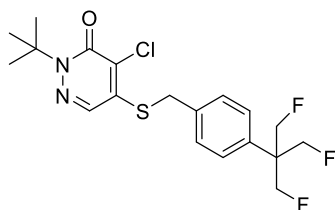
tert-Butylhydrazine hydrochloride (6.23 g, 50.0 mmol) was added to a solution of sodium hydroxide (1.90 g, 47.5 mmol) dissolved in a mixture of toluene (180 mL) and water (20 mL) at room temperature. Mucochloric acid (8.45 g, 50.0 mmol) was added in batches and stirred for 30 minutes. Acetic acid (2.72 mL, 47.5 mmol) was added dropwise and the reaction was heated for 45-50 °C and stirred for 18 hours. The solution was allowed to cool to room temperature and then diluted with water (80 mL). The organic layer was cooled to 0 °C and washed with 30% sodium hydroxide solution, concentrated hydrochloric acid solution and water. The organic layer was dried over magnesium sulfate, filtered and concentrated under vacuum to give the crude product as a red solid. The crude product was used without further purification (7.21 g, 68%). ^1H NMR (400 MHz, CDCl_3) δ 7.73 (1H, s, NCH), 1.64 (9H, s, CH_3). Data is in agreement with that reported in the literature.⁵

2-(*tert*-Butyl)-4-chloro-5-mercapto-4,5-dihydropyridazin-3(2H)-one (4.116)



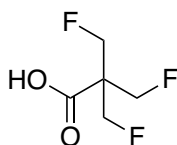
Sodium hydrosulfide hydrate (3.63 g, 64.8 mmol) was added to a solution of 2-(*tert*-butyl)-4,5-dichloropyridazin-3(2H)-one (7.54 g, 34.1 mmol) in ethanol (30 mL) in batches at 0 °C and the reaction mixture was stirred at room temperature for 2 hours. The mixture was poured into ice water and acidified with concentrated hydrochloric acid (23.4 mL). The yellow solid was collected, washed with ice water, dried and used without further purification (5.43 g, 72%). ^1H NMR (400 MHz, CDCl_3) δ 7.57 (1H, s, NCH), 4.00 (1H, s, SH), 1.63 (9H, s, CH_3). Data is in agreement with that reported in the literature.⁶

2-(*tert*-Butyl)-4-chloro-5-((4-(1,3-difluoro-2-(fluoromethyl)propan-2-yl)benzyl)thio)pyridazin-3(2H)-one (4.107)



1-(Bromomethyl)-4-(1,3-difluoro-2-(fluoromethyl)propan-2-yl)benzene (17.4 mg, 0.0619 mmol) and sodium carbonate (9.84 mg, 0.0929 mmol) were added to a solution of 2-(*tert*-butyl)-4-chloro-5-mercaptopyridazin-3(2H)-one (13.5 mg, 0.0619 mmol) in DMF (0.25 mL) and the reaction mixture was stirred for 18 hours at room temperature. The reaction mixture was extracted three times with ethyl acetate. The combined organic layers were washed with water, dried over magnesium sulfate, filtered and concentrated under vacuum to give the crude product. The crude product was purified by column chromatography over silica gel (hexane/ethyl acetate, gradient 0 to 10% ethyl acetate) to give the purified product as an orange solid (13.9 mg, 53%). m.p. 106-108 °C. IR $\nu_{\max}/\text{cm}^{-1}$ 2984 (C-H), 2361, 1653 (C=O), 1558 (C=C), 1506. ^1H NMR (400 MHz, CDCl_3) δ 7.60 (1H, s, CHN), 7.41-7.47 (4H, m, ArH), 4.79 (6H, dt, $J = 46.8, 1.5$ Hz, CH_2F), 4.26 (2H, s, SCH_2), 1.63 (9H, s, CH_3). ^{13}C NMR (101 MHz, CDCl_3) δ 131.9, 131.1, 129.4, 127.9, 83.1 (3C, dt, $J = 176.4, 5.2$ Hz, CH_2F), 35.4, 29.9, 27.8. $^{19}\text{F}\{^1\text{H}\}$ NMR (377 MHz, CDCl_3) δ -231.0 (3F, s, CH_2F). HRMS (ESI⁺) exact mass calculated for $\text{C}_{19}\text{H}_{22}\text{ON}_2^{35}\text{ClF}_3\text{SNa}^+$ [M+Na]⁺: 441.0986; found 441.0991.

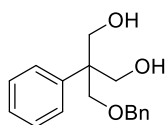
3-Fluoro-2,2-bis(fluoromethyl)propanoic acid (4.102)



To a mixture of (1,3-difluoro-2-(fluoromethyl)propan-2-yl)benzene (50 mg, 0.266 mmol), acetonitrile (1.04 mL), 1,2-dichloroethane (1.04 mL) and water (2.63 mL) were added ruthenium(III) chloride (10.5 mg, 0.0505 mmol) and sodium periodate (1.37 g, 6.38 mmol) sequentially. The reaction was stirred at 70 °C for 24 hours. The reaction was cooled to room temperature and filtered through celite, washing with DCM. The organic layer was separated and the aqueous layer was extracted with DCM. The combined organic layers

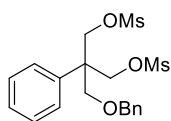
were dried over magnesium sulfate, filtered and concentrated to give the crude product. The crude product was purified by titration (hexane) to give the purified product as a white solid (9.77 mg, 24%). ^1H NMR (500 MHz, CDCl_3) δ_{H} 4.70 (6H, d, $J = 46.3$ Hz, CH_2F). ^{13}C NMR (126 MHz, CDCl_3) δ_{C} 173.7 (C=O), 79.6 (3C, dt, $J = 175.2, 6.1$ Hz, CH_2F), 53.8 (CCH_2F). $^{19}\text{F}\{^1\text{H}\}$ NMR (376 MHz, CDCl_3) δ_{F} -234.9 (3F, s, CH_2F). HRMS (ESI⁺) exact mass calculated for $\text{C}_5\text{H}_7\text{F}_3\text{O}_2\text{NH}_4^+ [\text{M}+\text{NH}_4]^+$: 174.0742; found 174.0299.

2-((Benzyloxy)methyl)-2-phenylpropane-1,3-diol (4.128)



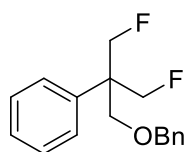
A solution of 2-hydroxymethyl-2-phenylpropane (100 mg, 0.547 mmol) in THF (0.2 mL) was added dropwise to a solution of sodium hydride (60% dispersion in mineral oil, 22.0 mg, 0.549 mmol) in THF (0.6 mL). The reaction mixture was refluxed for 1 hour, then benzyl bromide (71.8 μL , 0.604 mmol) was added and refluxing was continued for 16 hours. The reaction mixture was cooled to room temperature and water (0.1 mL) was added, followed by the removal of THF under reduced pressure. The residue was extracted with diethyl ether (3 x 2 mL), washed with water, brine and dried over magnesium sulfate. The solvent was removed under reduced pressure to give the crude product. The crude product was purified by column chromatography over silica gel (hexane/ethyl acetate, gradient 0 to 100% ethyl acetate) to give the purified product as a colourless oil (122.2 mg, 45%). ^1H NMR (400 MHz, d^6 -Acetone) δ 7.48-7.53 (2H, m, ArH), 7.24-7.35 (7H, m, ArH), 7.16-7.21 (1H, m, ArH), 4.53 (2H, s, CH_2Ph), 3.99 (2H, qd, $J = 10.9, 3.7$ Hz, CH_2OH), 3.92 (2H, s, $\text{CH}_2\text{OCH}_2\text{Ph}$), 3.71-3.79 (2H, m, $\text{CH}_2\text{OCH}_2\text{Ph}$). ^{13}C NMR (101 MHz, d^6 -Acetone) δ 143.0 (ArC), 139.7 (ArC), 129.0 (ArC), 128.7 (ArC), 128.4 (ArC), 128.2 (ArC), 128.1 (ArC), 126.8 (ArC), 73.9 (CH_2Ph), 73.5 ($\text{CH}_2\text{OCH}_2\text{Ph}$), 66.2 (CH_2OH), 49.8 (CCH_2O). HRMS (ESI) exact mass calculated for $\text{C}_{17}\text{H}_{20}\text{O}_3\text{Na}^+ [\text{M}+\text{Na}]^+$: 295.1310; found 295.1305.

2-((Benzyloxy)methyl)-2-phenylpropane-1,3-diyl dimethanesulfonate (4.129)



Triethylamine (84.5 mL, 0.606 mmol) was added to a solution of 1-(1,3-difluoro-2-(fluoromethyl)propan-2-yl)-4-methylbenzene (66.1 mg, 0.243 mmol) in dichloromethane (1.33 mL) at 0 °C. Methanesulfonyl chloride (47.0 mL, 0.606 mmol) was added and the reaction was warmed to room temperature. On completion, the reaction was quenched by the addition of saturated ammonium chloride solution (1.33 mL) and the aqueous layer was extracted with dichloromethane (3 x 7.2 mL). The combined organic layers were washed with brine (7.2 mL), dried over magnesium sulfate, filtered and concentrated under vacuum to give the crude product. The crude product was purified by column chromatography over silica gel (hexane/ethyl acetate, gradient 0 to 100% ethyl acetate) to give the purified product as a yellow oil (60.4 mg, 58%). IR $\nu_{\text{max}}/\text{cm}^{-1}$ 2988 (C-H), 2901 (C-H), 2361, 1352 (S=O), 1171 (S=O), 951, 822, 698. ^1H NMR (400 MHz, CDCl_3) δ 7.29-7.41 (8H, m, ArH), 7.23-7.28 (2H, m, ArH), 4.58 (4H, dd, $J = 11.1, 10.0$ Hz, OCH_2S), 4.53 (2H, s, OCH_2Ar), 3.82 (2H, s, $\text{CH}_2\text{OCH}_2\text{Ar}$), 2.85 (6H, s, SCH_3). ^{13}C NMR (126 MHz, CDCl_3) δ 137.4 (ArC), 137.3 (ArC), 129.0 (ArC), 128.7 (ArC), 128.1 (ArC), 127.9 (ArC), 126.7 (ArC), 73.8 (OCH_2Ar), 70.4 ($\text{CH}_2\text{OCH}_2\text{Ar}$), 69.9 (CH_2OS), 47.0 (CCH_2O), 37.3 (SCH_3). HRMS (ESI⁺) calculated for $\text{C}_{19}\text{H}_{24}\text{O}_7\text{S}_2\text{Na}^+$ $[\text{M}+\text{Na}]^+$: 451.0861; found 451.0856.

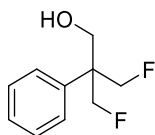
(1-(Benzyloxy)-3-fluoro-2-(fluoromethyl)propan-2-yl)benzene (4.130)



tert-Butylammonium fluoride (1.0 M in THF, 0.311 mL, 0.311 mmol) was added to a solution of 2-((benzyloxy)methyl)-2-phenylpropane-1,3-diyl dimethanesulfonate (33.4 mg, 0.0778 mmol) in acetonitrile (0.519 mL) and the reaction was stirred under reflux for 15 hours. The reaction was then cooled to room temperature and water (4.32 mL) was added. The mixture was extracted with ethyl acetate (3 x 3.24 mL). The combined organic layers were dried over magnesium sulfate, filtered and concentrated under vacuum to give the crude product. The

crude product was purified by column chromatography over silica gel (hexane/ethyl acetate, gradient 0 to 100% ethyl acetate) to give the purified product as a colourless oil (16.6 mg, 77%). ^1H NMR (400 MHz, CDCl_3) δ 7.23-7.44 (10H, m, ArH), 4.87 (2H, qd, $J = 9.3, 1.5$ Hz, CH_2F), 4.75 (2H, qd, $J = 9.3, 1.5$ Hz, CH_2F), 4.52 (2H, s, OCH_2Ar), 3.80 (2H, t, $J = 1.5$ Hz, CCH_2O). ^{13}C NMR (126 MHz, CDCl_3) δ 138.0 (ArC), 128.7 (ArC), 128.5 (ArC), 127.9 (ArC), 127.7 (ArC), 127.6 (ArC), 127.1 (ArC), 114.7 (ArC), 84.3 (2C, dd, $J = 175.3, 5.4$ Hz, CH_2F), 73.7 (OCH_2Ar), 72.1 (d, $J = 8.4$ Hz, CCH_2F), 70.6 (t, $J = 5.9$ Hz, CCH_2O). ^{19}F NMR (470 MHz, CDCl_3) δ -230.2 (2F, t, $J = 47.1$ Hz, CH_2F). HRMS (ESI $^+$) calculated for $\text{C}_{17}\text{H}_{18}\text{F}_2\text{ONa}^+$ $[\text{M}+\text{Na}]^+$: 299.1218; found 299.1212.

3-Fluoro-2-(fluoromethyl)-2-phenylpropan-1-ol (4.125)



(1-(Benzyloxy)-3-fluoro-2-(fluoromethyl)propan-2-yl)benzene (8.0 mg, 0.0203 mmol) was dissolved in ethanol (0.25 mL) and 10% palladium on carbon (2.0 mg) was added. The reaction was placed in an autoclave which was filled with hydrogen gas (50 bar). On completion, the reaction mixture was filtered through celite and the solvent removed under reduced pressure. The crude product was used for analytical purposes. ^1H NMR (400 MHz, CDCl_3) δ 7.22-7.44 (5H, m, ArH), 4.85 (4H, dt, $J = 47.1, 1.3$ Hz, CH_2F). ^{19}F NMR (376 MHz, CDCl_3) δ -230.7 (2F, t, $J = 47.1$ Hz, CH_2F).

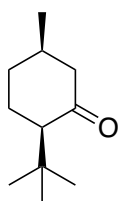
7.5 Chapter 5

(5R)-2-(tert-Butyl)-5-methylcyclohexan-1-one

Magnesium turnings (698 mg, 28.7 mmol) were placed in a dried RBF under argon equipped with a condenser. Dry diethyl ether (10 mL) was added, followed by iodomethane (1.79 mL, 28.7 mmol). Remaining pieces of magnesium were removed by filtration under inert atmosphere. The filtrate was cooled to 0 °C and copper iodide (375.3 mg, 1.97 mmol) was added and stirred for 30 minutes. A solution of (*R*)-(+)-pulegone (2.67 mL, 16.4 mmol) in dry diethyl ether (2.5 mL) was added and the reaction mixture was warmed to room temperature and stirred overnight. The reaction was cooled to 0 °C and water (3 mL) was

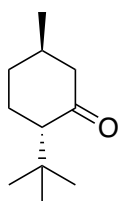
cautiously added, followed by saturated ammonium chloride solution (12.9 mL) and concentrated hydrochloric acid (1.82 mL). The mixture was extracted with diethyl ether (3 x 17.5 mL). The combined organic layers were washed with sodium thiosulfate (35 mL) and brine (35 mL), dried over magnesium sulfate, filtered and concentrated under reduced pressure. The crude product was purified by column chromatography over silica gel (hexane/ethyl acetate, gradient 0 to 5% ethyl acetate) to give the purified product as a diastereomeric mixture (*cis*- and *trans*- product ratio approximately 58:42) as a pale yellow oil (1.46 g, 53%).

(2*R*,5*R*)-2-(*tert*-Butyl)-5-methylcyclohexan-1-one (5.57)



$^1\text{H NMR}$ (400 MHz, CDCl_3) δ 2.47 (1H, ddd, $J = 12.9, 5.6, 1.2$ Hz), 2.28-2.31 (1H, m), 2.07-2.10 (1H, m), 2.02-2.05 (1H, m), 1.93-1.97 (1H, m), 1.89-1.96 (2H, m), 1.56-1.63 (1H, m), 0.99 (9H, s, $(\text{CH}_3)_3$), 0.95 (3H, d, $J = 7.0$ Hz, CH_3). Data is in agreement with that reported in the literature.²⁸⁰

(2*S*,5*R*)-2-(*tert*-Butyl)-5-methylcyclohexan-1-one (5.58)



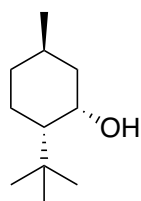
$^1\text{H NMR}$ (400 MHz, CDCl_3) δ 2.25 (1H, ddd, $J = 12.3, 4.0, 2.2$ Hz), 2.10-2.16 (1H, m), 2.03-2.07 (1H, m), 1.99 (1H, dd, $J = 12.3, 1.2$ Hz), 1.90-1.77 (2H, m), 1.41-1.46 (1H, m), 1.33 (1H, ddd, $J = 13.1, 3.1, 1.5$ Hz), 1.00 (3H, d, $J = 6.2$ Hz, CH_3), 0.98 (9H, s, $(\text{CH}_3)_3$). Data is in agreement with that reported in the literature.²⁸⁰

(5*R*)-2-(*tert*-Butyl)-5-methylcyclohexan-1-ol

Sodium borohydride (211.9 mg, 5.60 mmol) was added portionwise to a solution of (5*R*)-2-(*tert*-butyl)-5-methylcyclohexan-1-one (628.5 mg, 3.73 mmol) in anhydrous methanol (7 mL)

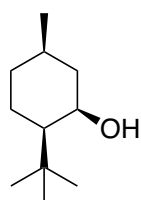
at 0 °C. The reaction was warmed to room temperature and stirred overnight. Water was added slowly to quench the reaction and the aqueous layer was extracted with diethyl ether. The combined organic layers were washed with brine, dried over sodium sulfate, filtered and concentrated under vacuum to give the crude product. The crude product was purified by column chromatography over silica gel (hexane/ethyl acetate) to give two separated diastereomeric products (322.4 mg, 51%).

(1*S*,2*S*,5*R*)-2-(*tert*-Butyl)-5-methylcyclohexan-1-ol (5.59)



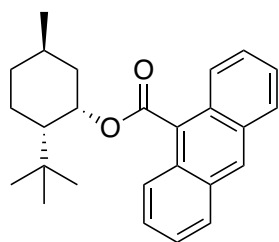
This product was isolated as a colourless liquid (204.0 mg). IR $\nu_{\max}/\text{cm}^{-1}$ 2956 (C-H), 1713, 1453, 1050 (C-O). ^1H NMR (400 MHz, CDCl_3) δ 4.21-4.25 (1H, m, CHOH), 1.68-1.81 (4H, m), 1.41-1.60 (2H, m), 1.04-1.17 (2H, m), 0.95 (9H, s, $(\text{CH}_3)_3$), 0.87 (3H, d, $J = 6.3$ Hz, CH_3). ^{13}C NMR (126 MHz, CDCl_3) δ 68.7 (CHOH), 50.8, 44.0, 35.7, 32.4, 28.8, 26.3, 22.5, 21.3. HRMS (ESI⁺) calculated for $\text{C}_{11}\text{H}_{22}\text{ONa}^+$ $[\text{M}+\text{Na}]^+$: 193.1604; found 193.1198.

(1*R*,2*R*,5*R*)-2-(*tert*-Butyl)-5-methylcyclohexan-1-ol (5.61)



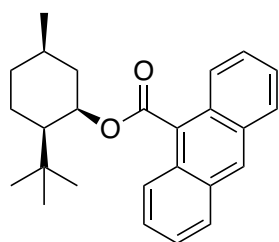
This product was isolated as a colourless liquid (118.4 mg). ^1H NMR (400 MHz, CDCl_3) δ 4.20-4.27 (1H, m, CHOH), 1.87-1.95 (1H, m), 1.63-1.72 (3H, m), 1.59-1.62 (1H, m), 1.47-1.57 (1H, m), 1.35-1.44 (1H, m), 1.16 (3H, d, $J = 7.4$ Hz, CH_3), 0.98-1.04 (1H, m), 0.96 (9H, s, $(\text{CH}_3)_3$). Data is in agreement with that reported in the literature.²⁸¹

(1*S*,2*S*,5*R*)-2-(*tert*-Butyl)-5-methylcyclohexyl anthracene-9-carboxylate (5.66)



Trifluoroacetic anhydride (0.326 mL, 2.34 mmol) was added to a solution of 9-anthracenecarboxylic acid (130.5 mg, 0.587 mmol) in toluene (3 mL). (1*S*,2*S*,5*R*)-2-(*tert*-Butyl)-5-methylcyclohexan-1-ol (100 mg, 0.587 mmol) was then added and the reaction was stirred for 3 hours. 10% Sodium hydroxide solution was added and the aqueous layer extracted. The organic layer was washed with water, dried over magnesium sulfate, filtered and concentrated under vacuum to give the crude product. The crude was purified by column chromatography over silica gel (hexane/ethyl acetate 10:1) to give the purified product as a yellow solid (158.5 mg, 72%). m.p. 154-156 °C. IR $\nu_{\text{max}}/\text{cm}^{-1}$ 2947 (C-H), 2361, 1709 (C=O), 1213, 1152 (C-O), 1003, 893, 731. ^1H NMR (500 MHz, CDCl_3) δ 8.51 (1H, s, ArH), 7.99-8.05 (4H, m, ArH), 7.46-7.54 (4H, m, ArH), 5.88-5.91 (1H, m, CHOCO), 2.57 (1H, dq, $J = 14.7, 3.4$ Hz), 1.86-2.00 (1H, m), 1.74-1.81 (1H, m), 1.52-1.60 (2H, m), 1.45 (1H, td, $J = 12.9, 3.4$ Hz), 1.36 (1H, ddd, $J = 14.7, 12.7, 2.4$ Hz), 1.23-1.29 (1H, m, CHCHOCO), 1.03 (3H, d, $J = 6.7$ Hz, CH_3), 0.91 (9H, s, $(\text{CH}_3)_3$). ^{13}C NMR (126 MHz, CDCl_3) δ 169.8 (C=O), 131.2 (2C, ArC), 128.8 (3C, ArCH), 128.6 (ArC), 128.0 (2C, ArC), 126.7 (2C, ArCH), 125.6 (2C, ArCH), 125.1 (2C, ArCH), 74.0 (CHOCO), 49.9 (CHCHOCO), 40.5, 35.5, 29.3, 28.8 (3C, $(\text{CH}_3)_3$), 27.5, 22.4, 22.3 (CH_3). HRMS (ESI⁺) calculated for $\text{C}_{26}\text{H}_{30}\text{O}_2\text{Na}^+$ $[\text{M}+\text{Na}]^+$: 397.2138; found 397.2133. $[\alpha]_{\text{D}}^{20} = +7.4^\circ$ ($c = 0.0126$, CHCl_3).

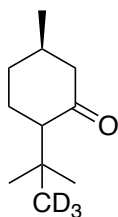
(1*R*,2*R*,5*R*)-2-(*tert*-Butyl)-5-methylcyclohexyl anthracene-9-carboxylate (5.65)



Trifluoroacetic anhydride (0.163 mL, 2.16 mmol) was added to a solution of 9-anthracenecarboxylic acid (120.3 mg, 0.541 mmol) in toluene (3.5 mL). (1*R*,2*R*,5*R*)-2-(*tert*-

Butyl)-5-methylcyclohexan-1-ol (92.2 mg, 0.541 mmol) was then added and the reaction was stirred for 3 hours. 10% Sodium hydroxide solution was added and the aqueous layer extracted. The organic layer was washed with water, dried over magnesium sulfate, filtered and concentrated under vacuum to give the crude product. The crude was purified by column chromatography over silica gel (hexane/ethyl acetate 10:1) to give the purified product as a yellow solid (145.7 mg, 72%). m.p. 159-161 °C. IR $\nu_{\text{max}}/\text{cm}^{-1}$ 2918 (C-H), 2359, 1670 (C=O), 1481, 1215, 1176 (C-O), 1003, 837. ^1H NMR (500 MHz, CDCl_3) δ 8.51 (1H, s, ArH), 7.99-8.08 (4H, m, ArH), 7.45-7.53 (4H, m, ArH), 5.92-5.95 (1H, m, CHOCO), 2.33 (1H, d, $J = 14.7$ Hz), 1.95-2.09 (2H, m), 1.50-1.63 (1H, m), 1.40-1.46 (1H, m), 1.27-1.34 (2H, m), 1.23-1.29 (1H, m, CHCHOCO), 1.04 (3H, d, $J = 7.2$ Hz, CH_3), 0.98 (9H, s, $(\text{CH}_3)_3$). ^{13}C NMR (126 MHz, CDCl_3) δ 161.4 (C=O), 131.2 (2C, ArC), 129.0 (2C, ArC), 128.6 (3C, ArCH), 127.6 (ArC), 126.3 (2C, ArCH), 125.9 (2C, ArCH), 125.6 (2C, ArCH), 74.5 (CHOCO), 50.2 (CHCHOCO), 37.2, 36.4, 32.7, 28.7 (3C, $(\text{CH}_3)_3$), 26.5, 21.7 (CH_3), 17.5. HRMS (ESI⁺) calculated for $\text{C}_{26}\text{H}_{30}\text{O}_2\text{Na}^+$ $[\text{M}+\text{Na}]^+$: 397.2138; found 397.2133. $[\alpha]_{\text{D}}^{20} = -13.9^\circ$ ($c = 0.0096$, CHCl_3).

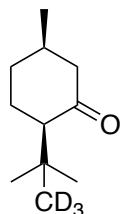
(5R)-5-Methyl-2-(2-methylpropan-2-yl-1,1,1-*d*3)cyclohexan-1-one



Magnesium turnings (139.5 mg, 5.74 mmol) were placed in a dried RBF under argon equipped with a condenser. Dry diethyl ether (2 mL) was added, followed by iodomethane- d_3 (0.357 mL, 5.74 mmol). Remaining pieces of magnesium were removed by filtration under inert atmosphere. The filtrate was cooled to 0 °C and copper iodide (75.0 mg, 0.328 mmol) was added and stirred for 30 minutes. A solution of (*R*)-(+)-pulegone (0.534 mL, 3.28 mmol) in dry diethyl ether (0.5 mL) was added and the reaction mixture was warmed to room temperature and stirred overnight. The reaction was cooled to 0 °C and water (0.60 mL) was cautiously added, followed by saturated ammonium chloride solution (2.58 mL) and concentrated hydrochloric acid (0.364 mL). The mixture was extracted with diethyl ether (3 x 3.5 mL). The combined organic layers were washed with sodium thiosulfate (7 mL) and brine (7 mL), dried over magnesium sulfate, filtered and concentrated under reduced

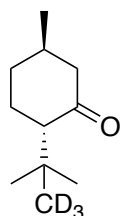
pressure. The crude product was purified by column chromatography over silica gel (hexane/ethyl acetate, gradient 0 to 5% ethyl acetate) to obtain two diastereomeric products (206.2 mg, 37%).

(2*R*,5*R*)-5-Methyl-2-(2-methylpropan-2-yl-1,1,1-*d*₃)cyclohexan-1-one (5.57a)



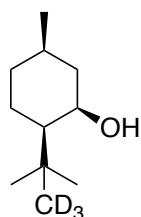
This product was isolated as a colourless liquid (66.1 mg). IR $\nu_{\max}/\text{cm}^{-1}$ 2361, 1658 (C=O), 1558, 1506. ¹H NMR (500 MHz, CDCl₃) δ 2.47 (1H, ddd, $J = 13.0, 5.6, 1.2$ Hz), 2.23-2.32 (1H, m), 2.07-2.13 (1H, m), 2.00-2.07 (1H, m), 1.90-1.97 (1H, m), 1.72-1.87 (2H, m), 1.56-1.63 (1H, m), 0.98 (6H, s, (CH₃)₃), 0.95 (3H, d, $J = 7.0$ Hz, CH₃). ¹³C NMR (126 MHz, CDCl₃) δ 213.2 (C=O), 59.4, 52.6, 50.5, 34.9, 32.6, 31.5 (2C, (CH₃)₂), 28.7, 28.1, 24.8 (CH₃). HRMS (EI) calculated for C₁₁H₁₇D₃O: 171.17; found 171.17. $[\alpha]_{\text{D}}^{20} = -54.0^\circ$ ($c = 0.001$, CHCl₃).

(2*S*,5*R*)-5-methyl-2-(2-methylpropan-2-yl-1,1,1-*d*₃)cyclohexan-1-one (5.58a)



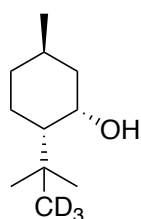
This product was isolated as a colourless liquid (140.1 mg). IR $\nu_{\max}/\text{cm}^{-1}$ 2954, 1709 (C=O), 1051. ¹H NMR (500 MHz, CDCl₃) δ 2.26 (1H, ddd, $J = 12.3, 4.0, 2.3$ Hz), 2.10-2.18 (1H, m), 2.07 (1H, ddd, $J = 12.7, 6.0$ Hz, 1.2 Hz), 2.01 (1H, td, $J = 12.3, 1.2$ Hz), 1.80-1.93 (2H, m), 1.44 (1H, qd, $J = 12.7, 3.0$ Hz), 1.27-1.38 (1H, m), 1.00 (3H, d, $J = 6.4$ Hz, CH₃), 0.98 (6H, s, (CH₃)₂). ¹³C NMR (126 MHz, CDCl₃) δ 212.4, 59.5, 52.6, 36.5, 34.9, 31.6, 28.7, 27.7 (2C, (CH₃)₂), 22.5 (CH₃), 19.7. HRMS (EI) calculated for C₁₁H₁₇D₃O: 171.17; found 171.17. $[\alpha]_{\text{D}}^{20} = +43.0^\circ$ ($c = 0.032$, CHCl₃).

(1*R*,2*R*,5*R*)-5-Methyl-2-(2-methylpropan-2-yl-1,1,1-*d*₃)cyclohexan-1-ol (5.61a)



Sodium borohydride (10.8 mg, 0.284 mmol) was added portionwise to a solution of (2*R*,5*R*)-5-methyl-2-(2-methylpropan-2-yl-1,1,1-*d*₃)cyclohexan-1-one (31.9 mg, 0.190 mmol) in anhydrous methanol (0.37 mL) at 0 °C. The reaction was warmed to room temperature and stirred overnight. Water was added slowly to quench the reaction and the aqueous layer was extracted with diethyl ether. The combined organic layers were washed with brine, dried over sodium sulfate, filtered and concentrated under vacuum to give the crude product. The crude product was purified by column chromatography over silica gel (20% ethyl acetate in petroleum ether) to give the purified product as a colourless liquid (19.3 mg, 58%). IR $\nu_{\max}/\text{cm}^{-1}$ 2916 (C-H), 2359, 1707, 1458, 1057 (C-O). ¹H NMR (500 MHz, CDCl₃) δ 4.22-4.25 (1H, m, CHOH), 1.87-1.96 (1H, m), 1.60-1.72 (3H, m), 1.59-1.62 (1H, m), 1.49-1.57 (1H, m), 1.36-1.42 (1H, m), 1.16 (3H, d, $J = 7.5$ Hz, CH₃), 0.98-1.04 (1H, m), 0.95 (6H, s, (CH₃)₃). ¹³C NMR (126 MHz, CDCl₃) δ 69.6 (CHOH), 51.2, 40.7, 32.8, 29.9, 28.7 (2C, (CH₃)₂), 26.6, 21.5 (CH₃), 16.3. HRMS (ESI⁺) calculated for C₁₁H₁₀D₃O⁺ [M+H]⁺: 190.1886; found 190.1897. $[\alpha]^{20}_{\text{D}} = -4.8^{\circ}$ ($c = 0.0021$, CHCl₃).

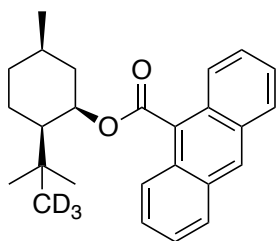
(1*S*,2*S*,5*R*)-5-Methyl-2-(2-methylpropan-2-yl-1,1,1-*d*₃)cyclohexan-1-ol (5.60a)



Sodium borohydride (33.3 mg, 0.880 mmol) was added portionwise to a solution of (2*S*,5*R*)-5-methyl-2-(2-methylpropan-2-yl-1,1,1-*d*₃)cyclohexan-1-one (98.7 mg, 0.587 mmol) in anhydrous methanol (1.1 mL) at 0 °C. The reaction was warmed to room temperature and stirred overnight. Water was added slowly to quench the reaction and the aqueous layer was extracted with diethyl ether. The combined organic layers were washed with brine,

dried over sodium sulfate, filtered and concentrated under vacuum to give the crude product. The crude product was purified by column chromatography over silica gel (20% ethyl acetate in petroleum ether) to give the purified product as a colourless liquid (62.1 mg, 61%). IR $\nu_{\max}/\text{cm}^{-1}$ 2956 (C-H), 2848, 2358, 1707, 1453, 1056 (C-O). ^1H NMR (500 MHz, CDCl_3) δ 4.21-4.24 (1H, m, CHOH), 1.68-1.80 (4H, m), 1.41-1.59 (2H, m), 1.05-1.14 (2H, m), 0.94 (6H, s, $(\text{CH}_3)_3$), 0.86 (3H, d, $J = 6.4$ Hz, CH_3). ^{13}C NMR (126 MHz, CDCl_3) δ 68.7 (CHOH), 50.8, 44.0, 35.7, 32.4, 29.8 (CD_3), 28.8 ($(\text{CH}_3)_2$), 26.3, 22.5 (CH_3), 21.3. HRMS (ESI⁺) calculated for $\text{C}_{11}\text{H}_{20}\text{D}_3\text{O}^+$ $[\text{M}+\text{H}]^+$: 190.1886; found 190.1897. $[\alpha]^{20}_{\text{D}} = +6.8^\circ$ ($c = 0.0072$, CHCl_3).

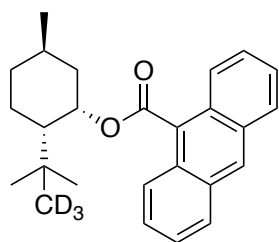
(1*R*,2*R*,5*R*)-5-Methyl-2-(2-methylpropan-2-yl-1,1,1-*d*₃)cyclohexyl anthracene-9-carboxylate (5.65a)



Trifluoroacetic anhydride (0.326 mL, 2.35 mmol) was added to a solution of 9-anthracenecarboxylic acid (130.5 mg, 0.587 mmol) in toluene (3 mL). (1*R*,2*R*,5*R*)-5-Methyl-2-(2-methylpropan-2-yl-1,1,1-*d*₃)cyclohexan-1-ol (100 mg, 0.587 mmol) was then added and the reaction was stirred for 3 hours. 10% Sodium hydroxide solution was added and the aqueous layer extracted. The organic layer was washed with water, dried over magnesium sulfate, filtered and concentrated under vacuum to give the crude product. The crude was purified by column chromatography over silica gel (hexane/ethyl acetate 10:1) to give the purified product as a yellow solid (165.5 mg, 75%). m.p. 155-157 °C. IR $\nu_{\max}/\text{cm}^{-1}$ 2957 (C-H), 2901, 2363, 1707 (C=O), 1213, 735. ^1H NMR (500 MHz, CDCl_3) δ 8.51 (1H, s, ArH), 7.99-8.10 (4H, m, ArH), 7.45-7.53 (4H, m, ArH), 5.92-5.95 (1H, m, CHOCO), 2.30-2.36 (1H, m), 1.96-2.09 (2H, m), 1.49-1.61 (1H, m), 1.40-1.45 (1H, m), 1.28-1.34 (2H, m), 1.24-1.27 (1H, m, CHCHOCO), 1.04 (3H, d, $J = 7.3$ Hz, CH_3), 0.98 (3H, s, CH_3), 0.97 (3H, s, CH_3). ^{13}C NMR (126 MHz, CDCl_3) δ 170.4 (C=O), 131.1 (2C, ArC), 129.6 (ArC), 128.6 (3C, ArCH), 127.6 (2C, ArC), 126.3 (2C, ArCH), 125.9 (2C, ArCH), 125.6 (2C, ArCH), 74.5 (CHOCO), 50.2 (CHCHOCO), 37.2, 32.7, 32.6, 29.8, 28.7 (2C, $(\text{CH}_3)_2$), 26.5, 21.7 (CH_3), 17.5. HRMS (ESI⁺) calculated for $\text{C}_{26}\text{H}_{27}\text{D}_3\text{O}_2\text{Na}^+$ $[\text{M}+\text{Na}]^+$: 400.2326; found 400.2320. $[\alpha]^{20}_{\text{D}} = -21.1^\circ$ ($c = 0.0055$, CHCl_3)

(1*S*,2*S*,5*R*)-5-Methyl-2-(2-methylpropan-2-yl-1,1,1-*d*₃)cyclohexyl anthracene-9-carboxylate

(5.66a)



Trifluoroacetic anhydride (0.326 mL, 2.34 mmol) was added to a solution of 9-anthracenecarboxylic acid (130.5 mg, 0.587 mmol) in toluene (3 mL). (1*S*,2*S*,5*R*)-5-Methyl-2-(2-methylpropan-2-yl-1,1,1-*d*₃)cyclohexan-1-ol (100 mg, 0.587 mmol) was then added and the reaction was stirred for 3 hours. 10% Sodium hydroxide solution was added and the aqueous layer extracted. The organic layer was washed with water, dried over magnesium sulfate, filtered and concentrated under vacuum to give the crude product. The crude was purified by column chromatography over silica gel (hexane/ethyl acetate 10:1) to give the purified product as a yellow solid (67.7 mg, 67%). m.p. 174-176 °C. IR ν_{max} /cm⁻¹ 2949 (C-H), 2926, 2361, 1709 (C=O), 1215, 893, 731. ¹H NMR (500 MHz, CDCl₃) δ 8.51 (1H, s, ArH), 7.98-8.05 (4H, m, ArH), 7.46-7.55 (4H, m, ArH), 5.88-5.91 (1H, m, CHOCO), 2.56 (1H, dq, *J* = 14.5, 3.3 Hz), 1.87-1.98 (1H, m), 1.74-1.80 (1H, m), 1.52-1.61 (2H, m), 1.45 (1H, td, *J* = 12.7, 3.3 Hz), 1.36 (1H, ddd, *J* = 14.8, 12.7, 2.4 Hz), 1.23-1.28 (1H, m, CHCHOCO), 1.03 (3H, d, *J* = 6.6 Hz, CH₃), 0.91 (3H, s, CH₃), 0.91 (3H, s, CH₃). ¹³C NMR (126 MHz, CDCl₃) δ 169.8 (C=O), 131.1 (2C, ArC), 129.3 (ArC), 128.8 (3C, ArCH), 127.4 (2C, ArC), 126.7 (2C, ArCH), 125.6 (2C, ArCH), 125.1 (2C, ArCH), 74.0 (CHOCO), 49.8 (CHCHOCO), 40.5, 35.4, 32.4, 28.8 (2C, (CH₃)₂), 28.7, 27.5, 22.4, 22.3 (CH₃). HRMS (ESI⁺) calculated for C₂₆H₂₈D₃O₂⁺ [M+H]⁺: 378.2512; found 378.2463. [α]_D²⁰ = +13.2° (c = 0.0079, CHCl₃).

7.6 Experimental details for computational analysis in Chapter 4

The accessible conformers of compounds **4.68**, **4.70**, **4.71** and **4.72** were explored using the iterative workflow approach with static metadynamics simulations (--v4 keyword) as implemented in CREST software^{282, 283} at the semiempirical GFN2-xTB level of theory.²⁸⁴ The resulting conformers were fully optimized with the hybrid Minnesota family functional M06-2X²⁸⁵ and Alrichs' triple ζ def2-TZVP basis set²⁸⁶ in Gaussian 16 rev C.01 program. Frequency

calculations confirmed all geometries as true energy minima, showing no imaginary frequencies. Molecular dipole moments were calculated for the global minima of **4.68**, **4.70**, **4.71** and **4.72** at the M06-2X/def2-TZVP level. The global minimum of **4.68** was used to explore the rotational energy profile (relaxed PES) around one C-CH₂F bond at the M06-2X/def2-TZVP theoretical level. Thermal corrections for each stationary point obtained from frequency calculations at standard temperature and pressure within the harmonic oscillator and rigid rotor models at the M06-2X/def2-TZVP theoretical level. No imaginary frequency was found for minima geometries, and a single imaginary frequency, corresponding to the C-CH₂F bond rotation, was found for the saddle points. NBO analysis (using the NBO 7.0 program^{287, 288} as implemented in Gaussian 16) was carried out at the M06-2X/def2-TZVP level of theory over optimised minima geometries, and NCI analysis²⁸⁹ calculated over the electron densities obtained at the same theoretical level.

Chapter 8 - References

- 1 S. Dehnen, L. L. Schafer, T. Lectka and A. Togni, *Inorg. Chem.*, **2021**, *60*, 17419–17425.
- 2 R. H. Langley and L. Welch, *J. Chem. Educ.*, **1983**, *60*, 759–761.
- 3 J. Flahaut and C. Viel, *J. Fluor. Chem.*, **1986**, *33*, 27–43.
- 4 H. Goldwhite, *J. Fluor. Chem.*, **1986**, *33*, 109–132.
- 5 L. Pauling, *J. Am. Chem. Soc.*, **1932**, *54*, 3570–3582.
- 6 D. O'Hagan, *Chem. Soc. Rev.*, **2008**, *37*, 308–319.
- 7 D. M. Lemal, *J. Org. Chem.*, **2004**, *69*, 1–11.
- 8 K. B. Wiberg and P. R. Rablen, *J. Am. Chem. Soc.*, **1993**, *115*, 614–625.
- 9 P. Ryberg and O. Matsson, *J. Org. Chem.*, **2002**, *67*, 811–814.
- 10 B. E. Smart, *J. Fluor. Chem.*, **2001**, *109*, 3–11.
- 11 T. Su, T. Zhang, S. Xie, J. Yan, Y. Wu, X. Li, L. Huang and H.-B. Luo, *Sci. Rep.*, **2016**, *6*, 21826.
- 12 P.-Y. Lien, R.-M. You and W.-P. Hu, *J. Phys. Chem. A*, **2001**, *105*, 2391–2400.
- 13 J. W. Banks, A. S. Batsanov, J. A. K. Howard, D. O'Hagan, H. S. Rzepa and S. Martin-Santamaria, *J. Chem. Soc., Perkin Trans. 2*, **1999**, *11*, 2409–2411.
- 14 B. J. van der Veken, S. Truyen, W. A. Herrebout and G. Watkins, *J. Mol. Struct.*, **1993**, *293*, 55–58.
- 15 R. J. Abraham, A. D. Jones, M. A. Warne, R. Rittner and C. F. Tormena, *J. Chem. Soc., Perkin Trans. 2*, **1996**, *4*, 533.
- 16 H. V. Phan and J. R. Durig, *J. Mol. Struct. Theochem*, **1990**, *209*, 333–347.
- 17 D. Wu, A. Tian and H. Sun, *J. Phys. Chem. A*, **1998**, *102*, 9901–9905.
- 18 A. Sun, D. C. Lankin, K. Hardcastle and J. P. Snyder, *Chem. Eur. J.*, **2005**, *11*, 1579–1591.
- 19 C. R. S. Briggs, M. J. Allen, D. O'Hagan, D. J. Tozer, A. M. Z. Slawin, A. E. Goeta and J. A. K. Howard, *Org. Biomol. Chem.*, **2004**, *2*, 732.
- 20 S. Purser, P. R. Moore, S. Swallow and V. Gouverneur, *Chem. Soc. Rev.*, **2008**, *37*, 320–330.
- 21 D. O'Hagan, *J. Fluor. Chem.*, **2010**, *131*, 1071–1081.
- 22 D. T. Wong, F. P. Bymaster and E. A. Engleman, *Life. Sci.*, **1995**, *57*, 411–441.

- 23 B. D. Roth, C. J. Blankley, A. W. Chucholowski, M. L. Hoefle, D. F. Ortwine, D. R. Sliskovic, M. W. Wilson, E. Ferguson, R. S. Newton, C. S. Sekerke and C. D. Stratton, *J. Med. Chem.*, **1991**, *34*, 357–366.
- 24 G. H. Phillipps, *Respir. Med.*, **1990**, *84 Suppl A*, 19–23.
- 25 J. Han, A. M. Remete, L. S. Dobson, L. Kiss, K. Izawa, H. Moriwaki, V. A. Soloshonok and D. O’Hagan, *J. Fluor. Chem.*, **2020**, *239*, 109639-109666.
- 26 W. K. Hagmann, *J. Med. Chem.*, **2008**, *51*, 4359–4369.
- 27 P. Shah and A. D. Westwell, *J. Enzyme Inhib. Med. Chem.*, **2007**, *22*, 527–540.
- 28 H. L. Yale, *J. Med. Pharm. Chem.*, **1959**, *1*, 121–133.
- 29 E. Moore, M. E. Fraley, I. M. Bell, C. S. Burgey, R. B. White, C.-C. Li, C. P. Regan, A. Danziger, M. Stranieri Michener, E. Hostetler, P. Banerjee and C. Salvatore, *J. Pharmacol. Exp. Ther.*, **2020**, *373*, 160–166.
- 30 S. J. Keam, *Drugs*, **2019**, *79*, 1797–1803.
- 31 J. Waugh and B. Jarvis, *Drugs Aging*, **2002**, *19*, 465–471.
- 32 F. Edelmann, *Pap. Proc. R. Soc. Tasmania*, **2016**, *150*, 45–49.
- 33 C. J. Giunta, *Bull. Hist. Chem.*, **2006**, *31*, 66–74.
- 34 M. J. Molina and F. S. Rowland, *Nature*, **1974**, *249*, 810–812.
- 35 S. C. Wofsy, M. B. McElroy and N. D. Sze, *Science (1979)*, **1975**, *187*, 535–537.
- 36 F. Watanabe and O. Shimomura, *Eisei kagaku*, **1991**, *37*, 337–346.
- 37 G. J. M. Velders, S. O. Andersen, J. S. Daniel, D. W. Fahey and M. McFarland, *Proc. Natl. Acad. Sci.*, **2007**, *104*, 4814–4819.
- 38 H. Sidebottom and J. Franklin, *Pure Appl. Chem.*, **1996**, *68*, 1757–1769.
- 39 S. A. Montzka, M. McFarland, S. O. Andersen, B. R. Miller, D. W. Fahey, B. D. Hall, L. Hu, C. Siso and J. W. Elkins, *J. Phys. Chem. A*, **2015**, *119*, 4439–4449.
- 40 H. Flerlage, G. J. M. Velders and J. de Boer, *Chemosphere*, **2021**, *283*, 131208.
- 41 C. B. Rivela, C. M. Tovar, M. A. Teruel, I. Barnes, P. Wiesen and M. B. Blanco, *Chem. Phys. Lett.*, **2019**, *714*, 190–196.
- 42 R. C. Buck, J. Franklin, U. Berger, J. M. Conder, I. T. Cousins, P. de Voogt, A. A. Jensen, K. Kannan, S. A. Mabury and S. P. van Leeuwen, *Integr. Environ. Assess. Manag.*, **2011**, *7*, 513–541.

- 43 Z. Wang, A. M. Buser, I. T. Cousins, S. Demattio, W. Drost, O. Johansson, K. Ohno, G. Patlewicz, A. M. Richard, G. W. Walker, G. S. White and E. Leinala, *Environ. Sci. Technol.*, **2021**, *55*, 15575–15578.
- 44 W. Nicole, *Environ. Health Perspect.*, **2010**, *118*, 1100–1108.
- 45 G. B. Post, P. D. Cohn and K. R. Cooper, *Environ. Res.*, **2012**, *116*, 93–117.
- 46 K. Steenland, T. Fletcher and D. A. Savitz, *Environ. Health Perspect.*, **2010**, *118*, 1100–1108.
- 47 H. Teng, *Appl. Sci.*, **2012**, *2*, 496–512.
- 48 G. J. Puts, P. Crouse and B. M. Ameduri, *Chem. Rev.*, **2019**, *119*, 1763–1805.
- 49 J. Blumm, A. Lindemann, M. Meyer and C. Strasser, *Int. J. Thermophys.*, **2010**, *31*, 1919–1927.
- 50 M. Sajid and M. Ilyas, *Environ. Sci. Pollut. Res.*, **2017**, *24*, 23436–23440.
- 51 A. P. Dobbs and M. R. Kimberley, *J. Fluor. Chem.*, **2002**, *118*, 3–17.
- 52 I. T. Horváth and J. Rábai, *Science (1979)*, **1994**, *266*, 72–75.
- 53 W. C. Smith, *Angew. Chem. Intl. Ed. Engl.*, **1962**, *1*, 467–475.
- 54 W. R. Hasek, W. C. Smith and V. A. Engelhardt, *J. Am. Chem. Soc.*, **1960**, *82*, 543–551.
- 55 W. J. Middleton, *J. Org. Chem.*, **1975**, *40*, 574–578.
- 56 R. P. Singh and J. M. Shreeve, *Synthesis (Stuttg.)*, **2002**, *2002*, 2561–2578.
- 57 P. A. Messina, K. C. Mange and W. J. Middleton, *J. Fluor. Chem.*, **1989**, *42*, 137–143.
- 58 G. S. Lal, G. P. Pez, R. J. Pesaresi, F. M. Prozonic and H. Cheng, *J. Org. Chem.*, **1999**, *64*, 7048–7054.
- 59 G. S. Lal, G. P. Pez and R. G. Syvret, *Chem. Rev.*, **1996**, *96*, 1737–1755.
- 60 W. E. Barnette, *J. Am. Chem. Soc.*, **1984**, *106*, 452–454.
- 61 T. Umemoto, K. Kawada and K. Tomita, *Tetrahedron Lett.*, **1986**, *27*, 4465–4468.
- 62 G. S. Lal, *J. Org. Chem.*, **1993**, *58*, 2791–2796.
- 63 Y. Takeyama, Y. Ichinose, K. Oshima and K. Utimoto, *Tetrahedron Lett.*, **1989**, *30*, 3159–3162.
- 64 K. Iseki, T. Nagai and Y. Kobayashi, *Tetrahedron Lett.*, **1993**, *34*, 2169–2170.
- 65 V. Aclav, M. Sek, A. Togni, V. Bizet and D. Cahard, *Org. Lett.*, **2011**, *13*, 5762–5765.
- 66 T. Umemoto and K. Adachi, *J. Org. Chem.*, **1994**, *59*, 5692–5699.
- 67 T. Umemoto, *Chem. Rev.*, **1996**, *96*, 1757–1777.
- 68 W. R. Dolbier, *Chem. Rev.*, **1996**, *96*, 1557–1584.

- 69 J. D. Park, F. E. Rogers and J. R. Lacher, *J. Org. Chem.*, **1961**, *26*, 2089–2095.
- 70 N. O. Brace, *J. Org. Chem.*, **1967**, *32*, 430–434.
- 71 X.-J. Tang and W. R. Dolbier, *Angew. Chem. Intl. Ed.*, **2015**, *54*, 4246–4249.
- 72 M. Pirtsch, S. Paria, T. Matsuno, H. Isobe and O. Reiser, *Chem. Eur. J.*, **2012**, *18*, 7336–7340.
- 73 Y. Fujiwara, J. A. Dixon, F. O’Hara, E. D. Funder, D. D. Dixon, R. A. Rodriguez, R. D. Baxter, B. Herlé, N. Sach, M. R. Collins, Y. Ishihara and P. S. Baran, *Nature*, **2012**, *492*, 95–99.
- 74 D. A. Nagib and D. W. C. MacMillan, *Nature*, **2011**, *480*, 224–228.
- 75 J. Wang, H. Xing, X. Qin, Q. Ren, J. Yang and L. Li, *J. Ethnopharmacol.*, **2020**, *262*, 113120.
- 76 M. Stoll, J. Hulstkamp and A. Rouvé, *Helv. Chim. Acta.*, **1948**, *31*, 543–553.
- 77 T. Yamamoto, A. Shimada, T. Ohmoto, H. Matsuda, M. Ogura and T. Kanisawa, *Flavour Fragr. J.*, **2004**, *19*, 121–133.
- 78 H. Walbaum, *J. Prakt. Chem.*, **1906**, *73*, 488–493.
- 79 L. Ruzicka, M. Stoll and H. Schinz, *Helv. Chim. Acta.*, **1926**, *9*, 249–264.
- 80 V. P. Kamat, H. Hagiwara, T. Katsumi, T. Hoshi, T. Suzuki and M. Ando, *Tetrahedron*, **2000**, *56*, 4397–4403.
- 81 P. Schwab, M. B. France, J. W. Ziller and R. H. Grubbs, *Angew. Chem. Intl. Ed. Engl.*, **1995**, *34*, 2039–2041.
- 82 E. Block, S. Jang, H. Matsunami, S. Sekharan, B. Dethier, M. Z. Ertem, S. Gundala, Y. Pan, S. Li, Z. Li, S. N. Lodge, M. Ozbil, H. Jiang, S. F. Penalba, V. S. Batista and H. Zhuang, *Proc. Natl. Acad. Sci. U. S. A.*, **2015**, *112*, E2766–E2774.
- 83 I. A. Solov’yov, P.-Y. Chang and K. Schulten, *Phys. Chem. Chem. Phys.*, **2012**, *14*, 13861–13871.
- 84 G. Bernardinelli and R. Gerdil, *Helv. Chim. Acta.*, **1982**, *65*, 1310–1317.
- 85 R. Callejo, M. J. Corr, M. Yang, M. Wang, D. B. Cordes, A. M. Z. Slawin and D. O’Hagan, *Chem. Eur. J.*, **2016**, *22*, 8137–8151.
- 86 M. J. Corr, R. A. Cormanich, C. N. von Hahmann, M. Bühl, D. B. Cordes, A. M. Z. Slawin and D. O’Hagan, *Org. Biomol. Chem.*, **2016**, *14*, 211–219.
- 87 G. Malcolm Dyson, *J. Soc. Chem. Ind.*, **1938**, *57*, 647–651.
- 88 R. H. Wright, *J. Theor. Biol.*, **1977**, *64*, 473–502.

- 89 L. Turin, *Chem. Senses*, **1996**, *21*, 773–791.
- 90 S. Gane, D. Georganakis, K. Maniati, M. Vamvakias, N. Ragoussis, E. M. C. Skoulakis and L. Turin, *PLoS One*, **2013**, *8*, e55780.
- 91 M. Shirasu, K. Yoshikawa, Y. Takai, A. Nakashima, H. Takeuchi, H. Sakano and K. Touhara, *Neuron*, **2014**, *81*, 165–178.
- 92 K. Touhara and L. B. Vosshall, *Annu. Rev. Physiol.*, **2009**, *71*, 307–332.
- 93 R. C. Araneda, A. D. Kini and S. Firestein, *Nat. Neurosci.*, **2000**, *3*, 1248–1255.
- 94 K. Mori, Y. K. Takahashi, K. M. Igarashi and M. Yamaguchi, *Physiol. Rev.*, **2006**, *86*, 409–433.
- 95 P. T. Lowe and D. O’Hagan, *J. Fluor. Chem.*, **2020**, *230*, 109420-109442.
- 96 M. Skibinski, Y. Wang, A. M. Z. Slawin, T. Lebl, P. Kirsch and D. O’Hagan, *Angew. Chem. Intl. Ed.*, **2011**, *50*, 10581–10584.
- 97 J. D. Dunitz and H. M. M. Shearer, *Helv. Chim. Acta.*, **1960**, *43*, 18–35.
- 98 F. A. L. Anet and T. N. Rawdah, *J. Am. Chem. Soc.*, **1978**, *100*, 7166–7171.
- 99 Y. Zhang, Y. Pan, H. Matsunami and H. Zhuang, *J. Visualized Exp.*, **2017**, *2017*, e55831.
- 100 H. Zhuang and H. Matsunami, *Nat. Protoc.*, **2008**, *3*, 1402–1413.
- 101 L. Ahmed, Y. Zhang, E. Block, M. Buehl, M. J. Corr, R. A. Cormanich, S. Gundala, H. Matsunami, D. O’Hagan, M. Ozbil, Y. Pan, S. Sekharan, N. Ten, M. Wang, M. Yang, Q. Zhang, R. Zhang, V. S. Batista and H. Zhuang, *Proc. Natl. Acad. Sci.*, **2018**, *115*, E3950–E3958.
- 102 N. Armanino, J. Charpentier, F. Flachsmann, A. Goeke, M. Liniger and P. Kraft, *Angew. Chem. Intl. Ed.*, **2020**, *59*, 16310–16344.
- 103 S. Fujimoto, K. Yoshikawa, M. Itoh and T. Kitahara, *Biosci. Biotechnol. Biochem.*, **2002**, *66*, 1389–1392.
- 104 C. Fehr, J. Galindo and O. Etter, *Eur. J. Org. Chem.*, **2004**, *2004*, 1953–1957.
- 105 D. Astruc, *New J. Chem.*, **2005**, *29*, 42–56.
- 106 R. H. Grubbs, *Tetrahedron*, **2004**, *60*, 7117–7140.
- 107 C. P. Casey and T. J. Burkhardt, *J. Am. Chem. Soc.*, **1974**, *96*, 7808–7809.
- 108 G. C. Fu, S. T. Nguyen and R. H. Grubbs, *J. Am. Chem. Soc.*, **1993**, *115*, 9856–9857.
- 109 P. Schwab, M. B. France, J. W. Ziller and R. H. Grubbs, *Angew. Chem. Intl. Ed. Engl.*, **1995**, *34*, 2039–2041.
- 110 P. Schwab, R. H. Grubbs and J. W. Ziller, *J. Am. Chem. Soc.*, **1996**, *118*, 100–110.

- 111 T. A. Kirkland and R. H. Grubbs, *J. Org. Chem.*, **1997**, *62*, 7310–7318.
- 112 M. Scholl, S. Ding, C. W. Lee and R. H. Grubbs, *Org. Lett.*, **1999**, *1*, 953–956.
- 113 G. C. Vougioukalakis and R. H. Grubbs, *Chem. Rev.*, **2010**, *110*, 1746–1787.
- 114 J. S. Kingsbury, J. P. A. Harrity, P. J. Bonitatebus and A. H. Hoveyda, *J. Am. Chem. Soc.*, **1999**, *121*, 791–799.
- 115 S. B. Garber, J. S. Kingsbury, B. L. Gray and A. H. Hoveyda, *J. Am. Chem. Soc.*, **2000**, *122*, 8168–8179.
- 116 P. Jean-Louis Hérisson and Y. Chauvin, *Makromol. Chem.*, **1971**, *141*, 161–176.
- 117 D. M. Jensen, *N. Engl. J. Med.*, **2011**, *364*, 1272–1274.
- 118 J. Kong, C. Chen, J. Balsells-Padros, Y. Cao, R. F. Dunn, S. J. Dolman, J. Janey, H. Li and M. J. Zacuto, *J. Org. Chem.*, **2012**, *77*, 3820–3828.
- 119 D. Martin, A. Weise and H.-J. Niclas, *Angew. Chem. Intl. Ed. Engl.*, **1967**, *6*, 318–334.
- 120 R. Bentley, *Chem. Soc. Rev.*, **2005**, *34*, 609.
- 121 L. Olbe, E. Carlsson and P. Lindberg, *Nat. Rev. Drug Discov.*, **2003**, *2*, 132–139.
- 122 Q. Zhou, X.-F. Yan, W.-S. Pan and S. Zeng, *World J. Gastroenterol.*, **2008**, *14*, 2617.
- 123 T. M. Engber, E. J. Koury, S. A. Dennis, M. S. Miller, P. C. Contreras and R. V Bhat, *Neurosci. Lett.*, **1998**, *241*, 95–98.
- 124 M. Darwish, M. Kirby, E. T. Hellriegel and P. Robertson, *Clin. Drug Investig.*, **2009**, *29*, 613–623.
- 125 D. A. Evans, M. D. Ennis and D. J. Mathre, *J. Am. Chem. Soc.*, **1982**, *104*, 1737–1739.
- 126 K. B. Sharpless, R. F. Lauer and A. Y. Teranishi, *J. Am. Chem. Soc.*, **1973**, *95*, 6137–6139.
- 127 R. N. Salvatore, R. A. Smith, A. K. Nischwitz and T. Gavin, *Tetrahedron Lett.*, **2005**, *46*, 8931–8935.
- 128 C. Fehr, J. Galindo, R. Haubiichs and R. Perret, *Helv. Chim. Acta.*, **1989**, *72*, 1537–1553.
- 129 A. Baur, *US Pat.*, US416710, **1889**.
- 130 O. R. P. David, *Eur. J. Org. Chem.*, **2017**, *2017*, 4–13.
- 131 K. M. Taylor, M. Weisskopf and J. Shine, *Environ. Health*, **2014**, *13*, 14.
- 132 E. Schnauffer and H. Hupfeld, *US Pat.*, US412545A, **1889**.
- 133 A. Baur, *US Pat.*, US481685, **1892**.
- 134 W. Mallmann, *Br. Pat.*, GB189404018A, **1894**.
- 135 S. Dörrich, J. B. Bauer, S. Lorenzen, C. Mahler, S. Schweetberg, C. Burschka, J. A. Baus, R. Tacke and P. Kraft, *Chem. Eur. J.*, **2013**, *19*, 11396–11408.

- 136 H. Barbier, *Helv. Chim. Acta.*, **1932**, *15*, 592–596.
- 137 H. Barbier, *Helv. Chim. Acta.*, **1936**, *19*, 1345–1354.
- 138 A. V. Grampoloff, *Helv. Chim. Acta.*, **1955**, *38*, 1263–1268.
- 139 M. S. Carpenter, *US Pat.*, US2072293A, **1935**.
- 140 M. S. Carpenter, *US Pat.*, US756798, **1947**.
- 141 P. S. Spencer, M. C. Bischoff-Fenton, O. M. Moreno, D. L. Opdyke and R. A. Ford, *Toxicol. Appl. Pharmacol.*, **1984**, *75*, 571–575.
- 142 V. Homem, I. Magalhães, A. Alves and L. Santos, *Environ. Pollut.*, **2017**, *226*, 190–197.
- 143 H. H. Schmeiser, R. Gminski and V. Mersch-Sundermann, *Int. J. Hyg. Environ. Health*, **2001**, *203*, 293–299.
- 144 B. Liebl and S. Ehrenstorfer, *Chemosphere*, **1993**, *27*, 2253–2260.
- 145 T. Yamagishi, T. Miyazaki, S. Horii and K. Akiyama, *Arch. Environ. Contam. Toxicol.*, **1983**, *12*, 83–89.
- 146 W. Butte, S. Schmidt and A. Schmidt, *Chemosphere*, **1999**, *38*, 1287–1291.
- 147 M. S. Carpenter, W. M. Easter and T. F. Wood, *J. Org. Chem.*, **1951**, *16*, 586–617.
- 148 G. Fráter, U. Müller and P. Kraft, *Helv. Chim. Acta.*, **1999**, *82*, 1656–1665.
- 149 L. Heeringa and M. Beets, *Br. Pat.*, GB991146A, **1965**.
- 150 O. R. P. David, *Chem. Eur. J.*, **2020**, *26*, 7537–7555.
- 151 T. F. Wood, W. M. Easter, M. S. Carpenter and J. Angiolini, *J. Org. Chem.*, **1963**, *28*, 2248–2255.
- 152 Th. Heberer, S. Gramer and H.-J. Stan, *Acta. Hydrochim. Hydrobiol.*, **1999**, *27*, 150–156.
- 153 R. Gatermann, J. Hellou, H. Hühnerfuss, G. Rimkus and V. Zitko, *Chemosphere*, **1999**, *38*, 3431–3441.
- 154 H. P. Hutter, P. Wallner, H. Moshhammer, W. Hartl, R. Sattelberger, G. Lorbeer and M. Kundi, *Chemosphere*, **2005**, *59*, 487–492.
- 155 T. Heberer, *Acta. Hydrochim. Hydrobiol.*, **2002**, *30*, 227–243.
- 156 P. Kraft, J. A. Bajgrowicz, C. Denis and G. Fráter, *Angew. Chem. Intl. Ed.*, **2000**, *39*, 2980–3010.
- 157 P. Kraft, V. Di Cristofaro and S. Jordi, *Chem. Biodivers.*, **2014**, *11*, 1567–1596.
- 158 V. Dacho, M. Babjak, J. Peřka and P. Szolcsányi, *Eur. J. Org. Chem.*, **2023**, *26*, e2023000.

- 159 M. Geyer, J. Bauer, C. Burschka, P. Kraft and R. Tacke, *Eur. J. Inorg. Chem.*, **2011**, 2011, 2769–2776.
- 160 P. Kraft and K. Popaj, *Eur. J. Org. Chem.*, **2008**, 2008, 4806–4814.
- 161 P. Kraft, S. Jordi, N. Denizot and I. Felker, *Eur. J. Org. Chem.*, **2014**, 2014, 554–563.
- 162 I. Felker, G. Pupo, P. Kraft and B. List, *Angew. Chem. Intl. Ed.*, **2015**, 54, 1960–1964.
- 163 K. Sonogashira, Y. Tohda and N. Hagihara, *Tetrahedron Lett.*, **1975**, 16, 4467–4470.
- 164 R. D. Stephens and C. E. Castro, *J. Org. Chem.*, **1963**, 28, 3313–3315.
- 165 D. Wang and S. Gao, *Org. Chem. Front.*, **2014**, 1, 556–566.
- 166 E. J. Corey, M. Chol. Kang, M. C. Desai, A. K. Ghosh and I. N. Houpis, *J. Am. Chem. Soc.*, **1988**, 110, 649–651.
- 167 W. Chodkiewicz and P. Cadiot, *C. R. Hebd. Seances. Acad. Sci.*, **1955**, 241, 1055–1057.
- 168 K. S. Sindhu, A. P. Thankachan, P. S. Sajitha and G. Anilkumar, *Org. Biomol. Chem.*, **2015**, 13, 6891–6905.
- 169 S. Radhika, N. A. Harry, M. Neetha and G. Anilkumar, *Org. Biomol. Chem.*, **2019**, 17, 9081–9094.
- 170 J.-X. Gong, H.-Y. Wang, L.-G. Yao, X.-W. Li and Y.-W. Guo, *Synlett.*, **2015**, 27, 391–394.
- 171 S. Wolfe, *Acc. Chem. Res.*, **1972**, 5, 102–111.
- 172 D. Rodrigues Silva, L. Azevedo Santos, T. A. Hamlin, C. Fonseca Guerra, M. P. Freitas and F. M. Bickelhaupt, *ChemPhysChem*, **2021**, 22, 641–648.
- 173 A. Abe, *J. Am. Chem. Soc.*, **1976**, 98, 6477–6480.
- 174 J. D. Dunitz and R. Taylor, *Chem. Eur. J.*, **1997**, 3, 89–98.
- 175 A. Karipides and C. Miller, *J. Am. Chem. Soc.*, **1984**, 106, 1494–1495.
- 176 C. Otake, T. Namba, H. Tabata, K. Makino, K. Hirano, T. Oshitari, H. Natsugari, T. Kusumi and H. Takahashi, *J. Org. Chem.*, **2021**, 86, 4638–4645.
- 177 S. Lobo, *Expert Opin. Drug Discov.*, **2020**, 15, 261–263.
- 178 P. D. Leeson and B. Springthorpe, *Nat. Rev. Drug Discov.*, **2007**, 6, 881–890.
- 179 A. K. Ghose, V. N. Viswanadhan and J. J. Wendoloski, *J. Comb. Chem.*, **1999**, 1, 55–68.
- 180 B. E. Smart, *J. Fluor. Chem.*, **2001**, 109, 3–11.
- 181 H.-J. Böhm, D. Banner, S. Bendels, M. Kansy, B. Kuhn, K. Müller, U. Obst-Sander and M. Stahl, *ChemBioChem*, **2004**, 5, 637–643.
- 182 A. Rodil, S. Bosisio, M. S. Ayoup, L. Quinn, D. B. Cordes, A. M. Z. Slawin, C. D. Murphy, J. Michel and D. O’Hagan, *Chem. Sci.*, **2018**, 9, 3023–3028.

- 183 Z. Fang, D. B. Cordes, A. M. Z. Slawin and D. O'Hagan, *Chem. Commun.*, **2019**, *55*, 10539–10542.
- 184 P. Bisel, L. Al-Momani and M. Müller, *Org. Biomol. Chem.*, **2008**, *6*, 2655–2665.
- 185 K. Strømgaard and K. Nakanishi, *Angew. Chem. Intl. Ed.*, **2004**, *43*, 1640–1658.
- 186 E. J. Corey and K. S. Rao, *Tetrahedron Lett.*, **1991**, *32*, 4623–4626.
- 187 C. Kotake, T. Yamasaki, T. Moriyama, M. Shinoda, N. Komiyama, T. Furumai, M. Konishi and T. Oki, *J. Antibiot.*, **1992**, *45*, 1442–1450.
- 188 T. A. van Beek and P. Montoro, *J. Chromatogr. A*, **2009**, *1216*, 2002–2032.
- 189 C. Kiewert, V. Kumar, O. Hildmann, J. Hartmann, M. Hillert and J. Klein, *Brain Res.*, **2008**, *1201*, 143–150.
- 190 Y. Deng, H.-C. Bi, L.-Z. Zhao, F. He, Y.-Q. Liu, J.-J. Yu, Z.-M. Ou, L. Ding, X. Chen, Z.-Y. Huang, M. Huang and S.-F. Zhou, *Xenobiotica*, **2008**, *38*, 465–481.
- 191 J.-L. Giner and C. Djerassi, *Phytochemistry*, **1991**, *30*, 811–814.
- 192 P. G. Middleton, M. A. Mall, P. Dřevínek, L. C. Lands, E. F. McKone, D. Polineni, B. W. Ramsey, J. L. Taylor-Cousar, E. Tullis, F. Vermeulen, G. Marigowda, C. M. McKee, S. M. Moskowitz, N. Nair, J. Savage, C. Simard, S. Tian, D. Waltz, F. Xuan, S. M. Rowe and R. Jain, *New Engl. J. Med.*, **2019**, *381*, 1809–1819.
- 193 V. A. Cullum, J. B. Farmer, D. Jack and G. P. Levy, *Br. J. Pharmacol.*, **1969**, *35*, 141–151.
- 194 T. I. Ng, P. Krishnan, T. Pilot-Matias, W. Kati, G. Schnell, J. Beyer, T. Reisch, L. Lu, T. Dekhtyar, M. Irvin, R. Tripathi, C. Maring, J. T. Randolph, R. Wagner and C. Collins, *Antimicrob. Agents Chemother.*, **2017**, *61*, e02558-16, 1-14.
- 195 K. Akinosoglou, G. Schinas and C. Gogos, *Viruses*, **2022**, *14*, 2540.
- 196 P. Remuzon, D. Bouzard, P. Di Cesare, M. Essiz, J. P. Jacquet, J. R. Kiechel, B. Ledoussal, R. E. Kessler and J. Fung-Tomc, *J. Med. Chem.*, **1991**, *34*, 29–37.
- 197 D. Ok, M. H. Fisher, M. J. Wyvratt and P. T. Meinke, *Tetrahedron Lett.*, **1999**, *40*, 3831–3834.
- 198 F. A. Davis, G. Venkat Reddy, M. Bental and C. J. Deutsch, *Synthesis (Stuttg.)*, **1994**, *7*, 701–702.
- 199 N. Miyaura and A. Suzuki, *J. Chem. Soc. Chem. Commun.*, **1979**, *19*, 866–867.
- 200 H. A. Dieck and R. F. Heck, *J. Org. Chem.*, **1975**, *40*, 1083–1090.
- 201 N. Miyaura, K. Yamada and A. Suzuki, *Tetrahedron Lett.*, **1979**, *20*, 3437–3440.
- 202 N. Miyaura, T. Yanagi and A. Suzuki, *Synth. Commun.*, **1981**, *11*, 513–519.

- 203 A. Suzuki, *J. Organomet. Chem.*, **1999**, 576, 147–168.
- 204 R. Rossi, A. Carpita and M. G. Quirici, *Tetrahedron*, **1981**, 37, 2617–2623.
- 205 N. K. Garg, D. D. Caspi and B. M. Stoltz, *J. Am. Chem. Soc.*, **2004**, 126, 9552–9553.
- 206 A. S. Guram, R. A. Rennels and S. L. Buchwald, *Angew. Chem. Intl. Ed. Engl.*, **1995**, 34, 1348–1350.
- 207 J. Louie and J. F. Hartwig, *Tetrahedron Lett.*, **1995**, 36, 3609–3612.
- 208 J. P. Wolfe, S. Wagaw and S. L. Buchwald, *J. Am. Chem. Soc.*, **1996**, 118, 7215–7216.
- 209 M. S. Driver and J. F. Hartwig, *J. Am. Chem. Soc.*, **1996**, 118, 7217–7218.
- 210 Y. Guari, D. S. van Es, J. N. H. Reek, P. C. J. Kamer and P. W. N. M. van Leeuwen, *Tetrahedron Lett.*, **1999**, 40, 3789–3790.
- 211 R. Dorel, C. P. Grugel and A. M. Haydl, *Angew. Chem.*, **2019**, 131, 17276–17287.
- 212 M. M. Heravi, Z. Kheilkordi, V. Zadsirjan, M. Heydari and M. Malmir, *J. Organomet. Chem.*, **2018**, 861, 17–104.
- 213 C. Schuster, C. Börger, K. K. Julich-Gruner, R. Hesse, A. Jäger, G. Kaufmann, A. W. Schmidt and H.-J. Knölker, *Eur. J. Org. Chem.*, **2014**, 2014, 4741–4752.
- 214 E. A. Abourashed, A. M. Clark and C. D. Hufford, *Curr. Med. Chem.*, **1999**, 6, 359–374.
- 215 K. Lisowska, J. Szemraj, S. Rozalska and J. Dlugonski, *FEMS Microbiol. Lett.*, **2006**, 261, 175–180.
- 216 D. Zhang, J. P. Freeman, J. B. Sutherland, A. E. Walker, Y. Yang and C. E. Cerniglia, *Appl. Environ. Microbiol.*, **1996**, 62, 798–803.
- 217 T. A. Ban, *Neuropsychiatr. Dis. Treat.*, **2007**, 3, 495–500.
- 218 K. Keller, M. Zalibera, M. Qi, V. Koch, J. Wegner, H. Hintz, A. Godt, G. Jeschke, A. Savitsky and M. Yulikov, *Phys. Chem. Chem. Phys.*, **2016**, 18, 25120–25135.
- 219 Q. A. Huchet, B. Kuhn, B. Wagner, H. Fischer, M. Kansy, D. Zimmerli, E. M. Carreira and K. Müller, *J. Fluor. Chem.*, **2013**, 152, 119–128.
- 220 P. Thordarson, *Chem. Soc. Rev.*, **2011**, 40, 1305–1323.
- 221 D. Brynn Hibbert and P. Thordarson, *Chem. Commun.*, **2016**, 52, 12792–12805.
- 222 K. Hirata, Y. Kawamura, M. Kudo and H. Igarashi, *J. Pestic. Sci.*, **1995**, 20, 213–221.
- 223 D. Suarez, G. Laval, S.-M. Tu, D. Jiang, C. Robinson, R. Scott and B. Golding, *Synthesis (Stuttg.)*, **2009**, 2009, 1807–1810.
- 224 M. Dang, M. Liu, L. Huang, X. Ou, C. Long, X. Liu, Y. Ren, P. Zhang, M. Huang and A. Liu, *J. Heterocycl. Chem.*, **2020**, 57, 4088–4098.

- 225 A. L. Henne and M. S. Newman, *J. Am. Chem. Soc.*, **1938**, *60*, 1697–1698.
- 226 P. H. J. Carlsen, T. Katsuki, V. S. Martin and K. B. Sharpless, *J. Org. Chem.*, **1981**, *46*, 3936–3938.
- 227 E. Harunari, H. Komaki and Y. Igarashi, *Beilstein J. Org. Chem.*, **2017**, *13*, 441–450.
- 228 H. G. Floss and S. Lee, *Acc. Chem. Res.*, **1993**, *26*, 116–122.
- 229 J. Lüthy, J. Rétey and D. Arigoni, *Nature*, **1969**, *221*, 1213–1215.
- 230 J. W. Cornforth, J. W. Redmond, H. Eggerer, W. Buckel and C. Gutschow, *Nature*, **1969**, *221*, 1212–1213.
- 231 H. Lenz and H. Eggerer, *Eur. J. Biochem.*, **1976**, *65*, 237–246.
- 232 F. A. L. Anet, D. J. O’Leary, J. M. Beale and H. G. Floss, *J. Am. Chem. Soc.*, **1989**, *111*, 8935–8936.
- 233 L. Mascaro, R. Hoerhammer, S. Eisenstein, L. K. Sellers, K. Mascaro and H. G. Floss, *J. Am. Chem. Soc.*, **1977**, *99*, 273–274.
- 234 R. W. Woodard, M. D. Tsai, H. G. Floss, P. A. Crooks and J. K. Coward, *J. Biol. Chem.*, **1980**, *255*, 9124–9127.
- 235 D. Arigoni, in *Ciba Foundation Symposium 60 - Molecular Interactions and Activity in Proteins*, **1978**, pp. 243–268.
- 236 A. Schweifer and F. Hammerschmidt, *Biochemistry*, **2018**, *57*, 2069–2073.
- 237 M. I. McLaughlin, K. Pallitsch, G. Wallner, W. A. van der Donk and F. Hammerschmidt, *Biochemistry*, **2021**, *60*, 1587–1596.
- 238 G. S. Baviera and P. M. Donate, *Beilstein J. Org. Chem.*, **2021**, *17*, 2028–2050.
- 239 C.-L. Wu, C.-H. Chang, Y.-T. Chang, C.-T. Chen, C.-T. Chen and C.-J. Su, *J. Mater. Chem. C*, **2014**, *2*, 7188–7200.
- 240 K. Okumoto, H. Kanno, Y. Hamaa, H. Takahashi and K. Shibata, *Appl. Phys. Lett.*, **2006**, *89*, 063504, 1-3.
- 241 S. F. Kouam, D. B. Yapna, K. Krohn, B. T. Ngadjui, J. Ngoupayo, M. I. Choudhary and B. Schulz, *J. Nat. Prod.*, **2007**, *70*, 600–603.
- 242 T. A. Corrêa, C. C. S. Alves, S. B. R. Castro, E. E. Oliveira, L. S. Franco, A. P. Ferreira and M. V. de Almeida, *Chem. Biol. Drug. Des.*, **2013**, *82*, 463–467.
- 243 R. C. Parish and L. M. Stock, *J. Org. Chem.*, **1965**, *30*, 927–929.
- 244 D. M. Smith and L. Levi, *J. Agric. Food Chem.*, **1961**, *9*, 230–244.
- 245 F. M. Menger and J. L. Sorrells, *J. Am. Chem. Soc.*, **2006**, *128*, 4960–4961.

- 246 J. L. Kellenberger, PhD thesis, ETH Zürich, **1997**.
- 247 H. Tokuyama, K. Yamada, H. Fujiwara, J. Sakata, K. Okano, M. Sappan and M. Isaka, *J. Org. Chem.*, **2017**, *82*, 353–371.
- 248 J. Xu, Y. Fu, D. F. Luo, Y. Y. Jiang, B. Xiao, Z. J. Liu, T. J. Gong and L. Liu, *J. Am. Chem. Soc.*, **2011**, *133*, 15300–15303.
- 249 R. W. Bates and S. Sridhar, *J. Org. Chem.*, **2011**, *76*, 5026–5035.
- 250 K. P. Jayasundera, S. J. Brodie and C. M. Taylor, *Tetrahedron*, **2007**, *63*, 10077–10082.
- 251 K. M. Joly, G. Mirri, Y. Willener, S. L. Horswell, C. J. Moody and J. H. R. Tucker, *J. Org. Chem.*, **2010**, *75*, 2395–2398.
- 252 M. A. S. Albert Padwa, Steven J. Coats, Scott R. Harring, Lazaros Hadjjarapoglou, *Synthesis (Stuttg.)*, **1995**, *8*, 973–984.
- 253 Y. Gan, P. Wang and T. A. Spencer, *J. Org. Chem.*, **2006**, *71*, 9487–9490.
- 254 Z. Wei, X. Wang, B. Seo, X. Luo, Q. Hu, J. Jones, M. Zeller, K. Wang, B. M. Savoie, K. Zhao and L. Dou, *Angew. Chem. Intl. Ed.*, **2022**, *61*, e202213840..
- 255 V. Percec, M. Glodde, M. Peterca, A. Rapp, I. Schnell, H. W. Spiess, T. K. Bera, Y. Miura, V. S. K. Balagurusamy, E. Aqad and P. A. Heiney, *Chem. Eur. J.*, **2006**, *12*, 6298–6314.
- 256 S. Karabiyikoglu, B. A. Boon and C. A. Merlic, *J. Org. Chem.*, **2017**, *82*, 7732–7744.
- 257 E. H. Sohn, B. G. Kim, J. S. Chung and J. C. Lee, *J. Colloid Interface Sci.*, **2010**, *343*, 115–124.
- 258 R. G. Salomon, D. J. Coughlin, S. Ghosh and M. G. Zagorski, *J. Am. Chem. Soc.*, **1982**, *104*, 998–1007.
- 259 D. Montes Vidal, A. L. von Rymon-Lipinski, S. Ravella, U. Groenhagen, J. Herrmann, N. Zaburannyi, P. H. G. Zarbin, A. R. Varadarajan, C. H. Ahrens, L. Weisskopf, R. Müller and S. Schulz, *Angew. Chem. Intl. Ed.*, **2017**, *56*, 4342–4346.
- 260 C. J. Sih, R. G. Salomon, P. Price, R. Sood and G. Peruzzotti, *J. Am. Chem. Soc.*, **1975**, *97*, 857–865.
- 261 Y. Hisanaga, Y. Asumi, M. Takahashi, Y. Shimizu, N. Mase, H. Yoda and K. Takabe, *Tetrahedron Lett.*, **2008**, *49*, 548–551.
- 262 S. Gnaim, Y. Takahira, H. R. Wilke, Z. Yao, J. Li, D. Delbrayelle, P.-G. Echeverria, J. C. Vantourout and P. S. Baran, *Nat. Chem.*, **2021**, *13*, 367–372.
- 263 H. Wu, S. Chen, D. Xiao, F. Li, K. Zhou, X. Yin, C. Liu, X. He and Y. Shang, *Org. Lett.*, **2023**, *25*, 1166–1171.

- 264 K. Ni, L.-G. Meng, H. Ruan and L. Wang, *Chem. Commun.*, **2019**, *55*, 8438–8441.
- 265 K. Nicholson, J. Dunne, P. DaBell, A. B. Garcia, A. D. Bage, J. H. Docherty, T. A. Hunt, T. Langer and S. P. Thomas, *ACS Catal.*, **2021**, *11*, 2034–2040.
- 266 K. Yasui, N. Chatani and M. Tobisu, *Org. Lett.*, **2018**, *20*, 2108–2111.
- 267 C. P. Tüllmann, Y.-H. Chen, R. J. Schuster and P. Knochel, *Org. Lett.*, **2018**, *20*, 4601–4605.
- 268 K. Osowska, T. Lis and S. Szafert, *Eur. J. Org. Chem.*, **2008**, *2008*, 4598–4606.
- 269 A. Vlasceanu, C. L. Andersen, C. R. Parker, O. Hammerich, T. J. Morsing, M. Jevric, S. Lindbæk Broman, A. Kadziola and M. B. Nielsen, *Chem. Eur. J.*, **2016**, *22*, 7514–7523.
- 270 Y.-J. Li, D.-G. Liu, J.-H. Ren, T.-J. Gong and Y. Fu, *J. Org. Chem.*, **2023**, *88*, 4325–4333.
- 271 G. C. Tsui, K. Villeneuve, E. Carlson and W. Tam, *Organometallics*, **2014**, *33*, 3847–3856.
- 272 F. H. Lutter and M. Jouffroy, *Chem. Eur. J.*, **2021**, *27*, 14816–14820.
- 273 R. Plamont, L. V. Graux and H. Clavier, *Eur. J. Org. Chem.*, **2018**, *2018*, 1372–1376.
- 274 A. C. A. D’Hollander and N. J. Westwood, *Tetrahedron*, **2018**, *74*, 224–239.
- 275 Y. Gu, S. N. Natoli, Z. Liu, D. S. Clark and J. F. Hartwig, *Angew. Chem. Intl. Ed.*, **2019**, *58*, 13954–13960.
- 276 J. E. D. Kirkham, T. D. L. Courtney, V. Lee and J. E. Baldwin, *Tetrahedron*, **2005**, *61*, 7219–7232.
- 277 B. M. Trost, V. S. Chan and D. Yamamoto, *J. Am. Chem. Soc.*, **2010**, *132*, 5186–5192.
- 278 Y. Chen, M. Leonardi, P. Dingwall, R. Labes, P. Pasau, D. C. Blakemore and S. V. Ley, *J. Org. Chem.*, **2018**, *83*, 15558–15568.
- 279 M. H. Nguyen and A. B. Smith, *Org. Lett.*, **2014**, *16*, 2070–2073.
- 280 A. M. Haydl and B. Breit, *Angew. Chem. Intl. Ed.*, **2015**, *54*, 15530–15534.
- 281 I. T. Crouch, R. K. Neff and D. E. Frantz, *J. Am. Chem. Soc.*, **2013**, *135*, 4970–4973.